An holistic bio-inspired approach for improving the performance of Unmanned Underwater Vehicles

Maryam Haroutunian

Doctor of Philosophy

School of Marine Science and Technology

24th July 2014

School of Marine Science and Technology
Armstrong Building
Newcastle University
NE1 7RU
United Kingdom

Abstract

This research, as a part of the Nature in Engineering for Monitoring the Oceans (NEMO) project, investigated bio-inspiration to improve the performance of Unmanned Underwater Vehicles (UUVs). Initially, the capabilities and performance of current AUVs were compared with Biological Marine Systems (BMSs), i.e. marine animals (Murphy & Haroutunian, 2011). This investigation revealed significant superiority in the capabilities of BMSs which are desirable for UUVs, specifically in speed and manoeuvring.

Subsequently, an investigation was carried out on BMSs to find means to make use of their superior functionality towards engineering improved UUVs. It was discovered that due to a mismatch between the purpose of each species evolution and the desired mission of an UUV, all desired characteristics are not evident in a single species. Moreover, due to the multi-functionality of biological systems, it is not possible to independently study each configuration. Therefore, an holistic approach to study BMSs as a system with numerous configurations was undertaken.

An evolutionary search and selection algorithm was developed to obtain the myriad of biological information and adjust them to engineering needs (Haroutunian & Murphy, 2012). This Optimum System Selector (OSS) was implemented to output aspects of the appropriate design combination for a bio-inspired UUV, based on its specified mission. The OSS takes into account the energetic cost of the proposed combination as well as the trade-off between size, speed and manoeuvrability. Appreciating the uncertainty in existing measured biological data, the developed code was successfully verified in comparison with BMSs data.

Energetic cost of transport is a key factor in selecting a design combination based on desired missions. This is key to the accuracy of the algorithm. Therefore, in another essential research theme, a sophisticated study has been carried out on the understanding, calculating, predicting and comparison of various biological and engineered underwater systems energetics (Phillips et al., 2012).

The results of the OSS compared with existing AUVs, showed improvements in the overall capabilities. Therefore, this method is an excellent guide to transform complex biological data for the future design and development of UUVs.

Acknowledgment

NEMO was a collaboration between Newcastle University (NCL), University of Southampton (UoS) and the National Oceanography Centre (NOC) and was sponsored by the Engineering and Physical Sciences Research Council (EPSRC) - Funding reference: EP/F066767/1.

Hereby, I would like to thank all the members of the NEMO team for their guidance and support. My special thanks to my supervisor Dr Alan J Murphy for selfless mentoring and support, to Professor Gwyn Griffiths for valuable knowledge and to Dr Alexander Phillips for all the brainstorming during my research.

Table of Contents

Table of Contents for the Appendices

List of Figures

List of Tables

Nomenclature

A_{fin}.....	Surface Area of the fin $[m^2]$
AR.....	Aspect Ratio
A_{WS}.....	Wetted Surface Area $[m^2]$
BD.....	Body Diameter $[m]$
BH.....…	Maximum Body Height $[m]$
BL.....	Body Length
BW.....…	Maximum Body Width $[m]$
C_D.....	Drag Coefficient
C_f.....	Friction Coefficient
COT.....…	Cost Of Transport $\left[{}^{J}/_{kg.m}\right]$
COT_{Net}.....	Net Cost Of Transport associated with propulsion
COT_{opt}.....	Cost Of Transport at optimum speed; also the minimum *COT*
$\mathrm{COT_{Total}}$...	Total Cost OF Transport
D_{BB}.....	Bare Body Drag $[N]$
D_{BF}.....	Bottom Fin Drag $[N]$
D_e.....	Equivalent Diameter $[m]$
D_G.....	Gills Drag $[N]$
D_{RF}.....	Dear Fin Drag $[N]$
D_S.....	Snout Drag $[N]$
$\mathrm{D_{SF}}$.....	Side Fin Drag $[N]$
$\mathrm{D_{StF}}$.....	Stabilising (Auxiliary) fin Drag $[N]$
D_{TF}.....	Top Fin Drag [N]
EL.....	Elliptical Length $[m]$
E_{fat}.....	specific Energy of fat
FF.....	Fitness Function
FM.....	Flexibility Measure
FR.....	Fineness Ratio
$\{Mass\}$.....	Mass $[kg]$
P_B.....	Brake Power $[W]$
P_E.....	Effective Power $[W]$

P_H..... Hotel Load $[W]$

P_M..... Muscle Power $[W]$

Q_{10}..... A temperature coefficient

Re..... Reynolds Number

R_s..... A chemical Reaction at a specific Temperature

R_{test}..... A chemical Reaction at the test Temperature

R_{Yaw}..... Yaw Radius$[m]$

$R_{Yaw_{TL}}$..... Length specific Yaw Radius $[TL]$

TL..... Total Length [m]

T_s..... Specific Temperature[℃]

T_{test}..... Test Temperature [℃]

U_{crit}..... Critical Speed $[^m/_s]$

U_{eco}..... Economic Speed $[^m/_s]$

U_{max}..... Maximum Speed$[^m/_s]$

U_{opt}..... Optimum Speed $[^m/_s]$

U_{Turn}..... Turning Speed $\left[^\circ/_s\right]$

V..... Volume $[m^3]$

$\propto_{SR}$..... Surface Roughness correction factor

$\propto_{\mathrm{TAE}}$..... Tri-Axial Ellipsoid correction factor

ρ..... Density $\left[^{kg}/_{m^3}\right]$

ρ_{SW}..... Density of sea water

η_m..... Motor/Muscle Efficiency

$\propto$..... Added Drag Coefficient

η_B..... Behind Efficiency

η_D..... Delivered Efficiency

η_H..... Hull Efficiency

η_{Ped}..... Peduncle Efficiency

η_{s}..... Shaft Efficiency

η_{Total}..... Total Efficiency

ξ..... A measure of efficiency equal to $\frac{\eta_{Total}}{c}$ where c is a correction factor

Abbreviations

AMR……..	Active Metabolic Rate
AUV……..	Autonomous Underwater Vehicle
BCF……....	Body and/or Caudal fin swimming mode
BDCF…….	Body and/or double caudal fin swimming mode
BMR……..	Basal Metabolic Rate
BMS……....	Biological Marine System
BUUUV….	Bio-inspired Unmanned Untethered Underwater Vehicle
CFD……....	Computational Fluid Dynamics
GA…….	Genetic Algorithm
FMR……..	Field Metabolic rate
N/A……	Not Available
OMPF……	Oscillation of median or pectoral fin swimming mode
OSS……....	Optimum System Selector
RMR……..	Routine Metabolic Rate
ROV……....	Remotely Operated Vehicle
SMR……..	Standard Metabolic Rate
UMPF……	Undulation of median or pectoral fin swimming mode

Chapter 1. Literature Review: Research background, state of the art of Autonomous Underwater Vehicles and a history of marine bio-inspiration

This chapter contains the background of the research. The history of ocean exploration and exploitation is discussed in this chapter. The concept of Autonomous Underwater Vehicles (AUVs) is introduced followed by their state of the art. Subsequently marine animals are introduced as the original inhabitants of the oceans with potential capabilities which could be a source of inspiration to improve the current capabilities of AUVs. The motivation of the research is presented and the aims and objectives are set. The methodology and the structure of the research are set out and finally the main achievements and novelties of the research are presented.

1.1 Introduction

Over three quarters of the earth's surface is covered with water. Therefore, the oceans are the habitat of the largest part of the earth's biodiversity (Madin, 2005). They are home to over 750,000 marine species. This has always intrigued humans to explore the oceans to discover the deepest depths. As a result, the history of ocean exploration and exploitation by mankind goes back to possibly 130,000 years ago; some stone tools discovered in the island of Crete suggest this (Strasser et al., 2010). The oceans' discoveries carried on with exploration by human divers in Greece and China, c.4500 B.C and the genesis of ship-borne deep-sea research carried out by the likes of Sir James Clark Ross in the 17th Century. Later on in the 20th Century, humans managed to descend to the deepest depths of the oceans by means of technological advances. A more recent example of manned descent is the journey of Jacques Piccard and Don Walsh to the deepest known place in the oceans which is in excess of 10000 *m*; this was in 1960 (Blidberg, 2001). Due to technical constraints and logistics in accessing the depths of the oceans, very few marine species are discovered in depths deeper than 2000 *m*. Aside the desire to solve the mysteries of the planet and its processes, many other reasons and resources attract humans to the oceans. The paramount necessity of having unlimited access to the most remote parts of the oceans is evident.

Oil is still the major source of energy on earth used by mankind. In search for new oil and gas reservoirs, the offshore industry will be exploiting deeper waters

extensively. Underwater platforms capable of exploring the deep oceans effectively will be required to facilitate this search. A thorough understanding of the impact of deep water intervention will be necessary to assess any environmental and biological damage (Gage, 2001). As well as exploration, surveying of the underwater structure will be of the upmost necessity. Means to make the survey of the structure and pipelines available with a high endurance of performance are in demand by the industry.

Apart from oil and gas, oceans also contain various minerals and other elements, which can be used in different sectors such as the food or pharmaceutical industry to treat many medical conditions. Some of these minerals are only found at certain depths. The discovery and retrieval of these resources economically is required by the food and pharmaceutical sectors.

Not only the biodiversity but also the animal behaviour and social life are of interest to many scientists. Platforms that can observe marine animals and track their movements while keeping up with their speed and manoeuvrability are in high demand. The observing platform must be accepted by the community or school of the observed animals, not injuring them or causing panic due to noise, etc.

All the demands from different sectors keen to explore and exploit the potentials in the oceans highlight that the persistent presence of mobile underwater platforms with diverse capabilities of speed, depth, manoeuvrability and endurance must be sought.

1.2 Ocean operations and the state of the art of Underwater Vehicles

Exploring the oceans to the extent which is possible today, has been facilitated by underwater vehicles. Access to deep waters where humans were previously unable to reach was initially improved by the design and application of manned submarines and later on, within the last half a century, by Unmanned Underwater Vehicles. Initially Remotely Operated Vehicles (ROVs) and more recently, with the increase in the sophistication of computers, Autonomous Underwater Vehicles (AUVs) have been designed and used. All these vehicles have made many underwater operations possible in scientific, military and industrial sectors.

The performance and capabilities of Unmanned Vehicles, specifically AUVs, have improved rapidly within the last few decades. Some good examples of AUV capabilities are that nowadays, AUVs exist that have reached or have the potential to reach the depths of 6000 m underwater (McPhail, 2009), whilst the deepest depths of the oceans are 11000 m. Furthermore, some glider type AUVs are able to operate months without

requiring refuelling which is a long range of operation. Some gliders have a required electrical power of less than 1 Watt (Griffiths et al, 2007). The two examples of fast AUVs are "Alister" (Figure 1.1) and "SeaOtter" (Figure 1.2) which have a maximum speed of 4.12 $\left[\frac{m}{s}\right]$ (Copros & Scourzic, 2011 and Somers, 2011), while the fastest AUV, Auv62-MR (Figure 1.3) has a maximum indicated speed of 10 $\left[\frac{m}{s}\right]$.

Figure 1.1. Alister REA AUV (AUVAC, 2010)

Figure 1.2. SeaOtter AUV (AUVAC, 2010)

Figure 1.3. AUV62-MR (SAAB, 2014)

However, generally, for AUVs a depth of up to only 1000 m and a speed of 1.5 $\left[\frac{m}{s}\right]$ are commonly achievable. As illustrated in Chapter 3 of this thesis only 13% of AUVs have a manufacturer's indicated depth of 6000 m and having a limited speed range, none of the AUVs have achieve speeds of more than 10$\left[\frac{m}{s}\right]$. From the AUVs performance data it is realised that currently there are restrictions in their capabilities mainly in terms of speed and depth capabilities, manoeuvrability and range of operation.

Therefore, there is always further demand to improve the underwater capabilities of AUVs beyond their current level of performance. The users of underwater vehicles demand more manoeuvrable vehicles to be able to reach, explore and operate in the deepest depths and harshest environments of the oceans at higher speeds. Having greater endurance coupled with lower possible cost is also a demand in many sectors.

AUVs are used in various sectors, each requiring different improvements and modifications. Offshore industry demands facilitated access to explore deep waters for surveying, inspections and maintenance. Different sectors of scientific communities

highly demand improved deep water capability of Underwater Vehicles for discovery journeys, to observe marine life, track marine species, gather pharmacological samples and perform environmental research. Furthermore, military sectors as well as security agencies strive constantly for improved performance and extended capabilities in all aspects of underwater technologies such as speed, endurance and especially stealth.

The demands or desired mission profile by various sectors are different and very diverse, concentrating on one, some or all aspects of AUV performance. To satisfy different mission profiles, AUV designs, parts and software must be tailored for different levels of improved manoeuvrability, speed capability or larger operating ranges. This must be coupled with lower weight and less cost both of which are desirable. Improved AUVs which are able to perform desired missions with more precision while being cost efficient, will satisfy these demands. Attempting to combine and benefit from the abilities of hybrid ROVs and intervention AUVs is another aim of new vehicle designs (Kermorgant & Scourzic, 2005).

1.2.1. Engineering Challenges

Conventional engineering methods are commonly used to improve the performance and capabilities of manmade machines. For AUVs, using lighter materials as well as a significant improvement in sensors and software have broadened their operational abilities and extent. Using common practice on engineering optimisation, some attempts including using lighter materials, more powerful sources of energy, and different buoyancy systems and optimised software have increased the capabilities of AUVs.

Although significant research attempts are carried out to improve the sensors and software in AUVs, little attempt has been made to manipulate the body design and propulsion modes of these vehicles, therefore turning them into "sensor taxis".

A challenge in the design of AUVs is the trade-off between various features and characteristics. For example, in current AUVs, having a larger size means being able to carry more battery mass and more payload, however size negatively affects the overall cost as well as other aspects of performance such as turning ability. It must also be noted that with variance in size there is also the scaling effect on drag. For larger vehicles, the Reynolds number (*Re*) is higher as it is directly proportional to the length. Flows at Reynolds numbers smaller that 5×10^3 are usually laminar while flows at higher Reynolds numbers are typically turbulent. In turbulent flows, unsteady vortices appear and interact with one another and skin friction drag increases. The change in the

structure of the boundary layer and the location of separation may result in less overall drag.

Some of the relatively new desired missions of AUVs are requiring levels of performance which was not originally applicable to AUVs. An example is animal tracking and observation. This requires a level of manoeuvrability unachievable by current AUVs. The new mission profiles require a review of original AUV design and an attempt to modify it to match the diverse range of desired missions. To improve the AUVs' capabilities, other possible means and sources of inspiration must be investigated.

1.3 Nature as a source of inspiration and the research motivation

Oceans are the habitat of about 90% of the living species. This makes the oceans the largest part of the earth's biodiversity (Madin, 2005). Marine Animals are the biological equivalent of AUVs. The 750,000 plus species living in the marine environment range in size from a few micrometre species to the Blue Whale which can grow to more than 30 meters in length. For simplicity and brevity, marine species are referred to in this research as Biological Marine Systems (BMSs).

It must be noted that the term "Marine" used throughout this research is referred to all species living both in freshwater and saltwater. The information on the living environment of each species can be found in the Appendix 1.2. 13.7% of the species studied in this research swim in freshwater.

For unity of calculation throughout this research, an average seawater density of 1025 $\left[\frac{kg}{m^3}\right]$ is used. Although the density of water varies between freshwater and saltwater (and can vary even with the temperature and salinity of the water), the effects of this change on the results of the calculations within this research are insignificant. For example, considering a unified water density of 1025 $\left[\frac{kg}{m^3}\right]$, for a 15cm goldfish, the bare body drag calculated in Chapter 5 is 0.0268 $[N]$. If the actual freshwater density of 1000 $\left[\frac{kg}{m^3}\right]$ would be used in the calculation, the drag of the same species would be 0.0268 $[N]$. This equals to an error of 2.2%. This verifies that the use of a unified water density does not affect the calculated results significantly.

All of the BMSs have adapted to thrive and survive through various underwater conditions in the ocean space, by different means. Some examples of specific underwater conditions are high water pressure and the lack of oxygen. BMSs have come

to their "successful" solution of survival and are improving continuously through the natural process of evolution. The ones that do survive in their habitat have superior performance and capacities over the ones that extinguish over time. Their superior characteristics, evolving through time, improve their survivability in their specific living environment.

Many BMSs exhibit functionalities and capabilities which are very much similar to the desired engineered features for underwater unmanned vehicles. These include, propulsion or in the case of marine species "locomotion", speed, high manoeuvrability and their resilience for operating and thriving at depth. It has been realised that this performance by BMSs is achieved through the multi-functionality of their systems.

Characteristics of interest in this research are speed and depth capability, manoeuvrability, range of operation and energetics. Some BMSs exhibit extremely high performance in one or more of the "characteristics of interest" of this project. Some examples of these BMSs include the sailfish (*Stiophorus platypterus*), which is able to swim at a speed of over 30 $\left[\frac{m}{s}\right]$ (compared to AUVs achieving speeds of no more than 10 $\left[\frac{m}{s}\right]$) and some marine animals like the snailfish (*Pseudoliparis amblystomopsis*) have been found at the extreme depths of the oceans.

There are many examples of BMSs which suggest that biological solutions picked by nature through evolution make BMSs exhibit superior performance and capabilities in comparison with the engineered alternatives. This suggests that inspiration from BMSs could be a possible approach towards the improvement of AUV performance and optimisation of the capabilities. However, different BMSs achieve their capabilities through diverse approaches. This means that the different aspects of BMSs' superior performance, the extent of their superior performance and the possible inspiration from biology must all be studied and investigated.

It is known from history (Vincent, 2001) that inspiration from nature by researchers and inventors traces back to at least the last three millennia. One of the simple and useful examples of bio-inspiration in the marine world is the swim fin, invented by Benjamin Franklin in 1717 (Fleming, 1972). Numerous types of studies and investigations are carried out on marine species with different purposes. These studies are discussed next.

1.4 Studying marine animals and marine bio-inspiration timeline

Several research works have studied and investigated BMSs from different sectors of science and engineering and with different aims and objectives. The combination of all types of these research works has led to bio-mimetic and bio-inspirational finding. Some classes of BMSs are studied more than others. As expected those species which are more easily available are investigated more than other species such as the Blue Whale which are rare and extremely large in size. Their size makes even simple measurements such as weight, very challenging. Therefore data for fish and small marine mammals is more available than other species such as rays and penguins.

Several studies and investigations of BMSs have been of interest to this project, some purely because they provide collectable data on BMSs and other because they provide a better understanding of the mechanism of some species. Although most of the data is raw and some use ambiguous terminology, they have become useful for the purpose of this research through manipulation or have been used for calculating other desirable parameters. Other studies have traces of either bio-mimicry or bio-inspiration within them and have been used to understand bio-inspiration. In this section different studies carried out on marine animals are discussed and the timeline of marine bio-inspiration and bio-mimicry is explained.

The studies on BMSs have been classified in this research into distinct groups as follows:

- Biological studies
- Specific biological features
- Biological comparisons
- Hydrodynamics and locomotion of BMSs
- The design, build and investigation of biomimetic examples based on marine species
- Bio-inspired investigation

These are each explained next.

1.4.1. Biological studies

These research works are usually performed by marine scientists to investigate the growth, reproduction and general behaviour and wellbeing of various BMSs. The biological studies either provide data on a specific individual(s) of the same species or the average values for a species. Data on specific individuals are more desirable when

comparing different systems as it provides a more precise estimate of the performance characteristics of that specific BMS, provided consistent terminology for the characteristics of all BMSs exists. However, as usually scientists are specialised in studying a certain group of BMSs and each class of BMSs are evolved differently, therefore studying each group and the terms used can be slightly different. For example, energetic Cost Of Transport (*COT*) of BMSs have been defined as energy consumed by kilogram of BMS's body per one meter of travel, $\left[\frac{J}{kg \times m}\right]$, or as the energy consumed for each kilogram of BMS's body per one stride of travel, $\left[\frac{J}{kg \times stride}\right]$, or as energy consumed per Newton per meter of travel, $\left[\frac{J}{N \times m}\right]$.

Therefore, data and results from these studies was used with due care, by unifying the terminology to compare similar terms.

1.4.2. Specific biological features

In some other studies, a specific aspect of BMSs characteristics has been investigated. For example, Altringham & Johnston, 1990, studied and measured the power output of the fast and slow muscle fibres of the bullrout (*Myoxocephalus scorpius L.*). These types of research give an understanding of a particular aspect of BMSs performance and the data gathered from them can be used for the purpose of understanding and comparing those aspects of the BMSs performance characteristics, either directly or after manipulation. In most cases these types of research only provide details of a single species, therefore many similar studies must be carried out to enable the comparison of results with other BMSs.

1.4.3. Biological comparisons

For the purposes of this thesis, "biological comparisons" is associated with research works in which certain characteristics of some BMSs are compared with each other or with other species (e.g. terrestrial animals). The results of these studies provide some data on the compared capabilities of BMSs. If the values are average values of the performance of the BMSs, i.e. do not belong to a single individual, the data are not as accurate as the data collected from a single individual. For some BMSs, these data are the only data available.

Some of these research works are looking into certain performance characteristics within a family of BMSs. The results of these studies provide an insight to the extent of

similarities and differences between BMSs with close genetic relations. As part of the present research it was realised that when the results, trends or empirical formulae used in biological comparison research works can be generalised for all or a group of BMSs, those formulae can be used to estimate some aspects of the performance characteristics of other BMSs in the same group for which the data in not available. An example is different regression lines obtained for the basal metabolism of some BMSs as discussed in Chapter 4.

1.4.4. Hydrodynamics and locomotion of BMSs

Hydrodynamics and locomotion of BMSs and specifically fish and relatively small marine mammals have been the subject of many research works. Studies on the hydrodynamics of marine mammals have been performed for example by Fish, 1993, 1996 and 1998. These research works were carried out on the hydrodynamics and swimming performance of some cetaceans to measure drag or measure and compare the power and thrust and therefore have estimates of the drag based on body and propulsion characteristics of the cetaceans. Also Fish & Rohr, 1999 investigated drag reduction while examining methods including viscous damping, dermal ridges, secretions and boundary layer heating based on the hydrodynamics of dolphins.

In similar studies for fish, Webb, 1975 studied general hydrodynamics of fish while Sfakiotakis et al., 1999 investigated different fish locomotion.

Some other studies have also been carried out on the prediction of hydrodynamics of a BMS by mathematical methods or computational fluid dynamics (CFD). Both methods can result in very sophisticated results but they are highly time consuming and therefore not possible to study multiple species simultaneously.

Reading about various definitions of propulsive efficiency in literature and encountering some unrealistically high values was a motivation to the present research work to introduce a unified terminology for various efficiencies within BMSs bodies for clarification and to avoid future confusions. This work is explained in Chapter 5 of this thesis.

1.4.5. The design, build and investigation of Biomimetic examples based on marine species

In more recent years some research works have been carried out to design and build a biomimetic prototype based on a BMS. Some of these prototypes are also known as bio-mimetic AUVs. An interesting aspect of these studies is the reproduction of

different aquatic locomotion modes as an alternative to AUV propulsion. Some of the many examples of these prototypes which have been built by the reproduction of body and caudal fin propulsion include, the lamprey-like BUR-002 (Ayres et al., 2000), the RoboTuna (Streitlien et al., 1996) and the RoboPike.

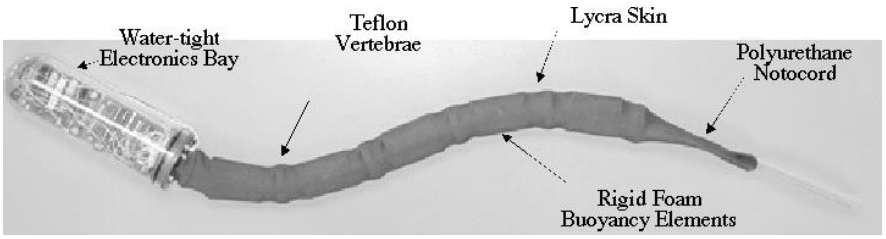

Figure 1.4. Lamprey-like prototype (Ayres et al., 2000)

Figure 1.5. Robotuna (Science museum, 2014)

Figure 1.6. Robopike (AUVAC, 2010)

There are also other research based on median or paired fins such as the JAMSTEC which is based on the swimming of a skate (Yamamoto, 2005) and the AquaPenguin (Figure 1.7) which is a prototype designed and built by Festo.

Figure 1.7. AquaPenguin by Festo (AUVAC, 2010)

The AquaPenguin is built mimicked from a penguin. However it has a speed of 1.39 $\left[\frac{m}{s}\right]$ which as part of this research is was realised that this speed is considerably lower than the speed of a same size penguin. Another example is the Subsea Glider (Figure 1.8) designed by EvoLogics which is a mimic of a ray. Other types of biomimetic AUVs also exist such as the Aqua Jelly (Figure 1.9) which was built based on a jelly fish by Festo.

Figure 1.8. Subsea Glider (AUVAC, 2010)

Figure 1.9. Aqua Jelly by Festo (AUVAC, 2010)

Aside from the design and build of biomimetic AUVs, research work has also been carried out on investigating some aspects of the performance of the biomimetic AUVs such as the work done by Anderson, 2002 on the manoeuvring capabilities of the RoboTuna. In another research work, Wen et al., 2012 tested the hydrodynamics of a self-propelled but clamped prototype based on an Atlantic mackerel in a water flume.

Although these prototypes are made very similar to the species itself but do not necessarily replicate the same capability of the species. This is a part of motivation for this research to investigate how the multi-functional biological systems can be used for engineering purposes and exhibit similar performance characteristics to the actual BMS.

Apart from the present performance, the above designs and studies have demonstrated potentials of the BMSs' propulsion modes and are the way forward in the design and build of BMS like propulsion systems which could be lighter than the equivalent AUV technologies and will produce considerable less noise.

1.4.6. Bio-inspired investigation

Although bio-inspiration and bio-mimetics are commonly used together, there is a principal difference between the two. Bio-inspiration attempts to understand the rational and mechanism behind a system in nature to perform a certain task, not necessarily mimicking the biological system as done so in bio-mimeitcs.

Relatively recently there have been attempts on the use of bio-inspiration in the design of AUVs. In these studies the focus is on one aspect of the performance and the

aim is to achieve the same capability and not necessarily the same design as a BMS. Fish et al., 2003 proposed the design of an AUV with multiple side control surfaces with improved turning capabilities. In another similar research Long et al., 2006 being inspired by marine turtles made a comparison between a two flippers and a four flippers propelled AUVs concluding that there would be a trade-off between surge acceleration and energetics. Therefore, the two flipper model would operate at lower required power while the four flipper model would have higher surge acceleration. The independent movements of the flippers also provided better manoeuvrability for the vehicle.

In some other research works the fin actuation has been of interest. Anderson et al., 1998, measured the thrust and power generated by an oscillating foil, concluding a high propulsive efficiency for the foil. Streitlien et al, 1996 investigated foil propulsion through vortex control. There have also been developments on propulsors by the use of smart materials (Quackenbush et al., 2003).

1.5 Research Motivation: The developments of bio-inspiration and marine animals as a possible source of inspiration to improve the performance of AUVs

Many bio-mimetic robots have been built which have introduced a new generation of light underwater AUVs with different levels of manoeuvrability and capabilities. Due to their fishlike swimming mode, these robots have been of the interest of both scientific and military sectors. Their body is made from aluminium, fibre glass or other lightweight materials and their manoeuvrability is sometimes improved through a flexible body or side control surfaces.

Currently, increasing number of different engineering disciplines are considering so called bio-mimetic or bio-inspiration in order to make progress in the design of engineered systems. Locomotive systems in nature (i.e. animals) are very versatile. They evolve and alter their strategies to adapt to their environment for better performance. Scientists in different sectors are being inspired through studying numerous biological systems, their locomotion, physiology, anatomy and their interactions with other systems as well as the environment. A testament to this is the IOP Journal of Bioinspiration and Biomimetics which was established in 2006. Research works published in this journal investigate all aspects of bio-inspiration and bio-mimetics from locomotion (bio-mechanics), biological sensors, materials, etc. and their application in aerial, terrestrial and marine sectors. There is a website dedicated to

marine bio-mimetics, and robotic fish (Robotic-fish.net, 2013). Some of the many examples of bio-mechanic/bio-mimetic vehicles include the RoboTuna, RoboPike, Bionic Manta and the Aqua Penguin. They all represent light robotic AUVs with alternative propulsion systems and different manoeuvring capabilities. These successfully built examples of bio-mimicked robots indicate that there are potentials of inspiration from marine species and extensive research is being carried out in this area.

As discussed, a huge amount of study is carried out on numerous BMSs which produce enormous amount of knowledge and understanding of their performance and characteristics, not all maybe useful from an engineering perspective. One thing all these studies have in common is restriction in the classes (groups) of BMSs which have been studied. Furthermore, prototypes or artificial fins bio-mimicked by a species are not usually made based on that specific species because the species is the best performing or the most efficient system but because that particular species has been of the most interest or within the speciality of the research work. Therefore, the bio-mimicked species are not "systematically" chosen.

The robotic AUVs do not perform any specific mission at the moment, except swimming and having visual sensors. Further research is required to realise how they can be used to perform AUV missions, therefore this became another motivation for this research to find a novel method for systematically choosing bio-inspired capabilities to fulfil engineering needs.

BMSs have a diverse set of capabilities, and have an equally diverse set of anatomical configurations. The contrast between BMSs' different anatomical configurations and general AUVs body form is significant, which suggests possible changes to the AUVs' structural design, control surface and propulsion modes should be investigated. The question that arises is that whether a bio-mimetic vehicle can be constructed that can exhibit improved AUV capability, and what would be the extent of any improvement.

Bar-Cohen, 2006 published a research work in the Bioinspiration and Biomimetics journal. The research work set out an approach to develop engineered solutions from sources found in nature that "sorts biological capabilities along technological categories". In present research it is proposed to extend this paradigm to extract elements and concepts from many BMSs to lead to novel engineering solutions which can be directed for a range of applications and diverse sets of mission profiles (Griffiths, 2009).

1.6 The rationale behind bio-inspiration for a new generation of AUVs

Nature has a lot of potentials to offer to improve engineering design techniques. Considering them, one may learn from nature, using the relevant novelties while leaving the undesirable ones, in order to relate engineering requirements to biological function.

However studying the available literature illustrates that there is a gap between the engineered underwater vehicle technologies and the scientific studies on BMSs; although, in some studies, reference has been made to AUV such as in Fish, 1997, AUVs and BMSs have not been challenged and compared with one another. Furthermore, although some studies have compared some performance aspects of genetically close species, very few have investigated a specific aspect of some classes of BMSs. There has not been a study looking thoroughly at approaching the marine animal kingdom as a system, and comparing the overall performance of numerous species. Comparing BMSs with each other as well as with current AUVs will result in realising what are the actual superiorities of BMSs over AUVs, how significant these advantages or disadvantages are, what are the reasons and sources of the differences in their performances and how BMSs technologies can be used to improve the engineered vehicles. Filling this gap was the foundation of this research.

In this research all classes of marine vertebrates have been investigated to get as thorough an understanding of various natural evolutions as possible to then compare them with current AUV performance.

1.7 Aims and Objectives of the research

Increasing demand in improved AUV performance and current restrictions in underwater vehicles capabilities emphasise that improvements to AUV performance and capabilities must be sought.

The aim of this research was to improve the performance of AUVs by investigating novel technologies and generating bio-inspired design techniques and implementation methods based on BMSs. This was performed by taking into account the diversity of BMSs as well as the diversity in the mission profiles desired for AUVs.

The aim was achieved by fulfilling two main objectives: Investigating bio-inspiration and the application of bio-inspiration.

Investigating bio-inspiration involved providing a greater understanding of marine biological organisms and systems for engineering application, and creating a new way of thinking in engineering design.

After bio-inspiration was investigated, lessons learned from nature needed to be applied to find design aspects with improved performance characteristics. In terms of vehicle specification, the principal engineering challenges associated with AUVs are propulsion, manoeuvring and depth capabilities, as well as the storage and efficient use of energy. Therefore, higher speed, greater endurance and depth of operation, reduced fuel consumption and advanced, cost-effective, designs and technologies are amongst the wish-list for AUVs demands. An optimum mixture of these features will result in a new generation of AUVs. These features of both AUVs and marine animals were analysed in this research.

1.8 Summary of Thesis Contribution

As AUV development is of interest to scientific, industrial and military sectors, the results of this work may be of interest to them all as a promising approach towards AUVs with improved capabilities.

In this research, the following summary of contributions has been made:

- Data collection and manipulation for BMS vs. AUVs
- Providing a guide for understanding bio-inspiration as an approach to improve the performance of engineered vehicles.
- Illustrating the important aspect of animal performance characteristics to be studied when investigating bio-inspiration.
- Identifying the superiorities of BMSs and the extent of it.
- Providing a guide on how to interpret the obtained results and knowledge from nature and use them towards engineering needs.

1.9 Synopsis of the methodology

In order to fulfil the objectives and achieve the aim of this research, several performance characteristics of AUVs and BMSs were compared. In order to perform the comparisons various data on the design and performance characteristics of AUVs and BMSs was collected and manipulated for comparison which are explained in Chapter 2. To capture the diverse capabilities of BMSs as much as possible it was decided to investigate all classes of marine vertebrates as well as a class of marine invertebrates. This was an interesting work as a comparison of this scale between the performance characteristics of AUVs and BMSs had not have been performed in the past. After sorting the data, a novel method was presented in this research to simplify the body

forms of BMSs as a tri-axial ellipsoid for easier comparison. Then, the body forms, speed capabilities, depth capabilities, energetic cost of transport and the manoeuvrability of AUVs and BMSs were compared as discussed in Chapter 3. Some parts of the research work done in Chapters 2 and 3 are published in Murphy & Haroutunian , 2011.

The power and therefore energy required for the operation of an AUV can be calculated by knowing the battery capacity and battery consumption of the vehicle. For BMSs the calculation of required energy was more complicated. Therefore, in another theme, means to estimate the energy consumption of BMSs was investigated and discussed in Chapter 4. Some parts of the research work carried out in Chapter 4 are published in Phillips et al., 2012.

When comparing the required power of different systems, the efficiency is also considered. Therefore, in Chapter 5 of this thesis, a novel method was presented to predict an indication of efficiency for BMSs through calculation of drag. In addition a comparison was made with current AUVs. Some parts of the research work done in Chapter 5 is submitted to the Bioinspiration and Biomimetics Journal and is under review (Phillips et al., 2013).

The other focus of this research was on bio-inspired manoeuvrability, therefore in Chapter 6, a novel method was presented for estimating the turning capability of various BMSs by introducing a measure of flexibility. After the body designs, speed, depth, energetics, efficiency and manoeuvrability of BMSs and AUVs were investigated, and BMSs with different superior performance characterises were identified, the first objective of the research was fulfilled.

When attempting to implement the bio-inspired knowledge for engineering purposes, it was realised that there was a mismatch between the purpose of BMSs and the desired mission for AUVs. In addition, not all superior performance characteristics were found in a single species and it was realised that there was a trade-off between various performance characteristics in BMSs. Moreover, due to the multi-functionality of the biological systems it was not possible to investigate each system separately.

Therefore, the concept of a novel search and selection algorithm was introduced in Chapter 7 which would take desired mission profiles as input and through a multi objective genetic algorithm which uses the formulas and equations developed in this research, outputs the bio-inspired design aspects of a Bio-inspired Unmanned Untethered Underwater Vehicle (BUUUV). The outputs include the body and control

surfaces design, propulsion mode, fuel and motor mass, and it will also output an estimate of the speed capabilities, required power and turning capability as an indication of manoeuvrability and overall efficiency for the BUUUV. The Optimum System Selector (OSS) was verified and tested as discussed in Chapter 8. The design output by the OSS shows potential overall improvements to the capabilities of AUVs. Some parts of the research work carried out in Chapters 7 and 8 are published in Haroutunian and Murphy, 2012.

1.10 Novelty and main achievements

In this research a thorough comparison on several performance characteristics of AUVs and BMSs was carried out. The comparison highlighted speed, manoeuvrability, mass specific depth and range of operation of BMSs to be significantly superior to AUVs. For each performance characteristics, the groups of BMSs with the highest performance were also identified.

Various methods which have been proposed and used within this research have made it possible to calculate or estimate the performance characteristics of BMSs. This is most useful where experiments and direct measurements are not available. These novel methods include:

- A method to estimate the mass using a tri-axial ellipsoid model
- Calculating the drag, the required power as well as an indication of the efficiency for BMSs. Analysing the calculated efficiencies of the BMSs indicated that similar efficiencies can be achieved by BMSs with different swimming modes, however at different speeds.
- Estimating the manoeuvring capability of BMSs in yaw axis using a novel flexibility measure.

Having numerous desired AUV missions in mind, to be able to use the multi-functional biological systems to fulfil engineering needs, a novel search and selection algorithm was developed which is able to output some aspects of the design as well as performance characteristics of a BUUUV based on a desired AUV mission profile. The results of the OSS demonstrate theoretically an overall improvement in the performance of equivalent AUVs using a bio-inspired design.

The findings of this research work can be used both to propose alternative bio-inspired designs to fulfil AUV desired mission profiles and also to predict the performance characteristics of BMSs without direct measurement.

Some aspects of this research which have already been published are listed below. For the full articles please refer to Appendix 2 of this thesis:

- Murphy, A.J. and Haroutunian, M. (2011). "Using Bio-Inspiration to Improve Capabilities of Underwater Vehicles". In: 17th International Unmanned Untethered Submersible Technology Conference (UUST 2011), 21-24 August, Portsmouth-USA. Curran Associates, Inc. Pp. 20-31. ISBN: 978-1-61839-927-4
- Murphy A.J. and Haroutunian M. (2011). "Nature in Engineering for Monitoring the Oceans: using inspiration from nature to improve the capability of Underwater vehicles to monitor the ocean space". In: 4th International Conference on Marine Science and Technology for Environmental Sustainability, ENSUS2011. Newcastle upon Tyne, UK.
- Phillips, A. B., Haroutunian, M., MAN, S. K., Murphy, A. J., Boyd, S. W., Blake, J. I. R. & Griffiths, G. (2012). "Nature in Engineering for Monitoring the Oceans: Comparison of the energetic costs of marine animals and AUVs". In: Sutton, R. and Roberts, G. (Ed.) Further Advances in Unmanned Marine Vehicles. The Institution of Engineering and Technology (IET). ISBN: 978-1-84919-479-2
- Haroutunian M. and Murphy A.J. (2012). "Mission based Optimum System Selector for Bio-inspired Unmanned Untethered Underwater Vehicles". In: Autonomous Underwater Vehicles (AUV2012) conference, 24th -27th September 2012. Southampton, UK.

Chapter 2. Nature and Engineering Data Collection and Manipulation

Persistence presence of marine animals in the oceans indicates that they have evolved to thrive underwater. Some aspects of the performance of BMSs is realised to be more advance compared to those of current AUVs. However, the extent of the superior performance of BMSs was not known. This emphasised on the necessity of precisely highlighting the aspects of their performance which are superior compared to engineered vehicles. Also it was required to then estimate how significant these superiorities are. For example, how much the efficiency can be increased and/or the power and energetic cost required reduced by using the biological system alternatives.

In order to highlight potential aspects of BMSs performance which are superior to AUVs and therefore a source of inspiration for improving the performance of the underwater vehicles, the performance characteristics of both AUVs and BMSs were required to be collected or calculated for comparison. The methods of collecting raw BMSs and AUVs data from numerous sources and manipulating them for cross comparison are explained in this chapter. In order to be able to investigate the evolution process for numerous BMSs leading to their specific performance characteristics and choose the ones best suited for the purpose of this research, all classes of marine vertebrates as well as few invertebrates were studied.

The data were used for comparing AUVs and BMSs in Chapter 3 and for verifying the OSS code in Chapter 8. Data on different design and performance characteristics of biological and engineered marine systems was gathered in this research. Due to the complexity of BMSs as well as different methods used in animal studies, various methods of gathering, measuring, calculating or estimating these data are also explained in this chapter.

2.1 Collecting data from literature

As the objective of the data collection was to capture as many different biological and engineered marine systems' performance and design characteristics, for both AUVs and BMSs various types of sources were used. The data collection for AUVs and BMSs are respectively discussed in Sections 2.1.1 and 2.1.2.

The general approach towards collecting data was to gather as much complete data on the body design and performance characteristics of AUVs and BMSs from literature

and then to fill the gaps within the database by other means. The alternative means included dissection (which is explained in Section 2.3 of this chapter), using BMSs photos and videos and also using trends or formula that resulted from analysing other BMSs or AUVs with more complete available data.

Measurements from videos were specifically time consuming and required careful attention. For each BMS, to obtain a precise measurement each frame of the video was viewed in order to find the frame in which the BMS was at zero angles at the appropriate view for taking measurements. The frame was then input into a CAD program, to draw the surfaces from the frame and to take the required measurements.

2.1.1 AUV data collection

Data on the capabilities of currently existing AUVs was collected from a wide variety of sources including AUV manufacturer's datasheets, journal and conference publications, as well as industry intelligence publications (e.g. Funnell, 2007 and AUVAC, 2010). The majority of gathered data for AUVs has been from specification sheets or existing trial results for the vehicle. For some AUVs (especially the ones that have been designed and built by mimicry from a certain species, i.e. biomimetic AUVs) data is not from trials but estimates of the manufacturer. These stated values which are not tested, have been used with the awareness of the uncertainty as the reliability and the accuracy of them is unknown. However, the data was assumed to be sufficiently accurate to perform a general comparison. Within this thesis, a note has been made where specific data in discussion have not resulted from experiment. The data collected for AUVs are listed in Table 2.1.

Table 2.1. Known parameters for each AUV

Known Characteristics	Parameters	Unit or description
Body design	Body Type	General form of the body known for AUVs; includes: Torpedo, teardrop, rectangular, oblate, open space and biomimetic.
	Dry Mass	$[kg]$
	Maximum body height (BH)	Greatest height of the AUV along the main body
	Maximum body width (BW)	Greatest width of the AUV along the main body
	Total Length (TL)	Overall length of the AUV [m]
Speed	Economical speed (1)	$Ueco[\frac{m}{s}]$
	Maximum Speed	$Umax\ [\frac{m}{s}]$
Manoeuvring	Turning (yaw) radius	R_{Yaw}
Diving	Maximum Depth	$[m]$
Energetics	Battery Rating	$[kWh]$
	Endurance	$[km]$ or $[h]$
	Hotel load	[Watt]

(1) The purpose for calculating the economic speed for AUVs was to compare it with the optimum speed of BMSs. However, for majority of AUVs the values for economic speed is not disclosed. As it will be explained later on, the situation is similar for BMSs. Therefore, in the majority of cases the cruising speed of the AUV replaces the economic speed. Having an estimate of the economic speed is important in terms of estimating the minimum energetics cost of transport.

The manufacturers datasheets, brochures and published papers linked within AUVAC, 2010, have been the major source of information and data for AUVs.

In addition, as this research is part of the collaboration with the National Oceanography Centre (NOC), more detailed information of the characteristics data for AUTOSUB 6000 was available to this research work which was not available for other AUVs. The database gathered for AUVs is presented in Appendix 1.3.

It must be noted that there are some challenges regarding gathering data for AUVs which are explained next:

1. Characteristics and especially performance data for many AUVs is not available in public domain, either due to commercialisation or confidentiality. For example, obtaining turning radius data for many AUVs is not possible.
2. Some performance data are based on the design calculations of the AUV (especially for biomimetic AUVs) and therefore have not been confirmed through trial. In the cases the data are “as stated by the manufacturer” and not tested, there is a possibility of exaggeration in the numbers and therefore, there will be a level of uncertainty when compared to other AUVs. As it is not always

clear whether a trial has been performed, one must accept the data unless otherwise proven to be inaccurate.

3. Many AUVs are improved and ungraded, which means through time their performance and characteristics change. Moreover, new AUVs are built with enhanced capabilities. This requires the data to be updated accordingly.

These challenges introduce some issues with the collected data. First of all, as data for all AUVs is not available, it is not possible to have an overall image of all AUVs' capabilities, a similar problem with marine species exist as well.

Secondly, different levels of accuracy in data affect the comparison. Therefore, the comparisons and conclusions can evolve as more information becomes available for different vehicles.

2.1.2 Biological marine systems data collection

A similar database was established for the "engineering" specifications of BMSs, including physical characteristics, anatomy, physiology, hydromechanics and their taxonomic relations and classifications. Gathered data for BMSs was based on experiments carried out on each animal by external sources or the authors' observations and measurements from videos and photos taken from the animals. Data was collected for different classes of marine animals including bony fish, fish with notochords (also known as "jaw-less fish"), sharks & rays, marine mammals, penguins, turtles and squids. Micro organisms are not studied in this research due to their size disparity to AUVs. Data has mainly been collected from either technical papers and books or online databases. "Fishbase" an online database for fish, shark and rays and "Sealifebase", a similar (but not as comprehensive) database to Fishbase for marine mammals and reptiles (Froese &, 2011) have been mainly used to gather data on many BMSs body characteristics, speed and oxygen consumption as well as taxonomy data. Digital Fish Library (Berquist et al., 2012) has been used to measure body dimensions of fish and sharks. A complete list of references used mainly for the purpose of data collection is presented in the "Database References" section of the references.

2.2 A general challenge in bio-inspiration

Where multiple data for a single species was collected from different sources, average values were derived and used. Furthermore, if all the data required for a species could not be obtained from a single source, multiple sources were used to gather the full

dataset for a given species. Therefore different individuals from the same species were used for various characteristics.

Individuals of the same species are different in geometry and performance. For example, their body shape is dependant to their environment conditions such as the time of the year or the applied stresses. Therefore, gathered data is a mean of all existing data for a certain species. The data are stored in a database for comparison.

Unlike engineered vehicles, which have a well-defined capability, the performance of a specific species is a variable depending on the physical and environmental parameters of the samples such as the BMS's body size. Consequently for a given species every characteristic is specified over a range and not given as a specific value and therefore, in many cases values are an average of multiple experiments.

Handling substantial amount of data on numerous individual species presented interesting challenges. It required addressing truly interdisciplinary literature, much of the published data regarding the capability of BMSs is not presented in engineering terms and is often presented for entirely different purposes. As explained in Chapter 1, BMSs have been studied through several approaches. A number of studies exist which use engineering terms, including publications on the hydrodynamics of few BMSs.

On the other hand, many other publications, while providing material of interest in this research are provided for the purposes of life-science and biological research. Moreover, it was acknowledged that the level of sophistication and precision in measuring or calculating some of the characteristics of some BMSs are different in various research works. For example, for measuring the turning radius, while many studies have only consider the turning circle to calculate the radius, Cheneval et al., 2007, also considered the change in the depth of the animal during turning, in order to obtain a more realistic value for the turning radius. It would be ideal if all data were measured with similar precision but due to the diversity of biological systems, having data with different precision were inevitable.

The number of individual species investigated in this research exceeded 300 from which a subset of 247 species with more complete data sets compared to the other BMSs are presented in Appendix 1.2. The amount of research carried out on various BMSs are different, hence the amount of data available for each BMS. Some BMSs have not been studied as thoroughly as others either due to accessibility difficulties (e.g. penguins and deep sea BMSs) or due to their size (e.g. the blue whale). On the other hand, some characteristics of some BMSs have been of the interest of many studies. As

a result, there are gaps in the data and therefore for comparing each characteristic, the subset of the BMSs' database with sufficient published data for comparison has been used. In these cases, taking into consideration the taxonomically close relationship between certain animals, investigating a species in a family is sufficient for the purpose of this research. By overcoming the abovementioned challenges, a database of BMSs has been gathered and the parameters are shown in Table 2.2.

Table 2.2. Known parameters for BMSs

Known Characteristics	Parameters	Unit or description
Body design	Body Form	General form of the body known for BMSs; e.g. Fusiform (1)
	Cross Section Type	General shape of the body cross sectional area (1)
	Average Mass	$[kg]$
	Maximum body height (BH)	Greatest height of the BMS along the main body
	Maximum body width (BW)	Greatest width of the BMS along the main body
	Elliptical Length (EL)	Length of the equivalent ellipsoid of the BMS body
	Total Length (TL)	Overall length from the snout to the end of the rear fin
	"a" & "b" factors (2)	$\{Mass\} = a(\{Length\})^b$
Taxonomy (3)	Full name	Common Name & Binominal Name
	Family, Order, Class	-
Swimming (only submerged swimming is considered)	Swimming Mode	Different body & rear fin or paired fin swimming modes; e.g. Thunniform
	Optimum Speed	$Uopt\ [\frac{m}{s}]$
	Maximum Speed	$Umax\ [\frac{m}{s}]$
Manoeuvring (4)	Turning (yaw) radius	R_{Yaw}
	Turning Speed	U_{Turn}
Control surfaces: (5) Rear fin (Caudal fin) Side fins (Pectoral Fins) Top fin(s) (Dorsal fin (s)) Bottom fin (s) (Anal or Ventral fins) Side stabilising fins (Pelvic fins)	Numbers or pairs	-
	Chord (6)	$[m]$
	Span (6)	$[m]$
	Area	$[m^2]$
	Aspect ratio	$AR = \frac{Span \times Chord}{Area}$
Diving	Maximum Depth	$[m]$
	Depth Range	$[m]$
Energetics	Cost of transport	$\left[\frac{J}{kg.m}\right]$
	Endurance (7)	$[km]$ or $[h]$
	Fat tissue storage	Can aid to estimate the energy reserve

Table 2.3 and Figure 2.1 provide some explanatory notes to Table 2.2.

Table 2.3. Explanatory notes to table 2.2

Note	Description
1	Since height to width ratio for many BMSs is unknown, body form and cross section type are very important and only by having these two parameters, it is possible to estimate the ratio for future calculations.
2	These empirical values are obtained for each species based on measurements (Froese & Pauly, 2011).
3	All data is not available for every species, therefore taxonomy helps to relate data collected to similar animals. In this research taxonomy data are coded numerically for simplicity.
4	Turning speed is inversely proportional to the speed of the animal, therefore maximum turning speed and lowest yaw radius is usually achieved by unpowered turns. An example of conducted experiments on several marine mammals illustrates this fact (Fish, 2002).
5	Gathering this set of data proved to be very difficult, especially since various studies have different definitions. For example, fin surface area could be considered as the projected area of both sides of the fin, one side of the fin or the actual area of the fin. Therefore for this research the area of BMSs control surfaces are measured using the species photo, 2D modelled in CAD software. The ratio is then taken compared to the 2D surface area of the body of the species in side view.
6	In this research and for the purpose of calculating the drag of a BMS, the chord of a fin is always considered parallel to the flow and the span is considered perpendicular to the flow. Refer to Figure 2.1 for an example of the chord and the span of the BMSs' control surfaces.
7	Usually measured during long migration.
Note that all parameters are not known for all BMSs in the database, therefore only the ones with available data are used when deriving calculations.	

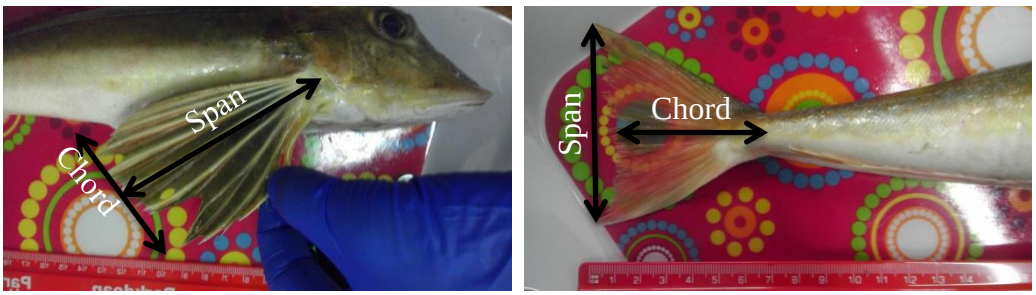

Figure 2.1. An example of chord and span measured for the control surfaces of BMSs as mentioned in Table 2.2 and note 6 of the same table.

2.2.1 Taxonomic coding

As mentioned in Section 2.2, where sufficient published data was not available for a BMS, considering genetic similarities, i.e. taxonomically close relationship between certain animals and realising the fact that genetically close BMSs often have similar characteristics, the performance characteristics of a BMS was predicted. Therefore, by knowing the taxonomic relationships between BMSs there was no need to thoroughly investigate every single species of marine animals.

To make easy use of animal taxonomy when applicable, the taxonomy of the BMSs was represented by a numerical code. A few types of taxonomic serial numbers already exist, such as the Taxonomic Serial Number (TSN) from the Integrated Taxonomic Information System (ITIS) which is in a 6 digit number format (ITIS, 2013) or the FAO Species Codes in a 3 letter followed by a 10 digit number format.

For the purpose of this research, a specific coding was made. The reason for this is that in this research interests are limited to the animal kingdom and only marine species with vertebrates. Moreover, there are limited number of species for which sufficient data is available. In addition, from an engineering perspective, the coding in aimed to categorise the species not only based on genetics which relates to the body design but also to capture some aspects of their performance characteristics such as their swimming mode. Therefore although based on taxonomical hierarchy, the coding is different compared to other coding available in literature and specific to this research. The taxonomy coding was used especially within the OSS as discussed in Chapter 7.

The taxonomy of a species is defined in the general hierarchy form of: Kingdom, phylum, class, order, family, genus and finally the species. Since all the species are animals, the coding starts from the "Class" level of taxonomical hierarchy in an "ABCC-EE" format; where:

- A represents the class/subclass as defined in Table 2.4.
- B divides the BMSs of the same class based on their swimming mode. If swimming mode of the BMS is not available, B is set to 0.
- CC represents the Order/Family level.
- EE represents the Genus/Species in the family.

The complete taxonomy table is presented in the Appendix 1.1.

Table 2.4. Taxonomy Coding of BMSs; representatives of the A value

A	Class	Definition
1	Actinopterygii and Agnatha (2 species)	Fish and "Jaw-less" fish
2	Chondrichthyes and Holocephali (1 species) (1)	Cartilaginous fish and "complete heads"
3	Mammalia	Mammals
4	Aves	Birds; specifically penguins
5	Reptilia	Reptiles
6	Cephalopoda	Head-feet; specifically squids

(1) The only one "Order" still surviving from subclass Holocephali is the "Chimera-forms".

The taxonomy data has been gathered from two main sources: WoRMS (Appeltans et al., 2012) and Fishbase (Froese & Pauly,2011) databases.

2.3 Engineering Dissection

On three separate occasions, data was gathered through the dissection of four different species. The collected data included the body dimensions but most importantly, the mass distribution within different body parts of the species which provided more detailed information compared to what was already available in literature. Knowing the mass distribution within the body of the BMSs was essential as it was used further on in the research to estimate the equivalents of motor mass, fuel mass and payload for BMSs. In addition, as discussed in Section 2.4 the samples gathered from the blubber of two of the species were further tested to estimate the specific energy of their fat.

A whiting (*Merlangius merlangus*), a spiny red gurnard (*Chelidonichthys spinosus*), a junior grey seal (*Halichoerus grypus*) and a junior white-beaked dolphin (*Lagenorhynchus albirostris*) were the four abovementioned species. The first two were bought from the fishmongers and the other two suffered injuries and starvation in the wild and had died. The reason for choosing these species was due to availability (in the case of the two marine mammals) and variety of their body shape and control surfaces.

The seal and the dolphin were dissected in the marine science laboratory in the Ridley building in Newcastle University (NCL) by specialists from the Zoological Society of London (ZSL) as their dissection required special expertise and also there was the possibility of contamination and the fact that the dissection was essential for

further investigation of the cause of death of the two species. The whiting and the gurnard were both dissected by the author to provide the detailed mass distribution which was required for the research. As the dissection of the whiting was part of a dissection training, the results are not as sophisticated as those of the gurnard.

2.3.1 A few considerations regarding "Engineering dissection"

Some aspects of the dissections performed in this research were unique to the research as the required data was different to those of scientific (conventional) dissection. Therefore, a few main points are made on "Engineering Dissection" as follows:

I. Before dissecting the gurnard, its volume was measured by placing it in a container full of water and then measuring the amount of lost water. This was performed during the dissection as attempting to model the species from measurements and photographs was extremely time consuming and possibly not as accurate. However, for the two marine mammals, this process was not possible due to the limits to the size of the container. The volume measured with this method was used in Chapter 3 to justify the use of tri-axial ellipsoids as a simplified shape for the body of BMSs.

II. At no point during measurement, should unnecessary pressure be put to the animal body since the flexibility might affect the precision of measured data. Precision is key, since the values are used for comparison, calculation and estimation further along.

III. Total body length, maximum height and maximum width have been measured. Body girths (circumferences) are often measured in scientific dissection and used for observing the growth of the species. These measurements are not useful since they do not indicate the ratio of height to width which is vital in drag and manoeuvring comparison and calculations.

IV. A camera was placed horizontally on top of the dissection table to take photos of each body part, especially the full body (top and side view) and control surfaces. These photos were then used to confirm measurements of lengths and also to calculate areas.

V. Each item and organ in the body was precisely separated and weighted since the exact mass was required; therefore no part should be mixed with the other; e.g. no flesh should remain attached to the bone. If separating flesh from the vertebrate, slight cooking of it will ease the process of separation but will affect the weight of the flesh.

Therefore the mix of bone and flesh have not been cooked in this research and the flesh has been separated from the bone with due care.

2.3.2 Presenting the dissection results

The three main views and the main measured body dimensions are illustrated in Figure 2.2.

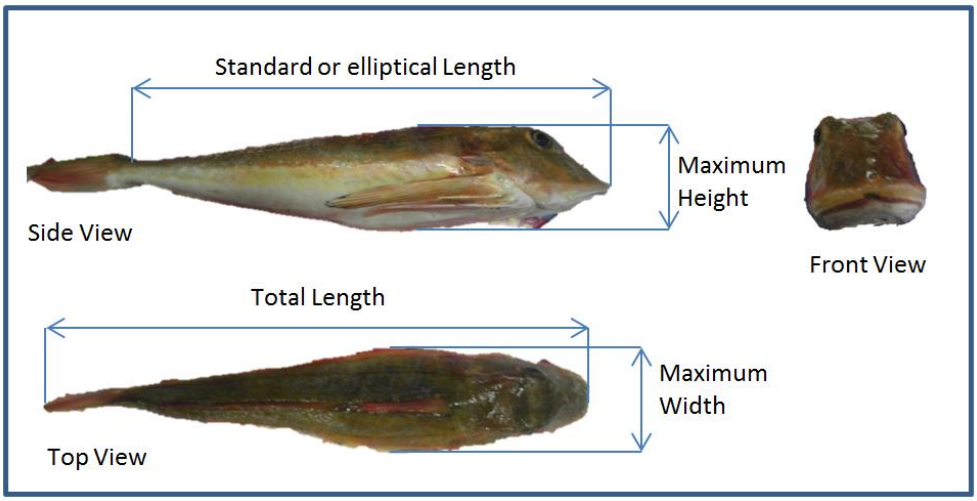

Figure 2.2. Side, Front and Top view of the gurnard (*Chelidonichthys spinosus*) prior to dissection with the main dimensions illustrated on the body

Tables 2.5 and 2.6 respectively show the detailed mass measurements of the body parts of the whiting and the gurnard. The tables are accompanied by Figures 2.3 through to Figure 2.6 which show different body parts of the two species. Figure 2.3 particularly shows the engineering dissection and arrangement of the species.

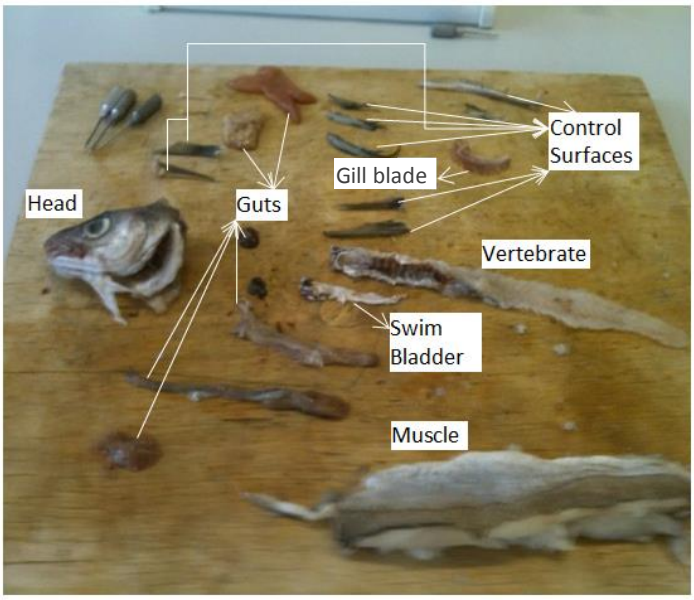

Figure 2.3. Dissected whiting (*Merlangius merlangus*)

Table 2.5. Mass Distribution of the whiting (*Merlangius merlangus*)

Body part	Sub parts	Mass [gr]	% of the total Mass	Note
Inside the gut		**20.9**	**9.33**	
	kidney	Not measured	Not measured	Very light; could not be measured by the scale
	stomach	4.8	2.14	
	liver	4.5	2.01	
	pyloric caeca	3.8	1.7	An additional organ for digestion in many fish
	intestines	7.8	3.48	
Head		**59.6**	**26.6**	
	brain	Not measured	Not measured	Very light; could not be measured by the scale
	gill blades	3.42	1.53	It had 6 blades
	heart	0.6	0.27	
1st Anal fin		**2.7**	**1.21**	
2nd Anal fin		**0.3**	**0.13**	
Caudal fin		**1.18**	**0.53**	
Pectoral fins		**1.64**	**0.73**	It had bits of flesh attached to it
Pelvic fins		**0.04**	**0.02**	
1st Dorsal fin		**1**	**0.45**	
2nd Dorsal fin		**1.25**	**0.56**	
3rd Dorsal fin		**0.3**	**0.13**	
Flesh (Muscle & fat mixture)		**118**	**52.7**	Contained red and white muscles
Vertebrate		**17.28**	**7.71**	
Sum of Masses		**224**	**100**	

A pie chart of the mass distribution for the whiting is presented in Figure 2.4

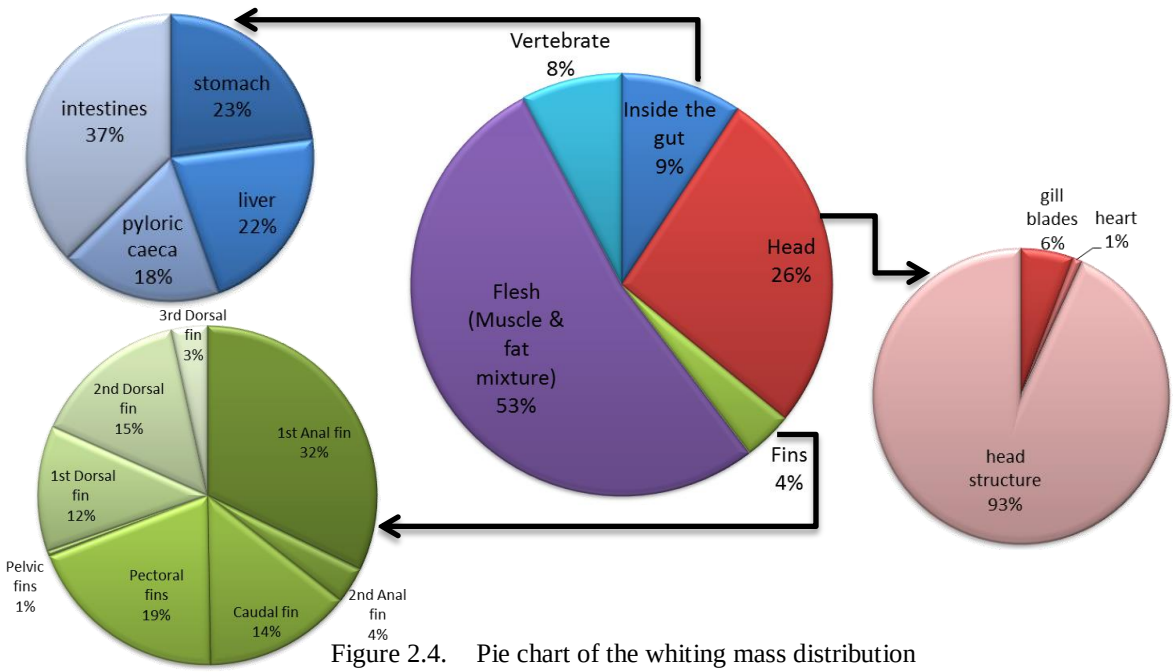

Figure 2.4. Pie chart of the whiting mass distribution

Table 2.6. Mass Distribution of the gurnard (*Chelidonichthys spinosus*)

Body part	Sub parts		Mass [kg]	% of the total Mass	Note
Inside the gut			**0.055**	**11.2**	
	1	kidney	0.002	0.4	
	2	gonads	0.008	1.6	
	3	unknown	0.009	1.8	
	4	oesophagus	0.008	1.6	
	5	stomach	0.016	3.3	
	6	liver	0.009	1.8	
	7	gall bladder	0.003	0.6	
Head			**0.091**	**18.6**	
	9	heart	0.002		
Anal fin			**0.001**	**0.2**	
Caudal fin			**0.005**	**1.0**	
Pectoral + pelvic area			**0.044**	**9.0**	**This included flesh mass connected to the fins**
	8	Right side	0.023		
		Left side	0.021		
Flesh (Muscle and fat mixture)			**0.22**	**45.0**	
	Total pectoral & pelvic area		0.027	5.5	White muscle
	end section		0.108	22.1	White and red muscles
	gut surrounding		0.085	17.4	White muscle
skin			**0.016**	**3.3**	
Vertebrate			**0.041**	**8.4**	Included the dorsal fins
	End section		0.024		
	Gut surrounding		0.017		
Sum of Masses			**0.473**	**96.7**	
Lost Mass (assumed blood)			0.016	3.3	

Figure 2.5 demonstrates the numerals in Table 2.6.

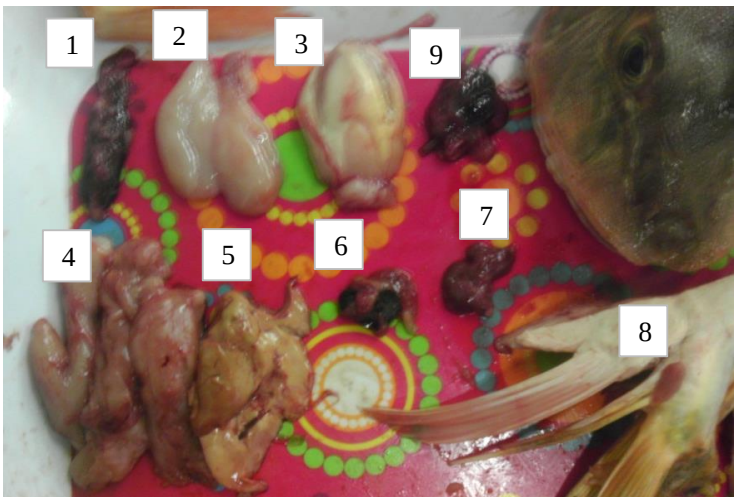

Figure 2.5. Numerated dissected gurnard body parts used it Table 2.6

A pie chart of the mass distribution for the gurnard is presented in Figure 2.6.

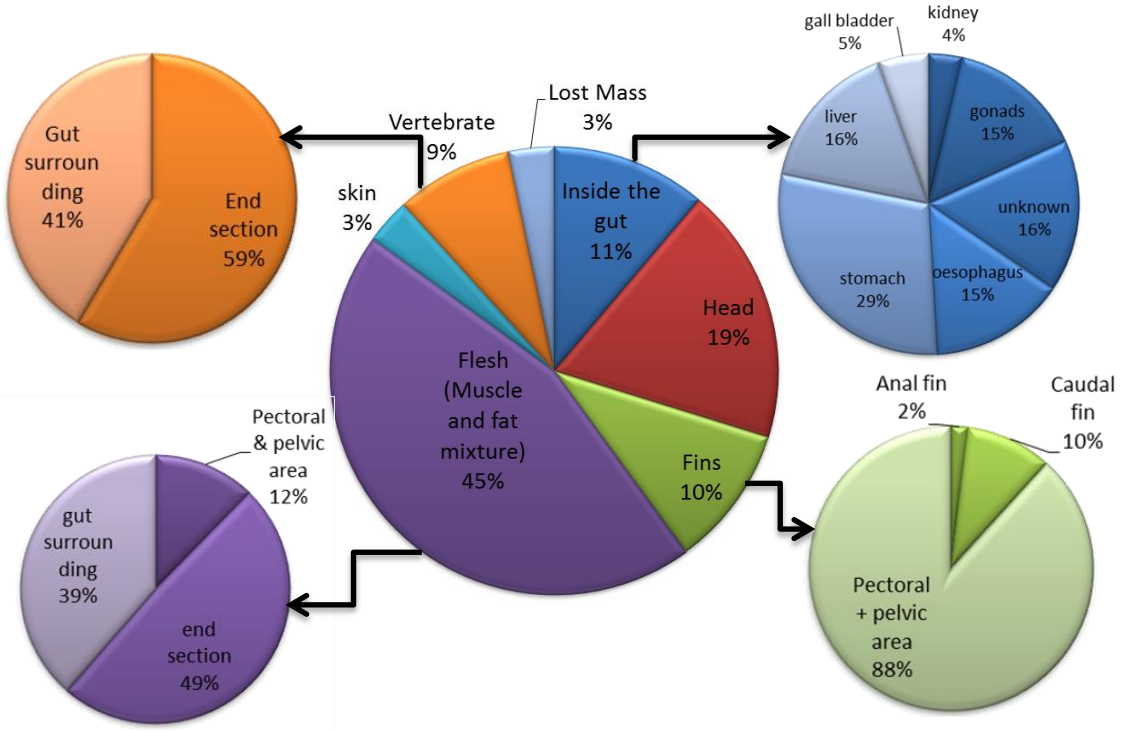

Figure 2.6. Pie chart of the gurnard mass distribution

The weight distribution of a 21.6 [*m*] female finback whale (*Balaenoptera physalus*) has also been collected from literature (Quiring, 1943).

Table 2.7. Mass distribution of the finback whale; raw data gathered from Quiring, 1943

Body part	Sub parts	Mass [kg]	% of the total Mass
Inside the gut		**3471.88**	**5.83**
	Adrenal	0.732	0.001
	Kidney	209	0.35
	Liver	809	1.36
	Heart	382	0.64
	Lung	394	0.66
	Stomach	310	0.52
	Intestine	1,009	1.7
	Diaphragm	250	0.42
	Uterus and Oviducts	103	0.17
	Ovaries	5.15	0.01
Head		**1731.82**	**2.91**
	Thyroid	3.97	0.01
	Brain	8.325	0.01
	Spleen	6.8	0.01
	Eyes	1.72	0.003
	Baleen	484	0.81
	Tongue	1,227	2.07
Muscle and fat		**22254**	**37.47**
	Muscle	9,863	16.61
	Fat and Muscle Bits	12,391	20.86
Blubber		**11,603**	**19.54**
Structure		**7604**	**12.8**
	Total rib weight	1,276	2.15
	Lower jaw	762	1.28
	Bone in the head	1,961	3.3
	Vertebrae	3,605	6.07
Scapula flukes, part of head		**523**	**0.88**
Tail vertebra and tail fin		**301**	**0.51**
Blood and body fluid		**11878.8**	**20**
Sum of Masses		**59367.5**	**99.94**
Lost Mass		26.503	0.06

A pie chart of the mass distribution for the finback whale is presented in Figure 2.7

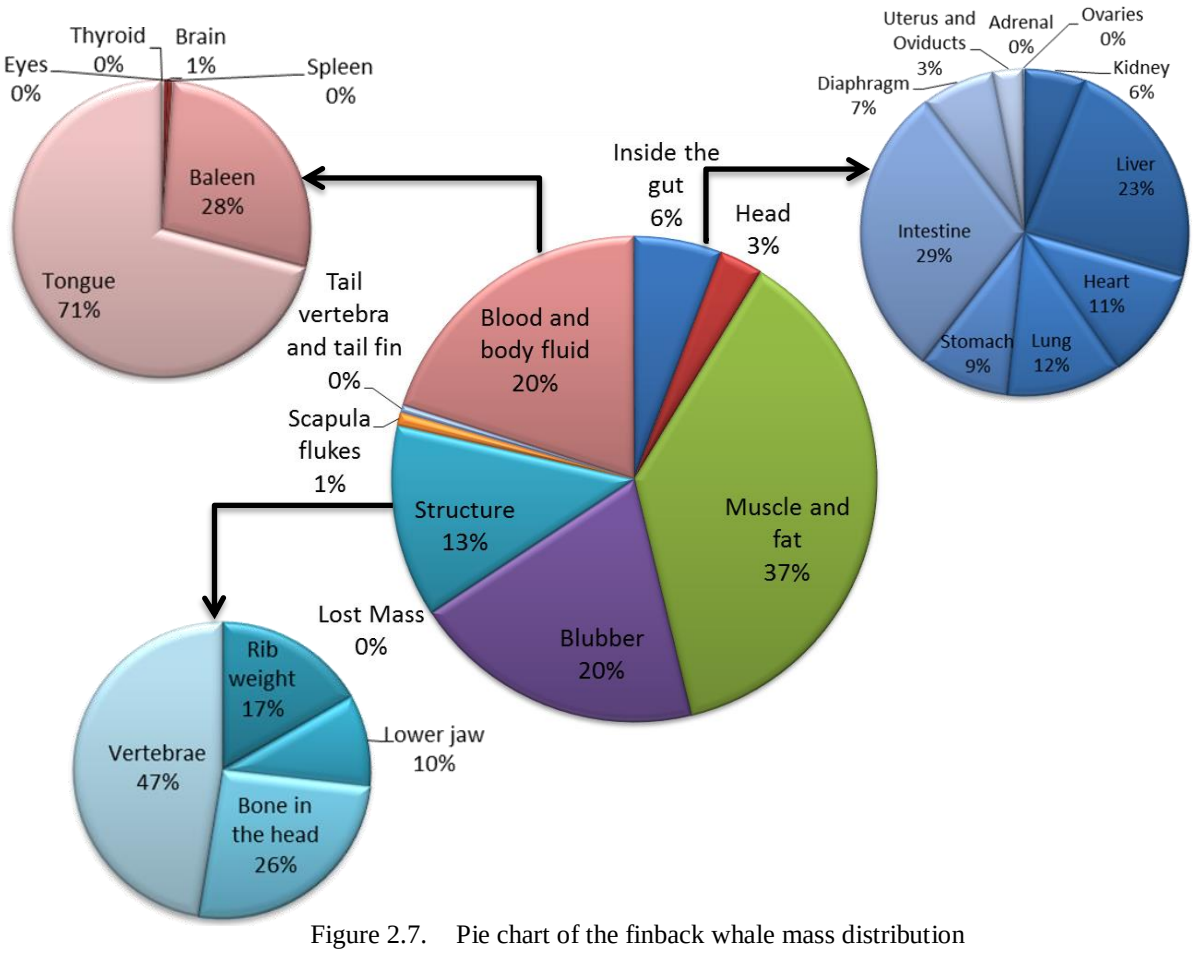

Figure 2.7. Pie chart of the finback whale mass distribution

Although dissection must be a common practice by marine scientists, the measurement data with the extent of detail performed in this research are scarce.

The main findings and usage of the dissections are as follows:

I. As the grey seal and the dolphin dissection was not performed by the author, the main results obtained were the overall mass and body dimensions of the two species; however samples of their fat was taken and tested; this is explained in section 2.4 of this chapter.

II. The measurements of the two fish were more sophisticated and provided details which are hardly found in the literature. The percentage of flesh mass to total mass; the measurement of body width as well as body height and the measurement and specially mass of control surfaces and the guts of the two fish and the whale from literature are used later on in the research when regenerating BMS data to then finding a possible bio-inspired design based on AUV missions.

III. The muscle mass provides an estimate of an equivalent to motor mass for fish and marine mammals, and the mass of the control surfaces and the guts have been used

to find the mass of bare body of BMS as well as to have an indication of corresponding payload for BMSs. These are later on explained in Chapters 5 and 7. As well as muscle, for fish, the flesh (edible part of the fish body) also contains the body fat. Sidwell et al., 1974 and Huss, 1995 published data for the flesh/fillet components of various fish. This has been used in this research to estimate the pure muscle mass and fat mass of the fish. Although, the mass distribution of a single animal does not represent the whole class, the data available at the present and for this research, provided the best estimate possible to be used with the search and selection algorithm in the final stage of the work.

Two more sources have been used in this research which presents some and not all mass data for some BMSs. Cherel et al., 1993 presented some mass data on king penguins (*Aptenodytes patagonicus*) and Lockyer,1976 measured some mass data on 6 species of whales. Table 2.8 shows a comparison of mass distribution of several BMSs of different classes. Mass distribution data for all BMS is not available. However the average values from Table 2.8 are used to have an estimate of mass distribution of other BMSs.

Table 2.8. Comparison of the mass Distribution of several BMSs

	% Muscle (Motor)	% Fat (Energy reserve)	Structure (bones & head)	Unwanted mass for AUVs	Control surfaces	Reference
Finback whale (*Balaenoptera physalus*)	37.47	19.54	12.80	8.73	1.39	Quiring, 1943
Whiting (*Merlangius merlangus*)	52	0.62 (3)	34.04	9.6	3.75	This study
Gurnard (*Chelidonichthys spinosus*)	52	Not measured (4)	29.88	14.3	3.2	This study
King penguin (*Aptenodytes patagonicus*)	32.3-37.8 (1)	15.8 – 17.5				Cherel et al., 1993
6 species of whales		15-43 (2)	12-17 (2)	8-13 (2)		Lockyer,1976

(1) This is the sum of the muscle mass of the pectoral fin (25.3%-28.8%) and the hind limb (7% -9%)

(2) These are the range of values for all the 6 whales

(3) Calculated based on Sidwell et al., 1974 which predict that about 1.2% of whiting flesh is fat.

(4) The mass data for the Gurnard were measured in this study. The mass of the fat was not measurable as due to the small amount of fat in the animal's body, it was not possible to separate the fat from the muscle to be measured separately.

Note that the mass of BMS sensors as illustrated for the whale is 0.02% of the total body mass, therefore insignificant to be considered. However, the organs inside the body cavity or the gut (also known as *viscera*) are not required for an AUV; therefore they can be considered as a corresponding to payload for AUVs.

It is apparent from Table 2.8 that regardless of the class of the animal, the sum of muscle and fat mass is usually between 50%-60% however, marine mammals and penguins have more than 15% of body fat and less than 40% muscle whereas for fish the amount of fat could be as low as 0.3% of the edible meat in cod (*Gadus morhua*) to 17.3% in various eels (Sidwell et al., 1974). Also for whale about 20% of body mass is body fluids which are required for circulation and thermoregulation. The mass of blood in fish body is not significant.

As illustrated in the Table 2.8, in this research the mass of BMSs has been divided as below:

$$\{Mass\}_{Total} = \{Mass\}_{Bare\ body\ (Triaxial\ ellipsoid)} + \{Mass\}_{control\ surfaces} + \{Mass\}_{other\ appendages}$$

Where:

$$\{Mass\}_{Bare\ body\ (Triaxial\ ellipsoid)} = \{Mass\}_{structure} + \{Mass\}_{fat\ (energy\ reserve)} + \{Mass\}_{muscle\ (motor)} + \{Mass\}_{guts\ (payload)} + \{Mass\}_{sensors\ (eyes,brain,etc)}$$

2.4 AUV vs. BMS mass breakdown

As this research is comparing biological and engineered underwater vehicles, it is interesting to also compare the mass distribution of the two. Furlong et al, 2008, published the mass breakdown for Delphin AUV, as shown in Table 2.9. The pie chart of the mass distribution is presented in Figure 2.8.

Table 2.9. Mass distribution of Delphin AUV (Furlong et al, 2008)

Body Part	Sub Part	Mass [kg]	% of the total Mass
Pressure Vessel		**13**	**48.85**
	Fore End Cap	1.56	5.86
	Aft End Cap	1.68	6.31
	Central Bulkhead	1.48	5.56
	Outer Tube	1.72	6.46
	Pressure Vessel Tubes	1.2	4.51
	Electronics	0.6	2.25
	Connectors	0.76	2.86
	Battery	4	15.03
Frame		**3.8**	**14.28**
	Bow	1.4	5.26
	Stern	2.4	9.02
Hull		**1.12**	**4.21**
	Bow Fairing	0.5	1.88
	Stern Fairing	0.62	2.33
Thrusters + Tubes & Mount		**6.4**	**24.05**
Duct + Fins + Servo-motors		**0.46**	**1.73**
Camera + Cable & Mount		**0.65**	**2.44**
Sonar & Mount		**0.5**	**1.88**
Kill Switch & Mount		**0.12**	**0.45**
Marker Droppers & Mount		**0.56**	**2.10**
Sum of masses		**26.61**	**100**

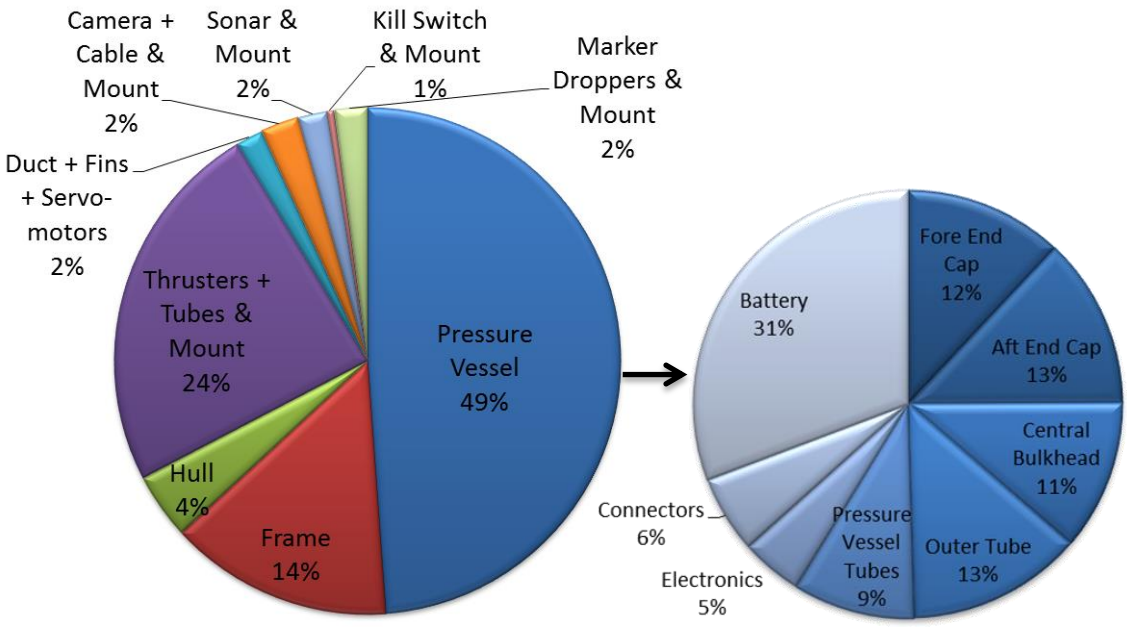

Figure 2.8. Pie chart of Delphin AUV mass distribution

Not all parts in AUVs and BMSs correspond to one another. However, in order to make a comparison, it was decided in the research that a suitable correspondence between AUV and BMS parts is as presented in Table 2.10.

Table 2.10. Corresponding parts for AUVs and BMSs

Body part	BMS corresponding part (s)	AUV corresponding part (s)
Motor	Muscle	Motor
Energy Reserve	Fat	Battery
Structure	Vertebrate, bones & head	Frame, hull and pressure vessel structure
Control surfaces & propulsors	Fins	Thrusters, ducts and fins
Sensors	brain	Electronics
	Eyes	Camera
	Others (e.g. ear, etc.)	Others (e.g. sonar, marker droppers, kill switch, etc.)
Connectors	Blood and nerves	Connectors and cables
Other	Inside the gut, spleen, baleen, etc.	not applicable

The corresponding masses of the sample BMSs and Delphin AUV are presented in a bar chart in Figure 2.9. Delphin AUV is not a representative of all available AUVs, neither are the three BMSs. However, the comparison adds new insights regarding the mass distribution of AUVs and BMSs.

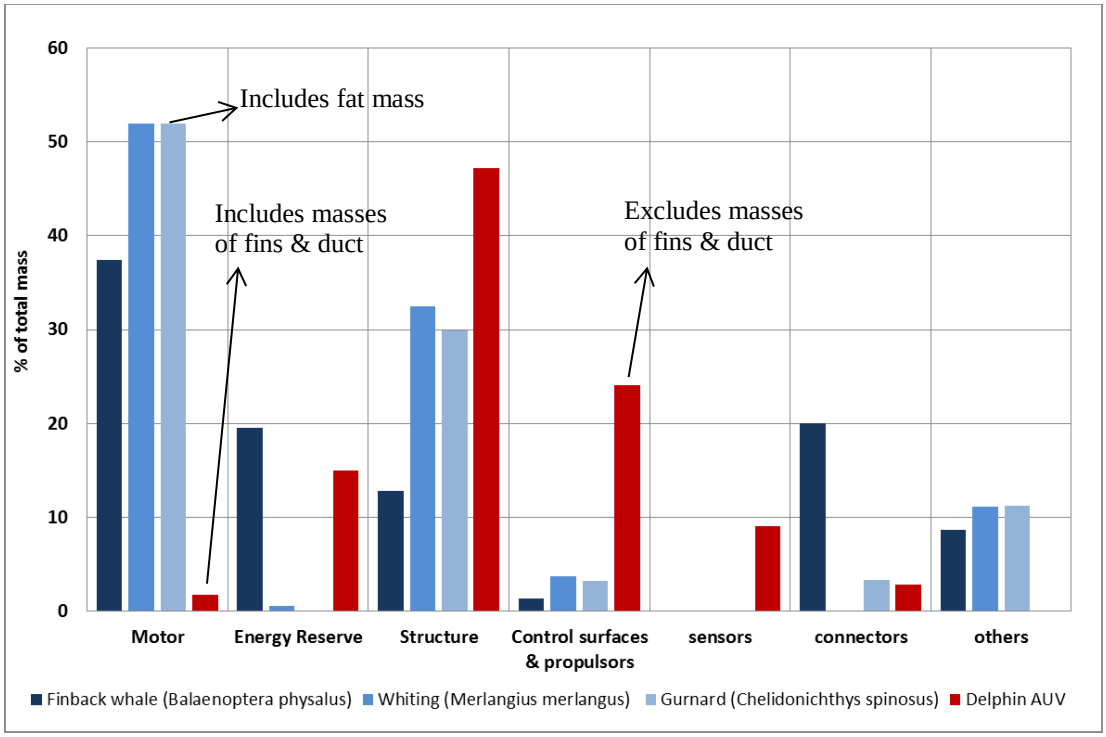

Figure 2.9. Bar chart comparison of masses of available BMSs and AUVs

As shown in Figure 2.9 Delphin AUV has considerably less motor mass (less than 2%) compared to the muscle mass of BMSs (in average more than 35%). Increasing the motor mass or muscle mass can have a significant impact on the speed capability of the vehicle or the animal.

Energy reserve of Delphin AUV is close to one of the finback whale and very similar to the king penguin average mentioned in Table 2.8, while the whiting has considerably lower energy reserve. Higher every reserve can provide higher endurance or the opportunity to consume more power for propulsion.

Most of the mass of Delphin AUV is invested on its structure and control surfaces (47.2%) while the highest value between BMS examples is 32.5%. Lighter materials available to BMSs make it possible for the remaining mass to be used for energy reserve and motor mass. Same statement can be made for the mass of control surfaces and proplusors. Maximum 3.75% control surface mass for BMSs compared to 24% for Delphin AUV.

Sensors are a crucial part of AUVs while in BMSs it is very low and almost negligible.

The connectors mass in Delphin AUV is close the lost mass for the gurnard which is assumed to be blood mass. While the whale being an endotherm has considerably higher blood mass.

About 10% of BMSs body mass which includes the contents of the gut have no correspondence to AUV mass.

From the comparison it is clear that the concentration of mass varies considerably between the AUV and the BMSs (as well as between the BMSs). Higher motor mass and reserved energy can provide more speed and endurance capability while lighter materials used for the structures and the control surfaces can reduce the overall mass or make room for increasing the mass of other parts.

2.5 Fat Specific Energy measurement

As well as the measured data, samples of the blubber of both marine mammals were taken to be tested for their calorific value. It is important to know the energetic value of BMSs fat. Combined with the amount of body fat, the energy reservoir of the BMSs can be calculated.

Samples were gathered horizontally and vertically to check whether the properties change through the depth of the blubber which later did not show any significant difference.

The blubber samples were tested in the calorie-meter of the school of Agriculture, Food and Rural Development. The results are shown in Table 2.11.

Table 2.11. Results of marine mammals' fat specific energy test

Energy Storage Type	Specific Energy (MJ/kg)	Reference
White beaked dolphin blubber	31.9	This research
Grey seal blubber	32.7	This research
Bowhead whale Blubber	36.4	U.S. Department of Agriculture, 2010

Both species where starved therefore the fat was yellowish and rubbery. If the tested sample provided the same calorific value as the blubber provided in the literature for bowhead whale (*Balaena mysticetus*), it would have meant that blubber would be pure burnable energy store; as shown in Table 2.9, both blubbers resulted in about 10% less specific energy. This could be due to being starved; however, almost similar results for two samples means that blubber has similar energetic value in pinnipeds and dolphins.

2.6 Discussion

There are many characteristics to be considered for each BMS or AUV and it is vital to be able to generalise the terminology and understand the differences between various research works and areas of research to be able to gather a reliable large scale database. After gathering and unifying all data, studies were carried out on means to compare BMSs with engineered vehicles, to investigate whether bio-inspiration is a promising approach. However, originally, animals are studied by scientists whereas engineers study vehicles. In bio-inspiration, the two are combined. In addition, since BMSs from different biological classes of species were investigated in this research, the key was to understand the mechanism of both engineered and biological systems and unify the definitions, in order to conduct a valid comparison.

Another interesting challenge was to handle the large size differences especially between numerous BMSs when comparing speed and depth capabilities which, due to

size and taxonomy differences for BMSs, required extra consideration. The comparison of various performance characteristics were carried out as discussed in Chapter 3.

Another important comparison between engineered and biological systems was the energetics. For vehicles, energetic cost is calculated from knowledge of the energy stored in the batteries and its subsequent consumption, which is well defined and specified. However for BMSs with limited available data, the calculation was rather complicated. Therefore, a formulation of the physical factors associated with biological and engineered systems energy usage was presented for energetic cost comparison (Phillips et al., 2012) which is discussed in Chapter 4 of this thesis.

The BMSs and AUVs databases as well as the taxonomy table of the BMSs which have been gathered, manipulated and used in this research have been presented in the Appendix 1 of this thesis for further information.

Chapter 3. A series of comparisons between BMSs and AUVs

In order to identify the aspects of the evolution and therefore performance of BMSs which are potentially an inspiration for engineered designs of AUVs to improve their performance, the characteristics of both AUVs and BMSs must be compared. The data which were collected and manipulated as explained in Chapter 2 are used to make the comparisons. In the present chapter, the methods for making the comparisons are explained, the comparisons are presented and interim discussion from the analysis of the comparisons is presented.

This analysis highlighted the relative superiority and possible limitations of both BMSs and AUVs. The main focus of the present research is to investigate possible improvements to the speed, manoeuvrability and depth capability of AUVs while attempting to reduce the mass and the cost. It was found that for BMSs the cost would be best associated with the energetic cost of their transport and their non-propulsive basal energetic cost. Where essential data is publicly available, energetic cost can also be calculated or estimated for AUVs. Therefore, corresponding to the focus of this research the following comparisons have been made:

- **Diversity of the body forms**
- **Speed and agility**
- **Depth capabilities**
- **Manoeuvrability**
- **Energetics**

Each of the above are considered next, in turn.

3.1 Diversity of the body forms

As various marine species have evolved differently for a variety of purposes and surviving modes, they exhibit very diverse performance. A novelty of this research has been to consider the biological marine systems as a system in which each of the species are a configuration. This required investigating as many species as possible. This was to capture a realistic and sophisticated understanding of the diversity and complexity in the marine biological designs and capabilities to then tailor them for the desired AUV performance. Taking this approach, presented the challenge of diversity in performance as well as in size and design. Overcoming this challenge as explained in this thesis

became a novelty of this research by providing better understanding of the reasons behind different designs of BMSs.

Both AUVs and BMSs have many diverse body forms. The diversity is greater in BMSs and they also exist in wide range of sizes. The size varies from fish with less than a meter of body length to the Blue Whale with an average body length of more than 25 meters. Therefore, before performing comparison of capabilities, the actual body shapes must be analysed for both AUVs and BMSs.

3.1.1 AUVs body shapes

AUV cross-sections are usually circular. Selecting circular cross-sections is mainly for ease of production as well as for hydrodynamic and drag reduction reasons. However, examples of rectangular or oval cross-sections exist as well. One factor on deciding the body shape and cross-section of AUVs is the inside volume required to carry the motor, batteries, sensors and other equipment.

As well as different cross-sections, there are seven main body types defined for AUVs which are studied in this research. These are classed in Table 3.1 that follows.

Table 3.1. Various body types of AUVs

Body Type	Description	Example
Biomimetic	The AUV is made in the shape of a marine animal	Bionic Manta AUV
Torpedo	As by the name, it is in shape of a torpedo with a circular cross section. This is the most used body type for AUVs.	AUTOSUB6000
Oblate	Similar to a torpedo but with an oval cross section	Sea otter MK2
Open space frame	Built with two main bodies connected to each other	Nereus AUV
Blended Wing	The vehicle has two extended side fins which blend with the main body. Similar examples of these wings are seen in nature, such as rays or bats.	XRAY Liberdade
Rectangular	Similar to a torpedo but with a rectangular cross section	Echo Ranger AUV
Teardrop	The body is in shape of a tear drop with a rather sharp rear section	Sea glider AUV

3.1.2 The rational for a unified body shape for BMSs

The main body measurements used for BMSs include Total Length (*TL*), Standard Length (*SL*) as well as maximum Body Height (*BH*) and maximum Body Width (*BW*). A generic example of BMS design in Figure 3.1 illustrates these measurements.

As the bodies of BMS are very diverse, a shape which could represent all BMSs to an acceptable extent was required. In this research, it is proposed that the best shape to describe the general body form of all BMSs which is used to compare them with each other as well as with AUVs, is a tri-axial ellipsoid.

A tri-axial ellipsoid is a 3D shape which will be an ellipse in all three views. This is illustrated in Figure 3.1. For the purpose of this research a new length is introduced. The Elliptical Length, *EL*. The Elliptical Length is the length of the main body which is simplified as a tri-axial ellipsoid. In this research, the Standard Length is corresponded to the Elliptical Length.

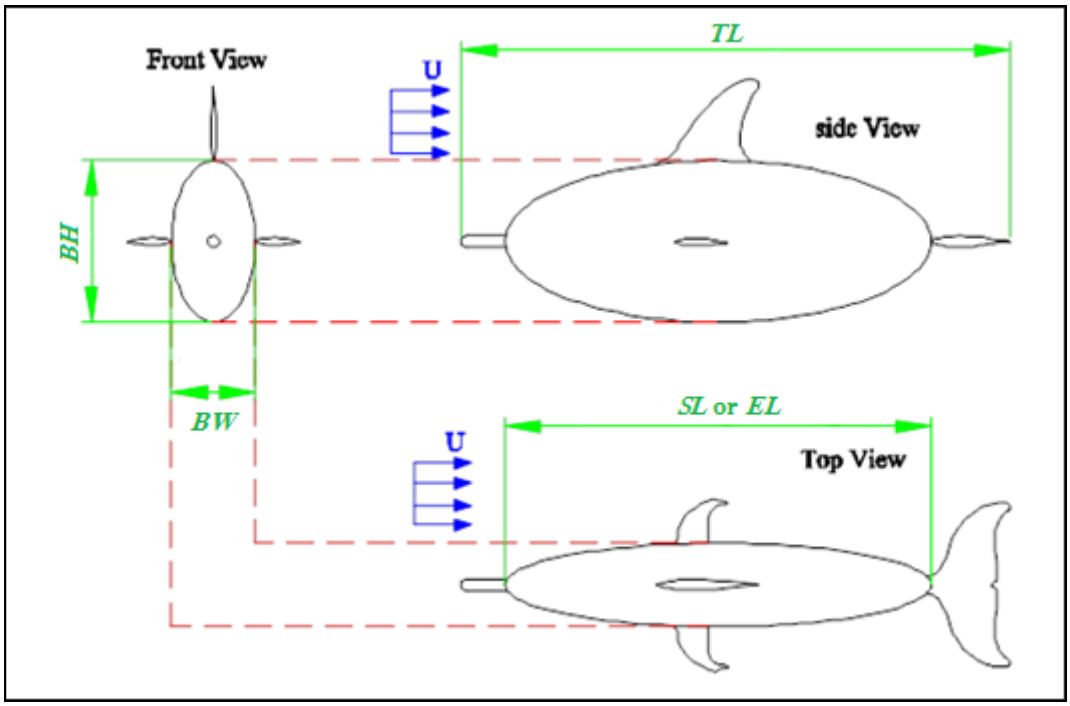

Figure 3.1. A presentation of the generic design of BMSs represented by a tri-axial ellipsoid

A major reason for considering BMSs main body shape as tri-axial ellipsoid is when calculating the drag as described in Chapter 5.

When considering the cross-sections and body forms of BMSs, similar to AUVs, BMSs are very diverse. Classifying the body forms of BMSs was more complicated compared to AUVs. Different classes of marine animals (i.e. fish, sharks, rays, marine

mammals, reptiles and invertebrates) studied in this research have different body forms as well as different control surface and other appendages.

The body forms and cross-sections studied in this work are explained in Tables 3.2 and 3.3 respectively. The cross-sections of BMSs body changes considerably along their body length. However, taking into account all the body segments of all BMSs is highly time consuming. Therefore, for the purpose of this research, the ratio of the largest body-height to body-width of the BMS, defines the cross-section type of the body. Five main body Cross-Sections (CSs) can be defined for BMSs as follows.

Table 3.2. Various body cross-sections of BMSs

Cross-Section	Description	BMSs mainly associate with this cross-section
Circular	A CS for which the width (*BW*) and the height (*BH*) are almost the same. A perfect circular CS is very rare for BMSs. Therefore, where $0.75 < \frac{BW}{BH} < 1.25$ (1), the CS is classified as circular	Marine mammals, penguins and eels
Oval	A CS for which either $0.50 < \frac{BW}{BH} \leq 0.75$ or $0.50 < \frac{BH}{BW} \leq 0.75$ (1)	Some fish and sharks
Oval box	Similar to oval CS. However the CS is not properly oval shaped and it more reassembles a rectangle with rounded corners.	Some fish such as the boxfish (genus Ostracion)
Compressed	A CS for which the $\frac{BH}{BW} > 2$ (1)	Some fish such as the sailfish (Stiophorus platypterus)
Flat	A CS for which the $\frac{BW}{BH} > 2$ (1)	Rays, turtles and flat fish

(1) These values are not formally defined in literature and were quantified by comparing the values from the BMSs within the database.

In addition, various body forms of the investigated BMSs were divided into six groups as presented in Table 3.3.

Table 3.3. Various body forms of BMSs

Body Form		Description	Example of BMSs
1	Anguilliform	Eel-like body form. Long bodies with relatively small CS compared to the body length	eels
2	Elongated	An elongated version of a fusiform body. The ratio of length to diameter is less than an eel but marginally more than a fusiform body. The body is not tapered at the end as such as the fusiform bodies.	Sailfish (*Stiophorus platypterus)*, barracuda (*Sphyraena barracuda*), Hammerhead shark (*Sphyrna lewini*), etc.
3	Fusiform	A body form which is rounded and tapered at both ends	Marine mammals, penguins and some fish
4	Short & High	A body type for which $\frac{BH}{EL} > 40\%$. BMSs associated with this body form usually have compressed body CSs	puffers and filefish (Tetraodontiformes)
5	Flat body	A body type for which $\frac{BW}{EL} > 50\%$. BMSs associated with this body form have flat CSs.	turtles and rays
6	Squid	The specific body shape of squids	squids

To make direct comparison between the main body types of BMSs, it would be ideal to have all the data on body width and body height of all BMSs and AUVs. However, due to insufficient data for both groups, it is not possible to make direct comparison in terms of length, width (breadth), height and volume. All measurements are not available for every BMS. For most BMSs only body length and height are measured, and for some only the body length. Therefore, the body dimensions which are unavailable must be estimated or accounted for by other means.

On the other hand, body length and mass are generally available. Furthermore, notwithstanding minor differences, BMSs and AUVs are approximately neutrally buoyant with the variation in density being relatively small (less than 2%), even between floating and sinking marine animals. Therefore in average it is possible to assume BMSs and AUVs have an average density of water $\left(\rho_{SW} = 1025\ {}^{Kg}/_{m^3}\right)$. In order to verify the tri-axial ellipsoid assumption, and find means to estimate the unavailable body dimensions, it was essential to test and observe whether the tri-axial ellipsoid model of a BMS would result in the same volume or mass as the real BMS. Noting the limitations, comparing some measure of fineness was desirable. Therefore, if the tri-axial ellipsoid model was validated for systems for which data was already available, it would be possible to populate it for all BMSs.

If the BMSs are idealised as tri-axial ellipsoids, by having body length, width and height data, the volume of the tri-axial ellipsoid can be calculated. Subsequently, by considering BMSs to be almost neutrally buoyant the mass can be calculated. The estimated mass can then be compared with the actual mass of the BMS. As:

$$\{Mass\}_{BMS} = \rho V_{BMS} \qquad 3.1$$

And the volume of a tri-axial ellipsoid is calculated as:

$$V_{BMS} = \frac{4\pi}{3}\left(\frac{EL \times BH \times BW}{8}\right) = \frac{\pi}{6}(EL \times BH \times BW) \qquad 3.2$$

Where *EL*, *BH* and *BW* represent the Elliptical Length, Body Height and Body Width, respectively.

Equation 3.2 is used to calculate the volume and hence the mass of the equivalent tri-axial ellipsoid which has the length *EL*. The total mass also includes the mass of the control surfaces (fins) of the BMS. However as shown in Tables 2.5, 2.6 and 2.7 the mass of the fins of the concerned BMSs is between 1.4 % of the total mass for the Whale and 3.8% of the total mass for the whiting. Therefore, it is assumed that the mass of the fins is negligible compared to the total mass.

Figure 3.2 illustrates the ratio between the mass of the BMSs within the database for which the actual mass was known, and the mass of the equivalent tri-axial ellipsoid. The blue line shows a 1:1 ratio line and the red line is the trend line of the actual data.

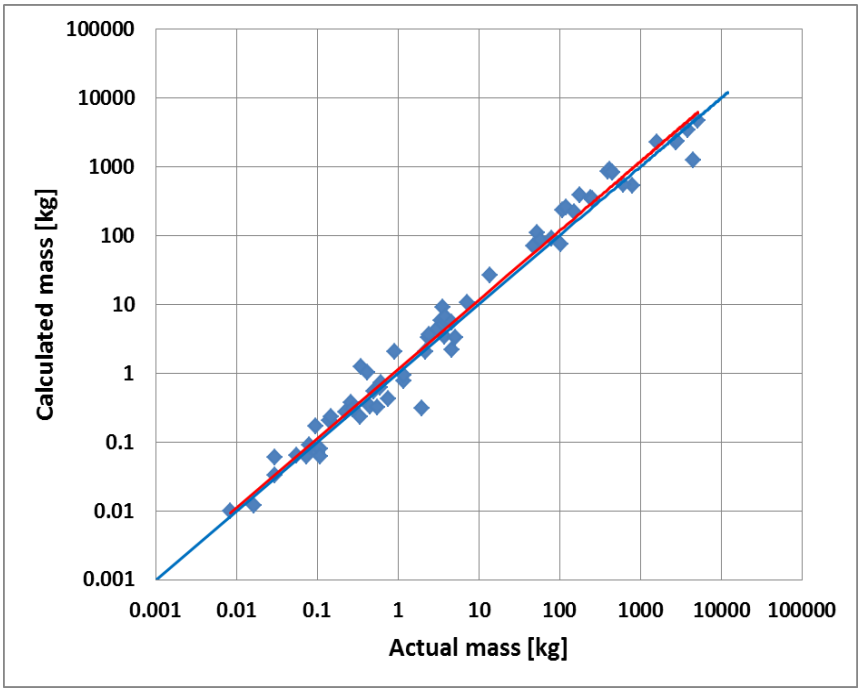

Figure 3.2. Log-log plot of actual mass of BMSs vs. calculated mass based on a tri-axial ellipsoid

Figure 3.2 highlights strong correlation between actual mass and the mass of the equivalent tri-axial ellipsoid for BMSs. Another proof that justified the use of tri-axial ellipsoids was the volume measured from the dissected Gurnard as discussed in Chapter 2. The difference between the actual volume of the Gurnard and the volume of the equivalent tri-axial ellipsoid was only 2.5%.

The analysis of Figure 3.2 as well as the results obtained from the volume comparison of the Gurnard justified the idea of representing BMSs as tri-axial ellipsoids.

A similar graph can also be plotted for AUVs as Figure 3.3

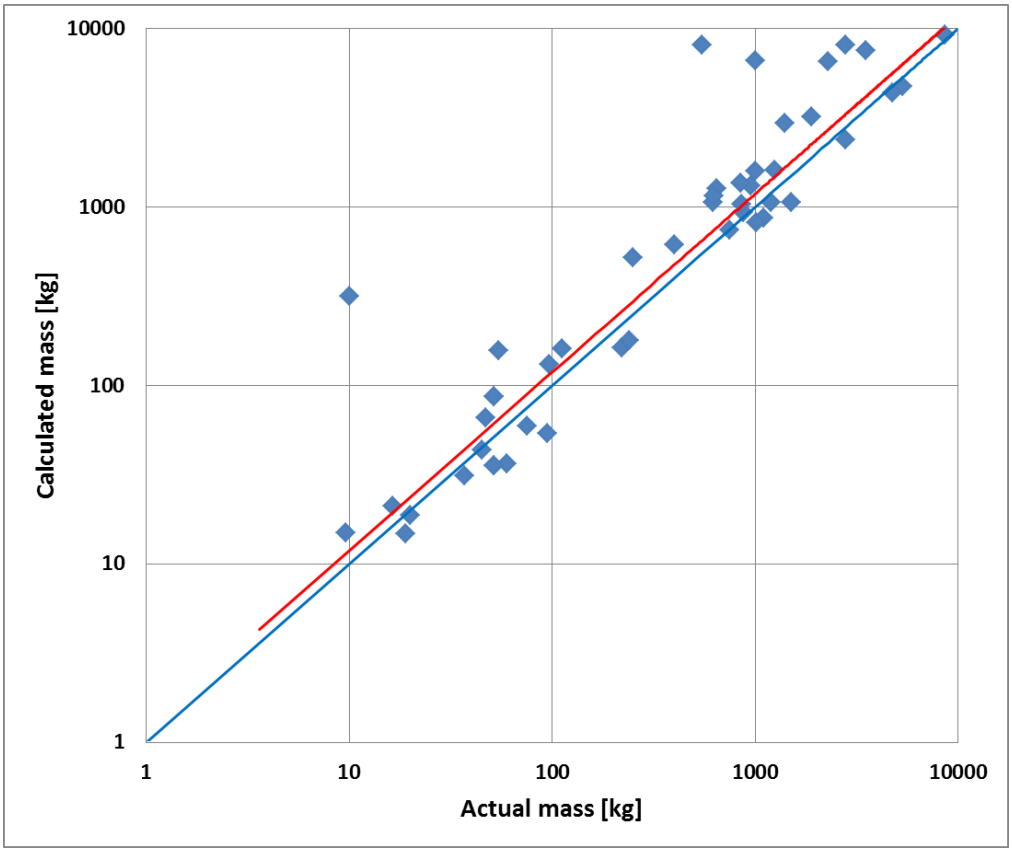

Figure 3.3. Log-log plot of actual mass of AUVs vs. calculated mass based on a tri-axial ellipsoid

It is observed from Figure 3.3 that as not many AUVs are built in a tapered shape which is similar to a tri-axial ellipsoid, some of the data points move further away from the 1:1 ratio line (the blue line). However, in overall the tri-axial ellipsoid model is a close representative of the shape of AUVs as a unified means.

3.1.3 Using the tri-axial ellipsoid model to compare the body forms of BMSs and AUVs

Unifying the approximate body shape of BMSs facilitated the comparisons between BMSs and AUVs. Equation 3.1 was used as a measure of body form comparison.

Another useful means for comparing the body shapes is the Fineness ratio (*FR*). *FR* is defined as length over diameter of the body.

$$FR = \frac{Length(L)}{Dimeter(D)} \tag{3.3}$$

This formula was used to classify different AUVs and BMSs.

As most BMSs as well as some AUVs have oval body cross sections which is defined by a *BH* and a *BW*, two different fineness ratios can be calculated. Therefore, an equivalent diameter was presented in this research to calculate only one value of *FR* which is comparable for both BMSs and AUVs. If the length of the system is kept the same (unchanged), the body with an equivalent diameter, which will therefore become a spheroid, must have the same volume as the tri-axial ellipsoid. Therefore:

$$V_{Spheroid} = V_{Ellipsoid} \tag{3.4}$$

This is written as:

$$\frac{4\pi \times \frac{\mathrm{EL}}{2} \times \left(\frac{D_e}{2}\right)^2}{3} = \frac{\pi}{6}(EL \times BH \times BW) \tag{3.5}$$

where D_e is the equivalent diameter.

By reforming the formula the equivalent diameter is calculated as:

$$D_e{}^2 = BH \times BW \tag{3.6}$$

which means:

$$D_e = \sqrt{BH \times BW} \tag{3.7}$$

Therefore the fineness ratio of AUVs and BMSs can be estimated as:

$$FR = \frac{EL}{\sqrt{BH \times BW}} \tag{3.8}$$

where BL is the elliptical length of the BMSs.

As for the BMSs for which body width and height are not available, the equivalent diameter is calculated by using the mass and length of the BMS, considering that based on the trend in Figure 3.2, the BMS fits with the ellipsoid model.

$$\{Mass\}_{ellipsoid} = \rho V_{ellipsoid} = \rho \frac{\pi}{6}(EL \times BH \times BW) \quad 3.9$$

By replacing $BH \times BW$ with the equivalent diameter from Equation 3.6 and rearranging the equation, D_e was calculated as:

$$D_e = \sqrt{\frac{6\{Mass\}_{ellipsoid}}{\rho\pi \times EL}} \quad 3.10$$

D_e vs. EL ratios for BMSs and D_e vs. TL ratios for AUVs are demonstrated in Figures 3.4 and 3.5, respectively. The dashed lines represent the base lines for different $\frac{EL}{D_e}$ values and the continuous lines represent the trend line for each body form of BMSs. The shapes adjacent to each dashed line represent the side view of an equivalent spheroid with the same *FR*.

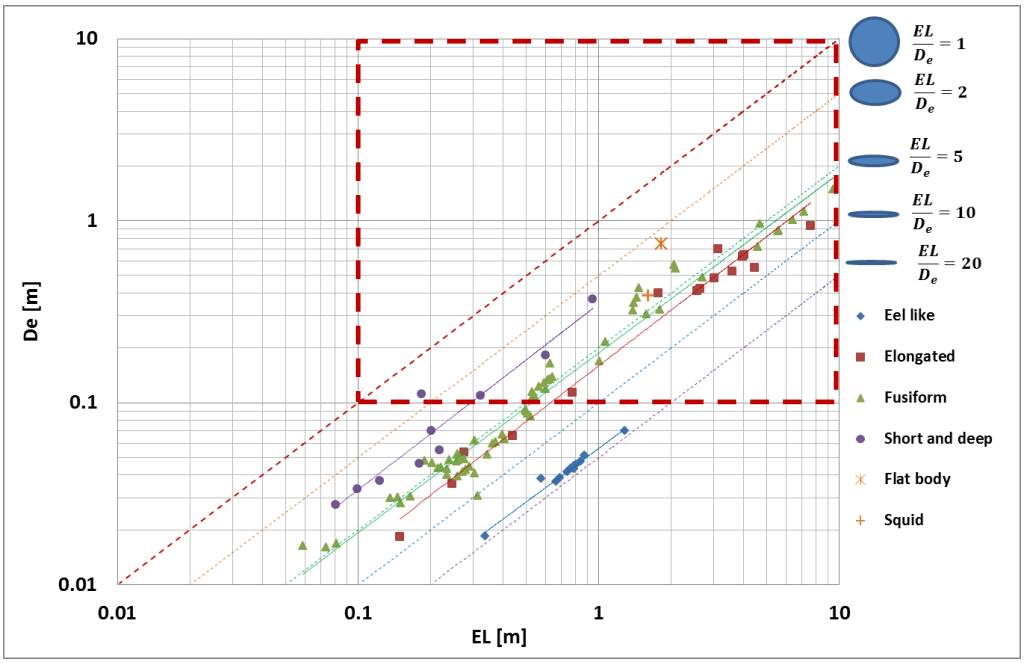

Figure 3.4. Length vs. equivalent diameter for BMSs with various body types. The red dashed frame is the boundary at which the AUVs exist and therefore Figure 3.4 demonstrates the area within this boundary

For turtles and squids there is a single data therefore no line is presented. Values of length-diameter or fineness ratio can be estimated from the trend lines in Figure 3.4 as in Table 3.4 below:

Table 3.4. Estimated values of fineness ratio for various body shapes of BMSs

Body form	Average $\frac{EL}{D_e} = FR$	R^2 Value
Eel like	17.83	0.97
Elongated	6.27	0.97
Fusiform	5.33	0.97
Short and deep	2.7	0.95
Flat (single data)	2.44	-

The only outlier in short and deep body forms (purple circles in Figure 3.4) belongs to striped burrfish *(Chilomycterus schoepfii)* which is a puffer fish, hence both deep and bluff. Its fineness ratio is 1.64. The haddock *(Melanogrammus aeglefinus)* is the outlier of fusiform bodies. Due to its slim body, it has a *FR* of 10.3.

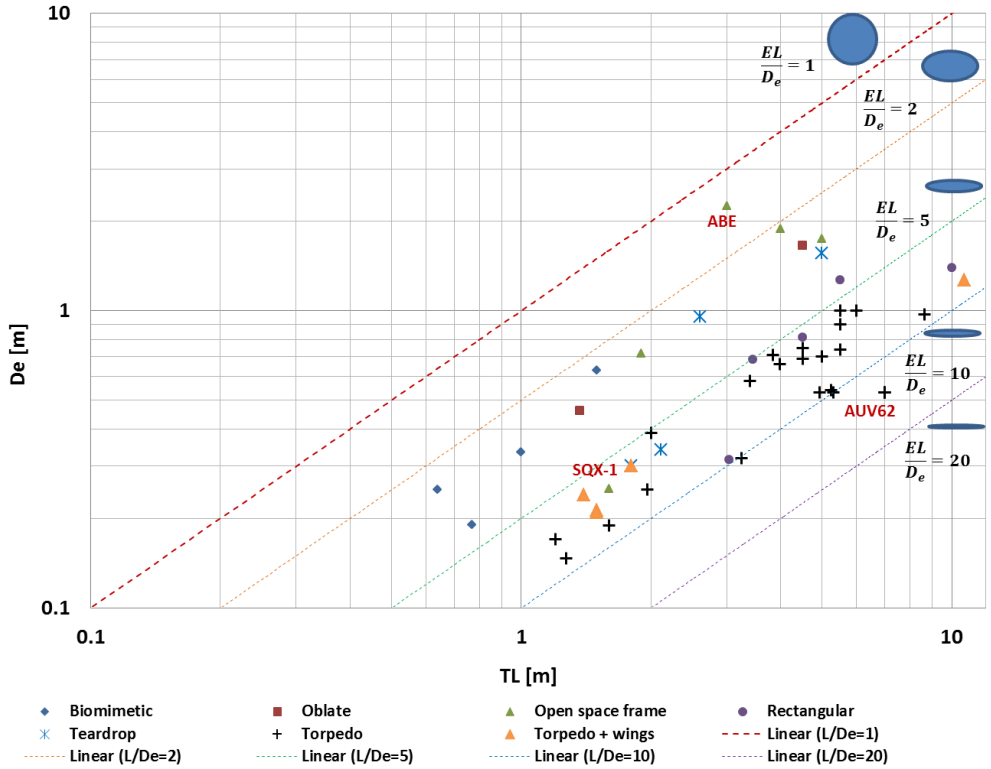

Figure 3.5. Length vs. equivalent diameter for AUVs with various body types
The blue ellipses represent the equivalent tri-axial ellipsoids modelled for BMSs with the indicated FR.

Figure 3.5 shows a large variance between the fineness ratios of AUVs with similar structure. However, three AUVs stand out as outliers. ABE and SQX-1 sit on the two far ends of the FR border line for space frame AUVs. This is due to the variance in the open space platforms. Although most have a similar box shape, ABE is a combination of two teardrops on top and a quasi-rectangular structure on the bottom all connected

together. Therefore ABE has the lowest *FR* off all AUVs at 1.34. SQX-1 is a combination of two connected torpedoes and has the highest FR of space frame AUVs at 6.4. One must notice that unlike BMSs, not all AUVs have ellipsoid body shapes. Especially space frame AUVs which have multiple bodies cannot be represented by an ellipsoid body design and they have been included in Figure 3.5 solely to have a varied range on AUVs in the plot. For a space frame AUV there could be several definitions of *FR* which will result in different answers; e.g. using length to width vs. length to depth ratio. In conclusion, the *FR* values obtained for non-ellipsoid shape AUVs are for body classification purposes and the complication mentioned above must be bore in mind.

Torpedoes and torpedoes with wings sit between the *FR*=5 and FR=10 lines. This is except for AUV62 which is a rather long thin AUV. Note that the widths of the wings are not included in the *FR* calculations as the *FR* is calculated for the main body.

The comparison between AUV and BMSs show that for AUVs the *FR* ranges between 1.34 and 13.2 while for BMSs the range is 1.6 to 18.4. More long and thin bodies exist in nature, all belonging to the species with eel like bodies. The FR ranges are summarised in Table 3.5 below. It is to be expected that the FR range of Fusiform BMSs is within the range of Teardrop AUVs. As for biomimetic AUVs their *FR* matches with the BMSs which they are built based on. For example the Aqua penguin with a fusiform body has a *FR* = 4.05 which is in the range of fusiform bodied BMSs.

Table 3.5. FR Ranges for BMSs and AUVs

AUV Body Type	Min FR	Max FR	BMS Body Type	Min FR	Max FR
Torpedo	5.16	13.2	Eel like	15.2	18.4
Rectangular	4.3	9.6	Elongated	4.4	6.9
Teardrop	2.7	6.2	Fusiform	3.5	7.5 (1)
Open space frame	1.34	6.4	Short and deep	1.6	3.9
Torpedo with wings	5.8	8.43			
Biomimetic	2.3	4.05			

(1) This is except for the Haddock with *FR*=10.3

In overall, it was concluded that for both AUVs and BMSs there is a large variation between body forms and cross-sections and considering their Fineness Ratio along with their body form provides a useful means to classify them. It was also realised that

despite the differences between body forms of AUVs and BMSs, as presented in Table 3.5, there are some body forms in BMSs that can be corresponded with one in AUVs. Table 3.5 also shows that the range of Fineness Ratio in BMSs is slightly larger than that of the AUVs.

Dorrington, 2006 performed a research work on the drag of spheroids and airships in which he investigates and compares the volumetric drag of spheroids and streamline bodies with regards to their Fineness Ratios. He mentions that the general assumption is that Fineness Ratios between 4 and 8 are best for minimising drag for streamline bodies. However, in practice the FR value is selected considering various parameters and not solely relying on minimising drag. Based on this, and considering space frame AUVs, it can be noted that as space frame AUVs are setup more for photographic surveys, they are generally low speed AUVs and use thrusters. Therefore, for these type of AUVs drag is not the most critical parameter to consider.

Dorrington's research illustrates that by using Hoerner, 1965 formula for volumetric drag it is observed that for FR values less than 3 the volumetric drag coefficient increases rapidly with minimising the FR. However, the changes in volumetric drag are insignificant when changing the FR between 3 and 10 (the range which has been investigated in the research). Another finding in his research is that higher FR certainly beneficial when targeting high cruising speed but the same cannot be said for certain when the target cruising speed is low. Looking into the FR values for BMSs while considering these findings it can be concluded that fusiform and elongated bodied BMSs which include marine mammals such as dolphins as well as fish such as the sailfish have evolved with body Fineness Ratios around 4 and 8 to minimise drag for high speed. However many other BMSs exist with much higher or lower FRs. As mentioned by Dorrington, other parameters could influence this, for example high manoeuvrability.

3.2 Speed and Agility

Speed and agility are parameters desired for AUVs operation especially when tracking and observing. To realise the difference in the agility of AUVs vs. BMSs, their speeds have been compared.

In the scope of this project, two main AUV speed are of interest. These are the economic speed, U_{eco}, and the maximum speed, U_{max}. U_{eco} is defined as the advance

speed of the AUV at which the energetic cost is minimum. U_{max} is defined as the maximum speed at which the AUV can move forward.

It must be noted that the data on the U_{eco} of AUVs is extremely hard to find and generally not available. Instead the manufacturers' cruising speed is available for most AUVs. Therefore, the cruising speed is instead used in present research to have an estimate of the lower energetic cost (Cost Of Transport, *COT*) values for AUVs. This means that the *COT* value estimated is higher than the actual *COT* for the vehicle. However, for most of BMSs the situation is similar; i.e. the optimum speed is not available and instead their voluntary cruising speed has been considered for *COT* calculations. Acknowledging the uncertainties and over estimation of minimum *COT*, the uncertainty is similar for both data sets. Therefore, the optimum *COT* results can be updated in future when more data on the economic speed of AUVs and optimum speed of BMSs become available.

Note that there is a third speed, minimum speed, U_{min}, which torpedo shaped AUVs must maintain to keep controllable which means the vehicle cannot keep stationary (Billingham, 2001). U_{min} has not been investigated in this research. However, it is worth mentioning that some BMSs also have a minimum speed. BMSs which are negatively buoyant must have a minimum speed to prevent them from sinking. These BMSs are sharks, rays and most of the marine mammals. For other BMSs, U_{min} is zero. This indicates that they can be still in the water.

For BMSs more speeds are defined as they have a larger speed range compared to AUVs. There are 5 specific speeds defined for BMSs as below:

- Minimum speed, U_{min}
- Optimum speed, U_{opt}
- Cruising speed, U_{Cruise}
- Critical speed, U_{crit}
- Maximum speed, U_{max}

There are as well 3 speed ranges defined for BMSs as follows:

- Sustained speeds,
- Prolonged speeds,
- Burst speeds

All these speeds and speed ranges are discussed next.

3.2.1 Different speeds and speed ranges in BMSs

Optimum speed for BMSs, U_{opt}, corresponds to U_{eco} in AUVs. U_{opt} is defined relative to the Cost Of Transport (*COT*) of the BMS. *COT* is explained in Section 3.5 and in detail in Chapter 4 of this thesis.

The optimum speed is the speed at which the energetic Cost Of Transport is minimum, $COT_{opt} = COT_{min}$. However, U_{opt} is usually lower than the voluntary cruising speed, U_{Cruise}, of BMSs. Therefore, most animals swim marginally faster than the speed with least *COT*.

In order to obtain a measure of minimum *COT* for comparison between various BMSs and AUVs, in this research where the optimum speed is not available or not specifically mentioned, the voluntarily forward swimming speed of the BMS (i.e. not routine movements or socialising locomotion) has been used instead.

It is difficult to quantify the difference between the two speeds as from the data gathered from various resources (e.g. Fishbase) it was realised that the voluntary cruising speed of BMSs could have a wide range. Therefore there is a degree of uncertainty on the similarity of the optimum speed and the voluntary cruising speed of BMSs.

Considering power is generally proportional to the speed cubed, on the assumption that optimum speed and cruising speed values are close, the required propulsion power for the two speeds will be similar. However, if the two speeds vary significantly, the powers will differ considerably. Considering the process of evolution tends to lead to a more "survivable design", which can be construed to imply that BMSs are evolved to their specific purpose, it is unlikely that they will tend to swim at speeds that will significantly increase their power consumption, unless they are forced to do it involuntarily. This is why any swimming under hypoxia, fasting, or other stresses has not been considered in this research.

U_{opt} and U_{Cruise} are both within a range of speeds known as sustained speed. This is the speed range at which only slow (red) muscles are operating. Therefore, due to the aerobic process, the animal does not endure fatigue. As stated by Viedler and Wardle, 1991, sustained speed can be endured by the animal for more than 3 hours (200 min) without muscle fatigue. If the BMS is pushed harder to swim within the prolonged range, fast (white) muscles start working and through anaerobic process, fatigue occurs. The critical speed, U_{crit}, is the border speed between pure aerobic and

aerobic/anaerobic process. Prolonged speeds can be endured between 200 minutes and 20 seconds. Highest speeds of BMS swimming fall within the burst speed range. It is usually endured less than 20 seconds. The BMS will be able to swim up to its maximum speed, U_{max}. This speed is corresponding to the maximum speed of AUVs. Therefore, U_{opt} and U_{max} are compared in this study.

Each individual of the same species has a different level of "fitness"; moreover many capabilities of a species are affected by their length nonlinearly. For example, collected data from Froese & Pauly, 2011, on the sustained speed of Atlantic mackerel (*Scomber scombrus*) showed that the sample with the elliptical length of 0.3 meters managed to sustain a swimming speed of 5.4 $\left[\frac{m}{s}\right]$ while another sample with *EL* of 0.38 meters only managed to sustain 3.04 $\left[\frac{m}{s}\right]$.

Therefore, in this research only in the case of relatively similar sizes individual of a species the average value of the speed or any other characteristics of that species are considered. If the size difference is significant or the test has been performed on a juvenile, all the individuals are considered separately.

Both the absolute speed as well as length specific speed of numerous BMSs and AUVs have been compared in this research. Length specific speed is the absolute speed divided by the total length of the BMS or the AUV.

The other consideration to be made when investigating BMSs is the diverse modes of their swimming. For AUVs the classification is simpler. There are three main types of AUVs, the ones propelled with propellers, biomimetic AUVs and gliders. However, BMSs have many diverse swimming modes. All the different swimming modes studied in this research are shown in Table 3.6. For ease of comparison the modes of swimming are coded based on their similarities.

Table 3.6. Various swimming mode of BMSs. BCF = Body and/or Caudal fin; UMPF =Undulation of median or pectoral fin; OMPF = Oscillation of median or pectoral fin; BDCF = Body and/or double caudal fin.

Swimming mode	Code
BCFAnguilliform	11
BCFSubcarangiform	12
BCFCarangiform	13
BCFThunniform	14
BCFOstraciiform	15
BDCF	16
UMPFRajiform	21
UMPFDiodontiform	22
OMPFLabriform	23
UMPFAmiiform	31
UMPFGymnotiform	32
UMPFBalistiform	33
OMPFTetraodontiform	34
JetForm (1)	41
Other	51

(1) Although squids are recognised for their unique jet propulsion, videos of their swimming illustrated that they use also their large side fins in a Rajiform mode to swim.

Different modes of BMS swimming is illustrated in Figure 3.6 (Sfakiotakis et al., 1999). These are divided into 3 main groups. As shown in Figure 3.6 all the swimming modes with the rear fin as the main propulsor are coded as 1x; e.g. 11 is the Anguilliform swimming. Those with paired side fin propulsion are coded as 2x and the ones with top or bottom fin propulsion are coded as 3x. This coding system was proposed in this research for ease of classification of swimming modes.

Two types of swimming which are not shown in Figure 3.6 are squid swimming and BDCF. Squid swimming is similar to jet propulsion hence, in this research it is defined as *Jet-form*. BDCF is the name given in this research to the swimming modes of BMSs with feet or hind limbs propulsion such as the sea otter. As shown in Figure 3.6, BCF propulsion modes range from the extreme body undulations of the Anguilliform swimmers to the rear fin (caudal fin) oscillation in the rigid bodies of Ostraciiform swimmers.

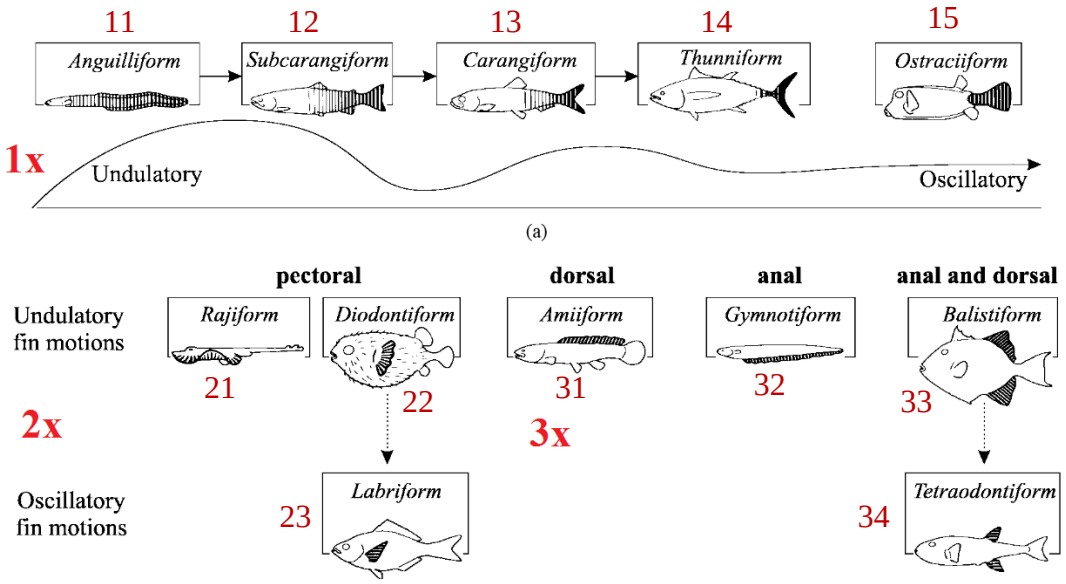

Figure 3.6. Various swimming modes of BMSs (copied and modified by adding the annotations from Sfakiotakis et al., 1999)

Those species of fish which do not use the rear fin while swimming at a sustained rate do in fact use their rear fin in transition to burst speeds and accelerating. Side fins as well as a mode of propulsion are also used for manoeuvring (Sfakiotakis et al., 1999). Moreover top fins are used in some BMSs to improve their upright stability.

Figure 3.6 clearly illustrates the swimming modes involving undulatory and oscillatory movement of median and/or paired fins. The Ostraciiform swimming mode involves the oscillation of the rear fin alone where the rigid body does not undulate and therefore does not particulate in propulsion. BMSs with this mode of swimming have rigid bodies. For the other four modes involving the rear fin it is apparent that from left to right in Figure 3.6 less of the length of the body is involved in the undulation, however more clarification is required. Both the length of the propulsive wave travelling along the body while swimming and also the length of the body which is involved in the undulatory movement are used to define and distinguish different rear (caudal) fin undulation swimming modes. These have been thoroughly explained by many scientists such as Webb, 1975, Blake, 1983 and Videler 1993. Table 3.7 below summarises the characteristics of each of the four swimming modes.

Table 3.7. Various BCF undulation swimming modes characteristics. $\%BL$ = Percentage of the body engaged in undulation/oscillation

Swim mode	$\%BL$	Specific wavelength of the body waves	Min. of the wave length present on the body	Max. of the wave length present on	Rear fin	BMS example
Anguilliform	100	<1	0.5	>1	Absent or very low aspect ratio (AR)	Eels
Subcarangiform	25-50	<1	0.5	<1*	Moderate AR	Goldfish
Carangiform	25-33	>1 slightly **	-	≤0.5	Moderate to high AR; usually forked type	Mackerel
Thunniform	<33***	1< & <2	-	<0.5	High AR; usually lunate type	Tuna

* Rarely more than1

** Maybe less than 1

***Just the caudal peduncle and the rear fin

In this section, realising that the propulsion or swimming modes of BMSs were varied considerably compared to those of the AUVs, different swimming modes of BMSs were reviewed. Having studied various swimming modes, the speeds of BMSs and AUVs were compared in the next section.

3.2.2 Comparing the optimum speed of BMSs and AUVs

To understand the different capabilities of the optimum or economic speed of AUVs and BMSs, the absolute and length specific optimum speeds, $U_{opt}\left[\frac{m}{s}\right]$ and $U_{opt}\left[\frac{TL}{s}\right]$ of numerous AUVs and BMSs with different swimming modes have been compared as illustrated in Figures 3.7 and 3.8 respectively. $U_{opt}\left[\frac{TL}{s}\right]$ or relative speed is the speed which is normalised in terms of body length per second. Due to the extensive body length range for BMSs, both figures are logarithmic on the abscissa. In Figure 3.7 the blue whale (*Balaenoptera musculus*) is an outlier within the Thunniform swimmers group and therefore is present outside the plot. Having a length of 27 m, the Blue whale has an optimum speed of 6.2 $\left[\frac{m}{s}\right]$.

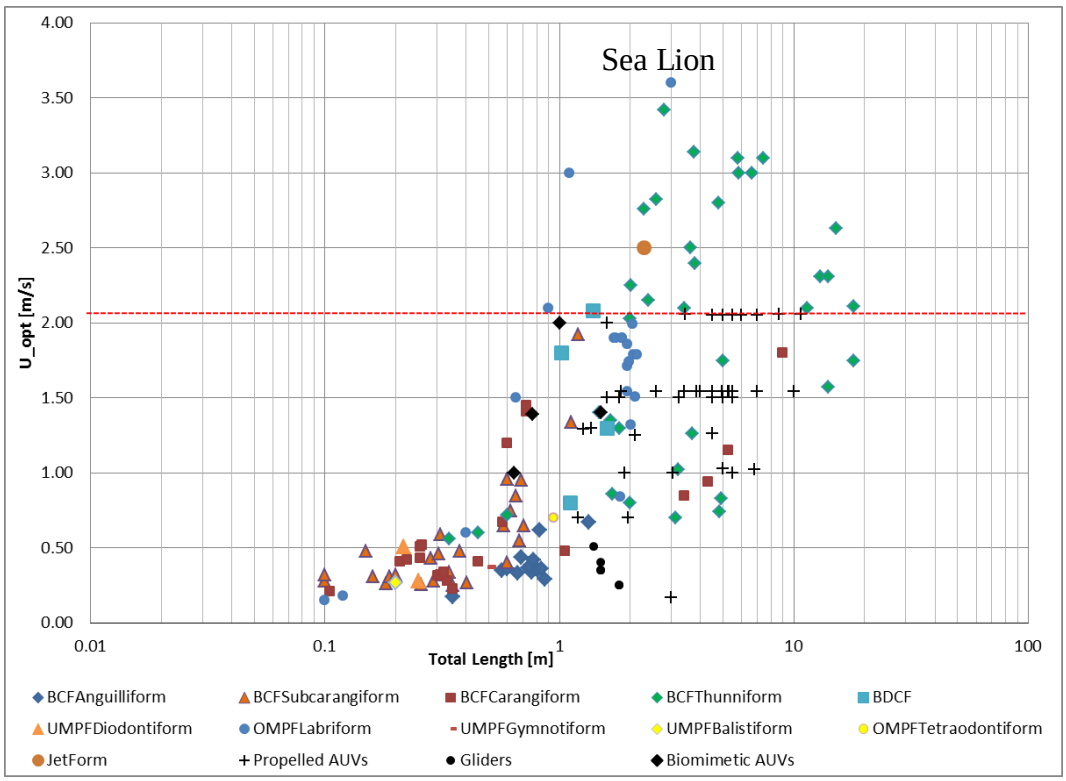

Figure 3.7. Absolute optimum speed capability of AUVs vs. BMSs. The red is the highest value of all AUVs in the database

As shown in Figure 3.7, the highest optimum speed of all AUVs is 2.06 m while the highest optimum speed for BMSs is 6.2 $\left[\frac{m}{s}\right]$. This value belongs to the 27 m long blue whale (*Balaenoptera musculus*). The Blue whale is an outlier within the Thunniform swimmers group and therefore is not present in the plot. Within the plot, the stellar sea lion (*Eumetopias jubatus*) has 175% higher optimum speed compared to the maximum for AUVs at 3.6 $\left[\frac{m}{s}\right]$. This is followed by the white-beaked dolphin (*Lagenorhynchus albirostris*) at 3.4 m/s. When comparing AUVs, it is clear that gliders are the slowest AUVs and propelled AUVs (i.e. AUVs which move forward using a rear propeller(s)) are the speediest. Naro-tartaruga a biomimetic AUV based on a turtle has a speed of 2 [m/s] very close to the maximum capability of AUVs.

Within the BMSs, Thunniform swimmers have the highest optimum speeds except for the sea lion which is a Labriform swimmer with a high optimum speed. The general trends are visible but due to the variety of data series they are not very clear in Figure 3.7. Therefore Figures 3.7.1 and 3.7.2 illustrate the data in clusters. The clusters are represented by 95% confidence enclosing ellipses. A 95% confidence enclosing ellipse is the smallest ellipse drawn around a set of data which would ensure to cover 95% of the points within that data set (Friendly et al., 2013). 95% confidence enclosing ellipses

are useful when obvious trend cannot be observed in a set of data. By enclosing the data set with the ellipse, a general trend for the data can be obtained by drawing a line across the longer diameter of the ellipse. Only series with more than two data points can be presented by the ellipsoids.

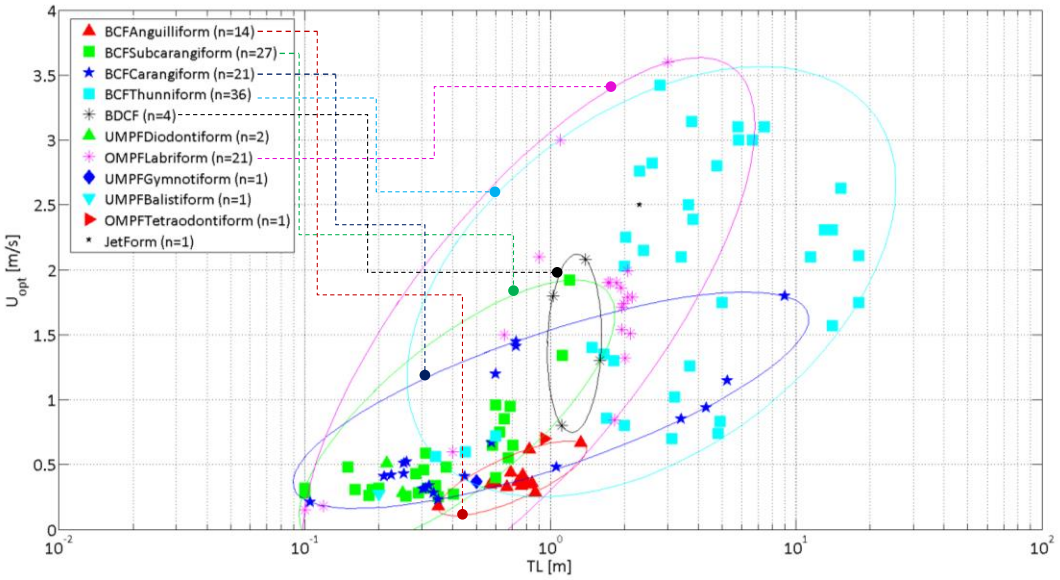

Figure 3.7.1 Absolute optimum speed capability of BMSs represented by 95% confidence ellipsoids

Figure 3.7.1 clearly illustrates that the BMSs larger than 10m present in the plot are Thunniform swimmers. This is due to the fact that except for whale sharks (*Rhincodon typus*), only marine mammals and more specifically Cetacean are found to be larger than 10 meters. Thunniform and Labriform swimmers have the highest speeds followed by Carangiform and Subcarangiform swimmers. Anguilliform swimmers have the lowest speeds.

The general trend for all groups shows an increase in speed with length. In fast swimmers, i.e. Thunniform and Labriform, the speed increases with a higher rate as a function of length compared to other types of swimming. Although Thunniforms and Labriforms are fast swimmers, for smaller BMSs, Carangiform and Subcarangiform swimming prove to be better in terms of speed, especially at body lengths less than one meter.

The only cluster which is aligned differently belongs to the feet swimmers (BDCF). The harbour seal (*Phoca witulina*) and elephant seal (*Mirounga leonina*) are the two higher points. The lowest point is the sea otter which although swims mainly with the feet, having a long tail its body is more adapted to terrestrial locomotion. The grey seal (*Halichoerus grypus*) although marginally larger in size has slightly less speed. The

reason being is that the data from William, 1999 suggests that this was the maximum speed of the flume therefore the optimum speed of the Grey seal could possibly be higher than measured in the experiment. As the body of Harbour seals and Grey seals are very similar, similar performance is expected from them as well.

Figure 3.7.2 demonstrates clusters of optimum speeds for AUVs. With the exception of the Autonomous Benthic Explorer (ABE) which is a slow propelled AUV with an economic speed of 0.17 $\left[\frac{m}{s}\right]$, gliders are in general the slowest of the AUVs. Although propelled AUVs have the highest speed but the biomimetic Naro-tartaruga (based on sea turtles) is very close to the high speed. It must be noted that the speed value presented for the Naro-tartaruga AUV was based on the estimation of the manufacturer and test data was not available at the time of this research.

From the plot, it was also realised that apparently AUVs are designed around certain speeds. These speeds were identified to be mainly $1\left[\frac{m}{s}\right]$, 1.5 $\left[\frac{m}{s}\right]$ and $2\left[\frac{m}{s}\right]$.

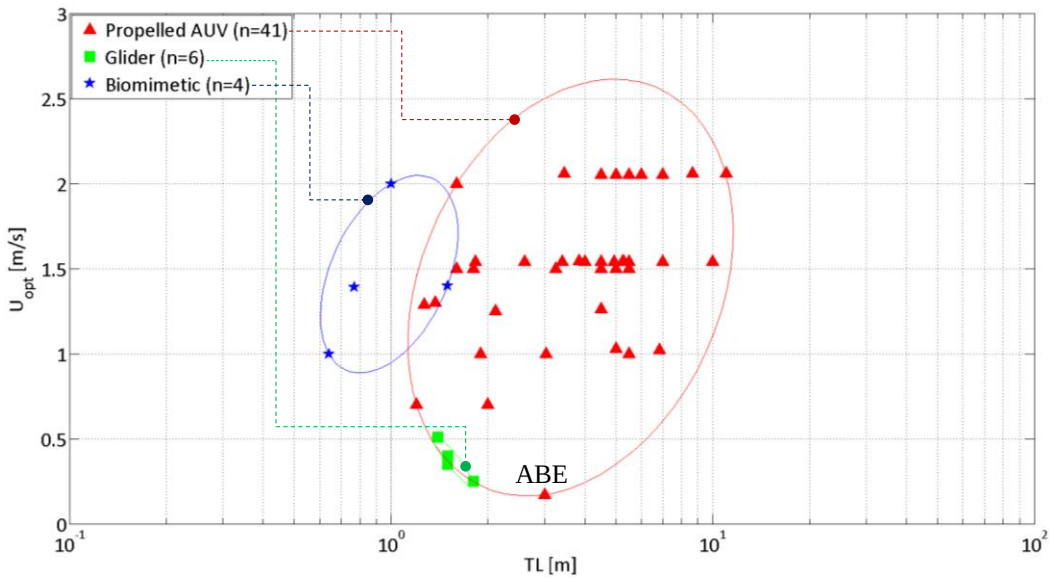

Figure 3.7.2 Absolute optimum speed capability of AUVs represented by 95% confidence ellipsoids

Besides the absolute speed, to make a parametric comparison, the length specific speeds of AUVs and BMSs have been compared as shown in Figure 3.8.

A general trend in the graph shows a reduction in length specific speed with the increase of body length. Relatively AUVs are sitting lower compared to BMSs, however, biomimetic AUVs have the best (highest) length specific speeds within the AUVs. In the case of the biomimetic Aqua Penguin and the Naro-tartaruga (points 1 and 2 in Figure 3.8), the data were also compared with the data from real corresponding

BMSs. The Naro-tartaruga has a significantly higher length specific speed compared to the leatherback turtle (*Dermochelys coriacea*) (point number 3). This could be due to the fact that in general larger BMSs have lower length specific speed. The value from the biomimetic turtle is impressive, however, this is the estimated manufacturer data and independent experiments have yet to confirm it, therefore the results must be considered with caution. As for the Aqua Penguin, the length specific speed is higher than all propeller AUVs but lower than real penguins (points 4 and 5). This is a proof that biomimetic AUVs have the capability to improve the capability of AUVs and there are yet improvements to be made to their design.

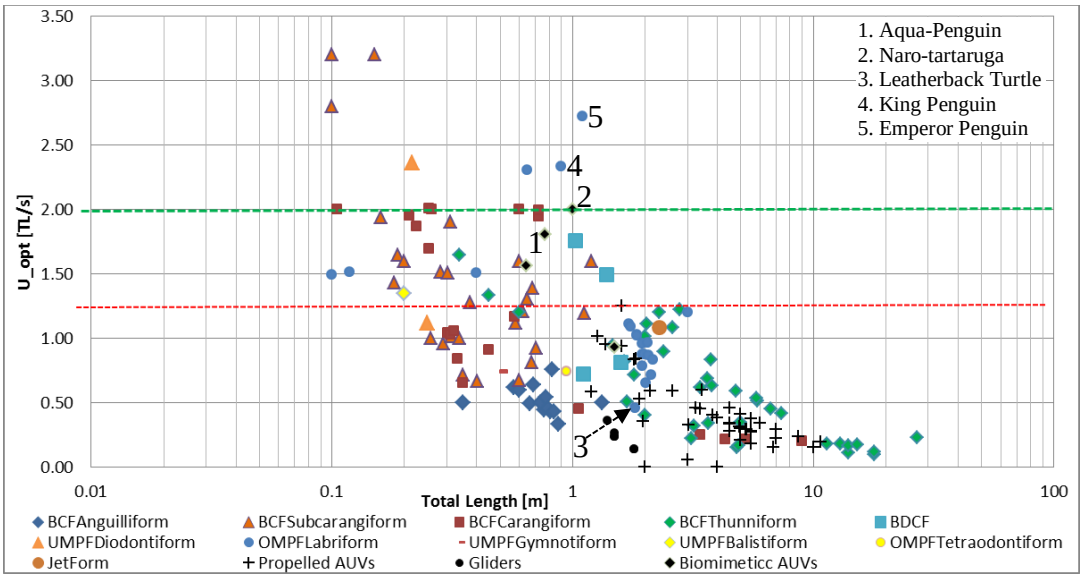

Figure 3.8. Length specific (relative) optimum speed capability of AUVs vs. BMSs. The red dashed line is the highest value of all conventional AUVs in the database. The green line is the highest value for biomimetic AUVs in the database

To investigate the relative speed further, same as the absolute speed, the data has been clustered with 95% confidence ellipsoids shown in Figures 3.8.1 and 3.8.2 for BMSs and AUVs respectively.

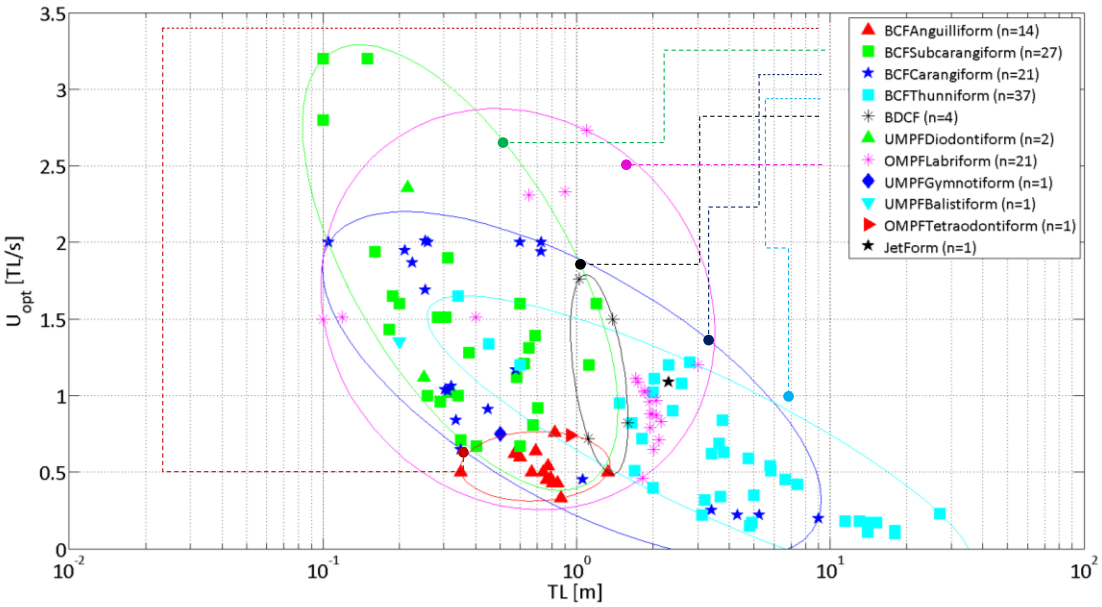

Figure 3.8.1 Relative optimum speed capability of BMSs represented by 95% confidence ellipsoids

All clusters show a reduction in relative speed with length unlike the absolute speed. The slope for BDCF swimmers is higher for the reasons explained when comparing absolute speeds. The smallest of the Subcarangiform swimmers have the highest relative speeds. It is interesting that increase in length does not seem to affect Anguilliform swimmers. This is to be expected as the body length range is small, the speed is generally low and also the range of available speeds is limited for Anguilliform swimmers.

As for AUVs, it was clear from Figure 3.8.2 that biomimetic AUVs have the highest relative speed. The reason for this is unclear and will require energetic cost data to become available for the biomimetic AUVs. When energetic cost data are measured, one can investigate on what cost do these AUVs swim considerably faster than conventional AUVs. Moreover, the speed data should be verified by the manufacturers through future trials. Similar to BMSs, similar general trend of lower relative speed at higher length exist for AUVs. This is to be expected as increase in size does not necessarily relate to increase in speed. As it is discussed in this research, there are several reasons to increase the size or length of an AUV, for example more payload or battery carrying capacity which for the former could contribute to more complex mission profiles and in the case of the latter, increase in endurance. More battery on-board could also contribute to more resources to increase the propulsion power.

However, considering the increase in size and mass of the vehicle, this will not necessarily result in higher length specific speeds.

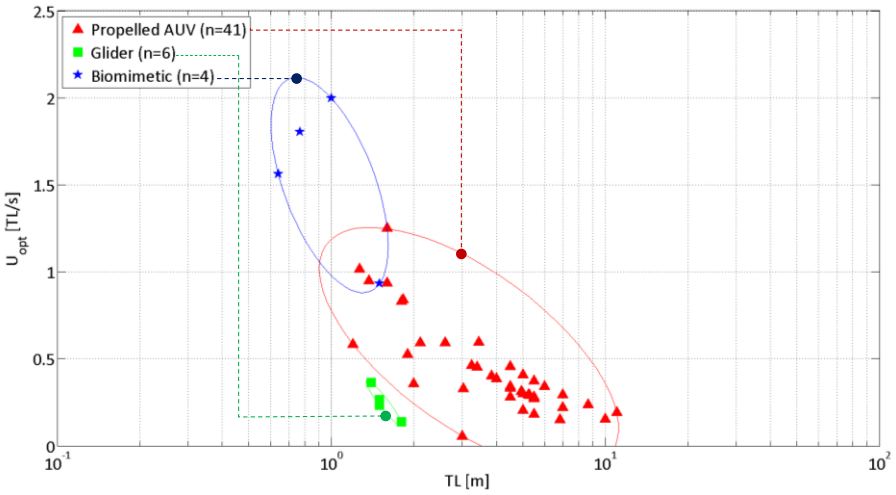

Figure 3.8.2 Relative optimum speed capability of AUVs represented by 95% confidence ellipsoids

Furlong et al., 2007 describes a theoretical model for the performance of an AUV. Based on this model there is a balance between the range and the speed of AUVs. Their work mentions that flight style AUVs (which use motor and propeller for propulsion) generally have cruising speeds of about 1-2.5 [m/s] while gliders have speeds of about 0.2-0.34 [m/s]. As it is explained later in Chapter 4, required propulsion power increases with the cube of speed, therefore the flight style AUVs required considerably more propulsion power compared to gliders. Moreover, gliders have very low non-propulsive propulsion power (refer to Chapter 4 for details). The sum of these two powers comprises the power consumption of the AUV, therefore gliders having lower power consumption can use their energy storage towards high endurance. That is why flight class AUVs have endurance of a few days while gliders can operate for months. Furlong et al., concludes that combining a flight class AUV with low non-propulsive power and reduced speed would have endurance comparable to gliders with the capability of larger speed ranges. It must be noted that minimising the non-propulsive power would also restrict the amount of sensors that the AUV can use on board. This subject will be discussed in-detail in the next chapter, Chapter 4.

3.2.3 *Comparing the maximum speed of BMSs and AUVs*

Figure 3.9 shows the comparison of maximum speed of AUVs and BMSs. It was observed that many BMSs which were mainly Thunniform swimmers had higher maximum speeds compared to AUVs. While the maximum speed of BMSs reaches 35 $\left[\frac{m}{s}\right]$ by the Thunniform swimming sailfish (*Stiophorus platypterus*), AUVs can reach a maximum speed of 10$\left[\frac{m}{s}\right]$. Therefore the fastest BMS has 350% the speed of the fastest AUV with less than half the body length. Thunniform swimmers are clearly evolved for fast swimming.

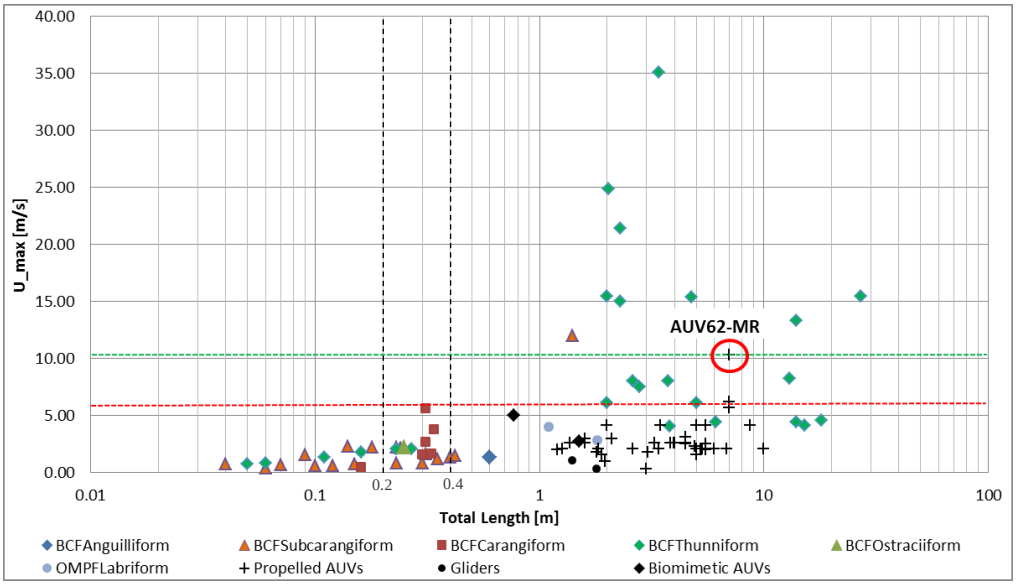

Figure 3.9. Absolute speed capability for AUVs and BMSs. The red line is the maximum speed for all AUVs except the AUV62-MR for which the maximum speed is on the green line

To make the data clearer, similar to the data for optimum swimming speeds, the data was clustered in Figure 3.9.1.

Following a similar trend as that observed when clustering the data on optimum speed, there was an increase in maximum speed capability with size. Although Thunniform swimmers swim at the highest speeds, at body lengths less than 0.4 m, Carangiform swimmers and at body lengths less than 0.2 m, Subcarangiform swimmers have higher speeds.

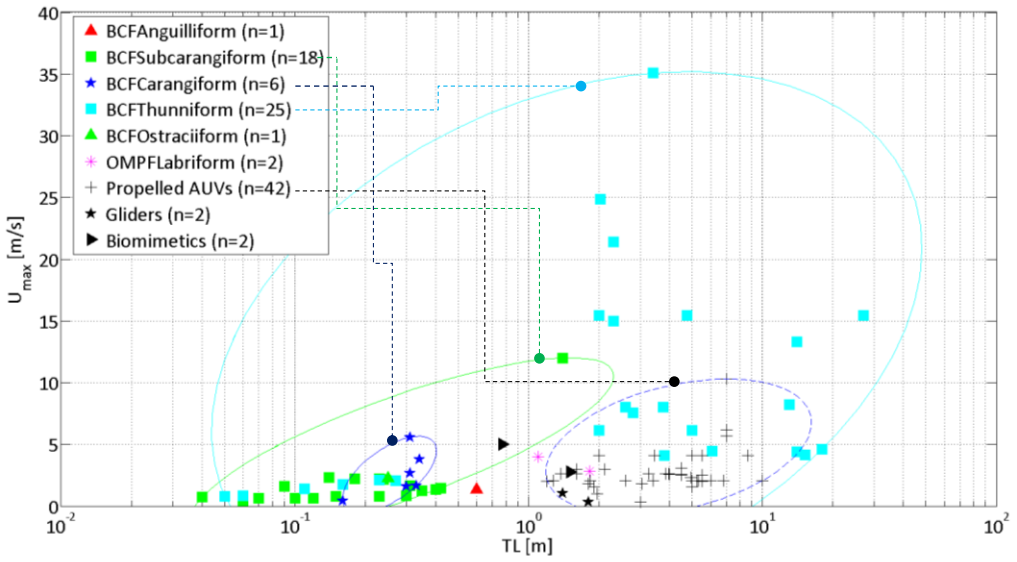

Figure 3.9.1. Maximum speed capability represented by 95% confidence ellipsoids

Fast swimmer BMSs generally have fusiform bodies with circular or oval cross-section; however some Thunniform swimmers such as the Sailfish with elongated body forms and compressed cross sections are amongst swimmers with the highest burst speeds. As for marine mammals, for fast swimming undulatory swimming is superior to oscillation of side flippers as performed by stellar sea lions (*Eumetopias jubatus*).

Figure 3.10 shows the comparison of length specific maximum speed for AUVs and BMSs with the clustered data shown in Figure 3.10.1

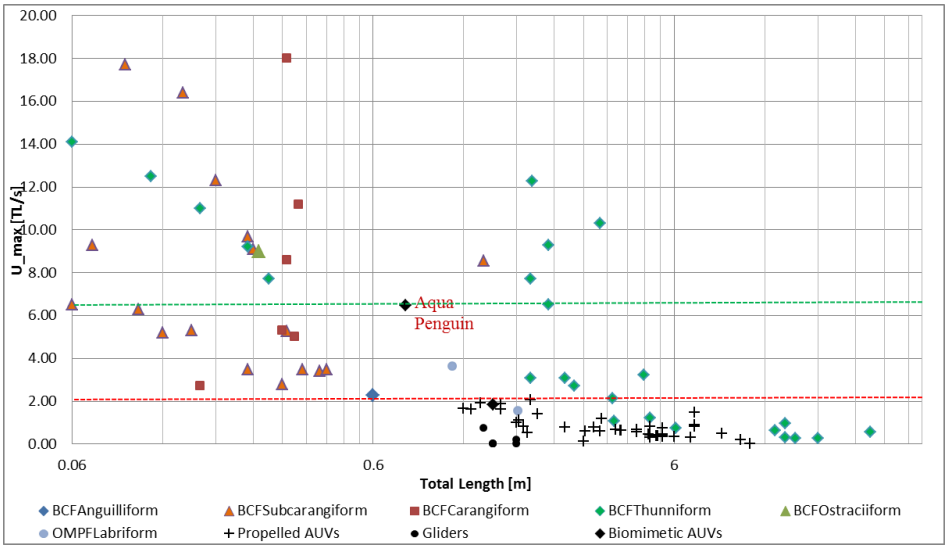

Figure 3.10. Length specific maximum speed capability of AUVs vs. BMSs

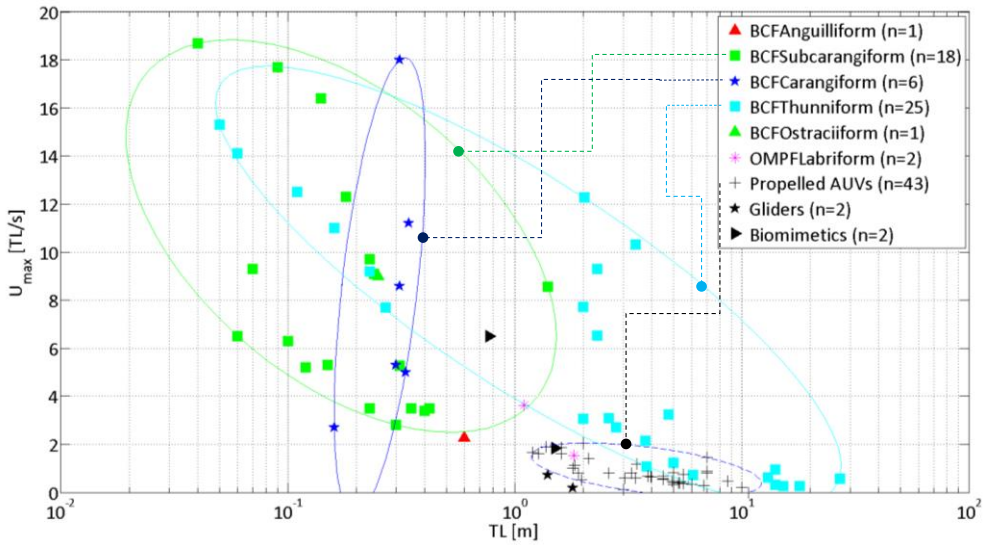

Figure 3.10.1 Maximum relative speed capability represented by 95% confidence ellipsoids

When comparing length specific speed $\left[\frac{TL}{s}\right]$, some relatively smaller marine animals which have Subcarangiform or Carangiform swimming modes, especially the Atlantic mackerel (*Scomber scombrus*), exhibit higher speeds. Although their absolute U_{max} is much less than those of Thunniform swimmers, at their size range they have the best performance. For example, the mackerel has a maximum speed of 5.58 $\left[\frac{m}{s}\right]$ and the highest length specific speed of 18 $\left[\frac{TL}{s}\right]$.

3.2.4 The effect of the Reynolds Number

A useful means when comparing the speed of numerous moving systems is the non-dimensional term Reynolds number (*Re*). As the Reynolds number is a function of both speed and body length, it is a useful means of comparison. Moreover, the Reynolds Number is used when calculating the frictional drag of moving systems. Therefore the value of *Re* can indicate the extent to which a moving system is affected by turbulence.

When comparing U_{opt} and considering the Reynolds number for Anguilliform swimmers, it was calculated that they swim at Reynolds numbers within the range of $2.1 \times 10^5 \leq Re \leq 7.4 \times 10^5$ (except for one juvenile eel at $Re = 5.1 \times 10^4$) . Therefore, Reynolds numbers are relatively low for Anguilliform swimmers compared to other BMSs with other modes of swimming and the range of *Re* is also small. Therefore, Anguilliform swimmers are less affected by turbulence compared to other modes of swimming. One important consideration is that regarding the relation between drag and speed for BMSs with different sizes, it must also be noted that drag is

proportionate to $\{Volume\}^{\frac{2}{3}}$ which means $drag \propto \{Mass\}^{\frac{2}{3}}$. This means that by increasing the size (i.e. body mass) of the BMS (while considering the speed increases linearly), the drag does not increase with the same rate. Consequently larger sized BMSs have less drag for their mass in comparison to smaller ones.

The Reynolds number ranges in which the BMSs and AUVs operate must also be considered. For example the Atlantic mackerel has a *Re* range of 9.09×10^4 to 1.44×10^6 while the fastest swimming BMS, the Sailfish, swims in Reynolds numbers up to 9.94×10^7. Figure 3.11 demonstrates different ranges of Reynolds numbers for AUVs and BMSs at their optimum and maximum speeds. Note that the *Re* range for maximum speed of Thunniforms starts at a smaller value compared to their optimum speed range. This is simply because some data for smaller BMSs in only available at their maximum speeds.

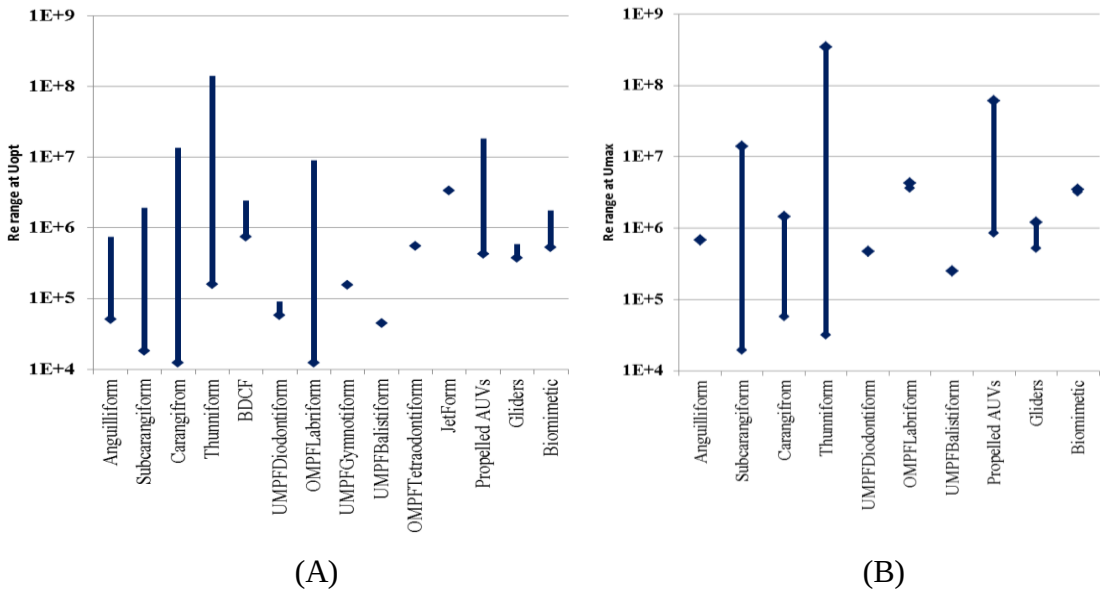

(A) (B)

Figure 3.11. Various ranges of *Re* for AUVs and BMSs at their optimum speeds (A) and maximum speeds (B). Single point means there has been only one data on that specific swimming mode

For BMSs with rear fin propulsion the Re range at optimum speed increases from Anguilliform to Thunniform. Propelled AUVs reach slightly above the range of Subcarangiform swimmers. However, as observed before, their speed is considerably less than those of Subcarangiforms. Gliders have the lowest Reynolds numbers of all AUVs.

For maximum speed not as many data is available. The Thunniforms have the highest *Re* number at 3.47×10^8 while the AUVs reach the $Re = 6.1 \times 10^7$ while gliders are still in the lowest range of Reynolds numbers.

As well as swimming mode, the form and fineness ratios of BMSs, may to some extent explain the high propulsion speed evident in nature. However this does not apply to all modes of swimming and it can be concluded that propulsion capability is the dominant factor affecting speed capability. However, fast swimmers with fusiform and elongated body forms have a fineness range of $4.4 < FR < 7.5$

It is clear that BMSs have higher speed capability and wider speed ranges compared to AUVs and as biomimetic AUV data shows there are potential improvements in terms of speed for AUVs. BMSs achieve their speed capabilities by different means which considering their superior performance requires further investigations. The investigation has been carried out and discussed in Chapter 5.

3.3 Depth Capabilities

The ability to reach the deepest depth of the oceans is an obvious capability desired for AUVs. Figure 3.12 is an indication of depth range per unit mass. Hence, the plotted data are based on a trade-off between absolute depth capability and mass as an indication of size. As shown in the plot, deep-water and especially mid-water fish have the highest depth range per mass capability. The BMSs with highest values of mass specific depth range are the Pacific viper fish (*Chauliodus macouni*) with a depth range ($\Delta Depth$) of $4365m$ $\left(\frac{\Delta Depth}{\{Mass\}} = 1.9 \times 10^5 \left[\frac{m}{kg}\right]\right)$, mid-water eelpout (*Melanostigma pammelas*) with a depth range of $2100m$ $\left(\frac{\Delta Depth}{\{Mass\}} = 2.1 \times 10^5 \left[\frac{m}{kg}\right]\right)$ and the sea lamprey (*Petromyzon marinus*) with $\Delta Depth$ $=2200m$ $\left(\frac{\Delta Depth}{\{Mass\}} = 8.5 \times 10^4 \left[\frac{m}{kg}\right]\right)$.

It is interesting that the swim bladder is present in the body of the deep diving Sea lamprey which proves not only shallow diving/living fish have swim a bladder. Most of the marine mammals and sharks have the lowest mass specific depth range. For BMSs, other than physical limits, motivation or "mission" of the animal is another key reason to perform a deep or shallow dive. Therefore, species do not always dive to their maximum capability. AUVs in Figure 3.12, are clustered within the same range as small marine mammals and sharks which have much less mass specific depth range capability compared to most of fish and penguins.

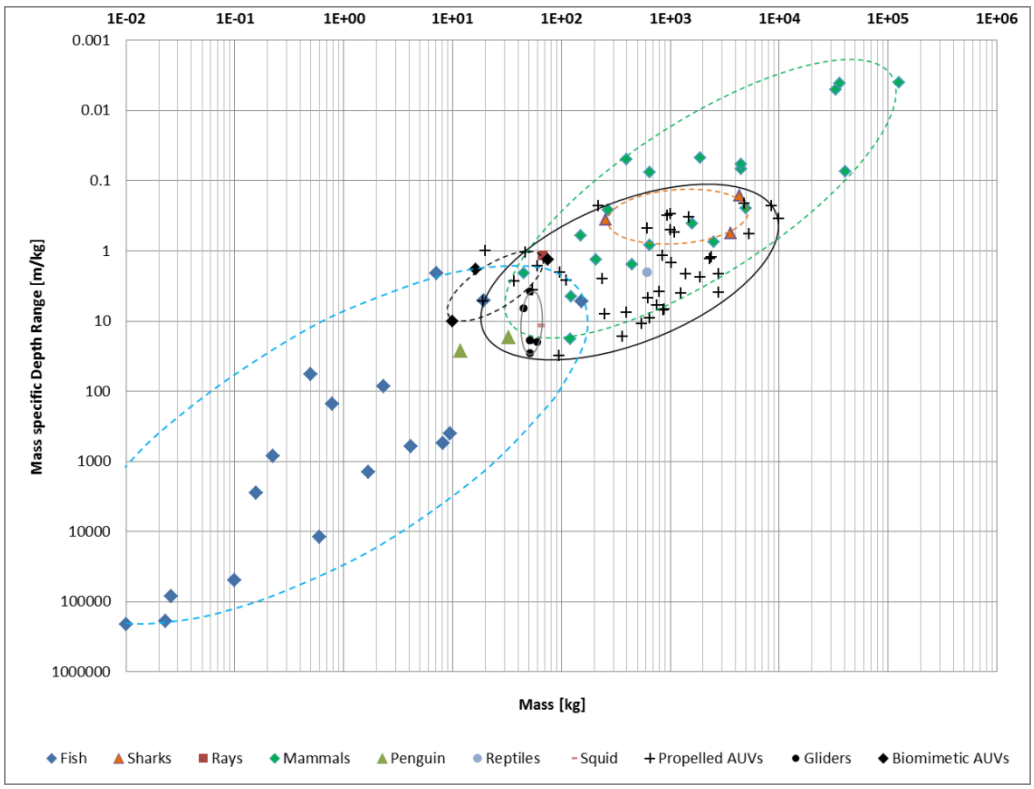

Figure 3.12. Depth range as a function of mass (Log-Log graph) comparison of BMSs and AUVs. If minimum depth for a BMSs in unknown, it has not been included in the plot

To obtain complete knowledge of depth capability of BMSs and AUVs, as well as depth range per kg of body mass, the absolute depth capability must also be considered. The rationale behind demonstrating the depth capability as a function of mass is that for AUVs the depth capability is generally dependant to the mass of the vehicle mainly as a result of the fuel carrying capacity of the vehicle. Therefore it was decided to compare the depth capability of all BMSs and AUVs as a function of mass.

Figures 3.13 and 3.14 demonstrate the absolute depth capability of BMSs and AUVs respectively. It is realised that AUVs can already reach great depths of 6000 m, and one vehicle, the Nereus Hybrid-ROV (i.e. can operate as an AUV [untethered] as well as an ROV[tethered]), has reached the depth of 10,903 m (Bowen et al., 2009) and it is claimed that the AUV has the capability to reach 11 km deep. It must be noted that Nereus has only been tested in AUV mode up to the depth of 2270 m and the 10,903 m dive has been performed in the ROV mode.

While there are many deep living BMSs, this does not indicate that they are always deep divers or have the ability to travel all the way up to the surface. The data suggests that AUVs perform with similar capability to marine mammals with the same mass; however, it is interesting that many marine animals including fish and penguins can

reach higher relative depth range with less mass. What is clear is that as well as different buoyancy control systems, deep-water fish have soft bodies and low $\frac{Mass}{Body\ Length}$ ratio compared to shallow water fish and air-breathing animals.

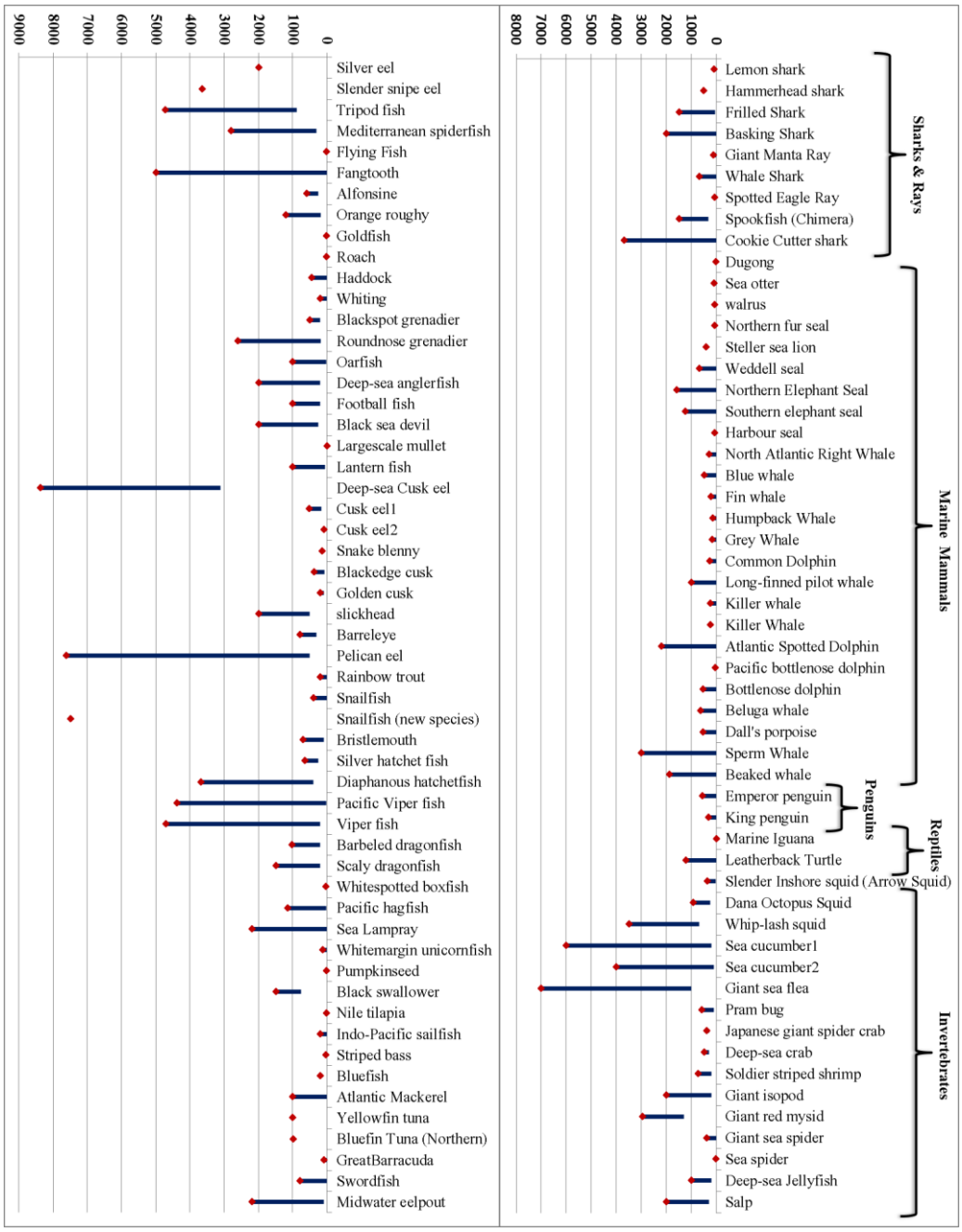

Figure 3.13. Depth range as a function of mass (Log-Log graph) comparison of BMSs and AUVs. If minimum depth for a BMSs in unknown, it has not been included in the plot

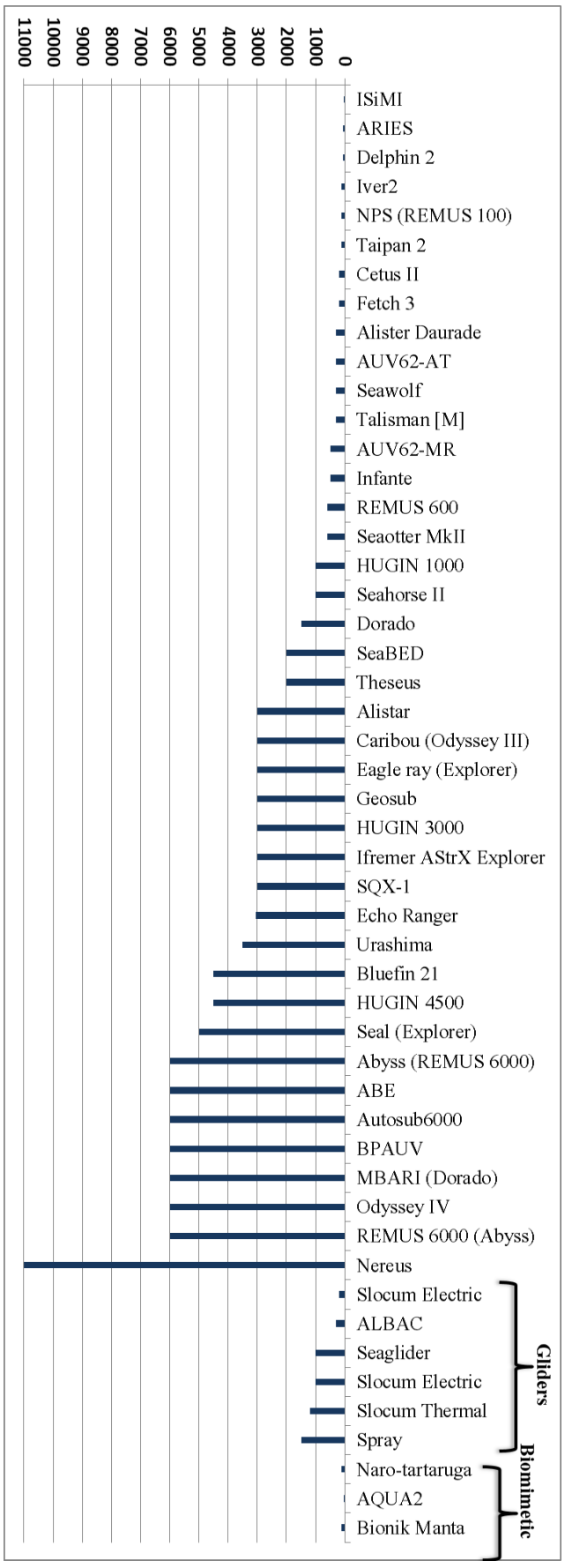

Figure 3.14. Depth range as a function of mass (Log-Log graph) comparison of BMSs and AUVs. If minimum depth for a BMSs in unknown, it has not been included in the plot

Figure 3.13 illustrates that fish (Actinopterygii) exist at the greatest depths and have been found at the widest depth ranges as well. Interestingly, some species belonging to the same family and therefore closely genetically related, have significantly different depth capabilities. The two most significant examples are snailfish and cusk eel; although most of the cusk eels have depth ranges not more than 600 meters, deep sea cusk eel (*Abyssobrotula galatheae*) swims in depth of 3110 to 8370 meters. And a recently discovered type of snailfish (*Pseudoliparis amblystomopsis*) has been found in the deepest depths of ocean trenches over 7500m (National Geographic, 2010), while *Agonopsis chiloensis* which is also a snailfish cannot swim deeper than 400 meters.

Marine mammals are the deepest air-breathing divers; they achieve their desired depth with less energetic cost compared to when they are forward swimming. This is achieved by shutting down their unused systems, reducing their heart rate and more important by gliding instead of swimming; in dives deeper than 300m, gliding is performed 60-95% of the total dive; this reduces their cost of diving to a great extent. (Williams et al., 2000)

Although the oxygen reserve and therefore size has a significant impact on the diving depth of air breathing BMSs, one key factor affecting their ability to dive and exist at depth or to migrate through a depth range is their buoyancy control mechanism. As indicated by Pelster, 2009, marine animals have various buoyancy control systems; these mainly include:

- Gas bladders: They are used by many fish usually living in shallow water,
- Lipid bladders: Examples are found in mid and deep-water fish such as Myctophids and the orange roughy (*Hoplostethus atlanticus*),
- Lipid in the liver mainly in sharks, and
- Hydrodynamic lift: This method is mainly used by marine mammals. However they also use the air in their lungs and possibly the change in the density of the lipid above their heads). Turtles adjust the depth with the remaining air in their lungs to remain neutrally buoyant. And finally, penguins remain positively buoyant. Therefore, they have a passive gliding surfacing. This also applies to right whales (such as the *Eubalaena glacialis*) as they are positively buoyant.

Biological buoyancy control systems are very diverse. However, for many BMSs, especially the ones living in the deepest depths of the ocean, their buoyancy control systems are still unknown and have not been studied. Therefore, there are many

questions to answer in terms of how some BMSs, mostly fish and some marine invertebrates can exist in deepest places in the ocean.

Depth capability is a subject with significant amount of investigation required to initially understand the mechanism behind BMSs capabilities which for many deep diving/living BMSs does not exist presently, the details of which are beyond the scope of this research. When the understanding is reached, it may result in bio-inspired divers.

3.4 Manoeuvrability

Underwater operations in narrow spaces, tracking fast moving and highly manoeuvrable marine animals, effective obstacle avoidance and many other desired missions, point to a high level of manoeuvrability required for AUVs.

One of the parameters to be considered as a manoeuvrability measure of a vehicle is the radius of turning circle, which is especially important in high speeds or when the vehicle mission is to chase and observe a marine animal.

AUVs are designed with up to 6 degrees of freedom to able them to turn more efficiently (with smaller radius). As well as turning radius or yaw radius (R_{Yaw}), rate of turn $[^{\circ}/_{S}]$ is a key factor to turning; rate of turn is the angle turned per second. AUTOSUB6000 has a rate of turn of 6.5 $[^{\circ}/_{S}]$. In comparison, the white spotted boxfish *(Ostracion meleagris)* (Walker, 2000) which in fact also has a rigid body, can turn up to about 200 $[^{\circ}/_{S}]$ or the Labriform swimmer Californian sea lion (*Zalophus californianus*) has a rate of turn of 690 $[^{\circ}/_{S}]$ (Fish et al., 2002). Some coral reef fish can have a rate of turn of up to 1200 $[^{\circ}/_{S}]$ while manoeuvring with side fins or up to 9200 $[^{\circ}/_{S}]$ is manoeuvring with the rear fin. Data on several cetaceans suggests that they have lower turning rates compared to other BMSs mentioned however the white sided dolphin (*Lagenorhynchus obliquidens*) can turn at about 453 $[^{\circ}/_{S}]$ (Walker, 2000). This means that BMSs can turn up to 1415 times faster than AUTOSUB6000 while the rigid bodied boxfish turns 33.5 times faster than AUTOSUB6000. This suggests a large gap between the turning capability of AUVs and BMSs.

Two main factors affecting this are the effective use of side fins in BMSs and more importantly the body flexibility. In order to take manoeuvrability of AUV to a higher level, thought must be put into flexible body AUVs. Figure 3.15 shows the extent of flexibility of the dissected gurnard (*Chelidonichthys spinosus*). As shown, the maximum extent of forced body flexibility for the gurnard is 139°.

Figure 3.15. Photo to measure the body flexibility of the gurnard

Data on manoeuvrability of AUVs is hard to find. However, due to the inflexible body of the vehicle, it is right to assume the turning circle and therefore turning radius of AUVs are relative to their length. Figure 3.16 illustrates the relationship between Body Length and turning radius in AUVs (An R^2 value of 0.8943 verifies the theory of a very good correlation). Therefore the R_{Yaw} of other studied AUVs has been estimated based on this correlation.

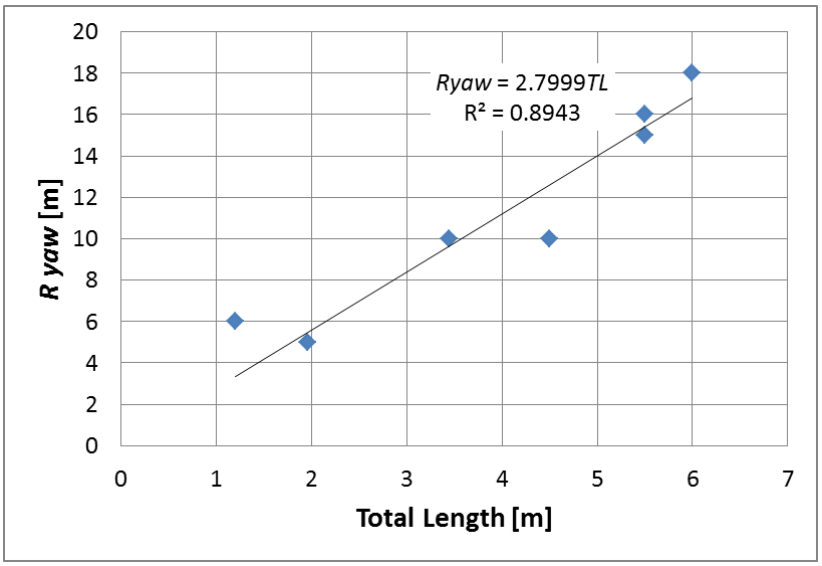

Figure 3.16. The correlation between total length and Yaw radius in AUVs

In different studies, turning radius is defined both as the radius of the path of the turning centre, $\frac{R_{path}}{Length}$, as well as the space required to turn, $\frac{R_{space}}{Length}$. Turning modes are different for different families of BMSs, due to swimming mode and flexibility.

Therefore these two terms must be defined and measured slightly different for some BMSs and sometimes in literature, it seems so that different definitions of turning radius for BMSs are being compared with each other, without taking into account the differences in body flexibility. For example the white spotted boxfish (*Ostracion meleagris*) makes an almost on the spot turn and therefore has a relatively small $\frac{R_{path}}{Length}$. However, due to its rigid body, to calculate $\frac{R_{space}}{Length}$, half the body length must be added to it. This is the same for turtles. However, Sea Lions have a highly flexible body and therefore their body takes almost the shape of their turning circle and for them:

$$\frac{R_{path}}{Length} = \frac{R_{space}}{Length}$$

3.4.1 Comparing the turning radius of BMSs and AUVs

A useful means to compare the turning capability of BMSs and AUVs is the length specific turning radius. Length specific turning radius is the radius of turning circle divided by the body length. Using the length specific turning radius is useful for comparison as the variation in size of the BMSs and AUVs is large.

Figure 3.17 is the plot of length specific turning radius data of BMSs and AUVs. For AUVs that the data is available, it is presented as black crosses. As the regression line in Figure 3.16 illustrated, the average length specific turning radius for AUVs can be assumed as 2.7999. Therefore a black dashed line showing this value is also presented in the Figure 3.17. For bio-mimetic AUVs, turning radius data is not yet available.

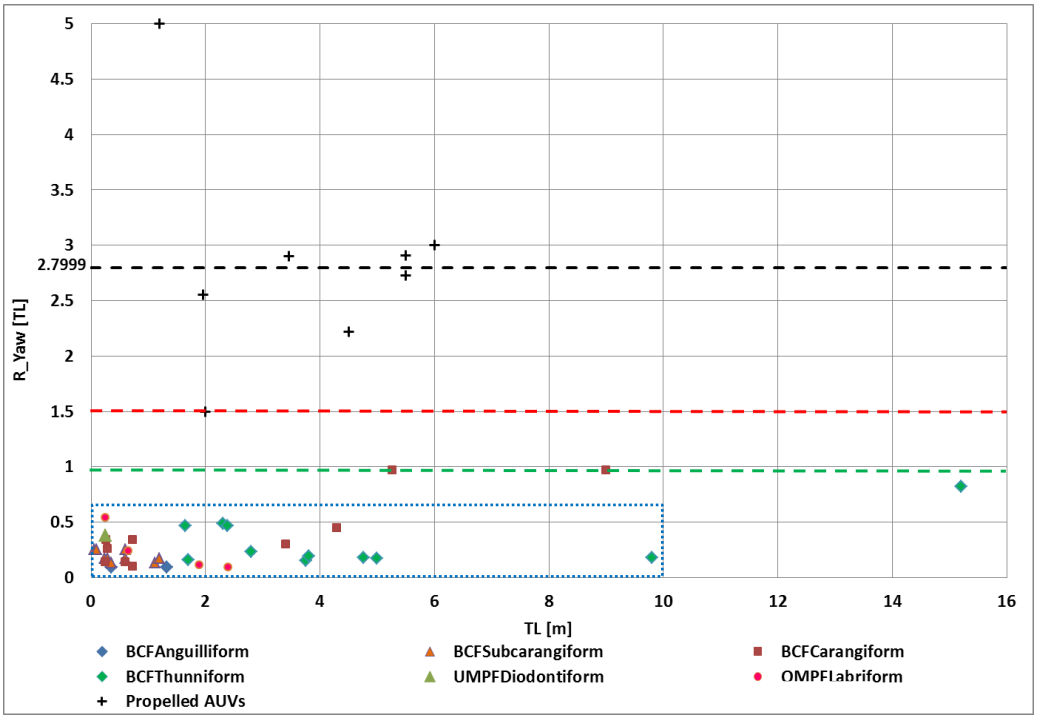

Figure 3.17. Length specific Yaw radius $(\mathrm{R}_{\mathrm{Yaw}_{TL}})$ or turning radius per unit length of AUVs and BMSs. The green dashes line is the highest radius for BMSs and the red dashed line the minimum radius for AUVs. The black dashed line represents the average value for $\mathrm{R}_{\mathrm{Yaw}_{TL}}$ of AUVs based on the regression line in Figure 3.16. The blue frame represents the area illustrated and discussed in Figure 3.18 to show the BMS data more clearly

As shown clearly in Figure 3.17, the relative turning radius of BMSs is less than 1.0. On the other hand for AUVs even of the same size it is larger than 2.1 times the total length. Only the Seawolf AUVs has an indicated turning radius of less than 3 m which means its relative R_{Yaw} is $1.5[TL]$. Therefore compared to the most manoeuvrable AUV, Seawolf, BMSs have up to 16.7 times less relative turning circle. High manoeuvrability in BMSs is achieved through multi jointed flexible bodies.

A closer look into the relative turning radius of BMSs has been taken as shown in Figure 3.18. For clarity of the data points, two species with large R_{Yaw} are not included in this figure; basking shark (*Cetorhinus maximus*) (two individuals with *BL*=5.3m and *BL*=8.5m, $R_{Yaw_{BL}}$ =0.97 $[TL]$) and humpback whale (*Megaptera novaeangliae*) (*BL*=15.2m, R_{Yaw}=0.82$[TL]$) which is a slow swimming marine mammal.

Clearly highly flexible eel like bodies have the lowest $R_{Yaw_{TL}}$. However, Labriform swimmers such as seals also have $R_{Yaw_{TL}}$ as low as 0.09 $[TL]$ in the same group, penguins are less manoeuvrable and turtles with rigid bodies are the least manoeuvrable of BMSs. However, rigid bodied BMSs such as turtles or the boxfish, have the lowest $\frac{R_{path}}{Length}$. Painted turtles have and average $\frac{R_{path}}{Length}$ =0.04 $[TL]$and the box fish 0.0015 $[TL]$.

This suggests that using their side fins (flippers) they almost turn on the spot. Thunniform swimmers are different in terms of their turning capability. Thunniform swimming fish have relatively rigid bodies with less flexibility and therefore their $R_{Yaw_{TL}}$ is as high as 0.49 $[TL]$. On the other hand marine mammals have more flexible bodies and therefore have better turning capability. It should be noted that there are arguments about the swimming mode of marine mammals and they have been corresponded both with Thunniform and Carangiform swimming modes. Carangiform and Subcarangiform swimmers have better manoeuvrability compared to Thunniform fish but not as well as eel like bodies or seals.

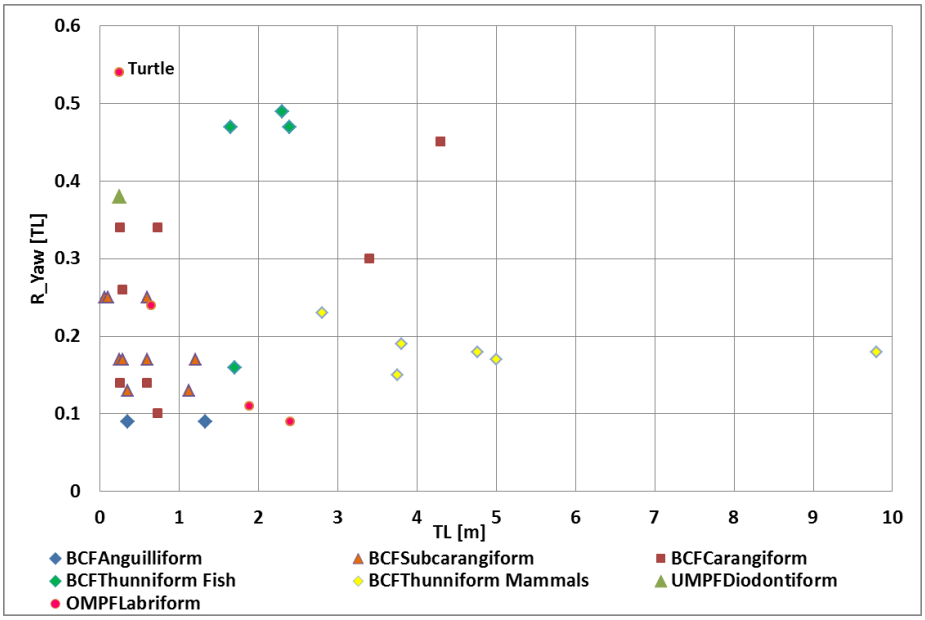

Figure 3.18. $R_{Yaw_{TL}}$ for various BMSs

Based on the conclusion from the comparisons made in this research and observing that body flexibility plays an important role in turning capability, through the collaboration within the NEMO project, a prototype of a flexible bodied AUV is being built in University of Southampton (Phillips et al., 2010).

3.5 Energetics

For most vehicles, cost is of upmost importance. Cost may be defined by various means; the financial cost, energy consumption, range of operation and so on. In this research, to correspond AUVs cost to an equivalent term for BMSs, energetics have been investigated, estimated and compared. Energetics can be investigated as energetic

Cost Of Transport (*COT*), or as energy storage capability which relates to endurance or range of operation.

Considering *COT*; this is a measure of energy expenditure required to swim at a given speed. For AUVs there are two main known speeds Economic Speed, U_{eco}, and maximum speed, U_{max}. On the other hand, BMSs have a long range of speeds. The speed ranges from their minimum speed (or still condition for neutrally buoyant BMSs) to their maximum speed. For comparing the energetic costs, there are two speeds which are particularly of interest; optimum speed, U_{opt} and maximum speed, U_{max}. As the *COT* vs. Speed curve is a U shape curve, it has a minimum; this occurs at what is known as the optimum *COT*, COT_{opt}. The corresponding speed to COT_{opt} is U_{opt}. In order to find the U_{opt}, it would be ideal that the *COT* is known at every speed; this data is not usually available. However, cruise speed or sustained speeds are available for most BMSs. Therefore, at these speeds, *COT* can be derived by measuring the oxygen consumption rate of the animals swimming at a given speed and converting it to energy as explained in Chapter 4.

For AUVs, *COT* can be calculating when the speed, weight, endurance and the battery capacity of the vehicle are known. The Cost Of Transport for the vehicle may also be defined as the energy required at each segment of time for each kilogram of the mass of the vehicle to move forward at a specific speed. By knowing the size and speed of the vehicle and the battery capacity, *COT* is calculated for AUVs as explained in Chapter 4.

Figure 3.18 shows that AUV are clustered within a small speed range but within this range, they have lower *COT* compared to BMSs. Glider AUVs have the lowest *COT* of all other marine underwater systems. This is to be expected due to their special low cost slow moving locomotion.

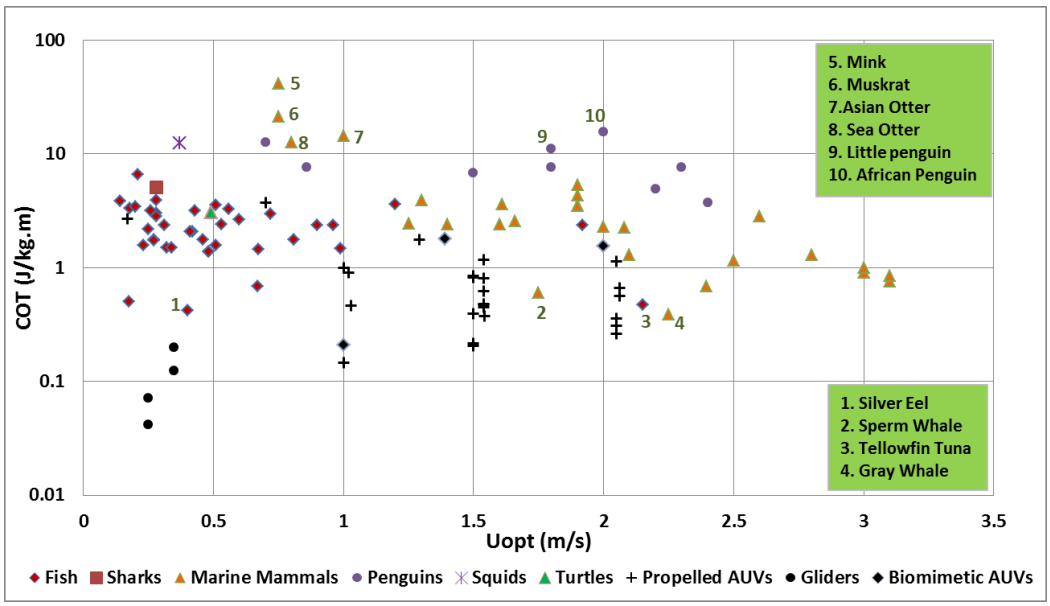

Figure 3.19. *COT* comparison of AUVs and BMSs

Figure 3.19 illustrates that large marine mammals and the Thunniform swimming Tuna have lower mass specific *COT* compared to other BMSs. Within the BMSs, the Grey Whale has the lowest *COT* at its optimum speed. The silver eel (*Anguilla anguilla*) and the sperm whale (*Physeter macrocephalus*) are associated with long range migrations (5000 - 6000 km). On the higher end of the plot sea otters (*Enhydra lutris*), the north American mink (*Neovison vison*) and the muskrat (*Ondatra zibethicus*) have *COT* higher than 10 $\left[\frac{J}{kg \times m}\right]$ as their bodies are not evolved specifically for aquatic locomotion. little penguin (*Eudyptula minor*) and African penguin (*Spheniscus demersus*) also have *COT* higher than 10 $\left[\frac{J}{kg \times m}\right]$.

Illustrating the *COT* at optimum speed as per Figure 3.18 is beneficial for the comparison between AUVs and BMSs. However, animals do not always operate at their optimum speed. Due to their high speed range capability, *COT* for animals, unlike AUVs, is a curve. This subject has been extensively studied and calculations carried out to produce the *COT* curve for numerous marine animals with different speed and *Re* ranges in the next chapter, chapter 4.

3.6 Conclusion

In this chapter several characteristics of AUVs and marine animals have been compared to highlight the relative superiority and limitations of biological and engineering systems. The main highlights of the comparisons are as follows.

- In terms of body forms, marine animals have slightly higher range of *FR* compared to AUVs. However, the range of *FR* for Teardrop AUVs and fusiform BMSs match with one another.
- Thunniform swimming is used for fast swimming by both fish and marine mammals. However, Labriform swimming mammals have high optimum speeds. Moreover, smaller fish with Carangiform swimming and some types of penguins with flapping swimming mode have high BL/s Speed. BMS have optimum speed capabilities of up to 175% higher compared to the highest optimum speeds of AUVs and maximum speed capability of up to 350% higher compared to the fastest AUVs.
- AUVs are relatively capable at deep diving. However, many fish can reach deeper depths with less mass. Therefore further research may clarify the reason by which they achieve this. One lesson to be learned from marine animals, especially marine mammals is to reduce the energy expenditure during diving by configuring the control surfaces for maximum gliding capability instead of swimming.
- In terms of manoeuvrability, the significant superior turning performance of marine animals is evident; this is achieved though their multi joint flexible bodies.
- Energetics is the most interrelated comparable characteristic between the two groups. It can be measured by *COT* or by endurance. The comparison shows that, although compared to many marine animals AUVs have less *COT* when swimming at their economic speed, their speed range is very limited.

The comparisons made in this chapter showed significant superiority of BMSs over AUVs in terms of their agility, manoeuvrability and swimming range. Therefore there are certainly potential bio-inspired improvements for AUVs in these aspects. However, it is apparent that the "raw" data is not in a form to allow all the comparisons as desired by the research; therefore further analysis was required to obtain the rest of the picture especially in terms of propulsion, energetics and manoeuvring of BMSs.

Even the traditional AUV designs are to some extent inspired by nature; however, in most cases the importance of nature has not been fully appreciated and the analysis has not been pursued as profound as it should have been to highlight the full potentials of inspiration from nature. This chapter highlighted general areas of superior performance of BMSs over AUVs. To understand the reasons behind the superior performance of BMSs, comprehensive studies were carried out on energetics and propulsion. These investigations are explained in Chapters 4 and 5.

Chapter 4. Energetics in detail

The amount of energy that an underwater system consumes to perform a task is very important. This affects the amount of energy storage (e.g. batteries in an AUV or fat in a BMS) that the vehicle requires to carry on-board, which consequently affects the amount of other equipment such as sensors (referred to as *payload*) which the vehicle can carry. This means that either the vehicle must be built heavier or will not be able to perform certain missions. Moreover, the energy consumption affects the range of operation or endurance of the vehicle. Therefore although energetics is not always a directly desirable characteristic, it affects other aspects of a vehicle's performance and it is especially important when comparing two systems with similar capabilities.

Therefore a clear understanding of the energetics of the vehicle is crucial. At the early comparison of the energetics of AUVs vs. BMSs, the *COT* at the optimum speed was compared as explained in Chapter 3. However, energetic cost is comprised of several components for both AUVs and BMSs and more in depth investigation was required to correspond different aspects of the energetics costs of AUVs and BMSs for comparison. This has been carried out as discussed in this chapter. Having the understating of *COT*, the range of operation is also estimated.

4.1 Cost Of Transport

Energetic Cost Of Transport (*COT*) can be defined as a mass normalised measure of the required energy to move a vehicle over a certain distance. The general equation for *COT* is as below:

$$COT = \frac{Energy}{Mass \times Distance} \tag{4.1}$$

Energy is power multiplied by time. Therefore Equation 4.1 can be written as:

$$COT = \frac{Power}{Mass \times Velocity} \tag{4.2}$$

The unit of *COT* is $\frac{kJ}{kg \times km}$ or its equivalent $\frac{J}{kg \times m}$.

In AUVs several types of batteries provide energy for different AUVs. Gliders on the other hand, have a buoyancy engine and therefore rely on small alternation in their buoyancy coupled with the use of side wings to propel themselves by converting vertical motion into horizontal. This, results in lower power consumption required for

propulsion. Therefore, operating at lower speeds compared to conventional AUVs, gliders require less battery mass to operate.

The battery capacity is measured in $kilo\,Watt \times hour$. If the battery capacity is divided by the time taken for the operation, the required power is calculated:

$$Power = \frac{Battery\ Capacity}{Time} \tag{4.3}$$

Therefore the battery provided *COT* for AUVs can be calculated as below:

$$COT = \frac{Battery\ Capacity}{Endurance \times Mass \times Speed} \tag{4.4}$$

Where:

- Mass is the mass of the vehicle
- Speed is the speed at which the vehicle operates
- Battery capacity is the specific energy of the battery multiplied by the amount of battery on board (battery mass)
- Endurance is measured as the time or distance travelled by the vehicle at the specified speed with the amount on-board battery without recharging. Endurance is measured in hours. This is explained in Section 4.3.

And therefore Equation 4.4 is re-written as:

$$COT\left[\frac{J}{kg \times m}\right] \tag{4.5}$$

$$= \frac{Mass_{Battery}\ [kg] \times Energy_{specific_{Battery}}\left[\frac{kWh}{kg}\right] \times 3.6 \times 10^6\left[\frac{J}{kWh}\right]}{Endurance[h] \times Mass_{Vehicle}\,[kg] \times Speed\left[\frac{m}{s}\right] \times 3.6 \times 10^3\left[\frac{s}{h}\right]}$$

Endurance data, if available, are usually measured during a trial or estimated by knowing the power required to run the AUV. The specific battery energy and battery mass are known for the AUV. The power required for the AUV to operate at a certain speed can be measured during a trial or can be calculated as the sum of propulsion power and hotel power. By having these data, the endurance of the AUV for a particular speed is calculated as $\frac{Mass_{Battery}\ [kg] \times Energy_{specific_{Battery}}\left[\frac{kWh}{kg}\right]}{AUV\ power\ consumption\ at\ a\ specific\ speed\ [kW]}$

COT of the AUV at that specific speed can then be calculated using Equation 4.5.

For BMSs, estimation of *COT* is more complicated and as explained in Section 3.2 of Chapter 3, there are three main swimming ranges at which they swim within. The *COT* can be also defined as the energy required for the muscle to operate. There are two types of muscle in Fish, the slow muscle and the fast muscle. These muscles are

commonly known as red muscles and white muscles respectively. The contribution of white muscles when the BMS is swimming within its sustained swimming range which includes the proximity of its optimum speed is negligible. Therefore, solely red muscles provide the propulsion through the rear fin and therefore only the energy required for the red muscles needs to be calculated at the sustained speeds range. These types of actuators are oxygen dependent and operate through an aerobic process. Direct measurement of energy consumption is not possible for BMSs. However, it is a fact that oxygen is consumed to burn fat and therefore produces energy. Therefore, for sustained speeds, the *COT* can be derived by measuring the rate of oxygen consumption of the animals swimming at a given speed. This is measured as mg of oxygen breathed by the BMS per unit time. Then the O_2 consumption is converted to energy based on the oxy-calorific value of oxygen. Elliott & Davison, 1975 measured this value to be equal to 13.59 $\left[\frac{J}{mg_{O2}}\right]$.

Therefore, to normalise the energy expenditure and make is comparable with the *COT* of engineered vehicles, the *COT* for BMSs at a sustained speed within the aerobic metabolism range (including optimum speed) is calculated at follows:

$$COT\left[\frac{J}{kg \times m}\right] = \frac{O_{2\,consumed}\ \left[\frac{mg}{kg \times h}\right] \times 13.59\left[\frac{J}{mg_{O2}}\right]}{U\left[\frac{m}{s}\right] \times 3600\left[\frac{s}{h}\right]} \qquad 4.6$$

As *COT* is a U shaped curve with a minimum, if the optimum speed of a species is not known, by measuring the *COT* at different sustained speeds and plotting the *COT* vs. Speed graph, the optimum *COT* and consequently the optimum speed can be estimated. Figure 4.1 illustrates a typical *COT* vs. Speed curve for a BMS up to the critical speed, U_{crit}, as explained in Section 3.2.

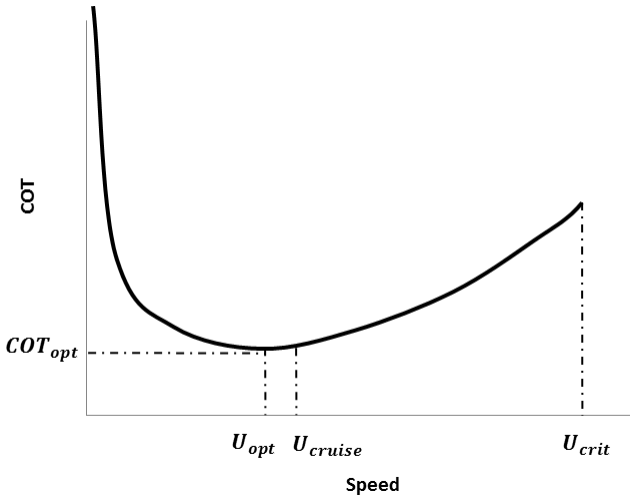

Figure 4.1. Typical Cost of Transport vs. speed plot of a BMS based on aerobic metabolism

In engineering terms required power is often calculated and indicated for various systems. By having the speed of the BMSs it is known that:

$$Power = COT \times U \times \{Mass\} \quad 4.7$$

Therefore by using Equation 4.6, required power is calculated as:

$$Power(Watts) = \frac{O_{2_{consumed}} \times 13.59 \times \{Mass\}}{3600} \quad 4.8$$

Various oxygen consumption rates and therefore metabolic rates are measured at different activity levels for BMSs. These include:

- Basal Metabolic Rate (BMR),
- Standard Metabolic Rate (SMR),
- Routine Metabolic Rate (RMR),
- Active Metabolic Rate (AMR), and
- Field Metabolic rate (FMR)

Each term is explained next.

- Basal Metabolic Rate (BMR): The metabolic rate measured for an endothermic BMS while satisfying 5 conditions proposed by Kleiber, 1975. The BMS must be and adult resting inactive (not asleep) but under no stress, in an environment within its neutral temperate, fasting so that no energy is consumed for digestion, not pregnant or lactating.
- Standard Metabolic Rate (SMR): Similar to BMR but measured for ectothermic BMSs. The metabolic rate measured for an ectothermic BMS while it is resting inactive at a specific temperature.
- Routine Metabolic Rate (RMR): The metabolic rate of a species which has some level on activity but not continuously swimming.
- Active Metabolic Rate (AMR): The metabolic rate of a species actively forward swimming at a certain speed.
- Field Metabolic rate (FMR): The metabolic rate of a species actively swimming; the speed may vary.

BMR and SMR are used when estimating non-propulsive energy consumption. AMR is the other measurement useful for the purpose of the research as the swimming

speed of BMS must be known so it can be used to estimate *COT* and power. Therefore FMR and RMR are not used within the scope of this research.

One consideration to be made is that to allow for direct comparison, the temperature of the water at which the BMS swims and the oxygen consumption has been measured must be taken into account. In order for the test to be valid for calculating *COT* and power, different measures need to made for endothermic and ectothermic BMSs. Endothermic BMSs are species that tend to maintain their body temperature at a temperature which is in favour metabolically, regardless of their environment. Endothermic BMSs include marine mammals, penguins and very few fish such as the tuna. On the other hand, the body temperature of ectothermic BMSs, such as most fish, reptiles and invertebrates, depends to the external environment. Therefore for endothermic BMSs, the temperature of the water should be in neutral thermal zone of that BMS so that no energy is consumed to regulate body temperature (Castellini, 2008). Similarly, because the BMR of ectothermic BMSs varies with temperature, they should all be tested at the same temperature.

Sometimes this is not possible as various fish live in different environments. If so, data gathered from different tests must be normalised to a specific unified temperature. To estimate the normalised metabolic rate, a temperature coefficient, Q_{10}, is used. (Winberg, 1971 and Schmidt-Nielsen, 1997). A chemical reaction (R_s) such as the metabolic rate at a specific temperature (T_s) is calculated as:

$$R_s = R_{test} \times Q_{10}^{\frac{T_s - T_{test}}{10}} \quad 4.9$$

Where R_{test} and T_{test} are the chemical reaction and the temperature from a test respectively. Q_{10} is a temperature coefficient which is a measure of the rate of change of a chemical reaction when the temperature is changed by 10 ℃.

Therefore, for the purpose of calculating the oxygen consumption, this can be rewritten as:

$$Consumed\ O_{2_s} = Consumed\ O_{2_{test}} \times Q_{10}^{\frac{T_s - T_{test}}{10}} \quad 4.10$$

Oxygen consumption data gathered from FishBase, (Froese and Pauly, 2011) are all normalised for 20℃. However, for some of the individual BMSs, the temperature at which data was collected was from other temperatures and no Q_{10} value was mentioned and therefore the data would have been biased due to the temperature. Therefore based

on 266 data of 12 species in Fishbase, the Q_{10} values were calculated and plotted against temperature in Figure 4.2. This is a good reference for converting oxygen consumption data from different temperatures within the range of 5℃-30℃ to 20℃. It is clear that oxygen consumption increases with temperature. However, note that these regression lines may only be used for conversion of oxygen consumption in ectothermic BMSs. Endothermic BMSs react differently to temperature changes and their oxygen consumption will increase if they are out of their neutral temperature zone, no matter whether it is a higher or lower temperature.

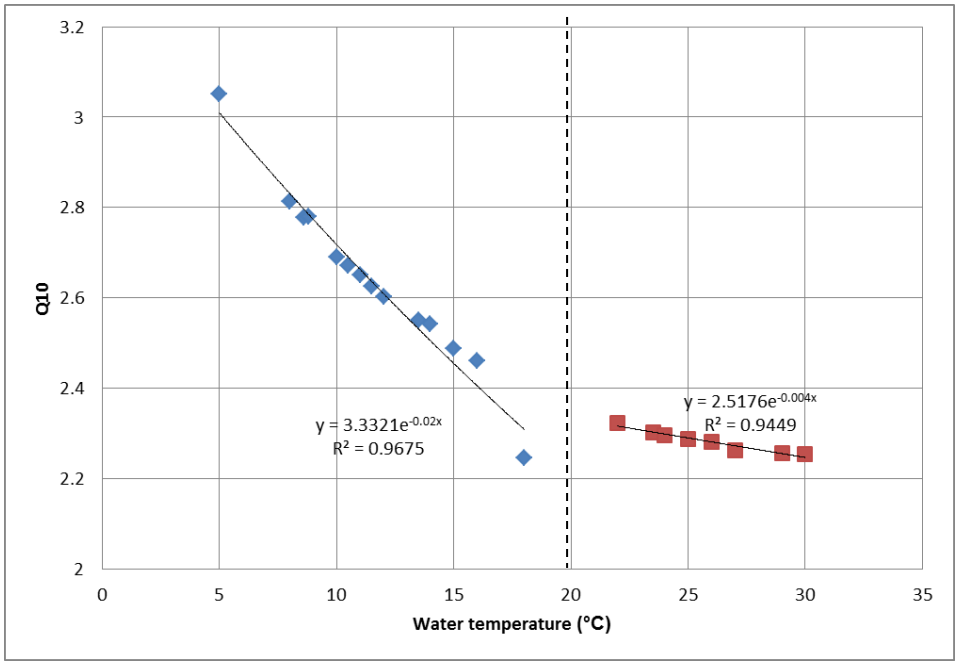

Figure 4.2. Q10 values as a function of water Temperature. The regression line passed through the blue points is for Q10 values at temperatures less than 20℃ while the line passed through the red points is for Q10 values at temperatures more than 20℃. As all oxygen consumption data are normalised for 20℃, the Q10 value at 20℃ equals to 1.

It should also be considered that animals are usually tested at a range of speeds at which they would voluntarily swim. Therefore the available data does not necessary reflect the complete range of swimming speeds of each BMS.

The methods explained above measures the aerobic metabolism for BMSs. This is most useful and accurate when the animal is swimming at speeds which the anaerobic metabolism is absent or minimal. If the speed increases to a point in which the fast twitching muscle are activated, then anaerobic metabolism occurs without oxygen and lactic acid is produced. Measuring the amount of produced lactic acid is complicated as over time some of the lactic acid is absorbed again. These data are not readily available. Therefore, calculating the anaerobic part of energy consumption is not possible for all

BMSs. However, it was realised in this research that if the maximum power capability of a muscle is known, the maximum *COT* maybe calculated. This is explained later on in Chapter 5.

Figure 4.3 illustrates the *COT* for BMSs over different Reynolds numbers. *COT* is proportional to speed; however, as the size of the BMSs varies considerably and Reynolds number is directly proportional to length and speed, it is appropriate to compare them over their Reynolds number ranges. Using the Reynolds number, different flow regimes in which various species swim are segregated. For many of the BMSs the data range is less or equal to their optimum speed as the tests have been carried out without putting stress on the species. It is realised that *COT* on its own is not a complete measure of the energy expenditure of a species. This is the reason to consider comparing *COT* within the speed range of BMSs. Figure 4.3 demonstrates that Thunniform fast swimmers such as tunas and marine mammals have lower optimum *COT* at a higher *Re* compared to Carangiform and Subcarangiforms swimmers. Silver eel which is an Anguilliform swimmer sits on the bottom of the graph, having the lowest optimum *COT* compared with other BMSs. For Carangiform and Subcarangiform swimmers it appears that body size affect *COT* as the bluefish, striped bass and the trout with similar body mass have *COT* of similar values. The general trend of the plot implies that larger body size or *Re* range, corresponds to lower *COT*; however, the Carp with larger body size compared to other Subcarangiform swimmers has higher *COT* as it is not swimming at its optimum range.

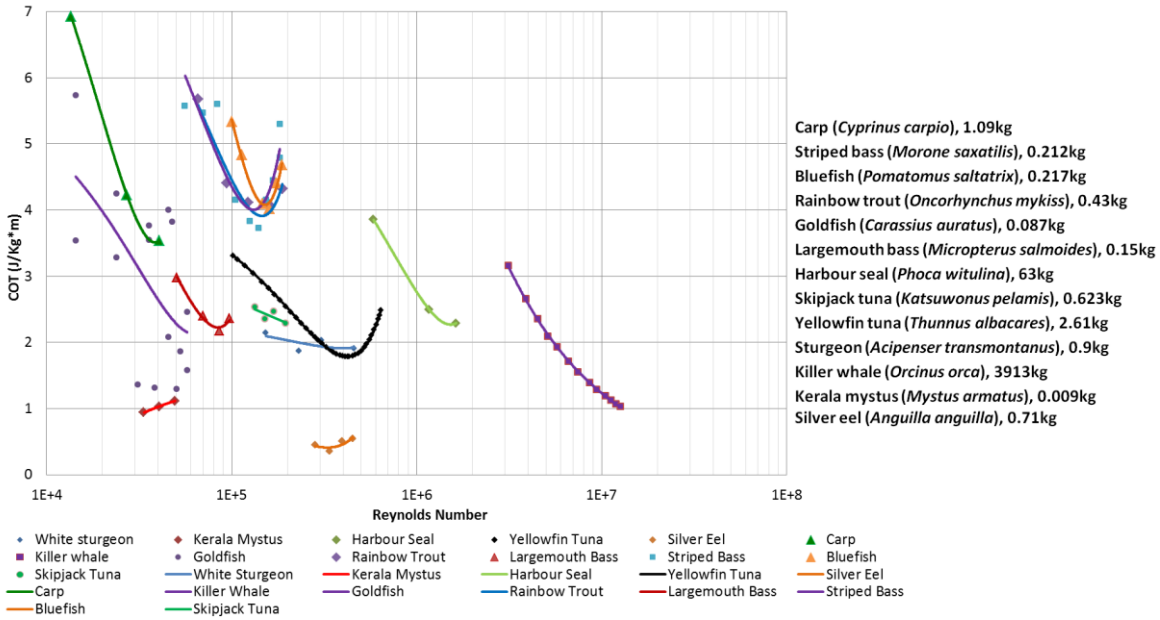

Figure 4.3. Semi-log plot of total COT vs. Reynolds number. Calculated from data in Davis et al., 1985; Dewar & Graham, 1994; Williams & Noren, 2009 and Froese & Pauly, 2011.

The most important conclusion from Figure 4.3 is that, the optimum speed at which the BMSs operate is an important factor in their energetics. Swimming at lower and higher speeds than the optimum speed can increase the *COT* considerably. For example, if extrapolating the data, the killer whale (*Orcinus orca*) has a high *COT* when compared with some fish at low Reynolds numbers which correspond to speeds less than $1\left[\frac{m}{s}\right]$, however its optimum speed is more than 2.5 $\left[\frac{m}{s}\right]$, at which it has *COT* even less than a sturgeon (*Acipenser transmontanus*). In addition the operation range of a killer whale in this plot is $3 \times 10^6 < Re < 2 \times 10^7$ which is the highest between the compared animals. Therefore although silver eel (*Anguilla anguilla*) has the lowest *COT* of all BMSs in the plot, if operating at the optimum speed of the killer whale, it will probably have higher *COT*. This does not come as a surprise; not only because BMSs with different swimming modes are evolved to swim more efficiently at different speeds, but also the drag scale effect mentioned in Section 3.2.4 in Chapter 3 explains the reason behind this phenomenon. As drag is proportionate to $\{Mass\}^{\frac{2}{3}}$, increase in mass does not increase the drag linearly. Therefore, it is expected for larger bodies to have proportionately less drag.

Figure 4.4 is the plot of total power for the BMSs in Figure 4.3 as well as the AUVs at their economic Reynolds number. AUV data is calculated from their *COT*. Figure 4.4 illustrates that total power is highly affected by the Reynolds number. AUVs have Reynolds Numbers within the range of marine mammals while gliders with $Re > 1 \times 10^6$ are close to smaller BMSs. Also speed affects the total power. Both of these factors must be investigated as the purpose of all these comparisons is to realise which system is operating more efficiently and less costly (energetic) at which range.

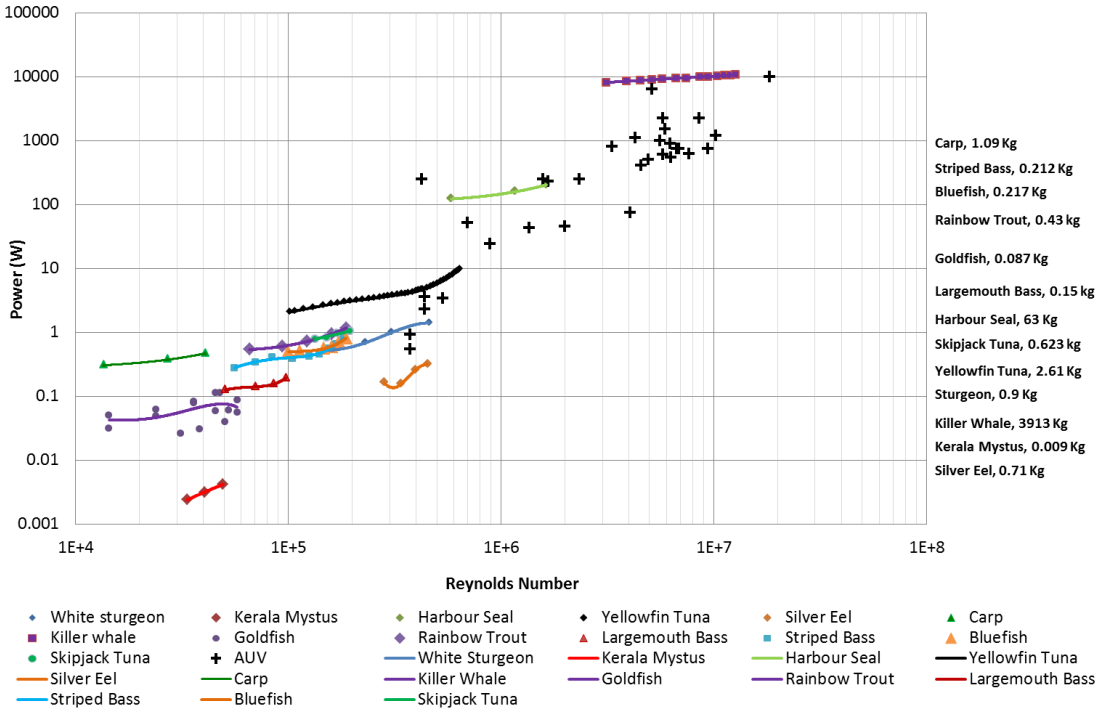

Figure 4.4. Total power vs. Reynolds Number for BMSs and AUVs

Figure 4.5 is the plot of total mass specific power of the systems in Figures 4.4.

This figure clearly shows that at their economic speed, AUVs have lower mass specific power compared to BMSs; however it is not clear whether this is due to higher propulsion power required for BMSs or higher hotel load. Both components have been investigated in Section 4.2.

Glider AUVs have the lowest mass specific power which was expected. As it is explained later in section 4.2, the two main components of power for an AUV are hotel power (non-propulsive) and propulsive power. Gliders are generally slow speed AUVs and as propulsion power increases with speed cubed, they have relatively lower propulsion power. Moreover, gliders usually carry less sensors compared to survey class AUVs which reduces their hotel load. In addition if no active buoyancy control system is present on board the hotel load will be less. As power is the sum of these two components, gliders are expected to have low power consumption compared to other AUVs.

Biomimetic AUVs have the highest total power among AUVs which is close to the range of the values for the harbour seal (*Phoca witulina*). However, both data belong to biomimetic AUVs with side fins as their main proplusors. The plot suggests that at higher speeds the propulsion power increases, however the rate of increase is

significantly higher when the systems is operating at speeds higher than its optimum speed.

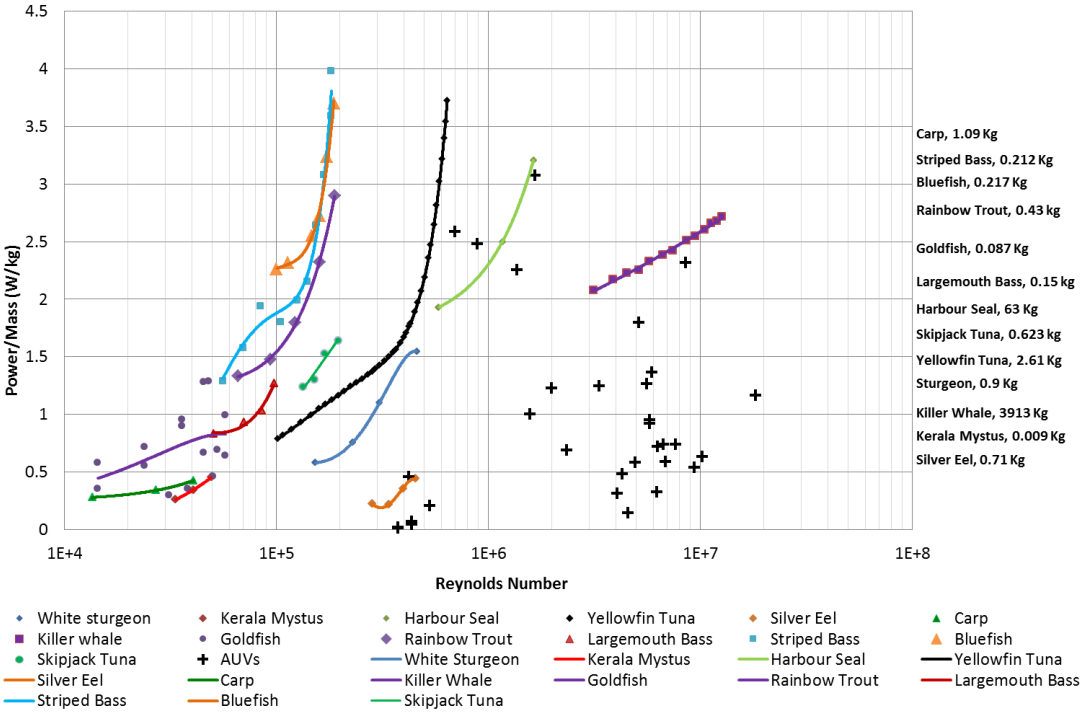

Figure 4.5. Mass specific total power vs. Reynolds Number for BMSs and AUVs

The comparison of *COT* and power suggests that hotel power and propulsion power must be compared separately to realise whether for different systems, the basal energetics of the body it high and dominating the *COT* or it is the propulsion power.

4.2 Components of Cost Of Transport

Vehicles require energy to move, however they also require a certain level of energy to perform non propulsive tasks. For BMSs, the overall required energy can be divided into six main components (Smith, 1976):

Total Energy =

Basal metabolism

+ Thermoregulation (for endothermic BMSs)

+ Voluntary activity

+ Specific Dynamic Action (heat produced by nutrient metabolism)

+ Growth fat and sexual products

+ Urine, gill exertion (for fish) and faeces

Note that Basal Metabolism of BMSs is calculated from the BMR for endothermic species or from the SMR for ectothermic BMSs. For simplicity, herein it is referred to as BMR. These six components as well can be divided into propulsive and non-propulsive required energy.

Therefore for any engineered or biological vehicle, the required energy is divided into two main parts: propulsive energy and non-propulsive energy. Both of these components must be studied separately as they affect the overall *COT* independently.

Basal metabolism, i.e. BMR for endothermic BMSs and SMR for ectothermic BMSs is the energy which is used to maintain the essential organs of the BMS as well as other life support systems and activities through basic level of respiration. Therefore it can be considered as the equivalent of hotel load in AUVs. Energy required for the propulsion power is often known as the "Net" Cost Of Transport therefore:

$$COT_{Total} = \frac{non\ propulsive\ energy\ consumption}{Mass \times Distance} + \ COT_{net} \qquad 4.11$$

Hotel load and propulsion power are explained next.

4.2.1 Hotel load

For both AUVs and BMSs, there is a base energetic cost to maintain non-propulsion related systems and activities. For engineered systems this base energetic cost is referred to as the hotel load. The hotel load is mainly associated with powering computers, hard drives and sensors (including buoyancy control system). This value, if available, is usually indicated by the manufacturer in watts.

The mission of an AUV dictates to a large extent its hotel load as hotel load comprises the power required for non-propulsive activities such as the computer, hardware and sensors which are all used to achieve the AUV's mission. Therefore, the more sophisticated the mission, higher value for hotel load is required. The assumption that survey class AUVs are designed for more sensor intensive missions, while gliders are usually designed towards high endurance, verifies the fact that gliders usually have lower hotel load.

Considering missions driving the hotel load of AUVs, the size of the AUV is not necessarily the driving factor for increase in hotel load as high endurance and therefore high battery capacity required will also increase the size of the AUV. However, the hotel load data from various survey class AUVs showed a general increase in hotel load

with mass. This tends to indicate that more complex missions require more sensors which leads to an increase in size as well as hotel load.

For BMSs this value can be calculated using the same method as explained in Section 1 of this chapter. To correspond with the hotel load of AUVs, base metabolism is calculated as power in Watts by using Equation 4.12 as below and for simplicity it is also going to be referred to as hotel load (P_H) for BMSs:

$$P_H\,[Watts] = \frac{Basal\ oxygen\ consumtion\left[\frac{mg}{kg \times h}\right] \times 13.59\ \times Mass[kg]}{3600} \qquad 4.12$$

Several studies have been carried out to derive empirical formulas by plotting regression lines for the hotel load of different BMSs. Two well-known pioneers are Kleiber, 1932 and Brody, 1945 who studied a wide range of terrestrial mammals and birds and demonstrated initially that the hotel load is very closely proportional to mass$^{0.75}$. This has since been modified by Kleiber and other scientists and several very close values of a and b have been proposed to be replaces in $a\{Mass\}^b$. They calculated the hotel load in $\left[\frac{\text{kcal}}{\{\text{day}\}}\right]$, to calculate P_H in watts:

$$\frac{kcal}{day} = \frac{4.184 \times 10^3}{24 \times 3600}\,[Watts] \qquad 4.13$$

As the interest in this research is on marine mammals, several proposed formulas by Kleiber, Brody and also McNab, 1988 are compared with some experimental data (Hoelsel, 2002) as plotted in Figure 4.6. While Kleiber mainly studied laboratory animals, McNab measured the BMR for wild marine mammals. As mentioned by Tomasi & Horton, 1992, for some captive animals and also large whales, the hotel load is twice the Kleiber value mainly due to stress. That is the reason for plotting also twice the Kleiber's regression line ($P_H = 6.78\{Mass\}^{0.75}$).

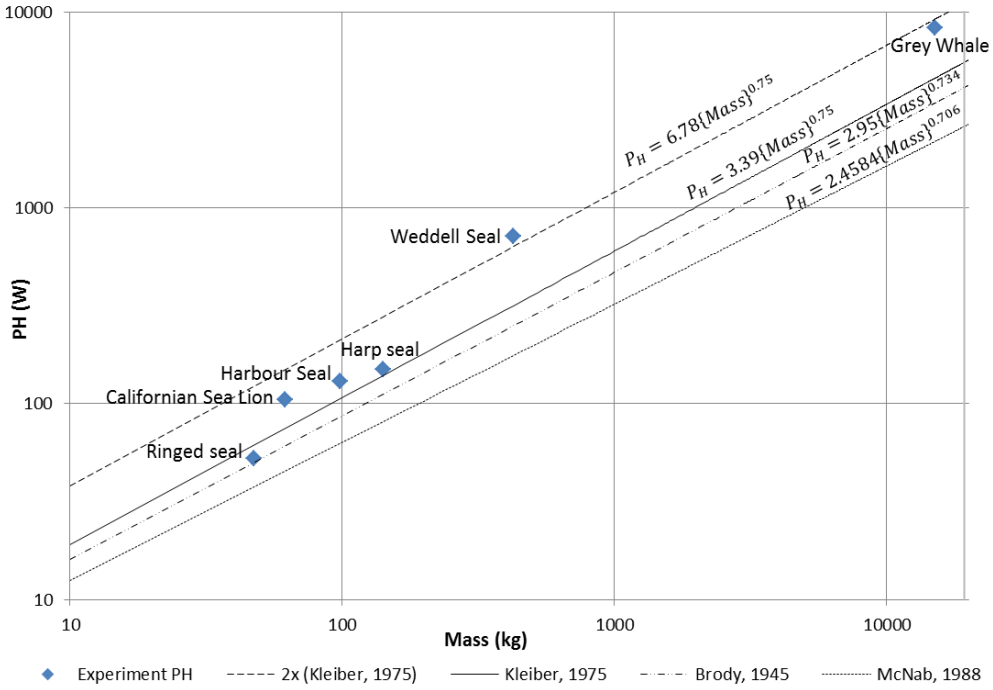

Figure 4.6. Comparison of various formulas (regression lines) for Hotel load as a function of Mass. The hotel load in regression line proposed by McNab has been converted from $\frac{cm^3_{O_2}}{g \times h}$ to $\frac{Watt}{kg}$ by Berta et al., 2005 and then to Watts in this research

As shown in Figure 4.6, most of the BMSs sit slightly above the Kleiber, 1975 line; this is mainly due to the fact that satisfying Kleiber conditions for some marine mammals is difficult if not impossible (Speakman et al., 1993), especially stress. There has also been proposed that BMSs have marginally higher hotel load compared to terrestrial mammals. This statement is debatable (Berta et al., 2005); however, the kleiber, 1975 regression line is closest to the actual value of hotel load for wild marine mammals.

Therefore in this research this line is used to estimate hotel load for marine mammals. Other similar regression lines have been proposed for other groups of BMSs. A list of the regression lines available for BMSs and AUVs is presented in Table 4.1.

Table 4.1. Regression lines of the empirical relationship between P_H (non-propulsive required power) and versus mass. R^2 values are presented where available

Groups of BMSs	Regression Line (W)	R^2	Source
Marine Mammals and birds	$P_H = 3.39Mass^{0.75}$		Kleiber, 1975
Teleosts(n=69) [2,4]	$P_H = 0.133Mass^{0.8}$	0.06	Clarke & Johnston , 1999
Teleosts (n=97) [1,4]	$P_H = 0.5072Mass^{1.0061}$	0.72	This reserach
Salmonoids (at 20°C)	$P_H = 0.313Mass^{0.855}$		Brett & Glass, 1973
Salmonoids (n=5) [1]	$P_H = 0.1579Mass^{0.7947}$	0.63	This research
Humboldt penguin (*Spheniscus humboldti*) (n=20) [3]	$P_H = 5.95Mass$	0.94	Luna-Jorquera & Culik, 2000
Penguins (n=3)	$P_H = 6.5547Mass^{0.818}$	0.92	This research
Eels (n=6) [1]	$P_H = 0.2341Mass^{1.2683}$	0.87	This research
Skipjack tuna (*Katsuwonus pelamis*) (n=6)	$P_H = 1.1224Mass^{1.2228}$	0.71	This research
Reptiles (including turtles)	$P_H = 0.378\ Mass^{0.83}$		Wallace & Jones, 2008
Conventional AUVs (n=8)	$P_H = 2.7653Mass^{0.6066}$	0.80	This research
Long Range AUVs & gliders (n=4)	$P_H = 1$		Phillips, et al., 2012

[1] Hotel load regression line was calculated from O_2 consumption data at different temperatures, normalised for 20 ℃.

[2] Hotel load regression line was converted from the equation in reference which is based on O_2 consumption in $\frac{mmol}{h}$ and mass in *grams*.

[3] Resting metabolic rate in water at 19℃. Their metabolic rate included heat loss which was associated with being submerged in water.

[4] Teleost fish or Teleostei are the main infraclass of the ray fined fish (Actinopterygii). The other two infraclasses are Holostei who show some primitive characteristics and Chondrostei which are primarily cartilaginous fish showing signs of laying down new bone material.

Figure 4.7 is a comparison between the hotel load of several AUVs and the base metabolism of numerous BMSs. The regression lines (empirical formulas) mentioned in Table 4.1 are also plotted on the graph.

The regression line proposed by Clarke & Johnston, 1999 for teleost fish shows the least hotel loads for the Teleosts. However, the findings of this research showed that eels have the lowest hotel load regression line at small masses (less than 0.5 kg). The regression line estimated for teleost fish in this research is higher than the one in the literature. This could be due to normalising data from other temperatures to 20°C, however the teleost fish data points from literature are all placed above the Clarke & Johnston line and some fit very well with the regression line proposed by this research. One reason for this is that similar to marine mammals, satisfying all the prerequisites for a BMR test is not always fully possible. For salmons (Salmonoids) as they are high fatty

fish different hotel load regression line was estimated in this research which is slightly less but close to the one predicted in literature with the same trend. The regression lines for turtles and the humboldt penguin are very close to the one predicted for teleost fish in this research. Marine mammals have the highest hotel load up to 100 kg body mass. AUVs have hotel loads between the salmons regression lines and marine mammals, and size wise they are close to marine mammals. However, most of them have less hotel load than marine mammals and a data for a glider shows very low hotel load, close to the eels regression line. The data points of the penguins sit higher than the regression line proposed by Luna-Jorquera & Culik, this may be due to the fact that only one species of penguin was tested in their research work.

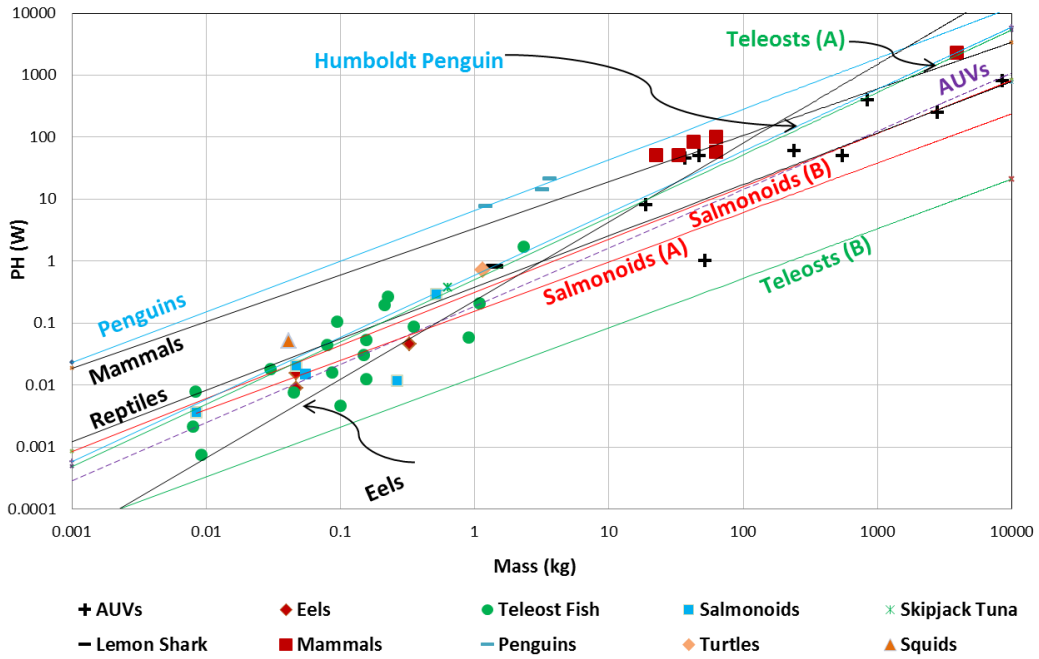

Figure 4.7. Hotel load as a function of mass for various BMSs and AUVs. Where there are two regression lines, those named (A) are from this research and those named (B) are from literature

As it is clear by Table 4.1, hotel load for all BMSs is not available. However, very close regression lines for various BMSs shows that with the regression lines already available, the hotel load for other BMSs can be estimated. For example the only data available for sharks, the lemon shark (*Negaprion brevirostris*) (average value of hotel load measured from several O_2 consumption data from seven Lemon Sharks of similar size from Scharold & Gruber, 1991) sits right on the regression line predicted for teleosts in this research.

All these regression lines are drawn assuming there is no size limit for all classes of BMSs. However, different classes of BMSs have different size range. Figure 4.7.1 is a modified plot of Figure 4.7, only showing regression lines within the range were the class of BMSs actually exist.

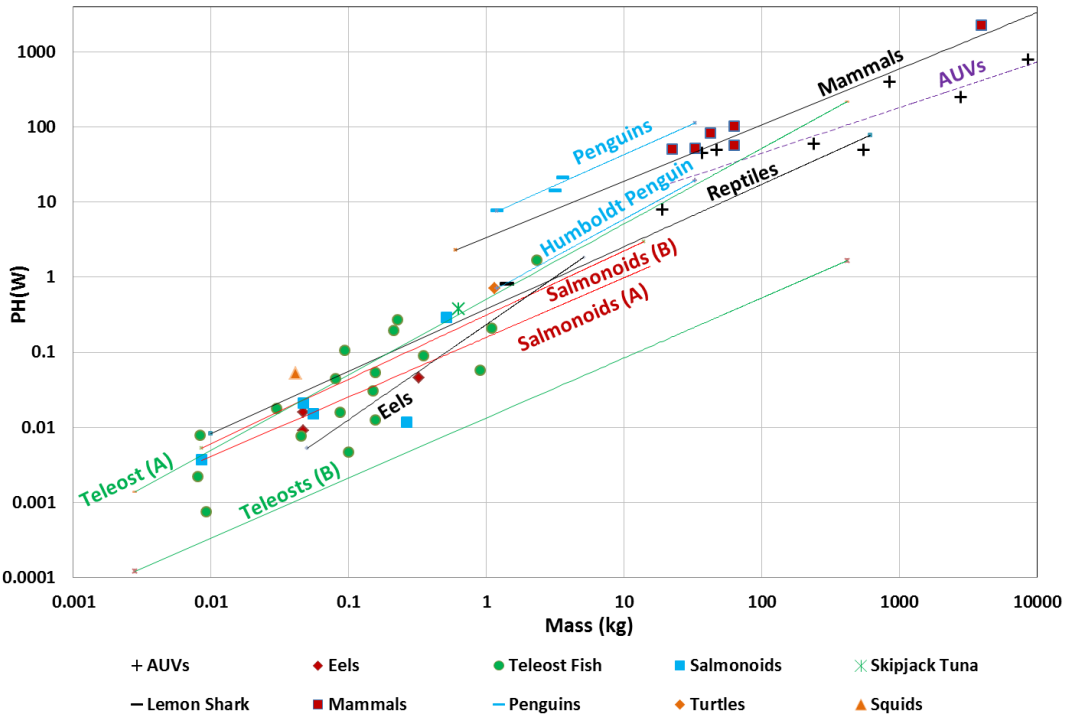

Figure 4.7.1 Hotel load as a function of mass for various BMSs and AUVs with regression lines only extended within the size range of each group of BMSs. Where there are two regression lines, those named (A) are from this research and those named (B) are from literature

Note that the size range is gathered from the 318 BMSs data within the database of this research.

Figure 4.7.1 shows that in reality all BMSs only exist in masses ranges less than a tonne except for marine mammals and sharks for which regression line is not available. AUVs hotel load falls between those of marine mammals and turtles. Another interesting data is the tuna, which despite showing endothermic characteristics has a hotel load which is in-line with other teleost fish.

AUVs regression line falls between reptiles and marine mammals. Marine mammals are expected to have high hotel loads as they are endotherms and as most of them are negatively buoyant, they consume energy not to sink. This is done by using their side fins to produce lift. AUVs are also required to control their buoyancy as they are positively buoyant while turtles (representing reptiles) alter the air volume in their lungs to keep neutrally buoyant (Peterson & Gomez, 2008). It is interesting that marine

mammals consume more non propulsive energy than AUVs, considering that especially survey class AUVs can be very sensor intensive. More detailed research is required to find the reason behind marine mammals high hotel load, whether it is in fact due to thermo regulation or other unaccounted stress during measurement.

In order to compare mass specific hotel load for BMSs and AUVs, the data and regression lines are plotted in Figure 4.8.

Except for the regression line for eels and the one proposed for teleost fish in this study, the rest of the regression lines suggest that mass specific hotel load decreases with size. The data set gathered in this research to draw the regression line for fish, included large fish with relatively high hotel load. The reason for this behaviour is not clear. However, the data points plotted on the graph do in fact agree with the trend. The lemon shark is again on the regression line for teleost fish. The data points for salmonoids show very different relative hotel loads in these fish which are genetically very close to one another, which proves that unless the test environment is exactly similar the resulting hotel load will be different to some extent. As the salmonoids data points fit between the data points of other teleosts, it is possible to use the regression lines of teleost for salmonoids as well.

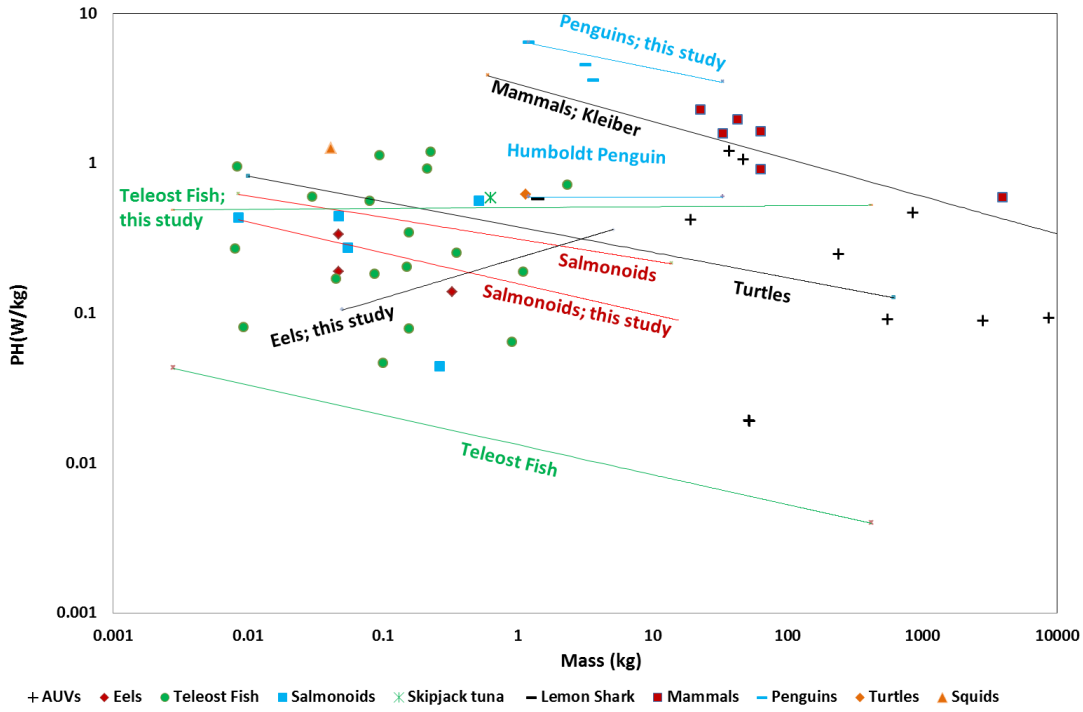

Figure 4.8. Mass specific hotel load for BMSs and AUVs

4.2.2 Propulsion power

Propulsive Cost Of Transport or net Cost Of Transport(COT_{net}) refers to energy required for the locomotion of a system. Therefore propulsion power is the corresponding power to the COT_{net}. Therefore total power required for a system is calculated as:

$$Power_{Total}(P_T) = Power_{Hotel}(P_H) + Propulsive_{power}(P_P) \quad 4.14$$

If hotel load or hotel power and the total power are known, the propulsion power is calculated as:

$$P_P = P_T - P_H \quad 4.15$$

It is also known that energy is power multiplied by time, so:

$$COT_{Total} = \frac{P_H + P_P}{\{Mass\} \times U} \quad 4.16$$

Where *U* the swimming/locomotive speed of the system. Therefore:

$$COT_{Net} = COT_{Total} - \frac{P_H}{\{Mass\} \times U} \quad 4.17$$

Based on the definition given in Sections 1 and 2 of this chapter, various components of the *COT* can be plotted typically as in Figure 4.9.

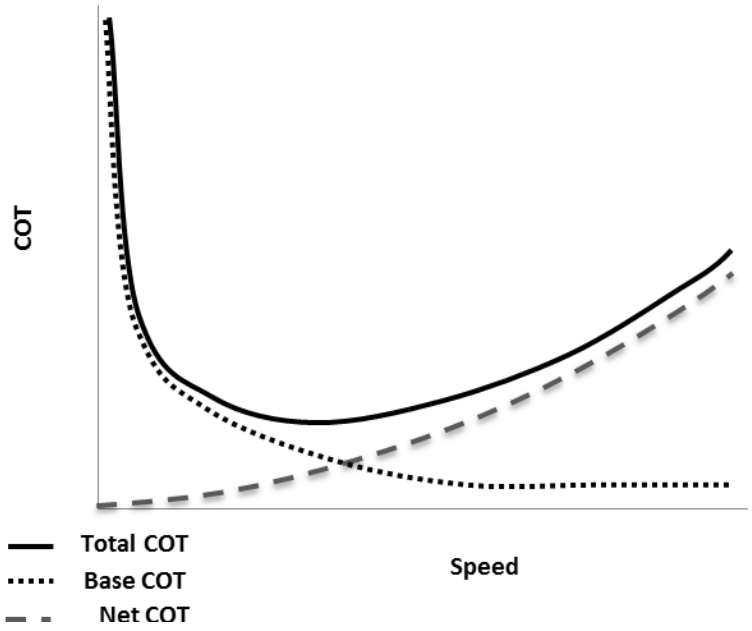

Figure 4.9. Total *COT*, base *COT* corresponding to Hotel load (P_H) and net *COT* corresponding to propulsion power and as a function of absolute speed [m/s]

Figure 4.10 and 4.11 illustrated the propulsion power and mass specific propulsion power of several BMSs and AUVs at their optimum speed. These values are estimated by using Equations 4.15 and 4.16 for the BMSs and AUVs for which the data was available.

It is clear that the range of operation for BMSs is significantly larger compared to AUVs. Gliders have propulsion powers very close to or less than 1 *Watt* while other AUVs operating at Reynolds numbers within the range of Marine Mammals, have similar propulsion powers to smaller marine mammals (the Harbour Seal). Fish operating at lower Reynolds ranges have considerably less propulsion power. However, when looking at mass specific propulsion power, most AUVs have required propulsion power less than 0.5 $\left[\frac{W}{kg}\right]$ similar to the silver eel. Note that the dotted line in Figure 4.10 shows the minimum *Re* for AUVs in the figure. Therefore, direct comparison between the propulsion power of AUVs and BMSs at *Re* less than 4.3×10^5 was not available.

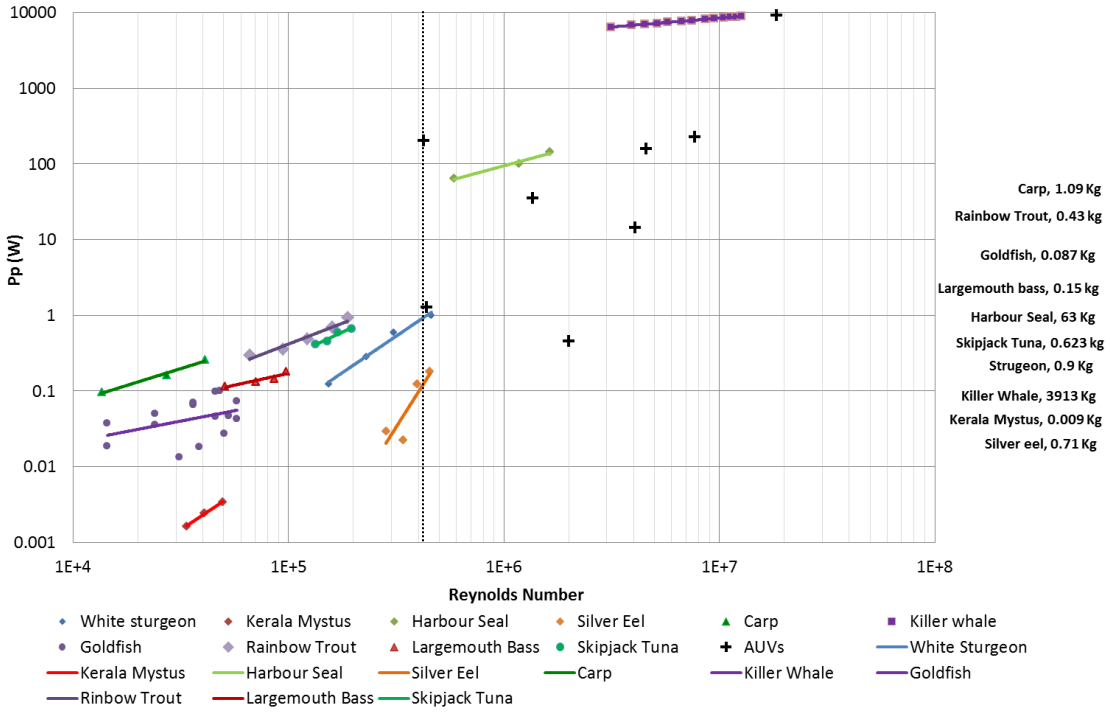

Figure 4.10. The propulsion power of various BMSs and AUVs at their Reynolds Numbers. The dotted line is the lowest *Re* (4.3×10^5) for the AUVs in the plot

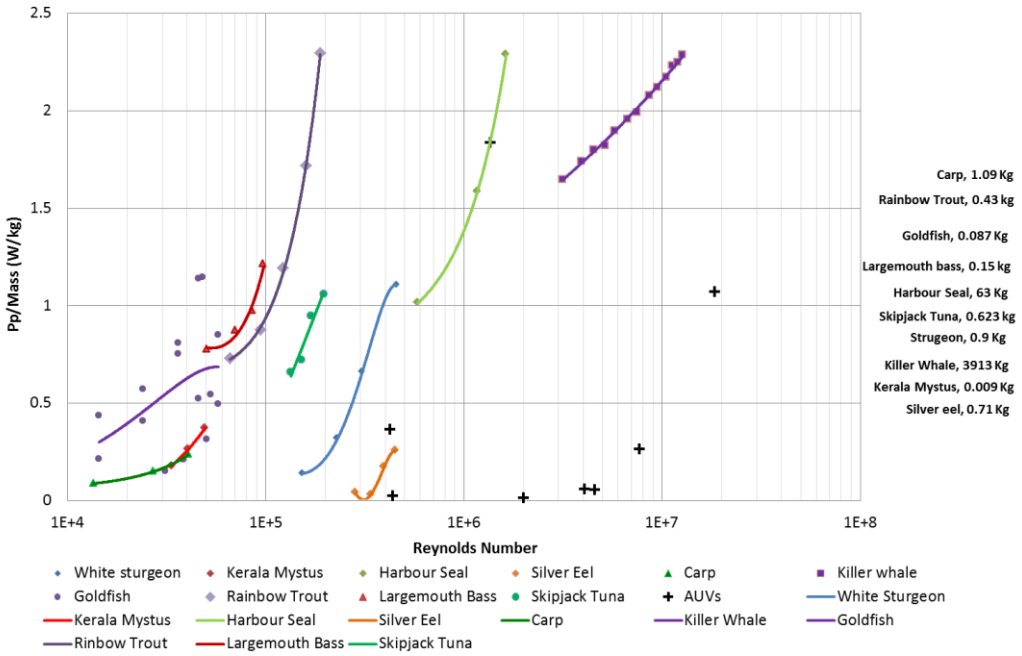

Figure 4.11. The mass specific propulsion power of various BMSs and AUVs at their *Re*

If both propulsive and non-propulsive components of the energetic cost are known, the COT_{Total} and corresponding power required can be calculated. Estimation of hotel load was discussed in Section 4.2.1. In order to calculate the propulsive cost for AUVs, many factors such as the thrust coefficient (k_T), torque coefficient(k_Q), the advance coefficient (J) and hull efficiency must be provided by the manufacturer (Lewis, 1989). For BMSs the propulsion power or propulsive energetics required for swimming is affected by several factors. Similar to AUVs (Allen et al., 2000), the propulsion power of BMSs varies due to their morphology, physiology and swimming/propulsion mode which clearly results in different propulsive efficiencies. However, as explained by Hammer, 1995 and Lighthill, 1969, their propulsive energetics is also affected by the environment in which they swim. This includes the characteristics of the water, the level of stress, etc. Therefore calculating the propulsion power for a BMS is not straight forward. However, as explained in Section 4.1 when total *COT* cannot be measured directly, using Equation 4.16 is the way to estimate *COT*. Considering every characteristics of water and the environment and the alteration of propulsion power as a consequence is very complicated and requires a separate research to be performed. The main factors affecting P_P are body characteristics (morphology and physiology) and swimming mode, therefore efficiency. These have been investigated in this research for different BMSs and as a result power and energetics estimated. This is thoroughly explained in Chapter 5.

4.3 Range and endurance

Endurance and range are both corresponded with the capability of a vehicle to operate with fixed amount of fuel on-board. Endurance is the time of operation, or it the case of BMSs, the time which they can swim and stay alive without feeding. Range is the distance which they can swim at the above condition.

Sometimes endurance or range are not defined as direct mission criteria and simply materialise when considering the scope of an operation. For example, inspecting pipelines does not have endurance as mission criteria; however it would be desirable if the vehicle is able to perform the operation completely before requiring a battery charge. For some missions though, endurance or range are direct criteria. For example a vehicle might be required to move to a certain point, perform a mission and return. Therefore, being able to estimate the endurance or range of vehicles is vital and clearly a vehicle with higher endurance is desirable, that is if the energetic cost is in the acceptable range. This is an example of trade-offs between various characteristics and capabilities of a vehicle which forces an AUV user to decide between two different vehicles. Considering these trade-offs and making a decision on the selection of a vehicle has been investigated extensively in this research and explained in Chapter 7.

Based on the description given in this section, endurance and range depend on the energy consumption, size, speed and also the reserved energy on the vehicle. This reserved energy is provided by batteries for AUVs. Conventional AUVs have a finite amount of energy stored (battery) on-board. Therefore, range is inversely proportional to *COT*. For AUVs, maximum endurance is gathered mainly through the data sheet provided by the manufacturer and occasionally from literature and personal communication. As such there is an unknown level of uncertainty in the accuracy of the results. By knowing the endurance and economic speed of the vehicle, the maximum range can be calculated as:

$$Range_{max}[km] = U_{eco}\left[\frac{m}{s}\right] \times Endurance\ [h] \times 3600\left[\frac{s}{h}\right] \times 0.001\left[\frac{km}{m}\right] \qquad 4.18$$

For marine animals, range is a challenging parameter to define as many species do not travel long distances without feeding. For BMSs the reserved energy usually exists in terms of body fat which is consumed when food is not readily available. Therefore in this research, the lipids and fatty acids stored in the body of BMSs are considered as

correspondence to the battery capacity in AUVs. These, when combined with known *COT* and swimming speed, provide a measure of endurance for BMSs.

It was mentioned that endurance is measured between two fuel recharges. This means that for BMSs it must be measured when the BMS is not eating and solely spending the reserved body fat. Some of the long migrating BMSs such as the sperm whales or eels do not eat during their long (~5000 km) migration and purely rely on their body reserves. However, most BMSs eat frequently to compensate for their energy loss during daily activities. One method of calculating the endurance of BMSs is by considering the eating pattern of all BMSs. In this research an alternative method was proposed. To estimate the maximum range or endurance of each BMS, it was assumed that the animals do not refuel and consume all the reserved fat while swimming at their optimum speed. This means that the total fat was considered as the total available fuel. Therefore, the maximum range is achieved when all the body fat is consumed. Consideration need to be made that in reality the animal will die when the fat reserve is very low and this calculation is carried out for the purpose of comparing different BMSs. One other consideration is that the studies have shown that BMSs also rely on their body protein to metabolise and provide energy to some extent (Palstra & Trillart, 2010). However this amount is not as significant as the energy produced by metabolised fat. For Example, in Plaice (*Pleuronectes platessa L.),* the amount of metabolised protein in only 10% of that of fat at the same time (Dawson & Grimm, 1980), bearing in mind that protein produces less energy. Furthermore, in this research as the muscle (protein) is considered as the motor of the BMS body, the energy is based solely on metabolised fat. As explained in Chapter 2, for some BMSs such as marine mammals, fat or lipids are easily distinguishable as they are in form of blubber.

However, for some BMSs especially most fish, fat is mixed with muscle fibres within the flesh and there is also fat in the skin. Although skin has fat, it does not get metabolised as this will make the body of the species vulnerable. Therefore only fat within the flesh is considered as burnable fat for the purpose of this research. Sharks have a concentration of fat in their liver. Between 40.6% of the liver mass of the silky shark is fat, while the liver mass is about 5.7% of the body mass. This average value of 2.3% of body mass extra fat is therefore added to the burnable fat in the body of sharks (values averaged from data measured by Navarro-Garcia et al., 2000). Fat tissue percentage is not available for all BMSs and therefore for BMSs the percentage of fat tissue is estimated based on the data available for genetically similar BMSs.

If the calorific value of BMSs fat is known, by knowing the amount of fat of the BMS, assuming it will not eat while swimming, the energy storage corresponding to that of the batteries in AUVs is calculated as:

$$Stored\ Energy\ [kWh] = \frac{\{Mass\}_{fat}[kg] \times E_{fat}\ \left[\frac{kJ}{kg}\right]}{3600\left[\frac{s}{h}\right]} \quad 4.19$$

Where E is the specific energy.

Therefore the maximum endurance at optimum speed can be calculated as below:

$$Endurance_{max}[h] = \frac{Stored\ Energy\ [kWh]}{COT_{Opt}\left[\frac{J}{kg.m}\right] \times U_{Opt}\left[\frac{m}{s}\right] \times \{Mass\}\ [kg]} \times 1000\left[\frac{W}{kW}\right] \quad 4.20$$

To use Equations 4.19 and 4.20 the E_{fat} must be known. Data on various sources of energy for both BMSs and AUVs is present in the literature and is listed in Table 4.2. As part of this research, the blubber of the two marine mammals mentioned in Chapter 2 was also tested to estimate their specific calorific value. The reason to perform the test was because both juvenile species were stranded and especially the white beaked dolphin suffered severe mal-nutrition. As a result of this the blubber had changed in texture in both cases. The texture was rubbery instead of jelly and colour had changed as well. Therefore due to this as well as the species being juveniles, there was the assumption that the resulting specific energy might have been less than one of a healthy adult animal. And this test must have been done to observe whether this does in fact occur. Blubber samples were taken from the middle body part of both the white beaked dolphin and the grey seal and were tested in the calorimeter.

Table 4.2. Comparison of the specific energy of various sources of energy storage for both biological and engineered systems. Shaded rows correspond to biological energy stores

Energy Storage Type	Used in	Specific Energy (MJ/kg)	Reference
Fish Oil (Cod Liver Oil)	BMSs	39.45	Liversey & Elia, 1988
Bowhead whale (*Balaena mysticetus*) subcutaneous fat (Blubber)	BMSs	36.4	US. Department of Agriculture, 2010
Grey seal (*Halichoerus grypus*) blubber	BMSs	32.7	This research
White beaked dolphin (*Lagenorhynchus albirostris*) blubber	BMSs	31.9	This research
PEM fuel cell	AUVs (Urashima)	~ 1.44	Griffiths, 2005
Lithium Polymer Battery	AUVs	0.70[1]	Griffiths, 2005
Lithium solid polymer Battery	AUVs (Autosub6000)	0.47-0.68	Griffiths, 2003
Lithium Ion Battery	AUVs[2]	0.324 -0.54	Griffiths, 2003
Mn Alkaline Battery	AUVs (seahorse II)	0.21-0.46[1]	Griffiths, 2005
Nickel Metal hydride (Ni-MH)	AUVs	0.28	Huggins, 2010
Sealed Lead-Acid Battery	AUVs (ALIVE)	0.07-0.11	Griffiths, 2003

[1]values calculated from data in literature

[2]Most common source of energy for AUVs

It is shown in Table 4.2 that the specific energy for the blubber and fish oil is more than 30 $\left[\frac{MJ}{Kg}\right]$. The blubbers tested in this research did produce 10%-15% less energy compared the value for bowhead whale in literature which suggests that at lowest quality, the blubber will still produce more than 30 $\left[\frac{MJ}{Kg}\right]$ of energy. When compared to batteries such as those used in AUVs (e.g. Lithium Polymer, 0.70$\left[\frac{MJ}{Kg}\right]$), or even the fuel cell used in Urashima, 1.44$\left[\frac{MJ}{Kg}\right]$, it becomes apparent that BMSs store and consume a high quality fuel. BMSs fuel has about 40 times more specific energy.

In order to have an understanding regarding the energy available to various BMSs and AUVs, the available energy content (or battery rating as it is called for AUVs) per kilogram of body mass [kWh/kg] has been plotted against the total body length for AUVs and BMSs in Figure 4.12. The battery rating for AUVs has been obtained from manufacturer's data or calculated from other data available by the manufacturer. For BMSs where the mass of fat tissue is known by assuming an average specific energy of 35 $\left[\frac{MJ}{kg}\right]$ for fat, the energy store is calculated from Equation 4.19 and divided by the body mass to obtain the mass specific energy content.

As illustrated in Figure 4.12, the mass specific energy content available to BMSs compared to similar length AUVs could be about 100 times higher. As explained the high specific energy of fat compared to the battery used in AUVs has a significant effect on the available energy for BMSs. Therefore, BMSs can benefit from higher endurance or can afford to use part of this energy to increase their speed.

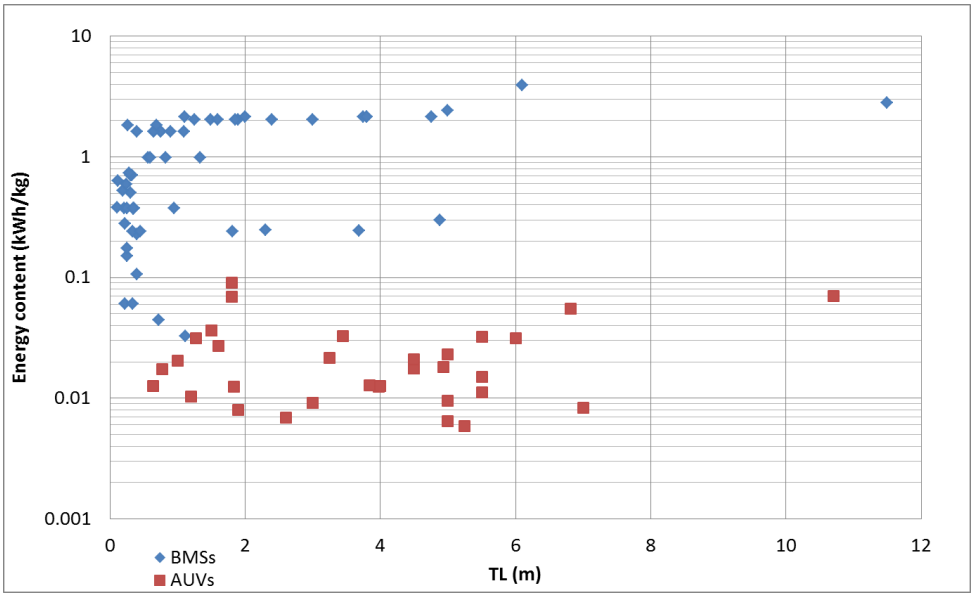

Figure 4.12. Mass specific energy content vs. total length for BMSs and AUVs. The graph is plotted for body lengths less than 12m where the AUVs within the database exist at.

By having an estimate of BMSs fat, the endurance $[h]$ can be calculated for BMSs. Endurance of several BMSs and AUVs are shown against length specific speed $\left[\frac{TL}{s}\right]$ in Figure 4.13. The size of the circle is an indication of the value of *COT*. It is evident by the plot that BMSs have significant higher endurance compared to AUVs. However, as stated before, their *COT* is generally higher. Two gliders, the Spray and the Seaglider have endurance over 1000 *h* with relatively small *COT*. However their speed is less than 0.2 $\left[\frac{TL}{s}\right]$ while BMSs have endurance higher than all conventional AUVs at length specific speeds higher than 3 $\left[\frac{TL}{s}\right]$.

Silver eel has the highest endurance of 11267 *h* or 15.6 months at the speed of 0.5 $\left[\frac{TL}{s}\right]$. Although, the African penguin with the fastest length specific speed of 3.07 $\left[\frac{TL}{s}\right]$, has an endurance of only 52 *h* with a very high *COT* of 15.5 $\left[\frac{J}{kg.m}\right]$ (as expected as Penguins do have comparatively high *COT*) and closely following is the sockeye salmon with a speed of 2.8$\left[\frac{TL}{s}\right]$ with 479 *h* of endurance at 3.92 $\left[\frac{J}{kg.m}\right]$. The

COT of most BMSs are higher than those of most AUVs as to be expected as the BMSs operate at a higher speed. Grey whale (*Eschrichtius robustus*) and sperm whale (*Physeter macrocephalus*) with endurance higher than 1000 *h* sit very close to gliders. However, their *COT* is higher than those of gliders. Sperm whales are migrating marine mammals and swim about 5000 *km*, while consuming the large energy storage in the form of blubber during long migrations.

Therefore, size is an important factor for marine mammals in order to store the required energy content. However, silver eels that also use their stored energy during migration, have marginally lower *COT* which reduces the amount of energy usage.

Details of eel migration still remain unknown till date. However, an interesting research by Aarestruo et al, 2009, tagging European eels (*Anguilla anguilla*) migrating from Europe to the Sargasso Sea has discovered that when swimming with the current, silver eels use the water current instead of swimming to go forward. This minimises their *COT* and increases their speed. One might suggest that this could mean the eels' *COT* is not as low as estimated. However, same research has discovered that as part of their journey, the eels swim against the current which can reduce their average daily speed to about 39%. Moreover, the research shows that eels also perform vertical migration in the water column during the day as well. Therefore, until more detailed information on the eels' migration becomes available, it can be inferred that in average the *COT* estimated for eels in present research is a good estimate which needs to be considered with the above notes bore in mind.

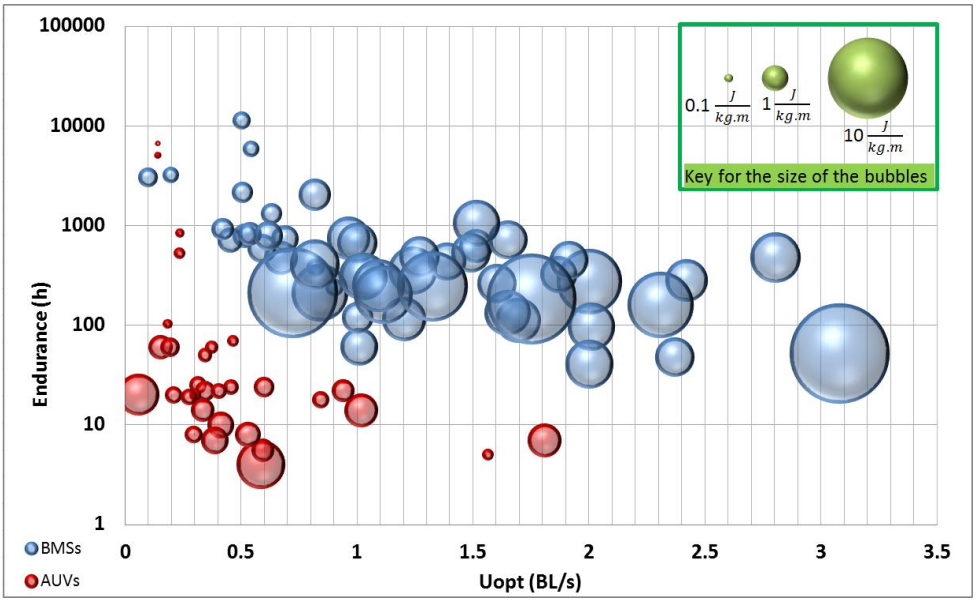

Figure 4.13. Endurance as a function of length specific speed for BMSs (blue circles) and AUVs (red circles)

4.4 Conclusion

In this chapter methods of gathering energetic cost data for BMSs and AUVs have been discussed and methods presented estimate the hotel load and propulsion power for BMSs to be compared with those of AUVs. The *COT*, propulsion power and hotel load of BMSs and AUVs have been compared. This shows that AUVs especially gliders have generally less *COT* compared to most BMSs. As there are no data for AUVs at Reynolds numbers less than 4.3×10^5, a cross comparison between AUVs and BMSs at lower Reynolds numbers was not possible. However, by comparing AUVs with BMSs within similar Reynolds number range, it was realised that AUVs had almost similar absolute propulsion power to BMSs with similar *Re*. However the mass specific propulsion power as well as hotel load of AUVs were lower compared to those of the BMSs. This explains their lower *COT*.

BMSs certainly have higher speed ranges and they benefit from high quality fuel.

In terms of endurance BMSs have definitely a significant superiority over AUVs. Although very few gliders have endurance higher than 1000*h* with very small *COT*, their speed is very low while BMSs have endurance higher than all conventional AUVs at length specific speeds higher than $3\left[\frac{TL}{s}\right]$. As discussed in Section 4.3, the mass specific energy content for BMSs could be as high as 100 times that of similar length AUV. This will result in higher endurance or if speed is crucial, part of this energy could be used towards increased cruising speed.

The energetics have been compared in this chapter, however to have an estimate of the efficiency of the systems, drag needs to be estimated for BMSs and compared with one another. This was carried out and explained in the next chapter, Chapter 5.

Chapter 5. Bio-Inspired Propulsion

In Chapter 4 the energetic costs and corresponding required powers for BMSs and AUVs were compared. When considering required propulsion power while comparing different systems, efficiency must also be considered. One objective of optimisation is to achieve higher system efficiency. To calculate efficiency, the drag of the system must be estimated.

The method for the estimation of drag for BMSs is discussed in this chapter. By having an estimate of drag, various efficiencies are defined for BMSs and estimated using energetics and drag. This is then followed by relevant discussion.

5.1 An estimate of the drag of BMSs

If an animal is physically available, it would be possible to measure its drag as done so in research works carried out by Webb, 1975 and Fish, 1998. Also research works such as those performed by, Anderson et al, 1997 and Read et al, 2002 have been looking into measuring forces and propulsive efficiencies on oscillating foils. These methods are useful for measuring the drag when the animal or the fins are available; this is not usually the case.

Therefore, having a method to be able to estimate the drag and therefore efficiency for comparison without the need for the actual animal was desirable. Therefore, a novel method for calculating drag and overall efficiency is presented in this research work. The method is explained next.

As shown in Equation 4.10 in Chapter 4, the energetic *COT* is the sum of hotel power and propulsion power divided by mass multiplied by speed. Propulsion power for AUVs and BMSs can be defined as:

$$P_P = \frac{D \times U}{\eta} \qquad 5.1$$

Where D is total drag of the AUV or the BMS while moving forward,

U is the forward speed,

η is the efficiency

As discussed in Chapter 3, the bare body of the BMSs has been associated with a tri-axial ellipsoid. However, in reality the body is not an exact tri-axial ellipsoid. Moreover, the bodies of different BMSs have different appendages which contribute to the drag. These are as follows:

- The top fin (s)
- The bottom fin (s)
- The side fins
- The rear fin (or twin fins if it is a BMS with feet)
- The gills (s)
- The eyes
- The long snout or the sword

Very few BMSs such as turtles, penguins and sea lions have small tails which can be considered as part of the tri-axial ellipsoid body. Therefore, in this research no extra drag is considered for tails.

Each of the above terms contribute to the total drag of the species however not all are present in all the BMSs.

Although the eyes contribute to the drag; their surface area in comparison to the bare body is very small. Therefore, as drag is directly proportional to the surface are, the contribution of the eyes to the total drag is very small and is calculated to be less than 1%. Therefore, although appreciating the existence of eyes' drag, the contribution can be considered insignificant. A similar consideration was made for the sword (long, thin snout) of some BMSs such as the swordfish (*Xiphias gladius*), the marlin (*Makaira indica*) or the sailfish (*Stiophorus platypterus*). The only exception is the hammerhead shark (*Sphyrna lewini*) for which the drag of the "hammer" is calculated as a flat plate as the surface are is significant.

As well as the body shape and appendages the roughness of the body skin mainly caused by hair attributes to the total drag as well. Finally, the BMS's bodies' are not still during swimming. Especially in BMSs that use their rear fin as the main source of propulsion, their body either yaws (e.g. in fish) or pitches (e.g. in marine mammals) during fin undulation. This affects the drag as well.

Therefore the total drag can be formulated as:

$$D_{Total} = \propto_{SR} (\propto_{TAE} D_{BB} + D_{TF} + D_{BF} + D_{SF} + D_{StF} + D_{RF} + D_G + D_S) \quad 5.2$$

Where each term is explained next:

$\propto_{SR}$is the factor of skin roughness. For majority of fish, the main body is covered with scales and for the rest such as the eels the body is slippery. For sharks, dolphins, whales and penguins the body surface is smooth in macroscopic levels. However, some marine mammals have hair on their body and some BMSs especially the larger ones, might have some smaller organisms stuck to their bodies, which will reduce the smoothness of the body surface. Measuring the skin roughness was not within the scope of this research, therefore the drag is measured without considering roughness. However, having the skin roughness will result in a more precise drag estimate.

$\propto_{TAE}$is the correction factor to compensate for the difference between the true shape of each BMS and a Tri-Axial Ellipsoid.

$D_{BB}$is the bare body drag of the BMS. As the bodies of BMSs are associated with tri-axial ellipsoid, D_{BB} is the drag of the corresponding tri-axial ellipsoid of the BMS.

D_{TF}, D_{BF}, D_{SF}, D_{StF} and D_{RF} are the drag of Top, Bottom, Side, Stabilising and Rear Fins respectively. In respect to the side fins, the drag might be less than the actual drag for some BMSs as measuring the actual chord of the fin from photos is not possible as the fin is usually not wide open.

D_G is the gills drag which is approximately 10% of the total drag at cruising speed (Videler, 1993), and

D_S is the snout drag.

In respect to each component in the drag formula some notes must be taken. In addition, the contribution of each component must be estimated. These are explained next.

There is another matter which can be both considered as correction factor or within the propulsive efficiency and that is considering the swimming mode. As explained in Section 5.1.2 in order to calculate drag, the body and the fins are considered static and the BMS gliding. However, this does not happen in reality and therefore means are required to account for different movements of BMSs mainly due to their swimming mode. In this research, the movement of BMSs for propulsion purpose is considered within the propulsive efficiency.

5.1.1 Adjusting the calculated drag for the BMSs

$\propto_{SR}$: The factor of skin roughness accounts for the skin roughness as well as the finlets in some BMSs such as the tuna (*Thunnus thynnus*). Similar to the eyes and the swords, the contribution of the finlets to the total drag is less than 0.5% and therefore not significant to be calculated as part of the total drag. Instead they are considered as part of the skin roughness.

$\propto_{TAE}$: As drag is calculated in general as:

$$D = 0.5\rho C_D A_{WS} U^2 \quad 5.3$$

Where C_D is the drag coefficient, A_{WS} is the wetted surface area and U is the speed, the $\propto_{TAE}$can be defined as:

$$\propto_{TAE} = \frac{A_{WS_{BMS}}}{A_{WS_{Tri-axial\ ellipsoid}}} \quad 5.4$$

For BMSs the actual area is unknown, however as area is volume to the power of 2/3 and volume is mass divided by density, by knowing the mass of the BMS and calculating the mass of the equivalent tri-axial ellipsoid, the $\propto_{TAE}$can be reformatted as:

$$\propto_{TAE} = \left(\frac{\{Mass\}_{BMS}}{\{Mass\}_{Tri-axial\ ellipsoid}}\right)^{\frac{2}{3}} \quad 5.5$$

5.2 Calculating components of the total drag

Two main drags which were calculated for BMSs were the bare body drag and the control surfaces (or fin) drag, both will be explained next.

5.2.1 Bare body drag

In engineering bare body drag, D_{BB}, is calculated as:

$$D_{BB} = 0.5\rho C_D A_{WS} U^2 \quad 5.6$$

Where:

C_D is the drag coefficient and A_{WS} is the wetted surface area and both must be estimated to calculate drag. As mentioned in Chapter 3, as part of this research it has been concluded that, for the purposes of providing sufficiently accurate drag estimates, BMSs body forms can be idealised using a tri-axial ellipsoid; from this wetted surface area and drag coefficient can be estimated.

Although no analytical formula is defined to calculate the surface area of a tri-axial ellipsoid, a number of approximation formulae exist and the one used in this research is the Knud-Thomsen formula (Michon, 2012) which estimates A_{WS} with less than 1% error.

The Knud-Thomsen formula for a BMS is:

$$A_{WS} = \pi \left(\frac{\left(EL(BW + BH)\right)^{1.6075} + (BW \times BH)^{1.6075}}{3} \right)^{\frac{1}{1.6075}} \quad 5.7$$

Where BW and BH are maximum body width and height and EL is the elliptical length. EL is used as the length of the main body, instead of total length, TL. This is because TL includes the rear fin.

The drag coefficient is in the form of $C_D = C_f(1 + k)$, where C_f is the friction coefficient and $(1 + k)$ is the form factor.

For turbulent flow (where vast majority of the vehicles and species studied in this research swim at) there are different methods to estimate C_f. These methods result in closely similar values. As an example, the C_f values calculated using the ITTC57 formula and the Prandtl-von Karman formula were compared in Figure 5.1. This figure shows that values from both methods are close especially at Re larger than 1×10^6. Thereore, in this research, C_f for vehicles was estimated using the Prandtl-von Karman formula, that is:

$$C_f = 0.072Re^{-0.2} \quad 5.8$$

This formula was also very useful when deriving Equation 5.19 which is explained later in this chapter.

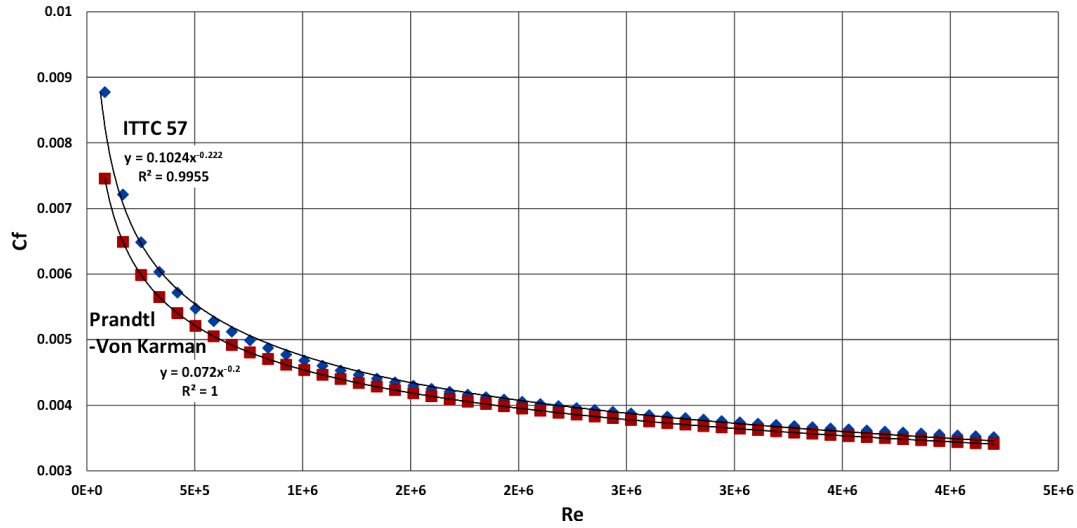

Figure 5.1. Comparing C_f values calculated using ITTC57 formula vs. Prandtl-von Karman formula

Where Re is the Reynolds Number and the kinematic viscosity is considered for sea water at 20℃ (ITTC, 2011) which is $\nu = 1.05 \times 10^{-6}\ \left[\frac{m^2}{s}\right]$.

The reason to consider water at 20℃ is because this is the standard temperature and therefore the temperature at which the oxygen consumption of BMSs has been corresponded to for comparison. It is appreciated that various BMSs live at different temperatures, but a unique temperature must be selected for comparison. Moreover, the kinematic viscosity changes for water temperatures between 0℃ and 50℃ which is greater than the range of temperature in the oceans, was published in ITTC, 2011. The kinematic viscosity ranges between 1.8×10^{-6} to $0.6 \times 10^{-6}\ \left[\frac{m^2}{s}\right]$. Considering its contribution to C_f which is to the power of 0.2 (i.e. $\nu^{0.2}$), this value will change between 0.07 and 0.06. Therefore, the difference in the kinematic viscosity is negligible for different temperatures of sea water.

The values obtained by using this formula were compared to examples tested in a Computational Fluid Dynamics (CFD) software and the results show less than 4% error.

The CFD analysis was performed by Dr. Alex B. Phillips, a collaborative party in the University of Southampton, based on conditions and characteristics requested by the author.

Hoerner, 1965 estimates the $(1 + k)$ value, for Spheroids:

$$1 + k = 1 + 1.5\left(\frac{BD}{EL}\right)^{\frac{3}{2}} + 7\left(\frac{BD}{EL}\right)^{3} \quad 5.9$$

where BD and EL are the diameter and length of the spheroid respectively.

As mention in Chapter 3, the equivalent diameter for a tri-axial ellipsoid can be calculated as $D_e = \sqrt{BH \times BW}$.

By substituting D_e for BD in Equation 5.9, the Form factor (1+k) was estimated for tri-axial ellipsoids. However, Horner, proposed the Equation 5.9 based on experiments on spheroid. Therefore to assure that the proposed formula would give acceptable results for a tri-axial ellipsoid, similar to the friction coefficient, samples were analysed in a CFD program. The results are shown in Figure 5.2. The two data points marked with a red cycle are spheroids ($BH/BW = 1$) and the other two data points are tri-axial ellipsoids with a $BH/BW = 5$. As illustrated in Figure 5.2, there is a close agreement between the k values of the two sets of data, which corresponds to the fineness ratio of the body and not the BH/BW values.

Therefore, results from Hoerner, 1965 formula are valid estimates of the form factor for a tri-axial ellipsoid.

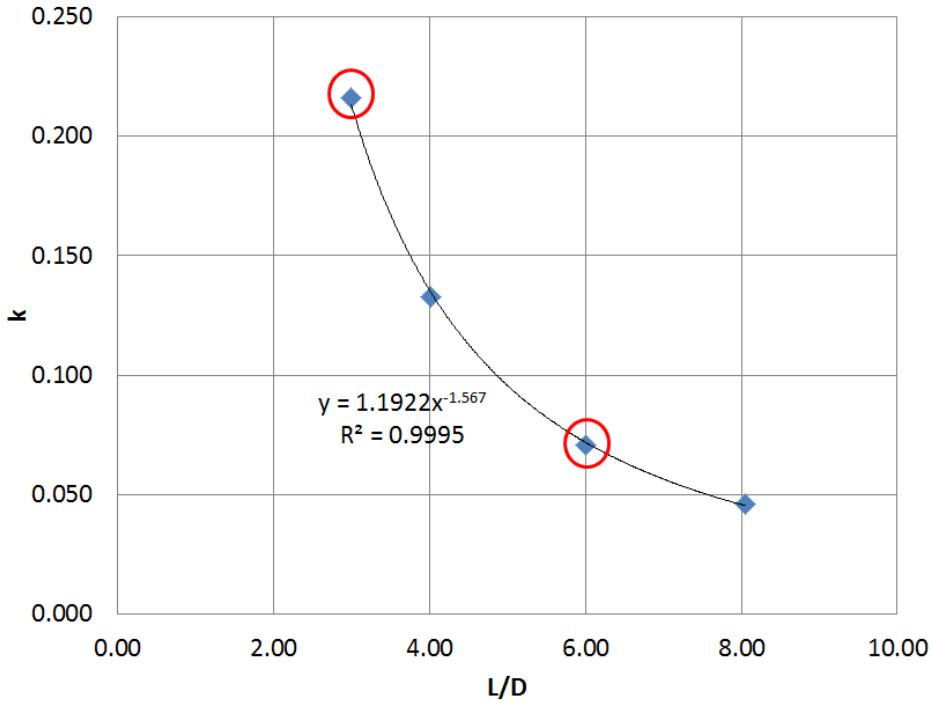

Figure 5.2. CFD results of the k value for spheroids and tri-axial Ellipsoids

5.2.2 Control surfaces (or fin) drag

In respect to fin drag, few considerations were made in order to calculate the drag and power. All fins are considered static (not moving). This is not true for BMSs as they tend to move their fins irregularly to steer themselves on their direct path. Therefore the sweep angle of the fin as well as the angle of attack changes continuously. However, considering the movements of different fins for each BMS and including that in the drag model requires a considerable extra amount of research work which is worthy of consideration for multiple future research projects in this field.

The span of the fin is measured as the projected length of the fin perpendicular to the flow when the BMS has the fin wide open. In some BMSs the surface area of the rear and the side fins shrinks while fast forward swimming to minimise drag however, in this research the size of the fins are considered non-changing. This is due to the fact that the amount of size change is different for each species and for different speeds therefore it is unclear from the collected data whether the fins have been opened or closed. An exaggerated example of this phenomena are seals which close their rear fin while gliding forward and open them completely when propelling. This will give them highest propulsion and less drag.

There are two simplifications made in this project to calculate the drag of the control surface of the BMSs body. Both of the simplifications are explained next.

1. Control surfaces of the BMS are considered thin flat plates. Although, only for fish the control surfaces are truly thin plates, measurements from the dissected white beaked dolphin (*Lagenorhynchus albirostris*) showed that the maximum thickness of the control surfaces to the span were about 5% for the fluke (rear fin) and about 10% for the dorsal fin (top fin). Therefore, considering that the data on the sections of the control surfaces of all BMSs is not widely available, all the control surfaces are considered thin plates. As for the wetted surface area of the fins (control surfaces), they are measured from photograph and videos of the BMSs and therefore the wetted surface area of the fins are in fact twice the surface area measure from photos.

2. The control surfaces are considered parallel to the flow, the movement of each fin not affecting the other as this would be different from species to species and taking into account the movements of each fin was not in the scope of this project.

The control surfaces of BMSs are: The rear fin, the top fin (could be absent or more than one in some BMSs), bottom fin (could be absent or more than one in some BMSs), side fins (in pair) and stabilising fins (in pair; could be absent in some BMSs).

Taking into account the considerations and simplifications the drag of the fins of each BMS is measured as:

$$D_{Contorl\ surfaces} = \sum^{All\ contorl\ surfaces} 0.5\rho C_{f_{fin}} A_{fin} U^2 \quad 5.10$$

Where U is the speed of the BMS, A_{fin} is the surface area of the fin and C_f is calculated from the Prandtl-von Karman formula as per Equation 5.8, where $Re_{fin} = \frac{U \times \{Chord\}_{fin}}{\nu}$

At this point all the components of drag are explained. Therefore by substituting Equation 5.1 in Equation 4.10:

$$COT = \frac{P_H}{MU} + \frac{D_{Total}}{\xi M} \quad 5.11$$

where M is the mass,

U is the speed,

D_{Total} is the Total drag,

P_H is the hotel load, and

$$\xi = \frac{\eta_{Total}}{c} \quad 5.12$$

where η_{Total} is the total efficiency and

c is a factor which accounts for the possible aspects of drag which could not be modelled such as the surface roughness. If the correction factor, *c*, can be assumed very close to 1 (if the skin roughness and other drag affecting terms are negligible) the total efficiency is calculated from Equation 5.12.

It is evident from literature that the definition of total efficiency is inconsistent when applied to BMSs and in some cases unclear; therefore to elaborate further on the definition of η_{Total}, this is given special treatment in the next section.

5.3 Definition of efficiency

This section provides a detailed explanation of propulsion energy usage for BMSs and AUVs. This is to resolve the issue of inconsistent and unclear definitions and use of propulsive efficiency when applied to BMSs. This leads to a clear and consistent definition of propulsive efficiency.

Batteries are the energy store of AUVs which correspond to food and fat for marine animals. As energy flows from the battery to eventually move the vehicle forward, some energy losses occur from the system. Figure 5.3a illustrates the flow of power and efficiency relationships in an AUV propulsion system and Figure 5.3b is the equivalent concept presented for a BMS. Table 5.1 provides explanatory notes to Figure 5.3.

From the descriptions in Table 5.1, it is realised that the total efficiency for BMSs, η_{Total}, is:

$$\eta_{Total} = \frac{DU_{BMS}}{P_M} \tag{5.13}$$

Where D is the drag,

U_{BMS} is the BMS speed and

P_M is the Muscle power. In Chapter 4 this term was called propulsion power to be distinguished from the hotel power, however from an engineering perspective; this power is in fact the equivalent of brake power in motors which is the muscle power.

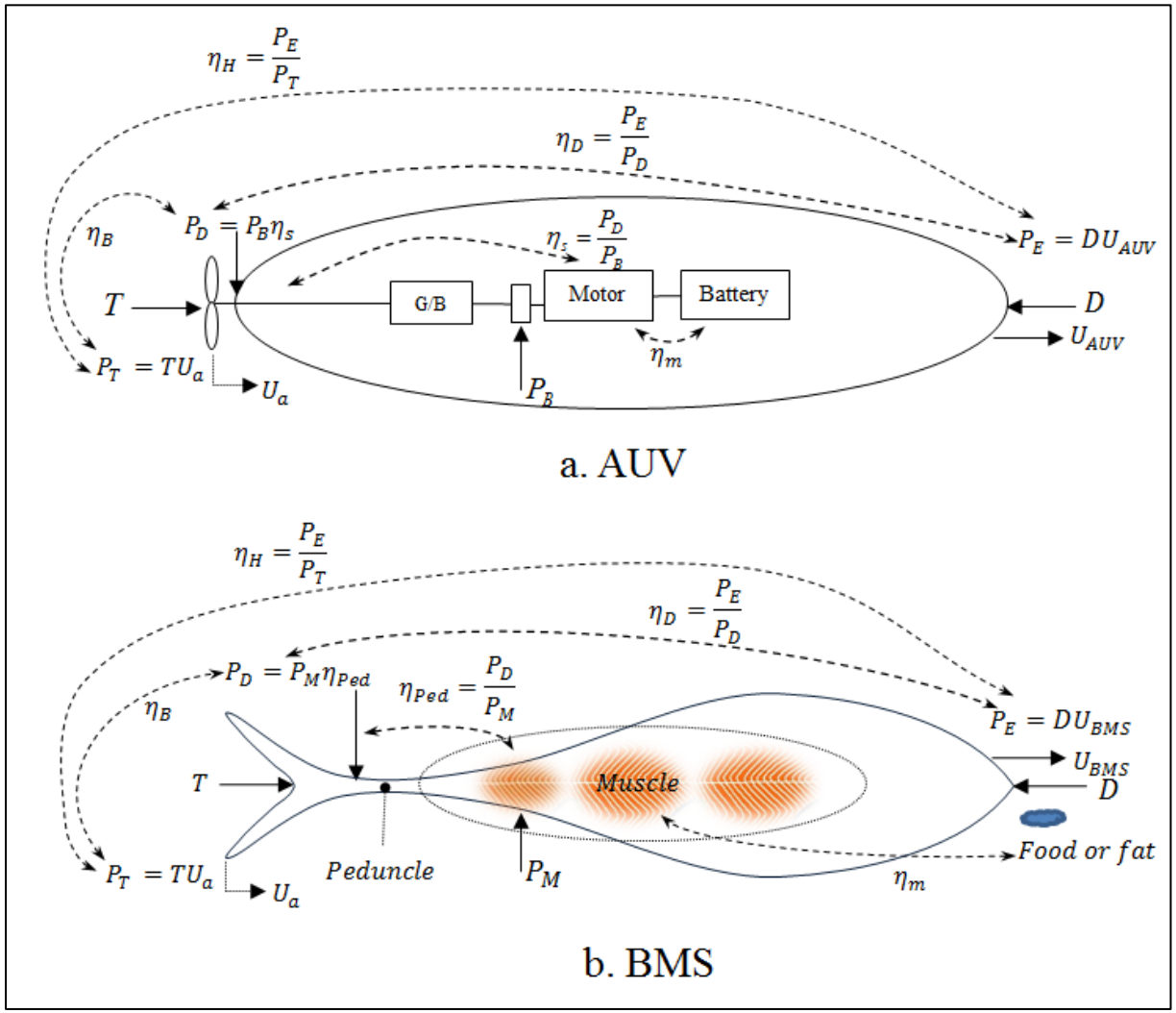

Figure 5.3. Comparison of power delivery in engineered vehicles and BMSs. Explaining notes to this figure are presented in Table 5.1

Table 5.1. Explanatory Notes To The Power Transitions And Efficiencies Illustrated In Figure 5.3

Process in AUV	**Corresponding Process in BMS**
Energy is lost when electrical energy is transferred to the motor from the batteries for operating the motor.	Energy loss when the energy obtained from food and fat are transferred to the muscle for operating the muscles.(1)
In this research the efficiency associated with this this energy loss is called the motor efficiency, η_m	The efficiency associated with this energy loss is the muscle efficiency, η_m
Energy is lost from friction when it is transferred through the drive chain to the propulsor.	Energy loss when energy is transferred from the muscle to the tail through the peduncle.(2)
The efficiency associated with this energy loss is known as the transmission, or shaft efficiency, η_s. $$\eta_s = \frac{P_D}{P_B}$$ Where P_D is the delivered power to the propeller and P_B is the brake power from the motor	The efficiency associated with this energy loss is the peduncle efficiency, η_{Ped}. $$\eta_{Ped} = \frac{P_D}{P_M}$$ Where P_D is the delivered power to the rear fin (the tail) and P_M is the muscle power
Energy is lost due to the propeller working in the flow field behind the AUV. In the desipline of naval architecture this is usually considered in two parts, namely with the propeller operating in the so-called open water condition with another adjustment for the effect of the wake behind the vehicle (Lewis, 1989)	Energy is lost due to the tail working in the flow field behind the BMS.
The efficiency associated with this energy loss is known as the "behind efficiency", η_B. $$\eta_B = \frac{P_T}{P_D}$$ Where P_T is the thrust power and is calculated as: $$P_T = TU_a$$ Where T is the thrust and U_a is the advance speed	In this research the efficiency associated with this energy loss is called the behind efficiency, η_B. $$\eta_B = \frac{P_T}{P_D}$$ Where P_T is the thrust power and is calculated as: $$P_T = TU_a$$ Where T is the thrust and U_a is the advance speed Note that T for a flapping tail is the mean net thrust derived over a complete oscillation.

Continued…

Continued from previous page…

Process in AUV	**Corresponding Process in BMS**
There is a difference between the power developped at the propeller as compared to the effective power of the AUV overcoming drag at a given AUV speed.	There is a difference between the power developped at the tail compared to the effective power of the BMS overcoming drag at a given speed.
This power loss is referred as the hull efficiency, η_H. $$\eta_H = \frac{P_E}{P_T}$$ Where P_E is the effective power and is calculated as: $$P_E = DU_{AUV}$$	This power loss can be referred to as the hull or BMS body efficiency, η_H. $$\eta_H = \frac{P_E}{P_T}$$ Where P_E is the effective power and is calculated as: $$P_E = DU_{BMS}$$
From the explanations given above:	
$$\eta_{Total} = \eta_m \times \eta_s \times \eta_B \times \eta_H$$ and in fact: $$\eta_B \times \eta_H = \eta_D = \frac{P_E}{P_D}$$ Where η_D is the delivered efficiency, therefore: $$\eta_{Total} = \eta_m \times \eta_s \times \eta_D = \frac{P_E}{P_B} = \frac{DU_{AUV}}{P_B}$$	$$\eta_{Total} = \eta_m \times \eta_{Ped} \times \eta_B \times \eta_H$$ and in fact: $$\eta_B \times \eta_H = \eta_D = \frac{P_E}{P_D}$$ Where η_D is the delivered efficiency, therefore: $$\eta_{Total} = \eta_m \times \eta_{Ped} \times \eta_D = \frac{P_E}{P_M} = \frac{DU_{BMS}}{P_M}$$
In BMS: (1) Food corresponds to the battery and muscle to the motor of an AUV. (2) Peduncle corresponds to the propeller shaft and the propulsion fin (e.g. the tail) to the propeller of an AUV	

In much of the literature which considers the locomotive and/or propulsive efficiency of BMSs, it is often unclear where the starting point in the energy flow in Figure 5.3 is. Therefore, claims of very high propulsive efficiency are often quoted as being a "total" efficiency, whereas, in reality they are more likely one of the sub-set of the efficiency terms illustrated in Figure 5.3 and explained in Table 5.1 which by definition will be higher than the real total efficiency.

As defined in Table 5.1:

$$\eta_{Total} = \eta_m \times \eta_{Ped} \times \eta_B \times \eta_H \qquad 5.14$$

Curtin & Woledge, 1993a,b measured the Muscle Efficiency to be 0.41 in fast muscle and 0.51 in slow muscles.

Also as measured for ships (Carlton, 2011) the energy losses in the shaft are small and therefore where there is no gearbox the shaft efficiency is between 0.98 & 0.99. Bearing in mind that for BMSs the peduncle (equivalent shaft) length is usually small as the muscle is spread along the body, it could be considered that the peduncle losses are small and similar efficiencies of the shaft applies to them. Therefore Equation 5.14 can be written for optimum and maximum speed as:

$$a)\ \eta_{Total_{Uopt}} = 0.502\eta_{B_{Uopt}} \times \eta_{H_{Uopt}} \qquad 5.15$$

and

$$b)\ \eta_{Total_{Umax}} = 0.404\eta_{B_{Umax}} \times \eta_{H_{Umax}}$$

Therefore if the total efficiency is known $\eta_B \times \eta_H$ can be calculated.

As optimum speed, U_{opt}, and maximum speed, U_{max}, are two particular speeds of interest, it is desirable if efficiency and *COT* can be estimated in these two speeds.

Having all the information required, ξ was calculated from Equation 5.11 as below:

$$\xi = \frac{D_{Total}}{Mass \times COT - \frac{P_H}{U}} \qquad 5.16$$

Where P_H is estimated from Table 4.1.

Equation 5.16 can be used to calculate ξ values up to the speed where the fast muscles are activated. As the fast muscles operate in the absence of oxygen, lactic acid formation must be included to calculate ξ values for those speeds.

There are two significant points to be made. First on energetics and second on speed, both are explained next.

5.3.1 Efficiency considerations

In Chapter 4, when comparing the hotel loads of BMSs, it was realised that many groups of BMSs had hotel loads within the same range of values and even some of the regression lines of different groups of BMSs had very similar trends. However, when using the regression lines to estimate the hotel load for then calculating efficiency, it was realised that to obtain a precise answer, it would be desirable to measure the hotel load of each individual (if possible) as using the regression line values for those BMSs for which the hotel load was not available in some cases resulted in negative propulsion power, which meant over estimating the hotel load. The opposite of this scenario could happen as well; if the hotel load is underestimated, the efficiency will be affected.

By analysing energetics data, it was realised that the overestimation or underestimation of powers occurs due to the fact that both the hotel load and the propulsion power of BMSs are affected by multiple factors. Temperature and salinity were two factors that were highlighted by analysing the fish data. In Chapter 4 it was mentioned that oxygen consumption and therefore hotel power increases with temperature for fish. Although this effect was normalised for ectoderms, for endotherms unless their neutral body temperature is known, normalising is not possible.

The effect of salinity is not as significant as the temperature. Results from a 0.21 m Rainbow trout showed that the mass specific hotel load increased by an average of 45% when salinity changed from 0 to 35 ppt (0 ppt begin the salinity of fresh water and 35 ppt the average ocean salinity). However, normalising power for salinity is not possible unless the salinity of the water at which all BMSs are swimming is known.

As for propulsion power, it was noted by Katz, 2002, that for ectodermic BMSs the muscle reaches a higher peak power output at a higher tailbeat frequency and at higher temperatures; i.e. higher the temperature, faster the tailbeat and therefore higher the speed. This is of course only valid up to the temperature at which the BMS can survive which is again different for each BMS. These changes are also different for endothermic BMSs. The effects of temperature is not quantified for all BMSs. Therefore, the temperature effects on propulsion power and consequently speed has not been considered in this research work. This discussion however, highlights the fact that BMSs have a temperature dependant motor.

Second point to be made is that for most BMSs, unless the *COT* has been measured at a range of speeds to precisely indicate the optimum speed, the indicated speed is a voluntary swimming speed. This means that the calculated measure of efficiency is not always the optimum efficiency.

Having noted the above, ξ values are calculated for BMSs, for which all data is available as shown in Figure 5.4.

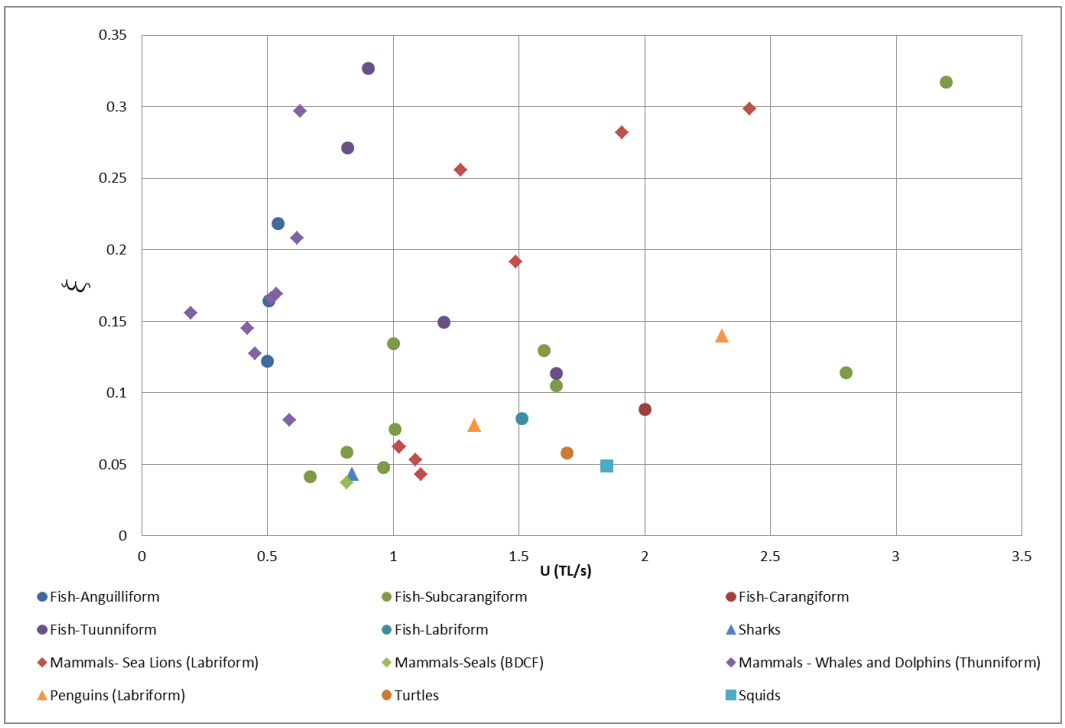

Figure 5.4. ξ values for Various BMSs as a function of relative speed

Figure 5.4 shows that BMSs have ξ values between 0.04 and 0.33, however the trends are not clear for all groups. Therefore, to clarify the data, ξ values are plotted against relative speed and also Reynolds numbers while also considering the size of the BMSs (the size of the bubbles are a measure of the mass of the BMSs) as marine mammals are relatively larger compared to other BMSs, the data points are divided into two groups for clarity of presentation. Therefore data for fish, a shark and a penguin are presented in Figure 5.5.1 and 5.5.2 and data for marine mammals are presented in Figures, 5.6.

Observing Figures 5.5.1 and 5.5.2, it was realised that eels representing Anguilliform swimming, swim at the lowest relative speed and have efficiencies between 0.12 and 0.22 which is higher compared to some other Fish swimming at relatively higher speeds at different swimming modes. For Subcarangiforms there is a trend of increases in efficiency with the increase of relative speed.

However, with the uncertainties explained earlier and as most Subcarangiforms BMSs have efficiencies between 0.04 and 0.13, there is a strong possibility that the data point for the goldfish (*Carassius auratus*) with the efficiency of 0.32 maybe an anomaly. The two data points of the Carangiform although different in size, have close efficiencies of

0.09. For Thunniform fish, efficiency increases with the Reynolds number as well as the size, however the yellowfin tuna (*Thunnus albacares*) with the highest efficiency of 0.33, swim only at 0.89 $\left[\frac{TL}{s}\right]$ which is relatively lower than smaller Thunniforms (as expected larger BMSs have relatively lower speed). The two penguins are of very similar size therefore the data point show an increase in efficiency with speed from 1.3 $\left[\frac{TL}{s}\right]$ to 2.3$\left[\frac{TL}{s}\right]$.

It is interesting that the three largest in this group, the 5.1*kg* eel (*Anguilla anguilla*), 3.8*kg* tuna (*Katsuwonus pelamis*) and 3.6*kg* penguin (*Spheniscus humboldti*) have very close values of overall efficiencies (0.14-0.16). However the eel swims at 0.5 $\left[\frac{TL}{s}\right]$, the tuna at 1.2 $\left[\frac{TL}{s}\right]$ and the penguin at 2.3 $\left[\frac{TL}{s}\right]$. Comparing these to the marine mammals data, the killer whales (*Orcinus orca*) swimming at about 0.5 $\left[\frac{TL}{s}\right]$, have the efficiencies within similar range to the three species mentioned above (0.14-0.17). However their size is considerably larger (2700-5000 *kg*).

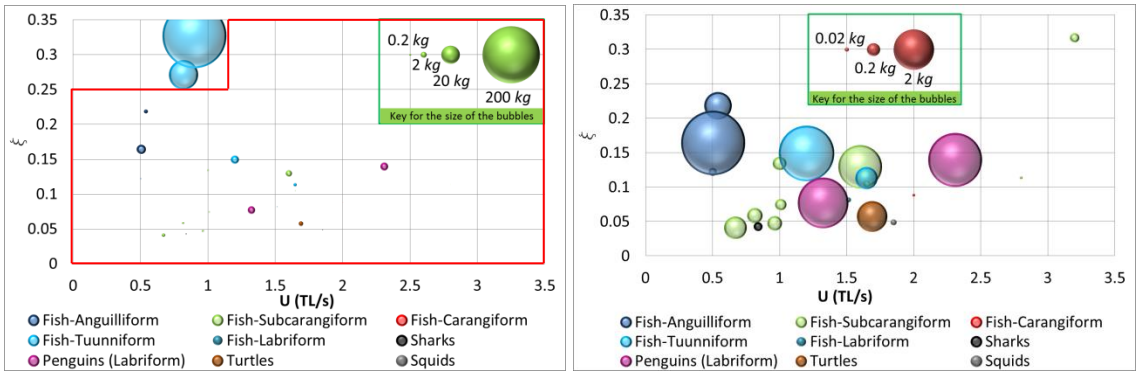

(A) (B)

Figure 5.5.1. ξ values for various fish, shark and a penguin as a function of relative speed with bubbles representing the mass. (B) presents only the data contained within the red boundary of Figure (A) with re-scaled bubble sizes to more clearly show the smaller BMSs

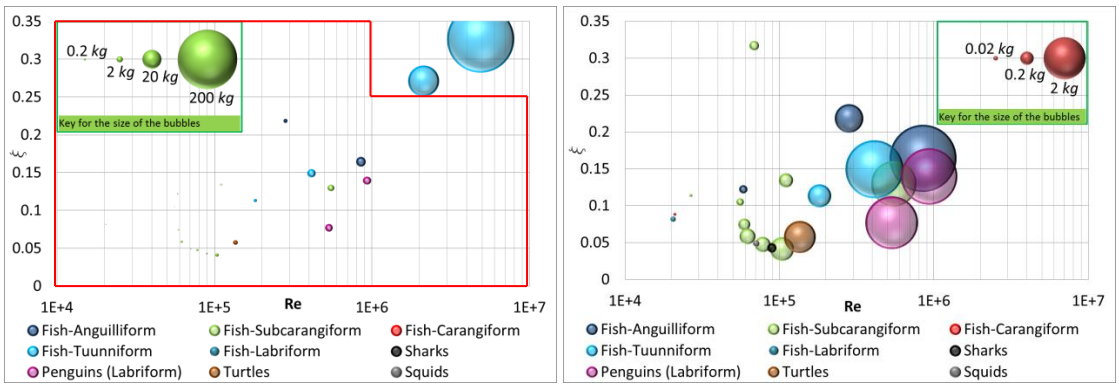

(A) (B)

Figure 5.5.2. ξ values for various fish, shark and a penguin as a function of *Re* with bubbles representing the mass. (B) presents only the data contained within the red boundary of Figure (A) with re-scaled bubble sizes to more clearly show the smaller BMSs

From Figure 5.6 it was realised that for sea lions efficiency increased from about 0.05 to 0.3 with the increase in relative speed (which is a similar trend to Subcarangiforms) and reduction in size. The seal (*Halichoerus grypus*) has the lowest efficiency of marine mammals at 0.037. The highest efficiency of about 0.3 was achieved by the bottlenose dolphin (*Tursiops truncatus*) and the California sea lion (*Zalophus californianus*); however the sea lion had a higher relative speed of at 2.4$\left[\frac{TL}{s}\right]$. As for whales and dolphins, as mentioned the two highest efficiencies belonged to the dolphins which are relatively smaller is size. The largest size data point, the grey whale (*Eschrichtius robustus*) (15 tonnes) had an efficiency of 0.16 at a very low speed of 0.2$\left[\frac{TL}{s}\right]$ while five data points of different killer whales showed that although having close sizes (2700-5000 kg) and relatively close speeds the efficiencies of the individuals ranged between 0.08 and 0.16.

There are several factors which can contribute to the variation in efficiency. The data presented, emphasises on the fact that unlike engineered vehicle, each individual BMS has different designs which affects the values of drag coefficient for each species. In addition each individual species has different levels of fitness and performance. Moreover, as mentioned previously, the level of uncertainty in the obtained values for hotel load and optimum speed of different BMSs could introduce an error value in the results. Therefore, several data points over the speed ranges of BMSs as well as detailed

information regarding the fitness and stress level of each species are required to observe the complete efficiency trends.

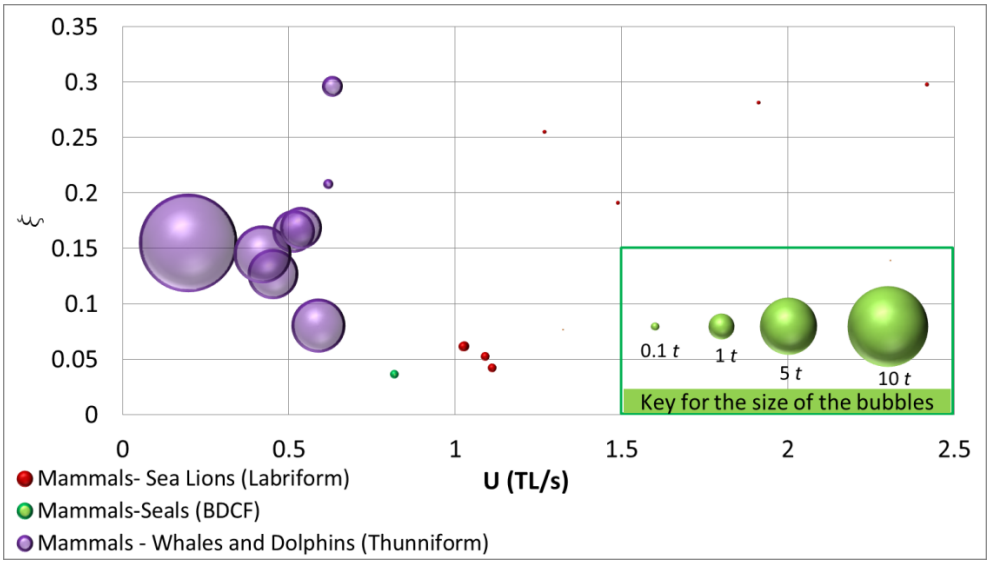

(A)

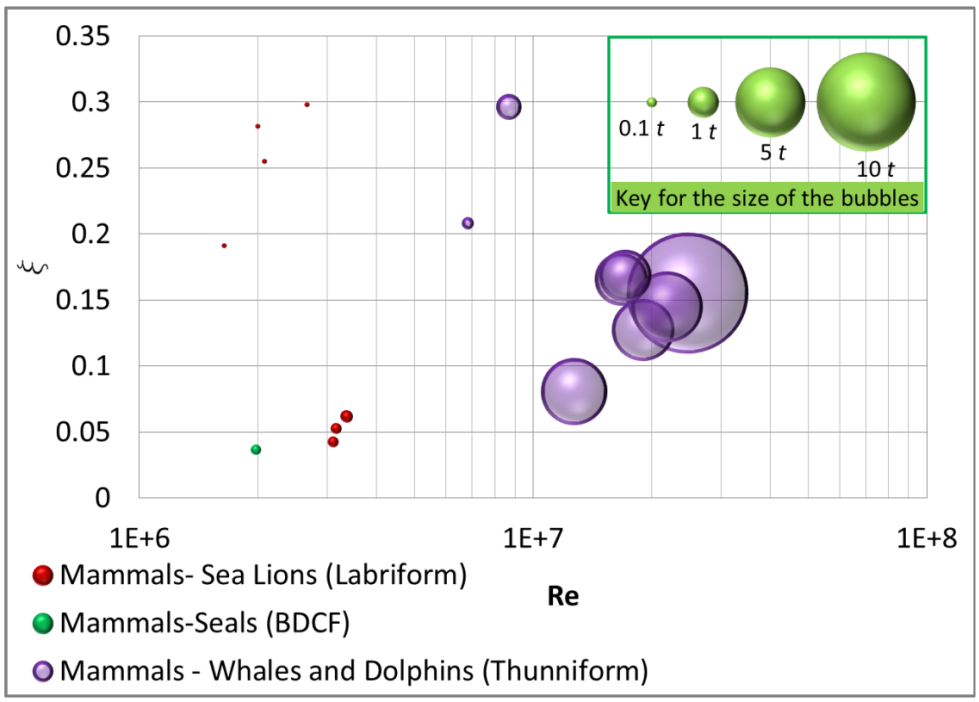

(B)

Figure 5.6. ξ values for various marine mammals as a function of relative speed (A) and Reynolds number (B) with bubbles representing the mass

In overall it was concluded that although a range of efficiencies were observed in different BMSs, similar efficiencies were found in BMSs with different swimming modes. This means that various BMSs have evolved to swim with different swimming modes and at different optimum speeds to achieving similar efficiencies. As observed fast swimming modes such as Thunniform and Labriform achieved higher efficiencies at higher speeds compared to swimming modes used for slower swimming such as Anguilliform. Moreover, it was observed that larger BMSs such as whales, achieved similar efficiencies to a tuna swimming with the same swimming mode. However, the whales having considerably larger sizes, swim at lower length specific speed compared to the tuna.

5.4 Estimate of ξ_{Uopt}

In Section 5.2 estimating ξ by having the speed, *COT* and drag was explained. However, *COT* is not always available. However, having an estimate of ξ and consequently *COT* for optimum and maximum speed (U_{opt}, and U_{max}) is essential for comparing different BMSs. Therefore, when *COT* is unavailable, ξ must be estimated by other means. In present research this has been done as follows:

$$COT = \frac{1}{\{\text{Mass}\}}\left(\frac{P_H}{U} + \frac{D_{Total}}{\xi}\right) \tag{5.17}$$

If considering the surface roughness to be considered within ξ, then:

$$D_{Total} = \propto_{TAE} D_{BB} + \sum D_{Fins} + D_G + D_S \tag{5.18}$$

$$= C_G \times 0.5\rho U^2\left(\propto_{TAE} C_D \mathrm{A_{WS}} + 2C_{F_{TF}}\mathrm{A}_{TF} + 2C_{F_{BF}}\mathrm{A}_{BF} + 2C_{F_{SF}}\mathrm{A}_{SF} + 2C_{F_{StF}}\mathrm{A}_{StF} + 2C_{F_{RF}}\mathrm{A}_{RF} + 2C_{F_S}\mathrm{A}_S\right)$$

where C_G is the gills' drag multiplier, which will be 1.1 for BMSs for which gills are present and 1 for those without gills (air breathers; i.e. mammals, penguins and reptiles).

Therefore as skin friction drag is $C_F = 0.072Re^{-0.2}$ by taking constant terms out of the parentheses, the equation was reformed to:

$$D_{Total} = C_G \times 0.5\rho \times 0.072\nu^{0.2}U^{1.8}\left(\propto_{TAE} EL^{-0.2}(1+k)\mathrm{A_{WS}} + 2\sum {Ch_{Fin}}^{-0.2}\mathrm{A}_{Fin}\right)$$

Where Ch_{Fin} is the chord of each fin and A_{Fin} is the surface area of the fin.

If

$$b = C_G \times 0.5\rho \times 0.072\nu^{0.2}\left(\propto_{TAE} EL^{-0.2}(1+k)\mathrm{A_{WS}} + 2\sum {Ch_{Fin}}^{-0.2}\mathrm{A}_{Fin}\right)$$

then,

$$D_{Total} = bU^{1.8}$$

Therefore, to estimate ξ at optimum speed, ξ_{Uopt}, *COT* was differentiated with respect to *U*:

$$\frac{dCOT}{dU} = \frac{1}{M}\left(\frac{-P_H}{U^2} + \frac{1.8 \times bU^{0.8}}{\xi}\right)$$

The *COT* at the optimum speed is minimum and therefore at U_{opt}:

$$\frac{dCOT}{dU} = 0$$

Therefore,

$$\xi_{Uopt} = \frac{1.8b{U_{opt}}^{2.8}}{P_H} \qquad 5.19$$

The above method proposed by the author can be used to calculate the ξ_{Uopt} when hotel load and the optimum speed (not any other speed) are known without requiring the *COT*.

The results of calculated efficiency vs. the one explained in Section 5.3 are shown in Figure 5.7. The plot shows that considering the uncertainties regarding the hotel load and speed, there is a good agreement between the results of the proposed method and the methods in Section 5.3. The average difference between the efficiencies predicted by the methods and the actual efficiencies is 45%. The highest over estimation is for a goldfish (*Carassius auratus*) data which is most probably due to the fact that the fish had a higher hotel load than predicted due to some applied stress. Also for the grey whale (*Eschrichtius robustus*) and grey seal (*Halichoerus grypus*) the over estimation is high as the Kleiber line is used for estimation; however, both the grey whale and especially the grey seal have a hotel load compared to other mammals of the same size.

The method proposed in this research in the form of Equation 5.19, is a novel method for predicting the overall efficiency at optimum speed, especially where *COT* is

not available. This method was used later on in Chapter 7 to calculate ξ_{Uopt} and sequentially the *COT* for the off-spring produced by a search and selection algorithm. If the exact value of the hotel load for a BMS is known, by comparing the results from the two methods the value of the optimum speed can be found as the two methods will output the same efficiency when the exact value of optimum speed is the input.

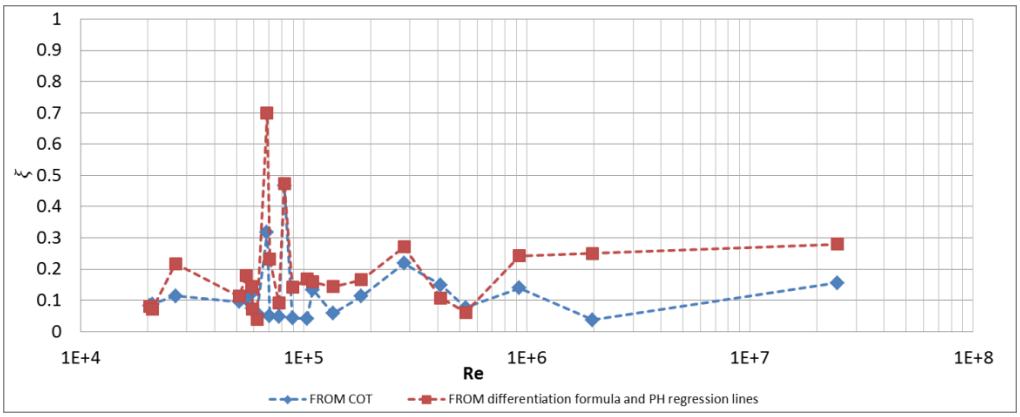

Figure 5.7. ξ_{Uopt} calculated from Equation 5.19 vs. results from Section 5.3

By replacing ξ_{Uopt} in the Equation 5.17 with Equation 5.19, the $COT_{U_{opt}}$ which is the minimum COT can be calculated as follows:

$$COT_{U_{opt}} = \left(\frac{2.8}{1.8}\right) \times \left(\frac{P_H}{\{Mass\}U_{opt}}\right) = \frac{1.5\dot{5}P_H}{\{Mass\}U_{opt}} \qquad 5.20$$

5.5 An estimate of ξ_{Umax}

For vehicles motor brake power is related to efficiency as follows:

$$P_B = U \times D_{BB} \times \frac{\propto}{\eta_{Total}}$$

Where P_B is the motor brake power; therefore:

$$\xi_{Umax} = \frac{Umax \times D_{Umax}}{P_{B\,Umax}} \qquad 5.21$$

To estimate ξ at maximum speed, ξ_{Umax}, the propulsion power at maximum speed must be quantified. For BMSs muscle power corresponds to the motor power in AUVs.

It would be ideal if similar to motors, a power value in terms of watt or $\frac{Watt}{kg\ of\ motor\ mass}$ could be defined for BMSs muscle.

If the power output of both the red and the white muscle fibres could have been measured or obtained from literature for BMSs, the ξ_{Umax} would have been estimated by substituting the maximum available muscle powers in Equation 5.21.

However, the characteristics and capabilities of white and red muscles in each BMS are different. The power output of both white and red muscles depends on several factors, which are mainly:

- The muscle contraction frequency: This is relative to the tailbeat frequency
- The amplitude of the muscle contraction. This can vary between 1% and 15% contraction for different speeds (2% and 30% total amplitude).
- The fitness and size of each BMS: Although it is expected that same species have similar characteristics, the quality of the muscle can be affected by the level of "fitness"; i.e. a species at a higher level of fitness has a better quality (more protein, less fatty) muscle. Furthermore, as smaller individuals of the same species swim at higher tailbeat frequencies, their maximum power output will occur at higher tailbeat frequencies.

The data on all the parameters involved in muscle power output are not available for all BMSs and therefore power output cannot be estimated at maximum speed. However having a measure of efficiency to compared BMSs at their maximum speed was desirable.

Although three main factors as explained affect the muscle power output, it is known that power is the work done per time. In the case of the BMSs, the work is the product of the force produced by the muscle and the distance which is the amplitude of muscle contraction. It is also apparent that the amplitude is proportional to the muscle length and hence the body length of the BMS; therefore,

$$A = k_1 EL \qquad 5.22$$

Where A is the amplitude of muscle contraction,

EL is the main body or the elliptical length of the BMS and

k_1 is a constant. As modelled by Medler & Hulme, 2009, the k_1 can be assumed the same across all BMSs for maximum power production. On the other hand, the force produced by the muscle is proportional to the muscle mass, hence,

$$F = k_2\{Mass\}_M \quad 5.23$$

Where F is the muscle force,

$\{Mass\}_M$ it the muscle mass of the BMS, and

k_2 is a constant. Similar to k_1, k_2 is assumed the same across all BMSs for maximum power production.

Therefore by using Equations 5.22 and 5.23 the power output of the muscle can be formulated as:

$$P_m = k_2\{Mass\}_M \times k_1 EL \times f \quad 5.24$$

Where P_m is the muscle output and f is the frequency of the tailbeat. The procedure for estimating the tailbeat frequency is explained later on in this section, part, 5.5.1

Therefore by using Equations 5.21 and 5.24 ξ_{Umax} can be estimated as:

$$\xi_{Umax} = \frac{Umax \times D_{Umax}}{k_2 \times k_1 \times \{Mass\}_M \times EL \times f}$$

or

$$\xi'_{Umax} = \frac{Umax \times D_{Umax}}{\{Mass\}_M \times EL \times f} \quad 5.25$$

Where ξ'_{Umax} is $\xi_{Umax} \times k_2 \times k_1$

Although this will not result in an absolute value for ξ_{Umax}, it is a means to compare efficiency at maximum speed for different BMSs.

Data on maximum speed of BMSs is not readily available; moreover the maximum recorded speed does not necessarily equal the maximum speed capability of the BMSs. However, the gathered data will give an understating of maximum speed efficiency of different BMSs. The ξ'at maximum recorded speed has been estimated for BMSs with Subcarangiform, Carangiform and Thunniform swimming modes as well as a turtle. The results are presented in Figure 5.8. It is apparent that for Thunniform and Subcarangiform Swimmers, ξ'_{Umax} is directly proportional to the relative maximum

speed with an R^2 values of 0.967 for Thuuniform swimmers and 0.986 for Subcarangiform swimmers.

For Thunniforms, $\xi'_{Umax} = 1.2297U_{max}\left[\frac{TL}{s}\right] - 0.2799$ and for Subcarangiforms, $\xi'_{Umax} = 0.2719U_{max}\left[\frac{TL}{s}\right] - 0.2567$.

For Thunniforms the slope is higher which means a Thunniform swimming BMSs would have a higher indication of maximum speed efficiency at the same relative maximum speed compared to a Subcarangiform. There is only one Carangiform data belonging to the Atlantic mackerel (*Scomber scombrus*) and if the regression line for Thunniforms is extended, the mackerel data is placed in between the two regression lines. This concludes that maximum speed efficiency of a Thunniform swimmer would be higher than that of a Carangiform swimmer, which is higher than that of a Subcarangiform swimmer, if they were to swim at the same relative speeds. To observe the effect of body mass, the data are re-plotted in Figure 5.9. The data are separated as the size of Thunniform swimmers is relatively larger and would disguise the smaller BMSs.

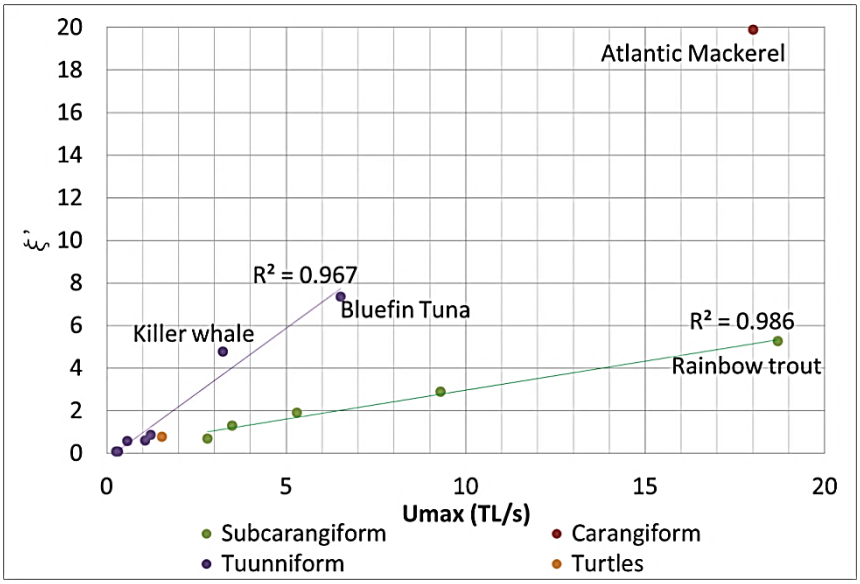

Figure 5.8. ξ'at maximum speed for BMSs as a function of relative speed

When observing data on Figures 5.9, it was realised that although some BMSs with relatively small size have low relative speed and therefore low indication of efficiency,

for both Subcarangiforms and Thunniforms it is the smaller BMSs is size which do swim at a relatively higher speed and have higher efficiency.

Comparing Figures 5.9.A and 5.9.B it was also realised that Thunniforms achieve similar indications of efficiency at lower relative speed as well as larger body size compared to Carangiforms. This means although the relatively smaller species in each swimming group travel at higher relative speeds and efficiencies the absolute size of Thunniform with similar efficiencies is larger than Subcarangiforms.

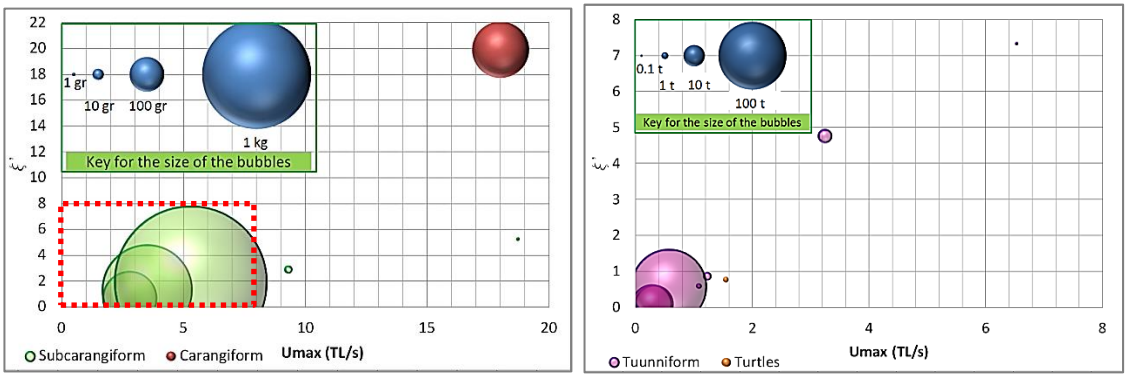

(A) (B)

Figure 5.9. ξ'at maximum speed for BMSs as a function of relative speed for Subcarangiforms and Carangiforms (A) and Thunniform and the turtle (B). The red frame in (A) is the area covered in (B)

5.5.1 Estimating the tailbeat frequency of BMSs

The frequency of oscillation/undulation varies for each species as well as for individuals of the same species with different sizes. In order to be able to calculate the fin beat speed, having an estimated of the frequency was essential. Therefore, data on the tail or flipper beat frequency, f, as a function of relative speed, U $\left[\frac{TL}{s}\right]$, has been presented in Figure 5.10 for 7 different groups of BMSs for which data was found. It is realised from the figure that there is a strong correlation ($R^2 > 0.75$ except for the penguins as per Table 5.2) between f and U. Although, the frequency depends on other factors such as fitness, etc., the correlation showed that considering f as a function of U was a reasonable approach.

BMSs with rear fin proplusors sit relatively closer to one another compared to Labriform swimmers (penguins) which have a relatively low flipper beat frequencies.

As moving from undulating bodies such as eels (Anguilliform) to more oscillating bodies such as the tunas (Thunniforms) the tailbeat frequency decreases for the same speed which could indicate better efficiency as less effort is required to achieve same relative speed.

The regression lines from each group as well as the R^2 values are presented in Table 5.2. For BMSs for which the equation is unknown the closest regression line has been used to estimate the frequency.

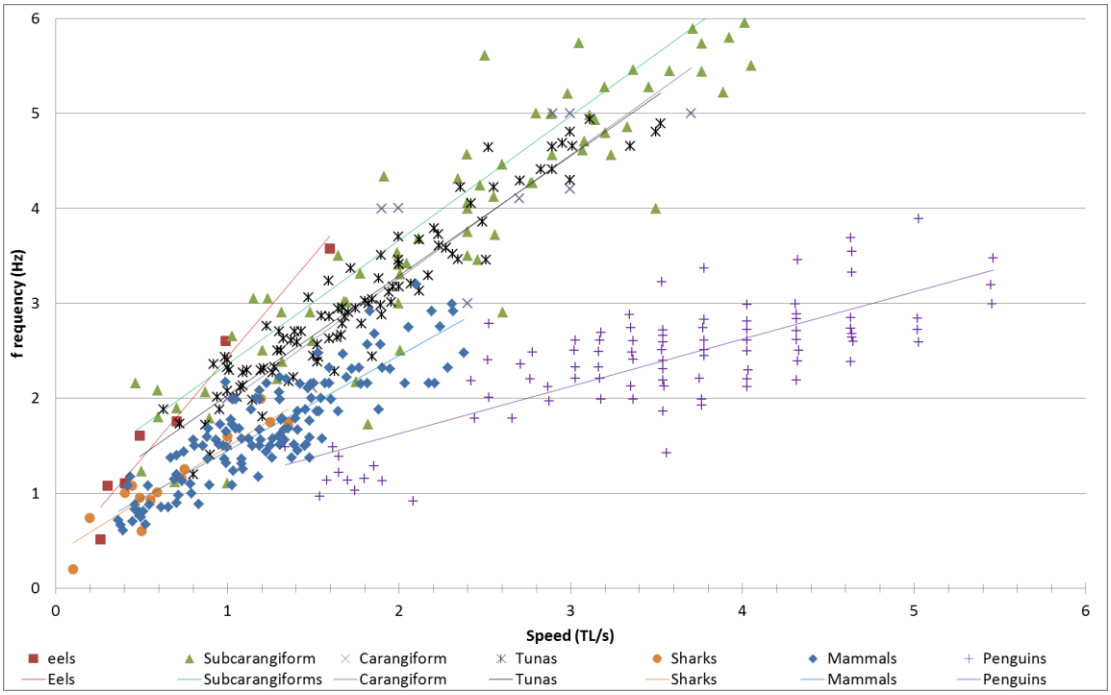

Figure 5.10. Tail or flipper beat frequency as a function of relative speed for various groups of BMSs. References are as follows as well as number of individuals (n) and number of species (s) where available: Eels (Shadwick, & Lauder, 2006), Subcarangiforms (Bainbridge, 1958 [n=4, s=1] and Shadwick, & Lauder, 2006), Carangiform (Shadwick, & Lauder, 2006), tunas (Shadwick & Syme, 2008 [n=12, s=1] and Shadwick, & Lauder, 2006), sharks (Jones, 1973 [n=1, s=1] and Shadwick, & Lauder, 2006), marine mammals (Fish, 1998 [n=19, s=4] and penguins (Clark & Bemis, 1979 [n=50, s=6])

Table 5.2. The regression line of finbeat frequency as a function of relative speed for various groups of BMSs presented in Figure 5.10

Group of BMSs / mode of swimming	Regression line equation	Regression line R^2 value
Eels (Anguilliform)	$f\ [Hz] = 2.1343U\left[\frac{TL}{s}\right] + 0.3021$	0.9601
Subcarangiform	$f\ [Hz] = 1.3092U\left[\frac{TL}{s}\right] + 1.0454$	0.9653
Carangiform	$f\ [Hz] = 1.3021U\left[\frac{TL}{s}\right] + 0.6605$	0.8007
Tunas (Thunniform)	$f\ [Hz] = 1.2595U\left[\frac{TL}{s}\right] + 0.7716$	0.9093
Sharks	$f\ [Hz] = 1.1261U\left[\frac{TL}{s}\right] + 0.3624$	0.8710
Mammals (Thunniform)	$f\ [Hz] = 1.0026U\left[\frac{TL}{s}\right] + 0.4474$	0.7534
Penguins (Labriform)	$f\ [Hz] = 0.4978U\left[\frac{TL}{s}\right] + 0.6323$	0.6182

5.6 Conclusions

In this chapter different components and correction factors contributing to the drag of BMSs were discussed and means were proposed to estimate each component. After defining the different efficiencies within the BMSs body, the total drag was calculated to obtain an indication of efficiency in BMSs, ξ. By analysing the results it was realised that the ξ value at sustained cruising speeds (close to the optimum speed) is between 0.04 and 0.33 when considering all BMSs. Moreover, it was found that some BMSs with different swimming modes are able to achieve similar ξ values, however at different speeds and different sizes. These results did not come as a surprise. One purpose of evolution is to improve the survivability of animals. Therefore, it is expected that each BMS would have evolved through time and developed certain characteristics such as a specific swimming mode which will give it the ability to swim efficiently at certain speeds. So, fast swimmers such as Thunniform swimmers would achieve a certain efficiency (or ξ value as an indication of it) at a higher speed compared to an eel which is evolved to be a relatively slow swimmer.

A method was proposed to estimate ξ at optimum speed without requiring the value of *COT*. Considering the uncertainties regarding the speed and hotel load of BMSs and appreciating the wide range of BMSs being included within the calculations, the proposed method gives a fair estimate of the ξ value. This method over predicts the

ξ_{opt} value is some cases. Having studied the base metabolic rate or hotel load of BMSs, this is expected. The hotel load of BMSs will increase, if they swim in conditions which are distant from their natural environment (such as changes in temperature and applied stresses). Therefore, it is possible to underestimate the hotel load and this is an important factor affecting the value of ξ_{opt}, hence over predicting it.

Another method was proposed to have an indication of efficiency at maximum speed, ξ'_{Umax}. The results showed a linear relationship between body length and ξ'_{Umax} for Thunniforms and Subcarangiform swimmers (for which enough data was available to predict a trend).

In order to estimate ξ'_{Umax}, based on data for several BMSs, equations based on regression lines were presented to estimate the frequency of the oscillation/undulation of the propulsive fins for different BMSs. These data are mostly available at speeds lower than the maximum speed or burst speeds of BMSs, however as speed does increase with the frequency of the tailbeat, it is assumed that the relationship remains constant. The results show that smaller BMSs swim at higher relative speeds $\left[\frac{TL}{s}\right]$ and tailbeat frequencies.

In this chapter the concentration was on methods to calculate drag and efficiency for BMSs. Knowing the values of ξ_{opt}, it is possible to compare the overall efficiency of BMSs with AUVs. As the hull efficiency can be considered very close to unity (Tupper & Rawson, 2001), Equation 5.15 (a) can be written as:

$$\eta_{Total_{Uopt}} \approx 0.502\eta_{B_{Uopt}}$$

As ξ_{opt} ranged between 0.04 and 0.33 for various BMSs, again if considering the *c* factor in Equation 5.12 to be very close to 1 (insignificant skin roughness) and therefore $\eta_{Total_{Uopt}} \approx \xi_{opt}$, then $\eta_{B_{Uopt}}$ would range between 0.08 and 0.66 for various BMSs. It was shown in Section 5.3.1 that different BMSs with various swimming modes can have similar overall efficiencies. Therefore, the reason for this large range is not yet known, and it is possible that the amount of uncertainties within the measured data, maybe the reason for this large range of efficiencies for BMSs.

Table 5.3 shows the comparison between the different efficiencies in BMSs and two AUVs. It is realised from the table that the overall efficiency of BMSs is lower

compared to the AUVs. However, the behind efficiency of BMSs can reach very close to the propulsive efficiency of the AUV (0.66 vs. 0.7). Therefore, the main difference is in the muscle efficiency which is considerably lower compared to the motor efficiency of the AUV. Considering the low noise and vibration produced by the swimming mode of BMSs compared to AUV propellers as well as the light weight of the propulsive fin, plus the similar efficiencies, a bio-inspired swimming mode, if designed to propel a BUUUV would be an alternative light weight option to propellers, especially for stealth.

Table 5.3. A Comparison between the efficiencies of BMSs and AUVs

Efficiencies at $Uopt$	BMSs	AUV[3]	Gliders
Total efficiency, η_{Total} [1]	0.04 - 0.33	0.53	0.5[4]
Muscle/Motor efficiency[2], η_M	0.502	0.8	-
Behind/propulsive efficiency	0.08-0.66	0.7	-
References	This research	Furlong et al, 2007	Griffiths, 2003

(1) Taking into account the considerations made regarding hull efficiency and the skin roughness

(2) Calculated as the product of motor efficiency and gearbox efficiency

(3) AUTOSUB long range

(4) The efficiency of the buoyancy engine

Chapter 6. The trade-off between Manoeuvrability and upright stability

In Chapter 3, it was realised that BMSs have relatively lower turning radius compared to AUVs of similar size and if was suggested that their flexible bodies was a key factor to this performance. However, in order to compare BMSs with one another in terms of manoeuvrability, a measure of flexibility must be sought.

When observing the swimming of different BMSs, it was realised that aside from their flexibility, they have various approaches to turning, due to their body structure and control surfaces. In order to explain further, BMSs have been grouped as below:

- **Fish**
- **Sharks**
- **Mantas**
- **Seals and sea lions**
- **Whales and dolphins**
- **Penguins**
- **Turtles**

Squids are left out of this analysis due to insufficient data. Hypothesis about the performance of each group is explained next and then an analysis to confirm the hypothesis is made.

- **Fish**

Fish are most flexible about the yaw axis and can use their rear fins as a rudder while turning about the yaw axis. Therefore, the main factor affecting the turning radius of fish is their swimming mode which is somewhat related to the flexibility of their bodies.

- **Sharks**

Sharks, similar to fish have a rear fin which acts as a rudder while turning, however as for sharks usually the body width is larger than the body height, their flexibility should be higher in the pitch axis compared to the yaw axis. However, due to their body structure (vertebrae) and their swimming mode, they do not have flexibility on the pitch

axis. Therefore the above factors makes sharks highly stable on both roll and yaw axis and consequently less favourable to turn.

- **Sea Lions and Seals**

Sea lions and seals have highly unstable bodies in roll axis and are more flexible in pitch axis. Therefore, during turning about the yaw axis, with the help of their side fins, they roll their bodies 90°. This way they use their flexible body to turn and use their side fins as rudders.

- **Mantas**

Although genetically closer to sharks, mantas have Roll unstable bodies. Therefore by using their large side fins they perform Yaw turns similar to seals and sea lions.

- **Whales and Dolphins**

Whale and dolphins are also more flexible in the pitch axis than Yaw axis. Therefore they either turn in the pitch axis or with the help of their Roll unstable bodies, Roll their body 90° to turn in the Yaw axis, where they can use their rear fins and their side fins to some extent to turn. The exception is for large baleen whales which do not have as much the flexibility of smaller whales and dolphins and therefore will have turning behaviours similar to sharks.

- **Penguins**

Similar to seals and sea lions, except that due to their positively buoyant bodies they experience different forces.

- **Turtles**

Turtles have rigid bodies and therefore their control surfaces are their main turning means. Therefore turtles can turn almost on spot and therefore have a turning radius of $0.5[TL]$.

6.1 A formula for turning radius of BMSs

BMSs were divided into seven groups based on their turning behaviour. However, means are required to estimate the turning radius of BMSs. It was hypothesised in this research that the low turning radius of BMSs is highly related to their flexible bodies.

Measuring the flexibility of the body of each BMSs (as done for the gurnard in Chapter 3) was not possible and data was not available. Moreover, the bodies of BMSs are very different but in order to test this hypothesis, having some measure of flexibility was desirable.

In Chapter 3 it was explained how a regression line for the turning radius of AUVs based on their total length was derived. Using the obtained formula, it is observed that with an R^2 value of 0.8943 the average length specific turning radius for AUVs which representing rigid bodies is 2.7999. By comparing this value to the actual length specific turning radius of the BMS, a measure of flexibility was estimated as follows:

$$Flexibility\ Measure\ (FM) = \frac{Actual\ BMS\ Length\ Specific\ Yaw\ Radius}{Average\ AUV\ Specific\ Yaw\ Radius} = \frac{Actual\ BMS\ Length\ Specific\ Yaw\ Radius}{2.7999} \quad 6.1$$

Therefore, $R_{yaw\ _{TL}} = 2.7999\,FM$. However, *FM* also must be estimated, as up to this point, *FM* was estimated based on the turning radius itself.

In order to estimate *FM* for BMSs, various groups of BMSs with different turning behaviours were separated and the values of *FM* for each group was plotted against the Total Length of the BMS in Figure 6.1. In order to show the data clearly, one data point which belonged to the humpback whale (*Megaptera novaeangliae*) was not shown on the plot as the whale had the largest FM of 0.29. Based on this research work it is realised that swimming mode in fish is related to their flexibility, therefore, fish were divided based on their swimming mode (not all swimming modes are included as data is not available for all modes of swimming).

As demonstrated in Figure 6.1, it was observed that the silver eel (*Anguilla anguilla*) representing Anguilliform fish and the Californian sea lion (*Zalophus californianus*) with a highly unstable body have the highest Flexibility (smallest *FM*) for their body length. The turtle (*Chrysemys picta*) and the boxfish (*Ostracion meleagris*) as expected have higher *FM* values compared to other BMSs with similar total length, as both species have inflexible bodies. The data point for the humboldt penguin (*Spheniscus humboldti*) is close to the regression line for Carangiform fish while tunas representing Thunniform swimming fish have the least flexibility between fish (Therefore the highest *FM*). Sharks as expected have low flexibility and the large baleen whale, the humpback whale, has the lowest flexibility of all BMSs is the plot.

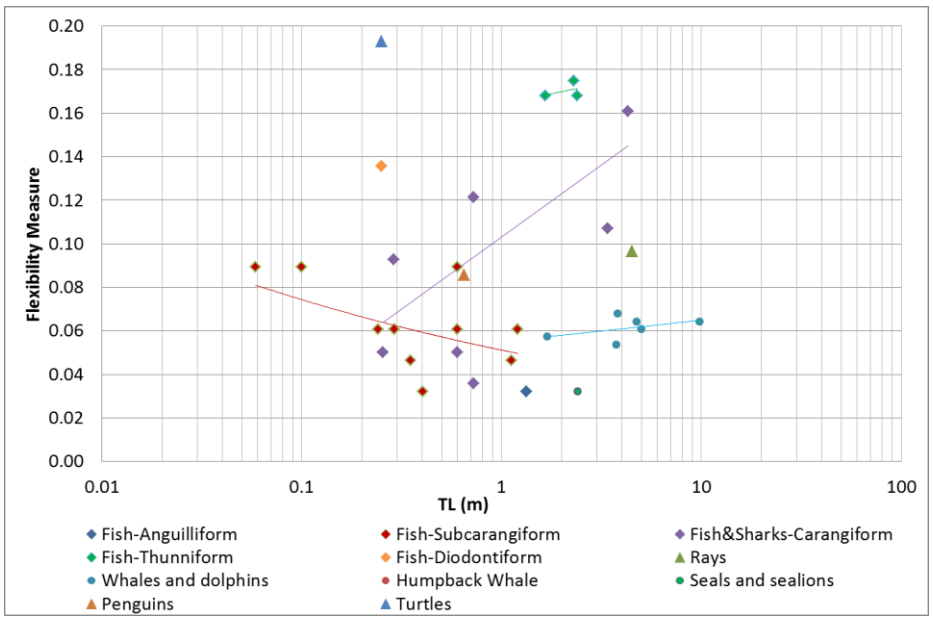

Figure 6.1. *FM* as a function of *TL* for various groups of BMSs

The regression lines and functions obtained from the data plotted in Figure 6.1 were presented in Table 6.1.

Table 6.1. FM as a function of TL for various groups of BMSs

BMS group		No. of species	Regression line formula	R^2 value
Fish & Sharks	Anguilliform	1 (silver eel, *Anguilla anguilla*)	$FM = 0.0241TL$	-
	Subcarangiform	10	$FM = 0.0511TL^{-0.162}$	0.22
	Carangiform	7	$FM = 0.0201TL + 0.0588$	0.53
	Thunniform	4	$FM = 0.1642TL^{0.0491}$	0.17
	Diodontiform	1 (boxfish, *Ostracion meleagris*)	$FM = 0.5428TL$	-
BMSs with cartilage	Rajiform (rays and skates)	1 (giant manta, *Manta birostris*)	$FM = 0.0214TL$	-
Marine Mammals	Labriform (sea Lions)	1 (California sea lion, *Zalophus californianus*)	$FM = 0.0134TL$	-
	Thunniform (whales and dolphins)	6	$FM = 0.0552TL^{0.0706}$	0.21
	Large Baleen whales	1 (humpback whale, *Megaptera novaeangliae*)	$FM = 0.0193TL$	-
Penguins		1 (humboldt penguin, *Spheniscus humboldti*)	$FM = 0.1318TL$	-
Turtles		1 (painted turtle, *Chrysemys picta*)	$FM = 0.7716TL$	-

In this section length specific turning radius of BMSs was presented as a function of flexibility which is itself represented as a function of the total length of BMSs. By observing the R^2 value for the regression lines presented in Table 6.1, it was concluded that swimming mode and length are not the only influential factors affecting the flexibility in BMSs. Moreover, turning radius is not solely a function of flexibility, but also relates to the movements of the body and control surfaces as well. The manoeuvring capabilities of BMSs suggest that investigating the mechanism of high manoeuvrability is a subject worthy of further research.

6.2 Conclusions of the comparison of biological and engineered system performance

Several characteristics of AUVs and BMSs have been compared in this research as discussed in Chapters 3, 4, 5 and the current chapter. The results highlighted significant superiority in terms of BMSs speed, speed range and manoeuvrability. *COT*, propulsion and turning capability were then investigated extensively, to understand the energy and power requirement of each BMS systems, the capability of different propulsion systems and an estimate for manoeuvrability of BMSs.

By the knowledge gained by this research, the capabilities of each BMS can be identified.

The second part of the main aim of this research work was to find means to use the bio-inspired knowledge to improve the design and therefore the performance of AUVs.

It became apparent that there are always trade-offs between different capabilities for BMSs. For example, some BMSs with lower *COT* have lower speed, or some highly manoeuvrable BMSs, have little upright stability. Therefore, in order to make use of the bio-inspired knowledge, the mission profile of the vehicle must be known. These missions must be then corresponded in a way with the mission or the purpose of BMSs to finally find the bio-inspired capability which is suited for the mission. These matters are discussed in the next Chapter.

Chapter 7. Implementing Bio-inspiration

The result of this research show that AUV technology has been improving rapidly and modern AUVs are built with improved capabilities in various aspects such as depth capability and energy consumption. Despite all the improvements, there are still limitations to AUV capabilities, which animals perform naturally such as high levels of manoeuvrability. Bio-inspiration is presented as an alternative approach to conventional engineered design.

In this research work, several characteristics of BMSs which have significance in the overall performance of the system with different importance have been studied, quantified and compared with those of the AUVs. The research highlighted the superior performance of BMSs, especially in terms of speed, speed range and manoeuvrability. There are still many unknowns regarding how exactly BMSs operate (e.g. buoyancy control system of many deep sea species), however as shown in this research, BMSs demonstrate their various capabilities due to their diverse and flexible multi-functional body design as well as various swimming modes which have evolved for different swimming speeds and manoeuvrability. The quality of fuel available to BMSs is also an influential factor in their speed and endurance, however considering solely the energy storage on board, not all BMSs have access to large amount of fuel (fish with little body fat).

By gaining the knowledge on the performance of BMSs and defining methods to calculate or estimate them, it is possible to make use of this bio-inspired knowledge. However, current bio-inspired AUVs are built based on mimicry from a specific species. One main purpose of this chapter is to introduce a method for systematic bio-inspired designs, not only mimicking nature but artificially evolving the design so that the end vehicle is optimised to fulfil a desired mission, inspired by nature.

Similar to any vehicle, in order to implement bio-inspired design, the mission profile or the purpose of the underwater vehicle must be known. The mission profile must then be compared with those of BMSs, to find the appropriate BMS for a specific AUV desired mission. AUV missions and their correspondence with the purpose of BMSs are discussed in this chapter and a method is presented to select an appropriate bio-inspired design to fulfil a desired AUV mission profile. In this method, bio-inspired formulas are used to select some aspects of the design of a Bio-inspired Unmanned Untethered

Underwater Vehicle (BUUUV). Therefore, this chapter makes use of the findings in the previous chapters of this bio-inspired research.

This method is at concept stage and when this thesis is being written no prototype has yet been being built based on the results of this method. It is possible to think that the idea might be futuristic, however that future is close. For example, this method outputs design options which make use of muscle instead of a motor. Already several type of artificial muscles exist which could be used for this purpose in the future. Also the proposition of using a flexible body for the BUUUV is an achievable aim as flexible bodied biomimetic AUVs already exist, such as the Robotuna.

Prior to implement the bio-inspired knowledge to AUV design, different AUV missions must be studied. This is explained next.

7.1 Mission definition for Underwater Vehicles

After various design aspects of the BMSs are understood, in order to apply the bio-inspired findings of this research to BUUUV design, the "purpose" or desired mission must be identified. The mission profile plays an important role in the design of any vehicle. For an AUV user, "best" option is not necessarily always the vehicle with the extreme capabilities. Therefore, instead of concentrating on a vehicle which has the maximum capability in any single performance characteristic, a vehicle is sought which has the requirements to fulfil the desired combination of characteristics. The main desired characteristics include speed capability and range, manoeuvrability, depth capability, endurance, energetic cost and weight. Therefore, the bio-inspired technology should attempt to find the optimum option that nature has to offer for a corresponding AUV mission. In order for this to become possible, the "missions" of BMSs must also be defined and understood so they can be corresponded with those of the AUVs.

While missions are not formally defined for BMSs, they are in fact a consequence of an evolutionary process, subject to highly varied evolutionary pressures. Consequently, some BMSs have evolved to be highly manoeuvrable such as Eels, some exhibit high speeds such as the Sailfish, and some have high acceleration characteristics, such as the Barracuda. Although animals are highly capable, their main aim is to survive and reproduce and the data gathered from them can always be biased by other factors such as the physical and mental condition of the BMS at the time of data collection.

On the other hand, AUV missions are varied and different to the ones of an animal. By gathering information available on various missions of different AUVs (AUVAC, 2011), 30 different principal missions were identified for the 189 AUVs studied. The table of the mission data is presented in Appendix 1.4.

These missions were identified across different industries with different levels of sophistication required. The missions varied from a general Oceanographic Survey which was mentioned in the mission profile of 49% of the studied AUVs to Anti-Submarine Warfare which was only within the mission profile of 3% of the AUVs.

Surprisingly, no strong correlation was found between body dimensions (length, depth, and height), mass and speed of the AUVs and their mission profiles. Even for very specific missions, AUVs with different designs parameters and capabilities are used. This is due to the fact that unlike ships which are designed for a specific purpose, e.g. to be a bulk-carrier, an oil tanker or a tug boat, AUVs are usually designed and built as "general purpose" and therefore used as "sensor taxis". This means that what gives an AUV the capability to perform a mission, apart from its motor, battery capacity and depth capability, are mainly the sensors on-board. Other aspects, such as the body design and propulsion are usually "off the shelf". The current designs might be simpler to build compared to a more sophisticated body design and therefore more convenient.

The method proposed in this chapter takes the payload mass as an input and also considers similar hotel loads for the same size AUV by using the regression line obtained in Chapter 4. In future it is possible to add a database of various sensors used in AUVs and their specific power requirements to be taken into consideration for a more accurate required power calculation.

Therefore at the present time the sensors are not specifically defined as there are numerous sensors that can be used for AUVs. The assumption made in this research is that the sensors fit within the optimising method through the hotel load regression line which accounts for the power required to operate average amount of sensors that are carried on board AUVs and the mass of payload which can be defined as an input and considered when calculating the mass for the proposed design.

However, although in the animal world, missions are very different and irrelevant to ones of the AUVs, it is evident that the evolution of animals is to some extend mission based. The variations in design are obvious in BMSs. Therefore, unconventional AUV designs are worthy of consideration. As AUVs are usually designed on generic basis, this research suggests that a more specific design based on a specific mission profile can

potentially improve the performance of the AUV and maybe reduce its energy consumption. Also, alternative technologies will equip AUVs with extra features. For example, an AUV propelled with an oscillating foil will have relatively lower vibration and noise which can be used both for scientific purposes and military missions.

As AUVs are made for general purpose, usually specific design characteristics are not mentioned in a mission profile. However, there are specific missions for which certain restrictions are imposed on the design of the AUV. For example, if an AUV is supposed to be carried by an aircraft, its mass is limited and the diameter may be required to be a specific value. Moreover, for the simplicity of transport, it is recommended to limit the maximum length of the AUV to an ISO shipping container length (Griffiths, 2012).

Therefore, to design an AUV for a specific mission, desired characteristics to perform the mission must be known. Therefore, the mission profile can include the size, speed, depth capability, manoeuvrability, range of operation and energetic costs. By knowing these, the AUV design can be modified for the mission.

7.2 Bio-inspired AUV design

In this research, the attempt is to modify the design of AUVs based on BMSs. However, AUV missions are varied and different to ones of an animal. In addition, as observed in the previous chapters, the superiority of BMSs is spread over a wide range of marine animals and they use different methods and systems which are interrelated with their other functions. This means that no specific BMS is able to fulfil all desired mission profiles of an AUV. In addition, unlike engineered vehicles, BMSs sub-systems are multi-functional, which makes it impossible to investigate them as stand-alone systems. Therefore, from an engineering perspective, it is not a complete BMS that is sought, rather particular sub-systems of BMSs. This was of course unnatural and defined the challenge that this research attempted to overcome.

In addressing this challenge a simple approach could have been to search the database of BMSs and find a BMS which would fulfil all engineering requirements for a specific mission.

As part of the research this simple approach was examined. Consider the algorithm in Figure 7.1 as the system selector for a BUUUV. For each mission scenario, mission requirements were input to the selector and the capabilities of BMSs were gathered in a

large database. These capabilities were then sorted based on fulfilling each mission requirement and the most capable BMSs were extracted.

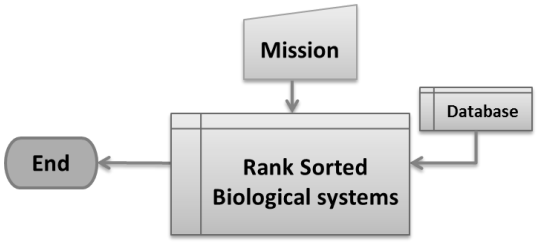

Figure 7.1. Simple algorithm to find best biological option

By implementing this algorithm, it was realised that:

1. For many mission profiles no BMS was fully able to fulfil all the mission requirements
2. Many of the BMSs were excluded from the sorting system due to failing even a single mission requirement.
3. Since overall ranking was calculated based on how much of the mission was fulfilled by the system, in many mission scenarios, systems with close ranks would vary considerably in capabilities.
4. This system only selected the existing best option and did not include any possible "optimisation".

This method therefore provided little useful insight to assist the design of a BUUUV.

7.3 The concept of the Optimum System Selector

Bearing in mind that the aim of this research was not to make a robotic fish, but to take the useful aspect of the BMSs (from an engineering perspective), and use them constructively for engineering purposes. Therefore, means were required to output the appropriate combination for a bio-inspired design based on a particular mission profile. Therefore, the simple algorithm was modified to the Optimum System Selector (OSS). OSS attempts to solve the abovementioned challenges of associating biological capability with engineering requirement.

Figure 7.2 shows the algorithm modified for the OSS. In this algorithm, for every input, the BMS database is compared against the desired mission specifications, similar to the initial algorithm in Figure 7.1. If the requirements are met by any BMS, then the corresponding system is the output. However, for many mission profiles that is not the

case as it was realised with the use of the simple algorithm. Instead the BMSs are ranked based on fulfilling the mission profile.

To optimise this initial generation, a decision maker was used. Nowadays, many methods of optimisation exist.

To decide on a method suitable for the purpose of this research, some considerations have been taken into account. Firstly, as part of this research, a rather large database of BMSs characteristics and performance was developed which includes many different designs with capabilities desirable for AUVs. So it would be preferable to choose an optimisation method which could use the database as part of its process. Secondly, many parameters (inputs) must be considered when defining a mission for an AUV. This requires an optimisation method which could optimise for multiple variables simultaneously. One possible optimisation tool that was investigated in this research which would consider the two abovementioned considerations was Artificial Neural Networks (ANN). It was possible to enter the current BMS database onto the ANN to train it while defining various dependent and independent variables to the network. However, as there are quite a few number of variables involved in the design of an AUV, the dataset required to train the ANN in order to find accurate connection between the inputs and the outputs, was considerably larger that the database that was collected in this research. This would considerably reduce the accuracy of the results produced by the ANN. Another optimisation method which is used in nature is through breeding and evolution. Therefore being inspired by nature, the decision maker was designed to accelerate evolution by using a Genetic Algorithm (GA). At present Genetic Algorithms are widely used in the field of design optimisation (Gen & Cheng, 2000), they can make use of the already developed database and can take into account multiple inputs (variables). Therefore it was decided that GA is the appropriate method to be used when attempting the optimisation of BMSs design.

GAs take an initial potential group as parents and breed a new generation. The off-spring are then evaluated and ones with superior performance are used as new parents for the next generation. The cycle carries on until the desired performance characteristics are fulfilled or until the continuation of the GA will not improve the results any further. In this research, due to numerous influencing factors, there are multiple equations to be solved simultaneously. Therefore, a Multiple Objective Genetic Algorithm (MOGA) was implemented within the OSS.

The desired mission specifications are input as the GA constrains and the BMS subset from the database of existing species is input as the first generation.

The performance characteristics of the first generation (actual BMSs) are calculated and compared against the desired mission profile. The decision maker then generates off-spring of the initial BMSs as a new generation, calculates their performance, and based on the mission input targets, decides which ones survive and the process continues until the desired results are achieved.

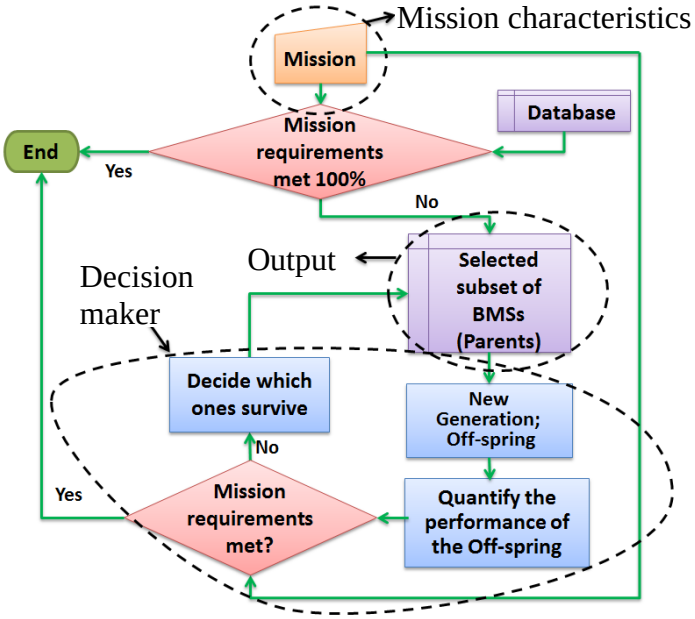

Figure 7.2. The algorithm modified for the OSS

The sub-algorithms of the OSS as indicated by dashed lines in Figure 7.2 are:

- ***The Mission characteristics (Section 7.3.1)***
- ***The Decision maker (Section 7.3.2)***
- ***The Output (Section 7.3.3)***

These are explained next.

7.3.1 The Missions characteristics

The desired AUV mission specifications are specified by the AUV user. These mission specifications are shown in Table 7.1 as input to the OSS. A manoeuvrability factor was included which may be achieved by using bio-inspired flexible bodies techniques as explained in Chapter 6.

The term "importance weight factor" for each mission specification is used to weight it against other inputs when evaluating the overall performance of systems and

making the decision on the optimum off-spring. These are used to derive the weight factor, w_i, in Equation 7.1.

Table 7.1. Mission Inputs

Input	*Sub-input(s)*	*Unit(s)*
Size	Total length *(TL)*	$[m]$
	Mass	$[kg]$
	Payload	$[kg]$
Speed	Optimum speed (U_{opt})	$\left[\frac{m}{s}\right]$
	Maximum speed (U_{Max})	$\left[\frac{m}{s}\right]$
Energetics	Total required power at U_{opt}	$[Watts]$
Endurance	Maximum range	$[km\ or\ h]$
Manoeuvrability	Turning Radius (R_{Yaw})	$[m\ or\ BL]$
Fuel	Battery type	$\left[\frac{MJ}{kg}\right]$
Importance weight factors		

7.3.2 The decision maker

The selected sub-set of BMSs is input to the decision maker where off-spring are produced with optimised performance.

In order to evaluate the performance of each individual (each parent or off-spring) within the GA, the GA code must be able to calculate or estimate the performance characteristics of that individual. Either that is a BMSs or the BUUUV offspring which is the bio-inspired chimera. The analysis of the comparisons made in Chapter 3 as well as the calculations in Chapters 4, 5 and 6 were used within the decision maker to calculate the performance of each individual.

The OSS is based on a genetic modification method, however although each off-spring is a combination of two parents, the off-spring will only survive (still remain in the generation) if it can meet all the criteria though the formula used within the OSS); that is how the new generation is validated.

Optimising the performance of the off-spring consists of minimising the energetic cost of the off-spring, as well as the trade-off between speed and propulsion and manoeuvrability due to the multi-functionality of the BMSs. These characteristics are known for the parents, but they must be calculated for the subsequent generations which are defined by the genetic algorithm. Since the decision maker makes the selection based on the estimated performance of the off-spring, it was crucial to minimise the calculation or estimation error. These calculations were based on the formula and

regression lines derived within this research. Therefore, with improved and more profound knowledge of more BMSs, these can be improved in the future.

As it is explained later in Section 8.2 in Chapter 8, after each iteration of the GA code, OSS plots the fitness function of the elite (the best possible design on that iteration). Therefore, it is visually clear whether the OSS is reaching to a conclusion or not as if it is not reaching a conclusion, the fitness function of the elite will not improve. The code can be run in two different modes in order to deal with an "impossible mission" situation. Firstly, as most of the runs with the OSS have reached an answer before the 30 iteration, it is possible to put a maximum number of iterations for the OSS (e.g. 100). In this mode when the OSS reaches the maximum iterations, it will stop running and as usual present the user with the data sheet including the details of all offspring in every iteration, the elite in each iteration as well as the final fitness function of the final elite. Therefore, by looking at each component of the overall fitness function it will be clear which desired capabilities have not been met.

Secondly, the OSS can be run while a limit has been set for the change in the fitness function of the elite; i.e. the OSS will stop running if the fitness function has not improved after a certain number of iterations. Similar to the first mode, it will be clear which desired capabilities have not been met by refereeing to the output data sheet. The details of the calculations and estimations within the decision maker are explained in Section 7.4. As the characteristics of the BMSs were known, all the formulae defined and used in this research were tested against the first generation of BMSs to ensure their validity.

7.3.3 The Output

The final off-spring generation produced by the decision maker is sorted in order by using linear programming which uses a Fitness Function (*FF*) (Kreyszing, 1999) in the form of:

$$a_1 w_1 + a_2 w_2 + \cdots + a_n w_n = FF \qquad 7.1$$

Where w_1 is the importance weight factor of each parameter and a_i is calculated as:

$$a_i = \frac{|Value_{Obtained} - Value_{Desired}|}{Value_{Desired}} \qquad 7.2$$

e.g. for speed a_i is calculated as:

$$a_i = \frac{\left|U_{off-spring} - U_{Desired}\right|}{U_{Desired}} \quad 7.3$$

Note that if the performance is better than what is required, e.g. the speed is higher than the desired speed, a_i will be set to zero. This means, there is no penalty for performing better than expected. Therefore, the GA attempts to find the design for which FF is zero.

The sorted collection will output specifications for body geometry, control surfaces & propulsion method and an estimate of speed and energetic cost. Outputs are shown in Table 7.2.

Table 7.2. Outputs of the OSS

Output from the OSS	Sub-Outputs	Unit
Size	TL, EL, BH, BW	$[m]$
	Mass	$[kg]$
	Payload	$[kg]$
	Fuel Mass, Muscle Mass	$[\%\ Mass]$
Speed	Propulsion mode	-
	U_{opt}, U_{max}	$\left[\frac{m}{s}\right]$
	Finbeat frequency [(2)]	$[Hz]$
Manoeuvrability	Flexibility Measure	-
	Turning Radius	$[m]$
Control surfaces [(1)]	Chord and Span of each fin	$[\%\ TL]$
	Aspect ratio of each fin	-
Energetics & Endurance	COT	$\left[\frac{J}{kg.m}\right]$
	Required power at U_{opt}	$[Watts]$
	Maximum range (at U_{opt})	$[km]$
Efficiency	ξ_{opt}	-

[(1)] The control surfaces are important for stability, diving and surfacing, propulsion & manoeuvring

[(2)] By knowing the speed, the frequency can be calculated from the regression lines in Table 5.2

As previously mentioned, the OSS is at its concept stage. However, implementing the BUUUV will be similar to AUVs with different technologies mentioned in this research. For example, the body form can be made from the dimensions obtained by the

OSS as the structure mass is accounted for within the OSS. Flexible materials have already been considered for biomimetic AUVs. However, another idea for introducing flexibility is to use inflexible material for the hull with flexible hinges depending on the swimming mode proposed by the OSS. For example, if the recommended swimming mode is Thunniform, two hinges are required; one at one third of the aft body length which is where the Thunniform bodies have the flexibility to move the rear fin, and the other at about one third fore body length where the head of the species moves. The mass of the sensors and payload is accounted for by an input to the OSS and the hotel load considered based on the hotel load of an AUV. Finally, artificial muscles operating with batteries will be used instead of motors.

Thus it is possible to implement the bio-inspired concept in a manner similar to traditional AUVs with different technologies and design approaches.

7.3.4 A note on breeding and mutation within the GA

Surviving parents in each generation within the GA must be combined or bred with one another to produce the off-spring. There are two main approaches to this. The characteristics of each parent can be considered as a binary code. In this approach the combination or "crossover" of two parents is performed by swapping a few *bits* within the binary code of one parent with the other to make two new children.

The second method handles real values as the characteristics of patents. Consider parents X and Y. The characteristics of each parent are represented as:

$$X = x_1, x_2, \dots x_n \quad \text{and} \quad Y = y_1, y_2, \dots y_n$$

where each x_i is a characteristics of parent X and each y_i is a characteristics of parent Y.

To breed the two parents, a random value between 0 and 1, r_i, is used for each characteristic. Therefore the i^{th} characteristic of the two new off-spring, U and W, are defined as below (Mühlenbein & Schlierkamp-Voosen, 1993):

$$u_i = r_i\, x_i + (1 - r_i)\, y_i \quad \text{and} \quad w_i = (1 - r_i)\, x_i + r_i\, y_i$$

As in this research, the characteristics of BMSs are real values, the second method was used within the OSS.

Another term used in GAs is "Elitism". This is where the best performing individuals (i.e. the ones with the smallest *FF* values in the OSS) are moved to the next generation directly without breeding. These individuals are known as the "Elite". The number of the elite can be altered to find the optimum number which will result to the

answer in the least amount of time. In this research the number of elite was considered as 2% of the total population. This value was found by analysing the results of the OSS. For a specific run, it took the OSS 150 seconds to give the final output when the elite was set to 2% while at elite =5% the same run took 6 minutes.

Similar to evolution some off-springs in some generations might mutate. In order to reflect this within a genetic algorithm, a mutation probability as well as a mutation amount was defined that the characteristics of an individual will mutate with that probability. It is standard for the mutation amount to be $\mp 10\%$. Therefore, this value was tested within the OSS. Mühlenbein & Schlierkamp-Voosen, 1993, mentioned that the mutation factor can be considered as $\frac{1}{n}$ where n is the number of characteristics of the parents which can be mutated. However as multiple functions had to be satisfied in the OSS and some characteristics were dependent on others, a mutation value has not been recommended for this situation. Therefore different values of mutation probability were tested and by analysing the data is was realised that the optimum value was $\frac{1}{3}$. A specific run took 37 seconds and 12 iteration to reach the final output with mutation probability of $\frac{1}{3}$ while the same run for mutation probabilities of $\frac{1}{2}, \frac{1}{4}$ and $\frac{1}{10}$ took 50, 58 and 118 seconds with 15, 17 and 28 iterations respectively, while all resulted in similar outputs.

7.4 The details of the decision maker within the OSS

Is section 7.3.2 it was briefly explained that the decision maker within the OSS uses the conclusions obtained in this research to estimate the performance of the off-spring. In this section, the calculations involved within the decision maker are explained in detail. These are required to calculate the fitness function for each individual which will determine their survival and eventually the BUUUV design for a specific mission profile. These parameters must be calculated for each individual.

- ***Mass and payload (Section 7.4.1)***
- ***Speed: U_{opt} and U_{max} (Section 7.4.2)***
- ***Energetics: COT_{opt}, $Range_{max}$ and ξ_{opt} (Section 7.4.3)***
- ***Manoeuvrability: R_{yaw} (Section 7.4.4)***

These are each explained next.

7.4.1 Mass and payload

The volume of each individual was calculated from Equation 3.2 $\left[V_{BMS} = \frac{\pi}{6}(EL \times BH \times BW)\right]$ based on a tri-axial ellipsoid. Then, by knowing the water density, mass was calculated. Note that for the first generation, which comprises the real BMSs, a "true tri-axial ellipsoid" factor is defined to compensate for the difference between the body of the BMS and the equivalent tri-axial ellipsoid. However, the off-spring are considered a true tri-axial ellipsoid. Therefore there are no correction factors.

As per Table 2.8 in Chapter 2, it was realised that although the mass of the muscle and fat varies for different BMSs, the sum of the two is within a similar range between very diverse species. The sum changed between 52% and 57%. Therefore as the average, the sum of fat and muscle contribution to the total mass is considered to be 55% across all BMSs. Considering the values presented in Table 2.8, this estimation is justified. Data of the percentage of body fat for BMSs were obtained from the literature. If the data was not available for a BMS, the values of BMSs which were either genetically similar or with the same swimming modes were used. The amount of fat varies between individuals of the same species and even for an individual it depends on many parameters such as the time of the year. Therefore the value is an average value for each species.

Payload which is a critical factor in the operation of some AUVs is not defined for BMSs. Therefore, to adjust payload for the bio-inspired design, as shown in chapter 2, the mass of BMSs' organs which are not required for an AUV - mainly the guts - are considered as payload. For the off-spring (BUUUVs), it is assumed that they use muscles (or in future, artificial muscles which are available) rather than motors. However, the muscle is considered as a standalone part, unlike animal muscle which depends on other organs (such as the organs in the guts) for survival. The reason for this assumption is that any existing artificial muscle is a standalone part. Therefore, the organs in the guts and their mass are ignored for the off-spring.

Table 7.3 demonstrates different corresponding body parts of AUVs and BMSs. As per Table 2.8 the average payload was estimated as 11% of total body mass. However, as within the OSS it is possible for the amount of fat to change (mutate) from one generation to the other, therefore it was considered that the sum of muscle mass, fat mass and payload should remain constant at 66% (55% +11% = 66%).

Table 7.3. The corresponding body parts between AUVs and BMSs

AUV	BMS
Structure + Outer shell + Control surfaces	Bone structure + Skin+ Fins
Motor	Muscle
Battery	Fat
Payload including sensors and control systems	Corresponding payload including brain, eyes and guts

7.4.2 Speed: U_{opt} and U_{max}

To precisely calculate the optimum and maximum speed of each individual within the OSS, a sophisticated method considering the thrust produced by the oscillation or undulation of the fin and body of the flexible BMS must be developed. Moreover, all the control surfaces of not only each species but each individual must be known. As an example, as shown in Figure 7.3 there are several Chum Salmons in the Subcarangiform group with relatively similar sizes (masses) and yet very different optimum speeds. Similarly, in Figure 7.4 several Atlantic mackerels (*Scomber scombrus*) of similar lengths have different speeds. Therefore, predicting the speed must be either based on thrust which requires details of the body and control surfaces of each individual, or based on experimental results which was not available for all BMSs and not feasible to do within the scope of this research.

Therefore, it was decided, for the purpose of the OSS to predict the speed as a function of size and more specifically the total length. These are shown in Figures 7.3 and 7.4. The equations of the regression lines in the two figures are available in Tables 7.4 and 7.5. Acknowledging the variance between the R^2 values obtained for the regression lines of different swimming modes and BMS groups, in general, the regression lines were in good agreement with the data and therefore using the regression lines provided sensible estimation of optimum and maximum speeds. Within the OSS, in order use the appropriate equation in Table 7.4 and similar equations which are related to different groups of BMSs, the taxonomy coding which was proposed in Chapter 2, Section 2.2 was used.

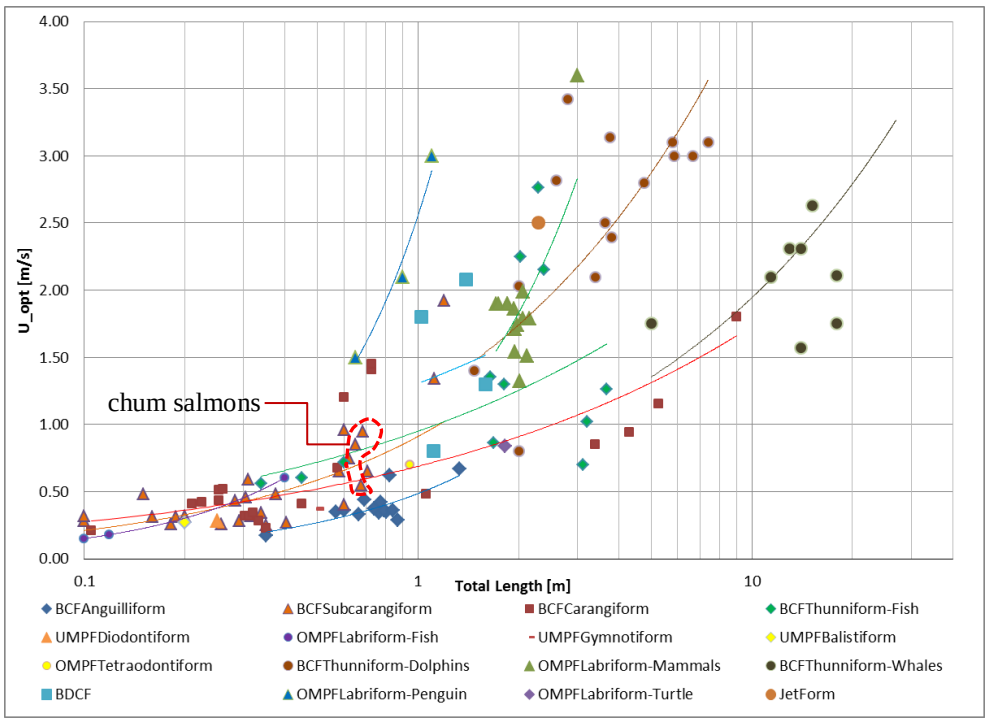

Figure 7.3. U_{opt} as a function of total length for various species. The Subcarangiforms within the red dashed line area are the chum salmons (*Oncorhynchus keta*)

Table 7.4. The equation of the regression lines for U_{opt} as a function of TL

Swimming mode	Regression line equation	R^2 value
Anguilliforms	$U_{opt} = 0.4849\{TL\}^{0.8518}$	0.607
Subcarangiforms	$U_{opt} = 0.9104\{TL\}^{0.6365}$	0.603
Carangiforms	$U_{opt} = 0.6882\{TL\}^{0.4008}$	0.560
Thunniform-Fish	$U_{opt} = 0.9494\{TL\}^{0.4007}$	0.353
Diodontiform	$U_{opt} = 1.12\{TL\}$	
Labriform-Fish	$U_{opt} = 1.5167\{TL\}^{1.004}$	0.999
Gymnotiform	$U_{opt} = 0.74\{TL\}$	
Balistiform	$U_{opt} = 1.35\{TL\}$	
Tetraodontiform	$U_{opt} = 0.741\{TL\}$	
BDCF	$U_{opt} = 1.3042\{TL\}^{0.3217}$	0.03
Thunniform-Whales	$U_{opt} = 0.5845\{TL\}^{0.5217}$	0.347
Thunniform-Dolphins	$U_{opt} = 1.1907\{TL\}^{0.5477}$	0.459
Labriform-Sea lion	$U_{opt} = 0.8658\{TL\}^{1.0787}$	0.413
Labriform - Penguins	$U_{opt} = 2.5556\{TL\}^{1.2903}$	0.977
Labriform - Turtles	$U_{opt} = 0.462\{TL\}$	
Jetform - Squids	$U_{opt} = 1.087\{TL\}$	

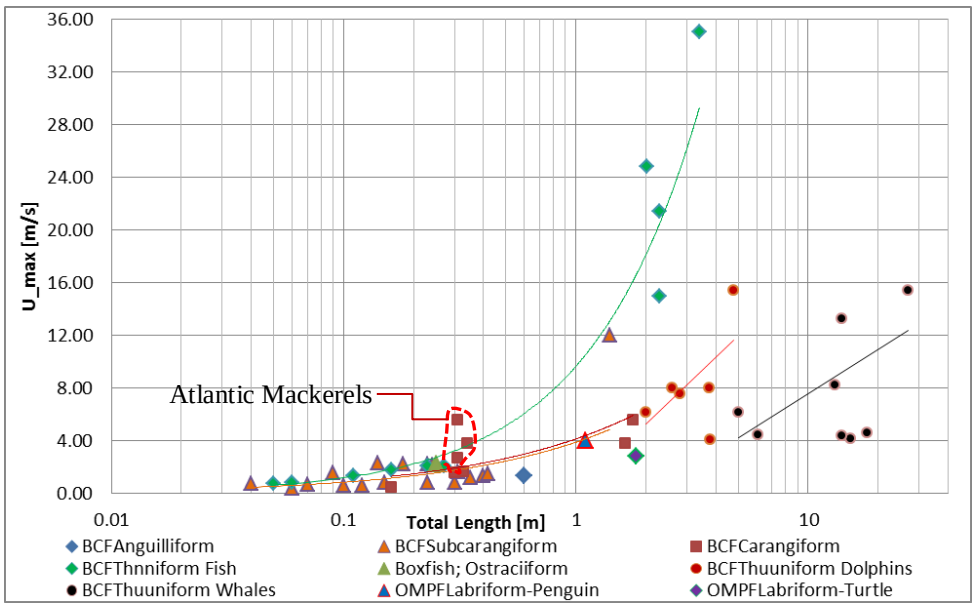

Figure 7.4. U_{max} as a function of total length for various species. The Carangiforms within the red dashed line area are the Atlantic mackerels (*Scomber scombrus*). In order to be able to associate the regression line for Carangiforms to larger BMSs as well, data of the maixmum speed of two lemon sharks (*Negaprion brevirostris*) was added to the plot (Sundstrom et al., 2001)

Data on maximum speed of fish with swimming modes which make use of fins other than the rear fin have not been thoroughly measured previously, maybe due to the fact that these fish are not associated with fast swimming. Moreover, by observing a video of a striped surf perch (*Embiotoca lateralis*), it was realised that although the fish uses a Labriform swimming mode for sustained speed, at burst speeds it in fact uses a Subcarangiform swimming mode. Therefore, as specific data on the maximum speed of fish with not rear fin propelled swimming modes have not been available to this research, the regression lines of Subcarangiform or Anguilliform swimming (for fish with *FR* similar to eels and Amiiform or Gymnotiform swimming modes during sustained swimming) have been used within the OSS. The one exception is the boxfish (*Ostracion meleagris*) for which maximum speed data is available. The boxfish has an interesting swimming technique. The boxfish has almost a Diodontiform swimming mode during sustained swimming. However, as its body is inflexible, it is unable to undulate or oscillate the body when swimming fast. Therefore instead it only oscillates the rear fin and swims with an Ostraciiform mode when sprinting. As demonstrated in Figure 7.4, the boxfish data fits well with the Thunniform regression line.

Table 7.5. The equation of the regression lines for U_{max} as a function of Total Length

Swimming mode	Regression line equation	R^2 value
Anguilliform-Eel	$U_{max} = 2.267TL$	
Subcarangiform	$U_{max} = 3.8832TL^{0.662}$	0.53
Carangiform	$U_{max} = 4.1322TL^{0.6358}$	0.41
Thunniform fish	$U_{max} = 9.6472TL^{0.9073}$	0.98
Whales	$U_{max} = 0.3722TL + 2.3665$	0.33
Dolphins	$U_{max} = 2.3033TL + 0.6454$	0.36
Labriform - Penguin	$U_{max} = 3.618TL$	
Labriform - Turtle	$U_{max} = 1.538TL$	

7.4.3 Energetics: $COT_{U_{opt}}$, Required power, $Range_{max}$ and ξ_{opt}

As U_{opt} was estimated in section 7.4.3, ξ_{opt} was calculated from Equation 5.19 $\left[\xi_{Uopt} = \frac{1.8bU_{opt}{}^{2.8}}{P_H}\right]$. If the OSS was to output a BMS chimera, the P_H would be estimated from the BMSs' regression line equations in Table 4.1. If on the other hand the OSS was to output a BUUUV, the regression line for an AUV of the same size has been used.

For the BUUUV output, the fuel used is battery, similar to AUVs. The type of the battery can be chosen as well. However, within the OSS for both the BMS output and the BUUUV output, muscles are considered as actuators. Although, OSS is at a concept stage, it is a fact that muscles can be stimulated with electricity and as it is explained in Section 8.4 in Chapter 8 many examples of artificial muscles already exist.

As both ξ_{opt} and U_{opt} were known, the *COT* at optimum speed which was also the minimum *COT* was then calculated by using Equation 5.20 $\left[COT_{U_{opt}} = \left(\frac{2.8}{1.8}\right) \times \left(\frac{P_H}{\{\text{Mass}\}U_{opt}}\right)\right]$. Consequently, the total required power at U_{opt} is calculated as $Power_{U_{opt}} = COT_{U_{opt}} \times U_{opt} \times \{Mass\}$.

In order to calculated maximum range $[km]$, the maximum Endurance $[h]$ measured at U_{Opt} needed to be calculated. Endurance was calculated form Equation 4.20 $\left[Endurance_{max} = \frac{Stored\ Energy}{COT_{opt} \times U_{opt} \times Mass} \times 1000\right]$. Within the OSS there is the capability to either use animals fat or different types of batteries usually used for AUVs as fuel. By knowing the amount of fat, the stored energy $[kWh]$ was calculated from Equation 4.19 $\left[Stored\ Energy = \frac{\{Mass\}_{fat} \times E_{fat}}{3600}\right]$.

Finally, maximum range was calculated by inserting Equations 4.13 and 4.14 in Equation 4.18 $\left[Range_{max} = U_{opt} \times Endurance \times 3600\right]$:

$$Range_{max} = \frac{\{Mass\}_{fat} \times E_{fat}}{COT_{opt} \times \{Mass\}} \times 1000 \qquad 7.4$$

As the main purpose of the OSS is to output BUUUV design aspects and characteristics, a list of batteries commonly used in AUVs is available to choose instead of BMSs fat. If a battery type is selected, $Range_{max}$ is calculated based on the battery capacity instead.

7.4.4 Manoeuvrability: R_{yaw}

As explained in Chapter 6, the turning capability of BMSs is related to their flexibility. Therefore the Flexibility Measure (*FM*) for each individual was estimated from Table 6.1. In order to be able to define flexibility for the off-spring within the OSS, it was decided that when breeding two parents, the child would get the swimming mode and therefore the taxonomy code of one parent. Therefore the same formula for *FM* was used for the child. By knowing the *FM*, $R_{yaw\ TL}$ was estimated from the Equation 6.1 $\left[R_{yaw\ TL} = 2.7999\, FM\right]$.

7.5 A note on stability, depth and future work

OSS has been written to find aspects of the Bio-inspired Unmanned Untethered Underwater Vehicle (BUUUV) design matching the mission inputs as per Table 7.1 and to output parameters as per Table 7.2. It is however possible to modify the OSS to consider other factors such as depth and stability. The mechanisms of BMSs buoyancy control and depth capabilities require further research. When sufficient knowledge is gathered on the depth capability of BMSs, the OSS will be able to include depth as another parameter.

Another possible future work is considering stability. At present stability is not considered within the OSS as stability has not been a focus of this project considering manoeuvrability in some degrees contradicts stability. For example, if a BMS is highly flexible in yaw axis, it is certainly unstable in that axis as it has a tendency to turn. However, if a measure of stability is known for a specific mission, it can be added as another influencing factor within the OSS. Both the body design and the control

surfaces can affect stability at different axis. Increasing the $\frac{BW}{BH}$ value will increase the upright stability. Side fins are used to provide life during diving and surfacing as well as roll stability. The top and bottom fin can also provide roll and yaw stability but would negatively affect the manoeuvrability in yaw axis. The body design can also be altered to give the body more stability. Therefore increasing the surface area of those fins will have a positive effect on stability but would also increase the drag. Therefore, there is always a trade-off between manoeuvrability and stability.

Within this chapter a method was presented to predict some aspects of BUUUV design based on bio-inspired knowledge. OSS would predict a different design for each mission profile. This could also be studied with an evolutionary approach. As the data of each generation is available with every run of the OSS, it can be observed how the BMS design would evolve into a BUUUV design with different mission profiles.

The analysis of the results obtained from the OSS is discussed in the next Chapter, 8, followed by the conclusions chapter of this thesis, Chapter 9.

Chapter 8. The Optimum System Selector in action

In Chapter 7 the concept of an Optimum System Selector (OSS) was explained which is designed to output some aspects of the design of a BUUUV based on bio-inspired knowledge while considering a mission profile.

In this Chapter, the details of the program are discussed, the program is verified and an AUV mission is set as input for the OSS and the result analysed to realise to what extend the design has been modified.

The OSS is a new concept in bio-inspired design and therefore at its early stages. Therefore with further bio-inspired research work, the code can be modified and also applied to other sectors.

As explained in Chapter 7, there are three main parts within the OSS: the mission characteristic, the decision maker and the output.

When the OSS is run, a page is presented to allow for the mission characteristics to be defined. A screenshot of this page is displayed in Figure 8.1. The constraint and importance of each characteristic can be defined and it can be decided whether to output BUUUVs or BMS chimeras. The main difference between BUUUVs and BMS chimeras is in the hotel load calculation and the gills drag. If BUUUVs are selected, the hotel load will be calculated from the AUVs regression line in Table 4.1 and there will not be any gills and therefore no gills drag. If batteries are chosen as fuel, there are nine types of batteries commonly used for AUVs which can be selected. However, if another type of fuel is required, the specific energy can be input as well.

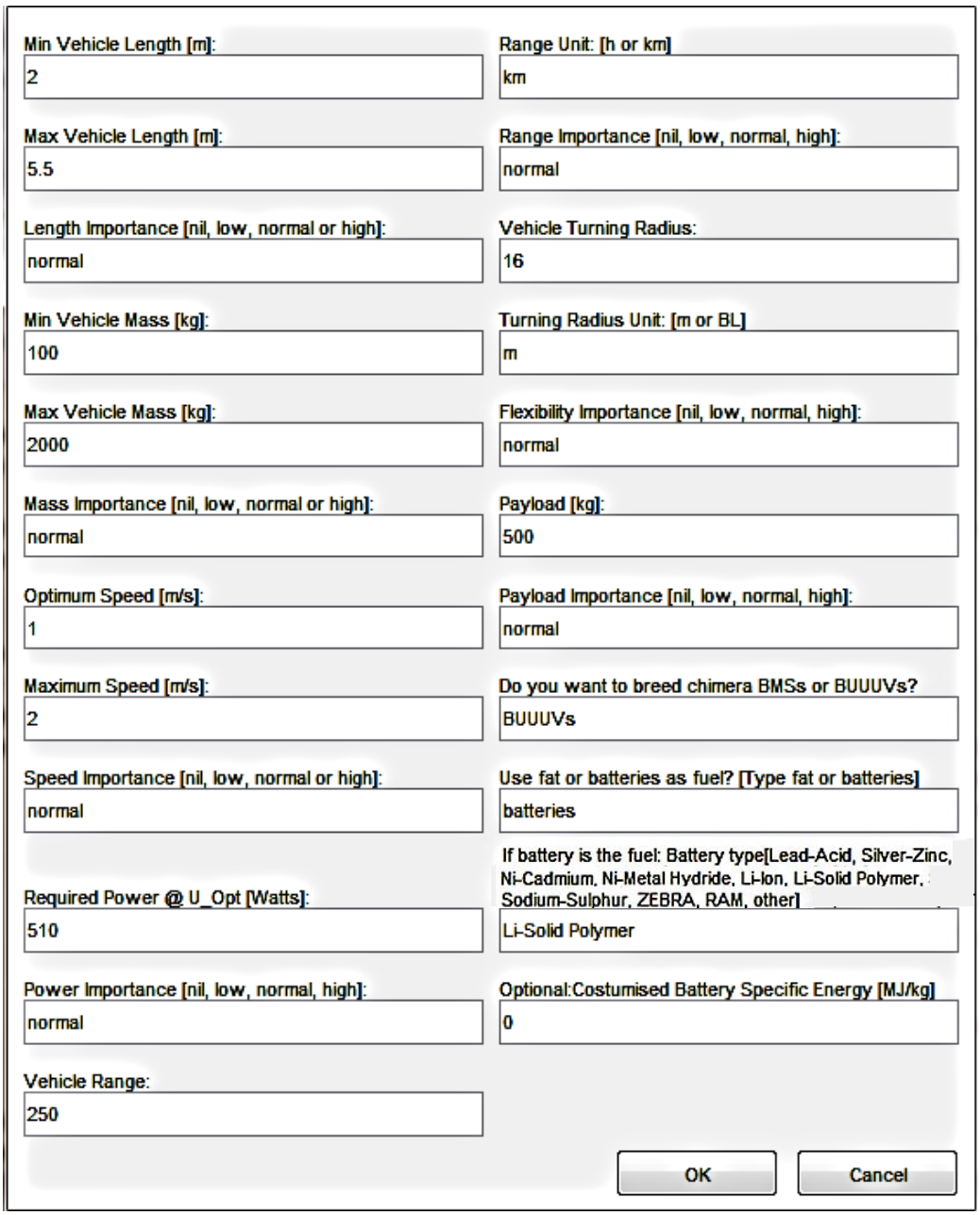

Figure 8.1. A screenshot of the mission input page within the OSS

8.1 OSS validation

As explained in Section 7.3 in Chapter 7, as well as the mission profile, the real BMSs are input to the OSS as the first generation. For the first generation the OSS then calculates their performance characteristics. In order to validate the performance of the OSS, the characteristics calculated by the OSS for the first generation were compared to the performance characteristics of the original BMS.

OSS writes the mission profile, results of each iteration including the design of each individual as well as their fitness at each iteration to an excel file. It also writes the elite of the iteration and the final output as well.

In order to perform a validation, in the mission selection page, the breeding was set to BMSs and the fuel to fat. 60 BMSs from different taxonomy classes and various swimming mode for which all the required data (body and control surfaces dimensions, fat and muscle mass, swimming mode and taxonomy) was available, have been set as the first generation.

Therefore, after running the OSS, the results of the calculation made for the first iteration were the performance characteristics for the real BMSs. The mass, U_{opt} and U_{max}, R_{Yaw} and $Power_{U_{opt}}$ obtained from the OSS were compared with those from literature for BMSs for which the data were available.

The OSS calculated the mass exactly the same as the mass of each BMS. For the other 4 characteristics, the calculated vs. literature values are plotted in Figures 8.2 – 8.5. The x-axis on all plots is the number of the BMS within the initial generation. The BMSs are listed based on their taxonomy. Therefore BMS number one is a silver eel (*Anguilla anguilla*), while BMS number 60 is a squid (*Taningia danae*).

The OSS calculated both U_{opt} and U_{max} values for all classes of BMSs based on the regression lines in Tables 7.3 and 7.4. In overall, the OSS follows the trend very well.

For the U_{opt} the data with obvious differences (as shown in Figure 8.2 by green dashed ovals) are for the blue whale (*Balaenoptera musculus*) (1) and the tunas (*Thunnus albacares* and *Thunnus thynnus*) (2), both of which had higher speeds than other BMSs in the same group based on the literature. Moreover, the blue whale was considerably larger than all other whales. The regression lines used to calculate speed were generalised for all the BMSs within a group, hence the difference in results for the outliers.

As for the U_{max} the two obvious difference were again for the Blue whale and the bluefin tuna (*Thunnus thynnus*). The speed was under predicted for the blue whale and over predicted for the tuna due to the fact that the speediest BMSs are within the Thunniform fish group such as the sailfish or the marlin. There is also always the possibility that the value from literature was not the true maximum speed of the tuna.

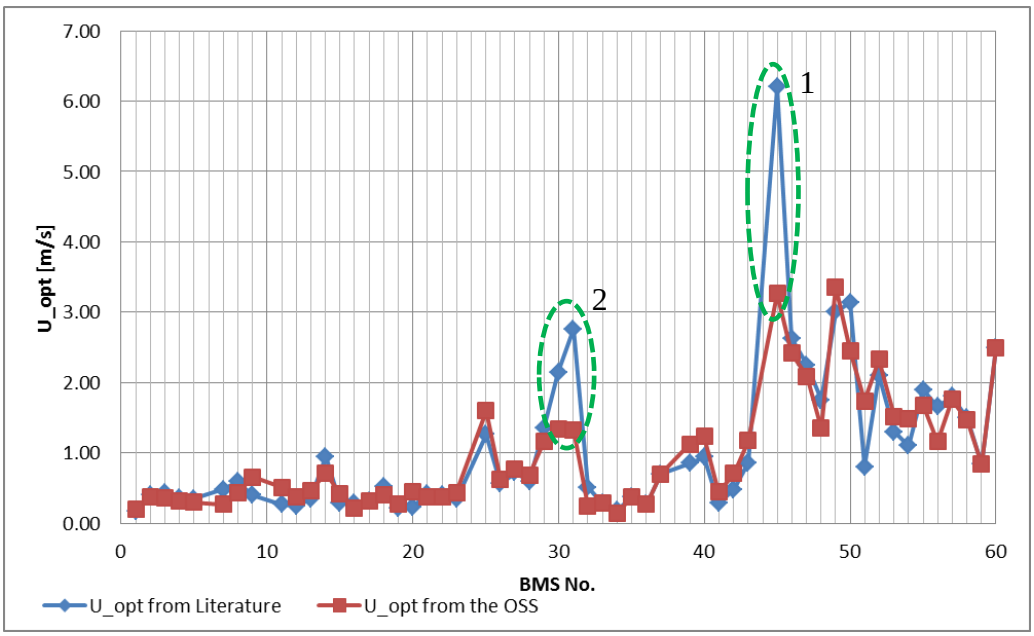

Figure 8.2. U_{opt} calculated by the OSS vs. the values from literature for various BMSs used as the first generation

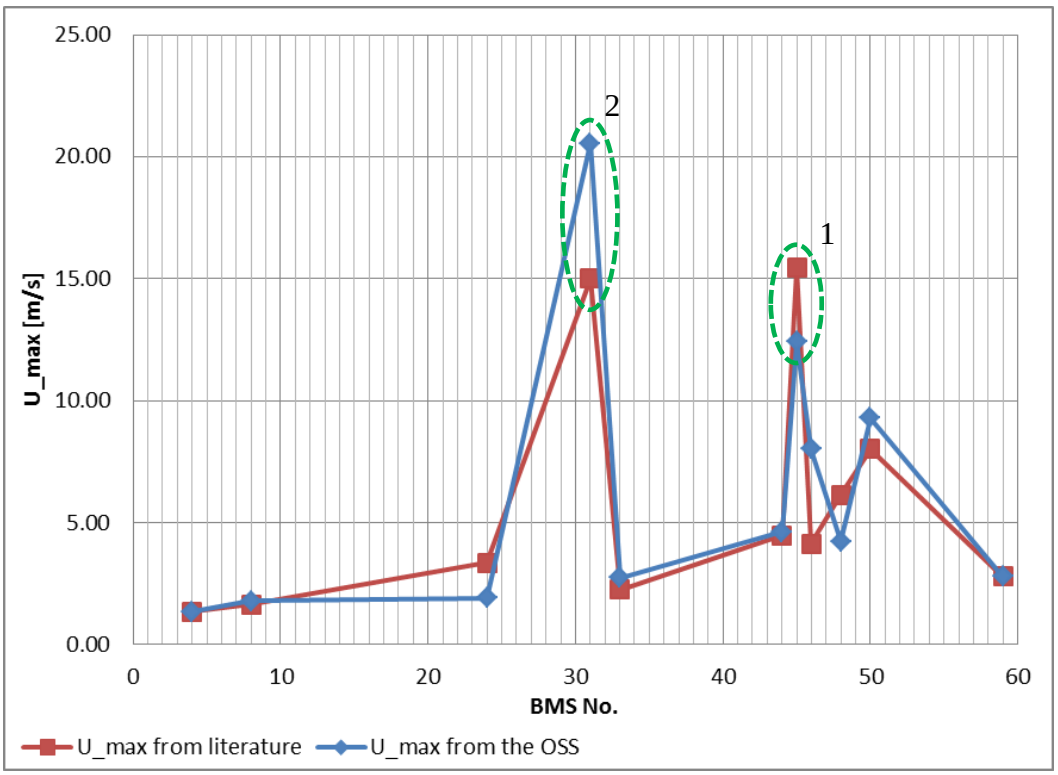

Figure 8.3. U_{max} calculated by the OSS vs. the values from literature for various BMSs used as the first generation

As demonstrated in Figure 8.4, the relative turning radius calculated by the OSS is very close to the data from literature with the mean error of $0.04TL$ over the range of all BMSs.

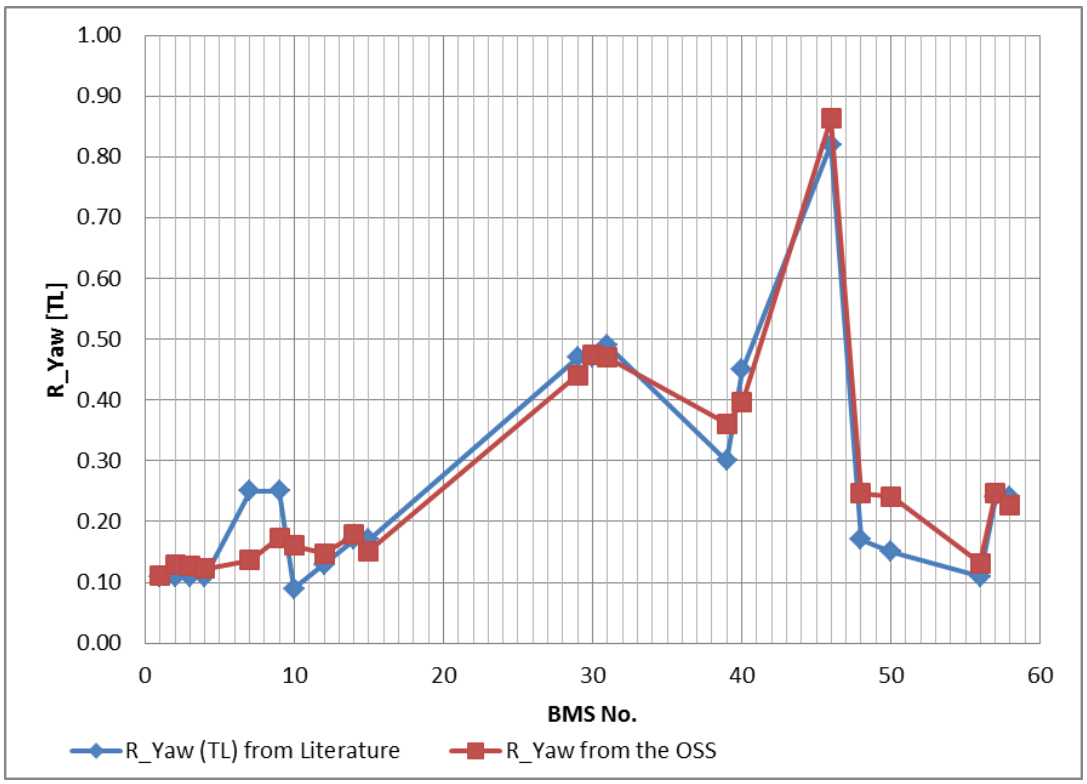

Figure 8.4. R_{Yaw} calculated by the OSS vs. the values from literature for various BMSs used as the first generation

As for the total power at optimum speed, the OSS again follows the trend well and the calculated results are close to the ones in literature in except for the data in the green dashed oval. These data all belong to marine mammals and the reason for the large difference is due to the under prediction of the hotel load. As explained in Chapter 4, the best hotel load regression line for marine mammals is that of Kleiber. However, the line usually under predicts the data as hotel load for BMSs in the field is higher than those tested in a laboratory under very specific conditions. Having noticed that, the uncertainties with the hotel load prediction does not affect the performance of the OSS when set to output a BUUUV as the hotel load will be calculated based on the regression line of AUVs' hotel load.

The performance of the OSS in calculating the performance of the BMSs was successful and therefore it was used to output a design based on a specific mission.

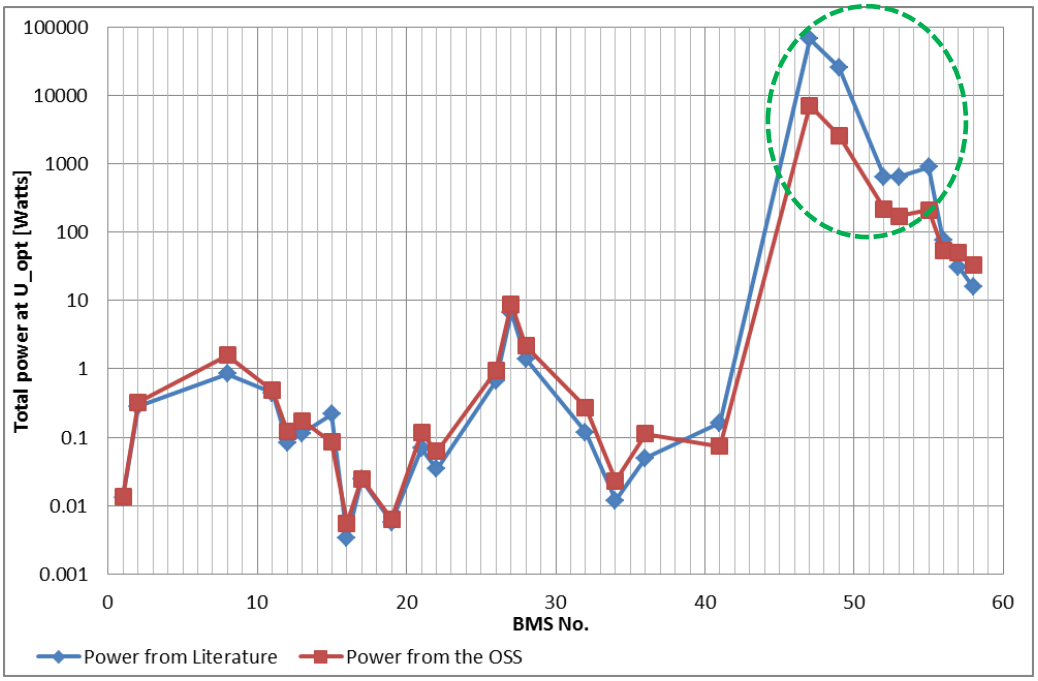

Figure 8.5. $Power_{U_{opt}}$ calculated by the OSS vs. the values from literature for various BMSs used as the first generation

8.2 An important note on normalising the components of the Fitness Function

In Chapter 7, it was explained that in general a fitness function made of multiple functions to be satisfied (zeroed in the case of the OSS) is formed as Equation 7.1 $[a_1w_1 + a_2w_2 + \cdots + a_nw_n = FF]$ were a_i is calculated as per Equation 7.2 $\left[a_i = \frac{|Value_{Obtained} - Value_{Desired}|}{Value_{Desired}}\right]$. Within the OSS, the *FF* comprises of 8 functions which related to TL, *Mass*, U_{opt}, U_{max}, $Power_{U_{opt}}$, Range, R_{Yaw} and payload. Therefore, $i = 8$. However, the values and ranges for each function are different. Therefore, these must be normalised. To normalise all functions, the maximum calculated value away from the desired value was found for each function and the maximum error was set to 1. The error for each individual was then calculated based on maximum error, as follows:

$$a_{i_{norm}} = \frac{\frac{|Value_{Obtained} - Value_{Desired}|}{Value_{Desired}}}{\frac{|Value_{maximum\ error} - Value_{Desired}|}{Value_{Desired}}} \quad 8.1$$

where $a_{i_{norm}}$ is the error value or the fitness value for function *i*.

For example, if the maximum desired BUUUV length was set to $5\,m$ but the maximum length for an individual was $33\,m$, the maximum error would be $\frac{|5-33|}{5}$. As

this value is the highest error, it was set to 1. Therefore, another individual with a length of 7 m would have a normalised error value of $\frac{\frac{|5-7|}{5}}{\frac{|5-33|}{5}} = 0.07$.

There are two ways to use the normalised method. Either use the ranges of values for the first generation and keep it for the entire run or change the normalised error for every generation. Both methods were tested within the OSS. OSS is set to plot the Fitness Function of the three best designs in each iteration. This is helpful as it demonstrates in real-time how the OSS is behaving and operating towards the final output. Having three best elite is useful to make sure the ranking of best individuals is done correctly.

Figure 8.6 demonstrates the performance of the OSS for the same mission profile run with constant normalised fitness (Figure 8.6 A) vs. changing normalised fitness (Figure 8.6 B). In the *FF* vs. iteration plots made by the OSS, the green line belongs to the best individual; the red line belongs to the second best individual and the blue line to the third best

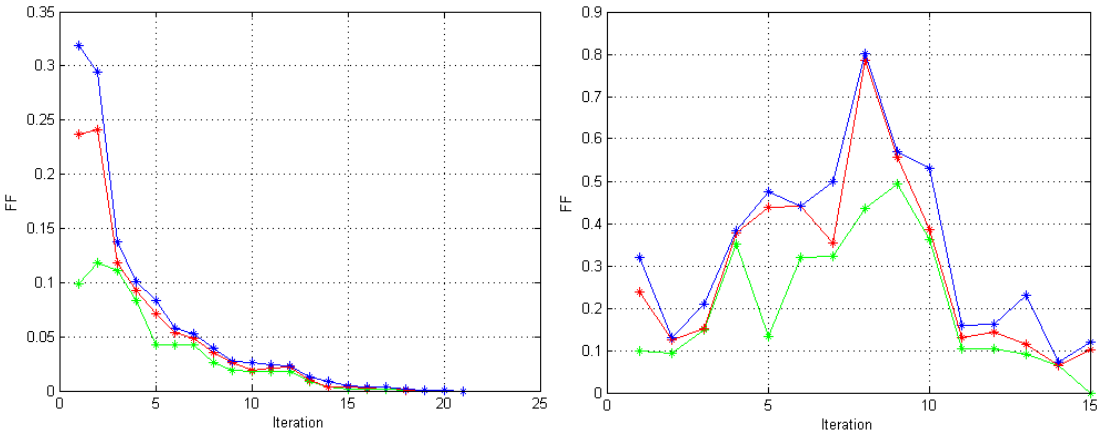

(A) (B)

Figure 8.6. The Fitness Function of the three best individuals plotted at each iteration. A is when the normalised fitness is constant and B when it changes at each iteration with the data range

The final output of the OSS is very similar for both runs. The design had the same swimming mode, fuel mass and very similar specifications. However, it took (A) 21 iterations and 76.6 seconds to get the results while (B) did it in 15 iterations and 47.6 seconds.

In (B) it might seem like the *FF* is worsening in some iterations, however this is not the case. As the normalisation is changing and the individuals are getting closer to the final result, the maximum error is reduced and therefore a smaller deviation from

desired values results in larger penalties. Therefore, the runtime of the OSS with changing normalised fitness was faster.

Then a similar mission profile was used as input, however in this run, the mission characteristics were set within a considerably more limited ranges. Table 8.1 demonstrates the different mission characteristics of the two mission profiles. The upper ranges of length and mass were kept the same to match the size of AUTOSUB6000 and the turning radius was reduced considerably.

Table 8.1. The difference in the mission profiles of the first and second test

Characteristic	First test	Second (more restricted range) test
Total Length $[m]$	2 -5.5	4.5 – 5.5
Mass $[kg]$	100 – 2000	1800 - 2000
Turning Radius $[m]$	< 16	< 4

Similar to the runs presented in Figure 8.6, the results from constant normalised errors and changing normalised error were very similar. However, in this test as shown in Figure 8.7, the constant normalisation reached the results in 19 iterations compared to 25 of changing normalisation. The reason being that when the range is limited, a very small variance from the desired value, will be penalised with a high value and this would make it more difficult for the OSS to reach the final output. However, both runs in the second test took longer than the first one. This indicates that when OSS is given a larger range for mission inputs it operates more efficiently.

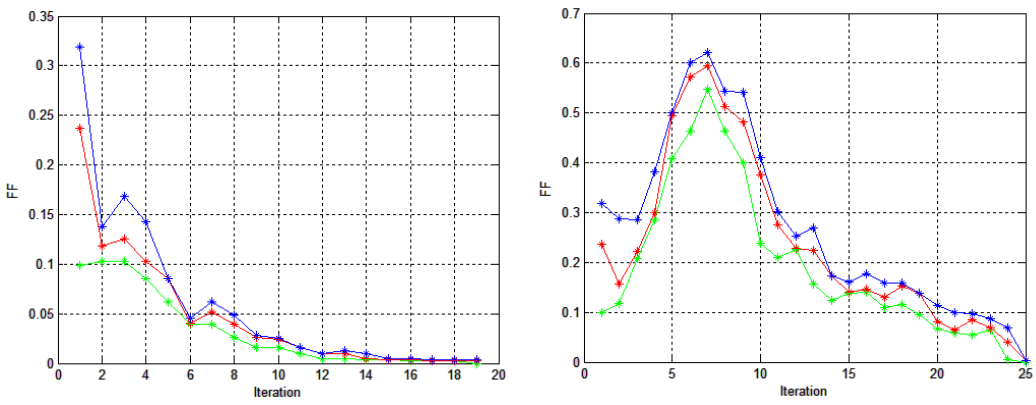

(A) (B)

Figure 8.7. The Fitness Function of the three best individuals plotted at each iteration for the AUTOSUB mission with stricter mission profile. “A” is when the normalised fitness is constant and “B” when it changes at each iteration with the data range

8.3 OSS output vs. AUTOSUB6000

After testing the OSS results against the performance characteristics of real BMSs and verifying that it was capable of predicting their performance characteristics with good accuracy, the OSS was used for its main purpose which was to predict the design and characteristics of a BUUUV. The mission characteristics were based on the mission profile of AUTOSUB6000. AUTOSUB6000 is used as the data for the vehicle was available through the collaboration with the National Oceanography Centre (NOC).

The main characteristics corresponding to the mission profile of AUTOSUB6000 are as shown in Figure 8.1. The OSS was run with that mission profile. The optimum design from the OSS was compared with the characteristics of AUTOSUB6000 as shown in Table 8.2.

Table 8.2. The performance and main body characteristics of BUUUV vs. AUTOSUB6000

Characteristic	AUTOSUB6000	BUUUV 2300103902* from the OSS	Improvement [%] $\frac{\lvert \boldsymbol{BUUUV - AUTOSUB} \rvert \times \mathbf{100}}{\boldsymbol{AUTOSUB}}$
Total Length [$\boldsymbol{m}$]	5.5	4.7	14.5
Mass [$\boldsymbol{kg}$]	2000	1927	3.7
Payload [kg]	500	533	6.6
Cruising Speed [$\boldsymbol{m/s}$]	1	1.31	31.0
Maximum Speed [$\boldsymbol{m/s}$]	2	4.12	106.0
Power [$\boldsymbol{Watts}$]	510	423	17.1
Range [$\boldsymbol{km}$]	250	428	71.2
Turning Radius [$\boldsymbol{m}$]	16	1.2	92.5

* This number is the BUUUV code. OSS is coded to generate this number in the format of IIAAABBBCC. II is number of the iteration, AAA and BBB are the first and the second parents from the previous generation and CC is the child number, either 01 or 02 as each couple make two off-spring. This is useful if it is required to track a particular individual back to analyse its evolution process.

To demonstrate what aspects of the vehicle design can be output by the OSS, the remaining characteristics of the BUUUV as predicted by the OSS are presented in Table 8.3. The OSS predicted that only a rear fin and a pair of side fins were required.

Table 8.3. The characteristics of the BUUUV not mentioned in Table 8.2

EL [%TL]	96.2
BW [%TL]	16.2
BH [%TL]	22.1
Propulsion mode	Thunniform
Muscle Mass [%Mass]	26
Fuel Mass [%Mass]	12.4
Battery Specific Energy [MJ/kg]	0.58
Taxonomy*	3403
COT_{opt} [J/(kg.m)]	0.17

Propulsion Power [W]	151
P_H[W]	272
Rear fin type	Forked
Rear fin Span [%TL]	21.9
Rear fin Chord [%TL]	7.8
Rear fin Aspect Ratio	4.18
Side fin Span [%TL]	16.4
Side fin Chord [%TL]	9.3
Side fin Aspect Ratio	2.9

* Taxonomy is in fact the taxonomy of the BMS on which the BUUUV was based. 3401 is a Whale.

The design parameters proposed by the OSS give higher flexibility to the BUUUV through the use of flexible materials or flexible segments on the body (the position of which is systematically chosen by the OSS considering the swimming mode of the BUUUV). The flexible body operating in conjunction with the rear fin and the side fin designs output by the OSS, reduces the turning radius for the BUUUV compared to AUTOSUB6000. The BUUUV output by the OSS is obtained by minimising the drag coefficient for the proposed speed range and therefore minimising the power consumption (while meeting other criteria). Also considering less body mass due to the use of lighter materials and a rear fin instead of a propeller will reduce the mass of the BUUUV and leave more space for payload and battery which can consequently increase the speed or endurance.

One must bear in mind that current AUVs are built with matured and tested available technologies while the bio-inspired AUV concept is rather new and many tests and trials are required for the future designed and built BUUUV to be operable. Therefore, the conclusions from the differences between the BUUUV and AUTOSUB6000 do not suggest an inferior design for AUTOSUB6000. AUV bodies are designed and built not solely for minimising drag but also considering ease of production and maintenance. The use of lighter materials for AUVs to bring the structure mass of AUV down and therefore increase the payload and battery capacity must be considered while also considering the strength of the material under pressure or impact.

Speed is based upon the regression lines of Figures 7.3 and 7.4. As mentioned previously, flexible fin oscillation needs to be studied in greater detail to obtain an

accurate formula, which is not yet available. Therefore speed calculations are the best estimate with the data available to date.

One more factor to bear in mind is that OSS proposes a mission specific design while AUVs are usually designed and built as general purpose, therefore realistically deciding which design is "superior" depends on whether a specific mission is in mind or the vehicle needs to have the flexibility to perform various missions.

In overall, as demonstrated in Table 8.2, in theory the BUUUV design which was output by the OSS showed improvements in different aspects of performance to fulfil the desired mission profile. Although this has not been implemented in reality, the results demonstrate a promising prospect for further exploration and implementation.

8.4 OSS Discussion

In this Chapter it was shown that despite the diverse performance of BMSs, it was possible to develop a search and selection algorithm to output some design aspects of a BUUUV based on a desired AUV mission.

The OSS was first tested and verified against calculating the performance characteristics of real BMSs. After verifying that the OSS is capable of predicting the performance of BMSs, it was used to output a bio-inspired design of a BUUUV which could match the capabilities of AUTOSUB6000. As shown in Table 8.2, it is theoretically possible to improve the overall performance of the vehicle by the use of bio-inspiration.

The OSS is developed as a novel and different approach to design. It takes into account the mission profile and attempts to tailor the design based on the desired characteristics while considering the bio-inspired capabilities. Another novelty within the OSS is the attempt to appreciate the multi-functionality of BMSs and trying to output a design which would satisfy multiple functions. The main interest of this research has been in the improvement of AUVs. However, its area of application can be extended to other uses. As the OSS has the ability to predict both BUUVs and BMSs designs, it can also be used for BMSs; e.g. to design a prosthetic limb for an injured BMS. Similarly it can be further developed and modified to be used for non-marine species.

Several aspects of the OSS can be modified and improved with further research. The quality of calculating the characteristics can be improved by obtaining data on more

BMSs which are measured in a unified manner so they correspond to one another and therefor minimise the uncertainties. Some aspects of the OSS are presently just a concept such as using muscles. However, this is a developing subject. In the case of muscles for example, some artificial equivalents already exist. Electro Active Polymers (EAPs) or muscle wires (Shape Memory Alloys) are two examples of the artificial muscles and the efficiency of EAPs at 38% (Bar-Cohen, 2004) is very similar to white muscles, 41%. Therefore, in this developing sector the OSS is worthy of future research and development as a means of bio-inspired implementation.

Chapter 9. Conclusions and recommendations for future work

This research work, as part of a collaborative project, NEMO (EPSRC funding reference: EP/F066767/1), was aimed to improve the performance of AUVs through design techniques and implementation methods inspired by nature. Realising the long term presence of marine animals in the oceans as well as studying the history and achievements in the field of bio-inspiration proved that bio-inspiration was a potentially promising approach. As explained in Chapters 1 and 2, the research intended to highlight the useful aspects of Biological Marine Systems (BMSs) design and leave the irrelative ones. Therefore, in order to achieve the aim of the project, two objectives were set: first to investigate bio-inspiration and second to implement it. As the improvement of the overall performance was sought, the main focus was set on the speed and agility, depth capabilities, endurance and energetics and size.

9.1 Novelties and Conclusions

The nature of this work demanded a new and different approach towards investigating marine animals and designing AUVs. The interim conclusions of each of the chapters have been discussed at the end of each chapter in this thesis. Therefore, below are the novelties introduced and overall conclusions made as part of this research work.

9.1.1 Comparing various performance aspects of different BMSs and AUVs

In order to capture the potentials of the marine animals, it was decided that various classes of marine animals must have been studied and compared with one another as well as with existing AUVs. Therefore, data on design and performance of more than 300 animals was collected alongside 58 AUVs. This was an interesting challenge as never before had this comparison been performed to this extent and therefore a fair amount of consideration was required to investigate animals from an engineering perspective. The body design, speeds, depth capabilities, manoeuvrability and energetics of AUVs and BMSs were required to be compared. This meant that comparable definitions and terms were required.

9.1.2 BMSs bodies considered as tri-axial ellipsoids

Each marine animal has a different body design. In order to be able to associate any performance to body design and size, a unified body design was required. As discussed in Chapter 3, it was realised that BMSs in overall would be best defined as a tri-axial ellipsoid. For drag calculations purposes further work was carried out as explained in Chapter 5 to verify the use of tri-axial ellipsoids. As a result, the bodies of BMSs were represented by tri-axial ellipsoids in this research and can be used in future research works. Comparing the bodies of AUVs and BMSs which were unified as tri-axial ellipsoids showed that the *FR* values ranges were similar, however eel like BMSs had the highest values of up to 18.4 compared to 13.2 for AUVs. Some similarities were also seen, such as fusiform BMSs with similar *FR*s as Teardrop AUVs.

9.1.3 Speed comparison

The economic speed of AUVs were compared with optimum or sustained speed of BMSs and it was realised that there was a general trend of increase in speed with size for BMSs. This was not as clear with AUVs as gliders irrelative to their size had very low speeds. BMSs reached higher speeds compared to AUVs and Thunniforms and Labriforms were the fastest swimmers.

The BMSs can energetically afford higher speed as they have access to fuel with higher specific energy. Moreover, their body design and dimensions as well as swimming mode have evolved for the speed range that they swim at, hence the observation that fast swimmers are either Thunniforms or Labriforms.

As for maximum speed, Thunniforms performed best with a significant superiority compared to AUVs.

For both optimum and maximum speeds, smaller size BMSs showed highest length specific speeds.

9.1.4 Energetics: Cost Of Transport (COT), endurance and range

Another interesting aspect of this research was the sophisticated work on the energetics of BMSs so there would be correspondence with AUVs for comparison. As explained in Chapter 4, as well as *COT*, the required power of some BMSs were calculated and therefore, the propulsion power of BMSs and AUVs were compared with one another.

By testing animal fat and concluding that regardless of the health of the BMS, the fat would almost retain its properties, an average specific energy value was set to calculate the range and endurance of BMSs to then be compared with AUVs.

Therefore, as concluded in Chapters 3 and 4, there was a considerable superiority in terms of speed, range of operation, manoeuvrability and size in BMSs. This is due to their swimming mode, specific body dimensions, flexibility and collaboration between the body and fins during swimming and manoeuvrability as well as lighter structure material and superior fuel type.

BMSs have higher speeds and especially maximum speeds regarding their size compared to AUVs. The highest speeds were seen in Thunniform and Labriform swimmers.

AUVs had good depth capabilities but many smaller BMSs had better mass specific depth capabilities. Some AUVs have an indicated maximum depth of up to 6000 m and Nereus AUV has reached the depth of 10,903 m in ROV mode. For AUVs depth was observed to be generally proportional to size. However this is not a definite trend. As previously mentioned, depth is not the sole reason for increasing the size of an AUV, as there are relatively large but shallow diving AUVs. These AUVs are larger either due to carrying more battery in order to increase their endurance or cruising speed, or they require the extra volume to carry more sensors for complex missions.

However, increasing the diving depth of an AUV will affect its size/mass as explained next. Deeper depth range means that the AUV must travel longer distance to and back from its maximum depth. Consequently, the vehicle requires more battery. The increase of battery power, increases the battery mass as well as the mass (and internal volume, therefore dimensions) of the AUV. The second is the use of a pressure vessel which can house the components of the AUV and is able to withstand the water pressure. At sea level the pressure (air pressure) is 1 *atm* which increases with water depth. This in conjunction with the change in density and temperature of water indicates that deep diving AUVs must have pressure vessels capable of withstanding relatively high pressures. For example an AUV diving to 6000 *m* must have a pressure vessel withstanding about 60 atm. This subsequently increases the thickness and therefore the mass of the pressure vessel.

Finally as AUVs are positively buoyant, they require some extra weight to counter the positive buoyancy. The buoyancy can be controlled dynamically. However the extra weight can also be added by physically adding weight such as lead weights to different

sections of the AUV. Clearly this will increase the mass (but not the volume) of the AUV. Therefore, although size does not always suggest more depth capability for AUVs, higher depth capability will increase the mass and the size of the vehicle.

The comparison of *COT*s highlighted that while locomotion at lower speeds, AUVs had generally lower *COT*s compared to BMSs. This was mainly down to higher hotel loads for BMSs. Comprehensive hotel load vs. mass graph was created which includes the regression lines for the hotel load of numerous BMSs as a function of their mass. Penguins and marine mammals had the highest hotel loads.

As mentioned in Chapter 4, the hotel load is mainly associated with powering computers, hard drives and sensors; i.e. non-propulsive required power. Therefore, larger AUVs have the volume (space) required for large number of sensors and consequently they will have higher hotel load. However, it must be notes that this is not a requirement. Therefore depending on the mission requirements, there are examples of comparatively large AUVs with small hotel loads.

It was also shown that animals benefit from a rather high energy density type of fuel with a very high specific energy compared to batteries used for AUVs and therefore their endurance was considerably higher than AUVs. If a fuel with higher energy density can be used on AUVs, it will increase their endurance as well. Higher energy density fuel may also have a positive impact on the speed of the vehicle as more energy would be available to be consumed for the propulsion of the vehicle. As shown with the results from the OSS (which was run assuming the BUUUV is running on batteries and not fat), this high energy density fuel when coupled with modifications to the body design for reduction in drag and possibly using alternative propulsion system can have even higher positive impact on the speed of the vehicle.

In terms of manoeuvrability, the BMSs were significantly superior, benefiting from a flexible body. It was noted that between BMSs there were more and less manoeuvrable species.

By performing the comparisons the superiorities in the performance of the BMSs were highlighted and investigating bio-inspiration was complete. However, when attempting to select an optimum system to use it to implement the bio-inspired knowledge, it was realised that the superiorities were spread over a range of BMSs. The multi-functionality of their biological systems indicated that means were required to capture the trade-off between various performance characterises to predict the performance of a BMS.

Therefore an holistic approach was taken towards marine animals, considering the animal kingdom as a system where each of the species was a specific configuration. Therefore each BMS consists of a combination of inter-related subsystems, so, all the performance characteristics including the efficiency, manoeuvrability and speed of the BMSs were required to be estimated and compared.

9.1.5 Calculating drag for BMSs and definition of efficiency for BMSs leading to the introduction of the ξvalue

Prior to estimating drag and efficiency, different energy losses and efficiencies within the body of a BMS were identified to clarify any possible confusion between various efficiencies in a BMS.

To estimate the efficiency, the drags of BMSs were calculated. To obtain precise answers, a method was proposed in this research for calculating all terms of drag in BMSs. Two correction factors were also introduced to compensate for skin roughness and the diversion from a true tri-axial ellipsoid body.

As skin roughness was not known for BMSs and there could be other possible drag terms such as parasites (for larger BMSs) which could not be determined, an indication of efficiency, ξ, term was defined to include these uncertainties.

Another novel approach introduced in this research was to calculate the ξ value at optimum speed without requiring the *COT*. This method can now be used in research works where the efficiency or the energetic cost of a BMS is required and experiments to measure them are not possible.

It was concluded from the results that although higher efficiencies are seen in some swimming modes such as Thunniform and Labriform more than others, similar efficiencies were calculated for similar size BMSs, with different swimming modes. The difference was in their speed.

Calculating the efficiency at maximum speed required having the maximum muscle capability of every BMS as the muscle characteristics can vary due to genetics, fitness, and more specific terms such as the amount of myoglobin, etc. To overcome this, another indicator of efficiency term, ξ', was introduced in this research which is an indication of efficiency related to the frequency of the finbeat, the amplitude of the muscle twitch which was directly proportional to the length of the BMS and the muscle

mass. The analysis highlighted that ξ' was directly proportional to the length specific maximum speed of BMSs.

9.1.6 Manoeuvrability of flexible bodies

Another novel part of this research was introducing a simplified method to estimate the yaw turning circle radius of flexible bodies. A flexibility measure was defined in this work which was directly proportional to the length specific yaw radius of BMSs. An empirical formula was also derived to estimate the yaw radius of AUVs. The higher manoeuvrability of BMSs was clear, however different groups of BMSs exhibited different manoeuvrability capabilities. Some Thunniform fish alongside turtles were within the least manoeuvrable while Anguilliform and Labriform marine mammals such as sea lions (*Zalophus californianus*) were within the most manoeuvrable BMSs.

9.1.7 The development of the Optimum System Selector (OSS)

The comparison of BMSs and AUVs highlighted the superiority of BMSs and a few methods were proposed to estimate the performance characteristics of BMSs. When attempting to implement the bio-inspired knowledge it was realised that although the purposes of BMSs were different to the mission profile of AUVs, but while investigating bio-inspiration it became clear that different BMSs have evolved to fulfil different purposes. Therefore the optimum system would be dependent on the mission profiles of AUVs. Therefore, being inspired by nature a novel evolutionary search and selection algorithm, the OSS, was proposed to output a bio-inspired design for AUVs based on their mission profile. The performance of the algorithm was tested by using it to calculate the performance characteristics of BMSs. Finally, the OSS was used to output a design for a BUUUV to perform similar to AUTOSUB6000. Comparing the characteristics of the BUUUV with AUTOSUB6000 it was realised that using bio-inspired design can theoretically improve the overall performance of AUVs. The potential improvements through the use of BUUUV are discussed as follows.

- Minimising the drag coefficient and therefore minimising the drag, energetic cost and required power for the mission profile. Specific design for the mission profile ensures that the BUUUV has enough space for the payload as well as the actuator and the batteries.

- Proposing the use of artificial muscles which reduces the “motor” mass. This in conjunction with the use of lighter materials for the structure can leave extra space for payload, sensors or battery which could lead to the increase in speed or endurance.
- Proposing the use of oscillating foils as an alternative to propellers. Although the efficiency has not been observed in this research to be as high as propellers, there are a few pros towards the use of oscillating foils for propulsion. Firstly, the foils have potentially less mass which is always appreciated for an AUV as mentioned above. Secondly, an oscillating foil has less noise and vibration which is beneficial for both stealth as well as animal observation. Finally, an oscillating foil can also contribute to manoeuvrability and reduce the necessity of using rudders as well as extra thrusters.
- Increasing the manoeuvrability and reducing the turning radius through systematic flexibility to the main body as well as the use of rear and side fins.

Therefore, there are several potential gains from considering bio-inspired designs for specific AUV mission profiles.

9.2 Impact of the research and Recommendations for future work

The aim of this research was to introduce a new method for the design of AUVs which could improve their overall performance using bio-inspiration. The OSS attempts to do that through evolution. Therefore, the OSS can be used as a mission based approach to the design of AUVs. The OSS as a concept can be used as a general method for mission based designs in different sectors. The focus of this work was to output alternative bio-inspired design for AUVs. In addition the OSS has the capability to be used to output designs for actual BMSs.

In overall, through this research marine animals were investigated as systems for which the performance characteristics can be calculated or estimated. Although the approach was from an engineering perspective, the findings of this research can be used to predict the performance characteristics of BMSs in terms of their speed, manoeuvrability, and energetics and depth capability. The estimation and calculation methods presented in this research will be useful if these characteristics cannot be measured directly. On the other hand, if experiments can be performed on several BMSs to measure different characteristics, the OSS can be modified accordingly.

Taking an holistic approach towards BMSs required tackling various performance characteristics. Some of the characteristics investigated in this research can be further studied. For example, in terms of depth there are still many unknowns about BMSs, especially those living in deepest parts of the oceans. If the buoyancy control systems of deep sea BMSs are known, it will be possible to answer the reason why small fish have very high mass specific depth capabilities.

In this research the speed was considered as a function of total length. If precise speed values are required, the speed can be calculated if the thrust produced from the propulsive fins are known. This requires the fins to be considered as flexible pendulums moving through water which is another research worthy of consideration.

While calculating the drag for each BMS, the fins were considered to be static. In reality the fins of BMSs have different movement patterns. Therefore, investigating different movements of various fins is another subject worthy of future research. Understanding the movements of fins and including that within the drag calculating model will result in more precise drag calculations and also will provide extra knowledge on the operation mechanism of different BMSs.

In overall, this research demonstrated that there are ways to approach animals from an engineering perspective and their performance can be considered to improve the performance of engineered vehicles to fulfil their missions. The results of the OSS compared with existing AUVs, showed improvements in the overall capabilities. Therefore, this method is an excellent guide to transform complex biological data for the future design and development of AUVs.

References

Aarestrup, K., Okland, F., Hansen, M.M., Righton, D., Gargan, P., Castonguay, M., Bernatchez, L., Howey, P., Sparholt, H., Pedersen, M.I. and McKinley, R.S. (2009). "Oceanic spawning migration of the European eel (Anguilla anguilla)". In: Science, 325(5948). doi: 10.1126/science.1178120. Erratun in: Nov 2009, 326 (5955).

Allen, B., Vorus, W.S. and Prestero, T. (2000). "Propulsion system performance enhancements on REMUS AUVs". OCEANS 2000 MTS/IEEE Conference and Exhibition. Providence, RI , USA.

Anderson, J. M. (2002). "Maneuvering and stability performance of a robotic tuna". Integrative and Comparative Biology, 42(1), pp. 118-126.

Anderson, J.M., Streitlien, K., Barrett, D.S. and Triantafyllou, M.S. (1998). "Oscillating foils of high propulsive efficiency". Journal of Fluid Mechanics, 360, pp. 41-72. Cambridge University Press.

Appeltans, W., Bouchet, P., Boxshall, G. A., Fauchald, K., Gordon, D. P., Hoeksema, B. W., Poore, G. C. B. , Van Soest, R. W. M., Stöhr, S., Walter, T. C., Costello, M. J. (eds.) (2010). World Register of Marine Species. Accessed at http://www.marinespecies.org on 2010.01.01

AUVAC (2010). "Autonomous Undersea Vehicle Applications Centre". URL: "www.AUVAC.org".

Ayers, J., Wilbur, C., and Olcott, C. (2000). "Lamprey robots". Proceedings of the International Symposium on Aqua Biomechanisms, Tokai University.

Bainbridge, R. (1958). "The speed of swimming of fish as related to size and to the frequency and amplitude of the tailbeat". Journal of Experimental Biology, 35, pp. 109-113.

Bar-Cohen, Y. (ed.) (2004). "Electroactive polymer (EAP) actuators as Artificial Muscles: Reality, Potential, and Challenges". Bellingham, WA, SPIE. The international Society for Optical Engineering.

Bar-Cohen, Y. (2006). “Bio-mimetics - using nature to inspire human innovation”. Bioinspiration and Biomimetics, 1(1), pp. 1-12.

Berta, A., Sumich, J.L. and Kovacs, K.M. (2005).” Marine Mammals: Evolutionary Biology”. 2nd edition. Academic Press. pps. 560. ISBN: 0080489346, 9780080489346.

Billingham, J. (2001). “Autonomous Underwater Vehicles (AUVs)”. Encyclopedia of Ocean Sciences. Academic Press. pp. 212-216. doi:10.1006/rwos. 2001.0303

Blake, R.W. (1983). “Fish Locomotion”. CUP Archive. pps. 208. ISBN: 0521243033, 9780521243032.

Blidberg, D. R. (2001) "The Development of Autonomous Underwater Vehicles (AUV); A Brief Summary", International Conference on Robotics and Automation (ICRA). Seoul, Korea, May 2001. P. 12.

Bowen, A.D., Yoerger, D.R., Taylor, C., McCabe, R., Howland, J., Gomez-Ibanez, D., Kinsey, J.C., Heintz, M., McDonald, G., Peters, D.B., Bailey, J., Bors, E., Shank, T., Whitcomb, L.L., Martin, S.C., Webster, S.E., Jakuba, M.V., Fletcher, B., Young, C., Buescher, J., Fryer, P. and Hulme, S. (2009). “Field trials of the Nereus hybrid underwater robotic vehicle in the challenger deep of the Mariana Trench”. OCEANS 2009, MTS/IEEE Biloxi, pp. 1 – 10.

Brett, J.R. and Glass, N.R. (1973). “Metabolic Rates and Critical Swimming Speeds of Sockeye Salmon (*Oncorhynchus nerka*) in Relation to Size and Temperature”. Journal of the Fisheries Research Board of Canada, 30(3), pp. 379-387.

Brody, S. (1945). “Bioenergetics and Growth”. Reinhold Publication Corporation, New York

Carlton, J. (2011). “Marine Propellers and Propulsion”. Butterworth-Heinemann. pps. 560. ISBN: 0080549233, 9780080549231

Castellini, M. (2008). “Thermoregulation”. Perrin, W.F., Wursig, B. and Thewissen, J.G.M. (eds.), Encyclopaedia of Marine Mammals. London, Academic Press.

Cheneval, O., Blake, R.W., Trites, A.W. and Chan, K.H.S. (2007). “Turning Maneuvers in Stellar Sea Lions (*Eumatopias Jubatus*)”. Marine Mammal Science, 23(1), pp. 94-109. The Society for Marine Mammalogy. DOI: 10.1111/j.1748-7692.2006.00094.x

Cherel, Y., Charrassin, J.B. and Handrich, Y. (1993). “Comparison of Body Reserve Buildup in Prefasting Chicks and Adults of King Penguins (*Aptenodytes patagonicu*)”. Physiological Zoology, .66(5), pp. 750-770. The University of Chicago Press. Stable URL: http://www.jstor.org/stable/30163822

Clark, B.D. and Bemis, W. (1979). “Kinematics of swimming of penguins at the Detroit Zoo”. Journal of Zoology London, 188, pp. 411-428.

Clarke, A. and Johnston, N.M. (1999). “Scaling of metabolic rate with body mass and temperature in teleost fish”. Journal of animal ecology, 68, pp. 893-905.

Copros, T and Scourizic, D. (2011). “Alister – Rapid Environment Assessment AUV (Autonomous Underwater Vehicle)”. In: Ceccaldi, H.J., Dekeyser, I., Girault , M. and Stora, G. (eds), Global Change: Mankind-Marine Environment Interactions. Proceedings of the 13th French-Japanese Oceanography Symposium. pp. 233-238. DOI: 10.1007/978-90-481-8630-3_40. Print ISBN: 978-90-481-8629-7

Curtin, N. A. and Woledge, R. C. (1993a). “Efficiency of energy conversion during sinusoidal movement of red muscle fibres from the dogfish *Scyliorhinus canicula*”. Journal of Experimental Biology, 185, pp. 195-206.

Curtin, N. A. and Woledge, R. C. (1993b) “Efficiency of energy conversion during sinusoidal movement of white muscle fibres from the dogfish *Scyliorhinus canicula*”. Journal of Experimental Biology, 183, pp.137-147.

Davis, R. W., Williams, T. M. & Kooyman, G. L. (1985). "Swimming metabolism of yearling and adult Harbor Seals *Phoca vitulina*". Physiological Zoology, 58, 590-596.

Dawson, A. S. and Grimm, A. S. (1980). “Quantitative seasonal changes in the protein, lipid and energy content of the carcass, ovaries and liver of adult female plaice, *Pleuronectes platessa L*.”. Journal of Fish Biology, 16 (5), pp. 493-504. Blackwell

Publishing Ltd. DOI: 10.1111/j.1095-8649.1980.tb03729.x

De Blasio, F.V. (2011). “Introduction to the Physics of Landslides: Lecture notes on the dynamics of mass wasting”. Springer, pps.423. ISBN: 9400711220, 9789400711228

Dewar, H. & Graham, J. B. (1994) "Studies of tropical tuna swimming performance in a large water tunnel". I. Energetics. Journal of Experimental Biology, 192, 13-31.

Don Stevens, E., Lam, H.M. and Kendall, J. (1974). “Vascular Anatomy of the Counter-Current Heat Exchanger of Skipjack Tuna”. Journal of Experimental Biology, 61, pp. 145-153.

Dorrington, G.E. (2006). “Drag of Spheroid-Cone Shaped Airship”. In: Journal of Aircraft, 43(2), pp. 363-371. Doi: 10.2514/1.14796.

Elliott, J. M. & Davison, W. (1975) "Energy equivalents of oxygen consumption in animal energetics Oecologia", 19, 195-201.

Fish, F.E. (1993). “Power Output and Propulsive Efficiency of swimming Bottlenose Dolphin (*Tursiops Truncatus*)”. Journal of Experimental Biology. 185, pp. 179-193.

Fish, F.E. (1997). “Biological Designs for Enhanced Manoeuvrability: Analysis of Marine Mammal Performance”. Tenth International Symposium on Unmanned Untethered Submersible Technology: Special Session on Bio-Engineering Research Related to Autonomous Underwater Vehicles. New England Centre, University of NH, Durham. Organized by AUSI and ONR

Fish, F.E. (1998). "Comparative kinematics and hydrodynamics of odontocete cetaceans: Morphological and ecological correlates with swimming performance". The Journal of Experimental Biology. 22-Sep-1998 ed., The Company of Biologists Limited.

Fish, F. E. (2002). “Balancing Requirements for Stability and Manoeuvrability in Cetaceans” Integrative and Comparative Biology, 42(1), pp. 85-93

Fish, F.E. (2006). “The myth and reality of Gray's paradox: implication of dolphin drag reduction for technology”. Bioinspiration and Biomimetics, 1(2), pp. 17-25.

Fish, F.E., Lauder, G.V., Mittal, R., Techet, A.H., Triantafyllou, M.S., Walker, J.A. and Webb, P.W. (2003). “Conceptual Design for the Construction of a Biorobotic AUV Based on Biological Hydrodynamics”. Proceedings of the 13th International Symposium on Unmanned Untethered Submersible Technology, Durham, NH.

Fish, F.E. and Rohr, J.J. (1999). “Review of dolphin hydrodynamics and swimming performance”. Technical report 1801, SPAWAR systems.

Fleming, T.J. (1972). “Benjamin Franklin”. Four Winds Press.

Friendly, M., Monette, G. and Fox, J. (2013). “Elliptical Insights: Understanding Statistical Methods through Elliptical Geometry”. Statistical Science, 28(1), pp. 1-39. DOI:10.1214/12-STS402.

Froese, R. & Pauly, D. (2011) "FishBase: version (02/2011)", World Wide Web www.fishbase.org.

Funnell, C. Ed. (2007). "Jane’s Underwater Technology 2006-2007", Ninth Edition, Surrey: Jane’s Information Group.

Furlong, M., McPhail, S.D. and Stevenson, P. (2007). “A Concept Design for an Ultra-Long-Range Survey Class AUV”. In: IEEE OCEANS 2007 – Europe. Print ISBN: 978-1-4244-0635-7. Doi: 10.1109/OCEANSE.2007.4302453

Gage, J. D. (2001). "Deep-sea benthic community and environmental impact at the Atlantic frontier." Continental Shelf Research, 8, pp. 957-986

Gen, M. and Cheng, R. (2000). “Genetic Algorithms and Engineering Optimization”. Wiley-Interscience publication: Engineering Design and Automation, 7, pps. 495. John Wiley & Sons. ISBN: 0471315311, 9780471315315.

Griffiths, G. (ed.) (2003). “Technology and applications of Autonomous Underwater Vehicles”. Ocean Science and Technology, Taylor & Francis, London.

Griffiths, G. (2005). “Cost vs. performance for fuel cells and batteries within AUVs”. UUVS 2005, Southampton, September, 2005

Griffiths, G.J., C.; Ferguson, J.; Bose, N. (2007) 'Undersea gliders', Journal of Ocean

Technology, 2(2), pp. 64-75.

Griffiths, G. (2009). “Nature in Engineering for Monitoring the Oceans (NEMO)”. Case of support for the EPSRC grant, pps.8. Unpublished.

Griffiths, G. (2012). Skype video-conference on the 01 October 2012, Newcastle University.

Hammer, C. (1995). “Fatigue and exercise tests with fish”. Comparative Biochemistry and Physiology Part A: Physiology, 112(1), pp. 1-20.

Haroutunian M. and Murphy A.J. (2012). “Mission based Optimum System Selector for Bio-inspired Unmanned Untethered Underwater Vehicles”. Autonomous Underwater Vehicles (AUV2012) conference, 24th-27th September 2012. Southampton, UK.

Hoelsel, A. R. (2002). "Marine Mammal Biology; an evolutionary approach".

Hoerner, S. F. (1965). “Fluid-Dynamic Drag. Theoretical, experimental and statistical information”. Hoerner Fluid Dynamics.

Huggins, R. A. (2010). “Energy Storage”, Springer.

Huss, H.H. (1995). “Quality and changes in fresh fish”. FAO Fisheries Technical Paper, T348, pps. 195. ISBN: 9251035075.

ITTC, (2011). “ITTC – Recommended Procedures: Fresh Water and Seawater Properties”. International Towing Tank Conference, pp.1-45. Article stable URL: http://ittc.sname.org/CD 2011/pdf Procedures 2011/7.5-02-01-03.pdf

Jones, F.R.H. (1973). Tailbeat frequency, amplitude, and swimming speed of a shark tracked by sector scanning sonar”. Journal of Cons. Int. Explor. Mar., 35(1), pp. 95-97.

Jefferson, T. A., Leatherwood, S. & Webber, M. A. (1993). "FAO Species Identification Guide; Marine mammals of the world". In Department, F. A. A. (Ed.).

Katz, S.L. (2002). “Review: Design of heterothermic muscle in fish”. Journal of

Experimental Biology, 205, pp. 2251-2266.

Kleiber, M. (1932). “Body size and metabolism”. Hilgardia: A Journal of Agriculture Science. 6(11), pp. 315-352.

Kleiber, M. (1975). “The Fire of Life: An Introduction to Animal Energetics”. R.E. Kteiger Publishing Co., Huntington, New York.

Kermorgant, H. & Scourzic, D. (2005). "Interrelated functional topics concerning autonomy related issues in the context of autonomous inspection of underwater structures", Proc. IEEE Oceans 2005.

Kreyszing, E. (1999). “Advanced Engineering Mathematics”. John Wiley & Sons. 8th Edition, p.994. ISBN-10: 047133328X.

Lewis, Edward V. (ed.) (1989). “Principles of Naval Architecture”. The Society of Naval Architects and Marine Engineers, Volume II.

Lighthill, M.J. (1969). “Hydromechanics of aquatic animal propulsion”. Annual Review of Fluid Mechanics, 1, pp. 413-446.

Liversey, G. and Elia, M. (1988). “Estimation of energy expenditure, net carbohydrate utilization, and net fat oxidation and synthesis by indirect calorimetry: evaluation of errors with special reference to the detailed composition of fuels”. The American Society for Clinical Nutrition, Inc, 47(4), pp. 608-628.

Lockyer, C. (1976). “Body weights of some species of large whales”. ICES Journal of Marine Science, 36(3), pp. 259-273

Long, J. H., Schumacher, J., Livingston, N., and Kemp, M. (2006). “Four flippers or two? Tetrapodal swimming with an aquatic robot”. Bioinspiration and Biomimetics, 1(1), pp. 20-29.

Luna-Jorquera, G. and Culik, B.M. (2000). “Metabolic rates of swimming Humboldt penguins”. Marine Ecology Progress Series. 203, pp. 301-309

Madin, L. (2005). "Discovering life and sustaining habitats". Oceanus, Ocean life institute, Woods Hole Oceanographic Institution.

McPhail, S. (2009) 'Autosub6000: A Deep Diving Long Range AUV', Journal of Bionic Engineering, 6(1), p. 6.

Medler, S. and Hulme, k. (2009). “Frequency-dependant power output and skeletal muscle design”. In: Comparative biochemistry and physiology. Molecular and integrative physiology, 152 (3), pp. 407-417.

Meyer-Rochow, V.B. and Ingram, J.R. (1993). “Red-White muscle distribution and fibre frowth dynamics: A comparison between Lacustrine and Riverine populations of the Southern Smelt *Retropinna retropinna Richardson*”. Proceedings of the Royal Society London B, 252, pp. 85-92. DOI: 10.1098/rspb.1993.0050.

Michon, G. P. (2012). “Final Answers”.
URL: http://www.numericana.com/answer/ellipsoid.htm. [Accessed: 04.2012]

Mühlenbein, H. and Schlierkamp-Voosen, D. (1993). ” Predictive Models for the Breeder Genetic Algorithm: I. Continuous Parameter Optimization”. Evolutionary Computation, 1(1), pp. 25-49.

Murphy, A.J. and Haroutunian, M. (2011). “Using Bio-Inspiration to Improve Capabilities of Underwater Vehicles”. In: 17th International Unmanned Untethered Submersible Technology Conference (UUST 2011), 21-24 August, Portsmouth-USA

National Geographic, (2010). "Ghost of the deep".
URL:http://news.nationalgeographic.com/news/2010/10/photogalleries/101014-deep-fish-seen-snailfish-eel-ocean-pictures. [Accessed January 2011]

Navarro-Garcia, G., Pacheco-Aguilar, R., Vallejo-Cordova, B., Ramirez-Suarez, J.C. and Bolaños, A. (2000). “Lipid Composition of the Liver Oil of Shark Species from the Caribbean and Gulf of California Waters”. Journal of Food Composition and Analysis, 13(5), pp. 791-798, ISSN 0889-1575.

Pelster, B., (2009). “Buoyancy control in Aquatic Vertebrates”. In: Cardio-Respiratory Control in Vertebrates: Comparative and Evolutionary Aspects”. GLASS, M. L. AND WOOD, S. C. Springer Dordrecht Heidelberg London New York. ISBN: 978-3-540-93984-9

Peterson, C.C. and Gomez, D. (2008). “Buoyancy Regulation in Two Species of Freshwater Turtle”. In: Herpetologica, 64(2), pp. 141-148. Print ISSN: 0018-0831. doi: http://dx.doi.org/10.1655/07-050.1

Phillips, A. B., Haroutunian, M., Man, S. K., Murphy, A. J., Boyd, S. W., Blake, J. I. R. & Griffiths, G. (2012). “Nature in Engineering for Monitoring the Oceans: Comparison of the energetic costs of marine animals and AUVs”. SUTTON, R. and ROBERTS, G. (eds.) Further Advances in Unmanned Marine Vehicles. The Institution of Engineering and Technology (IET). ISBN: 978-1-84919-479-2

Phillips, Alexander B., Blake, J.I.R., Smith, B., Boyd, S.W. and Griffiths, G. (2010) “Nature in engineering for monitoring the oceans: towards a bio-inspired flexible AUV operating in an unsteady flow”. Proceedings of the Institution of Mechanical Engineers, Part M, Journal of Engineering for the Maritime Environment, 224 (4), pp. 267-278. doi:10.1243/14750902JEME201

Quackenbush, T. R., Usab, W. J., and Carpenter, B. F. (2003). “Ducted propulsors with streerable outflow using smart material technology”. Proceedings of the International Conference on Advanced Marine Materials: Technology and Applications, Royal Institution of Naval Architects, London, UK

Quiring, D.P. (1943). “Weight Data on Five Whales”. Journal of Mammalogy, 24 (1), pp. 39-45. American Society of Mammalogists. Article Stable URL: http://www.jstor.org/stable/1374778

Read, D.A., Hover, F.S. and Triantafyllou, M.S. (2003). “Forces on oscillating foils for propulsion and maneuvering”. Journal of Fluids and Structures, 17, pp. 163–183

Rivera, G., Rivera, A. R. V., Dougherty, E. E. and Blob, R. W. (2006). “Aquatic turning performance of painted turtles (*Chrysemys picta*) and functional consequences of a rigid body design”. The Journal of Experimental Biology 209, 4203-4213. doi:10.1242/jeb.02488

Robotic-fish.net (2013). “Robotic Fish Of All Species”. URL: http://www.robotic-fish.net

Rome, L.C. (1998). “Some advances in integrative muscle physiology”. Comparative

Biochemistry and Physiology, Part B, 120, pp.51 – 72

Roper, C.F.E. and Vecchione, M. (1993). “A geographic and taxonomic review of Taningia danae Joubin, 1931 (Cephalopoda: Octopoteuthidae), with new records and observations on bioluminescence”. In: Okutani, T., O'Do, R.K. and Kubodera, T. (eds.) Recent Advances in Cephalopod Fisheries Biology. Tokai University Press, Tokyo. pp. 441–456.

SAAB (2014). “AUV62-MR, AUV system for mine reconnaissance”. URL: www.saabgroup.com/en/Naval/Underwater-Security/Autonomous-Underwater-Vehicles/AUV62-MR_AUV_System_for_Mine_Reconnaissance/Features. Accessed: [22-05-2014]

Scharold, J. and Gruber, S.H. (1991). "Telemetered Heart Rate as a Measure of Metabolic Rate in the Lemon Shark, Negaprion brevirostris" Copeia, 1991 (4), pp. 942-953.

Schmidt-Nielsen, K. (1997). “Animal Physiology: Adaptation and Environment”, 5th edition. Cambridge University Press, Cambridge, UK.

Science Museum (2014). “Robotuna, c.2000”. URL: www.sciencemuseum.org.uk/objects/oceanography/L2000-4475.aspx. Accessed: 22-05-2014]

Sfakiotakis, M., Lane, D.M. and Davies, J.B.C (1999). “Review of Fish Swimming Modes for Aquatic Locomotion”. IEEE Journal Of Oceanic Engineering, 24(2), pp. 237-252

Shadwick, R.E. and Lauder, G.V. (eds.) (2006).”Fish Physiology: Fish Biomechanics”. Fish Physiology, 23, pps. 560. ISBN: 0080477763, 9780080477763.

Shadwick, R.E. and Syme, D.A. (2008). “Thunniform swimming: muscle dynamics and mechanical power production of aerobic fibres in yellowfin tuna (*Thunnus albacares*)”. Journal of Experimental Biology, 211, pp. 1603-1611. doi:10.1242/jeb.013250

Sidwell, V. D., Foncannon, P. R., Moore, N. S and Bonnet, J. C. (1974). “Composition of the edible portion of raw fresh or frozen crustaceans, finfish and mollusks. 1.

Protein, fat, moisture, ash, carbohydrate, energy value, and cholesterol". Marine Fisheries Review, 36(3), pp. 21-35.

Smith, R.R (1976). "Studies on the energy metabolism of cultured fish". PhD thesis. Ithaca, New York, Cornell University Press.

Somers, W. (2011) Doppler-Based Localization for Mobile Autonomous Underwater Vehicles. The state University of New Jersey

Speakman, J.R., McDevitt,R.M. and Cole, K.R. (1993). "Measurement of Basal Metabolic Rates: Don't Lose Sight of Reality in the Quest for Comparability". Physiological Zoology, 66(6), pp. 1045-1049.

Strasser, T.F., Pangopoulou, E., Runnels, C.N., Murray, P.M., Thompson, N., Karkanas, P., McCoy, F.W. and Wegman, K.W. (2010). "Stone Age Seafaring in the Mediterranean: Evidence from the Plakias Region for Lower Paleolithic and Mesolithic Habitation of Crete". The Journal of the American School of Classical Studies at Athens. 79 (2), pp. 145–190.

Streitlien, K., Triantafyllou, G. S., and Triantafyllou, M. S., (1996). "Efficient foil propulsion through vortex control". AIAA Journal, 34, pp. 2315-2319

Sundstrom, L.F., Gruber, S.H., Clermont, S.M., Correia, J.P.S., de Marignac, J.R.C., Morrissey, J.F., Lowrance, C.R., Thomassen, L. and Oliveira, M.T. (2001). "Review of elasmobranch behavioral studies using ultrasonic telemetry with special reference to the lemon shark, Negaprion brevirostris, around Bimini Islands, Bahamas". Environmental Biology of Fishes, 60, pp. 225–250. Kluwer Academic Publishers. Printed in the Netherlands

Thillart, G. V. D., Palstra, A. & Ginneken, V. V. (2007). "Simulated migration of European silver eel; swim capacity and cost of transport". Journal of Marine Science and Technology, 1-16.

Tomasi, T.E. and Horton, T.H. (ed.) (1992). "Mammalian Energetics: Interdisciplinary Views of Metabolism and Reproduction". Cornell University Press. pps. 276. ISBN: 0801426596, 9780801426599.

Tupper, E.C. and Rawson, K.J. (2001). “Basic Ship Theory, Volume 2”. Butterworth-Heinemann, pps. 368. ISBN: 0080499864, 9780080499864.

U.S. Department of Agriculture (2010). “USDA national nutrient database for standard reference”, release 23. Nutrient data laboratory URL: www.ars.usda.gov/nutrientdata

Videler, J.J. (1993). “Fish Swimming”. Springer.

Vincent J. F. V. (2001). "Stealing ideas from nature". In: Deployable Structures (ed. S Pellegrino), Springer-Verlag, Vienna, pp. 51-58

Wallace, B.P. and Jones, T.T. (2008). “What makes marine turtles go: A review of metabolic rates and their consequences”. Journal of Experimental Marine Biology and Ecology, 356, pp. 8-24. Elsevier

Webb, P.W. (1975). “Hydrodynamics and energetics of fish propulsion”. Department of the Environment Fisheries and Marine Service, Bulletin 190

Wen, L., Wang, T.M., Wu, G.H. and Liang, J.H. (2012). “Hydrodynamic investigation of a self-propelled robotic fish based on a force-feedback control method”. Bioinspiration & Biomimetics, 7, pp. 17. IOP publishing. doi:10.1088/1748-3182/7/3/036012

Williams, R. & Noren, D. P. (2009) "Swimming speed, respiration rate, and estimated cost of transport in adult killer whales". Marine Mammal Science, 25, 327-350.

Williams, T. M., Davis, R. W., Fuiman, A., Francis, J., Boeuf, B. J. L., Horning, M., Calambokidis, J. & Croll, D. A. (2000). "Sink or Swim: Strategies for Cost-Efficient Diving by Marine Mammals". Science magazine, 288, 133-136.

Winberg, G.G. (ed.) (1971). “Methods for the Estimation of Production of Aquatic Animals”. Academic press, London & Newyork.

Yamamoto, I. (2005). “Research and development of autonomous underwater vehicles”. Proceedings of the Unmanned Underwater Vehicle Showcase, Southampton, UK.

Database References

The references in this section are not cited in the main body of the thesis. However, they are used in the creation of the database and are cited in Appendix 2.

Aoyama, J., Hissmann, K., Yoshinaga, T., Sasai, s., Uto, T. and Ueda, Hiroshi (1999). "Swimming depth of migrating silver eels Anguilla japonica released at seamounts of the West Mariana Ridge, their estimated spawning sites". Marine Ecology Progress Series, 186: pp. 265-269.

Berquist, R.M, Gledhill K.M, Peterson, M.W, Doan, A.H, Baxter, G.T, Yopak, K.E., Kang, N., Walker, H.J., Hastings, P.A. and Frank, L.R. (2012) "The Digital Fish Library: Using MRI to Digitize, Database, and Document the Morphological Diversity of Fish". PLoS ONE, 7(4), e34499. doi:10.1371/journal.pone.0034499

Behrens, J.W., Præbel, K. and Steffensen, J.F. (2005). "Swimming energetics of the Barents Sea capelin (*Mallotus villosus*)". Journal of Experimental Marine Biology and Ecology, 331(2), pp.208-216

Berta, A., Sumich, J.L. and Kovacs, K.M. (eds.) (2006). "Marine Mammals Evolutionary Biology", Elsevier inc.

Blake, R.W. and Chan, K.H.S. (2006). "Models of the turning and fast-start swimming dynamics of aquatic vertebrates". Journal of Fish Biology, 69, pp. 1824–1836. doi:10.1111/j.1095-8649.2006.01251.x.

Borgwardt, N. and Culik, B.M. (1999). "Asian small-clawed otters (*Amblonyx cinerea*): resting and swimming metabolic rates". Journal of Comparative Physiology and Biology, 169: pp. 100-106.

Bowen, A.D.; Yoerger, D.R.; Taylor, C.; McCabe, R.; Howland, J.; Gomez-Ibanez, D.; Kinsey, J.C.; Heintz, M.; McDonald, G.; Peters, D.B.; Fletcher, B.; Young, C.; Buescher, J.; Whitcomb, L.L.; Martin, S.C.; Webster, S.E. and Jakuba, M.V. (2008). "The Nereus hybrid underwater robotic vehicle for global ocean science operations to 11,000m depth," OCEANS 2008, pp.1-10, 15-18 September 2008. doi: 10.1109/OCEANS.2008.5151993

Boyd, I.L., Reid, K. and Bevan, R.M. (1995). "Swimming speed and allocation of time during the dive cycle in Antarctic fur seals. Animal Behaviour, 50: pp. 769-784.

Breen, M., Dyson, J., O'neill, F. G. O., Jones, E. and Haigh, M. (2004). "Swimming endurance of haddock (*Melanogrammus aeglefinus*) at prolonged and sustained swimming speeds, and its role in their capture by towed fishing gears". ICES Journal of Marine Science, 61, pp. 1071-1079.

Brill, R.W., Block, B. A., Boggs, C. H., Bigelow, K. A., Freund, E. V. and Marcinek, D. J.(1999). "Horizontal movements and depth distribution of large adult yellowfin tuna (*Thunnus albacares*) near the Hawaiian Islands, recorded using ultrasonic telemetry: implications for the physiological ecology of pelagic fishes". Marine Biology. 133: pp. 395-408.

Brisbin, I.L. Jr. (1972). "Seasonal variations in the libe weights and major body components of captive box turtles". Herpetologica, 28, pp. 70-75

Bruce, B.D., J.D. Stevens, and H. Malcom, (2006). "Movements and swimming behaviour of white sharks (Carcharodon carcharias) in Australian waters". Marine Biology, 150: pp. 161-172.

Bruce, B.D., Stevens, J.D. and Malcom, H. (2006). "Movements and swimming behaviour of white sharks (*Carcharodon carcharias*) in Australian waters". Marine Biology, 150: pp. 161-172.

Castellini, M. (2000). "History of polar whaling: insights into the physiology of the great whales", Comparative Biochemistry and Physiology, Part A, 126, pp. 153-159.

Clark, T.D. and Seymour, R.S. (2006). "Cardiorespiratory physiology and swimming energetics of a high-energy-demand". Journal of Experimental Biology, 209 (19), pp. 3940-3951

Domenici, P. and Blake, R. W. (1997). "The kinematics and performance of fish fast-start swimming". The Journal of Experimental Biology, 200, pp. 1165-1178.

Domenici, P. (2001). "Review: The scaling of locomotor performance in predator-prey encounters: from fish to killer whales." Comparative Biochemistry and Physiology Part A, 131. pp. 169-182.

Fish, F. E. and Hui, C. A. (1991). "Dolphin Swimming - a review." Mammal Review, 4, pp. 181-195.

Fish, F.E., Hurley, J., Costa, D.P. (2002). "Maneuverability by the sea lion Zalophus californianus: turning performance of an unstable body design". The Journal of Experimental Biology, 206, pp. 667-674. DOI: 10.1242/jeb.00144

Fish, F. E. and Lauder, G. V. (2006). "Passive and active flow control by swimming fishes and mammals." Annual Review of Fluid Mechanics, 38, pp. 193-224.

He, P. and Wardle, C.S. (1986). "Tilting Behaviour of the Atlantic Mackeral, *Scomber scombrus* at low swimming speeds". Fish Biology, 29: pp. 223-323.

Hoelzel, A.R. (ed.) (2002). "Marine mammal biology: An Evolutionary Approach". Wiley. ISBN 0632052325

Hui, C.A. (1985). "Maneuverability of the Humboldt penguin (*Spheniscus humboldti*) during swimming". Canadian Journal of Zoology, 63, pp. 2165-2167. DOI: 10.1139/z85-318

Jobling, M. and Johansen, S.J.S. (2003). "Fat Distribution in Atlantic Salmon *Salmo Salaar L.* in relation to body size and feeding regime". Aquaculture Research, 34(4), pp. 331-316.

Jun, B.H., Park, J.Y., Lee, F.Y., Lee, P.M., Lee, C.M., Kim, K., Lim, Y.K. and Oh, J.H. (2009). "Development of the AUV 'ISiMI' and a free running test in an Ocean Engineering Basin". Ocean Engineering, 36, pp. 2-14. Elsevier

Kawabea, R., Naitob, Y., Satob, K., Miyashitac, K and Yamashitaa, N. (2004). "Direct measurement of the swimming speed, tailbeat, and body angle of Japanese flounder (*Paralichthys olivaceus*)". ICES Journal of Marine Science. 61: pp. 1080-1087.

Korsmeyer, K.E., Steffensen, J.F. and Herskin, J. (2002). "Energetics of median and paired fin swimming, body and caudal fin swimming, and gait transition in

parrotfish (*Scarus schlegeli*) and triggerfish (*Rhinecanthus aculeatus*)". Journal of Experimental Biology, 205: pp. 1253-1263.

Kongsberg (2009). "Autonomous underwater vehicle - HUGIN AUV" http://www.km.kongsberg.com.

Lowe, C. G. (2002). "Bioenergetics of free-ranging juvenile scalloped hammerhead sharks (Sphyrna lewini) in Kane'ohe Bay, O'ahu, Hawaii". Journal of Experimental Marine Biology and Ecology, 278, pp. 141-156.

Luna-Jorquera, G. and Culik, B.M. (2000). "Metabolic rates of swimming Humboldt penguins". Marine Ecology Progress Series, 203: pp. 301-309.

Maeda, T., Ishiguro, S., Yokohama, K., Hirokawa, K., Hashimoto, A., Okuda, Y. and Tani, T. (2004). "Development of Fuel Cell AUV "URASHIMA"". Mitsubishi Heavy Industries Technical Review, 41(6), pp.1-5.

Marty, P. (2004). "ALIVE: An Autonomous Light Intervention Vehicle". Scandinavian OIL.GAS Magazine. 11/12, 2004

Ohlberger, J., Staaks, G. and Hölker, F. (2006). "Swimming efficiency and the influence of morphology on swimming costs in fishes". Journal of Comparative Physiology B: Biochemical, Systemic, and Environmental Physiology, 176(1): pp. 17-25.

Otani, S., Naito, Y., Kato, A. and Kawamura, A. (2001). "Oxygen consumption and swim speed of the harbor porpoise *Phocoena phocoena*". Fisheries Science, 67: pp. 894-898.

Palstra, A., van Ginneken, V. and van den Thillart, G. (2008). “Cost of transport and optimal swimming speed in farmed and wild European silver eels (*Anguilla anguilla*)”. Comparative Biochemistry and Physiology Part A: Molecular & Integrative Physiology. 151(1): pp. 37-44.

Parsons, G.R. (1990). “Metabolism and swimming efficiency of the bonnethead shark *Sphyrna tiburo*”. Marine Biology. 104(3): pp. 363-367.

Pepperell, J.G. and Davis, T.L.O. (1999). “Post-release behaviour of black marlin, *Makaira indica*, caught off the Great Barrier Reef with sportfishing gear”. Marine Biology, 135: pp. 369-380.

Rosen, D.S. and Trites, A. (2002). “Cost of transport in steller sea lions, *Eumetopias jubatus*”. Marine Mammal Science, 18(2): pp. 513-524.

Sato, K., Naito, Y., Kato, A., Niizuma, Y., Watanuki, Y., Charrassin, J.B., Bost, C.A., Handrich, Y. and Maho, Y. L (2002). “Buoyancy and maximal diving depth in penguins: do they control inhaling air volume? “. The Journal of Experimental Biology, 205, pp. 1189–1197. The Company of Biologists Limited

Sato, K., Watanuki, Y., Takahashi, A., Miller,P.J.O., Tanaka, H., Kawabe, R., Ponganis, P.J., Handrich, Y., Akamatsu, T., Watanabe, Y., Mitani, Y., Costa,D.P., Bost, C., Aoki, K., Amano,M., Trathan,P., Shapiro, A. and Naito, Y. (2007). "Stroke frequency, but not swimming speed, is related to body size in free-ranging seabirds, pinnipeds and cetaceans". Proceedings of the Royal Society of London. Series B, Biological Sciences, 274(1609): pp. 471-477.

Sepulveda, C.A., Dickson, K.A. and Graham, J.B. (2003). "Swimming performance studies on the eastern Pacific bonito Sarda chiliensis, a close relative of the tunas (family Scombridae) I. Energetics". Journal of Experimental Biology, 206: pp. 2739-2748.

Sims, D.W. (2000). “Filter-feeding and cruising swimming speeds of basking sharks compared with optimal models: they filter-feed slower than predicted for their size”. Journal of Experimental Marine Biology and Ecology. 249: pp. 65-76.

Steinhausen, M.F., Steffensen, J.F. and Andersen, N.G. (2005).”Tail beat frequency as a predictor of swimming speed and oxygen consumption of saithe (*Pollachius virens*) and whiting (*Merlangius merlangus*) during forced swimming”. Marine Biology, 148: pp. 197-204.

Steenson, L.V., Phillips, A.P., Furlong, M.E., Rogers, E. and Turnock, S.R. (2011). "Maneuvering of an Over-Actuated Autonomous Underwater Vehicle using both Through-Body Tunnel Thrusters and Control Surfaces". UUST2011

Stobutzki, I. C. and Bellwood, D. R. (1997). "Sustained swimming abilities of the late pelagic stages of coral reef fishes". Marine Ecology Progress Series, 149, pp.31-41.

Sumich, J.L. (1983). "Swimming velocities, breathing patterns, and estimated costs of locomotion in migrating grey whales, *Eschrichtius robustus*". Canadian Journal of Zoology, 61(3): p. 647-652.

Syme, D.A., Gollock, M., Freeman, M.J. and Gamperl, a.K. (2008). "Power Isn't Everything: Muscle Function and Energetic Costs during Steady Swimming in Atlantic Cod (*Gadus morhua*). Physiological and Biochemical Zoology. 81(3): pp. 320-335. doi: 10.1086/528784.

Tanaka H, Takagi Y, and Naito Y. (2001). "Swimming speeds and buoyancy compensation of migrating adult chum salmon *Oncorhynchus keta* revealed by speed/depth/acceleration data logger". Journal of Experiemental Biology. 204: pp. 3895-3904.

Tudorache, C., O'Keefe, R.A. and Benfey, T.J. (2011). "Optimal swimming speeds reflect preferred swimming speeds of brook charr (*Salvelinus fontinalis Mitchill*, 1874)". Fish Physiology Biochemisty. 37: pp. 307-315.

Tytell, E. D. (2007). "Do trout swim better than eels? Challenges for estimating performance based on the wake of self-propelled bodies." Experimental Fluids, 43, pp. 701-712.

Van den Thillart, G., Palstra, A. and Van Ginneken, V. (2007). "Simulated Migration of European Silver Eel; Swim Capacity and Cost Of Transport". Journal of Marine Science and Technology, Special Issue, 2007, pp.1-16.

Van Ginneken, V., Antonissen, E., Muller, K.U, Booms, R., Eding, E., Verreth, J. and Van den Thillart, G. (2005). "Eel migration to the Sargasso: remarkably high swimming efficiency and low energy costs". The Journal of Experimental Biology, 208, pp. 1329-1335.

Videler, J. J. and Nolet, B.A. (1990). "Costs of Swimming Measured at Optimum Speed: Scale effects, Differences Between Swimming Styles, Taxonomic Groups and Submerged and Surface Swimming". Comparative Biochemistry and

Physiology, 97A(2), pp.91-99

Videler, J. J. and Wardle, C. S. (1991). "Fish swimming stride by stride". Reviews in Fish Biology and Fisheries, 1, pp.23-41

Walker, J. A. (2000). "Does a rigid body limit maneuverability?". The Journal of Experimental Biology, 203, pp.3391-3396.

Watanabe, Y. and Sato, K. (2008). "Functional Dorsoventral Symmetry in Relation to Lift-Based Swimming in the Ocean Sunfish *Mola mola*". PLoS ONE, 3(10).

Webb, P.W. (1977). "Energetics of size on performance and energetics of fish, in Scale effects in locomotion". (ed) Pedley, T.J., Academic Press. pp. 315-331.

Westerberg, H.k., Lagenfelt, I. and Svedang H. (2007). "Silver eel migration behaviour in the Baltic". ICES Journal of Marine Science, 64: pp. 1457-1462.

Williams, R. and Noren, D.P. (2009). "Swimming speed, respiration rate, and estimated cost of transport in adult killer whales". Marine Mammal Science, 25(2): p. 327-350.

Williams, T.M. (1999). "The evolution of cost efficient swimming in marine mammals: limits to energetic optimization". Philosophical Transactions of the Royal Society B: Biological Sciences, 354(1380): pp. 193-201.

Woodward, B.L., Winn, J.P., Fish, F.E. (2006). "Morphological Specialisation of Baleen Whales Associated With Hydrodynamic Performance and Ecological Niche". Journal of Morphology, 267, pp. 1284-1294.

Yazdi, P., Kilian, A. and Culik, B.M. (1999) "Energy expenditure of swimming bottlenose dolphins (Tursiops truncatus)". Marine Biology, 134, pp. 601-607. Springer-Verlag 1999

Yoshida, H., Hyakudome, T., Ishibahis, S., Sawa, T., Tsukioka, S., Aoki, T., Tani, T., Iwata, M. and Moriga, T. (2010). "A Compact High Efficiency PEFC System for Underwater Platforms". Williams, N., Krist, K. and Garland, N. (eds.), ECS transactions: Electrochemical Society, Fuel Cell Seminar 2009, 26(1), pp. 67-76.

Appendix

Appendix 1. BMSs and AUVs databases

The legend below is a legend for the entire Appendix 1.

1	Mean (average) Value
2	Voluntary Swimming Speed
3	Mode of the swimming speed
4	The BMS was a juvenile
5	Sustained speed
6	Highest burst speed recorded for the species
7	Less than
8	More than
9	Actual value from manufacturer experiment
10	Mass estimated from $Mass = 0.99L^{3.09}$(Webb, 1977)
11	Calculated from the mass-length relationship
13	Indicated value by the manufacturer; no trial records found
14	Values from genetically similar species

Also, note that for Appendix 1.2, the legend below is associated with various cross-sections.

1	Circular
2	Oval
2.5	Oval box
3	Compressed
3.5	Flat

Appendix 1.1. The Taxonomy table

Class	Order	Family (Sub Order if applicable)	BinominalName	CommonName	Taxa Code	Taxa No
Actinopterygii (Fish)	Beryciformes	Anoplogastridae	*Anoplogaster cornuta*	fangtooth	1001	1
	Beryciformes	Berycidae	*Beryx decadactylus*	alfonsine	1002	1
	Beryciformes	Trachichthyidae	*Hoplostethus atlanticus*	orange roughy	1003	1
	Lophiiformes	Ceratiidae	*Cryptopsaras couesi*	deep-sea anglerfish	1004	1
	Lophiiformes	Himantolophidae	*Himantolophus albinares*	football fish	1005	1
	Lophiiformes	Melanocetidae	*Melanocetus johnsonii*	Black sea devil	1006	1
	Myctophiformes	Myctophidae	*Diaphus rafinesquii*	lantern fish	1007	1
	Osmeriformes	Opisthoproctidae	*Opisthoproctus soleatus*	barreleye	1008	1
	Osmeriformes	Osmeridae	*Mallotus villosus*	barents sea capelin	1009	1
	Perciformes	Chiasmodontidae	*Chiasmodon niger*	black swallower	1010	1
	Perciformes	Scaridae	*Scarus schlegeli*	parrotfish	1011	1
	Perciformes	Sciaenidae	*Cynoscion neblosus*	spotted seatrout	1012	1
	Perciformes	Sciaenidae	*Scaenops ocellatus*	red drum	1012	2

Class	Order	Family (Sub Order if applicable)	BinominalName	CommonName	Taxa Code	Taxa No
	Perciformes	Sparidae	*Archosargus probatocephalus*	sheepshead	1013	1
	Stomiiformes	Gonostomatidae	*Gonostoma denudatum*	bristlemouth	1014	1
	Anguilliformes	Anguillidae	*Anguilla anguilla*	silver eel	1101	1
	Anguilliformes	Anguillidae	*Anguilla japonica*	Japanese eel	1101	2
	Anguilliformes	Nemichthyidae	*Nemichthys scolopaceus*	slender snipe eel	1102	1
	Aulopiformes	Ipnopidae	*Bathypterios grallator*	tripod fish	1103	1
	Aulopiformes	Ipnopidae	*Bathypterios mediterraneus*	Mediterranean spiderfish	1103	2
	Ophidiiformes	Ophidiidae	*Abyssobrotula galatheae*	deep-sea cusk eel	1105	1
	Ophidiiformes	Ophidiidae	*Lepophidium marmoratum*	cusk eel4	1105	2
	Ophidiiformes	Ophidiidae	*Neobythites sivicola*	cusk eel3	1105	3
	Ophidiiformes	Ophidiidae	*Ophidion barbatum*	snake blenny	1105	4
	Ophidiiformes	Ophidiidae	*Ophidion muraenolepis*	blackedge cusk	1105	5
	Ophidiiformes	Ophidiidae	*Sirembo imberbis*	golden cusk	1105	6
	Perciformes	Zoarcidae	*Melanostigma pammelas*	midwater eelpout	1106	1
	Pleuronectiformes	Paralichthyidae	*Paralichthys*	Japanese flounder	1108	1

Class	Order	Family (Sub Order if applicable)	BinominalName	CommonName	Taxa Code	Taxa No
			olivaceus			
	Saccopharyngiformes	Eurypharyngidae	*Eurypharynx pelecanoides*	pelican eel	1109	1
	Stomiiformes	Stomiidae	*Chauliodus macouni*	Pacific viper fish	1110	1
	Stomiiformes	Stomiidae	*Chauliodus sloani*	viper fish	1110	2
	Stomiiformes	Stomiidae	*Melanostomias melanops*	barbeled dragonfish	1110	3
	Stomiiformes	Stomiidae	*Stomias boa*	scaly dragonfish	1110	4
	Cypriniforme	Cyprinidae	*Leuciscus leuciscus*	common dace	1201	1
	Cypriniformes	Cyprinidae	*Carassius auratus*	goldfish	1201	2
	Cypriniformes	Cyprinidae	*Cyprinus carpio*	carp	1201	3
	Cypriniformes	Cyprinidae	*Rutilus rutilus*	roach	1201	4
	Esociformes	Esocidae	*Esox lucius*	pike	1202	1
	Gadiformes	Gadidae	*Gadus morhua*	atlantic cod	1203	1
	Gadiformes	Gadidae	*Melanogrammus aeglefinus*	haddock	1203	2
	Gadiformes	Gadidae	*Merlangius merlangus*	whiting	1203	3
	Gadiformes	Gadidae	*Pollachius virens*	saithe	1203	4
	Gadiformes	Macrouridae	*Coelorhynchus coelorhynchus*	blackspot grenadier	1204	1
	Gadiformes	Macrouridae	*Coryphaenoides rupestris*	roundnose grenadier	1204	2

Class	Order	Family (Sub Order if applicable)	BinominalName	CommonName	Taxa Code	Taxa No
	Osmeriformes	Alepocephalidae	*Alepocephalus umbriceps*	slickhead	1205	1
	Perciformes	Sphyraenidae	*Sphyraena barracuda*	greatbarracuda	1206	1
	Salmoniformes	Salmonidae	*Coregonus artedi*	cisco	1207	1
	Salmoniformes	Salmonidae	*Coregonus clupeaformis*	lake whitefish	1207	2
	Salmoniformes	Salmonidae	*Oncorhynchus keta*	chum salmon	1207	3
	Salmoniformes	Salmonidae	*Oncorhynchus mykiss*	rainbow trout	1207	4
	Salmoniformes	Salmonidae	*Oncorhynchus nerka*	sockeye salmon	1207	5
	Salmoniformes	Salmonidae	*Salvelinus fontinalis*	brook charr	1207	6
	Acipenseriformes	Acipenseridae	*Acipenser fulvescens*	lake sturgeon	1301	1
	Beloniformes	Exocoetidae	*Exocoetus*	flying fish	1302	1
	Characiformes	Chaeracidae	*Metynnis argenteus*	silver dollar	1303	1
	Clupeiformes	Clupeidae	*Sardinops sagax*	south American pilchard	1304	1
	Mugiliformes	Mugilidae	*Liza macrolepis*	largescale mullet	1305	1
	Osteoglossiformes	Mormyridae	*Gnathonemus petersii*	elephantnose fish	1306	1
	Perciformes	Carangidae	*Seriola lalandi*	yellowtail kingfish	1307	1

Class	Order	Family (Sub Order if applicable)	BinominalName	CommonName	Taxa Code	Taxa No
	Perciformes	Centrarchidae	*Micropterus salmoides*	largemouth bass	1308	1
	Perciformes	Centrarchidae	*Micropterus dolomieu*	smallmouth bass	1308	2
	Perciformes	Cichlidae	*Oreochromis niloticus*	Nile tilapia	1309	1
	Perciformes	Cichlidae	*Oreochromis niloticus*	Nile tilapia	1309	1
	Perciformes	Moronidae	*Morone saxatilis*	striped bass	1310	1
	Perciformes	Pomatomidae	*Pomatomus saltatrix*	bluefish	1311	1
	Perciformes	Scombridae	*Scomber scombrus*	Atlantic mackerel	1312	1
	Perciformes	Scombridae	*Scomber japonicus*	chub mackerel	1312	2
	Perciformes	Carangidae	*Trachurus symmetricus*	Pacific jack mackerel	1401	1
	Perciformes	Coryphaenidae	*Coryphaena hippurus*	dolphinfish	1402	1
	Perciformes	Istiophoridae	*Makaira indica*	black marlin	1403	1
	Perciformes	Istiophoridae	*Stiophorus platypterus*	Indo-Pacific sailfish	1403	2
	Perciformes	Scombridae	*Katsuwonus pelamis*	skipjack tuna	1404	1
	Perciformes	Scombridae	*Sarda chiliensis*	Pacific bonito	1404	2
	Perciformes	Scombridae	*Thunnus*	yellowfin tuna	1404	3

Class	Order	Family (Sub Order if applicable)	BinominalName	CommonName	Taxa Code	Taxa No
			albacares			
	Perciformes	Scombridae	*Thunnus thynnus*	bluefin tuna (northern)	1404	4
	Perciformes	Xiphiidae	*Xiphias gladius*	swordfish	1405	1
	Stomiiformes	Sternoptychidae	*Sternoptyx diaphana*	diaphanous hatchetfish	1501	1
	Stomiiformes	Sternoptychidae	*Argyropelecus hemigymnus*	silver hatchet fish	1501	2
	Tetraodontiformes	Diodontidae	*Chilomycterus schoepfi*	striped burrfish	1601	1
	Tetraodontiformes	Ostraciidae	*Ostracion cubicus*	boxfish	1602	1
	Tetraodontiformes	Ostraciidae	*Ostracion meleagris*	whitespotted boxfish	1602	2
	Perciformes	Acanthuridae	*Naso annulatus*	whitemargin unicornfish	1701	1
	Perciformes	Acanthuridae	*Acanthurus bahianus*	ocean surgeonfish	1701	2
	Perciformes	Centrarchidae	*Lepomis gibbosus*	pumpkinseed	1702	1
	Perciformes	Embiotocidae	*Cymatogaster aggregata*	shiner perch	1703	1
	Perciformes	Embiotocidae	*Cymatogaster aggregata*	shiner perch	1703	1
	Perciformes	Labridae	*Thalassoma bifasciatum*	bluehead wrasse	1704	1
	Perciformes	Labridae	*Oxyjulis californica*	señorita	1704	2

Class	Order	Family (Sub Order if applicable)	BinominalName	CommonName	Taxa Code	Taxa No
	Perciformes	Pomacentridae	*Stegastes leucostictus*	beaugregory damselfish	1705	1
	Perciformes	Pomacanthidae	*Centropyge multifasciata*	angelfish	1705	2
	Scorpaeniformes	Agonidae	*Agonopsis chiloensis*	snailfish	1706	1
	Lampriformes	Regalecidae	*Regalecus glesne*	oarfish	1801	1
	Gymnotiformes	Apteronotidae	*Apteronotus albifrons*	black ghost	1802	1
	Perciformes	Chaetodontidae	*Chaetodon capistratus*	foureye butterflyfish	1901	1
	Tetraodontiformes	Balistidae	*Rhinecanthus aculeatus*	picasso triggerfish	1902	1
	N/A	N/A	*Pseudoliparis amblystomopsis*	snailfish(new)	1903	1
	Tetraodontiformes	Molidae	*Mola mola*	ocean sunfish	1904	1
Agnatha (Fish with notochord)	Myxiniformes	Myxinidae	*Eptatretus stoutii*	Pacific hagfish	1104	1
	Petromyzontiformes	Petromyzontidae	*Petromyzon marinus*	sea lamprey	1107	1
Chondrichthyes (Cartilaginous fish)	Hexanchiformes	Chlamydoselachidae	*Chlamydoselachus anguineum*	frilled shark	2101	1
	Squaliformes	Squalidae	*Squalus acanthias*	dogfish	2102	1
	Squaliformes	Dalatiidae	*Isistius brasiliensis*	cookie cutter shark	2103	1

Class	Order	Family (Sub Order if applicable)	BinominalName	CommonName	Taxa Code	Taxa No
	Carcharhiniformes	Triakidae	*Triakis henlei*	mustelus henlei	2201	1
	Carcharhiniformes	Triakidae	*Triakis semifasciata*	leopard shark	2201	2
	Orectolobiformes	Rhincodontidae	*Rhincodon typus*	whale shark	2203	1
	Carcharhiniformes	Carcharhinidae	*Carcharhinus leucas*	bull shark	2301	1
	Carcharhiniformes	Carcharhinidae	*Carcharhinus melanoterus*	blacktip reef shark	2301	2
	Carcharhiniformes	Carcharhinidae	*Negaprion brevirostris*	lemon shark	2301	3
	Carcharhiniformes	Sphyrnidae	*Sphyrna lewini*	hammerhead shark	2304	1
	Carcharhiniformes	Sphyrnidae	*Sphyrna tiburo*	bonnethead shark	2304	2
	Lamniformes	Cetorhinidae	*Cetorhinus maximus*	basking shark	2305	1
	Orectolobiformes	Ginglymostomatidae	*Ginglymostoma cirratum*	nurse shark	2306	1
	Lamniformes	Lamindae	*Carcharodon carcharias*	white shark	2401	1
	Myliobatiformes	Mobulidae	*Manta birostris*	giant manta ray	2601	1
	Rajiformes	Myliobatidae	*Aetobatus narinari*	spotted eagle ray	2602	1

Class	Order	Family (Sub Order if applicable)	BinominalName	CommonName	Taxa Code	Taxa No
Holocephali	Chimaeriformes	Rhinochimaeridae	*Rhinochimaera pacifica*	spookfish (chimera)	2202	1
Mammalia(Mammals)	Sirenia	Dugongidae	*Dugong dugon*	dugong	3301	1
	Cetacea	Balaenidae (Mysticeti)	*Balaena mysticetus*	bowhead whale	3401	1
	Cetacea	Balaenidae (Mysticeti)	*Eubalaena glacialis*	north Atlantic right whale	3401	2
	Cetacea	Balaenopteridae (Mysticeti)	*Balaenoptera acutorostrata*	minke whale	3402	1
	Cetacea	Balaenopteridae (Mysticeti)	*Balaenoptera borealis*	sei whale	3402	2
	Cetacea	Balaenopteridae (Mysticeti)	*Balaenoptera brydei*	bryde's whale	3402	3
	Cetacea	Balaenopteridae (Mysticeti)	*Balaenoptera musculus*	blue whale	3402	4
	Cetacea	Balaenopteridae (Mysticeti)	*Balaenoptera physalus*	fin whale	3402	5
	Cetacea	Balaenopteridae (Mysticeti)	*Megaptera novaeangliae*	humpback whale	3402	6
	Cetacea	Balaenopteridae (Mysticeti)	*Eschrichtius robustus*	grey whale	3403	1
	Cetacea	Monodontidae (Odontoceti)	*Delphinapterus leucas*	beluga whale	3404	1
	Cetacea	Physeteridae (Odontoceti)	*Physeter macrocephalus*	sperm whale	3405	1
	Cetacea	Ziphiidae	*Hyperoodon*	beaked whale	3406	1

Class	Order	Family (Sub Order if applicable)	BinominalName	CommonName	Taxa Code	Taxa No
		(Odontoceti)	*ampullatus*			
	Cetacea	Delphinidae (Odontoceti)	*Orcinus orca*	killer whale	3407	1
	Cetacea	Delphinidae (Odontoceti)	*Pseudorca crassidens*	false killer whale	3407	2
	Cetacea	Delphinidae (Odontoceti)	*Cephalorhynchus commersonii*	commerson's dolphin	3407	3
	Cetacea	Delphinidae (Odontoceti)	*Delphinus delphis*	common dolphin	3407	4
	Cetacea	Delphinidae (Odontoceti)	*Globicephala*	long-finned pilot whale	3407	5
	Cetacea	Delphinidae (Odontoceti)	*Lagenorhynchus acutus*	white sided dolphin	3407	6
	Cetacea	Delphinidae (Odontoceti)	*Stenella frontalis*	Atlantic spotted dolphin	3407	7
	Cetacea	Delphinidae (Odontoceti)	*Tursiops truncatus*	bottlenose dolphin	3407	8
	Cetacea	Delphinidae (Odontoceti)	*Tursipos truncatus gillii*	Pacific bottlenose dolphin	3407	8
	Cetacea	Phocoenidae (Odontoceti)	*Phocoena phocoena*	harbour porpoise	3408	1
	Cetacea	Phocoenidae (Odontoceti)	*Phocoena phocoena*	harbour porpoise	3408	1
	Cetacea	Phocoenidae (Odontoceti)	*Phocoenoides dalli*	dall's porpoise	3408	2
	Carnivora	Mustelidae	*Enhydra lutris*	sea otter	3501	1

Class	Order	Family (Sub Order if applicable)	BinominalName	CommonName	Taxa Code	Taxa No
	Carnivora	Odobenidae (Pinnipedia)	*Odobenus rosmarus*	walrus	3502	1
	Carnivora	Phocidae (Pinnipedia)	*Halichoerus grypus*	grey seal	3503	1
	Carnivora	Phocidae (Pinnipedia)	*Leptonychotes weddellii*	weddell seal	3503	2
	Carnivora	Phocidae (Pinnipedia)	*Mirounga angustirostris*	northern elephant seal	3503	3
	Carnivora	Phocidae (Pinnipedia)	*Mirounga leonina*	southern elephant seal	3503	4
	Carnivora	Phocidae (Pinnipedia)	*Phoca witulina*	harbour seal	3503	5
	Carnivora	Phocidae (Pinnipedia)	*Pusa sibirica*	baikal seal	3503	6
	Rodentia	Cricetidae (Pinnipedia)	*Ondatra zibethicus*	muskrat	3504	1
	Carnivora	Otariidae (Pinnipedia)	*Arctocephalus gazella*	Antarctic fur seal	3701	1
	Carnivora	Otariidae (Pinnipedia)	*Calorhinus ursinus*	northern fur seal	3701	2
	Carnivora	Otariidae (Pinnipedia)	*Eumetopias jubatus*	steller sea lion	3701	3
	Carnivora	Otariidae (Pinnipedia)	*Eumetopias jubatus*	steller sea lion	3701	3
	Carnivora	Otariidae (Pinnipedia)	*Zalophus californianus*	California sea lion	3701	4

Class	Order	Family (Sub Order if applicable)	BinominalName	CommonName	Taxa Code	Taxa No
	Carnivora	Mustelidae	*Amblonyx cinerea*	asian small- clawed otters	3702	1
	Carnivora	Mustelidae	*Neovison vison*	north American mink	3702	2
Aves (Birds: Penguins)	Sphenisciformes	Spheniscidae	*Aptenodytes forsteri*	emporer penguin	4701	1
	Sphenisciformes	Spheniscidae	*Aptenodytes patagonicus*	king penguin	4701	2
	Sphenisciformes	Spheniscidae	*Eudyptula minor*	little penguin	4701	3
	Sphenisciformes	Spheniscidae	*Pygoscelis adeliae*	adelie penguin	4701	4
	Sphenisciformes	Spheniscidae	*Pygoscelis antarctica*	chinstrap penguin	4701	5
	Sphenisciformes	Spheniscidae	*Pygoscelis papua*	gentoo pinguin	4701	6
	Sphenisciformes	Spheniscidae	*Spheniscus demersus*	African penguin	4701	7
	Sphenisciformes	Spheniscidae	*Spheniscus humboldti*	humboldt penguin	4701	8
	Sphenisciformes	Spheniscidae	*Eudyptes chrysolophus*	macaroni penguin	4701	9
Reptilia (Reptiles)	Sauria	Iguanidae	*Amblyrhynchus cristatus*	marine iguana	5101	1
	Testudines	Dermochelyidae (Cryptodira)	*Dermochelys coriacea*	leatherback turtle	5701	1
	Testudines	Cheloniidae (Cryptodira)	*Chelonia mydes*	green sea turtle	5702	1
	Testudines	Emydidae (Cryptodira)	*Chrysemys picta*	painted turtle	5703	1

Class	Order	Family (Sub Order if applicable)	BinominalName	CommonName	Taxa Code	Taxa No
Cephalopoda(head feet)	Teuthida	Loliginidae	*Loligo plei*	slender inshore squid (arrow squid)	6001	1
	Teuthida	Loliginidae	*Loligo opalescens*	opalescent inshore squid	6001	2
	Oegopsida	Architeuthidae	*Architeuthis x*	giant squid	6002	1
	Oegopsida	Octopoteuthidae	*Taningia danae*	dana octopus squid	6003	1
	Teuthida	Mastigoteuthidae	*Mastigoteuthis flammea*	whip-lash squid	6004	1

Appendix 1.2. BMSs' Database

1.Taxonomy			2.Swimming				3.Manoeuvrability			4.Depth Capability [m]		5.Energetics			6.Body Characteristics		
CommonName	Taxa Code	Taxa-No	Swimming Mode	Swim Mode	Uopt [m/s]	Umax [m/s]	R-Yaw (m)	R-Yaw (/L)	R-path (L)	Min Depth	Max Depth	COT-Opt (J/(kg*m))	Endurance (h)	FatTissue Percentage	Body Form	Cross-Section	TL (m)
fangtooth	1001	1								2	4992				4	3	0.18
alfonsine	1002	1								250	600				4	3	
orange roughy	1003	1								180	1200				4	3	0.57
deep-sea anglerfish	1004	1								200	2000				4	3	
football fish	1005	1								200	1000				4	2	0.265
Black sea devil	1006	1								250	2000				4	2	
lantern fish	1007	1								50	1000				2		
barreleye	1008	1								300	800				3	2	
barents sea capelin	1009	1			0.28							3.01			2	3	0.1693 [(11)]
black swallower	1010	1								750	1500				3	3	
parrotfish	1011	1			0.53							2.39	47.8935	0.624	3	3	0.224 [(11)]
spotted seatrout	1012	1			0.81							1.77			3	1	0.299 [(11)]
red drum	1012	2			0.90							2.35			3	2	0.32 [(11)]
sheepshead	1013	1			0.99							1.47			4	3	0.273 (11)
bristlemouth	1014	1								100	700				2	3	0.161
silver eel	1101	1	BCFAnguilliform	11	0.67			0.09			2000	0.68	2163.81	10.14	1	1	1.33
silver eel	1101	1	BCFAnguilliform	11	0.18						2000	0.50	11266.7	10.14	1	1	0.35
silver eel	1101	1	BCFAnguilliform	11	0.40							0.42	5868.06	10.14	1	1	0.74
silver eel (european)	1101	1	BCFAnguilliform	11	0.62									10.14	1	1	0.82 (11)
Japanese eel	1101	2	BCFAnguilliform	11	0.44 [(1)]										1	1	0.69 (11)

1.Taxonomy			2.Swimming				3.Manoeuvrability			4.Depth Capability [m]		5.Energetics			6.Body Characteristics		
CommonName	Taxa Code	Taxa-No	Swimming Mode	Swim Mode	Uopt [m/s]	Umax [m/s]	R-Yaw (m)	R-Yaw (/L)	R-path (L)	Min Depth	Max Depth	COT-Opt (J/(kg*m))	Endurance (h)	FatTissue Percentage	Body Form	Cross-Section	TL (m)
slender snipe eel	1102	1	BCFAnguilliform	11							3656				1	3	1.3
tripod fish	1103	1	BCFAnguilliform	11						878	4720				2	3	1.531
Mediterranean spiderfish	1103	2								300	2800				2	3	0.24
Pacific hagfish	1104	1	BCFAnguilliform	11						16	1155				1	1	0.43
deep-sea cusk eel	1105	1	BCFAnguilliform	11						3110	8370				1	2	0.165
cusk eel4	1105	2	BCFAnguilliform	11						155	525				1	3	
cusk eel3	1105	3	BCFAnguilliform	11						75	100				1	3	0.26
snake blenny	1105	4	BCFAnguilliform	11							150				1	3	0.26
blackedge cusk	1105	5	BCFAnguilliform	11						80	370				1	3	0.159
golden cusk	1105	6	BCFAnguilliform	11						100	200				2	3	0.21
midwater eelpout	1106	1	BCFAnguilliform	11						96	2195				1		0.11
sea lamprey	1107	1	BCFAnguilliform	11	0.36	1.36				1	2200			10.14	1	2	0.6
Japanese flounder	1108	1	BCFAnguilliform	11	0.35(3)									10.14	3	3	0.568 (11)
pelican eel	1109	1	BCFAnguilliform	11						500	7625				1	3	1
Pacific viper fish	1110	1	BCFAnguilliform	11						25	4390				2	2	0.25
viper fish	1110	2								200	4700				2	3	0.36
barbeled dragonfish	1110	3								200	1024				2	3	0.298
scaly dragonfish	1110	4	BCFAnguilliform	11						200	1500				1	3	
common dace	1201	1	BCFSubcarangiform	12		1.59									3	2	0.09
goldfish	1201	2	BCFSubcarangiform	12	0.32			0.25			20	1.49			3	2	0.1
goldfish	1201	2	BCFSubcarangiform	12	0.48							1.3734			3	2	0.15
goldfish	1201	2	BCFSubcarangiform	12		0.65								1.092	3	2	0.07
goldfish	1201	2	BCFSubcarangiform	12				0.25						1.092	3	2	0.0587159
carp	1201	3	BCFSubcarangiform	12	0.59	1.64								1.092	3	3	0.31

1.Taxonomy			2.Swimming				3.Manoeuvrability			4.Depth Capability [m]		5.Energetics			6.Body Characteristics		
CommonName	Taxa Code	Taxa-No	Swimming Mode	Swim Mode	Uopt [m/s]	Umax [m/s]	R-Yaw (m)	R-Yaw (/L)	R-path (L)	Min Depth	Max Depth	COT-Opt (J/(kg*m))	Endurance (h)	FatTissue Percentage	Body Form	Cross-Section	TL (m)
carp	1201	3	BCFSubcarangiform	12	0.26									1.092	3	3	0.182 (11)
carp	1201	3	BCFSubcarangiform	12	0.32									1.092	3	3	0.315 (11)
roach	1201	4	BCFSubcarangiform	12	0.40			0.25		15	15			1.092	3	3	0.6
roach	1201	4	BCFSubcarangiform	12	0.32									1.092	3	3	0.2(11)
roach	1201	4	BCFSubcarangiform	12	0.43									1.092	3	3	0.284(11)
pike	1202	1	BCFSubcarangiform	12				0.09						1.092	2	2	0.402 (11)
Atlantic cod	1203	1	BCFSubcarangiform	12	0.27							1.77	476.041	2.34	3	2	0.403(11)
Atlantic cod	1203	1	BCFSubcarangiform	12		1.47								2.34	3	2	0.42
Atlantic cod	1203	1	BCFSubcarangiform	12		0.84								2.34	3	2	0.3
haddock	1203	2	BCFSubcarangiform	12	0.25			0.13		10	450	2.16	60.9047	0.338	3	1	0.248
haddock	1203	2	BCFSubcarangiform	12	1.34			0.13			450			0.338	3	1	1.12
whiting	1203	3	BCFSubcarangiform	12	0.34					10	200	1.50	118.954	0.624	3	2	0.34
saithe	1203	4	BCFSubcarangiform	12	0.48							1.37			3	1	0.3755 (11)
saithe	1203	4	BCFSubcarangiform	12		1.23									3	1	0.35
saithe	1203	4	BCFSubcarangiform	12		1.36									3	1	0.4
blackspot grenadier	1204	1	BCFSubcarangiform	12						200	500				2	1	
roundnose grenadier	1204	2	BCFSubcarangiform	12						180	2600				2	1	1.1
slickhead	1205	1	BCFSubcarangiform	12						500	2000				2	2	
greatbarracuda	1206	1	BCFSubcarangiform	12		12.00				1	100				2	3	1.4
cisco	1207	1			0.23							1.57	2037.06	7.566	3	2	0.282 (11)
lake whitefish	1207	2	BCFSubcarangiform	12	0.46							1.77	620.923	5.2	3	2	0.3044 (11)
chum salmon	1207	3	BCFSubcarangiform	12	0.95(3)									18.85	3	3	0.685

1.Taxonomy			2.Swimming				3.Manoeuvrability			4.Depth Capability [m]		5.Energetics			6.Body Characteristics		
CommonName	Taxa Code	Taxa-No	Swimming Mode	Swim Mode	Uopt [m/s]	Umax [m/s]	R-Yaw (m)	R-Yaw (/L)	R-path (L)	Min Depth	Max Depth	COT-Opt (J/(kg*m))	Endurance (h)	FatTissue Percentage	Body Form	Cross-Section	TL (m)
rainbow trout	1207	4	BCFSubcarangiform	12				0.17						6.084	3	3	0.2415 (11)
rainbow trout	1207	4	BCFSubcarangiform	12	0.28			0.17			200	2.84	743.838	6.084	3	3	0.291
rainbow trout	1207	4	BCFSubcarangiform	12	0.96			0.17		0	200	2.35	262.19	6.084	3	3	0.6
rainbow trout	1207	4	BCFSubcarangiform	12	1.92			0.17			200			6.084	3	3	1.2
rainbow trout	1207	4	BCFSubcarangiform	12		0.75								6.084	3	3	0.04
sockeye salmon	1207	5	BCFSubcarangiform	12	0.31							2.35	721.727	5.408	3	3	0.188
sockeye salmon	1207	5	BCFSubcarangiform	12	0.28							3.92	479.025	5.408	3	3	0.1
brook charr	1207	6	BCFSubcarangiform	12	0.26							-		18.85	3	3	0.258 (11)
lake sturgeon	1301	1	BCFCarangiform	13		0.43									2	1	0.16
flying fish	1302	1	BCFCarangiform	13							20				2	2	
silver dollar	1303	1	BCFCarangiform	13			0.0131								4	3	
south American pilchard	1304	1	BCFCarangiform	13		0									3	3	0.14
largescale mullet	1305	1	BCFCarangiform	13	1.45			0.34						3.9	3	2	0.726
largescale mullet	1305	1	BCFCarangiform	13	0.52			0.34		10	10			3.9	3	2	0.26
largescale mullet	1305	1	BCFCarangiform	13	0.21							6.57	274.818	3.9	3	2	0.105
elephantnose fish	1306	1	BCFCarangiform	13	0.23				0.04					3.79	2	3	0.35
yellowtail kingfish	1307	1	BCFCarangiform	13	0.67							1.45			3	3	0.5752 (11)
largemouth bass	1308	1	BCFCarangiform	13	0.42							2.06	323.625	2.88	3	2	0.225
smallmouth bass	1308	2					0.0261								3	2	
Nile tilapia	1309	1	BCFCarangiform	13	1.41			0.10		5	20			0.4602	4	3	0.725
Nile tilapia	1309	1	BCFCarangiform	13	0.41							2.06		0.4602	4	3	0.21
striped bass	1310	1	BCFCarangiform	13	0.43			0.26		30	30	3.14	112.329	1.56	3	2	0.254

1.Taxonomy			2.Swimming				3.Manoeuvrability			4.Depth Capability [m]		5.Energetics			6.Body Characteristics		
CommonName	Taxa Code	Taxa-No	Swimming Mode	Swim Mode	Uopt [m/s]	Umax [m/s]	R-Yaw (m)	R-Yaw (/L)	R-path (L)	Min Depth	Max Depth	COT-Opt (J/(kg*m))	Endurance (h)	FatTissue Percentage	Body Form	Cross-Section	TL (m)
bluefish	1311	1	BCFCarangiform	13	0.51			0.14			200	3.53	96.882	1.794	3	3	0.254
bluefish	1311	1	BCFCarangiform	13	1.20			0.14		0	200	3.58	40.5998	1.794	3	3	0.6
Atlantic mackerel	1312	1	BCFCarangiform	13	0.34(2)									7.2228	3	2	0.3209 (11)
Atlantic mackerel	1312	1	BCFCarangiform	13		5.58				0	1000			7.2228	3	2	0.31
chub mackerel	1312	2	BCFCarangiform	13		0								7.2228	3	2	0.3
Pacific jack mackerel	1401	1	BCFThunniform	14		0.77									3	2	0.05
dolphinfish	1402	1	BCFThunniform	14			0.0134								3	3	
black marlin	1403	1	BCFThunniform	14	1.26(1)									2.5	2	2	3.68(11)
Indo-Pacific sailfish	1403	2	BCFThunniform	14		35.07				0	200			0	2	3	3.4
skipjack tuna	1404	1	BCFThunniform	14	0.56							3.24	133.745	2.496	3	2	0.34 (11)
skipjack tuna	1404	1	BCFThunniform	14	0.72							2.94	114.638	2.496	3	2	0.6 (11)
Pacific bonito	1404	2	BCFThunniform	14	0.60							2.65		2.496	3	2	0.449 (11)
yellowfin tuna	1404	3	BCFThunniform	14				0.47						2.496	3	2	0.347 (11)
yellowfin tuna	1404	3	BCFThunniform	14	1.35			0.47		1	1000	0.47	380.188	2.496	3	2	1.65
yellowfin tuna	1404	3	BCFThunniform	14	2.15			0.47			1000	0.4728	238.723	2.496	3	2	2.39
yellowfin tuna	1404	3	BCFThunniform	14	1.3									2.496	3	2	1.809 (11)
bluefin tuna (northern)	1404	4	BCFThunniform	14	2.76	15.00		0.49			985			2.548	3	2	2.3
bluefin tuna (northern)	1404	4	BCFThunniform	14		21.4								2.548	3	2	2.3
swordfish	1405	1	BCFThunniform	14	2.25	24.86				0	800				2	3	2.026
diaphanous hatchetfish	1501	1	BCFOstraciiform	15						400	3676			3.85	4	3	0.055
silver hatchet fish	1501	2								250	650			3.85	4	3	
striped burrfish	1601	1	UMPFDiodontiform	22	0.51							1.57		3.85	4	1	0.216 (11)

1.Taxonomy			2.Swimming				3.Manoeuvrability			4.Depth Capability [m]		5.Energetics			6.Body Characteristics		
CommonName	Taxa Code	Taxa-No	Swimming Mode	Swim Mode	Uopt [m/s]	Umax [m/s]	R-Yaw (m)	R-Yaw (/L)	R-path (L)	Min Depth	Max Depth	COT-Opt (J/(kg*m))	Endurance (h)	FatTissue Percentage	Body Form	Cross-Section	TL (m)
boxfish	1602	1	UMPFDiodontiform	22			0.0493							3.85	4	2.5	
whitespotted boxfish	1602	2	UMPFDiodontiform	22	0.28	2.25		0.38	0.00	1	30			3.85	4	2.5	0.25
whitemargin unicornfish	1701	1	OMPFLabriform	23						1	122			3.85	3		0.36
ocean surgeonfish	1701	2					0.0039		0.011					3.85	4	3	0.35
pumpkinseed	1702	1	OMPFLabriform	23	0.6				0.05		15			6.53	4	3	0.4
pumpkinseed	1702	1	OMPFLabriform	23	0.18				0.05			3.34	1055.99	6.53	4	3	0.119
shiner perch	1703	1	OMPFLabriform	23	0.14							3.83	94.2849	0.52	4	3	
shiner perch	1703	1	OMPFLabriform	23	0.26							3.14	61.925	0.52	4	3	
bluehead wrasse	1704	1	OMPFLabriform	23			0.0044		0.022						2	2	0.2
señorita	1704	2			0.20							3.43			3	3	
beaugregory damselfish	1705	1	OMPFLabriform	23			0.0026		0.026						4	3	0.1
angelfish	1705	2					0.0046		0.023						4	3	0.2
snailfish	1706	1	OMPFLabriform	23						3	400				2	2	0.14
oarfish	1801	1	UMPFAmiiform	31						20	1000				1	3	
black ghost	1802	1	UMPFGymnotiform	32	0.37				0.03					3.85	2	3	0.5
foureye butterflyfish	1901	1	UMPFBalistiform	33			0.0033		0.022						4	3	0.15
picasso triggerfish	1902	1	UMPFBalistiform	33	0.27							1.74			4	3	0.2 (11)
snailfish(new)	1903	1	UMPFBalistiform	33	1.20	2.00				7500	7500				1	2.5	0.15
ocean sunfish	1904	1	OMPFTetraodontiform	34	0.7[(1)]									3.85	4	3	0.945 (11)
frilled shark	2101	1	BCFAnguilliform	11						50	1500				3	2	1.96
dogfish	2102	1	BCFAnguilliform	11			0.0391								3	3	

1.Taxonomy			2.Swimming				3.Manoeuvrability			4.Depth Capability [m]		5.Energetics			6.Body Characteristics		
CommonName	Taxa Code	Taxa-No	Swimming Mode	Swim Mode	Uopt [m/s]	Umax [m/s]	R-Yaw (m)	R-Yaw (/L)	R-path (L)	Min Depth	Max Depth	COT-Opt (J/(kg*m))	Endurance (h)	FatTissue Percentage	Body Form	Cross-Section	TL (m)
cookie cutter shark	2103	1	BCFAnguilliform	11						1	3700				2	3	0.42
mustelus henlei	2201	1	BCFSubcarangiform	12		0									2	2	0.24
leopard shark	2201	2	BCFSubcarangiform	12		0									2	2	0.98
spookfish (chimera)	2202	1	BCFSubcarangiform	12						330	1490				2	1	
whale shark	2203	1	BCFSubcarangiform	12						0	700				2	2	10
bull shark	2301	1	BCFCarangiform	13		0									3	2	2
blacktip reef shark	2301	2	BCFCarangiform	13		0									2	2	0.97
lemon shark	2301	3	BCFCarangiform	13	0.85			0.30		0	92				3	2	3.4
lemon shark	2301	3	BCFCarangiform	13		0									3	2	2
hammerhead shark	2304	1	BCFCarangiform	13	0.94			0.45			512				2	2	4.3
hammerhead shark	2304	1	BCFCarangiform	13	-			0.45			512				2	2	4.3
bonnethead shark	2304	2	BCFCarangiform	13	-							1.6736		3.08	2	2	4.8765 (11)
bonnethead shark	2304	2	BCFCarangiform	13	0.28[2]							5.06	211.353	3.08	2	2	0.3341828
bonnethead shark	2304	2	BCFCarangiform	13	0.48[2]									3.08	2	2	1.0594735
basking shark	2305	1	BCFCarangiform	13	1.8			0.97		0	2000				2	1	9
basking shark	2305	1	BCFCarangiform	13	1.15			0.97							2	1	5.2626 (11)
nurse shark	2306	1	BCFCarangiform	13		0									2	2	2
white shark	2401	1	BCFThunniform	14	0.86[1]										3	1	1.69 (11)
giant manta ray	2601	1	UMPFRajiform	21				0.27		0	120				5	3.5	4.5
spotted eagle ray	2602	1	UMPFRajiform	21						1	80				5	3.5	1.23
dugong	3301	1	BCFCarangiform	13						0	20				3	1	3.3
bowhead whale	3401	1	BCFThunniform	14	2.11	4.61									3	1	18
north Atlantic right whale	3401	2	BCFThunniform	14		4.47				0	305			40.5	3	1	6.1

1.Taxonomy			2.Swimming				3.Manoeuvrability			4.Depth Capability [m]		5.Energetics			6.Body Characteristics		
CommonName	Taxa Code	Taxa-No	Swimming Mode	Swim Mode	Uopt [m/s]	Umax [m/s]	R-Yaw (m)	R-Yaw (/L)	R-path (L)	Min Depth	Max Depth	COT-Opt (J/(kg*m))	Endurance (h)	FatTissue Percentage	Body Form	Cross-Section	TL (m)
minke whale	3402	1	BCFThunniform	14	2.11	7.24								15	3	1	
sei whale	3402	2	BCFThunniform	14	2.31	13.30								18	3	1	14
bryde's whale	3402	3	BCFThunniform	14	2.31	8.23				0				23	3	1	13
blue whale	3402	4	BCFThunniform	14	6.20	15.44				0	500			27	3	1	27
fin whale	3402	5	BCFThunniform	14	2.51	10.30				0	230			24	3	1	
humpback whale	3402	6	BCFThunniform	14	2.63	4.14		0.82		0	148			27	3	2	15.2
grey whale	3403	1	BCFThunniform	14	1.57	4.41				0	170			29	3	1	14
grey whale	3403	1	BCFThunniform	14	2.25							0.39	3213.04	29	3	1	11.5
beluga whale	3404	1	BCFThunniform	14	1.75	6.13		0.17		0	647			25	3	1	5
sperm whale	3405	1	BCFThunniform	14	1.75					0	3000	0.60	3055.56	33	3	1	18
beaked whale	3406	1	BCFThunniform	14						0	1888				3	1	7
killer whale	3407	1	BCFThunniform	14	2.80	15.42		0.18		0	260	1.30	587.607	22	3	1	4.76
killer whale	3407	1	BCFThunniform	14	-			0.18			260	-		22	3	1	9.8
killer whale	3407	1	BCFThunniform	14	3.00							0.90	792.181	22	3	1	5.8402546
killer whale	3407	1	BCFThunniform	14	3.00							1.00	712.963	22	3	1	6.6502088
killer whale	3407	1	BCFThunniform	14	3.10							0.75	919.952	22	3	1	7.3999118
killer whale	3407	1	BCFThunniform	14	3.10							0.84	821.386	22	3	1	5.7897281
false killer whale	3407	2	BCFThunniform	14	3.14	8.03		0.15						22	3	1	3.75
commerson’s dolphin	3407	3	BCFThunniform	14				0.16							3	1	1.7
common dolphin	3407	4	BCFThunniform	14	2.82	8.03				0	280				3	1	2.6
long-finned pilot whale	3407	5	BCFThunniform	14						0	1000				3	1	6.1
white sided dolphin	3407	6	BCFThunniform	14	3.42	7.56		0.23							3	1	2.8
Atlantic spotted dolphin	3407	7	BCFThunniform	14	0.80					0	2200			22	3	1	2
bottlenose dolphin	3407	8	BCFThunniform	14	2.39	4.10		0.19		0	535	0.68	1313.88	22	3	1	3.8

1.Taxonomy			2.Swimming				3.Manoeuvrability			4.Depth Capability [m]		5.Energetics			6.Body Characteristics		
CommonName	Taxa Code	Taxa-No	Swimming Mode	Swim Mode	Uopt [m/s]	Umax [m/s]	R-Yaw (m)	R-Yaw (/L)	R-path (L)	Min Depth	Max Depth	COT-Opt (J/(kg*m))	Endurance (h)	FatTissue Percentage	Body Form	Cross-Section	TL (m)
bottlenose dolphin	3407	8	BCFThunniform	14	2.5							1.16	737.548	22	3	1	3.6331406
bottlenose dolphin	3407	8	BCFThunniform	14	2.1							1.3	783.476	22	3	1	3.4059164
Pacific bottlenose dolphin	3407	8	BCFThunniform	14						0	50			22	3	1	3.8
harbour porpoise	3408	1	BCFThunniform	14	1.40							2.41			3	1	1.476 (11)
harbour porpoise	3408	1	BCFThunniform	14	2.03	6.13									3	1	2
dall's porpoise	3408	2	BCFThunniform	14		15.43				0	550				3	1	2
sea otter	3501	1	BDCF	16	0.80							12.60	212.191	22	3	1	1.11 (11)
sea otter	3501	1	BDCF	16						0	95				3	1	1.48
walrus	3502	1	BDCF	16						0	90				3	1	3.6
grey seal	3503	1	BDCF	16	1.30							3.90	403.654	21.05	3	1	1.5943161
weddell seal	3503	2	BDCF	16						0	700				3	1	2.9
weddell seal	3503	2	BDCF	16	1.5[(1)]										3	1	2.8562452
northern elephant seal	3503	3	BDCF	16	1.8[(1)]										3	1	1.0233776
northern elephant seal	3503	3	BDCF	16						0	1581				3	1	5
southern elephant seal	3503	4	BDCF	16						0	1255				3	1	5.8
southern elephant seal	3503	4	BDCF	16	1.3[(1)]										3	1	3.7140872
harbour seal	3503	5	BDCF	16	1.25							2.45	668.254	21.05	3	1	1.25
harbour seal	3503	5	BDCF	16	1.61							3.60	353.093	21.05	3	1	1.3
harbour seal	3503	5	BDCF	16	2.08							2.26	435.357	21.05	3	1	1.5
harbour seal	3503	5	BDCF	16	2.20									21.05	3	1	1.0992498
harbour seal	3503	5	BDCF	16						0	90			21.05	3	1	1.9

1.Taxonomy			2.Swimming				3.Manoeuvrability			4.Depth Capability [m]		5.Energetics			6.Body Characteristics		
CommonName	Taxa Code	Taxa-No	Swimming Mode	Swim Mode	Uopt [m/s]	Umax [m/s]	R-Yaw (m)	R-Yaw (/L)	R-path (L)	Min Depth	Max Depth	COT-Opt (J/(kg*m))	Endurance (h)	FatTissue Percentage	Body Form	Cross-Section	TL (m)
baikal seal	3503	6	BDCF	16	1.1[(1)]									21.05	3	1	1.495 (11)
muskrat	3504	1	BDCF	16	0.75							21.40			3	1	
Antarctic fur seals	3701	1	OMPFLabriform	23	1.99[(1)]										3	1	2.0576648
northern fur seal	3701	2	OMPFLabriform	23						0	70				3	1	2.1
steller sea lion	3701	3	OMPFLabriform	23	3.6									21.05	3	1	3
steller sea lion	3701	3	OMPFLabriform	23	1.90							3.50	307.749	21.05	3	1	1.857173
steller sea lion	3701	3	OMPFLabriform	23	1.90							3.50	307.749	21.05	3	1	1.851163
steller sea lion	3701	3	OMPFLabriform	23	1.90							4.30	250.493	21.05	3	1	1.7438241
steller sea lion	3701	3	OMPFLabriform	23	1.90							5.30	203.23	21.05	3	1	1.7114688
steller sea lion [(4)]	3701	3	OMPFLabriform	23	1.90						424	3.50	307.749	21.05	3	1	1.851163
California sea lion	3701	4	OMPFLabriform	23				0.09						21.05	3	1	2.4
California sea lion	3701	4	OMPFLabriform	23			0.1564							21.05	3	1	1.85 (11)
California sea lion	3701	4	OMPFLabriform	23	1.6			0.11				2.4	532.95	21.05	3	1	1.08 (11)
California sea lion	3701	4	OMPFLabriform	23	1.66			0.11				2.55	483.47	21.05	3	1	1.31
California sea lion	3701	4	OMPFLabriform	23	2			0.11				2.3	444.897	21.05	3	1	1.05 (11)
California sea lion	3701	4	OMPFLabriform	23	2.6			0.11				2.8	281.116	21.05	3	1	1.08 (11)
California sea lion	3701	4	OMPFLabriform	23				0.11						21.05			1.89
asian small- clawed otters	3702	1	OMPFLabriform	23	1							14.42	148.328	22	3	1	
north American mink	3702	2	OMPFLabriform	23	0.75							41.10	69.3881	22	3	1	
emperor penguin	4701	1	OMPFLabriform	23	3.00	3.98				0	564			16.65	3	1	1.1
emporer penguin	4701	1	OMPFLabriform	23	1.7[(1)]									16.65	3	1	
king penguin	4701	2	OMPFLabriform	23	2.1[(1)]					0	318			16.65	3	1	0.9(1)

1.Taxonomy			2.Swimming				3.Manoeuvrability			4.Depth Capability [m]		5.Energetics			6.Body Characteristics		
CommonName	Taxa Code	Taxa-No	Swimming Mode	Swim Mode	Uopt [m/s]	Umax [m/s]	R-Yaw (m)	R-Yaw (/L)	R-path (L)	Min Depth	Max Depth	COT-Opt (J/(kg*m))	Endurance (h)	FatTissue Percentage	Body Form	Cross-Section	TL (m)
little penguin	4701	3	OMPFLabriform	23	0.70							12.65	182.806	16.65	3	1	0.4
little penguin	4701	3	OMPFLabriform	23	1.8							11.1	81.0185	16.65	3	1	
little penguin	4701	3	OMPFLabriform	23	1.8(1)							11.10	81.0185	16.65	3	1	
adelie penguin	4701	4	OMPFLabriform	23	2.2							4.9	150.162	16.65	3	1	
adelie penguin	4701	4	OMPFLabriform	23	2.0(1)							4.90	165.179	16.65	3	1	
chinstrap penguin	4701	5	OMPFLabriform	23	2.4							3.7	182.292	16.65	3	1	
chinstrap penguin	4701	5	OMPFLabriform	23	2.3(1)							3.70	190.217	16.65	3	1	
gentoo penguin	4701	6	OMPFLabriform	23	1.8							7.6	118.33	16.65	3	1	0.75
gentoo penguin	4701	6	OMPFLabriform	23	2.3(1)							7.60	92.6058	16.65	3	1	0.75
gentoo pinguin	4701	6	OMPFLabriform	23										16.65	3	1	0.75
African penguin	4701	7	OMPFLabriform	23	2.00							15.50	52.2177	16.65	3	1	0.65
African penguin	4701	7	OMPFLabriform	23	0.86							7.65	245.99	16.65	3	1	0.65
humboldt penguin	4701	8	OMPFLabriform	23	1.50			0.24				6.80	158.701	16.65	3	1	0.65
macaroni penguin	4701	9	OMPFLabriform	23	2.0(1)									16.65	3	1	
marine iguana	5101	1	BCFAnguilliform	11						0	12				3	2	1.3
marine iguana (jouvenile)	5101	1	BCFAnguilliform	11											3	2	
leatherback turtle	5701	1	OMPFLabriform	23	0.84	2.80				0	1230				5	3.5	1.82
green sea turtle	5702	1	OMPFLabriform	23	0.49							3.04			5	3.5	0.29
painted turtle	5703	1	OMPFLabriform	23				0.54	0.042						5	3.5	0.25
slender inshore squid (arrow squid)	6001	1	JetForm	41						20	370				6		
opalescent inshore squid	6001	2	JetForm	41	0.37							12.46			6		0.2
giant squid	6002	1	JetForm	41											6		
dana octopus squid	6003	1	JetForm	41	2.50					240	940			1.4	6		2.3
whip-lash squid	6004	1	JetForm	41						700	3500				6		

1.Taxonomy			2.Swimming				3.Manoeuvrability			4.Depth Capability [m]		5.Energetics			6.Body Characteristics			
CommonName	Taxa Code	Taxa-No	Swimming Mode	Swim Mode	Uopt [m/s]	Umax [m/s]	R-Yaw (m)	R-Yaw (/L)	R-path (L)	Min Depth	Max Depth	COT-Opt (J/(kg*m))	Endurance (h)	FatTissue Percentage	Body Form	Cross-Section	TL (m)
sea cucumber1	7001	1	Other	51						200	6000						
sea cucumber2	7001	2	Other	51						100	4000						
giant sea flea	7002	1	Other	51						1000	7000						
pram bug	7003	1	Other	51						100	600						
Japanese giant spider crab	7004	1	Other	51						300	400						
deep-sea crab	7005	1	Other	51						300	500						
soldier striped shrimp	7006	1	Other	51						200	750						
giant isopod	7007	1	Other	51						200	2000						
giant red mysid	7008	1	Other	51						1300	2950				5		
giant sea spider	7009	1	Other	51						5	400						
sea spider	7010	1	Other	51						15	24						
deep-sea jellyfish	7011	1	JetForm	41						200	1000						
salp	7012	1	Other	51						300	2000						

1.Taxonomy			6.Body Characteristics						7. Control Surfaces (Span and Chord are measure as % of TL)								
CommonName	Taxa Code	Taxa-No	EL (%TL)	Mass	aMass_L (Mass [gr])	bMass_L (TL [cm])	BW [%TL]	BH [% TL]	Rear Fin Span%	Rear Fin Chord %	Rear fin Aspect Ratio (Span^2/Area)	Rear fin type	Side Fin Span%	Side Fin Chord %	Side fin Aspect Ratio (Span^2/Area)	Top Fin Span%	Top Fin Chord %
fangtooth	1001	1		0.1				41.1									
alfonsine	1002	1															
orange roughy	1003	1															
deep-sea anglerfish	1004	1															
football fish	1005	1						48.7									
black sea devil	1006	1															
lantern fish	1007	1															
barreleye	1008	1															
barents sea capelin	1009	1	87.88	0.027	0.0037	3.14		13.31			1.724						
black swallower	1010	1															
parrotfish	1011	1	90.6	0.232[(1)]	0.03090	2.87		30.3			1.161						
spotted seatrout	1012	1	88.5	0.35	0.01310	3.000		18.7			1.411						
red drum	1012	2	86.4	0.35	0.0087	3.06		24.1			1.488						
sheepshead	1013	1	79.6	0.35	0.01478	3.045		38.1			1.441						
bristlemouth	1014	1						12.3									
silver eel	1101	1	96.34	5.106	0.0009	3.18	4.57	6				Eel_like	3.471	1.6638	2.3591639	1.2809	74.983
silver eel	1101	1	96.34	0.075	0.0011	3.13	4.57	6				Eel_like	3.471	1.6638	2.3591639	1.2809	74.983
silver eel	1101	1	96.34	0.914			4.57	6				Eel_like	3.471	1.6638	2.3591639	1.2809	74.983
silver eel (european)	1101	1	96.34	1.18	0.0008	3.22	4.57	6				Eel_like	3.471	1.6638	2.3591639	1.2809	74.983
Japanese eel	1101	2	100	0.54	0.00053	3.268	5.5	6				Eel_like	3.471	1.6638	2.3591639	1.2809	74.983
slender snipe eel	1102	1															
tripod fish	1103	1		9.535				11.16									

1.Taxonomy			6.Body Characteristics						7. Control Surfaces (Span and Chord are measure as % of TL)								
CommonName	Taxa Code	Taxa-No	EL (%TL)	Mass	aMass_L (Mass [gr])	bMass_L (TL [cm])	BW [%TL]	BH [% TL]	Rear Fin Span%	Rear Fin Chord %	Rear fin Aspect Ratio (Span^2/Area)	Rear fin type	Side Fin Span%	Side Fin Chord %	Side fin Aspect Ratio (Span^2/Area)	Top Fin Span%	Top Fin Chord %
Mediterranean spiderfish	1103	2		4.12				12									
Pacific hagfish	1104	1															
deep-sea cusk eel	1105	1															
cusk eel4	1105	2															
cusk eel3	1105	3						20.3									
snake blenny	1105	4		0.065				12.1									
blackedge cusk	1105	5						14.6									
golden cusk	1105	6						14.7									
midwater eelpout	1106	1		0.01													
sea lamprey	1107	1	96.2	0.449			4.07	7.2	4.1	9.29	0.783	Truncate				2.3	10.99
Japanese flounder	1108	1	88.9	2.2	0.012	3	6.25	37	23.84	12.37	2.243	Truncate	10.25	7.46	1.748419	6.99	75.39
pelican eel	1109	1		0.6				4.6									
Pacific viper fish	1110	1		0.023													
viper fish	1110	2		8.2				12.7									
barbeled dragonfish	1110	3						11.99794026776652									
scaly dragonfish	1110	4															
common dace	1201	1															
goldfish	1201	2	81.08	0.017	0.0149	3.047	12.3	22.43	38.914	19.328	1.9	Truncate	16.86	7.3488	2.8071752	12.214	33.489
goldfish	1201	2	81.08	0.1	0.0148	3.07	12.3	22.43	38.914	19.328	1.9	Truncate	16.86	7.3488	2.8071752	12.214	33.489
goldfish	1201	2		0.0058 (11)	0.0148	3.07	12.3	22.43	38.914	19.328	1.9	Truncate	16.86	7.3488	2.8071752	12.214	33.489
goldfish	1201	2	81.08	0.003	0.0245	2.732	12.3	22.43	38.914	19.328	1.9	Truncate	16.86	7.3488	2.8071752	12.214	33.489

1.Taxonomy			6.Body Characteristics						7. Control Surfaces (Span and Chord are measure as % of TL)								
CommonName	Taxa Code	Taxa-No	EL (%TL)	Mass	aMass_L (Mass [gr])	bMass_L (TL [cm])	BW [%TL]	BH [% TL]	Rear Fin Span%	Rear Fin Chord %	Rear fin Aspect Ratio (Span^2/Area)	Rear fin type	Side Fin Span%	Side Fin Chord %	Side fin Aspect Ratio (Span^2/Area)	Top Fin Span%	Top Fin Chord %
carp	1201	3	82.7	2	0.0105	3.14	9.45	24.42	26.036	19.13	1.846	Forked	19.09	6.8239	3.5760251	11.874	32.825
carp	1201	3	82.7	0.11	0.0214	2.95	9.45	24.42	26.036	19.13	1.846	Forked	19.09	6.8239	3.5760251	11.874	32.825
carp	1201	3	82.7	0.56	0.0214	2.95	9.45	24.42	26.036	19.13	1.846	Forked	19.09	6.8239	3.5760251	11.874	32.825
roach	1201	4	82.6	4.7	0.053	3.35	8.7	26.1	22.96	15.578	1.49	Forked	15.42	4.8362	4.1975869	15.384	14.649
roach	1201	4	82.6	0.11	0.0074	3.21	8.7	26.1	22.96	15.578	1.49	Forked	15.42	4.8362	4.1975869	15.384	14.649
roach	1201	4	82.6	0.34	0.0074	3.21	8.7	26.1	22.96	15.578	1.49	Forked	15.42	4.8362	4.1975869	15.384	14.649
pike	1202	1	87.5	0.408	0.0045	3.09	7.87	14.9	20.43	15.8	1.921	Forked	12.92	9.44	1.5822408	15.66	13.15
Atlantic cod	1203	1	92.5	0.621(1)	0.0085	3.03	13	17.29	15.035	16.645	1.297	Truncate	12.78	5.8745	2.9518411	10.786	12.989
Atlantic cod	1203	1	92.94	0.704 (11)			8.54	20.29	15.035	16.645	1.635	Truncate	12.78	5.8745	2.9518411	10.786	12.989
Atlantic cod	1203	1	92.94	0.255 (11)			8.54	20.29	15.035	16.645	1.635	Truncate	12.78	5.8745	2.9518411	10.786	12.989
haddock	1203	2	89.7	0.156	0.0062	3.1150	9.44	22.42	15.035	16.645	1.635	Truncate	12.78	5.8745	2.9518411	10.786	12.989
haddock	1203	2	89.7	15	0.0062	3.1150	9.44	22.42	15.035	16.645	1.635	Truncate	12.78	5.8745	2.9518411	10.786	12.989
whiting	1203	3	89.9	0.224	0.006	3.07	9.08	15.7	11.96	14.022	1.054	Truncate	11.32	11.82	1.1422927	12.455	13.237
saithe	1203	4	91.5	0.485	0.0095	2.99		22.6			1.663	Forked					
saithe	1203	4										Forked					
saithe	1203	4										Forked					
blackspot grenadier	1204	1															
roundnose grenadier	1204	2		1.69				14.6									
slickhead	1205	1						17.1									
greatbarracuda	1206	1		19.41													
cisco	1207	1	85	0.28	0.0081	3.13	14.4	20.1			3.18						

1.Taxonomy			6.Body Characteristics						7. Control Surfaces (Span and Chord are measure as % of TL)								
CommonName	Taxa Code	Taxa-No	EL (%TL)	Mass	aMass_L (Mass [gr])	bMass_L (TL [cm])	BW [%TL]	BH [% TL]	Rear Fin Span%	Rear Fin Chord %	Rear fin Aspect Ratio (Span^2/Area)	Rear fin type	Side Fin Span%	Side Fin Chord %	Side fin Aspect Ratio (Span^2/Area)	Top Fin Span%	Top Fin Chord %
lake whitefish	1207	2	85.2	0.364	0.0063	3.21		21.7			1.8						
chum salmon	1207	3	91.3	3.75			14.5	26.3	25.23	13.28	3.175	Truncate	12.12	5.53	2.7990549	11.08	11.78
rainbow trout	1207	4		0.174	0.0089	3.096		22.81	24.68	14.04	3.131	Truncate	9.82	6.06	2.4969549	9.31	12.4
rainbow trout	1207	4	89	0.264	0.01	3.02	14	22.81	24.68	14.04	3.131	Truncate	9.82	6.06	2.4969549	9.31	12.4
rainbow trout	1207	4	89	2.344 (11)	0.01	3.02	14	22.81	24.68	14.04	3.131	Truncate	9.82	6.06	2.4969549	9.31	12.4
rainbow trout	1207	4	89	13.9			14	22.81	24.68	14.04	3.131	Truncate	9.82	6.06	2.4969549	9.31	12.4
rainbow trout	1207	4		0.0011 (11)			14	22.81	24.68	14.04	3.131	Truncate	9.82	6.06	2.4969549	9.31	12.4
sockeye salmon	1207	5	89.4	0.055	0.01555	3	16.6	22.82	24.68	14.04	3.131	Truncate	9.82	6.06	2.4969549	9.31	12.4
sockeye salmon	1207	5	89.4	0.009	0.01555	3	16.6	22.82	24.68	14.04	3.131	Truncate	9.82	6.06	2.4969549	9.31	12.4
brook charr	1207	6	90.8	0.2	0.0102	3.04		26.4			1.538						
lake sturgeon	1301	1															
flying fish	1302	1															
silver dollar	1303	1		0.005													
south American pilchard	1304	1															
largescale mullet	1305	1	82.7	4.53	0.0167	2.962	16.8	22.1	25.65	16.63	2.631	Forked	10.72	4.446	2.8912949	12.347	9.585
largescale mullet	1305	1	82.7	0.216	0.0167	2.962	16.8	22.1	25.65	16.63	2.631	Forked	10.72	4.446	2.8912949	12.347	9.585
largescale mullet	1305	1	82.7	0.008			16.8	22.1	25.65	16.63	2.631	Forked	10.72	4.446	2.8912949	12.347	9.585
elephantnose fish	1306	1	79	0.75			11.3	20.62	16.98	13.51	1.914	Forked	12.3	7.37	1.8821846	9.78	21.18
yellowtail kingfish	1307	1	86.8	2.1[(1)]	0.028 (12)	2.77		20			3.49						
largemouth bass	1308	1	87.4	0.15	0.0107	3.11	16.9	29.1	25.1	16.66	2.46	Forked	12.39	11.57	1.3265823	3.59	14.34
smallmouth bass	1308	2		0.162													

1.Taxonomy			6.Body Characteristics						7. Control Surfaces (Span and Chord are measure as % of TL)								
CommonName	Taxa Code	Taxa-No	EL (%TL)	Mass	aMass_L (Mass [gr])	bMass_L (TL [cm])	BW [%TL]	BH [% TL]	Rear Fin Span%	Rear Fin Chord %	Rear fin Aspect Ratio (Span^2/Area)	Rear fin type	Side Fin Span%	Side Fin Chord %	Side fin Aspect Ratio (Span^2/Area)	Top Fin Span%	Top Fin Chord %
Nile tilapia	1309	1	82.7	7.15	0.0366	2.844	17.3	36.4	26.29	14.02	1.919	Truncate	25.84	12.19	3.7364611	11.17	52.14
Nile tilapia	1309	1	82.7	0.08	0.0347	2.87	17.3	36.4	26.29	14.02	1.919	Truncate	25.84	12.19	3.7364611	11.17	52.14
striped bass	1310	1	89.5	0.212	0.0065	3.09		22.5			2.3						
bluefish	1311	1	87	0.225	0.01356	2.899		25.37			2.66	`					
bluefish	1311	1	87	1.94	0.01356	2.899		25.37			2.66						
Atlantic mackerel	1312	1	90.2	0.3	0.0062	3.11	12.4	17.3	21.78	7.36	5.267	Forked	9.23	4.16	3.0923013	8.51	13.43
Atlantic mackerel	1312	1	90.2				12.4	17.3	21.78	7.36	5.267	Forked	9.23	4.16	3.0923013	8.51	13.43
chub mackerel	1312	2	90.2	0.288 (11)			12.4	17.3	21.78	7.36	5.267	Forked	9.23	4.16	3.0923013	8.51	13.43
pacific jack mackerel	1401	1															
dolphinfish	1402	1		26.27													
black marlin	1403	1	82.4	180	0.00458	2.96	10.8	16.1	37.49	7.57	9.039	Lunate	15.66	3.51	6.698596	10.33	49.73
Indo-Pacific sailfish	1403	2						10.19									
skipjack tuna	1404	1	89.9	0.6	0.0074	3.26	13.8	23.9	26.82	5.83	7.743	Lunate	12.43	6.56	4.4119046	13.15	24.51
skipjack tuna	1404	1	89.9	3.8	0.0074	3.26	13.8	23.9	26.82	5.83	7.743	Lunate	12.43	6.56	4.4119046	13.15	24.51
pacific bonito	1404	2	88.8	1.19(1)	0.0105	3.06	10.5	20.9	20.96	6.19	4.707	Lunate	7.35	4.91	2.1044994	9.47	28.53
yellowfin tuna	1404	3	87.5	0.835			19.7	26.3	27.65	5.73	7.793	Lunate	24.7	6.14	8.8	12.12	20.6
yellowfin tuna	1404	3	87.5	52.95	0.0147	3.013	19.7	26.3	27.65	5.73	7.793	Lunate	24.7	6.14	8.8	12.12	20.6
yellowfin tuna	1404	3	87.5	253.3	0.0214	2.974	19.7	26.3	27.65	5.73	7.793	Lunate	24.7	6.14	8.8	12.12	20.6
yellowfin tuna	1404	3	87.5	77.8 (1)	0.0297	2.91	19.7	26.3	27.65	5.73	7.793	Lunate	24.7	6.14	8.8	12.12	20.6
bluefin tuna (northern)	1404	4	89.3	244 (1)	0.0187	2.93	21	28.7	25.26	7.04	5.588	Lunate	17.01	5.31	4.9383871	9.57	19.85
bluefin tuna (northern)	1404	4		244 (1)			21	28.7	25.26	7.04	5.588	Lunate	17.01	5.31	4.9383871	9.57	19.85
swordfish	1405	1	87.7	153	0.00135	3.447		17	32.1	5.5988	5.21	Lunate					

1.Taxonomy			6.Body Characteristics						7. Control Surfaces (Span and Chord are measure as % of TL)								
CommonName	Taxa Code	Taxa-No	EL (%TL)	Mass	aMass_L (Mass [gr])	bMass_L (TL [cm])	BW [%TL]	BH [% TL]	Rear Fin Span%	Rear Fin Chord %	Rear fin Aspect Ratio (Span^2/Area)	Rear fin type	Side Fin Span%	Side Fin Chord %	Side fin Aspect Ratio (Span^2/Area)	Top Fin Span%	Top Fin Chord %
diaphanous hatchetfish	1501	1						69.5									
silver hatchet fish	1501	2															
striped burrfish	1601	1	84.9	0.35	0.0236	3.124	51.8	51.8	10.89	14.14	0.914	Truncate	12.05	21.08	0.6475028	14.46	15.01
boxfish	1602	1		0.047													
whitespotted boxfish	1602	2	80.7	0.5			27.8	28.57	24.79	21.32	1.481	Round	16.84	12.93	1.4911431	13.26	15.63
whitemargin unicornfish	1701	1		0.79				34									
ocean surgeonfish	1701	2		0.004													
pumpkinseed	1702	1	80.8	0.9	0.006	3.238	17	44.1	21.19	16.9	1.619	Forked	19.05	14.97	1.7152834	15.29	44.3
pumpkinseed	1702	1	80.8	0.03	0.01	3.19	17	44.1	21.19	16.9	1.619	Forked	19.05	14.97	1.7152834	15.29	44.3
shiner perch	1703	1		0.03													
shiner perch	1703	1		0.035													
bluehead wrasse	1704	1		0.003													
señorita	1704	2		0.07													
beaugregory damselfish	1705	1		0.004													
angelfish	1705	2		0.009													
snailfish	1706	1						15.2									
oarfish	1801	1															
black ghost	1802	1	87.91	0.42	0.0027	3.07	10	17.34	3.429	12.093	0.284	Pointed	6.679	8.1526	0.851769	5.501	72.797
foureye butterflyfish	1901	1		0.004													
picasso triggerfish	1902	1	90	0.143(1)	0.0522	2.641	13.4	40	23.12	17.06	1.759	Round	11.94	10.06	1.5236037	9.79	8.35
snailfish(new)	1903	1															
ocean sunfish	1904	1	82.93	48	0.045400	3.050	23	66.91	55.62	17.06	3.762	Round	13.54	12.39	1.3740938	36.61	18.5
frilled shark	2101	1															

1.Taxonomy			6.Body Characteristics						7. Control Surfaces (Span and Chord are measure as % of TL)								
CommonName	Taxa Code	Taxa-No	EL (%TL)	Mass	aMass_L (Mass [gr])	bMass_L (TL [cm])	BW [%TL]	BH [% TL]	Rear Fin Span%	Rear Fin Chord %	Rear fin Aspect Ratio (Span^2/Area)	Rear fin type	Side Fin Span%	Side Fin Chord %	Side fin Aspect Ratio (Span^2/Area)	Top Fin Span%	Top Fin Chord %
dogfish	2102	1		0.754													
cookie cutter shark	2103	1						10.6									
mustelus henlei	2201	1															
leopard shark	2201	2															
spookfish (chimera)	2202	1															
whale shark	2203	1	81.6	4300			19.5	18.6	26.94	9.1	5.055	Assymetric	14.56	10.46	2.3113127	7.64	12.57
bull shark	2301	1															
blacktip reef shark	2301	2															
lemon shark	2301	3	79.3	254.3	0.0053	3.16	14.7	13.8	12.11	14.12	1.044	Assymetric Hi	14.76	11.96	2.3100159	8.05	9.66
lemon shark	2301	3							12.11	14.12	1.044	Assymetric Hi	14.76	11.96	2.3100159	8.05	9.66
hammerhead shark	2304	1	72.9	450			11.7	22.73	16.18	11.72	1.922	assymetric Hi	9.97	9.21	1.8716042	14.81	12.1
hammerhead shark	2304	1	72.9	450	-		11.7	22.73	16.18	11.72	1.922	assymetric Hi	9.97	9.21	1.8716042	14.81	12.1
bonnethead shark	2304	2	73.6	800	0.00069	3.372	9.66	11.93	16.18	11.72	1.922	assymetric Hi	9.97	9.21	1.8716042	14.81	12.1
bonnethead shark	2304	2	73.6	0.095	0.00069	3.372	9.66	11.93	16.18	11.72	1.922	assymetric Hi	9.97	9.21	1.8716042	14.81	12.1
bonnethead shark	2304	2	73.6	4.65	0.00069	3.372	9.66	11.93	16.18	11.72	1.922	assymetric Hi	9.97	9.21	1.8716042	14.81	12.1
basking shark	2305	1	84.6	3600				13.7			3.25	Assymetric					
basking shark	2305	1	84.6	720[10]	0.00494	3		13.7			3.25	Assymetric					
nurse shark	2306	1															
white shark	2401	1	82.7	80	0.00766	3.15	20	21.5	27.06	9.69	4.013	Assymetric	20.29	12.6	3.4665216	10.78	17.12
giant manta ray	2601	1			0.0164	3											

1.Taxonomy			6.Body Characteristics						7. Control Surfaces (Span and Chord are measure as % of TL)								
CommonName	Taxa Code	Taxa-No	EL (%TL)	Mass	aMass_L (Mass [gr])	bMass_L (TL [cm])	BW [%TL]	BH [% TL]	Rear Fin Span%	Rear Fin Chord %	Rear fin Aspect Ratio (Span^2/Area)	Rear fin type	Side Fin Span%	Side Fin Chord %	Side fin Aspect Ratio (Span^2/Area)	Top Fin Span%	Top Fin Chord %
spotted eagle ray	2602	1		67.6	0.0059	3.13											
dugong	3301	1		400													
bowhead whale	3401	1	96.18	22745 (11)	0.0039	3											
north Atlantic right whale	3401	2	96.18	4500			21.8	21.83	37.39	10.49	6.029	Forked	15.64	10.08	2.0701557		
minke whale	3402	1	96.18														
sei whale	3402	2	96.18	17000	0.0062	3											
bryde's whale	3402	3	96.18	12000													
blue whale	3402	4	96.18	1E+05	0.0064	3	15.7	15.7	21.521	7.0066	5.576	Forked	13.15	5.2322	3.922362	1.5038	3.7594
fin whale	3402	5	96.18		0.005	3											
humpback whale	3402	6	96.18	36287			23.8	23.78	34.148	9.6438	3.947	Forked	30.81	8.8324	5.1471435		
grey whale	3403	1	96.18	33200			17.7	17.74	24.41	8.3118	3.63	Forked	17.41	8.8836	2.9626013		
grey whale	3403	1	96.18	15000	0.0014	3.28	17.7	17.74	24.41	8.3118	3.63	Forked	17.41	8.8836	2.9626013		
beluga whale	3404	1	93.92	1590			19.5	18.75	25.19	10.3	3.096	Forked	10.05	8.7281	1.4741472		
sperm whale	3405	1	93.92	40800	0.0092	3											
beaked whale	3406	1	93.92	2500													
killer whale	3407	1	96.18	4500	0.208	2.577	15	15	25	8.19	3.791	Forked	11.66	9.0261	2.0641234	19.147	13.269
killer whale	3407	1	96.18	8500	0.208	2.577	15	15	25	8.19	3.791	Forked	12.69	6.9718	2.0641234	19.147	13.269
killer whale	3407	1	96.18	2800	0.208	2.577	15	15	25	8.19	3.791	Forked	12.69	6.9718	2.0641234	19.147	13.269
killer whale	3407	1	96.18	3913	0.208	2.577	15	15	25	8.19	3.791	Forked	12.69	6.9718	2.0641234	19.147	13.269
killer whale	3407	1	96.18	5153	0.208	2.577	15	15	25	8.19	3.791	Forked	12.69	6.9718	2.0641234	19.147	13.269
killer whale	3407	1	96.18	2738	0.208	2.577	15	15	25	8.19	3.791	Forked	12.69	6.9718	2.0641234	19.147	13.269
false killer whale	3407	2	96.18	379.7	0.0072	3	16	16	23	6.93	3.791	Forked	11.34	6.45	2.2584405	7.58	15.66
commerson’s dolphin	3407	3	88.53	86													

1.Taxonomy			6.Body Characteristics						7. Control Surfaces (Span and Chord are measure as % of TL)								
CommonName	Taxa Code	Taxa-No	EL (%TL)	Mass	aMass_L (Mass [gr])	bMass_L (TL [cm])	BW [%TL]	BH [% TL]	Rear Fin Span%	Rear Fin Chord %	Rear fin Aspect Ratio (Span^2/Area)	Rear fin type	Side Fin Span%	Side Fin Chord %	Side fin Aspect Ratio (Span^2/Area)	Top Fin Span%	Top Fin Chord %
common dolphin	3407	4	88.53	209.2	0.0119	3											
long-finned pilot whale	3407	5	88.53					24.4									
white sided dolphin	3407	6	88.53														
Atlantic spotted dolphin	3407	7	88.53	121.5			13.1	13.08	24.8	8	3.919	Forked	8.24	5.48	2.2708227	12.97	12.73
bottlenose dolphin	3407	8	88.53	650			14.6	19.77	24.8	8	3.919	Forked	8.24	5.48	2.2708227	12.97	12.73
bottlenose dolphin	3407	8	88.53	176	0.00367	3											
bottlenose dolphin	3407	8	88.53	145	0.00367	3	14.6	19.77	24.8	8	3.919	Forked	8.24	5.48	2.2708227	12.97	12.73
Pacific bottlenose dolphin	3407	8	88.53	650													
harbour porpoise	3408	1	88.53	42.5[(1)]	0.083	2.632											
harbour porpoise	3408	1	88.53	94.49	0.083	2.632											
dall's porpoise	3408	2	88.53	122.4													
sea otter	3501	1		20	0.0147	3											
sea otter	3501	1		45													
walrus	3502	1		1900													
grey seal	3503	1	86.9	104	0.0522	2.86	20	20	22.268	15.921	1.951	Round Feet	12.63	5.8197	0.4619053		
weddell seal	3503	2	86.9	450													
weddell seal	3503	2	86.9	330	0.202	2.53											
northern elephant seal	3503	3	86.9	33.5	0.0281	3.023											
northern elephant seal	3503	3	86.9														
southern elephant seal	3503	4	86.9	5000													
southern elephant seal	3503	4	86.9	236.7	0.00462	3											
harbour seal	3503	5	86.9	42.5	0.0404	2.89											

1.Taxonomy			6.Body Characteristics						7. Control Surfaces (Span and Chord are measure as % of TL)								
CommonName	Taxa Code	Taxa-No	EL (%TL)	Mass	aMass_L (Mass [gr])	bMass_L (TL [cm])	BW [%TL]	BH [% TL]	Rear Fin Span%	Rear Fin Chord %	Rear fin Aspect Ratio (Span^2/Area)	Rear fin type	Side Fin Span%	Side Fin Chord %	Side fin Aspect Ratio (Span^2/Area)	Top Fin Span%	Top Fin Chord %
harbour seal	3503	5	86.9	33	0.0404	2.89											
harbour seal	3503	5	86.9	63	0.0404	2.89											
harbour seal	3503	5	86.9	32	0.0404	2.89											
harbour seal	3503	5	86.9	150													
baikal seal	3503	6	82.67	70.1	0.2585	2.4984	29.3	29.33	37.8	24.18	3.868	Round Feet	21.27	8.7178	3.614382		
muskrat	3504	1		0.6													
Antarctic fur seals	3701	1		34.5	0.00396	3											
northern fur seal	3701	2		270													
steller sea lion	3701	3	78.93	650	0.0363	2.89	23	23.01	21.069	14.942	1.95	Round Feet	29.96	14.019	3.5596613		
steller sea lion	3701	3	78.93	140	0.0332	2.92	23	23.01	21.069	14.942	1.95	Round Feet	29.96	14.019	3.5596613		
steller sea lion	3701	3	78.93	138.7	0.0332	2.92	23	23.01	21.069	14.942	1.95	Round Feet	29.96	14.019	3.5596613		
steller sea lion	3701	3	78.93	116.5	0.0332	2.92	23	23.01	21.069	14.942	1.95	Round Feet	29.96	14.019	3.5596613		
steller sea lion	3701	3	78.93	110.3	0.0332	2.92	23	23.01	21.069	14.942	1.95	Round Feet	29.96	14.019	3.5596613		
steller sea lion [(4)]	3701	3	78.93	138.7			23	23.01	21.069	14.942	1.95	Round Feet	29.96	14.019	3.5596613		
California sea lion	3701	4	78.93	390	0.0039	3.3309	23	23.01	21.069	14.942	1.95	Round Feet	29.96	14.019	3.5596613		
California sea lion	3701	4	78.93	140	0.0039	3.3309	23	23.01	21.069	14.942	1.95	Round Feet	29.96	14.019	3.5596613		
California sea lion	3701	4	78.93	23	0.0039	3.3309	23	23.01	21.069	14.942	1.95	Round Feet	29.96	14.019	3.5596613		
California sea lion	3701	4	78.93	22.5	0.0039	3.3309	23	23.01	21.069	14.942	1.95	Round Feet	29.96	14.019	3.5596613		
California sea lion	3701	4	78.93	21	0.0039	3.3309	23	23.01	21.069	14.942	1.95	Round Feet	29.96	14.019	3.5596613		

1.Taxonomy			6.Body Characteristics						7. Control Surfaces (Span and Chord are measure as % of TL)								
CommonName	Taxa Code	Taxa-No	EL (%TL)	Mass	aMass_L (Mass [gr])	bMass_L (TL [cm])	BW [%TL]	BH [% TL]	Rear Fin Span%	Rear Fin Chord %	Rear fin Aspect Ratio (Span^2/Area)	Rear fin type	Side Fin Span%	Side Fin Chord %	Side fin Aspect Ratio (Span^2/Area)	Top Fin Span%	Top Fin Chord %
California sea lion	3701	4	78.93	23	0.0039	3.3309	23	23.01	21.069	14.942	1.95	Round Feet	29.96	14.019	3.5596613		
California sea lion	3701	4	78.93	137.8	0.0039	3.3309	23	23.01	21.069	14.942	1.95	Round Feet	29.96	14.019	3.5596613		
asian small- clawed otters	3702	1		3.1[(1)]													
north American mink	3702	2		1													
emperor penguin	4701	1	100	33													
emporer penguin	4701	1	100	24.5													
king penguin	4701	2	100	11.9					9.9611	22.125	0.894	Round Feet	42.32	8.2722	5.92765		
little penguin	4701	3	100	1.2													
little penguin	4701	3	100	1.2													
little penguin	4701	3	100	1.2													
adelie penguin	4701	4	100	4													
adelie penguin	4701	4	100	4.2													
chinstrap penguin	4701	5	100	3.8													
chinstrap penguin	4701	5	100	3.8													
gentoo penguin	4701	6	100	5.5			28	28	9.9611	22.125	0.894	Round Feet	42.32	8.2722	5.92765		
gentoo penguin	4701	6	100	5.5					9.9611	22.125	0.894	Round Feet	42.32	8.2722	5.92765		
gentoo pinguin	4701	6	100	5.5					9.9611	22.125	0.894	Round Feet	42.32	8.2722	5.92765		
African penguin	4701	7	100	3.2													
African penguin	4701	7	100	3.17													
humboldt penguin	4701	8	96.42	3.6			25	25.3	9.9611	22.125	0.894	Round Feet	42.32	8.2722	5.92765		
macaroni penguin	4701	9	100	3.3													
marine iguana	5101	1			0.0458	3											

1.Taxonomy			6.Body Characteristics						7. Control Surfaces (Span and Chord are measure as % of TL)								
CommonName	Taxa Code	Taxa-No	EL (%TL)	Mass	aMass_L (Mass [gr])	bMass_L (TL [cm])	BW [%TL]	BH [% TL]	Rear Fin Span%	Rear Fin Chord %	Rear fin Aspect Ratio (Span^2/Area)	Rear fin type	Side Fin Span%	Side Fin Chord %	Side fin Aspect Ratio (Span^2/Area)	Top Fin Span%	Top Fin Chord %
marine iguana (jouvenile)	5101	1															
leatherback turtle	5701	1	100	612			53.2	31.7	19.331	13.541	1.941	Round Feet	39.86	14.81	3.5960382		
green sea turtle	5702	1	100	1.15													
painted turtle	5703	1	100														
slender inshore squid (arrow squid)	6001	1															
opalescent inshore squid	6001	2		0.041													
giant squid	6002	1															
dana octopus squid	6003	1	69.57	61.4			16.9	16.85	16.854	39.326	0.857	Squid	31.21	56.18	1.1111111		
whip-lash squid	6004	1															
sea cucumber1	7001	1															
sea cucumber2	7001	2															
giant sea flea	7002	1															
pram bug	7003	1															
Japanese giant spider crab	7004	1															
deep-sea crab	7005	1															
soldier striped shrimp	7006	1															
giant isopod	7007	1															
giant red mysid	7008	1															
giant sea spider	7009	1															
sea spider	7010	1															
deep-sea jellyfish	7011	1															
salp	7012	1															

1.Taxonomy			7. Control Surfaces (Span and Chord are measure as % of TL)												
CommonName	Taxa Code	Taxa-No	Top fin Aspect Ratio (Span^2/Area)	Auxillary Side Fin Span%	Auxillary Side Fin Chord%	Auxillary Side fin Aspect Ratio (Span^2/Area)	Bottom FinSpan %	Bottom FinChord %	Bottom FinAspect Ratio (Span^2/Area)	Rear Fin 2 or sword Span%	Rear Fin Chord %	Rear fin Aspect Ratio (Span^2/Area)	Top Fin2 Span %	Top Fin2 Chord %	Top fin2 Aspect Ratio (Span^2/Area)
fangtooth	1001	1													
alfonsine	1002	1													
orange roughy	1003	1													
deep-sea anglerfish	1004	1													
football fish	1005	1													
black sea devil	1006	1													
lantern fish	1007	1													
barreleye	1008	1													
barents sea capelin	1009	1													
black swallower	1010	1													
parrotfish	1011	1													
spotted seatrout	1012	1													
red drum	1012	2													
sheepshead	1013	1													
bristlemouth	1014	1													
silver eel	1101	1	0.0170826				1.2809	64.6231	0.02						
silver eel	1101	1	0.0170826				1.2809	64.6231	0.02						
silver eel	1101	1	0.0170826				1.2809	64.6231	0.02						
silver eel (european)	1101	1	0.0170826				1.2809	64.6231	0.02						
Japanese eel	1101	2	0.0170826				1.2809	64.6231	0.02						
slender snipe eel	1102	1													
tripod fish	1103	1													
Mediterranean spiderfish	1103	2													
Pacific hagfish	1104	1													

1.Taxonomy			7. Control Surfaces (Span and Chord are measure as % of TL)												
CommonName	Taxa Code	Taxa-No	Top fin Aspect Ratio (Span^2/Area)	Auxillary Side Fin Span%	Auxillary Side Fin Chord%	Auxillary Side fin Aspect Ratio (Span^2/Area)	Bottom FinSpan %	Bottom FinChord %	Bottom FinAspect Ratio (Span^2/Area)	Rear Fin 2 or sword Span%	Rear Fin Chord %	Rear fin Aspect Ratio (Span^2/Area)	Top Fin2 Span %	Top Fin2 Chord %	Top fin2 Aspect Ratio (Span^2/Area)
deep-sea cusk eel	1105	1													
cusk eel4	1105	2													
cusk eel3	1105	3													
snake blenny	1105	4													
blackedge cusk	1105	5													
golden cusk	1105	6													
midwater eelpout	1106	1													
sea lamprey	1107	1	0.4181818										4.01	24.64	0.3340278
Japanese flounder	1108	1	0.116678	8.79	4.11	3.40821	7.94	54.75	1.151481						
pelican eel	1109	1													
Pacific viper fish	1110	1													
viper fish	1110	2													
barbeled dragonfish	1110	3													
scaly dragonfish	1110	4													
common dace	1201	1													
goldfish	1201	2	0.451006	15.902	10.8205	2.29522	13.327	14.8233	1.256848						
goldfish	1201	2	0.451006	15.902	10.8205	2.29522	13.327	14.8233	1.256848						
goldfish	1201	2	0.451006	15.902	10.8205	2.29522	13.327	14.8233	1.256848						
goldfish	1201	2	0.451006	15.902	10.8205	2.29522	13.327	14.8233	1.256848						
carp	1201	3	0.7014301	13.062	9.75205	2.1672	13.142	9.85764	2.030139						
carp	1201	3	0.7014301	13.062	9.75205	2.1672	13.142	9.85764	2.030139						
carp	1201	3	0.7014301	13.062	9.75205	2.1672	13.142	9.85764	2.030139						
roach	1201	4	2.1389866	10.682	6.99601	2.31672	12.684	9.41745	2.27123						
roach	1201	4	2.1389866	10.682	6.99601	2.31672	12.684	9.41745	2.27123						

1.Taxonomy			7. Control Surfaces (Span and Chord are measure as % of TL)												
CommonName	Taxa Code	Taxa-No	Top fin Aspect Ratio (Span^2/Area)	Auxillary Side Fin Span%	Auxillary Side Fin Chord%	Auxillary Side fin Aspect Ratio (Span^2/Area)	Bottom FinSpan %	Bottom FinChord %	Bottom FinAspect Ratio (Span^2/Area)	Rear Fin 2 or sword Span%	Rear Fin Chord %	Rear fin Aspect Ratio (Span^2/Area)	Top Fin2 Span %	Top Fin2 Chord %	Top fin2 Aspect Ratio (Span^2/Area)
roach	1201	4	2.1389866	10.682	6.99601	2.31672	12.684	9.41745	2.27123						
pike	1202	1	2.7130833	11.57	3.62	3.15125	11.45	11.18	1.327486						
Atlantic cod	1203	1	1.3198241	8.8933	5.67688	4.08988	12.075	14.3775	7.539934				10.578	20.756	1.022047
Atlantic cod	1203	1	1.3198241	8.8933	5.67688	4.08988	12.075	14.3775	7.539934				10.578	20.756	1.022047
Atlantic cod	1203	1	1.3198241	8.8933	5.67688	4.08988	12.075	14.3775	7.539934				10.578	20.756	1.022047
haddock	1203	2	1.3198241	8.8933	5.67688	4.08988	12.075	14.3775	7.539934				10.578	20.756	1.022047
haddock	1203	2	1.3198241	8.8933	5.67688	4.08988	12.075	14.3775	7.539934				10.578	20.756	1.022047
whiting	1203	3	2.9261829	9.65	4.5	4.65845	5.9395	32.9761	0.308567				8.2357	20.749	1.1278734
saithe	1203	4													
saithe	1203	4													
saithe	1203	4													
blackspot grenadier	1204	1													
roundnose grenadier	1204	2													
slickhead	1205	1													
greatbarracuda	1206	1													
cisco	1207	1													
lake whitefish	1207	2													
chum salmon	1207	3	1.3246267	9.72	7.14	2.1936	9.39	12.99	1.081203						
rainbow trout	1207	4	1.1442389	10.16	7.25	2.10966	10.85	11.14	1.54532						
rainbow trout	1207	4	1.1442389	10.16	7.25	2.10966	10.85	11.14	1.54532						
rainbow trout	1207	4	1.1442389	10.16	7.25	2.10966	10.85	11.14	1.54532						

1.Taxonomy			7. Control Surfaces (Span and Chord are measure as % of TL)												
CommonName	Taxa Code	Taxa-No	Top fin Aspect Ratio (Span^2/Area)	Auxillary Side Fin Span%	Auxillary Side Fin Chord%	Auxillary Side fin Aspect Ratio (Span^2/Area)	Bottom FinSpan %	Bottom FinChord %	Bottom FinAspect Ratio (Span^2/Area)	Rear Fin 2 or sword Span%	Rear Fin Chord %	Rear fin Aspect Ratio (Span^2/Area)	Top Fin2 Span %	Top Fin2 Chord %	Top fin2 Aspect Ratio (Span^2/Area)
rainbow trout	1207	4	1.1442389	10.16	7.25	2.10966	10.85	11.14	1.54532						
rainbow trout	1207	4	1.1442389	10.16	7.25	2.10966	10.85	11.14	1.54532						
sockeye salmon	1207	5	1.1442389	10.16	7.25	2.10966	10.85	11.14	1.54532						
sockeye salmon	1207	5	1.1442389	10.16	7.25	2.10966	10.85	11.14	1.54532						
brook charr	1207	6													
lake sturgeon	1301	1													
flying fish	1302	1													
silver dollar	1303	1													
south American pilchard	1304	1													
largescale mullet	1305	1	2.040754	11.727	8.309	1.95219	11.747	9.97	1.967902				10.816	7.174	2.89693
largescale mullet	1305	1	2.040754	11.727	8.309	1.95219	11.747	9.97	1.967902				10.816	7.174	2.89693
largescale mullet	1305	1	2.040754	11.727	8.309	1.95219	11.747	9.97	1.967902				10.816	7.174	2.89693
elephantnose fish	1306	1	0.7891131	7.93	4.44	2.49741	10.1	24.61	0.650201						
yellowtail kingfish	1307	1													
largemouth bass	1308	1	0.2971662	11.25	4.87	2.87838	11.5	14.7	1.330617				8.56	19.49	0.518641
smallmouth bass	1308	2													
Nile tilapia	1309	1	0.2997307	11.26	13.56	1.25025	14.21	19.69	0.9728						
Nile tilapia	1309	1	0.2997307	11.26	13.56	1.25025	14.21	19.69	0.9728						
striped bass	1310	1													
bluefish	1311	1													
bluefish	1311	1													
Atlantic mackerel	1312	1	1.5125334	7.26	5.05	3.17899	4.91	9.17	0.934785				5.34	9.09	1.228062

1.Taxonomy			7. Control Surfaces (Span and Chord are measure as % of TL)												
CommonName	Taxa Code	Taxa -No	Top fin Aspect Ratio (Span^2/Area)	Auxillary Side Fin Span%	Auxillary Side Fin Chord%	Auxillary Side fin Aspect Ratio (Span^2/Area)	Bottom FinSpan %	Bottom FinChord %	Bottom FinAspect Ratio (Span^2/Area)	Rear Fin 2 or sword Span%	Rear Fin Chord %	Rear fin Aspect Ratio (Span^2/Area)	Top Fin2 Span %	Top Fin2 Chord %	Top fin2 Aspect Ratio (Span^2/Area)
Atlantic mackerel	1312	1	1.5125334	7.26	5.05	3.17899	4.91	9.17	0.934785				5.34	9.09	1.228062
chub mackerel	1312	2	1.5125334	7.26	5.05	3.17899	4.91	9.17	0.934785				5.34	9.09	1.228062
Pacific jack mackerel	1401	1													
dolphinfish	1402	1													
black marlin	1403	1	1.0676228				8.65	13.21	2.026063				2.47	7.5	0.6289588
Indo-Pacific sailfish	1403	2													
skipjack tuna	1404	1	2.0039692	9.98	4.59	3.53068	6.82	4.37	3.291748				6.59	7.01	2.3980177
skipjack tuna	1404	1	2.0039692	9.98	4.59	3.53068	6.82	4.37	3.291748				6.59	7.01	2.3980177
pacific bonito	1404	2	0.772645	5.2	3.49	2.26846	7.25	7.62	2.535576				6.29	10.83	1.491859
yellowfin tuna	1404	3	2.5153151	8.97	7.08	3.14915	13.48	7.53	4.882063				14.09	5.97	6.276576
yellowfin tuna	1404	3	2.5153151	8.97	7.08	3.14915	13.48	7.53	4.882063				14.09	5.97	6.276576
yellowfin tuna	1404	3	2.5153151	8.97	7.08	3.14915	13.48	7.53	4.882063				14.09	5.97	6.276576
yellowfin tuna	1404	3	2.5153151	8.97	7.08	3.14915	13.48	7.53	4.882063				14.09	5.97	6.276576
bluefin tuna (northern)	1404	4	1.7697565	8.47	5.67	2.98796	7.16	8.16	2.805999				7.62	8.38	3.172918
bluefin tuna (northern)	1404	4	1.7697565	8.47	5.67	2.98796	7.16	8.16	2.805999				7.62	8.38	3.172918
swordfish	1405	1													
diaphanous hatchetfish	1501	1													
silver hatchet fish	1501	2													
striped burrfish	1601	1	1.2880651				14.75	10.29	1.753688						
boxfish	1602	1													
whitespotted boxfish	1602	2	1.0525447				15.18	13.07	1.52352						
whitemargin unicornfish	1701	1													
ocean surgeonfish	1701	2													
pumpkinseed	1702	1	0.5476192	8.71	13.2	1.06581	20.84	10.45	2.852395						

1.Taxonomy			7. Control Surfaces (Span and Chord are measure as % of TL)												
CommonName	Taxa Code	Taxa-No	Top fin Aspect Ratio (Span^2/Area)	Auxillary Side Fin Span%	Auxillary Side Fin Chord%	Auxillary Side fin Aspect Ratio (Span^2/Area)	Bottom FinSpan %	Bottom FinChord %	Bottom FinAspect Ratio (Span^2/Area)	Rear Fin 2 or sword Span%	Rear Fin Chord %	Rear fin Aspect Ratio (Span^2/Area)	Top Fin2 Span %	Top Fin2 Chord %	Top fin2 Aspect Ratio (Span^2/Area)
pumpkinseed	1702	1	0.5476192	8.71	13.2	1.06581	20.84	10.45	2.852395						
shiner perch	1703	1													
shiner perch	1703	1													
bluehead wrasse	1704	1													
señorita	1704	2													
beaugregory damselfish	1705	1													
angelfish	1705	2													
snailfish	1706	1													
oarfish	1801	1													
black ghost	1802	1	0.0922726												
foureye butterflyfish	1901	1													
picasso triggerfish	1902	1	2.2165611				10.22	19.1	0.549902				9.26	23.22	0.4396862
snailfish(new)	1903	1													
ocean sunfish	1904	1	3.1771016												
frilled shark	2101	1													
dogfish	2102	1													
cookie cutter shark	2103	1													
mustelus henlei	2201	1													
leopard shark	2201	2													
spookfish (chimera)	2202	1													
whale shark	2203	1	1.2531043				5.31	6.79	1.638356				3.07	4.87	1.1550123
bull shark	2301	1													
blacktip reef shark	2301	2													
lemon shark	2301	3	1.1630025				5.18	10.12	0.985037				8.47	6.59	1.9054688

1.Taxonomy			7. Control Surfaces (Span and Chord are measure as % of TL)												
CommonName	Taxa Code	Taxa-No	Top fin Aspect Ratio (Span^2/Area)	Auxillary Side Fin Span%	Auxillary Side Fin Chord%	Auxillary Side fin Aspect Ratio (Span^2/Area)	Bottom FinSpan %	Bottom FinChord %	Bottom FinAspect Ratio (Span^2/Area)	Rear Fin 2 or sword Span%	Rear Fin Chord %	Rear fin Aspect Ratio (Span^2/Area)	Top Fin2 Span %	Top Fin2 Chord %	Top fin2 Aspect Ratio (Span^2/Area)
lemon shark	2301	3	1.1630025				5.18	10.12	0.985037				8.47	6.59	1.9054688
hammerhead shark	2304	1	3.9691658				3.94	9.01	1.02466	20.21	18.06	1.6348227	5.13	4.63	2.4435376
hammerhead shark	2304	1	3.9691658				3.94	9.01	1.02466	20.21	18.06	1.6348227	5.13	4.63	2.4435376
bonnethead shark	2304	2	3.9691658				3.94	9.01	1.02466	20.21	18.06	1.6348227	5.13	4.63	2.4435376
bonnethead shark	2304	2	3.9691658				3.94	9.01	1.02466	20.21	18.06	1.6348227	5.13	4.63	2.4435376
bonnethead shark	2304	2	3.9691658				3.94	9.01	1.02466	20.21	18.06	1.6348227	5.13	4.63	2.4435376
basking shark	2305	1													
basking shark	2305	1													
nurse shark	2306	1													
white shark	2401	1	1.2510324												
giant manta ray	2601	1													
spotted eagle ray	2602	1													
dugong	3301	1													
bowhead whale	3401	1													
north atlantic right whale	3401	2													
minke whale	3402	1													
sei whale	3402	2													
bryde's whale	3402	3													
blue whale	3402	4	0.8												
fin whale	3402	5													
humpback whale	3402	6													
grey whale	3403	1													
grey whale	3403	1													
beluga whale	3404	1													
sperm whale	3405	1													

1.Taxonomy			7. Control Surfaces (Span and Chord are measure as % of TL)												
CommonName	Taxa Code	Taxa-No	Top fin Aspect Ratio (Span^2/Area)	Auxillary Side Fin Span%	Auxillary Side Fin Chord%	Auxillary Side fin Aspect Ratio (Span^2/Area)	Bottom FinSpan %	Bottom FinChord %	Bottom FinAspect Ratio (Span^2/Area)	Rear Fin 2 or sword Span%	Rear Fin Chord %	Rear fin Aspect Ratio (Span^2/Area)	Top Fin2 Span %	Top Fin2 Chord %	Top fin2 Aspect Ratio (Span^2/Area)
beaked whale	3406	1													
killer whale	3407	1	3.10061												
killer whale	3407	1	3.10061												
killer whale	3407	1	3.10061												
killer whale	3407	1	3.10061												
killer whale	3407	1	3.10061												
killer whale	3407	1	3.10061												
false killer whale	3407	2	1.035064												
commerson’s dolphin	3407	3													
common dolphin	3407	4													
long-finned pilot whale	3407	5													
white sided dolphin	3407	6													
Atlantic spotted dolphin	3407	7	2.84013												
bottlenose dolphin	3407	8	2.84013												
bottlenose dolphin	3407	8													
bottlenose dolphin	3407	8	2.84013												
Pacific bottlenose dolphin	3407	8													
harbour porpoise	3408	1													
harbour porpoise	3408	1													
dall's porpoise	3408	2													
sea otter	3501	1													
sea otter	3501	1													
walrus	3502	1													

1.Taxonomy			7. Control Surfaces (Span and Chord are measure as % of TL)												
CommonName	Taxa Code	Taxa-No	Top fin Aspect Ratio (Span^2/Area)	Auxillary Side Fin Span%	Auxillary Side Fin Chord%	Auxillary Side fin Aspect Ratio (Span^2/Area)	Bottom FinSpan %	Bottom FinChord %	Bottom FinAspect Ratio (Span^2/Area)	Rear Fin 2 or sword Span%	Rear Fin Chord %	Rear fin Aspect Ratio (Span^2/Area)	Top Fin2 Span %	Top Fin2 Chord %	Top fin2 Aspect Ratio (Span^2/Area)
grey seal	3503	1								22.2678	15.921	1.9511927			
weddell seal	3503	2													
weddell seal	3503	2													
northern elephant seal	3503	3													
northern elephant seal	3503	3													
southern elephant seal	3503	4													
southern elephant seal	3503	4													
harbour seal	3503	5													
harbour seal	3503	5													
harbour seal	3503	5													
harbour seal	3503	5													
harbour seal	3503	5													
baikal seal	3503	6													
muskrat	3504	1													
Antarctic fur seals	3701	1													
northern fur seal	3701	2													
steller sea lion	3701	3								21.0686	14.942	1.95			
steller sea lion	3701	3								21.0686	14.942	1.95			
steller sea lion	3701	3								21.0686	14.942	1.95			
steller sea lion	3701	3								21.0686	14.942	1.95			
steller sea lion	3701	3								21.0686	14.942	1.95			

1.Taxonomy			7. Control Surfaces (Span and Chord are measure as % of TL)												
CommonName	Taxa Code	Taxa -No	Top fin Aspect Ratio (Span^2/Area)	Auxillary Side Fin Span%	Auxillary Side Fin Chord%	Auxillary Side fin Aspect Ratio (Span^2/Area)	Bottom FinSpan %	Bottom FinChord %	Bottom FinAspect Ratio (Span^2/Area)	Rear Fin 2 or sword Span%	Rear Fin Chord %	Rear fin Aspect Ratio (Span^2/Area)	Top Fin2 Span %	Top Fin2 Chord %	Top fin2 Aspect Ratio (Span^2/Area)
steller sea lion (4)	3701	3								21.0686	14.942	1.95			
California sea lion	3701	4								21.0686	14.942	1.95			
California sea lion	3701	4								21.0686	14.942	1.95			
California sea lion	3701	4								21.0686	14.942	1.95			
California sea lion	3701	4								21.0686	14.942	1.95			
California sea lion	3701	4								21.0686	14.942	1.95			
California sea lion	3701	4								21.0686	14.942	1.95			
California sea lion	3701	4								21.0686	14.942	1.95			
Asian small- clawed otters	3702	1													
north American mink	3702	2													
emperor penguin	4701	1													
emporer penguin	4701	1													
king penguin	4701	2								9.96108	22.125	0.8943544			
little penguin	4701	3													
little penguin	4701	3													
little penguin	4701	3													
adelie penguin	4701	4													
adelie penguin	4701	4													
chinstrap penguin	4701	5													
chinstrap penguin	4701	5													

1.Taxonomy			7. Control Surfaces (Span and Chord are measure as % of TL)												
CommonName	Taxa Code	Taxa-No	Top fin Aspect Ratio (Span^2/Area)	Auxillary Side Fin Span%	Auxillary Side Fin Chord%	Auxillary Side fin Aspect Ratio (Span^2/Area)	Bottom FinSpan %	Bottom FinChord %	Bottom FinAspect Ratio (Span^2/Area)	Rear Fin 2 or sword Span%	Rear Fin Chord %	Rear fin Aspect Ratio (Span^2/Area)	Top Fin2 Span %	Top Fin2 Chord %	Top fin2 Aspect Ratio (Span^2/Area)
gentoo penguin	4701	6								9.96108	22.125	0.8943544			
gentoo penguin	4701	6								9.96108	22.125	0.8943544			
gentoo pinguin	4701	6								9.96108	22.125	0.8943544			
African penguin	4701	7													
African penguin	4701	7													
humboldt penguin	4701	8								9.96108	22.125	0.8943544			
macaroni penguin	4701	9													
marine iguana	5101	1													
marine iguana (jouvenile)	5101	1													
leatherback turtle	5701	1								19.3307	13.541	1.9408483			
green sea turtle	5702	1													
painted turtle	5703	1													
slender inshore squid (arrow squid)	6001	1													
opalescent inshore squid	6001	2													
giant squid	6002	1													
dana octopus squid	6003	1													
whip-lash squid	6004	1													
sea cucumber1	7001	1													
sea cucumber2	7001	2													
giant sea flea	7002	1													
pram bug	7003	1													

1.Taxonomy			7. Control Surfaces (Span and Chord are measure as % of TL)												
CommonName	Taxa Code	Taxa-No	Top fin Aspect Ratio (Span^2/Area)	Auxillary Side Fin Span%	Auxillary Side Fin Chord%	Auxillary Side fin Aspect Ratio (Span^2/Area)	Bottom FinSpan %	Bottom FinChord %	Bottom FinAspect Ratio (Span^2/Area)	Rear Fin 2 or sword Span%	Rear Fin Chord %	Rear fin Aspect Ratio (Span^2/Area)	Top Fin2 Span %	Top Fin2 Chord %	Top fin2 Aspect Ratio (Span^2/Area)
Japanese giant spider crab	7004	1													
deep-sea crab	7005	1													
soldier striped shrimp	7006	1													
giant isopod	7007	1													
giant red mysid	7008	1													
giant sea spider	7009	1													
sea spider	7010	1													
deep-sea jellyfish	7011	1													
salp	7012	1													

1.Taxonomy			7. Control Surfaces (Span and Chord are measure as % of TL)						8. Environment	9.References
CommonName	Taxa Code	Taxa-No	Top Fin3 Span%	Top Fin3 Chord%	Top fin3 Aspect Ratio (Span^2/Area)	Bottom Fin2 Span%	Bottom Fin2 Chord%	Bottom Fin2 Aspect Ratio (Span^2/Area)	-	References other than Froese & Pauly, 2011
fangtooth	1001	1							Marine	
alfonsine	1002	1							Marine	
orange roughy	1003	1							Marine	
deep-sea anglerfish	1004	1							Marine	
football fish	1005	1							Marine	
black sea devil	1006	1							Marine	
lantern fish	1007	1							Marine	
barreleye	1008	1							Marine	
barents sea capelin	1009	1							Marine	Behrenset al., 2005
black swallower	1010	1							Marine	
parrotfish	1011	1							Marine	Korsmeyer et al., 2002
spotted seatrout	1012	1							Marine	Videler, 1993
red drum	1012	2							Marine	Videler, 1993
sheepshead	1013	1							Marine	Videler, 1993
bristlemouth	1014	1							Marine	
silver eel	1101	1							Marine	Tytell, 2007
silver eel	1101	1							Marine	Van Den Thillart et al., 2007 , Rivera, 2006
silver eel	1101	1							Marine	Van Ginneken et al., 2005
silver eel (european)	1101	1							Marine	Palstra et al., 2008
japanese eel	1101	2							Marine	Aoyama et al., 1999
slender snipe eel	1102	1							Marine	
tripod fish	1103	1							Marine	
Mediterranean spiderfish	1103	2							Marine	
Pacific hagfish	1104	1							Marine	
deep-sea cusk eel	1105	1							Marine	

1.Taxonomy			7. Control Surfaces (Span and Chord are measure as % of TL)						8. Environment	9.References
CommonName	Taxa Code	Taxa-No	Top Fin3 Span%	Top Fin3 Chord%	Top fin3 Aspect Ratio (Span^2/Area)	Bottom Fin2 Span%	Bottom Fin2 Chord%	Bottom Fin2 Aspect Ratio (Span^2/Area)	-	References other than Froese & Pauly, 2011
cusk eel4	1105	2							Marine	
cusk eel3	1105	3							Marine	
snake blenny	1105	4							Marine	
blackedge cusk	1105	5							Marine	
golden cusk	1105	6							Marine	
midwater eelpout	1106	1							Marine	
sea lamprey	1107	1							Marine	
japanese flounder	1108	1							Marine	Kawabe et al., 2004
pelican eel	1109	1							Marine	
pacific viper fish	1110	1							Marine	
viper fish	1110	2							Marine	
barbeled dragonfish	1110	3							Marine	
scaly dragonfish	1110	4							Marine	
common dace	1201	1							Freshwater	Viedeler & Wardle, 1991
goldfish	1201	2							Freshwater	Rivera, 2006; Videler & Wardle,1991
goldfish	1201	2							Freshwater	Videler, 1993; Videler & Nolet, 1990
goldfish	1201	2							Freshwater	Viedeler & Wardle, 1991
goldfish	1201	2							Freshwater	Blake & Chan, 2006
carp	1201	3							Freshwater	
carp	1201	3							Freshwater	Ohlberger et al., 2006
carp	1201	3							Freshwater	Ohlberger et al., 2006
roach	1201	4							Freshwater	Rivera, 2006; Videler & Nolet,1990
roach	1201	4							Freshwater	Ohlberger et al., 2006
roach	1201	4							Freshwater	Ohlberger et al., 2006
pike	1202	1							Freshwater	Rivera, 2006

1.Taxonomy			7. Control Surfaces (Span and Chord are measure as % of TL)						8. Environment	9.References
CommonName	Taxa Code	Taxa-No	Top Fin3 Span%	Top Fin3 Chord%	Top fin3 Aspect Ratio (Span^2/Area)	Bottom Fin2 Span%	Bottom Fin2 Chord%	Bottom Fin2 Aspect Ratio (Span^2/Area)	-	References other than Froese & Pauly, 2011
Atlantic cod	1203	1	9.1008	15.5583	1.2061299	11.18083	9.5503953	2.0244175	Marine	Syme et al., 2008
Atlantic cod	1203	1	9.1008	15.5583	1.2061299	11.18083	9.5503953	2.0244175	Marine	Viedeler & Wardle, 1991
Atlantic cod	1203	1	9.1008	15.5583	1.2061299	11.18083	9.5503953	2.0244175	Marine	Viedeler & Wardle, 1991
haddock	1203	2	9.1008	15.5583	1.2061299	11.18083	9.5503953	2.0244175	Marine	Rivera, 2006; Videler, 1993; Videler & Nolet,1990
haddock	1203	2	9.1008	15.5583	1.2061299	11.18083	9.5503953	2.0244175	Marine	Videler & Nolet,1990; Breen et al., 2004
whiting	1203	3	6.9888	13.4487	1.3407734	4.0774862	13.329066	0.5242695	Marine	Steinhausen et al., 2005
saithe	1203	4							Marine	Steinhausen et al., 2005
saithe	1203	4							Marine	Viedeler & Wardle, 1991
saithe	1203	4							Marine	Viedeler & Wardle, 1991
blackspot grenadier	1204	1							Marine	
roundnose grenadier	1204	2							Marine	
slickhead	1205	1							Marine	
great barracuda	1206	1							Marine	
cisco	1207	1							Marine / Freshwater	Videler, 1993
lake whitefish	1207	2							Freshwater	Videler, 1993
chum salmon	1207	3							Marine / Freshwater	Tanaka et al., 2001 ; Jobling and Johansen, 2003
rainbow trout	1207	4							Marine / Freshwater	Blake & Chan, 2006
rainbow trout	1207	4							Marine / Freshwater	Videler, 1993; Videler & Nolet,1990
rainbow trout	1207	4							Marine / Freshwater	Blake & Chan, 2006
rainbow trout	1207	4							Marine / Freshwater	Videler & Nolet,1990; Viedeler & Wardle, 1991
rainbow trout	1207	4							Marine / Freshwater	Viedeler & Wardle, 1991
sockeye salmon	1207	5							Marine /	Videler, 1993; Jobling and Johansen, 2003; Videler & Nolet,1990

1.Taxonomy			7. Control Surfaces (Span and Chord are measure as % of TL)						8. Environment	9.References
CommonName	Taxa Code	Taxa-No	Top Fin3 Span%	Top Fin3 Chord%	Top fin3 Aspect Ratio (Span^2/Area)	Bottom Fin2 Span%	Bottom Fin2 Chord%	Bottom Fin2 Aspect Ratio (Span^2/Area)	-	References other than Froese & Pauly, 2011
									Freshwater	
sockeye salmon	1207	5							Marine / Freshwater	Videler, 1993; Jobling and Johansen, 2003; Videler & Nolet,1990
brook charr	1207	6							Marine / Freshwater	Tudorache et al., 2011; Jobling and Johansen, 2003
lake sturgeon	1301	1							Freshwater	Viedeler & Wardle, 1991
flying fish	1302	1							Marine	
silver dollar	1303	1							Freshwater	Blake & Chan, 2006
south American pilchard	1304	1							Marine	Viedeler & Wardle, 1991
largescale mullet	1305	1							Marine / Freshwater	Videler & Nolet,1990
largescale mullet	1305	1							Marine / Freshwater	Rivera, 2006
largescale mullet	1305	1							Marine / Freshwater	Videler, 1993; Videler & Nolet,1990
elephantnose fish	1306	1							Freshwater	Rivera, 2006
yellowtail kingfish	1307	1							Marine	Clark & Seymour, 2006
largemouth bass	1308	1							Freshwater	Videler, 1993; Cooke & Philipp, 2009; Videler & Nolet,1990
smallmouth bass	1308	2							Freshwater	Blake & Chan, 2006
nile tilapia	1309	1							Freshwater	Videler & Nolet,1990
nile tilapia	1309	1							Freshwater	Videler, 1993; Videler & Nolet,1990
striped bass	1310	1							Marine / Freshwater	Videler, 1993; Videler 1990; Rivera, 2006; Videler & Nolet,1990
bluefish	1311	1							Marine	Videler & Nolet,1990; Rivera, 2006; Videler, 1993
bluefish	1311	1							Marine	Videler, 1993; Rivera, 2006
Atlantic mackerel	1312	1							Marine	He & Wardle, 1986
Atlantic mackerel	1312	1							Marine	Viedeler & Wardle, 1991
chub mackerel	1312	2							Marine	Viedeler & Wardle, 1991

1.Taxonomy			7. Control Surfaces (Span and Chord are measure as % of TL)						8. Environment	9.References
CommonName	Taxa Code	Taxa-No	Top Fin3 Span%	Top Fin3 Chord%	Top fin3 Aspect Ratio (Span^2/Area)	Bottom Fin2 Span%	Bottom Fin2 Chord%	Bottom Fin2 Aspect Ratio (Span^2/Area)	-	References other than Froese & Pauly, 2011
pacific jack mackerel	1401	1							Marine	Viedeler & Wardle, 1991
dolphinfish	1402	1							Marine	Blake & Chan, 2006
black marlin	1403	1				3.21	4.8	1.090381	Marine	Pepperell & Davis, 1999
Indo-Pacific sailfish	1403	2							Marine	
skipjack tuna	1404	1							Marine	Videler, 1993
skipjack tuna	1404	1							Marine	Videler, 1993
Pacific bonito	1404	2							Marine	Sepulveda et al., 2003
yellowfin tuna	1404	3							Marine	Blake & Chan, 2006
yellowfin tuna	1404	3							Marine	Rivera, 2006
yellowfin tuna	1404	3							Marine	Dewar 1994; Korsmeyer et al., 2002
yellowfin tuna	1404	3							Marine	Brill et al., 1999
bluefin tuna (northern)	1404	4							Marine	Videler & Wardle, 1991; Dewar & Graham,1994; Korsmeyer et al., 2002; Rivera, 2006
bluefin tuna (northern)	1404	4							Marine	Viedeler & Wardle, 1991
swordfish	1405	1							Marine	
diaphanous hatchetfish	1501	1							Marine	
silver hatchet fish	1501	2							Marine	
striped burrfish	1601	1							Marine	Videler, 1993
boxfish	1602	1							Marine	Blake & Chan, 2006
whitespotted boxfish	1602	2							Marine	Blake & Chan, 2006; Videler & Nolet,1990; Stobutzki & Bellwood, 1997; Walker, 2000
whitemargin unicornfish	1701	1							Marine	
ocean surgeonfish	1701	2							Marine	Blake & Chan, 2006
pumpkinseed	1702	1							Freshwater	Videler & Nolet,1990; Rivera, 2006; Cooke & Philipp, 2009
pumpkinseed	1702	1							Freshwater	Videler, 1993; Cooke & Philipp, 2009; Videler & Nolet,1990
shiner perch	1703	1							Marine / Freshwater	Videler, 1993

1.Taxonomy			7. Control Surfaces (Span and Chord are measure as % of TL)						8. Environment	9.References
CommonName	Taxa Code	Taxa-No	Top Fin3 Span%	Top Fin3 Chord%	Top fin3 Aspect Ratio (Span^2/Area)	Bottom Fin2 Span%	Bottom Fin2 Chord%	Bottom Fin2 Aspect Ratio (Span^2/Area)	-	References other than Froese & Pauly, 2011
shiner perch	1703	1							Marine / Freshwater	Videler, 1993
bluehead wrasse	1704	1							Marine	Blake & Chan, 2006
señorita	1704	2							Marine	Videler, 1993
beaugregory damselfish	1705	1							Marine	Blake & Chan, 2006
angelfish	1705	2							Marine	Blake & Chan, 2006
snailfish	1706	1							Marine	
oarfish	1801	1							Marine	
black ghost	1802	1							Freshwater	Rivera, 2006; Videler & Nolet,1990
foureye butterflyfish	1901	1							Marine	Blake & Chan, 2006
picasso triggerfish	1902	1							Marine	Korsmeyer et al., 2002
snailfish(new)	1903	1							Marine	
ocean sunfish	1904	1							Marine	Watanabe & Sato, 2008
frilled shark	2101	1							Marine	
dogfish	2102	1							Marine	Blake & Chan, 2006
cookie cutter shark	2103	1							Marine	
mustelus henlei	2201	1							Marine	Viedeler & Wardle, 1991
leopard shark	2201	2							Marine	Viedeler & Wardle, 1991
spookfish (chimera)	2202	1								
whale shark	2203	1				2.38	5.7	0.7978028	Marine	Froese & Pauly, 2011 , Colman, J.G.
bull shark	2301	1							Marine / Freshwater	Viedeler & Wardle, 1991
blacktip reef shark	2301	2							Marine	Viedeler & Wardle, 1991
lemon shark	2301	3				7.95	4.79	2.9273969	Marine	Rivera, 2006; Videler & Nolet,1990; Videler & Wardle, 1991
lemon shark	2301	3				7.95	4.79	2.9273969	Marine	Viedeler & Wardle, 1991
hammerhead shark	2304	1							Marine	Rivera, 2006

1.Taxonomy			7. Control Surfaces (Span and Chord are measure as % of TL)						8. Environment	9.References
CommonName	Taxa Code	Taxa-No	Top Fin3 Span%	Top Fin3 Chord%	Top fin3 Aspect Ratio (Span^2/Area)	Bottom Fin2 Span%	Bottom Fin2 Chord%	Bottom Fin2 Aspect Ratio (Span^2/Area)	-	References other than Froese & Pauly, 2011
hammerhead shark	2304	1							Marine	Lowe 2002
bonnethead shark	2304	2							Marine	Parsons, 1990
bonnethead shark	2304	2							Marine	Parsons, 1990
bonnethead shark	2304	2							Marine	Parsons, 1990
basking shark	2305	1							Marine	Rivera, 2006; Sims, 2000
basking shark	2305	1							Marine	Sims, 2000
nurse shark	2306	1							Marine	Viedeler & Wardle, 1991
white shark	2401	1							Marine	Bruce et al., 2006
giant manta ray	2601	1							Marine	Rivera, 2006
spotted eagle ray	2602	1							Marine	Froese & Pauly, 2011
dugong	3301	1							Marine	
bowhead whale	3401	1							Marine	
north Atlantic right whale	3401	2							Marine	
minke whale	3402	1							Marine	
sei whale	3402	2							Marine	
bryde's whale	3402	3							Marine	
blue whale	3402	4							Marine	Woodward et al., 2006
fin whale	3402	5							Marine	
humpback whale	3402	6							Marine	Rivera, 2006; Castellini 2000; Berta et al., 2006, Woodward et al., 2006
grey whale	3403	1							Marine	ideler & Nolet,1990; Fish, 1997; Berta et al., 2006, Woodward et al., 2006
grey whale	3403	1							Marine	Williams, 1999; Sumich, 1983, Woodward et al., 2006; Videler & Nolet,1990
beluga whale	3404	1							Marine	Rivera, 2006; Fish, 1997; Castellini 2000; Berta et al., 2006
sperm whale	3405	1							Marine	Berta et al., 2006
beaked whale	3406	1							Marine	
killer whale	3407	1							Marine	Williams & Noren, 2009; Rivera, 2006

1.Taxonomy			7. Control Surfaces (Span and Chord are measure as % of TL)						8. Environment	9.References
CommonName	Taxa Code	Taxa-No	Top Fin3 Span%	Top Fin3 Chord%	Top fin3 Aspect Ratio (Span^2/Area)	Bottom Fin2 Span%	Bottom Fin2 Chord%	Bottom Fin2 Aspect Ratio (Span^2/Area)	-	References other than Froese & Pauly, 2011
killer whale	3407	1							Marine	Domenici & Blake,1997; Domenici 2001; Berta et al., 2006
killer whale	3407	1							Marine	Williams & Noren, 2009
killer whale	3407	1							Marine	Williams & Noren, 2009
killer whale	3407	1							Marine	Williams, 1999
killer whale	3407	1							Marine	Williams, 1999
false killer whale	3407	2							Marine	Rivera, 2006
commerson’s dolphin	3407	3							Marine	Fish, 2002
common dolphin	3407	4							Marine	
long-finned pilot whale	3407	5							Marine	
white sided dolphin	3407	6							Marine	Fish,2002
Atlantic spotted dolphin	3407	7							Marine	
bottlenose dolphin	3407	8							Marine	Fish,2002; Rivera, 2006; Fish & Hui, 1991; Fish, 1997; Berta et al., 2006; Fish & Lauder, 2006
bottlenose dolphin	3407	8							Marine	Yazdi et al., 1999
bottlenose dolphin	3407	8							Marine	Williams, 1999
Pacific bottlenose dolphin	3407	8							Marine	
harbour porpoise	3408	1							Marine	Otani et al., 2001
harbour porpoise	3408	1							Marine	
dall's porpoise	3408	2							Marine	
sea otter	3501	1							Marine	Williams, 1999
sea otter	3501	1							Marine	
walrus	3502	1							Marine	
grey seal	3503	1							Marine	Williams,1999
weddell seal	3503	2							Marine	
weddell seal	3503	2							Marine	Sato et al., 2007

1.Taxonomy			7. Control Surfaces (Span and Chord are measure as % of TL)						8. Environment	9.References
CommonName	Taxa Code	Taxa-No	Top Fin3 Span%	Top Fin3 Chord%	Top fin3 Aspect Ratio (Span^2/Area)	Bottom Fin2 Span%	Bottom Fin2 Chord%	Bottom Fin2 Aspect Ratio (Span^2/Area)	-	References other than Froese & Pauly, 2011
northern elephant seal	3503	3							Marine	Sato et al., 2007
northern elephant seal	3503	3							Marine	
southern elephant seal	3503	4							Marine	
southern elephant seal	3503	4							Marine	Sato et al., 2007
harbour seal	3503	5							Marine	Videler, 1993; Videler & Nolet,1990
harbour seal	3503	5							Marine	Williams,1999; Videler & Nolet,1990
harbour seal	3503	5							Marine	Videler, 1993; Videler & Nolet,1990
harbour seal	3503	5							Marine	Williams,1999
harbour seal	3503	5							Marine	
baikal seal	3503	6							Marine	Sato et al., 2007
muskrat	3504	1							Freshwater	Williams, 1999
Antarctic fur seals	3701	1							Marine	Boyd et al., 1995
northern fur seal	3701	2							Marine	
steller sea lion	3701	3							Marine	Domenici & Blake,1997; Domenici 2001; Berta et al., 2006
steller sea lion	3701	3							Marine	
steller sea lion	3701	3							Marine	Rosen &Trites, , 2002
steller sea lion	3701	3							Marine	Rosen &Trites, , 2002
steller sea lion	3701	3							Marine	Rosen &Trites, , 2002
steller sea lion [4]	3701	3							Marine	
California sea lion	3701	4							Marine	Rivera, 2006
California sea lion	3701	4							Marine	Blake & Chan, 2006
California sea lion	3701	4							Marine	Williams,1999; Fish et al., 2002
California sea lion	3701	4							Marine	Videler, 1993; Fish et al., 2002; Videler & Nolet,1990
California sea lion	3701	4							Marine	Williams,1999; Fish et al., 2002
California sea lion	3701	4							Marine	Williams,1999; Fish et al., 2002

1.Taxonomy			7. Control Surfaces (Span and Chord are measure as % of TL)						8. Environment	9.References
CommonName	Taxa Code	Taxa-No	Top Fin3 Span%	Top Fin3 Chord%	Top fin3 Aspect Ratio (Span^2/Area)	Bottom Fin2 Span%	Bottom Fin2 Chord%	Bottom Fin2 Aspect Ratio (Span^2/Area)	-	References other than Froese & Pauly, 2011
California sea lion	3701	4							Marine	Fish et al., 2002
Asian small- clawed otters	3702	1							Freshwater	Borgwardt & Culik, 1999
north American mink	3702	2							Freshwater	Williams, 1999
emperor penguin	4701	1							Marine	
emporer penguin	4701	1							Marine	Sato et al., 2007
king penguin	4701	2							Marine	Sato et al., 2002
little penguin	4701	3							Marine	Videler, 1993
little penguin	4701	3							Marine	Luna-Jorquera & Culik, 2000
little penguin	4701	3							Marine	Sato et al., 2007
adelie penguin	4701	4							Marine	Luna-Jorquera & Culik, 2000
adelie penguin	4701	4							Marine	Sato et al., 2007
chinstrap penguin	4701	5							Marine	Luna-Jorquera & Culik, 2000
chinstrap penguin	4701	5							Marine	Sato et al., 2007
gentoo penguin	4701	6							Marine	Luna-Jorquera & Culik, 2000
gentoo penguin	4701	6							Marine	Sato et al., 2007
gentoo pinguin	4701	6							Marine	BBC Science & Nature
African penguin	4701	7							Marine	Luna-Jorquera & Culik, 2000
African penguin	4701	7							Marine	Luna-Jorquera & Culik, 2000
humboldt penguin	4701	8							Marine	Hui, 1985; Luna-Jorquera & Culik, 2000
macaroni penguin	4701	9							Marine	Sato et al., 2007
marine iguana	5101	1							Marine	
marine iguana (jouvenile)	5101	1							Marine	
leatherback turtle	5701	1							Marine	
green sea turtle	5702	1							Marine	
painted turtle	5703	1							Freshwater	Rivera, 2006

1.Taxonomy			7. Control Surfaces (Span and Chord are measure as % of TL)						8. Environment	9.References
CommonName	Taxa Code	Taxa-No	Top Fin3 Span%	Top Fin3 Chord%	Top fin3 Aspect Ratio (Span^2/Area)	Bottom Fin2 Span%	Bottom Fin2 Chord%	Bottom Fin2 Aspect Ratio (Span^2/Area)	-	References other than Froese & Pauly, 2011
slender inshore squid (arrow squid)	6001	1							Marine	
opalescent inshore squid	6001	2							Marine	
giant squid	6002	1							Marine	
dana octopus squid	6003	1							Marine	Roper & Vecchione, 1993
whip-lash squid	6004	1							Marine	
sea cucumber1	7001	1							Marine	
sea cucumber2	7001	2							Marine	
giant sea flea	7002	1							Marine	
pram bug	7003	1							Marine	
Japanese giant spider crab	7004	1							Marine	
deep-sea crab	7005	1							Marine	
soldier striped shrimp	7006	1							Marine	
giant isopod	7007	1							Marine	
giant red mysid	7008	1							Marine	Monterey Bay Aquarium
giant sea spider	7009	1							Marine	
sea spider	7010	1							Marine	
deep-sea jellyfish	7011	1							Marine	
salp	7012	1							Marine	

Appendix 1.3. AUVs' Database

	Dimensions (m)					Speed		Manoeuvre	Depth	Energetics				Reference
Name	**BL (m)**	**W (m)**	**R-Yaw (m) From formula**	**Mass (kg)**	**Body type**	**U-Eco (m/s)**	**U-max (m/s)**	**R-Yaw (m) From formula**	**Depth (m)**	**Endurance-max (h)**	**Battery Rating (kWh)**	**COT (J/Kg*m)**	**Battery Type**	**References other than AUVAC, 2011**
Bionik Manta (subsea glider)	1.5	1.57	-	10	Biomimetic	1.4	2.78		100	24				
AquaPenguin	0.77	0.19		9.6	Biomimetic	1.39	5			7	0.1665	1.78		
naro-tartaruga	1	0.45		75	Biomimetic	2			100		1.536	1.536		
AQUA2	0.64	0.44		16.5	Biomimetic	1			30	5	0.2074	0.20736		
Robo-pike	0.81			3.63	Biomimetic									
Cetus II	1.37	0.71	3.84	54.5	Oblate	1.3	2.6	3.84	200					
Talisman [M]	4.5	2.5	12.60	1000	Oblate	1.54	2.57	12.60	300				Li-Ion	
ALIVE	4	2.2	11.20	3500	Open space frame	1.54	2.57	11.20		7	44	1.17	Lead acid	Marty, 2004
Autonomous Benthic Explorer (ABE)	3	2	8.40	550	Open space frame	0.17	0.34	8.40	6000	20	5	2.67		
Nereus	5	2	14.00	2800	Open space frame	1.5	1.54	14.00	11000 (13)	20	18	0.21	Li-Ion	Bowen et al., 2008
SeaBED	1.9	0.34	5.32	250	Open space frame	1	1.54	5.32	2000	8	2	1.00		

	Dimensions (m)					Speed		Manoeuvre	Depth	Energetics				Reference
Name	**BL (m)**	**W (m)**	**R-Yaw (m) From formula**	**Mass (kg)**	**Body type**	**U-Eco (m/s)**	**U-max (m/s)**	**R-Yaw (m) From formula**	**Depth (m)**	**Endurance-max (h)**	**Battery Rating (kWh)**	**COT (J/Kg*m)**	**Battery Type**	**References other than AUVAC, 2011**
SQX-1	1.6	0.25	4.48	95	Open space frame	2	3	4.48	3000	8			Li-Ion	
Autonomous Benthic Explorer (ABE)	3	2	8.40	550	Open space frame	0.17	0.34	8.40	6000	20	5	2.67		
ARIES	3.04	0.4	8.51	220	Rectangular	1	1.8	8.51	50	8				
Echo Ranger	5.5	1.27	15.40	5308	Rectangular	1.54	4.12	15.40	3050	28				
Infante	4.5	1.1	12.60	1000	Rectangular	1.26	2.5	12.60	500	18.4				
Seaotter MkII	3.45	0.98	10[9]	1100	Rectangular	2.06	4.12	10[9]	600	24	36	0.66		
Urashima	10	1.3	-	10000	Rectangular	1.54	2.06		3500	54			Fuel cell	Maeda et a, 2004
Alistar	5	1.68	14.00	2300	Teardrop	1.03	2.06	14.00	3000	20	22	0.46	Li-Ion	Copros & Scourzic, 2011
Fetch 3	2.11	0.34	5.91	97	teardrop	1.25	3	5.91	200	10				
Odyssey IV	2.6	0.7	7.28	650	Teardrop	1.54	2.06	7.28	6000	5.56	4.5	0.81	Li-Ion	
Seaglider (iRobot configuration)	1.8	0.3	-	52	Teardrop	0.25			1000	5111	4.72	0.07	Lithium	
Abyss (REMUS 6000)	4	0.66	11.14	880	Torpedo		2.6	11.14	6000	24	11			

	Dimensions (m)					Speed		Manoeuvre	Depth	Energetics				Reference
Name	**BL (m)**	**W (m)**	**R-Yaw (m) From formula**	**Mass (kg)**	**Body type**	**U-Eco (m/s)**	**U-max (m/s)**	**R-Yaw (m) From formula**	**Depth (m)**	**Endurance-max (h)**	**Battery Rating (kWh)**	**COT (J/Kg*m)**	**Battery Type**	**References other than AUVAC, 2011**
Alister Daurade	5	0.7	14.00	950	Torpedo	2.05	4.11	14.00	300	10	22	1.13	Li-Ion	Copros & Scourzic, 2011
Autosub6000	5.5	0.9	16[9]	2000	Torpedo	1	2	16[9]	6000	103	42	0.15	Li-Ion Polymer	Yoshida et al., 2010
AUV 62-AT	7	0.53	19.60	620	Torpedo	2.05	6.17	19.60	300	12				
AUV 62-MR	7	0.53	19.60	1500	Torpedo	2.05	10.3	19.60	500	12				
AUV 62-VBSS	7	0.53	19.60	1200	Torpedo	1.54	5.66	19.60			10			
Bluefin 21	4.93	0.53	13.80	750	Torpedo	1.54	2.3	13.80	4500	25	13.5	0.47		
BPAUV	1.83		5.12	362.87	Torpedo	1.54	2.06	5.12	6000	18	4.5	0.45	Li-Ion	
Caribou (Odyssey III)	3.4	0.58	9.52	400	Torpedo	1.54	2.06	9.52	3000	20			Li-polymer	
Delphin 2	2	0.25	5[9]	47	Torpedo	0.7	1	5[9]	50	8				Steenson et al., 2011
Dorado	5.24	0.54	14.67	1018	Torpedo	1.54	2.06	14.67	1500	8	6	0.48	Li-Ion	
Eagle ray (Explorer)	4.5	0.69	12.60	630	Torpedo	1.54	2.57	12.60	3000	22	13.2	0.62	Li-Ion	
Geosub	6.82	-	19.10	2400	Torpedo	1.02	2.05	19.10	3000	60	132	0.90	Li-Ion	
HUGIN 1000	4.5	0.75	10[9]	850	Torpedo	2.05	3.08	10[9]	1000	24	15	0.36	Li-Polymer	Kongsberg, 2009

	Dimensions (m)					Speed		Manoeuvre	Depth	Energetics				Reference
Name	**BL (m)**	**W (m)**	**R-Yaw (m) From formula**	**Mass (kg)**	**Body type**	**U-Eco (m/s)**	**U-max (m/s)**	**R-Yaw (m) From formula**	**Depth (m)**	**Endurance-max (h)**	**Battery Rating (kWh)**	**COT (J/Kg*m)**	**Battery Type**	**References other than AUVAC, 2011**
HUGIN 3000	5.5	1	15[9]	1400	Torpedo	2.05	2.05	15[9]	3000	60	45	0.26	Al/HP semi fuelcell	Kongsberg, 2009; Yoshida et al., 2010
HUGIN 4500	6	1	18[9]	1900	Torpedo	2.05	2.05	18[9]	4500	50	60	0.31	Al/HP semi fuelcell	Kongsberg, 2009
Ifremer AStrX Explorer	4.5		12.60	793	Torpedo	1.5	2.5	12.60	3000	14	14	0.84	Li-Ion	
ISiMI	1.2	0.17	6[9]	20	Torpedo	0.7	2	6[9]	20	4	0.207	3.70	Li-Polymer	Jun et al., 2009
Iver2	1.27	0.147	3.56	19	Torpedo	1.29	2.06	3.56	100	14	0.6	1.75		
MBARI (Dorado)	5.3	0.53	14.84		Torpedo	1.54	2.06	14.84	6000	17.5				
NPS (REMUS 100)	1.6	0.19	4.48	37	Torpedo	1.5	2.6	4.48	100	22	1	0.82	Li-Ion	
REMUS 600	3.25	0.32	9.10	240	Torpedo	1.5	2.6	9.10	600	70	5.2	0.21	Li-Ion	
REMUS 6000 (Abyss)	3.84	0.71	10.75	862	Torpedo	1.543	2.6	10.75	6000	22	11	0.38	Li-Ion	
Seahorse II	8.66	0.97	24.25	4763	Torpedo	2.06	4.12	24.25	1000	72			Alcaline Duracel	
Seal (Explorer)	5.5	0.74	15.40	1250	Torpedo	1.5	2.5	15.40	5000	19	14	0.39	Li-Ion	

	Dimensions (m)					Speed		Manoeuvre	Depth	Energetics				Reference
Name	**BL (m)**	**W (m)**	**R-Yaw (m) From formula**	**Mass (kg)**	**Body type**	**U-Eco (m/s)**	**U-max (m/s)**	**R-Yaw (m) From formula**	**Depth (m)**	**Endurance-max (h)**	**Battery Rating (kWh)**	**COT (J/Kg*m)**	**Battery Type**	**References other than AUVAC, 2011**
Seawolf	2	0.3	3[9]	112	Torpedo		4.12	3[9]	300	3				
Taipan 2	1.8		5.04	60	Torpedo	1.5	1.8	5.04	100	2				
ALBAC	1.4	0.24	-	45	Torpedo + wings	0.51	1.03		300	1				
Slocum Electric (1km, science)	1.5	0.21	-	52	Torpedo + wings	0.35			1000	528	1.9005	0.20	Alkaline C cell or Li	
Slocum Electric (Coastal Configuration, science)	1.5	0.21	-	52	Torpedo + wings	0.35			200	840	1.9005	0.12	Alkaline C cell or Li	
Slocum Thermal	1.5	0.213	-	60	Torpedo + wings	0.4			1200	2778				
Spray	1.8	0.3	-	51.8	Torpedo + wings	0.25	0.35		1500	6666	3.6111	0.04		
Theseus	11	1.27	29.96	8600	Torpedo + wings	2.06		29.96	2000	60	600	0.56	Li-Ion	

Appendix 1.4. AUVs' Mission Database

The abbreviations for the missions presented in Appendix 1.4 are as bellows:

AUV mission	Abbreviation	AUV mission	Abbreviation
Anti-Submarine Warfare	ASW	Mine Countermeasures	MC
Beach Survey	BS	Mineral field Survey	MFS
Cable Deployment	CD	Marine Science Survey	MSS
Coastal Mapping	CM	Oil and Gas Survey	OGS
Cable Route Survey	CRS	Oceanographic Survey	OS
Environmental Monitoring	EM	Pipeline Route Survey	PRS
Explosive Ordnance Disposal	EOD	Rapid Environmental Assesment	REA
Freshwater Mapping	FM	Search and Recovery	S&R
Force Protection	FP	Search, Classify and Map	SCM
Geophysical Survey	GS	Sensor Development	SD
Hydro-acoustic Research	HAR	Seabed Mapping	SM
Hull Inspection	HI	Scientific Research	SR
Harbor and Port Security	HPS	Surf Zone Surveillance	SZS
Inspection Maintenance and Repair	IMR	Vehicle Research	VR
Intelligence, Surveillance, and Reconnaissance	ISR	Wind Park Construction Survey	WCS

AUV	Body Type	TL [m]	BW [m]	BH [m]	BW [% TL]	BH [% TL]	Mass [kg]	Max Depth [m]	U_Eco [m/s]	Range [h]
Abyss configuration	Torpedo	4	0.66	0.7	17%	17%	880	6000		20
ACFR Seaglider configuration	Teardrop						52	1,000	0.25	5113
ACFR Slocum Gliders configuration	Torpedo with Wings						52	200	0.35	720
ALBAC configuration	Torpedo with Wings	1.4	1.2	0.3	86%	24%	45		0.51	1
ALISTAR configuration	Teardrop	5	1.68	1.5	34%	29%	2300	3000	1.03	20
Alister REA configuration	Torpedo	4.8	0.7	1.2	15%	25%	800	300	2.06	12
APL/UW Seaglider configuration	Teardrop	3.2	1	0.3	31%	9%	52	1,000	0.25	7200
Aqua Explorer 2000 configuration	Oblate	3	1.3	0.9	43%	30%	300	2,000		16
Aqua2 configuration	Biomimetic	0.6	0.44	0.1	69%	20%	16.5	30	0.51	5.5
AquaPenguin configuration	Biomimetic	0.8	0.66	0.2	86%	25%	9.6		1.39	7
ARCS configuration	Torpedo with Wings						1360	304.8	2.05	10
Arctic Explorer configuration	Torpedo	7.4	0.74	0.7	10%	10%	2,200	5,000	1.5	
Aries configuration	Rectangular	3	0.4	0.3	13%	8%	220	50	1	8
Aster configuration	Torpedo						973	3,000		
Autonomous Benthic Explorer configuration	Open Space Frame	3	2	2.5	67%	83%	550	6000	0.17	14
Autonomous Underwater Vertical Profiler (AUVeP) configuration	Open Space Frame						30	20		
Autosub Long Range configuration	Torpedo with Wings							6000	0.4	4400
Autosub3 configuration	Torpedo	7	0.9	0.9	13%	13%	2400	1600		72
Autosub6000 configuration	Torpedo	5.5	0.9	0.9	16%	16%	2000	6000	1	70
AUV Leucathea configuration	Torpedo	1.3	0.15	0.2	12%	12%	19	100	1.29	16
AUV-150 configuration	Torpedo	4.8	0.5	0.5	10%	10%	490		2.06	
AUV62 configuration	Torpedo	7	0.53	0.5	8%	8%	1000	500	3	
Benthic Rover configuration	Open Space Frame	2.5	1.5	1.2	60%	48%	1400	6000	0.02	
Bluefin-12D configuration	Torpedo	4.3	0.32	0.7	7%	15%	260	1,500	2	30
Bluefin-12S configuration	Torpedo	3.8	0.32	0.7	8%	19%	213	200	2	26
Bluefin-21 configuration	Torpedo	4.9	0.53	0.8	11%	16%	750	4500	1.54	25
Bluefin-9 Sealion configuration	Torpedo	1.7	0.24	0.2	15%	15%	50	200	1.52	12
BlueStar configuration	Torpedo	1.7	0.2	0.2	12%	12%	45	100	1.54	6
BPAUV configuration	Torpedo	3.3	0.53	0.5	16%	16%	363		1.54	18
Cal Poly Remus Vehicle configuration	Torpedo								1.54	

AUV	Body Type	TL [m]	BW [m]	BH [m]	BW [% TL]	BH [% TL]	Mass [kg]	Max Depth [m]	U_Eco [m/s]	Range [h]
Caribou configuration	Torpedo	3.5	0.58	0.6	17%	17%	400	3000	1.54	20
CMOP Remus 100 configuration	Torpedo						37	100	1.54	10
CMOP Slocum Glider Phoebe configuration	Torpedo with Wings						52	200	0.35	720
C-Surveyor II configuration	Torpedo	6.2	1	1	16%	16%	1400	3000	1.54	50
C-Surveyor III configuration	Torpedo	6.4	1	1	16%	16%	1500	4500	1.54	50
C-Surveyor IV configuration	Torpedo	4.6	1	1	22%	22%	1400	3000	1.54	
C-Surveyor V configuration	Torpedo	6.2	1	1	16%	16%	1400	3000	1.54	
Cuttthroat LSV-2 configuration	Model Submarine	34	10	10	30%	30%	185,520			
Delphin2 configuration	Torpedo	2	0.25	0.3	13%	13%	47	50		8
DEPTHX configuration	Open Space Frame	4.3	3.04	3	71%	71%	1300	1000	0.2	8
DNS Pegel configuration	Torpedo	3.1	0.55	0.6	18%	18%	300	6,000	2	
DOF Subsea Hugin configuration	Torpedo	5.5	1	1	18%	18%	1,400	3,000	1.54	60
DORA configuration	Torpedo						80	1000	1	4
Double Eagle configuration	Oblate	2.9	1.3	1	45%	34%	540	3000	2	10
Eagle Ray configuration	Torpedo	4.5	0.69	0.7	15%	15%	630	3,000	1.54	22
Echo Mapper II configuration	Torpedo	4.1	0.53	0.5	13%	13%	525	4,500	1.54	25
Echo Ranger configuration	Rectangular	5.5	1.27	1.3	23%	23%	5308	3050	1.54	28
Echo Surveyor I configuration	Torpedo	5.4	1	1	19%	19%	1,450	3,000	1.54	60
Echo Surveyor II configuration	Torpedo	5.4	1	1	19%	19%	1,450	3,000	1.54	60
Endurance configuration	Oblate	2.1	1.52	0.8	71%	37%	1,043	1,000		6
Epaulard configuration	Teardrop	4	1.1	2	28%	50%	2900	6000	0.51	7
ERI Slocum Gliders configuration	Torpedo with Wings						52	200	0.35	720
Exocetus Coastal Glider configuration	Torpedo with Wings	2	0.32	0.3	16%	16%	120		1.03	336
Explorer configuration	Torpedo	4.5	0.69	1.8	15%	40%	750	5000	1.5	22
Fetch 3 configuration	Teardrop	2.1	0.34	0.3	16%	16%	97	200		10
Fetch configuration	Teardrop	1.9	0.29	0.3	15%	15%	99	150		18
Folaga configuration	Torpedo	2	0.16	0.2	8%	8%	31	80	1.03	6
Gavia Defence configuration	Torpedo	1.8	0.2	0.3	11%	17%	49	1000	1	7
Gavia Offshore Surveyor configuration	Torpedo	1.8	0.2	0.3	11%	17%	49	1000	1	5
Gavia Scientific configuration	Torpedo	1.8	0.2	0.3	11%	17%	49	1000	1	6
GeoSwath Plus Remus 100 configuration	Torpedo							100	1.54	12

AUV	Body Type	TL [m]	BW [m]	BH [m]	BW [% TL]	BH [% TL]	Mass [kg]	Max Depth [m]	U_Eco [m/s]	Range [h]
Girona 500 configuration	Open Space Frame	1.5	1	1	67%	67%	140	500	0.5	8
GOSL SQX-1 configuration	Open Space Frame	1.6	0.25	0.8	16%	52%	95	3000	2	8
HarborScan configuration	Torpedo	2.5	0.19	0.2	8%	8%	52.6	300	1.29	
Henry Bigelow configuration	Torpedo with Wings						52		0.35	720
Horizon Marine Slocum Gliders configuration	Torpedo with Wings						52	1,000	0.35	720
Hovering AUV configuration	Open Space Frame	1	0.71	0.4	72%	39%	82			3
Hugin 1000 configuration	Torpedo	4.7	0.75	0.8	16%	16%	850	3000	1.54	24
Hugin 3000 configuration	Torpedo	5.5	1	1	18%	18%	1400	3000	1.54	60
Hugin 4500 configuration	Torpedo	6	1	1	17%	17%	1900	4500	1.54	60
Intelligent Hybrid Underwater Vehicle configuration	Oblate	3	1.1	0.7	37%	23%	350	50		
iRobot 1KA Seaglider configuration	Teardrop	2.8	1	0.4	36%	14%	52	1000	0.25	7200
ISIMI AUV100 configuration	Torpedo	1.5	0.2	0.2	13%	13%	38	100	1.5	
Iver2 configuration	Torpedo	0.1	0.01	0	8%	8%	19	100	1.29	24
Jaguar configuration	Open Space Frame	1.9	0.34	1.8	18%	94%	250	6,000	1	8
Knifefish configuration	Torpedo								1.54	
Kokanee LSV-1 configuration	Model Submarine	27	3	3	11%	11%	140,270			
Light Autonomous Vehicle LAUV configuration	Torpedo	1.1	0.15	0.2	14%	14%	15	50	1.5	8
LMRS configuration	Torpedo	6	0.53	0.5	9%	9%	1244	1000		60
Lucille configuration	Open Space Frame								1	
MACO configuration	Open Space Frame	1.5	0.44	0.6	29%	41%	70	60	0.9	2.5
MANO configuration	Torpedo	3.8	0.32	0.3	8%	8%	204	200	2	19.5
Mano configuration	Torpedo								2	
Manta Test Vehicle configuration	Oblate	10	4.72	1.8	45%	17%	14060	243	2.32	4
MARES configuration	Torpedo	1.5	0.2	0.2	13%	13%	32	100	1.11	10
Marlin Mk 1 configuration	Oblate	1.5	0.8	0.8	53%	53%	454	304	2.06	10
Marlin MK 2 configuration	Oblate	3	1.5	1.3	50%	43%	954	4,000	2	20
Marlin MK 3 configuration	Oblate	4.9	1.5	1.3	31%	27%	1590	4000	2	60
Mary Ann and Ginger configuration	Torpedo	3.8	0.71	0.7	18%	18%	862	6000		22
Maya configuration	Torpedo with Wings	1.7	0.23	0.2	13%	13%	55	200	1.5	7.2

AUV	Body Type	TL [m]	BW [m]	BH [m]	BW [% TL]	BH [% TL]	Mass [kg]	Max Depth [m]	U_Eco [m/s]	Range [h]
MBARI Seafloor Mapping AUV configuration	Torpedo	5.3	0.53	0.5	10%	10%	680	6000	1.54	17.5
MBARI Upper Water Column AUV configuration	Torpedo	3.7	0.54	0.5	15%	15%	476	6000	1.54	20
Midsize Automated Reconfigurable Vehicle configuration	Torpedo						226	457	3	26
MIT LAMSS Bluefin 21 configuration	Torpedo	4.9	0.53	0.5	11%	11%			1.54	
Mk 18 Mod 2 Kingfish configuration	Torpedo	3.9	0.66	0.7	17%	17%	282	600	1.5	
MolaMola configuration	Open Space Frame	1.9	0.34	1.8	18%	94%	200	2,000	1	8
Morpheus configuration	Rectangular						35	200	1.03	
Multi AUV Test Bed configuration	Torpedo						29.48	100	1.29	4
MUN Explorer AUV configuration	Torpedo						700	3,000	1.5	6
MUN Hybrid Glider configuration	Torpedo with Wings							200	0.35	
MUN Slocum Gliders configuration	Torpedo with Wings							200	0.35	
Muscle configuration	Torpedo								1.54	
NCS Offshore Surveyor configuration	Torpedo						80	1,000	1	5
Nessie VT configuration	Torpedo	1.6	0.28	0.3	18%	18%	40	100	1.5	22
nfante configuration	Rectangular	4.5	1.9	0.6	42%	13%	1000		1.26	18.4
NOAA Remus 100 configuration	Torpedo	1.6	0.19	0.2	12%	12%	45	100	1.54	10
NPS Remus 100 configuration	Torpedo						37	100	1.54	22
NRC IOT Slocum Gliders configuration	Torpedo with Wings						52	1,000	0.35	720
NURC Remus 100 configuration	Torpedo with Wings								0.51	
NUWC 21UUV configuration	Torpedo	6.3	0.53	0.5	8%	8%	750	457	6	10
NUWC Ecomapper configuration	Torpedo								1.29	8
NUWC Remus 600 configuration	Torpedo							600	1.5	
NUWC SAUV configuration	Other						200	500	0.51	
NUWC SAUV configuration	Other								0.51	
Odyssey IV configuration	Torpedo	2.6	1.5	1.4	58%	54%	650	6,000	1.54	8
Offshore Works Huggin 1000 configuration	Torpedo	4.9	0.75	0.8	15%	15%	775	3,000	1.54	29
OKPO 300 configuration	Torpedo	1.8	0.26	0.3	14%	14%	55	300	1.54	10
OKPO 6000 configuration	Torpedo	3.8	0.7	0.7	18%	18%	950	6000	1.54	10
OSU Seaglider configuration	Teardrop						52	1,000	0.25	7200

AUV	Body Type	TL [m]	BW [m]	BH [m]	BW [% TL]	BH [% TL]	Mass [kg]	Max Depth [m]	U_Eco [m/s]	Range [h]
OSU Slocum Gliders configuration	Torpedo with Wings						52	200	0.35	720
Pelagia configuration	Torpedo with Wings						52	200	0.35	720
Phoenix 21 inch AUV configuration	Torpedo						1,650	1,500	1.54	25
Picasso configuration	Torpedo with Wings	2	0.8	0.8	40%	40%	200	1,000	0.51	
Pirajuba configuration	Torpedo	1.8	0.23	0.2	13%	13%			1	4
Powered Tow Body configuration	Torpedo	3.6	0.32	0.3	9%	9%	127	300	7	
Puma configuration	Open Space Frame	1.9	0.34	1.8	18%	94%	250	6,000	1	8
R1 configuration	Torpedo	8.2	1.1	1.1	13%	13%	3,628	400	1.85	24
R2D4 configuration	Rectangular	4.4	1.08	0.8	25%	18%	1,630	4,000	1	24
Ranger configuration	Torpedo	0.9	0.09	0.1	10%	10%	9.07	5		8
Razor configuration	Oblate	1.7	0.76	0.3	45%	17%		100		12
RedStar configuration	Torpedo	1.7	0.2	0.2	12%	12%	45	100	1.54	6
Reef Explorer I configuration	Open Space Frame									
Reef Explorer II configuration	Open Space Frame						50	20		8
Remus 100 configuration	Torpedo	1.6	0.19	0.2	12%	12%	37	100	1.54	10
Remus 100-S configuration	Torpedo	1.8	0.19	0.2	10%	10%	45	100	1.54	10
Remus 600 configuration	Torpedo	3.3	0.32	0.3	10%	10%	240		1.5	70
Remus 6000 configuration	Torpedo	3.8	0.71	0.7	18%	18%	862	6000		22
Remus 600-S configuration	Torpedo	4.3	0.32	0.3	7%	7%	326	600	1.5	24
RESL Slocum Glider configuration	Torpedo with Wings						52		0.35	
Rutgers Slocum Gliders configuration	Torpedo with Wings						52	1,000	0.35	720
Sabertooth Single Hull configuration	Oblate	3	0.4	0.5	13%	15%	250	3,000	2.05	3
Sabretooth Double Hull configuration	Oblate	3	0.9	0.5	30%	15%	650	3,000	2.05	8
SAUV II configuration	Other	2.3	1.1	0.5	48%	22%	200		0.51	8
SAUVIM configuration	Oblate	6.1	2.1	1.8	34%	30%	6500	6000		
Scripps Spray Glider configuration	Torpedo with Wings	1.8	1.01	0.3	56%	17%	51.8	1500	0.25	6666
Sea Maverick configuration	Torpedo	9.1	1.22	1.5	13%	16%		1,000	2.57	
Sea Stalker configuration	Torpedo with Wings	8.7	0.97	1	11%	11%	4,763	1,000	0.51	
SeaBED configuration	Open Space Frame	1.9	0.34	1.5	18%	79%	250	2,000	1	8
SeaBED configuration	Open Space Frame							2,000	1	10
SeaCat configuration	Torpedo						130	300	2	6

AUV	Body Type	TL [m]	BW [m]	BH [m]	BW [% TL]	BH [% TL]	Mass [kg]	Max Depth [m]	U_Eco [m/s]	Range [h]
SeaExplorer configuration	Teardrop	2.9	0.6	0.3	21%	9%	59	700	0.26	
Seahorse configuration	Torpedo	8.7	0.97	1	11%	11%	4,763	1,000	2.06	72
SEAL configuration	Torpedo	5.5	0.74	1.3	13%	23%	1250	5000	1.5	19
SeaOtter configuration	Rectangular	3.5	0.98	0.5	28%	14%	1100	600	2.06	
SeaWolf configuration	Torpedo	2	0.3	0.5	15%	25%	112	300	4.12	3
Sirius configuration	Open Space Frame	2	1.5	1.5	75%	75%		700	1	
Slocum Electric Glider Coastal configuration	Torpedo with Wings	1.8	1.01	0.5	56%	27%	52	200	0.35	720
Slocum Electric Glider configuration	Torpedo with Wings	1.8	1.01	0.5	56%	27%	52	1000	0.35	720
Slocum Thermal Glider configuration	Torpedo with Wings	1.8	1.01	0.5	56%	27%	60	1200	0.35	43
SOG Seagliders configuration	Teardrop						52		0.25	7200
Spray Glider configuration	Torpedo with Wings	2.1	1.01	0.3	47%	14%	52	1500	0.2	4320
SQX-500 configuration	Open Space Frame	1.6	0.25	0.8	16%	52%	95	500	2	8
SRI AUV configuration	Torpedo						550	600	2	
Starbug configuration	Other	1.2	0.45	0.2	38%	13%	26	100	0.7	4
Subsea Glider configuration	Biomimetic	3.5	1.5	0.5	43%	14%	10	100	1.39	24
Swordfish Mk 18 Mod 1 configuration	Torpedo							100	1.54	
Talisman L configuration	Oblate						50			
Talisman M configuration	Oblate	4.5	2.5	1.1	56%	24%	1000	300		
Tantan configuration	Rectangular	2	0.75	0.8	38%	38%	180	150	1	12
TAVROS SAUV configuration	Other	2.3	1.1	0.5	48%	22%	200	500	0.51	8
Tethys configuration	Torpedo	2.3	0.31	0.3	13%	13%	110		0.5	740
Theseus configuration	Torpedo with Wings						8600	2000	2.06	60
Tri-Dog 1 configuration	Open Space Frame	1.9	0.58	0.5	31%	29%	170	100	0.72	3
TriMARES configuration	Open Space Frame	1.3	0.8	0.5	62%	38%	70	100	1.11	10
Twin Burger configuration	Open Space Frame	1.5	0.86	0.5	56%	35%	120	50	0.51	2
UAF ANT Littoral Glider configuration	Torpedo with Wings	2	2	0.3	100%	16%	120	200	1.03	
UAF Slocum Gliders configuration	Torpedo with Wings	1.5	1.01	0.5	67%	33%	52	200	0.35	720
UBC Gavia configuration	Torpedo	1.8	0.2	0.3	11%	17%	49	1000	1	6
UConn Gliders- Bill and Frank configuration	Torpedo with Wings						52	200	0.35	720
Urashima configuration	Rectangular	10	1.3	1.5	13%	15%	7,257	3,500	1.54	18
USM Underwater Glider configuration	Torpedo with Wings	1.3	1	0.2	77%	13%				2

AUV	Body Type	TL [m]	BW [m]	BH [m]	BW [% TL]	BH [% TL]	Mass [kg]	Max Depth [m]	U_Eco [m/s]	Range [h]
UTEC Gavia configuration	Torpedo	2.7	0.2	0.3	7%	11%	80	1,000	1	5
VT 475 AUV configuration	Torpedo	0.9	0.12	0.2	14%	28%	8.3		1.54	8
VT Self Mooring AUV configuration	Torpedo	2.3	0.18	0.2	8%	8%		500	2.06	25
Waldo configuration	Torpedo with Wings						52	1,000	0.35	720
WHOI Remus 6000 configuration	Torpedo	3.8	0.71	0.7	18%	18%	862	6,000		22
WHOI Tunnel Inspection Vehicle configuration	Torpedo	2.7	0.4	0.4	15%	15%				16
Yellowfin configuration	Torpedo	0.9	0.12	0.1	13%	13%	7.71		1.02	10
YSI EcoMapper configuration	Torpedo	0.2	0.01	0	7%	7%	20.4	200	1.29	8

AUV	ASW	BS	CD	CM	CRS	EM	EOD	FM	FP	GS	HAR	HI	HPS	IMR	ISR	MC	MFS	MSS	OGS	OS	PRS	REA	S&R	SCM	SD	SM	SR	SZS	VR	WCS
Number of AUVs perofrming the mission	5	14	1	33	13	89	6	18	2	29	7	7	16	14	16	26	8	51	24	94	23	22	9	29	11	70	27	1	47	2
Percent of AUVs performing the mission	3 %	7 %	1 %	17 %	7 %	47 %	3 %	9 %	1 %	15 %	4 %	4 %	8 %	7 %	8 %	14 %	4 %	27 %	13 %	49 %	12 %	12 %	5 %	15 %	6 %	37 %	14 %	1 %	25 %	1 %
Abyss configuration																				OS						SM				
ACFR Seaglider configuration						EM														OS										
ACFR Slocum Gliders configuration						EM														OS										
ALBAC configuration						EM														OS										
ALISTAR configuration					CRS					GS				IMR					OGS		PRS									
Alister REA configuration				CM											ISR	MC						REA				SM				
APL/UW Seaglider configuration						EM														OS										
Aqua Explorer 2000 configuration			CD		CRS	EM				GS								MSS	OGS		PRS					SM				
Aqua2 configuration		BS				EM		FM				HI						MSS						SCM			SR	SZS	VR	
AquaPenguin configuration																											SR			

ARCS configuration																													VR	
Arctic Explorer configuration																											SM			
Aries configuration																									SD				VR	
Aster configuration				CM		EM		FM										MSS		OS		REA								
Autonomous Benthic Explorer configuration										GS																SM				
Autonomous Underwater Vertical Profiler (AUVeP) configuration						EM														OS										
Autosub Long Range configuration						EM														OS										
Autosub3 configuration						EM				GS								MSS		OS						SM	SR			
Autosub6000 configuration										GS								MSS		OS						SM			VR	
AUV Leucathea configuration						EM												MSS		OS		REA				SM				
AUV-150 configuration															ISR											SM				
AUV62 configuration						EM										MC										SM				

Benthic Rover configuration										GS							MFS													
Bluefin-12D configuration	AS W			CM		EM	EOD			GS						MC		MSS		OS			S&R	SCM		SM				
Bluefin-12S configuration		BS		CM		EM		FM					HPS			MC		MSS		OS		REA			SD	SM	SR		VR	
Bluefin-21 configuration	AS W					EM	EOD			GS					ISR	MC		MSS		OS			S&R	SCM		SM				
Bluefin-9 Sealion configuration		BS		CM			EOD						HPS			MC														
BlueStar configuration																													VR	
BPAUV configuration																MC								SCM						
Cal Poly Remus Vehicle configuration						EM																								
Caribou configuration		BS		CM		EM		FM		GS	HAR							MSS		OS		REA			SD	SM	SR		VR	
CMOP Remus 100 configuration																		MSS		OS										
CMOP Slocum Glider Phoebe configuration						EM														OS										
C-Surveyor II configuration																			OGS		PRS									
C-Surveyor III configuration																			OGS		PRS									

C-Surveyor IV configuration																			OGS		PRS										
C-Surveyor V configuration																			OGS		PRS										
Cuttthroat LSV-2 configuration											HAR																			VR	
Delphin2 configuration																										SD				VR	
DEPTHX configuration																											SM			VR	
DNS Pegel configuration																														VR	
DOF Subsea Hugin configuration					CRS														OGS		PRS						SM				
DORA configuration						EM																					SM				
Double Eagle configuration																MC											SM				
Eagle Ray configuration						EM														OS											
Echo Mapper II configuration										GS										OS							SM				
Echo Ranger configuration					CRS	EM				GS					ISR		MFS	MSS	OGS	OS	PRS	REA		SCM	SD	SM	SR		VR	
Echo Surveyor I configuration																			OGS		PRS					SM				
Echo Surveyor II configuration					CRS														OGS		PRS					SM				

Endurance configuration						EM		FM		GS																		SR		VR	
Epaulard configuration																					OS					SM			VR	
ERI Slocum Gliders configuration																		MSS			OS									
Exocetus Coastal Glider configuration						EM									ISR										SCM					
Explorer configuration										GS								MSS			OS				SCM		SM	SR		
Fetch 3 configuration																					OS					SM				
Fetch configuration						EM															OS									
Folaga configuration						EM								IMR																
Gavia Defence configuration	AS W	BS		CM		EM							HPS		ISR	MC									SCM		SM			
Gavia Offshore Surveyor configuration					CRS	EM		FM		GS							MFS	MSS	OGS	OS	PRS	REA					SM			
Gavia Scientific configuration		BS		CM		EM		FM		GS							MFS	MSS		OS		REA					SM	SR		VR	
GeoSwath Plus Remus 100 configuration		BS		CM				FM																							
Girona 500 configuration				CM								HI											S&R	SCM		SM			VR	

GOSL SQX-1 configuration														IMR					OGS		PRS										
HarborScan configuration				CM		EM		FM				HI	HPS			MC		MSS		OS		REA	S&R	SCM		SM				
Henry Bigelow configuration																		MSS		OS										
Horizon Marine Slocum Gliders configuration																		MSS		OS										
Hovering AUV configuration							EOD					HI	HPS																	
Hugin 1000 configuration				CM	CRS	EM				GS								MSS	OGS	OS	PRS			SCM			SR			
Hugin 3000 configuration				CM	CRS	EM				GS							MFS	MSS	OGS	OS	PRS			SCM		SM	SR			
Hugin 4500 configuration				CM	CRS	EM				GS								MSS	OGS	OS	PRS			SCM		SM				
Intelligent Hybrid Underwater Vehicle configuration						EM																				SM				
iRobot 1KA Seaglider configuration													HPS		ISR					OS										
ISIMI AUV100 configuration																													VR	
Iver2 configuration				CM		EM		FM														REA								
Jaguar configuration					CRS			FM										MSS	OGS	OS	PRS			SCM		SM				

Knifefish configuration																MC														
Kokanee LSV-1 configuration											HAR																		VR	
Light Autonomous Vehicle LAUV configuration				CM		EM		FM	FP	GS			HPS			MC		MSS		OS		REA	S&R	SCM		SM				
LMRS configuration				CM						GS						MC										SM				
Lucille configuration						EM												MSS		OS						SM				
MACO configuration										GS																			VR	
MANO configuration																													VR	
Mano configuration																									SCM	SD				VR	
Manta Test Vehicle configuration																														VR	
MARES configuration						EM														OS										
Marlin Mk 1 configuration														IMR	ISR															
Marlin MK 2 configuration														IMR	ISR															
Marlin MK 3 configuration														IMR	ISR															

Mary Ann and Ginger configuration																				OS			S&R			SM				
Maya configuration						EM														OS										
MBARI Seafloor Mapping AUV configuration				CM																						SM				
MBARI Upper Water Column AUV configuration						EM														OS		REA								
Midsize Automated Reconfigurable Vehicle configuration																													VR	
MIT LAMSS Bluefin 21 configuration																								SCM	SD				VR	
Mk 18 Mod 2 Kingfish configuration		BS		CM			EOD						HPS			MC							S&R	SCM	SD	SM				
MolaMola configuration																				OS						SM				
Morpheus configuration		BS		CM		EM		FM								MC		MSS		OS		REA								
Multi AUV Test Bed configuration																													VR	
MUN Explorer AUV configuration				CM														MSS		OS						SM			VR	
MUN Hybrid Glider configuration																				OS					SD		SR		VR	

MUN Slocum Gliders configuration																				OS					SD		SR			
Muscle configuration											HAR					MC											SR		VR	
NCS Offshore Surveyor configuration																			OGS		PRS					SM				
Nessie VT configuration						EM							HPS					MSS		OS										
nfante configuration						EM																								
NOAA Remus 100 configuration				CM																										
NPS Remus 100 configuration											HAR																		VR	
NRC IOT Slocum Gliders configuration						EM														OS										
NURC Remus 100 configuration													HPS			MC											SR			
NUWC 21UUV configuration						EM					HAR									OS							SR		VR	
NUWC Ecomapper configuration						EM																								
NUWC Remus 600 configuration				CM		EM					HAR							MSS		OS					SD	SM	SR		VR	
NUWC SAUV configuration																													VR	

NUWC SAUV configuration																														VR	
Odyssey IV configuration																					OS									VR	
Offshore Works Huggin 1000 configuration					CRS					GS											OS	PRS					SM				
OKPO 300 configuration		BS		CM	CRS	EM		FM		GS		HI	HPS			MC	MFS	MSS	OGS	OS	PRS	REA		SCM		SM	SR			WCS	
OKPO 6000 configuration										GS							MFS	MSS		OS											
OSU Seaglider configuration						EM														OS											
OSU Slocum Gliders configuration						EM														OS											
Pelagia configuration						EM														OS											
Phoenix 21 inch AUV configuration	AS W																						S&R			SM					
Picasso configuration						EM												MSS		OS											
Pirajuba configuration						EM																								VR	
Powered Tow Body configuration																MC								SCM		SM					
Puma configuration						EM												MSS		OS											

R1 configuration																				OS						SM				
R2D4 configuration																				OS						SM				
Ranger configuration						EM														OS									VR	
Razor configuration		BS		CM		EM			FP			HI	HPS							OS		REA								
RedStar configuration																										SM			VR	
Reef Explorer I configuration						EM												MSS												
Reef Explorer II configuration						EM												MSS												
Remus 100 configuration						EM							HPS			MC				OS				SCM		SM	SR			
Remus 100-S configuration				CM				FM										MSS		OS						SM				
Remus 600 configuration		BS		CM		EM		FM		GS								MSS						SCM		SM	SR			
Remus 6000 configuration				CM		EM				GS							MFS	MSS	OGS	OS	PRS			SCM		SM	SR			
Remus 600-S configuration				CM	CRS													MSS	OGS	OS	PRS	REA	S&R	SCM		SM				WCS
RESL Slocum Glider configuration						EM														OS										

Rutgers Slocum Gliders configuration						EM														OS											
Sabertooth Single Hull configuration														IMR																	
Sabretooth Double Hull configuration														IMR																	
SAUV II configuration						EM												MSS		OS							SR		VR		
SAUVIM configuration												HI		IMR															VR		
Scripps Spray Glider configuration						EM														OS											
Sea Maverick configuration															ISR																
Sea Stalker configuration															ISR																
SeaBED configuration										GS									OGS						SM						
SeaBED configuration				CM														MSS					SCM		SM						
SeaCat configuration														IMR	ISR			MSS				REA									
SeaExplorer configuration						EM												MSS		OS											
Seahorse configuration						EM									ISR			MSS		OS					SM						

SEAL configuration						EM														OS						SM					
SeaOtter configuration																MC										SM					
SeaWolf configuration				CM				FM		GS			HPS			MC		MSS	OGS	OS	PRS	REA									
Sirius configuration						EM																				SM					
Slocum Electric Glider Coastal configuration						EM														OS		REA					SR				
Slocum Electric Glider configuration						EM														OS		REA					SR				
Slocum Thermal Glider configuration																				OS									VR		
SOG Seagliders configuration	AS W																														
Spray Glider configuration						EM														OS		REA									
SQX-500 configuration						EM									ISR	MC		MSS		OS				SCM		SM					
SRI AUV configuration						EM							HPS													SM					
Starbug configuration		BS				EM												MSS		OS											
Subsea Glider configuration				CM		EM		FM						IMR				MSS		OS				SCM							

Swordfish Mk 18 Mod 1 configuration		BS		CM			EOD						HPS			MC								SCM		SM					
Talisman L configuration																MC										SM					
Talisman M configuration															ISR	MC															
Tantan configuration						EM																							VR		
TAVROS SAUV configuration						EM														OS		REA									
Tethys configuration						EM														OS									VR		
Theseus configuration																		MSS		OS						SM					
Tri-Dog 1 configuration														IMR															VR		
TriMARES configuration														IMR					OGS												
Twin Burger configuration																											SR		VR		
UAF ANT Littoral Glider configuration						EM												MSS		OS							SR				
UAF Slocum Gliders configuration						EM												MSS		OS							SR				
UBC Gavia configuration						EM				GS										OS											

UConn Gliders- Bill and Frank configuration						EM														OS										
Urashima configuration																				OS						SM				
USM Underwater Glider configuration						EM														OS										
UTEC Gavia configuration						EM													OGS		PRS									
VT 475 AUV configuration						EM																							VR	
VT Self Mooring AUV configuration						EM																							VR	
Waldo configuration						EM														OS										
WHOI Remus 6000 configuration																				OS				SCM		SM				
WHOI Tunnel Inspection Vehicle configuration														IMR																
Yellowfin configuration						EM																							VR	
YSI EcoMapper configuration						EM														OS						SM				

Appendix 2. Publications

Appendix 2.1. Using Bio-Inspiration to Improve Capabilities of Underwater Vehicles

Murphy, A.J. and Haroutunian, M. (2011). "Using Bio-Inspiration to Improve Capabilities of Underwater Vehicles". In: 17th International Unmanned Untethered Submersible Technology Conference (UUST 2011), 21-24 August, Portsmouth-USA. Curran Associates, Inc. Pp. 20-31. ISBN: 978-1-61839-927-4

USING BIO-INSPIRATION TO IMPROVE CAPABILITIES OF UNDERWATER VEHICLES

Dr Alan J Murphy [(1)] and **Maryam Haroutunian** [(2)]

School of Marine Science and Technology, Armstrong Building, Newcastle University, NE1 7RU, Newcastle upon Tyne - UK

(1) Lecturer, a.j.murphy@ncl.ac.uk

(2) PhD Student, maryam.haroutunian@ncl.ac.uk

ABSTRACT

There are over 750,000 marine species ranging in size from a few micrometers to dozens of meters, all of which, through the natural process of evolution, have arrived at "successful" solutions to surviving and operating in the ocean space.
Many of these species have capabilities and functionality which have much in common with the engineered capabilities required for underwater vehicles e.g. propulsion/locomotion, manoeuvrability/agility and the ability & resilience to operate at depth. Indeed, in many examples, it appears the biological solutions exhibit superior performance compared to the technological alternative, yet in biology these capabilities are achieved by different and diverse means.
In this research an extensive study on the capabilities of marine animals has been conducted in relation to the equivalent capability on AUVs. And the biological solutions to propulsion, agility, depth and vehicle (or animal) architecture have been focused on. This paper will present the approach adopted, some specific studies and key results from using a bio-inspired approach to improving AUV engineering capabilities.

Acknowledgments
This research is part of a collaborative project, "Nature in Engineering for Monitoring the Oceans" (NEMO), including the National Oceanography Centre and the University of Southampton and is funded by the Engineering and Physical Sciences Research Council (EPSRC, 2009).
The authors would like to acknowledge that the data collected on AUV characteristics and capabilities has been a collaborative work with NEMO colleagues in the University of Southampton.

Nomenclature

s	Second
AUV	Autonomous Underwater Vehicle
BL	Body Length
C_B	Block Coefficient
COT	Cost of Transport
D	Diameter (Subscripts as relevant)
D_d	Derived Diameter
Eco (Speed)	Economic (speed)
FR	Fineness Ratio
L	Length
M	Mass (Subscripts as relevant)
MA	Marine animal
Re	Reynolds Number
ROV	Remotely Operated Vehicle
R_{Yaw}	Yaw Radius
kg	Kilo gram
U	Speed (Subscripts as relevant)
V	Volume (Subscripts as relevant)
ρ	Density
ρ_{SW}	Density of sea water

INTRODUCTION

Man-kind has a long history in ocean exploration and exploitation; from early exploration with divers in Greek and Chinese cultures, c.4500 B.C., to the genesis of ship-borne deep-sea research in the 17th Century by the likes of Sir James Clark Ross. In the 19th Century technological advances have seen human descents to the deepest regions of the ocean, when in 1960, Jacques Piccard and Don Walsh reached a manned decent to the deepest known place in the oceans in excess of 10km (Blidberg, 2001).

The current Status of AUV Technology

Improved access for deep water exploration has been facilitated by Unmanned Underwater Vehicles, initially ROVs and more recently, with increased sophistication of computers, Autonomous Vehicles. Nevertheless, there is still further demand for improved underwater capability beyond that currently possible with existing AUVs. For

example, in the offshore industry there is demand for accessing and exploring deep waters for survey, inspections and maintenance. Similarly, there is high demand in the scientific community for improved deep-water capability for discovery and study of deep-water species, pharmacological sampling and environmental research. Furthermore, military and security agencies are constantly striving for improved capabilities in all aspects of underwater technology.

More agile and manoeuvrable AUVs with larger operating ranges can satisfy these demands by performing desired missions with more precision and cost-efficiency. Benefiting from the collective abilities of hybrid ROVs and intervention underwater vehicles is another aim of new vehicle designs (Kermorgant & Scourzic, 2005). However, currently there are restrictions in AUV capabilities including depth capabilities, speed, manoeuvrability and power. For example, the gathered database in this research shows that only 29% of the AUV types operate deeper than 3000m, whereas the deepest waters are 8000–11000m deep. In the UK, AUTOSUB6000 is the deepest diving AUV, to a depth of 5600m (Thaindian News, 2009). Furthermore, compared to other marine vehicles, AUVs are relatively slow and have limited speed ranges, with even the fastest, e.g. "Alister" and "SeaOtter" at 4.12m/s, being below 10m/s) (AUVAC, 2010).

Possible inspiration from nature

Nature has been a source of inspiration for researchers and inventors over the last three millennia (Vincent, 2001) and systems found in nature are continuously evolving, with those surviving in their specific environment having superiority over those extinguished over time. The greatest part of Earth's biodiversity, ~90% of the major groups of living species, is in the oceans (Madin, 2005) and marine animals have specifically adapted to thrive in underwater conditions (e.g. high water pressure, lack of air, etc.). Initial research in this project has identified marine animals with specific superior characteristics; e.g. high-speed or large depth range. Furthermore, examples of superior overall performance are evident; this being achieved through multi-functionality in biological systems. The *Sailfish*, for example can achieve a speed of over 30m/s and marine animals have been found at the extremes of the oceans' depth.

The research challenge

This paper is reports on research carried-out at Newcastle University. The aim of this research is to improve the performance of AUVs by investigating novel technologies, inspired by marine animals, as well as generating bio-inspired design techniques and implementation methods. To achieve this aim, two main objectives are being pursued:

- Investigating bio-inspiration
  - ✓ Provide a greater understanding of marine biological organisms and systems for engineering application
  - ✓ Create a new way of thinking in engineering design
  - ✓ Use biological systems to improve engineering technology
- Application of bio-inspiration
  - ✓ to applied the lessons learned from nature to improve depth, speed and manoeuvrability of AUVs

(NEMO, 2011)

A brief on Bio-Inspiration

Considering all the potentials nature has to offer to improve engineering design techniques, one may learn from nature, using the relevant novelties while leaving the undesirable ones, in order to relate engineering requirements to biological function. This is different from mimicking nature; therefore NEMO is not aiming to build a robotic fish.

METHODOLOGY

In terms of vehicle specification, the principal engineering challenges associated with AUVs are propulsion, manoeuvring and depth capabilities, as well as the storage and efficient use of energy. Therefore, more speed, greater endurance and depth of operation, more agility, reduced fuel consumption and advanced, cost-effective, designs and technologies are amongst the wish-list for AUVs demands; however, an optimum mixture of these features will result in a new generation of AUVs. These features of both AUVs and marine animals were analysed in this research.

Investigating marine animals and AUV capabilities

Data on the existing capabilities of 73 types of AUV was collected from a wide variety of sources, including AUV manufacturers, journal and conference publications and industry intelligence publications (e.g. Funnell, 2007 and AUVAC, 2010). The majority of gathered data for AUVs has been from specification sheets or existing trial results for the vehicle. For some AUVs (especially the bio-mimicking ones) data is not from trials but predictions of the manufacturer, which is assumed to be sufficiently accurate to perform a general comparison.

In addition, a similar database was established for the "engineering" specifications of marine animals, including physical characteristics, anatomy, physiology, hydromechanics and their taxonomic relations and classifications. Data is collected for 10 different classes of marine animals including bony fish, marine mammals, sharks & rays, penguins, etc. micro organisms are not studied in this research due to their size disparity to AUVs.

Data has mainly been collected from either technical papers and books (e.g. Thillart et al, 2007, Rivera et al, 2006, Hoelsel, 2002, Fish, 1998 and Jefferson et al, 1993) as well as databases published over the internet (e.g. Froese, 2011 and Appeltans et al, 2010). Where multiple data for a single species has been collected from different sources, average values have been derived and used. Furthermore, multiple sources are sometimes used to gather the full dataset for a given species. In some cases, dimensions have been derived from photos of the species, where the scale factor is known.

This presented interesting challenges; because it required addressing truly interdisciplinary literature and much of the published data regarding the capability of marine animals is not presented in engineering terms and is often presented for entirely different purposes. There are a number of studies which are in engineering terms, including various publications of marine animal hydrodynamics whereas many other publications, while providing material of interest in this research are provided for the purposes of life-science and biological research.

The number of species investigated was originally over 200, from which a subset of 127 with sufficient published data for comparison has been entered in the final database; this is due to some species being unreachable or not have been completely studied. In these cases, by considering taxonomically close relationship between certain animals, investigating a species in a family is sufficient for the purpose of this research.

Individuals of the same species are different in geometry and performance (e.g. their body shape is dependant to their environment and emotional conditions); therefore, gathered data is a mean of all existing data for a certain species. The data are stored in a database for constant use, comparison and update. The database includes data on general characteristics (dimensions, kinematics, depth of operation, etc.), structure, mechanisms and taxonomy.

A CONTRAST BETWEEN MARINE ANIMALs and AUVs

To highlight the relative superiority and limitations of biological systems and AUVs, the stored data have been analysed to make the following comparisons:

- Variations in body forms
- Speed and agility
- Depth capabilities
- Manoeuvrability
- Energetics

These are considered next, each in turn.

Variations in body forms

AUVs and especially marine animals have many different body forms and large variation in size; it would be ideal to compare their body forms to include resistance characteristics to the study. However, due to insufficient data for both groups, it is not possible to make direct comparison in terms of length, breadth, height and volume. On the other hand, Body Length and mass are generally available; furthermore, notwithstanding minor differences, MAs and AUVs are approximately neutrally buoyant (the variation of density is relatively small, even between floating and sinking marine animals); therefore they have an average density of water ($\rho_{SW} = 1025\,{}^{Kg}/_{m^3}$).

Noting the limitations, comparing some measure of fineness is desirable. If we idealise any marine animal as an elliptical body of revolution (many MAs have fusiform body shapes which are wide in the middle section and tapered at both ends) and fit the same volume of the animal to it and keep the body length the same, by working out the equivalent diameter, D_d, the ratio of overall length to this equivalent diameter, $\frac{L}{D_d}$ is expected to be an indication of fineness ratio. To test this approach, it is first applied to AUVs for which body diameter is known. That is by comparing the fineness ratio ($\frac{L}{quoted\ D_{max}}$) of an AUV with the one of a neutrally buoyant elliptical body of revolution of the same length, if the assumption regarding density is correct, the expectations are, to see a correlation between the two values.

Considering the elliptical body of revolution as Figure 1, the derived diameter is calculated as follows:

Block coefficient of a cylindrical AUV is defined in the form of:

$$C_B = \frac{V_{AUV}}{\frac{\pi}{4}D^2 L} \quad (1)$$

$$M_{AUV} = \rho V_{AUV} = \frac{\pi D^2}{4} L C_B \rho \quad (2)$$

$$D = \sqrt{\frac{4M}{\pi \rho L}} \quad (3)$$

And $$D_d = \sqrt{3/2}\, D = \sqrt{\frac{6M}{\pi \rho L}} \quad (4)$$

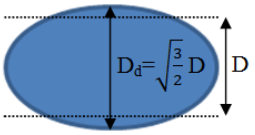

Figure 1: Side view of an elliptical body of revolution showing D_d as compared to the diameter, D of the cylinder with the same volume and length

The results are illustrated in Figure 2 which highlights strong correlation between derived and actual fineness ratios based on actual diameter of the AUV.

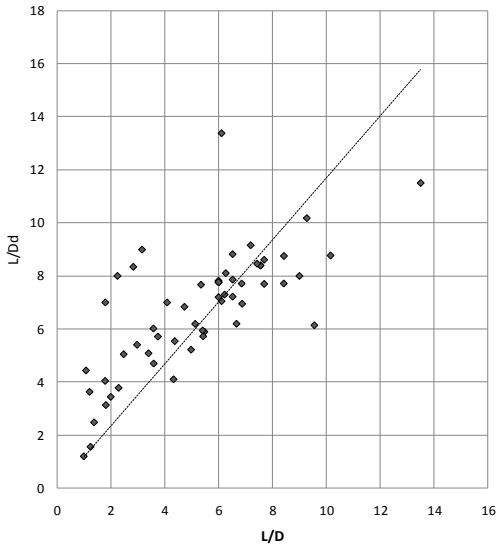

Figure 2: Fineness ratios of AUVs vs. equivalent elliptical bodies of revolution of the same length

By knowing the actual diameter of AUVs and validating the approach, same steps are performed for marine animals; the results of fineness ratios are illustrated in Figures 3 (for AUVs) and 4 (for MAs). Due to the large size variance in marine animals, the graph only illustrates MAs with BL<10m, with larger animals being whales (with fusiform bodies) and whale shark (elongated body); these large animals follow the same trend as smaller ones except for the 27m Fin whale which is more slender than other fusiforms ($\frac{L}{D_d}$<11.9) and whale shark being more slender than other animals with elongated oval cross-sectioned bodies ($\frac{L}{D_d}$<11.2). Note that contours for different L/D_d (also known as Fineness ratio (FR)) have been placed with side views of the equivalent elliptical bodies of revolution provided for clarity.

By comparing the Figures 3 & 4, marine animals exhibit higher fineness ratios; while AUVs have 1<$\frac{L}{D_d}$<15, animals range between 2.8< $\frac{L}{D_d}$<67 with leatherback turtle and sea lamprey having the lowest and highest values in respect. The space-frame AUVs have the lowest fineness ratios while torpedoes have the highest. The only fusiform body animal with $\frac{L}{D_d} > 15$ is marine iguana; the reason being the consideration of its long tail in overall length. As expected, auguilliform species have the highest ratios.

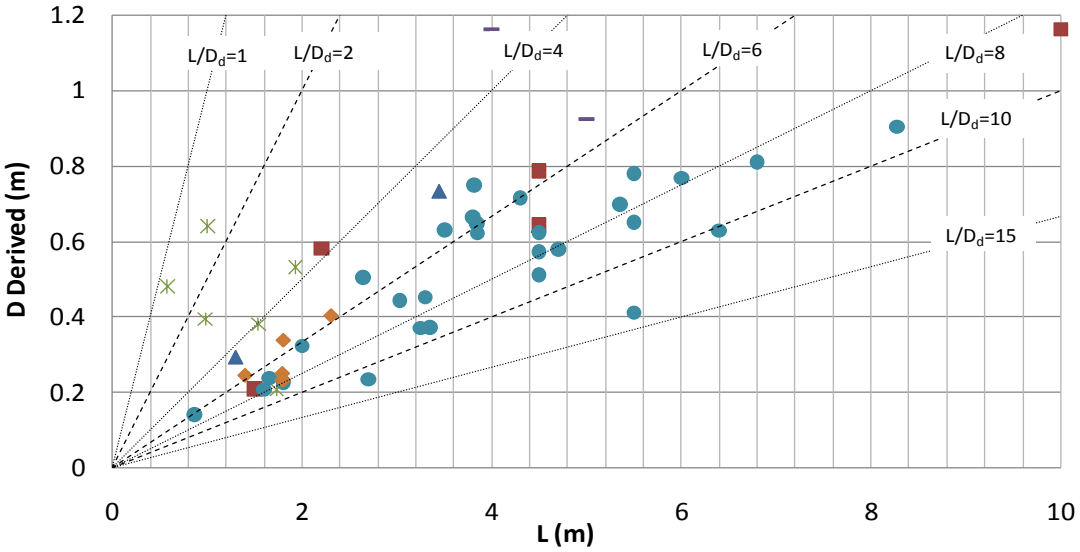

Figure 3: Length vs. D_d for AUVs; note that Triangle=Oblate; Square=Rectangular; Star=Space Frame; Short line=Tear drop; Circle=Torpedo; Kite=Torpedo+ gliderwing

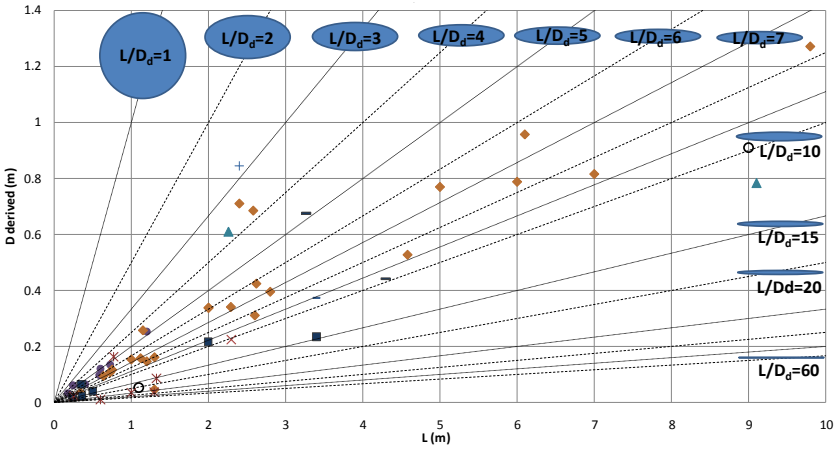

Figure 4: Length vs. D_d for marine animals; Circle=Short & deep; Triangle=Rayform; Kite=Fusiform; Short line=Elongated with oval cross-section (CS); Square= Elongated with compressed CS; Open circle= Elongated with circular CS; Star=Auguilliform (eel-like); Plus=Turtle; Cross=Squid

Speed and Agility

Figure 5 illustrates the absolute speed of marine animals with different modes of swimming while the two dashed lines represent the highest economic and maximum speed of all AUVs in the database. Figure 6 is the equivalent presentation in terms of relative speed; i.e. speed has been normalised in terms of Body Length per second (BL/s).

Comparing AUVs and animals the superior speed capability of marine animals is very significant. While the maximum economic speed of all AUVs is 2.5m/s and their maximum speed capability 4.12m/s marine animals can have optimum speeds more than 6m/s and with their maximum capability up to 35m/s. (Optimum speed is the speed at which the animal has lowest energy expenditure.)

When considering absolute speed, thunniform swimmers (in which only less than 1/3 of the body is involved in the swimming and propulsion power is mainly produced by oscillation of the rear fin) have the highest values. Both in terms of their maximum capability (the highest point) and also their optimum speed, indicated as the lowest point or the start of the line on the figure. Fast swimmers have generally fusiform body shapes with circular or oval cross-section; however some animals with elongated body forms and compressed cross sections that have thunniform swimming mode are amongst highest burst speed swimmers (e.g. Sailfish). As for marine mammals, undulatory swimming is superior to oscillation (flapping) of side flippers as performed by stellar sea lions.

However, when comparing relative speed (BL/s), some relatively smaller marine animals which have subcarangiform or carangiform swimming mode (which are similar to thunniform in terms of caudal fin (rear fin) oscillation but a larger proportion of the body contributes to the oscillation of the tail and the muscle distribution is different as well) such as Atlantic Mackerel, have superior capability, although their U_{opt} (speed with lowest energy expenditure) is much less (e.g. for the Mackerel, maximum relative speed is 26.15 BL/s while the optimum is only 5.05 BL/s). AUVs capabilities are very low compared to animals; the highest relative economic speed is 0.96 BL/s with the highest maximum speed not exceeding 2.06 BL/s.

The Reynolds number (Re) in which the animal swims should also be considered; e.g. Atlantic Mackerel has a Re range of 7.69×10^5 to 3.98×10^6 while sailfish swims in Re up to1.14×10^8. As for AUVs, when considering U_{opt} , they have a Re range of $2.8 \times 10^5 < \mathrm{Re} < 2.1 \times 10^7$with Hammerhead AUV which has the highest economic speed has a $\mathrm{Re} < 7.1 \times 10^6$.

As discussed in the previous section the relatively high fineness ratios of animals compared to AUVs, may to some extent explain the high propulsion speed evident in nature. It is also realised that when analysing burst speeds, lift base swimmers especially penguins as well as thunniform swimmers with high speed capability have higher FR; however this does not comply to other forms of swimming and it can be concluded that propulsion capability is the dominant factor affecting speed capability. However, fast swimmers (U> 5 BL/s) have a fineness range of 4< FR <15.

Legend for Figure 5 & 6
1100_BCFAnguilliform,
1200_BCFSUbcarangiform,
1300_BCFCarangiform,
1400_BCFThunniform,
1500_BCFOstraciiform,
2111_OMPLabriform,
2112_OMPFLiftbaseFlapping,
2300_UMPFGymnotiform,
2400_UMPFBalastiform,
3000_JetForm

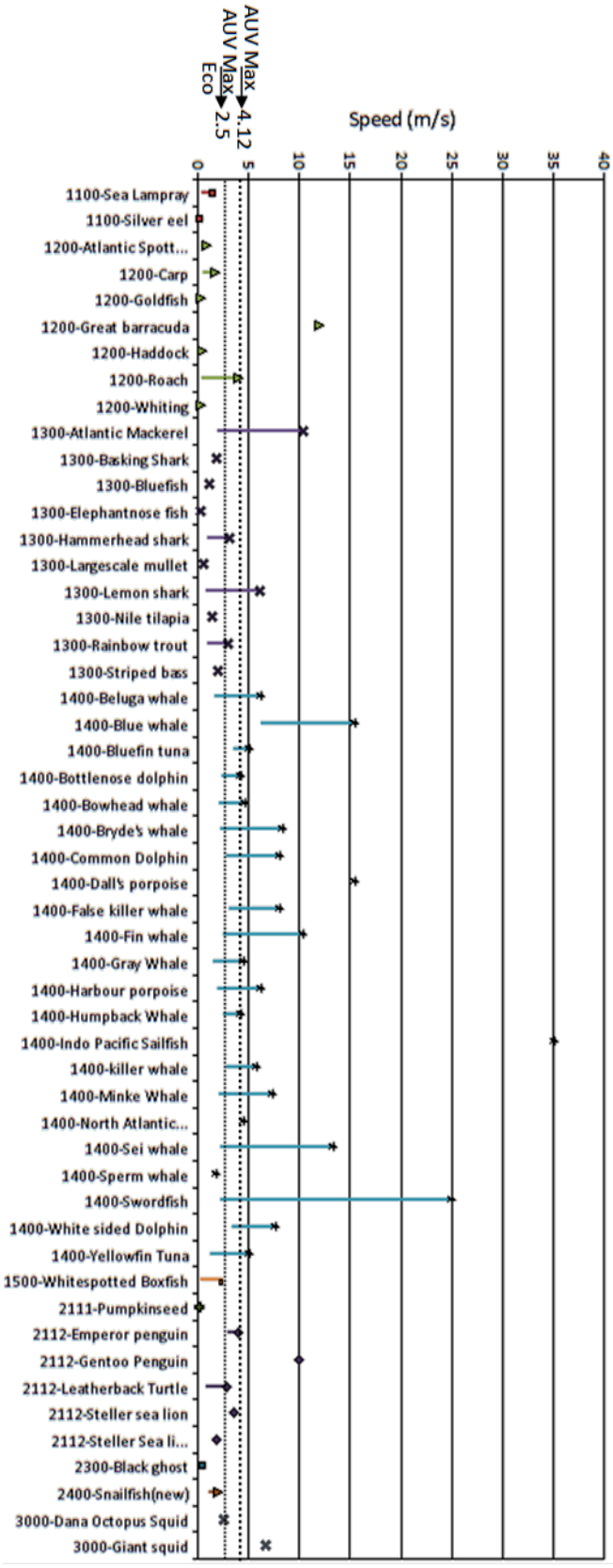

Figure 5: Absolute speed capability

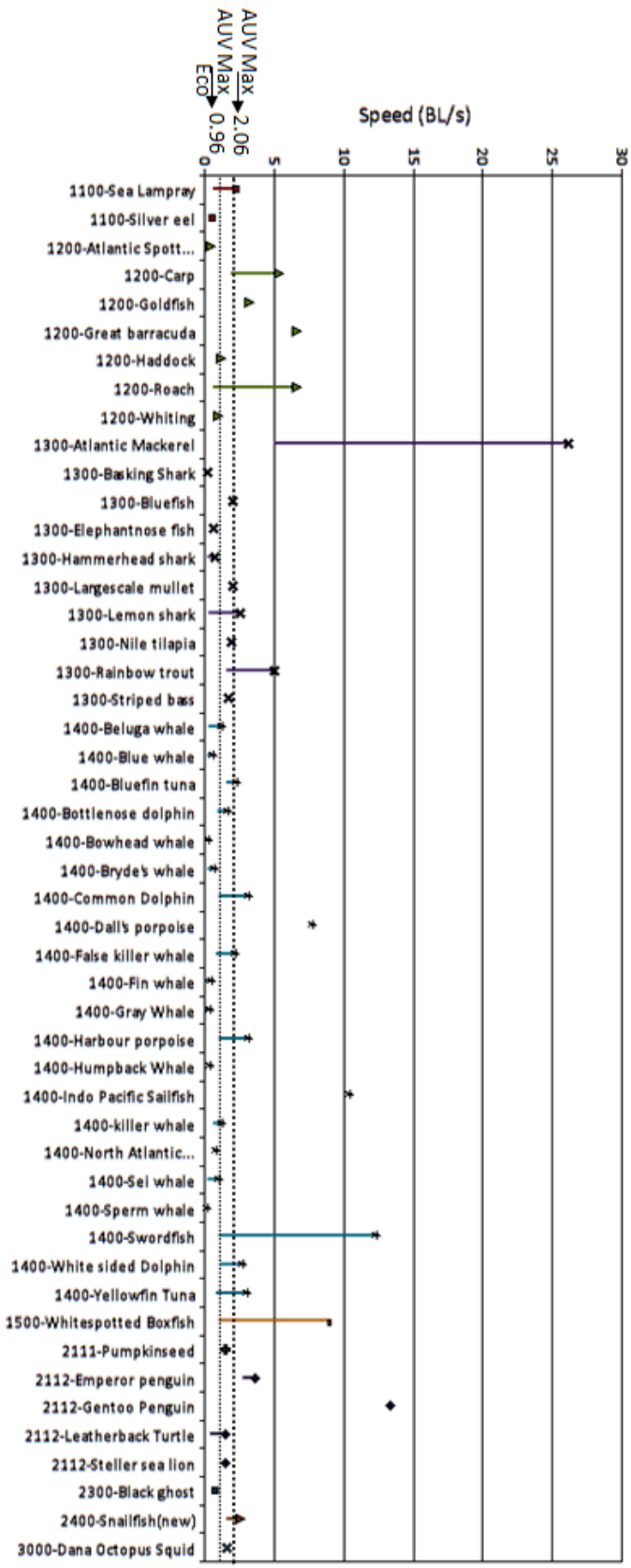

Figure 6: BL/s speed capability

(Legend explained on previous page)

Depth Capabilities

For marine animals, one of the factors affecting their ability to exist at depth or to migrate through a depth range is their buoyancy control mechanism. As indicated by Pelster, 2009, marine animals have various buoyancy control systems; these include: gas bladders (used by many fish usually living in shallow water), lipid bladders (e.g. in mid and deep-water fish such as myctophids and orange roughy), lipid in the liver (e.g. in sharks), hydrodynamic lift (e.g. marine mammals; however they also use the air in their lungs and possibly the change in the density of the lipid above their heads). Turtles adjust the depth (in which they are neutrally buoyant) with the remaining air in their lungs. And finally, penguins remain positively buoyant, therefore they have a passive gliding surfacing; this also applies to Right whales which are positively buoyant. Figure 7 is an indication of depth range per unit mass; so the results are based on a trade off between absolute depth capability and mass (an indication of size). The figure shows that deep-water especially mid-water fish (e.g. the largest values belong to pacific viper fish (ΔD =4365m), mid-water eel pout (ΔD=2100m) and Sea Lampray (ΔD=2200m) which has a swim bladder) have the best depth range/mass capability with most of the mammals and sharks having the lowest capability, however, other than physical limits, motivation or "mission" of the animal is another key reason for deep or shallow diving; i.e. species do not always dive to their maximum capability. AUVs in Figure 7, are clustered within the same range of small marine mammals, which have superior relative depth range over larger animals, however much less capable compared to most of fish.

Figures 8 and 9 show the absolute depth capability of AUVs and MAs; it is realised that AUVs can already reach great depths and while there are many deep living animals, this does not indicate that they are always deep divers or that they can travel all the way up to the surface. The data suggest that AUVs perform with similar capability to marine animals with the same mass; however, it is interesting that many marine animals including many fish and some penguins can reach higher relative depth range with less mass; therefore further study is required to clarify the mechanism of this behaviour and possible bio-inspired techniques. As well as different buoyancy control systems, deep-water fish have soft bodies and low $\frac{M}{BL}$ ratio compared to shallow water fish and air-breathing animals.

Fish exist at the greatest depths and are found at the widest depth range. Interestingly, some species belonging to the same family (therefore closely genetically related) have significantly different depth capabilities. The two most significant examples are snailfish and cusk eel; although most of the cusk eels have depth ranges not more than 600 meters, deep sea cusk eel swims in depth of 3110 to 8370 meters. And a recently discovered type of snailfish has been found in the deepest depths of ocean trenches over 7500m (National Geographic, 2010), while Agonopsis chiloensis which is also a snailfish cannot swim deeper than 400 meters.

Marine mammals are the deepest air-breathing divers; they achieve their desired depth with less energetic cost compared to when they are forward swimming. This is achieved by shutting down their unused systems, reducing their heart rate and more important by gliding instead of swimming; in dives deeper than 300m, gliding is performed 60-95% of the total dive; this reduces their cost of diving to a great extent. (Williams et al, 2000)

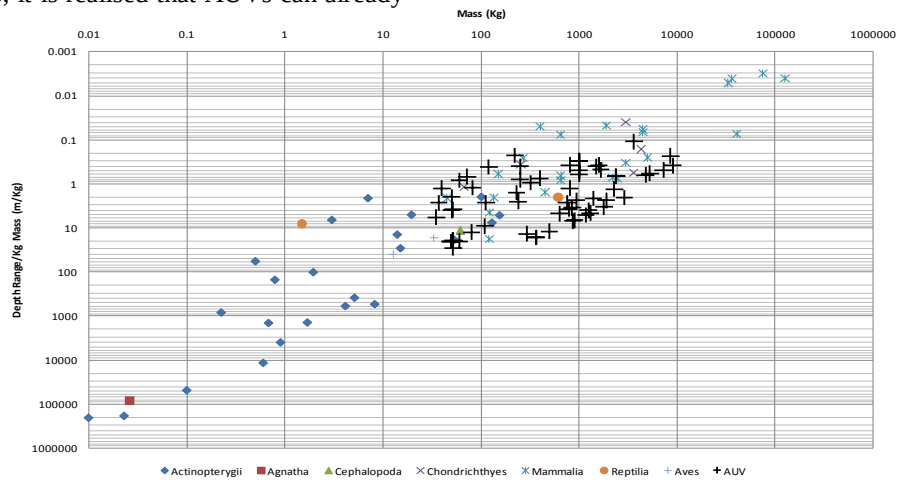

Figure 7: Depth range as a function of mass (Log-Log graph) comparison of Marine Animals and AUVs (shown with crosses) – Graph excludes species seen in one depth and therefore have no depth range

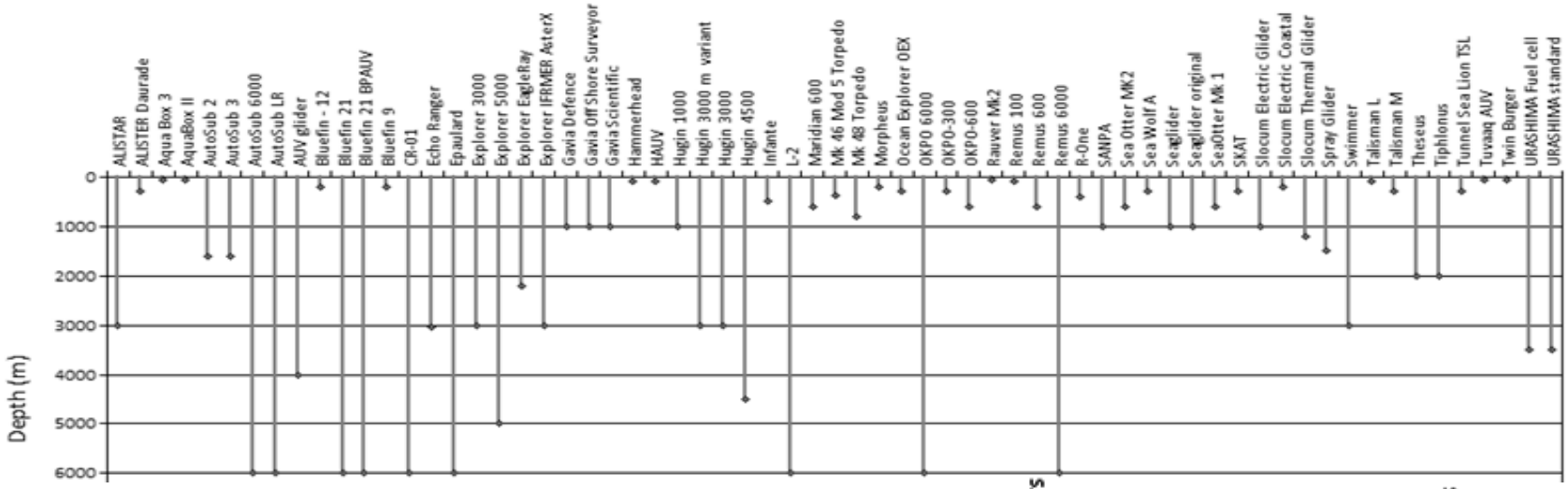

Figure 8: Depth capability of AUVs

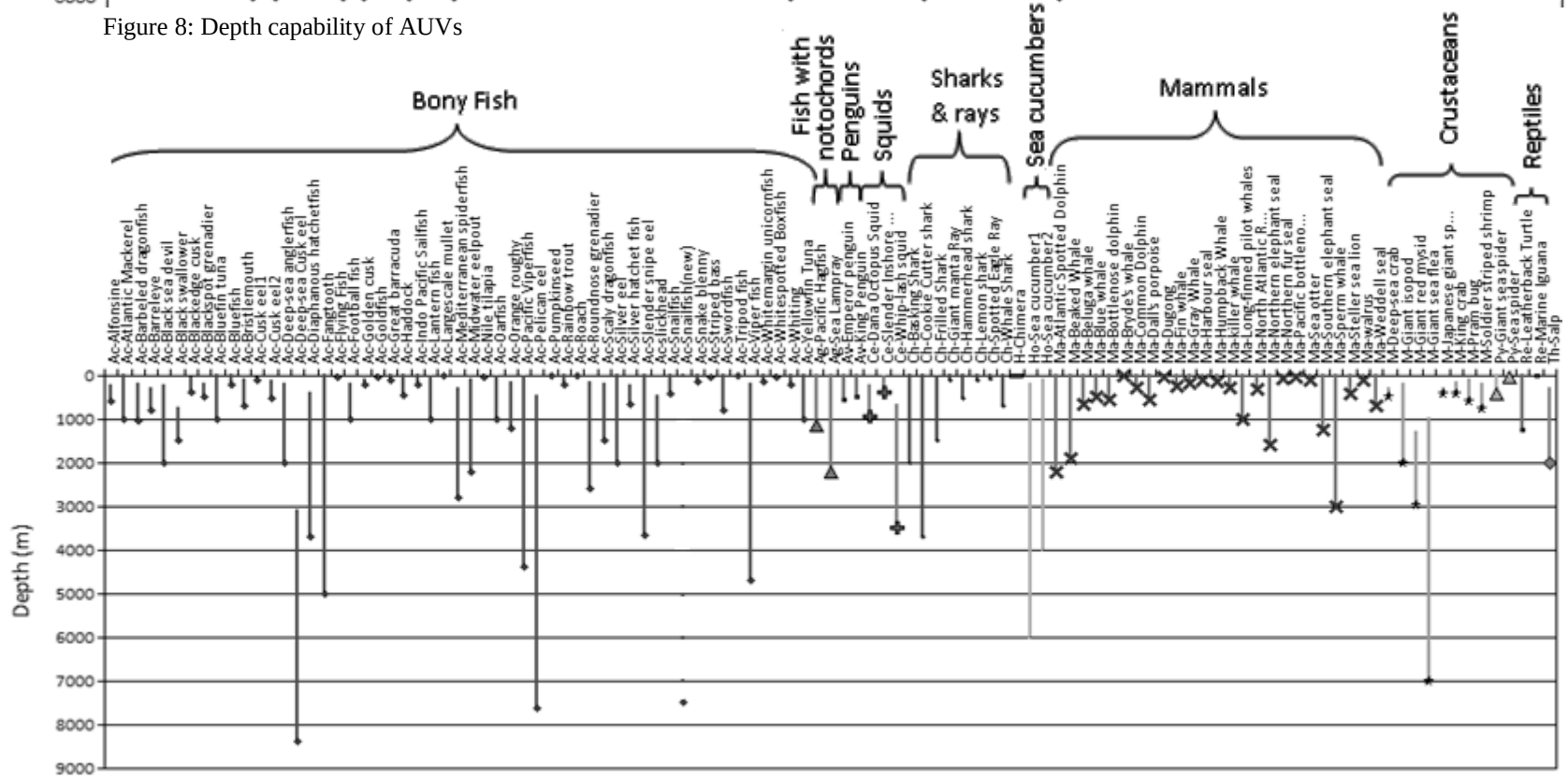

Figure 9: Depth capability of MAs

Manoeuvrability

One of the parameters to be considered as a manoeuvrability measure of a vehicle is the radius of turning when changing directions, which is especially important in high speeds or when the vehicle mission is to chase and observe a marine animal.

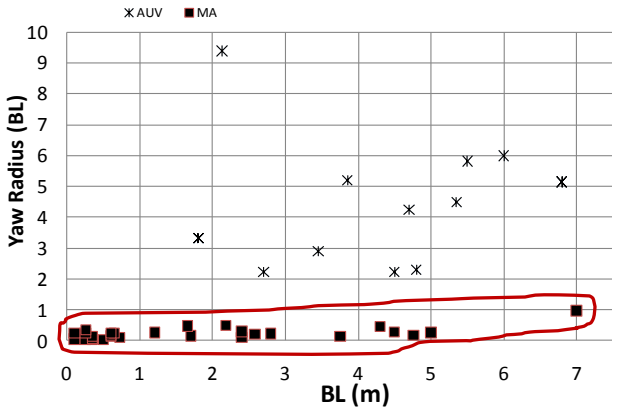

Figure 10: Yaw radius (R_{Yaw}) or turning radius per unit length of AUVs and MA

As the ring in Figure 10 encompassing the marine animal data highlights, AUVs have very large R_{Yaw} in comparison with marine animals; this makes them less manoeuvrable. High manoeuvrability is achieved by multi joint flexible bodies, so that as shown in Figure 11, flexible bodies such as black ghost and elephantnose fish have R_{Yaw} <0.05BL while for fast swimming fish with more rigid bodies such as tunas R_{Yaw} >0.45BL which is even more than some marine mammals and sharks. Figure 11 shows the turning data in Figure 10, in range consistent with the most of the data within the ring.

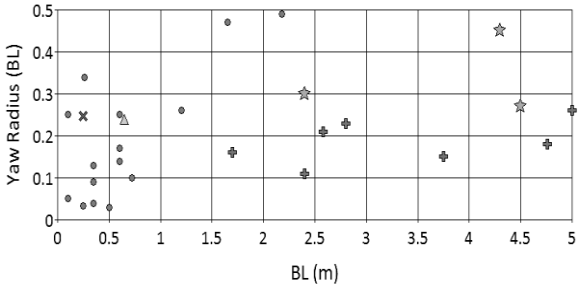

Figure 11: R_{Yaw} for various classes of MAs; Circle=Fish, Plus=Shark, Star=Mammal, Cross=Turtle, Triangle=Penguin

For clarity, two species with large R_{Yaw} are not included in this figure; Basking shark (BL=7m, R_{Yaw} =0.97BL) and Humpback whale (BL=15.2m, R_{Yaw}=0.82BL) which is a slow swimmer.

Energetics

Energetics can be investigated as Cost of transport (COT), or as energy storage capability which relates to endurance.

Considering COT; this is a measure of energy expenditure required to swim at a given speed. It is measured as Joules per metre kilogram body mass $\left(\frac{J}{kg \times m}\right)$. For marine animals, it is derived by measuring the oxygen consumption rate of the animals swimming at a given speed and converting O_2 consumption to produced energy by using the oxy-calorific value of oxygen (13.59 kJ/mg_{O2}, Elliott and Davison (1975)). Figure 12 shows that AUV are clustered within a small speed range but within this range, they have lower COT compared to many of the marine animals. This however excludes larger marine animals such as whales which indicates that larger the animal size, lower the mass specific COT.

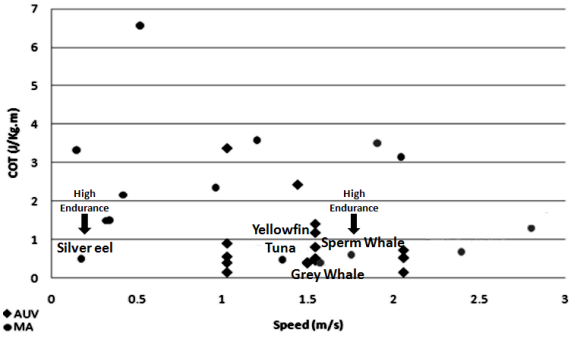

Figure 12: COT comparison of AUVs and MAs

Although, illustrating the COT at optimum speed (as presented in Figure 12) is beneficial for AUVs vs. MAs comparison, however, animals do not always operate at their optimum speed. Due to their high speed range capability, COT for animals, unlike AUVs, is a curve. This subject has been extensively studied and calculations carried out to produce the COT curve for different marine animals in various speed and Re ranges in Phillips et al, 2011; therefore, complete details are not provide in this paper.

Figure 13 illustrates the COT for MAs over various speed ranges; it is realised that COT on its own is not a complete measure of the energy expenditure of a species, speed range should also be considered; e.g. killer whale has a high COT when compared with fish at speeds less than 1m/s however its optimum speed is more than 2.5m/s, at which it has COT even less than a sturgeon. In addition the operation range of a killer whale is $3 \times 10^6 < Re < 2 \times 10^7$ which is the highest between the compared animals.

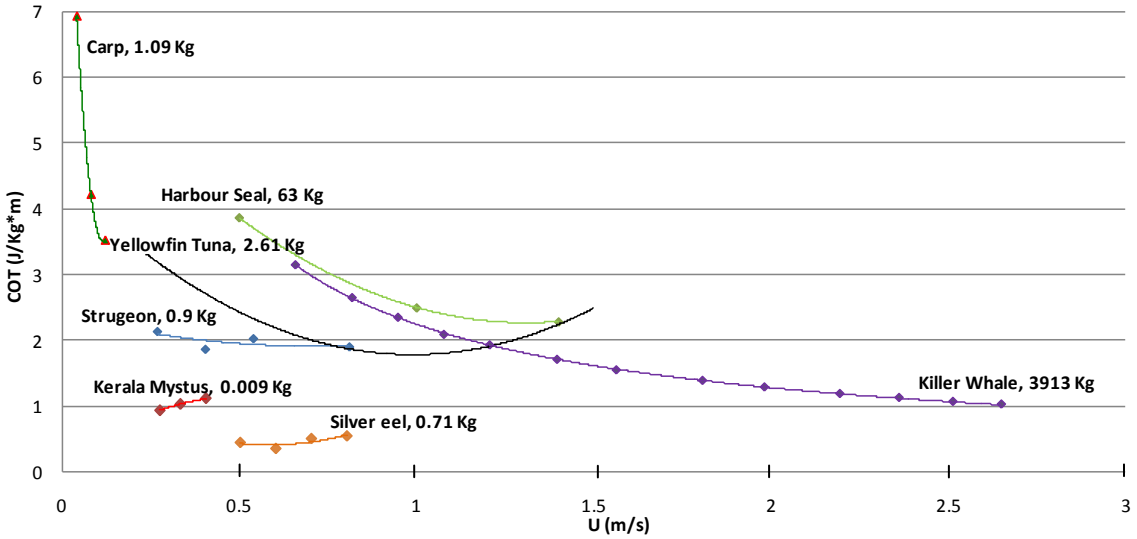

Figure 13: Total COT of various marine animals tested in a speed range. Calculated from data in Davis et al. (1985); Dewar and Graham (1994); Williams and Noren (2009); Froese and Pauly (2011). (Figure copied from Phillips et al, 2011)

Endurance: Endurance refers to the time an animal can continue living normally without feeding and where there is data available, it is provided in analogy with power reserves of AUVs. So this is an indication of energy storage capability. Energy is stored in animals in the form of lipids and fatty acids and consumed when food is not readily available. The fat and sugar reserves of a fish represent its equivalent 'battery' capacity and provide a measure of autonomy when combined with known COT and optimum speed values.

As part of this research, specific calorific value testing of the blubber of two marine mammals was conducted in a laboratory experiment; the result show specific energy of more than 30 MJ/Kg for the blubbers; this value compared to batteries such as Lithium Polymer or Nickel Metal hydride with less than 0.5 MJ/Kg (Huggins, 2010)) highlights that marine animals consume a high quality fuel. (Phillips et al, 2011).

Endurance (h) of several marine animals (light circle) and AUVs (dark circle) are shown in Figure 15, in which the size of the circle is an indication of COT value. The graph shows a significant high endurance within marine animals compared to AUVs. Sperm whale with the highest endurance (5000 Km) and other marine mammals that are long migrators, have large energy storage as blubber which is consumed during long migrations; therefore size is important for these animals in order to store the required energy content. However silver eels also use their stored energy during migration but they have a very low COT which reduces the amount of energy usage and where possible, they use the water current instead of swimming to go forward.

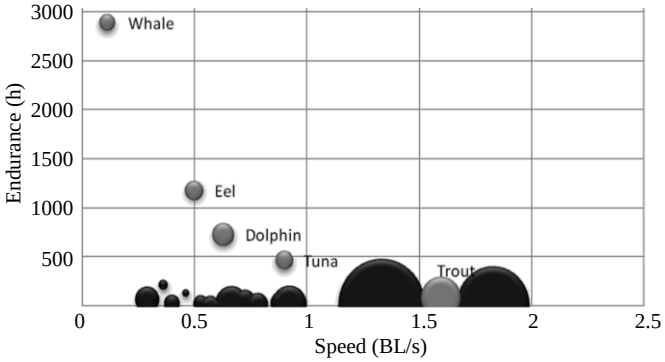

Figure 15: Endurance as a function of relative speed for MAs (light circles) and AUVs (dark circles)

OPTIMUM SYSTEM SELECTION

After comparing the capabilities of biological and engineering systems, it is realised that there are systems in certain species, or a group of species exist that under certain circumstances exhibit superior to AUVs in one or more of the studied capability (i.e. speed, depth, etc.); this are usually achieved by various approaches. However, in some cases, given the scarcity of the available data and the ambiguity of the data, the challenge is how to take the data on MAs and use it to improve AUVs. Bearing in mind the aim of this research is not to make a robotic fish, but to take good bits, and use them constructively for engineering purpose. For optimum and multi dimensional use of the available data and various biological systems, an algorithm is being developed in order to highlight optimum performing system,

systems or species. This is by giving the user the ability to set limits for optimum and maximum speeds, depth of operation, turning radius as well as body size and COT. In addition, it also provides the feature of weighting the importance of each criterion based on the intended mission profile. (Figure 16 shows an example of user input values)

Uopt (m/s)		Umax (m/s)		Depth (m)		Yaw R (x BL)		Length (m)		Weight (Kg)	
Min	Max	Min	Max	Min	Max	Min	Max	Min	Max	Min	Max
0.05	21	0.1495	41.2	12	8370	0.03	4.69	0.055	33.53	0.01	6E+05
	6.20		16.00						11.00		
OK	OK	OK	OK	OK	OK	OK	OK	OK	OK	OK	OK
IMPORTANCE											
1		1		1		1					
Percentage											
25.0		25.0		25.0		25.0					

Figure 16: The limits that user may alter and their weight (Importance)

As a result marine animals and AUVs closest to the chosen mission profiles or circumstances are highlighted (e.g. in Figure 17) and a detailed list, illustrates the collaboration of each criterion to the overall rating for the animal. This gives a more precise understanding of the overall performance of each system while pointing out the geometry as well.

%	Name	Uopt	Umax	Depth-m	BL-m	W-Kg	YawR-L	Δdepth
59	killer whale	2.8	15.4	260	9.8	8500	0.41	260
48	Bluefin tuna	3.6	5	1000	4.5	1197	0.49	N/A
42	Beluga whale	1.75	6.13	647	5	1590	0.26	647
41	Bottlenose dolphin	2.394	4.1	535	3.8	650	0.32	535
39	Yellowfin Tuna	1.35	5	1000	2.39	253	0.47	N/A
36	Lemon shark	0.85	6.1	92	3.4	254	0.3	92
36	Baskin Shark	1.8	1.8	2000	9	3600	0.97	N/A
35	Striped bass	2.04	2.04	N/A	2	100	0.26	N/A
33	Rainbow trout	0.96	3	200	1.2	13.9	0.17	200
33	Hammerhead shark	0.94	3.1	512	4.3	450	0.45	N/A

Figures 17: Example of 10 best matches of MA with the same given criteria as above (the best match in this case is 59% of what required)

CONCLUSION

In this paper various characteristics of AUVs and marine animals have been compared to highlight the relative superiority and limitations of biological and engineering systems. The comparisons mainly highlight that:

- In terms of body forms, marine animals have significantly higher fineness ratios compared to AUVs while most of the high speed animals have a fineness ratio range of 4< FR <15.
- Thunniform swimming is used for fast swimming by both fish and marine mammals, however smaller fish with carangiform swimming and some types of penguins with flapping swimming mode have high BL/s Speed.
- Although, AUVs are relatively capable at deep diving, many fish can reach deeper depths with less mass, therefore further research may clarify the reason by which they achieve this. One lesson to be learned from marine animals, especially marine mammals is to reduce the energy expenditure during diving by configuring the control surfaces for maximum gliding capability instead of swimming.
- In terms of manoeuvrability, the significant superior turning performance of marine animals is evident; this is achieved by their multi joint flexible bodies.
- Energetics is the most interrelated comparable characteristic between the two groups. It can be measured by COT (energy consumption during swimming) or by endurance. The comparison shows that, although compared to many marine animals, AUVs have less COT when swimming at their economic speed, however their speed range is very limited.

Many characteristics have been studied in this paper, which all seem significant with different importance, in order to accomplish a defined mission. Therefore an optimum selection means has being developed to collect all of these criteria together for a better overall comparison.

The comparisons show that optimisation is required and necessary; bio inspiration is a different approach because even the traditional AUV designs are to some extent inspired by nature; however, in most cases the inspiration has only been a first start (idea) but maybe the importance of nature has not always been appreciated and the analysis not been pursued as profound as it should have been.

REFERENCES

APPELTANS, W., BOUCHET, P., BOXSHALL, G. A., FAUCHALD, K., GORDON, D. P., HOEKSEMA, B. W., POORE, G. C. B. , VAN SOEST, R. W. M., STÖHR, S., WALTER, T. C., COSTELLO, M. J. (eds.) (2010). World Register of Marine Species. Accessed at http://www.marinespecies.org on 2010.01.01

AUVAC (2010). "Autonomous Undersea Vehicle Applications Centre". URL: "www.AUVAC.org".

BLIDBERG, D. R. (2001) "The Development of Autonomous Underwater Vehicles (AUV); A Brief Summary", International Conference on Robotics and Automation (ICRA). Seoul, Korea, May 2001. pp.

DAVIS, R. W., WILLIAMS, T. M. & KOOYMAN, G. L. (1985). "Swimming metabolism of yearling

and adult harbor seals Phoca vitulina". Physiological Zoology, 58, 590-596.

DEWAR, H. & GRAHAM, J. B. (1994) "Studies of tropical tuna swimming performance in a large water tunnel". I. Energetics. Journal of Experimental Biology, 192, 13-31.

ELLIOTT, J. M. & DAVISON, W. (1975) "Energy equivalents of oxygen consumption in animal energetics Oecologia", 19, 195-201.

EPSRC (2009). "Engineering and Physical Science Research Council grants on the web. URL: http://gow.epsrc.ac.uk. [Accessed December 2009]

FISH, F. E. (1998). "Comparative kinematics and hydrodynamics of odontocete cetaceans: Morphological and ecological correlates with swimming performance". The Journal of Experimental Biology. 22-Sep-1998 ed., The Company of Biologists Limited.

FROESE, R. & PAULY, D. (2011) "FishBase: version (02/2011)", World Wide Web www.fishbase.org.

FUNNELL, C. Ed. (2007). "Jane's Underwater Technology 2006-2007", Ninth Edition, Surrey: Jane's Information Group.

HOELSEL, A. R. (2002). "Marine Mammal Biology; an evolutionary approach".

HUGGINS, R. A. (2010). "Energy Storage", Springer.

JEFFERSON, T. A., LEATHERWOOD, S. & WEBBER, M. A. (1993). "FAO Species Identification Guide; Marine mammals of the world". In Department, F. A. A. (Ed.).

KERMORGANT, H. & SCOURZIC, D. (2005). "Interrelated functional topics concerning autonomy related issues in the context of autonomous inspection of underwater structures", Proc. IEEE Oceans 2005.

MADIN, L. (2005). "Discovering life and sustaining habitats". Oceanus, Ocean life institute, Woods Hole Oceanographic Institution.

NATIONAL GEOGRAPHIC, (2010). "Ghost of the Deep".URL:http://news.nationalgeographic.com/news/2010/10/photogalleries/101014-deep-fish-seen-snailfish-eel-ocean-pictures. [Accessed January 2011]

NEMO, (2011). "Nature in Engineering for Monitoring the Oceans". Accessed at: http://www.sesnet.soton.ac.uk/NEMO/

PELSTER, B., (2009). "Buoyancy control in Aquatic Vertebrates". In: Cardio-Respiratory Control in Vertebrates: Comparative and Evolutionary Aspects". GLASS, M. L. AND WOOD, S. C. Springer Dordrecht Heidelberg London New York. ISBN: 978-3-540-93984-9

PHILLIPS, A. B., HAROUTUNIAN, M., MAN, S. K., MURPHY, A. J., BOYD, S. W., BLAKE, J. I. R. & GRIFFITHS, G. (2011). "Nature in Engineering for Monitoring the Oceans: Comparison of the energetic costs of marine animals and AUVs". In SUTTON, R. and ROBERTS, G. (eds.) Recent Advances in Unmanned Marine Vehicles. The Institution of Engineering and Technology (IET). (In press)

RIVERA, G., RIVERA, A. R. V., DOUGHERTY, E. E. & BLOB, R. W. (2006). "Aquatic turning performance of painted turtles (Chrysemys picta) and functional consequences of a rigid body design". The Journal of Experimental Biology, 209, 4203-4213.

THAINDIAN NEWS, (2009). "Britain's deepest diving autonomous underwater vehicle completes trail run successfully". URL: www.thaindian.com. [Accessed February 2010]

THILLART, G. V. D., PALSTRA, A. & GINNEKEN, V. V. (2007). "Simulated migration of European silver eel; swim capacity and cost of transport". Journal of Marine Science and Technology, 1-16.

VINCENT J. F. V. (2001). "Stealing ideas from nature". In Deployable Structures (ed. S Pellegrino), Springer-Verlag, Vienna, pp. 51-58

WILLIAMS, T. M., DAVIS, R. W., FUIMAN, A., FRANCIS, J., BOEUF, B. J. L., HORNING, M., CALAMBOKIDIS, J. & CROLL, D. A. (2000). "Sink or Swim: Strategies for Cost-Efficient Diving by Marine Mammals". Science magazine, 288, 133-136.

WILLIAMS, R. & NOREN, D. P. (2009) "Swimming speed, respiration rate, and estimated cost of transport in adult killer whales". Marine Mammal Science, 25, 327-350.

Appendix 2.2. Nature in Engineering for Monitoring the Oceans: Comparison of the energetic costs of marine animals and AUVs

Phillips, A. B., Haroutunian, M., MAN, S. K., Murphy, A. J., Boyd, S. W., Blake, J. I. R. & Griffiths, G. (2012). "Nature in Engineering for Monitoring the Oceans: Comparison of the energetic costs of marine animals and AUVs". In: Sutton, R. and Roberts, G. (Ed.) Further Advances in Unmanned Marine Vehicles. The Institution of Engineering and Technology (IET). ISBN: 978-1-84919-479-2

(An actual copy from the Book is presented in this thesis)

Chapter 17

Nature in engineering for monitoring the oceans: comparison of the energetic costs of marine animals and AUVs

A.B. Phillips[1], *M. Haroutunian*[2], *S.K. Man*[1], *A.J. Murphy*[2], *S.W. Boyd*[1], *J.I.R. Blake*[1] *and G. Griffiths*[3]

17.1 Introduction

Three billion years of evolution has led to numerous methods of marine animal propulsion adapted to movement in three dimensions. The term swimming encompasses the movement of marine mammals and fish, the motions of cephalopods and medusae and the slow diurnal vertical migration of zooplankton. Swimming performance is considered a main trait in determining fitness in many aquatic animals (Plaut, 2001). Swimming is the only alternative for most aquatic animals to find food, escape predators and successfully reproduce (Videler, 1993). Averaged over a period, the amount of energy acquired by an individual through feeding must exceed the amount of energy expended by daily activities, growth and reproduction. Based on optimal foraging theory, natural selection should operate to maximize the ratio of energy income to energy expenditure (Townsend and Winfield, 1985).

Underwater vehicles operate in the same environment, often in a similar manner to their natural counterparts. One of the first recorded designs for an underwater vehicle was detailed by William Bourne in 1578 (Bourne, 1578; Stefoff, 2006). Four hundred and fifty years of development has led to a range of vehicles encompassing large nuclear submarines, smaller manned submarines, remotely operated vehicles (ROVs) and autonomous underwater vehicles (AUVs). As complex mechatronic artefacts, there are a myriad of sub-systems within AUVs that could be amenable to bio-inspired design including, among others, sonar waveforms and signal processing based on marine mammal vocalization (Reijniers and Peremans, 2007); bio-inspired swarm intelligence algorithms, for example, for autonomous networking (Dressler, 2005); bio-inspired energy sources (e.g. microbial 'fuel cells' coupled to artificial muscle) (Anderson *et al.*, 2011).

[1]University of Southampton, Southampton, UK
[2]Newcastle University, Newcastle, UK
[3]National Oceanography Centre, University of Southampton Waterfront Campus, Southampton, UK

However, care needs to be taken when looking for inspiration from biological systems to understand that:

1. the biological system is optimized for the applications of interest, for example many physiological adaptations are due to attracting a mate or other reasons, which may not be the desired outcome, and
2. inspiration should be sought from biological systems that are more efficient than their engineered equivalent.

There appears to be a view in much of the literature that marine animals are energetically more efficient than engineered systems (Zhou *et al.*, 2007; Gao *et al.*, 2009). The data presented in this chapter contradict this argument. In part, this misconception may be due to the outcomes, in isolation, of studies on drag reduction through bio-mimicry (e.g. Anthony *et al.*, 2000; Fish, 2006) or to studies showing high *propulsive* efficiencies for marine animal and bio-inspired propulsors (e.g. Bose and Lien, 1989; Fish, 1993, 1996; Anderson *et al.*, 1998). For ships the propulsive efficiency is conventionally defined as the ratio of useful power obtained overcoming resistance at a certain speed to the power delivered to the propeller shaft where torque may be directly measured, as such it incorporates loses in the wake, thrust deduction and loses in the shaft (typically of the order of 1%) (Comstock, 1977).

$$\eta_P = \frac{\text{Resistance} \times \text{Velocity}}{\text{Shaft Delivered Power}} \tag{17.1}$$

For marine animals the propulsive efficiency is typically inferred from among others: wake studies (Tytell and Lauder, 2004), Lighthill's elongated body theory (Lighthill, 1970; Weihs, 1989), strip theories (Bose and Lien, 1989) and blade element theories (Blake, 1979). As such it only considers losses in the wake.

$$\eta_P = \frac{\text{Thrust} \times \text{Velocity}}{\text{Mechanical Power Delivered}} \tag{17.2}$$

Both the above approaches neglect the energy lost converting chemical energy to mechanical energy. By concentrating only on one aspect of the vehicle/animal system, the overall questions of cost of transport and efficiency of energy consumption are rarely completely addressed. Figure 17.1 illustrates the flow of energy for both an AUV and a fasting, migratory silver eel, starting with potential chemical energy and ending with propulsion power, highlighting energy losses at each stage. This chapter uses a system approach to explain why many AUVs have a lower cost of transport than marine animals of similar size.

17.2 Cost of transport

Cost of transport (COT) is a normalized measure of the energy required to transport the animal's or vehicle's mass over a unit distance. The general formulation of cost of transport is given by:

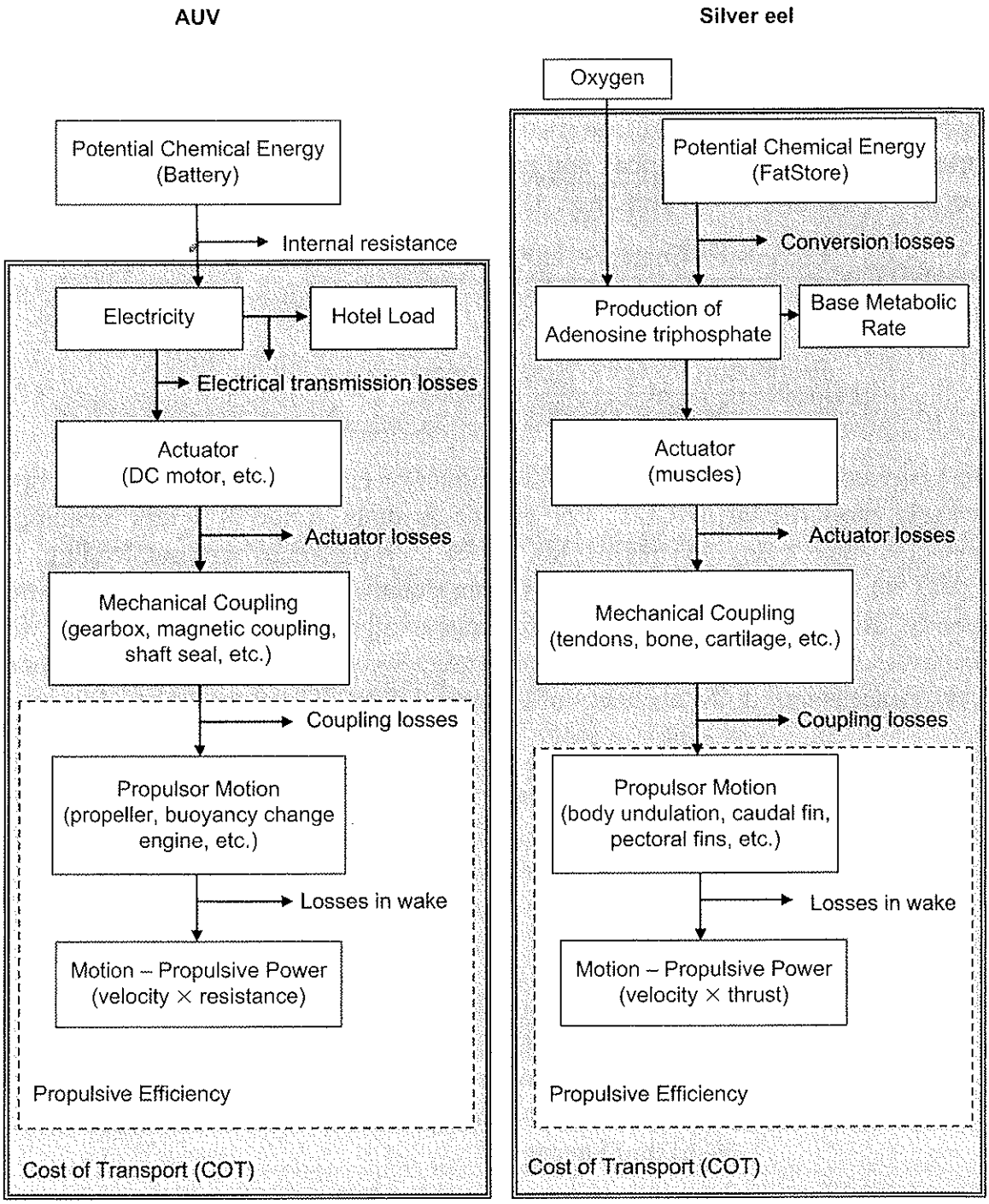

Figure 17.1 Diagrammatic comparison of the energy flow for an AUV (left) and a Silver eel (right). Silver eels provide a useful comparison with AUVs since they fast on their 5500 km migration to their spawning ground (van Ginneken and Maes, 2005)

$$\text{COT} = \frac{\text{Energy}}{\text{Mass} \times \text{Distance}} = \frac{\text{Power}}{\text{Mass} \times \text{Velocity}} \tag{17.3}$$

Cost of transport has units of J/kg/m or equivalently kJ/kg/km.

For both AUVs and marine animals, there is a base energetic cost to maintain a number of non-propulsion systems as well as energetic costs of propulsion.

For engineered systems, the base energetic cost is referred to as the hotel load and is associated with powering computers, hard drives and sensors.

The energetic costs of propulsion (swimming) are influenced by a variety of environmental factors, propulsion method (swimming modes) and associated efficiency as well as physiological and morphological characteristics of the vehicle (species) (Lighthill, 1969; Hammer, 1995; Allen *et al.*, 2000).

$$\text{COT} = \frac{\text{Propulsion Energy} + \text{Hotel Energy}}{\text{Mass} \times \text{Distance}}$$

$$= \frac{\text{Propulsion Power} + \text{Hotel Power}}{\text{Mass} \times \text{Velocity}} \tag{17.4}$$

Since conventional AUVs have a finite amount of energy stored onboard, range is inversely proportional to COT. For marine animals, range is a less meaningful parameter since many species do not travel long distances without feeding. For AUVs, the COT for each vehicle has been determined based on quoted battery capacity, displaced mass and maximum range available from manufacturer's websites, available literature or personal communications. As such there is an unknown level of uncertainty in the accuracy of the results for COT values deduced from:

$$\text{COT} = \frac{\text{Total Stored Energy}}{\text{Range} \times \text{Mass}} \tag{17.5}$$

In animals, the total energy used can be divided into the following components (Smith, 1976):

$$\begin{aligned}\text{Energy}_{\text{Total}} = {} & \text{Basal Metabolism} + \text{Thermoregulation (endotherms)} \\ & + \text{Voluntary Activity} + \text{Specific Dynamic} \\ & \quad \text{Action (heat produced by nutrient metabolism)} \\ & + \text{Growth of Fat and Sexual Products} + \text{Urine, Gill Excretion} \\ & \quad \text{(fish) and Faeces}\end{aligned}$$

Animals' basal metabolism (generally calculated from the base metabolic rate (BMR) for endothermic animals or standard metabolic rate (SMR) for ectothermic animals), referred to herein as BMR for simplicity), which is the equivalent of Hotel Load in AUVs, is the energy used to maintain essential organs and other life support systems and activities through base levels of respiration. For these measurements, animals should be resting, under no stress, and fasting so that energy is not expended for digestion.

Since direct measurement of energy consumption is not possible for marine animals, the amount of oxygen consumption (mg) is measured in order to calculate the energy expenditure. This is based on the fact that oxygen is consumed to burn fat and produce energy. To normalize the data and allow comparison with engineered systems, the following calculations have been performed:

$$\text{Power}_{\text{Total}}\ (\text{watts}) = \frac{\text{O}_2\,\text{Consumption at } 20^{\circ}\text{C}\left(\frac{\text{mg}}{\text{kg}\cdot\text{h}}\right) \times 13.59 \times \text{Mass (kg)}}{3600} \tag{17.6}$$

where 13.59 J/mg is the O_2 calorific value (Elliott and Davison, 1975).

$$\text{COT}\left(\frac{\text{J}}{\text{kg}\cdot\text{m}}\right) = \frac{\text{Power}_{\text{Total}}}{\text{Mass} \times \text{Speed}} \tag{17.7}$$

$$\text{Base Metabolic Rate (watts)} = \frac{\text{BMR}\left(\frac{\text{mg}}{\text{kg}\cdot\text{h}}\right) \times 13.59 \times \text{Mass (kg)}}{3600} \tag{17.8}$$

$$\text{Power}_{\text{Propulsion}} = \text{Power}_{\text{Total}} - \text{Base Metabolic Rate} \tag{17.9}$$

$$\text{COT}_{\text{Net}} = \text{COT}_{\text{Total}} - \frac{\text{Base Metabolic Rate}}{\text{Mass} \times \text{Speed}} \tag{17.10}$$

To allow direct comparison, the temperature of the tests is important. For endotherms, the temperature should be in their neutral thermal zone so that energy is not consumed to regulate body temperature (Casellini, 2008). For comparison, ectotherms should also be tested at the same temperature (because their BMR changes with temperature); if this is not possible, data gathered from different tests should be normalized to a unique temperature (data gathered from FishBase (Froese and Pauly, 2011) are normalized for 20°C). The normalized metabolic rate is calculated using the temperature coefficient (Q_{10}) (Winberg, 1971; Schmidt-Nielsen, 1997):

$$R_2 = R_1 \times \text{Q}_{10}^{\frac{T_2 - T_1}{10}} \tag{17.11}$$

where R_1 and R_2 are the rates of a chemical reaction at temperature one (T_1) and temperature two (T_2), respectively. Therefore, for our purpose this can be re-written as:

$$\text{O}_2\text{Consumption}_{T_2} = \text{O}_2\text{Consumption}_{T_1} \times \text{Q}_{10}^{\frac{T_2 - T_1}{10}} \tag{17.12}$$

It should be considered that generally animals are tested at the range of speeds at which they would voluntarily swim; therefore, the available data does not reflect the complete range of operation of each species.

Figure 17.2 illustrates an idealized COT plot. At low speeds the hotel load (BMR), which is invariant to forward speed, dominates, driving the COT to infinity at zero forward speed. At high speeds the propulsion power term dominates and the

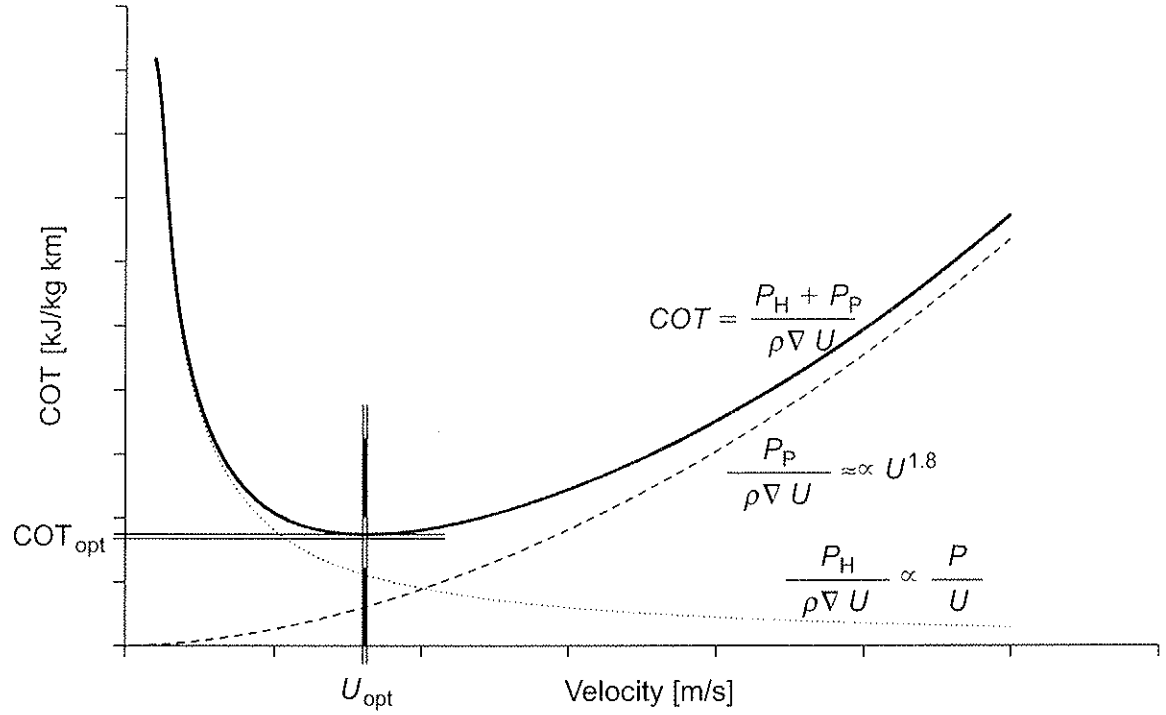

Figure 17.2 Idealized cost of transport curve, illustrating the propulsion power (P_P) and hotel power (P_H)

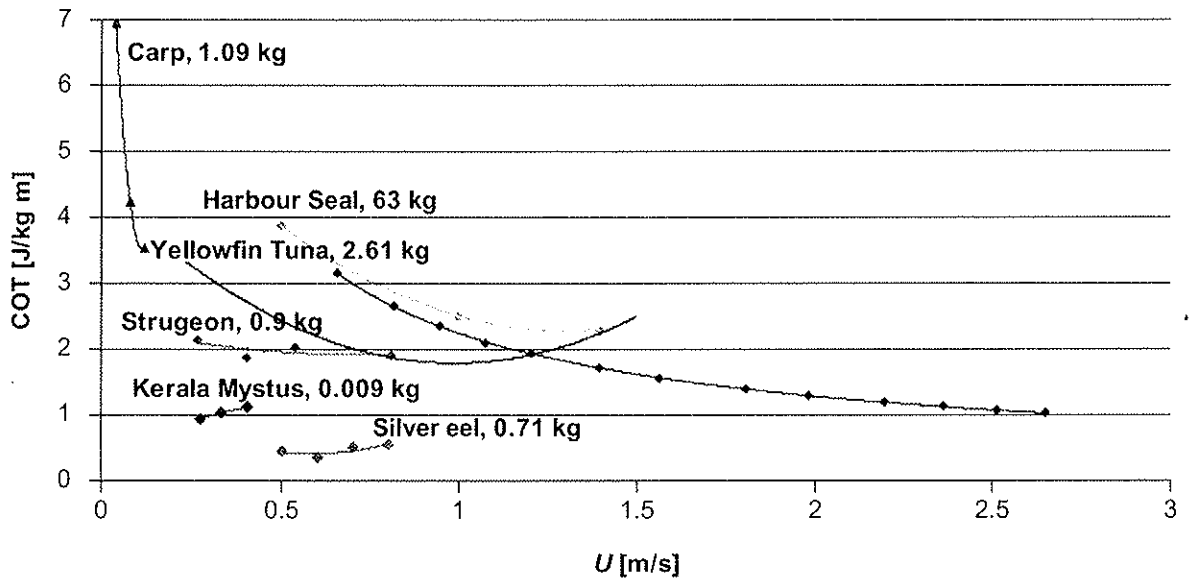

Figure 17.3 Total COT of various marine animals (Davis et al., 1985; Dewar and Graham, 1994; Williams and Noren, 2009; Froese and Pauly, 2011)

COT rises with increase in speed. Between these two extremes lies an optimum speed which corresponds to a minimum energetic cost per unit distance, U_{opt}. U_{opt} also corresponds to the speed with the longest associated range. COT_{opt} and U_{opt} are accepted values for comparing energetic costs of marine animals (Videler, 1993).

Figure 17.3 illustrates the significant variations in the COT experienced by many marine animals. Where there is sufficient data available over a large speed

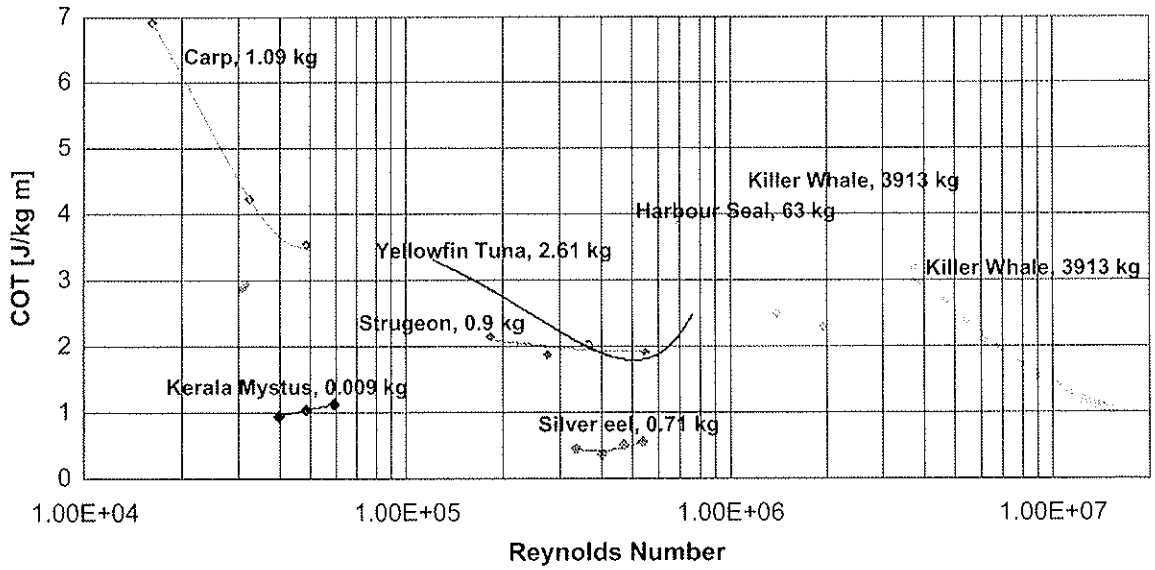

Figure 17.4 COT of various animals considering their Reynolds number (UL/v). Data taken from (Davis et al., 1985; Dewar and Graham, 1994; Williams and Noren, 2009; Froese and Pauly, 2011)

range, the mean curves exhibit the expected 'U' shape. The results show clear variation with respect to, for example, animal size, taxonomy, and endothermic or ectothermic animals. The causes of these variations are discussed in the following sections. One interesting result is that the silver eel has a COT substantially lower than animals of equivalent size (see Figure 17.3) or Reynolds number (see Figure 17.4).

To illustrate the influence that parameters such as size, speed and hotel load (BMR) have on the COT calculations, the simplified case of a self-propelled prolate spheroid is considered. It is important to note that while this discussion is presented using engineering terminology, the concepts discussed are equally applicable to marine animals. The prolate spheroid can be defined using two variables, the polar radius, b (or $L/2$), and the equatorial radius, a (or $D/2$), where L is the polar diameter and D is the equatorial diameter of the spheroid. The angular eccentricity of the spheroid, e_a, is calculated by taking the arccosine of the ratio of equatorial radius and polar radius.

$$e_a = \arccos(a/b) = \arccos(D/L) \tag{17.13}$$

The surface area is given by:

$$A = 2\pi\left(\left(\frac{D}{2}\right)^2 + \frac{D/2 \times L/2 \times e_a}{\sin e_a}\right) \tag{17.14}$$

The volume of a prolate spheroid is given by:

$$\nabla = \frac{1}{6}\pi D^2 L \tag{17.15}$$

Assuming neutral buoyancy in seawater of density ρ, the displaced mass of the system is given by:

$$\text{Mass} = \rho \frac{1}{6} \pi D^2 L \tag{17.16}$$

An estimate of the propulsive power is given by:

$$P_{\text{P}} = \frac{1}{2\eta_{\text{P}}\eta_{\text{a}}} C_{\text{D}} \rho A_W U^3 \tag{17.17}$$

where C_{D} is the drag coefficient, A_{w} is the wetted surface area, η_{p} is the propulsive efficiency, which is taken as the ratio of the effective power delivered by the propulsor compared to the power delivered to the propulsor by the 'shaft'. It accounts for hull efficiency, propulsor efficiency and the influence on the propulsor of operating behind a vessel. η_{a} is the actuator efficiency and represents the efficiency of transferring electrical energy into mechanical energy, and U is the spheroid's velocity. At first glance, it appears that the propulsion power requirement increases with velocity cubed. In practice both propulsive efficiency and drag coefficient are Reynolds number, and hence velocity dependent. For streamlined bodies experiencing laminar flow, the drag coefficient is proportional to $Re^{-0.5}$, and $Re^{-0.2}$ for turbulent flows (Alexander, 2005). Thus, for low Reynolds numbers ($Re < 100{,}000$), the propulsive power is proportional to $velocity^{2.5}$, and $velocity^{2.8}$ at turbulent Reynolds numbers.

The total drag acting on a submerged body away from the free surface is a combination of skin friction drag and pressure drag. For ships, it is normal to use the ITTC'57 correlation line to estimate the skin friction coefficient for a towed body (SNAME, 1957).

$$C_{\text{f}} = \frac{0.075}{(\log_{10}(Re) - 2)^2} \tag{17.18}$$

This formulation includes the influence of Reynolds number ($Re = UL/\nu$), which indicates the local flow regime, laminar flow leads to a rapid increase in the skin friction coefficient below a Reynolds number of 100,000. To estimate the pressure drag component it is normal practice for naval architects to use a form factor $(1 + k)$ as a multiplier on the frictional drag coefficient to estimate the total drag coefficient (Comstock, 1977), thus:

$$C_{\text{D}_{\text{h}}} = C_{\text{f}}(1 + k) \tag{17.19}$$

For a streamlined body the form factor can be estimated from (Hoerner, 1965):

$$(1 + k) = 1 + 1.5\left(\frac{D}{L}\right)^{3/2} + 7\left(\frac{D}{L}\right)^3 \tag{17.20}$$

Such an approach provides a fair estimate of the naked hull resistance of typical torpedo style AUVs (Phillips *et al.*, 2007). To make allowance for the drag

of control surfaces and other appendages, the bare hull drag is increased by 20%. The total COT may thus be estimated from:

$$\mathrm{COT} = \frac{1.2/(2\eta_p\eta_a)\frac{0.075}{(\log_{10}(UL/\upsilon)-2)^2}\left[1+1.5\left(\frac{D}{L}\right)^{3/2}+7\left(\frac{D}{L}\right)^3\right]\rho 2\pi\left((D/2)^2+\frac{DLe_a}{4\sin e_a}\right)U^3+P_H}{\rho\frac{2}{6}\pi D^2 L\times U} \tag{17.21}$$

where $e_a = \arccos(D/L)$

Hence,

$$\mathrm{COT} = f\left(L, \frac{L}{D}, U, P_H, \eta_p, \eta_a, \upsilon, \rho\right) \tag{17.22}$$

The density and kinematic viscosity are properties of the surrounding fluid rather than the AUV or marine animal. The influence of the remaining six parameters is illustrated in Figure 17.5.

Since drag is proportional to volume to the power two-thirds, increasing vehicle size reduces the propulsion power requirements per unit mass and hence the cost of transport drops, and so does the associated U_{opt}. At low speeds ($U < U_{opt}$), the COT is highly sensitive to hotel load. The magnitude of COT_{opt} is also highly sensitive to hotel load. As the hotel load tends to zero so does the magnitude of COT_{opt}. A hotel load of zero will result in $U_{opt} = 0$; clearly this is not a practical transit speed. Thus, the operator will have to make a compromise between selecting a suitable speed to transit between two points and the energy cost associated with that speed.

Increase in propulsion system efficiency significantly reduces the COT at higher speeds ($U > U_{opt}$), where propulsion power dominates; at speeds less than U_{opt} the propulsion system efficiency has limited influence on COT.

Length/diameter ratio influences the volumetric drag of the vehicle; at low L/D ratio the frictional drag component is small while the pressure drag component is large. At high L/D ratios the frictional drag is large while the pressure drag is small. Using the above formulations, the minimum drag is obtained at L/D ratio of 6.36. Departures from this value lead to higher drag coefficients, which lead to increases in COT at high speeds, $U > U_{opt}$. In fish, body shape (fineness ratio) has been shown to be an important factor for energy-reducing strategies for fish operating at speeds higher than U_{opt} (Ohlberger *et al.*, 2006).

17.2.1 Hotel power/metabolic rate

The non-propulsion power requirements dominate the COT calculation at speeds below U_{opt} and have a significant impact on the maximum range of an AUV. To understand the biological equivalent in an example class of marine animals, the Kleiber relationship (Kleiber, 1932) is typically used by biologists to predict the basal metabolic rate of marine mammals:

$$\mathrm{BMR} = 3.39\ \mathrm{mass}^{0.75} \tag{17.23}$$

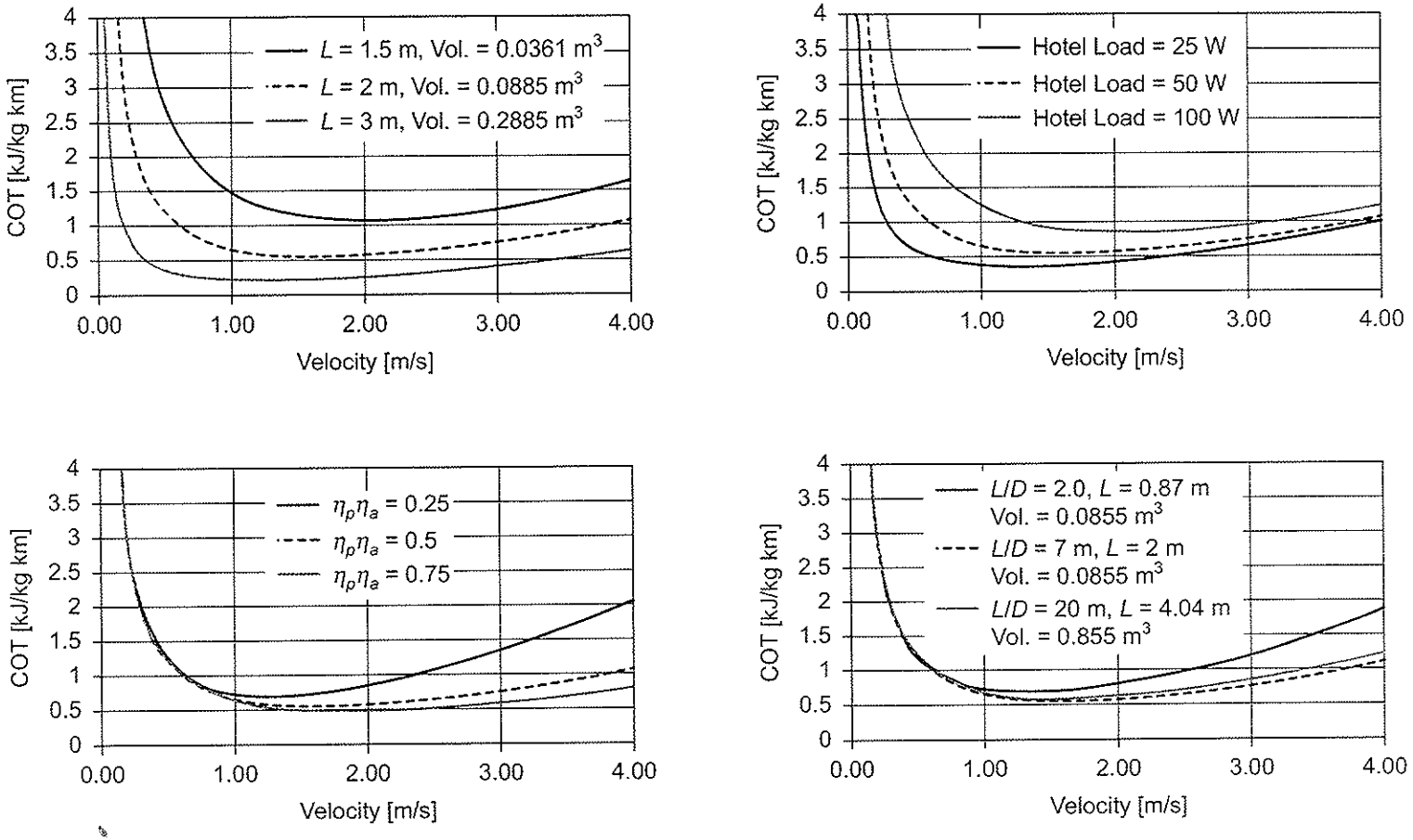

Figure 17.5 *Influence of various parameters on the cost of transport (COT). Unless otherwise identified, calculations are based on $L = 2$ m, $P_H = 50$ W, $\eta_p\eta_a = 0.5$, $L/D = 7$, $\rho = 1025$ kg/m^3 and $\nu = 1.19 \times 10^{-6}$ m^2/s. Influence of vehicle size (top left); influence of hotel load (top right); influence of total propulsion system efficiency $\eta_p\eta_a$ (bottom left); influence of length/diameter ratio (bottom right)*

BMR in a resting, thermoneutral, post-absorptive, non-growing individual is often assumed to be the lowest stable metabolic rate of an individual (Boyd, 2002). For marine mammals, this may not be comparable with the AUV hotel load since thermoregulation also needs to be considered. An alternative metric is the field metabolic rate (FMR); this is the metabolic rate of free ranging animals in the field, but it may incorporate some level of swimming activity. Boyd (2002) notes that for larger animals, the FMR tends to the BMR predicted by the Kleiber relationship, suggesting that for larger marine mammals thermoregulation costs less energy per unit mass. It is worth noting that unlike man-made actuators, biological muscles will consume energy at rest, which contributes to the metabolic rate of animals. Typical values for humans show that muscle consumes 54.4 kJ/kg/day at rest, which is significantly higher than bone (9.6 kJ/kg/day) and adipose tissue (18.8 kJ/kg/day). However, it is much lower than the remainder of the internal organs (or high metabolic residual mass) which consume 225.9 kJ/kg/day (Heymsfield *et al.*, 2002).

Figure 17.6 compares the field metabolic rate of marine mammals (data collated from various sources by Boyd (2002)) with the hotel load of AUVs; note the log, log scale. Typically, marine mammals have a power requirement not associated with propulsion of one order of magnitude greater than AUVs of similar mass. Gliders and long-range vehicles with very low hotel loads have non-propulsion power requirements of two or three orders of magnitude smaller than marine mammals of similar size. These long-range vehicles have sacrificed linear or area coverage rate and limited the choice of sensors to low-power devices in order to minimize the hotel load. Note the lower BMR of various eel species compared to salmonoid fish.

The relationship between field metabolic rate and marine mammal mass has a good correlation ($R^2 = 0.8609$). However, the AUVs (excluding long-range vehicles) demonstrate significant scatter ($R^2 = 0.4043$). This may be attributed to the range of available instruments each vehicle may be fitted with in order to complete their mission; for example, a fluxgate heading sensor such as PNI TCM5 (0.01 W) (PNI, 2011), or a fibre optic gyro such as IXSEA PHINS (IXSEA, 2011), inertial navigation system (INS) (15 W) or a Persistor CF2 (<0.2 W) (Persistor Instruments Inc., 2010), may be the controller for vehicles from tens to hundreds of kilograms in mass.

17.2.2 Propulsion power

Propulsion power costs make a significant contribution to the COT at speeds greater than U_{opt}. Energy lost by propulsion system inefficiencies can account for a large portion of energy expenditure in an AUV. Along with under-predicting the drag and over-predicting the mass of batteries that may be carried, over-predicting the propulsion system efficiency is a common cause of an AUV being unable to achieve the design range at the desired speed (Stevenson *et al.*, 2007). There are losses in every stage of the propulsion system (see Figure 17.1) from power source to propeller. Some of these losses are caused by inefficiency in energy conversion, from chemical energy to electricity (e.g. internal resistance in batteries), from

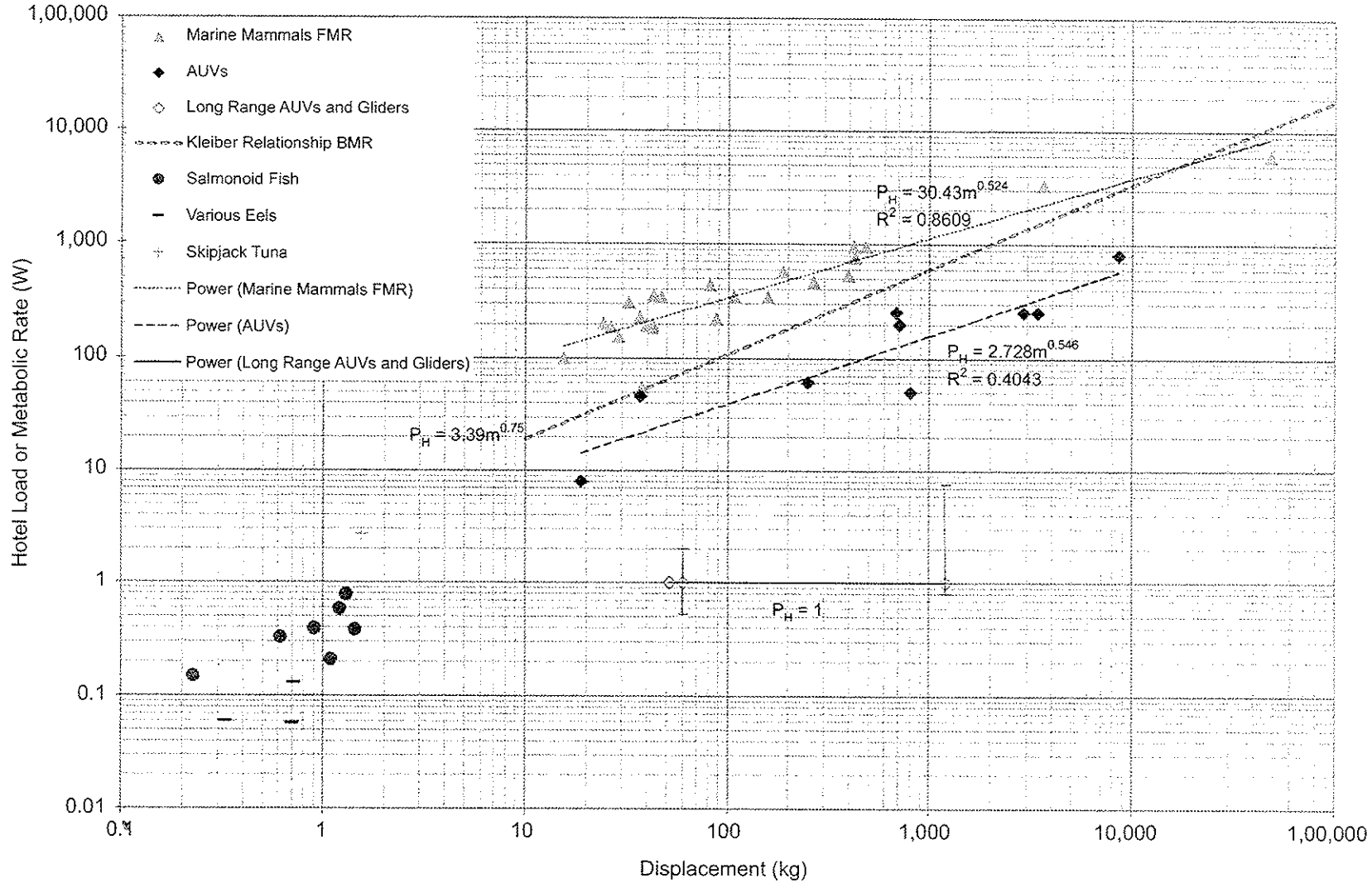

Figure 17.6 Comparison of AUV (n = 12) hotel load, marine mammal (n = 25) field metabolic rate and fish BMR. For AUVs, the mass quoted is the displaced mass corresponding to the outer hull volume and thus includes the mass of water in free flooding spaces in the hull. Data for marine mammals collated from various sources by (Boyd, 2002). Fish data calculated from O_2 consumption values from (Froese and Pauly, 2011). Example error bars are presented for the Seaglider (ca 60 kg) and AutosubLR (ca 1000 kg) vehicles

electricity to mechanical energy, shaft losses and, finally, from mechanical energy in the propulsor to that in the fluid. Other losses come from powering support systems such as motor controller and power regulators.

At a fundamental level, the power is required to overcome the hydrodynamic drag experienced by the animal or vehicle. Good-quality drag data for marine animals and AUVs are limited. However, *L/D* ratios are more widely available and give a good indication of the level of streamlining of the hull (body) which in turn is indicative of the drag; see Figure 17.7, where the 'diameter' for marine animals is the largest cross-sectional depth or height measured along the body. All but one of the marine animals considered have *L/D* ratios in the range of 3–7.5; although the sample is small compared to the total number of species, the species for which data is available tend to have good swimming performance. The exception is the silver eel with a *L/D* ratio of 16.6. The AUVs exhibit greater variation, with about 80% of them having *L/D* ratios larger than 3; those with an *L/D* less than 3 are generally box frame AUVs, which are more ROV-like in their appearance and operation.

Returning to Eqs. (17.13) through (17.22), an estimate of the towed naked hull drag of a 3.5 m^3 volume prolate spheroid travelling at 2 m/s has been performed; the results are shown in Figure 17.8. While the drag rises rapidly at *L/D* ratios of below 3 due to separation at the stern of the vehicle increasing the pressure drag component, the drag only varies by less than 20% for *L/D* ratios between 3 and 12 and by less than 5% for *L/D* ratios between 4 and 12. Obviously, naked hull drag is not the complete story, as control surfaces or fins and other protuberances such as aerials can add substantially to the total drag (Phillips *et al.*, 2010).

Numerous authors have quoted high propulsive efficiencies (η_D) for marine animals using carangiform and thunniform type propulsion (high-speed long-distance swimmers in which virtually all movement is in the caudal fin). For example, the propulsive efficiencies of pseudo killer whales at 0.9 (Fish, 1996), bottlenose dolphins at 0.81 (Fish, 1993), and fin whale at 0.85 (Bose and Lien, 1989) are high compared with that of a typical propeller (Wageningen B5-75) open water efficiency of 0.5–0.7 (Carlton, 2007). Anderson *et al.* (1998) and Read *et al.* (2003) examined the thrust produced by a NACA0012 foil (60 cm by 10 cm with end plates) heaving and pitching in a manner similar to thunniform propulsion at a range of Strouhal numbers and maximum foil incidence angles. Anderson *et al.* (1998) measured a peak propulsive efficiency of 0.87 with proper selection of Strouhal number, angle of attack, heave amplitude ratio and phasing of the heave and pitch motions. However, Read *et al.* (2003) were unable to replicate these results, achieving a lower maximum efficiency of 0.715. Lower aspect ratio oscillating foils experience significant end effects due to the presence of tip vortices, which reduce both thrust production and efficiency compared to the infinite foil case (Dong, 2005).

Other swimming approaches have less impressive propulsive efficiencies: the American eel (*Anguilla rostrata*), which uses anguilliform motion (undulatory body waves initiated at the nose with maximum amplitude at the tail), has a propulsive efficiency estimated at 0.43–0.54 based on wake studies (Tytell and

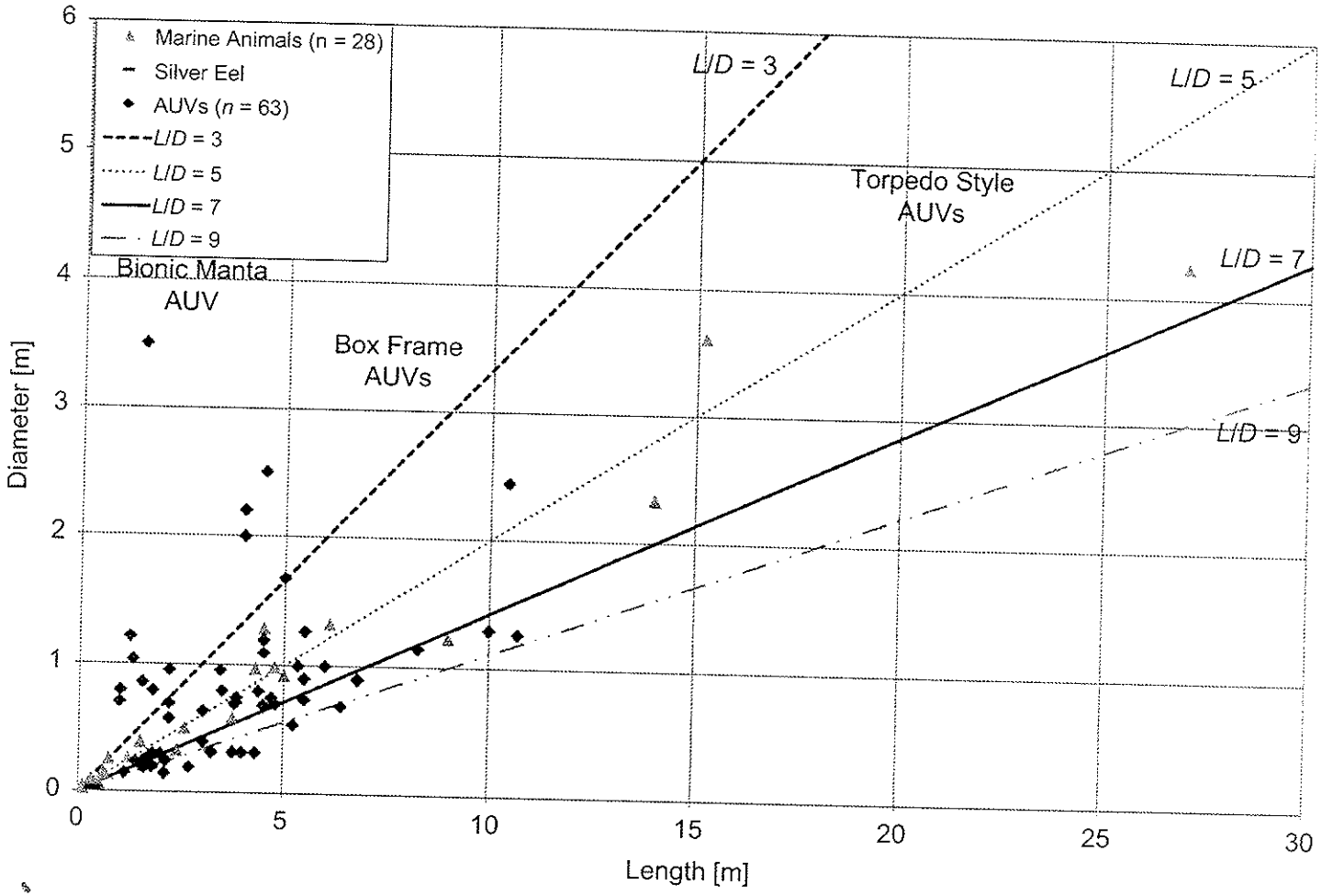

Figure 17.7 Comparisons of diameter (or widest lateral dimension) versus length for a selection of AUVs (n = 28) and marine animals (n = 28). The shaded areas highlight the type of vehicle configuration

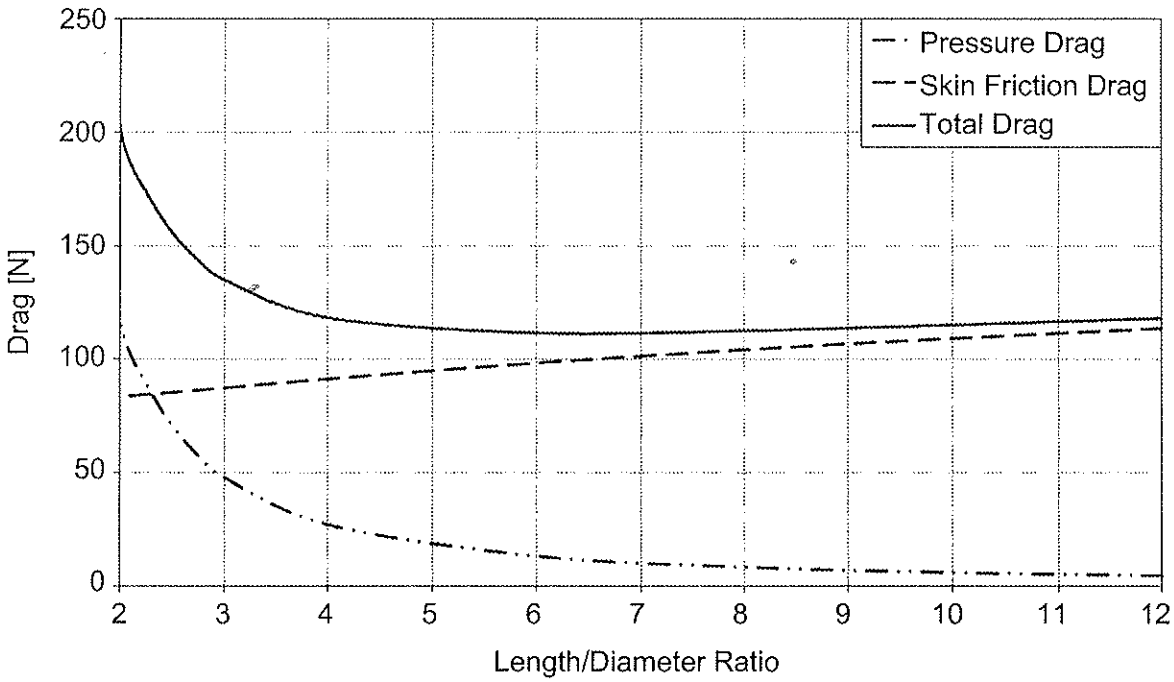

Figure 17.8 Influence of length/diameter ratio on a 3.5 m^3 streamlined hull travelling at 2 m/s

Lauder, 2004). The labriform swimming (a type of median and/or paired fin (MPF) propulsion in which the species uses a control surface other than the tail to swim) has significantly lower propulsive efficiencies in the range of 0.15–0.2 for a bluegill sunfish (*Lepomis macrochirus*) (Jones *et al.*, 2007). However, labriform swimming is largely performed by non-pelagic fish where increased manoeuvrability is required to negotiate complex environments. Labriform swimmers swim primarily with their pectoral fins, using their caudal fin to assist only at higher speeds. These species possess a swim bladder and are thus able to maintain neutral buoyancy. The transition, from pectoral to pectoral and caudal fin gaits, termed the pectoral-caudal gait transition speed (Drucker, 1996), occurs at a threshold speed that varies between species and individual size (Mussi *et al.*, 2002). The ability to maintain the pectoral and caudal fin gait for long periods also varies between species (Korsmeyer *et al.*, 2002). Drucker and Lauder (2000) measured the gait transition speed for black surfperch (*Embiotoca jacksoni*) and the bluegill sunfish (*Lepomis macrochirus*); for individuals of 20 cm length the $U_{p\text{-}c}$ was 2.0 BL/s (body lengths per second) for the surfperch and 1.5 BL/s for the sunfish.

High potential propulsive efficiencies have led to significant research effort being applied to mimicking biological propulsion systems in preference to the more conventional screw propeller. For example, see Draper Laboratory VCUUV robotic tuna (Anderson and Chhabra, 2002), robotic dolphin (Yu *et al.*, 2009), Finnegan robotic turtle (Wolf *et al.*, 2006), Biomimetic Tuna (Suleman and Crawford, 2008) and the review by Roper *et al.* (2011). However, the propulsive efficiency considers only the ability of the motion of the propulsor to generate hydrodynamic thrust (and shaft losses for AUVs). No account is made for the additional losses incurred generating the shaft motion, or energy losses earlier in the energy flow (see Figure 17.1).

In nature, motion is created using muscles. Biological muscles for vertebrates can be separated into four groups: fast and slow skeletal muscles, smooth muscles and cardiac muscles (Oota and Saitou, 1999). Skeletal muscles will be the main interest for studying propulsion, as it is the only type that can be consciously controlled, and is responsible for actuating all limbs or propulsors. Skeletal muscles are made up of two types of muscle fibres: slow twitch (Type I) and fast twitch (Type II). Biological muscles are not very efficient compared to rotary electric motors, but their efficiency is superior to that of man-made linear actuators. Typically, skeletal muscles are only 0.3 efficient, although certain types can reach 0.5 (Curtin and Woledge, 1993a). Adenosine triphosphate (ATP) is the main energy source for the majority of cellular functions. Contraction of the muscle fibres is powered by the energy released by the breakdown of ATP to adenosine diphosphate (ADP) and a phosphate ion. The energy released in cells by the breaking down of foodstuffs can be used to recombine the ADP and phosphate ion to reform ATP; this process is only 0.5 efficient (Alexander, 2003). Study of biological muscles in robotics is often restricted to being the target for comparison with man-made systems (Caldwell, 1993). However, attempts have been made to graft living biological muscle to actuate underwater vehicles (Herr and Dennis, 2004). The field of biomechatronics is still in its infancy, and sustaining the living muscle ex-vivo is a considerable challenge.

For engineered artefacts, there are a number of technologies used in converting stored chemical energy into kinetic energy. These can be divided into two groups, namely rotary or linear. The rotary actuators are the most common and can be subdivided into three types: electric motors, hydraulic motors and heat engines. Linear actuators are less common but include a large variety of actuation technologies. These include shape memory alloys, electroactive polymers and hydraulic pistons. Linear actuators are mainly used in bio-inspired propulsion systems. Also, linear actuation may be achieved using rotary actuators. Often these include a conversion component, such as pulleys, rack and pinion, screws, and hydraulic pumps. Table 17.1 provides a guide to typical actuator efficiencies.

Most biomimetic propulsion systems require oscillating or reciprocating motion. In the majority of systems, this is achieved by using a rotary electric motor connected to a gearing system. Some control the motions electronically by varying motor output through a sinusoidal cycle (Licht *et al.*, 2004a), but others achieve it using a cam and cranks (Yu *et al.*, 2009). Pneumatic and hydraulic cylinders are common in land robot systems but less common in AUVs.

The typical rotation speeds of DC motors or engine output shafts are too fast for efficiently driving a propeller, thus a reduction gearbox is often used. Exceptions include the direct drive motors used on the Autosub3 and Autosub6000 vehicles. The efficiency of different gearboxes varies: a one-stage planetary gear can be over 90% efficient, while a worm drive can be as little as 40%. Generally, the greater the reduction ratio, the lower the gearbox efficiency (Maxon, 2011).

An alternative actuation and propulsion method is the buoyancy engine used on glider vehicles. A pump is used to effect buoyancy changes to make the glider system positively or negatively buoyant. The resulting potential energy is converted to kinetic energy through the use of wings. The total system efficiency for a glider is

Table 17.1 Typical actuator efficiencies (shaded rows correspond to biological actuators)

Actuator type	Typical efficiencies	Comments	Source
Direct current (DC) motor	0.6–0.9	It is a commonest form of actuator used to propel an AUV. The quoted efficiencies are maximum motor efficiencies at optimum continuous loading. Efficiency varies with size and motor design	Maxon (2011)
Pneumatic cylinders	<0.67	However, the efficiency is highly dependent on other variables and highly dependent on other components in the pneumatic system, so most are much less efficient than this theoretical maximum	Prior and White (1995)
Dogfish (*Scyliorhinus canicula*) red muscle fibres (Type I)	<0.507	Muscle fibres isolated from the dogfish were electrically stimulated at 12°C. The resulting efficiency for sinusoidal motion varies with frequency, with maximum efficiency at 0.61–0.95 Hz and maximum power at 1.02 Hz	Curtin and Woledge (1993a)
Dogfish (*Scyliorhinus canicula*) white muscle fibres (Type II)	<0.41	Muscle fibres isolated from the dogfish were electrically stimulated at 12°C. The resulting efficiency for sinusoidal motion varies with frequency, with maximum efficiency at 2.0–2.5 Hz and maximum power at 3.5 Hz	Curtin and Woledge (1993b)
Diesel engine	<0.4	The chief advantage of a heat engine is that combustion fuels typically have much higher specific energy than batteries. However, they do require a source of oxygen, which may be taken from the air using a snorkel. University of Tokyo's R-one robot is one of a handful of AUVs that uses an air-independent internal combustion engine. R-one robot carries a closed cycle diesel engine and liquid oxygen	Ura and Obara (1999)
Bluegill sunfish (*Leponis macrochirus*) propulsion muscles	0.37–0.26	Efficiency estimate is at maximum labriform swimming speed, based on the upper and lower estimates of available mechanical power, respectively. Total swimming power required was estimated based on oxygen consumption	Jones *et al.* (2007)

(Continued)

Table 17.1 (Continued)

Actuator type	Typical efficiencies	Comments	Source
Electroactive polymers	<0.38	Electroactive polymer (EAP) is a new form of polymer linear actuator which changes shape when a current is applied. There are two types of EAP, electronic and ionic. The main difference between the two types of EAP is that the former uses Coulomb forces and the latter uses ion movement	Bar-Cohen (2004)
Shape memory alloys	<0.1	Shape memory alloy (SMA) actuators function by heating and cooling the alloy to induce a phase transition. The resultant change in the crystal lattice causes a change in the overall shape of the SMA, which results in a force. The speed of the actuation depends on heating and cooling rate and in general is much slower than electric motor. SMA actuators suffer heavy loss through hysteresis as heating and cooling phase transitions occur at different temperatures	Humbeeck (2001)

Table 17.2 Comparison of propulsion system efficiencies

Buoyancy engine		Propeller system	
Propulsive system efficiency	<0.5	Propulsive efficiency	0.7
		Shaft efficiency	0.95
		Gearbox efficiency	0.9
		Motor efficiency	0.9
		Propulsion system efficiency	0.53

at best 0.5 (occurring for the deepest depth range) (Griffiths, 2003). Using a well-matched propeller, motor and gearbox system, it should be possible to achieve similar propulsive system efficiencies (Furlong *et al.*, 2007) (see Table 17.2).

Assuming ATP conversion efficiency of 0.5 and a muscle efficiency of 0.5, a pseudo killer whale with a propulsive efficiency of 0.9 will have a propulsion system efficiency of 0.225, significantly lower than the 0.5 that can be achieved with an engineered propeller or buoyancy change system. For subcarangiform

swimmers, Webb (1975) suggests that total propulsion system efficiencies (overall aerobic efficiency) are commonly in the range of 0.15–0.30.

As such, extreme care must be made when designing a propulsion system to ensure that the actuator efficiency is sufficiently high. However, the objective of this type of research is not always to make efficient actuators but to investigate the hydrodynamics, logic and mechanism of biological systems, for example simple mimicry, in which many underwater vehicles with biomimetic propulsors either quote poor total propulsion system efficiencies (Yu *et al.*, 2009) or total propulsion system efficiency is not quoted at all (Suleman and Crawford, 2008; Cai *et al.*, 2010). In many cases a propeller-driven AUV would be able to achieve the same speed as a vehicle using bio-inspired propulsion but at a lower propulsive system power (Licht *et al.*, 2004b).

17.3 Optimum cost of transport

For both pelagic marine animals and AUVs, it is common to transit at or near U_{opt} minimizing the COT, and in the case of AUVs maximizing the range (Sato *et al.*, 2010). Figure 17.9 compares the optimum cost of transport, COT_{opt}, for various marine animals and AUVs.

Also included in the figure are three regression lines. For salmonoid fish, Brett (1964) presents an extrapolated regression:

$$COT_{opt} = 2.15 \ \text{mass}^{-0.25} \tag{17.24}$$

Williams (1999) suggests the following regression line ($R^2 = 0.83$) for marine mammals from 21 to 15,000 kg:

$$COT_{opt} = 7.79 \ \text{mass}^{-0.29} \tag{17.25}$$

Fitting an equivalent regression line through all the AUV data highlights the scatter and variation in the data. The resulting line (not plotted in Figure 17.9 for clarity) has the form:

$$COT_{opt} = 0.4149 \ \text{mass}^{-0.123} \tag{17.26}$$

This line has an R^2 value of 0.043, which shows there is negligible correlation between mass and COTopt for the entire AUV dataset. By removing the three gliders and the AutosubLR from the data (as arguably these form a different class of vehicle), a more meaningful regression line is generated:

$$COT_{opt} = 1.813 \ \text{mass}^{-0.285} \tag{17.27}$$

which has an R^2 value of 0.5248. This line corresponds to a faster reduction in COT with increasing size than the regression lines for salmonoid fish, while the exponents for AUVs and marine mammals are essentially identical. Based on the

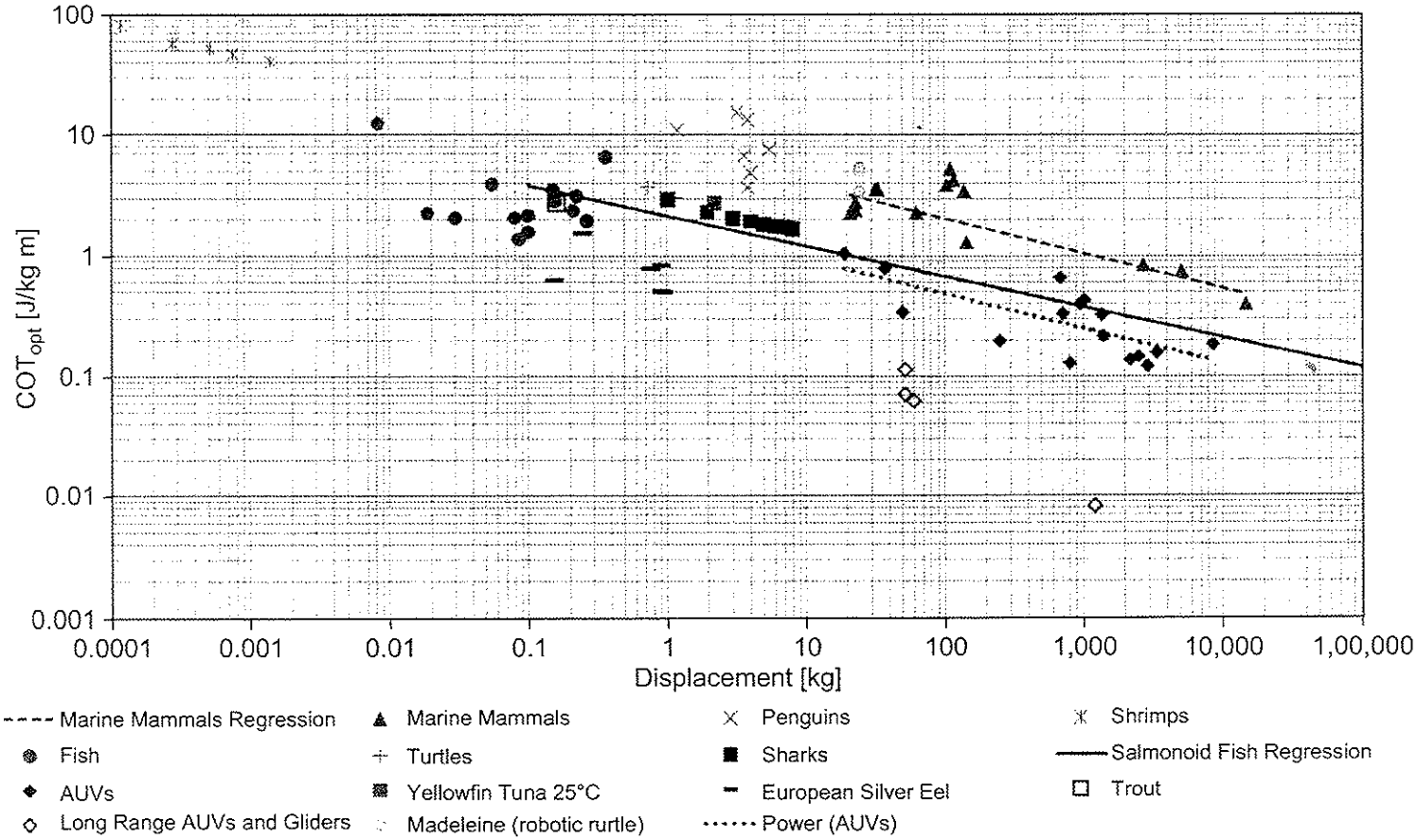

Figure 17.9 Comparison of the optimum cost of transport versus mass for various types of marine animals (n = 56) and AUVs (n = 22). For AUVs, the mass quoted is the displaced mass corresponding to the outer hull volume and thus includes the mass of water in free flooding spaces in the hull. Data for Madeleine, a robotic turtle, are taken from (Long Jr et al., 2006). Data for shrimps, turtles, and fish are summarized in (Videler and Nolet, 1990). For mammals, the data is taken from (Videler and Nolet, 1990; Williams, 1999; Rosen and Trites, 2002). Data for yellowfin tuna are taken from (Dewar and Graham, 1994) and for squid from (Webber and O'Dor, 1986). Data for penguins are summarized in (Luna-Jorquera and Culik, 2000). Bonnethead shark (the smallest of the hammerhead sharks) data are taken from (Parsons, 1990). Silver eel data are taken from (van Ginneken et al., 2005) and collated by (Palstra and van den Thillart, 2010), where multiple measurement techniques are used an average value has been taken. Trout data are taken from (van Ginneken et al., 2005). Regression line for salmonoid fish is taken from (Brett, 1964), and for marine mammals from (Williams, 1999). The apparently anomalous data point at ~1100 kg and <0.01 COT_{opt} corresponds with the AutosubLR, which is currently under development; its position on the graph is clarified in Figure 17.10, where its COT_{opt} is consistent with its mass and hotel load (1 W design)

regression lines a typical AUV has a COT 4.3 times smaller than a marine mammal of similar displacement.

While there is significant scatter in the data for both the AUVs and marine mammals, as expected from the simplified model, increasing displaced mass tends to lead to a reduction in COT_{opt}. It is also apparent that the AutosubLR and gliders have significantly lower cost of transport than normal AUVs of similar size; this is required for these vehicles to achieve their desired ranges – their designers have accepted that all non-propulsion power requirements including science sensors should be low (order 1 W) and that the forward speed will also be low (order 0.3 to 0.4 m/s) to ensure operation at COT_{opt}.

There is a notable distinction between the COT_{opt} for warm-blooded and cold-blooded marine animals. Williams (1999) also noted that the COT_{opt} of transport for marine mammals is considerably higher than those extrapolated for salmonoid fish of the same mass. This was attributed to the difference in maintenance cost (hotel load) between the two groups due to the inherent difference in endothermy. By removing the energetic cost of maintaining endothermy, Williams (1999) showed that the COT_{opt} of marine mammals tended to those of salmonoid fish.

Similarly, the measured metabolic rates of tuna exceed those of other well-studied fish (salmonoids) by approximately threefold (Korsmeyer and Dewar, 2001), thus explaining the higher COT_{opt} of yellowfin tuna compared to salmonoid fish. The high COT_{opt} of penguins may be attributed to the reports that some diving birds incur high substantial thermoregulatory energetic costs (Leeuw *et al.*, 1998; Grémillet *et al.*, 2005).

Note the comparatively low COT of the silver eel compared to the trout (both data points are for similar sized animals). This may initially seem at odds with the previously stated observation that carangiform propulsion (as for the trout) has a high propulsive efficiency compared to anguilliform propulsion (for the eel) (Tytell and Lauder, 2004), but this is an example where the whole system efficiency is what is reflected in the COT. Since neither the trout nor the silver eel have high drag body shapes, it is probable that the difference is due to high metabolic efficiency (low BMR) in the silver eel (van Ginneken *et al.*, 2005; also see Figure 17.6). Such an argument is supported by Clarke and Johnston (1999) who illustrate the low-resting O_2 consumption of eels compared to other common fish types. Similarly, Pettersson and Hedenstrom (2000) illustrated that increased propulsive power requirements of high drag bodies may be offset by reducing the BMR to achieve similar COT values.

For most bio-inspired AUVs, there is insufficient data to calculate COT; the robotic turtle Madeleine (Long Jr *et al.*, 2006) is an exception. COT data is available for a range of gaits based on either two or four flipper locomotion; these COT values are similar in magnitude to marine animals of similar sizes, but higher than similar sized AUVs.

Considering the similarity in form and propulsion method of most AUVs, there is surprising scatter in the AUV COT_{opt} data, which covers a much wider range of COT_{opt} compared to marine animals of the same size. As highlighted in the previous section, COT_{opt} is highly sensitive to the hotel load. Figure 17.10 shows the

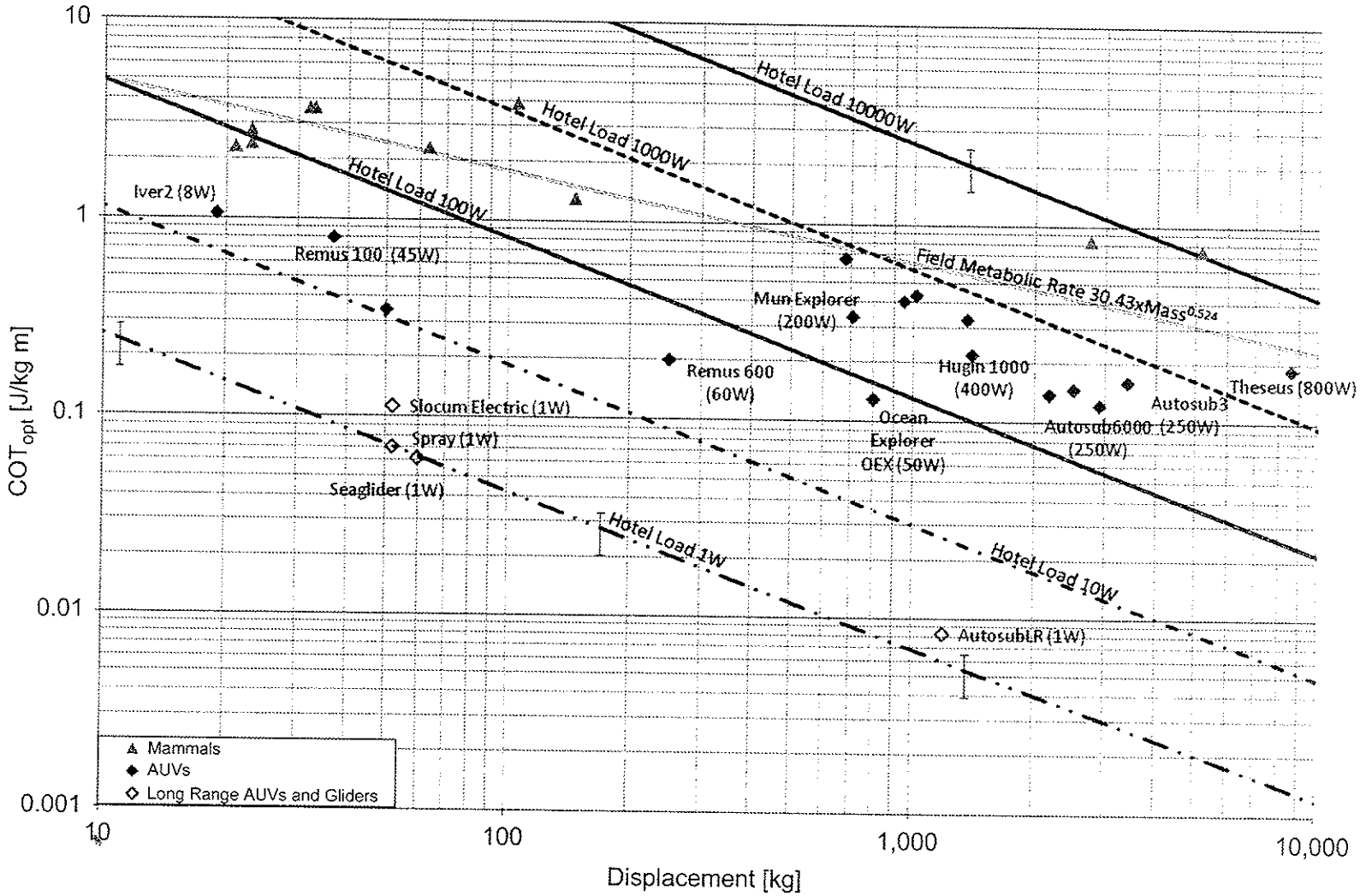

Figure 17.10 *Influence of hotel load on COT_{opt}. The mass quoted is the displaced mass corresponding to the outer hull volume and thus includes the mass of water in free flooding spaces in the hull. The diagonal black lines represent the predicted COT_{opt} for various hotel loads assuming $\eta_D\eta_a = 0.5$, $L/D = 7$, $P_H = 50$ W, $\rho = 1025$ kg/m^3 and $\nu = 1.19 \times 10^{-6}$ m^2/s. The field metabolic rate is the resting metabolic rate in the field; field metabolic rate relationship is taken from (Boyd, 2002). Included in the hotel load 1 W line and the hotel load 10,000 W line are error bars indicating the influence of reducing the propulsion power by a factor of two and increasing the propulsion power by a factor of two*

influence of hotel load on COT_{opt}, using the same methodology as before, assuming, $\rho = 1025$ kg/m^3, $\nu = 1.19 \times 10^{-6}$, $L/D = 7$ and $\eta_D \eta_a = 0.5$.

Also, where known the hotel load of the various vehicles are indicated on the plot. From this plot, it becomes clear that the variability in the COT_{opt} of AUVs is closely linked to the variability of their hotel loads, which range from the order of 1000 W for Theseus (Butler, 1999) to an actual hotel load of approximately 1 W for the three commonest gliders and the design hotel load for AutosubLR (currently ~7 W). Comparing the AUV data points to the predicted COT_{opt} with different hotel loads suggests that the simple model captures well the observed variation. The simple model is also relatively well able to capture the COT_{opt} for marine mammals by assuming that the FMR is equivalent to hotel load and using the regression line from Boyd (2002).

Traditionally, survey style AUVs have been designed with a cruising speed of around 2 m/s as a compromise between maximizing the range and the need to make reasonable progress (Stevenson *et al.*, 2007). For many vehicles this velocity is close to U_{opt}. With a reduction in hotel load, U_{opt} also reduces and may well reduce significantly below 2 m/s (e.g. to ~0.3 m/s for AutosubLR at 1 W hotel load). With this, many AUVs may start to operate routinely at speeds higher than U_{opt}, where both propulsive efficiency and drag coefficient play an important role in the COT of the vehicle. Petterson and Hedenstrom (2000) showed that low drag fish can use a broader range of swimming velocities without substantial increase in energetic cost, whereas high drag fish have a marked increase in swimming costs. Similar results are observed for AUVs with low C_{Dv} and high propulsive efficiencies (Figure 17.5d).

17.4 Discussion

The data presented in this chapter correct the common misconception that marine animals have greater propulsion system efficiencies than engineered systems of an equivalent size. This highlights that when searching for inspiration from nature to enhance engineered artefacts, it is important to identify biological solutions which are either superior to their engineered equivalent or have the potential to be. For example, for AUV designers interested in metrics other than level flight performance, such as manoeuvring, bio-inspired propulsion systems have clearly demonstrated improved performance (Anderson *et al.*, 1998).

The discussion in this chapter focuses on COT and energetic requirements while travelling in a straight line. For the marine animals, no account has been taken of potential penalties associated with high manoeuvrability, such as large control fins, which may lead to increased drag for straight ahead swimming, or adaptations to improve reproduction success rates. Also, energy expenditure associated with maintaining depth for non-neutrally buoyant systems has not been considered explicitly; this is an issue for animals and AUVs.

Away from free-stream operating conditions the preference of fish to use unsteady flow features has been observed in both the laboratory (Webb, 1998; Liao *et al.*, 2003) and the field (Fausch, 1993; McLaughlin and Noakes, 1998; Hinch and Rand, 2000). The potential of replicating such behaviours with AUVs is discussed in Philips *et al.* (2010).

Along with its COT, another key metric in determining the ability of an AUV to obtain its design range is the amount of energy stored on board the vehicle. Conventional AUVs carry a finite amount of chemical energy (batteries or fuel) which is used for both propulsion and hotel load. Hence, to maximize the vehicle's range at a specific speed, the AUV designer must minimize the COT while optimizing the specific energy of the power source. There are many types of power sources. Often the selection is determined by the choice of propulsion system, mission requirement and size and weight limitations. The most common power sources in AUVs are electrical batteries in which potential chemical energy is stored. Batteries can be approximately modelled as a voltage source in series with a resistance; this internal resistance of a battery is dependent on the specific battery's size, chemical properties, age, temperature and the discharge current. However, other types of power source do exist; these include chemical fuel, such as diesel, Otto fuel II and compressed hydrogen among others. Fuller discussions of engineered technologies may be found in (Hasvold *et al.*, 2006; Bradley *et al.*, 2001; Griffiths *et al.*, 2004). The specific energy of some common forms of energy storage in the natural and engineered world is compared in Table 17.3. The fats used in nature as energy stores have significantly higher specific energies than current battery technologies; for example, fish oils have a specific energy over 60 times greater than lithium polymer batteries.

Typically, batteries account for between 5% and 45% of an AUV's mass, dependent on mission, range, depth and speed requirements (Griffiths *et al.*, 2004).

Table 17.3 Comparison of specific energy of various energy storage methods, both biological and engineered (shaded rows correspond to biological energy stores)

Energy storage type	Specific energy (MJ/kg)	Reference
Diesel	40.0	Larminie and Lowry (2003)
Fish oil (cod liver oil)	39.45	Liversey and Elia (1988)
Bowhead whale (*Balaena mysticetus*) subcutaneous fat (blubber)	36.4	U.S. Department of Agriculture (2010)
Grey seal (*Halichoerus grypus*) blubber	32.7	This study[1]
White-beaked dolphin (*Lagenorhynchus albirostris*) blubber	31.9	This study[1]
Otto fuel II (monopropellant)	5.04	Luo *et al.* (2008)
Lithium polymer battery	0.47	Huggins (2010)
Nickel metal hydride (Ni-MH)	0.28	Huggins (2010)

[1]Tested in a calorimeter, blubber samples were taken from the middle body part of a white-beaked dolphin and a grey seal, both stranded, and specially the dolphin suffered from malnutrition; therefore, the blubber had changed in texture (rubbery instead of jelly) and colour, hence there is the assumption that the resulting specific energy might be less than one of a healthy animal.

Marine animals are able to acquire additional energy through feeding to replenish the energy used through routine behaviours, so the energy stored by various marine animals varies with species, sex, season, migratory stage, feeding behaviour and age among other variables (Jonsson *et al.*, 1997; Anthony *et al.*, 2000; Struntz *et al.*, 2004). In a study in Prince William Sound, Alaska, shrimps and octopus had the lowest average fat content at ~1%, whereas the highest fat content was found in adult eulachon (25%) and adult herring (21%) (Iverson *et al.*, 2002). In bottlenose dolphins (*Tursiops truncatus*), blubber accounts for between 15% and 27% of an adult animal's total mass (Struntz *et al.*, 2004). Blubber not only provides an energy store for marine mammals, but it is multifunctional, providing buoyancy, streamlining and functions in thermoregulation (Struntz *et al.*, 2004).

It is assumed that silver eels make the 6000 km journey back to their spawning ground without feeding (Schmidt, 1923; van Ginneken and Maes, 2005). van Ginneken *et al.* (2005) simulated a 5500 km migration by placing female silver eels in a swim tunnel. Nine individuals with an average mass of 914.7 g completed the simulated migration at 0.5 BL/s (~0.37 m/s) using an average of 3.45 MJ/kg. The fat content of silver eels prior to migration ranges from 10% to 28% (Svedang and Wickstrom, 1997). Assuming a fat energetic content of 39.45 MJ/kg, the silver eel will have remaining fat reserves to allow for reproduction on arrival. Based on the above energetic values, no current secondary battery technology would allow a 1 kg engineered silver eel with 20% mass of batteries with equivalent propulsion and hotel power requirements to complete more than around 200 km.

Similar to the feeding behaviour of marine animals, not all AUVs rely solely on their onboard energy supply for the whole duration of their mission; for example the Naval Underwater Warfare Center's SAUV is solar powered (Crimmins *et al.*, 2006) and Teledyne's Slocum Thermal Glider (Webb *et al.*, 2001) uses the vertical ocean temperature gradient to generate volume changes.

17.5 Conclusions

Optimum cost of transport provides a useful metric for comparing the total energetic requirements of marine animals and AUVs. AUVs in general have a much wider range of COT_{opt} compared to marine animals; this is attributed to the much greater variability in AUV hotel load per unit mass than marine animal BMR per unit mass. In general, AUVs have a lower COT_{opt} than equivalent sized marine animals, and are therefore, as complete systems, more energy efficient than their natural counterparts.

Marine animals and AUVs with low drag coefficients and high propulsion system efficiencies are able to operate over a wide range of speeds around U_{opt} without incurring significant energetic penalties, unlike those with high drag or low propulsion system efficiencies. Consequently, for AUVs which operate above U_{opt}, minimizing the propulsive power requirements has a significant impact on the range of the vehicle.

Typically, Seaglider AUVs have achieved long ranges in excess of 4900 km by reducing their hotel load below 1 W. Other long-range gliders and AUVs have also adopted the approach of minimizing their hotel load to maximize the range. To reduce the hotel load sufficiently, significant sacrifices are required in terms of type and frequency of measurements that may be taken. Marine animals can achieve equivalent migrations (e.g. silver eels at 5500 km) by having high metabolic efficiencies (low base metabolic rates) and taking advantage of high specific energy fat stores which have specific energies 60 times that of the best secondary battery technologies.

When assessing the propulsive power requirements of an AUV or marine animal, it is vital that all aspects of the system are considered, from actuator and shafts to the propulsor's interaction with the fluid. The high propulsive efficiency of thunniform propulsion (in which thrust is produced by oscillation of the tail involving very little bending of the body) coupled with the comparatively poor efficiency of muscle results in an overall efficiency that may be significantly lower than a conventional propeller and DC motor combination.

Acknowledgements

This research was supported by the EPSRC through grant number EP/F066767/1 entitled 'Nature in Engineering for Monitoring the Oceans (NEMO)', a joint project between the University of Southampton, Newcastle University and the National Oceanography Centre. The overall aim of this project is to find and synthesize novel design and implementation concepts for deep-diving and agile unmanned underwater vehicles (UUV) to meet offshore industry, environmental monitoring and scientific research needs based on inspiration from marine organisms to achieve increased functionality, lower weight and energy requirements and lower capital and operational costs.

References

Alexander, R. M. (2003) *Principles of Animal Locomotion*. Princeton, NJ, Princeton University Press

Alexander, R. M. (2005) Models and scaling of energy costs for locomotion. *Journal of Experimental Biology*, **208**, 1645–1652

Allen, B., Vorus, W. S. & Prestero, T. (2000) Propulsion system performance enhancements on REMUS AUVs. In *Oceans 2000 MTS/IEEE Conference and Exhibition*, Providence, RI, USA, 11–14 September

Anderson, I. A., Ieropoulos, I. A., Mckay, T., O'brien, B. & Melhuish, C. (2011) Power for robotic artificial muscles. *IEEE/ASME Transactions on Mechatronics*, **16**, 107–111

Anderson, J. M. & Chhabra, N. K. (2002) Maneuvering and stability performance of a robotic tuna. *Integrative and Comparative Biology*, **42**, 118–126

Anderson, J. M., Streitlien, K., Barrett, D. S. & Triantafyllou, M. S. (1998) Oscillating foils of high propulsive efficiency. *Journal of Fluid Mechanics*, **360**, 41–72

Anthony, J. A., Roby, D. D. & Turco, K. R. (2000) Lipid content and energy density of forage fishes from the northern Gulf of Alaska. *Journal of Experimental Marine Biology and Ecology*, **1**, 53–78

Bar-Cohen, Y. (Ed.) (2004) *Electroactive polymer (EAP) actuators as Artificial Muscles: Reality, Potential, and Challenges*. Bellingham, WA, SPIE – The International Society for Optical Engineering

Blake, R. W. (1979) The mechanics of labriform locomotion in the angelfish (*Pterophyllum eimekei*): An analysis of the power stroke. *Journal of Experimental Biology*, **82**, 255–271

Bose, N. & Lien, J. (1989) Propulsion of a fin whale (*Balaenoptera physalus*): Why the fin whale is a fast swimmer. *Proceedings of the Royal Society of London. Series B, Biological Sciences*, **237**, 175–200

Bourne, W. (1578) *Inventions or devices. Very necessary for all generalles and captaines, as wel by sea as by land.* Published by the Author, London

Boyd, I. L. (2002) Energetics: Consequences for fitness. In Hoelzel, A. R. (Ed.), *Marine Mammal Biology: An Evolutionary Approach.* Blackwell Publishing, Malden, Oxford and Carlton, pp. 247–277

Bradley, A. M., Feezor, M. D., Singh, H. & Sorrell, F. Y. (2001) Power systems for autonomous underwater vehicles. *IEEE Journal of Oceanic Engineering*, **26**, 526–538

Brett, J. R. (1964) The respiratory metabolism and swimming performance of young sockeye salmon. *Journal of Fisheries Research Board Canada*, **21**, 1183–1226

Butler, B. (1999) *Field trials of the Theseus AUV*, http://www.ise.bc.ca/auv1002.html, 18/02/2011

Cai, Y., Bi, S. & Zheng, L. (2010) Design and experiments of a robotic fish imitating cow-nosed ray. *Journal of Bionic Engineering*, **7**, 120–126

Caldwell, D. G. (1993) Natural and artificial muscle elements as robot actuators. *Mechatronics*, **3**, 269–283

Carlton, J. (2007) *Marine Propellers and Propulsion.* Butterworth-Heinemann, Oxford

Casellini, M. (2008) Thermoregulation. In Perrin, W. F., Wursig, B. & Thewissen, J. G. M. (Eds.), *Encyclopedia of Marine Mammals.* London, Academic Press

Clarke, A. & Johnston, N. M. (1999) Scaling of metabolic rate with body mass and temperature in teleost fish. *Journal of Animal Ecology*, **68**, 893–905

Comstock, J. P. (1977) *Principles of Naval Architecture, 4th Edition.* Society of Naval Architects & Marine Engineers, New York

Crimmins, D. M., Patty, C. T., Beliard, M. A., Baker, J., Jalbert, J. C., Komerska, R. J., *et al.* (2006) Long-endurance test results of the solar-powered AUV system. In *Oceans 2006,* Boston, MA, USA, 18–21 September, pp. 1–5

Curtin, N. A. & Woledge, R. C. (1993a) Efficiency of energy conversion during sinusoidal movement of red muscle fibres from the dogfish *Scyliorhinus canicula. Journal of Experimental Biology*, **185**, 195–206

Curtin, N. A. & Woledge, R. C. (1993b) Efficiency of energy conversion during sinusoidal movement of white muscle fibres from the dogfish *Scyliorhinus canicula*. *Journal of Experimental Biology*, **183**, 137–147

Davis, R. W., Williams, T. M. & Kooyman, G. L. (1985) Swimming metabolism of yearling and adult harbor seals *Phoca vitulina*. *Physiological Zoology*, **58**, 590–596

Dewar, H. & Graham, J. B. (1994) Studies of tropical tuna swimming performance in a large water tunnel – Energetics. *Journal of Experimental Biology*, **192**, 13–31

Dong, H. (2005) Wake structure and performance of finite aspect-ratio flapping foils In *43rd AIAA Aerospace Sciences Meeting and Exhibit*, Reno, NV, USA, January 10–13

Dressler, F. (2005) Efficient and scalable communication in autonomous networking using bio-inspired mechanisms – an overview. *Informatica*, **29**, 183–188

Drucker, E. G. (1996) The use of gait transition speed in comparative studies of fish locomotion. *American Zoology*, **36**, 555–566

Drucker, E. G. & Lauder, G. V. (2000) A hydrodynamic analysis of fish swimming speed: Wake structure and locomotor force in slow and fast labriform swimmers. *Journal of Experimental Biology*, **203**, 2379–2393

Elliott, J. M. & Davison, W. (1975) Energy equivalents of oxygen consumption in animal energetics. *Oecologia*, **19**, 195–201

Fausch, K. D. (1993) Experimental analysis of microhabitat selection by juvenile steelhead (*Oncorhynchus mykiss*) and coho salmon (*O. kisutch*) in a British Columbia stream. *Canadian Journal of Fisheries and Aquatic Sciences*, **50**, 1198–1207

Fish, F. E. (1993) Power output and propulsive efficiency of swimming bottlenose dolphins (*Tursiops truncatus*). *Journal of Experimental Biology*, **185**, 179–193

Fish, F. E. (1996) Transitions from drag-based to lift-based propulsion in mammalian swimming. *American Zoology*, **36**, 628–641

Fish, F. E. (2006) The myth and reality of Gray's paradox: Implication of dolphin drag reduction for technology. *Bioinspiration & Biomimetics*, **1**(2), R17–R25

Froese, R. & Pauly, D. (2011) *FishBase: Version (02/2011)*, http://www.fishbase.org

Furlong, M. E., Mcphail, S. D. & Stevenson, P. (2007) A concept design for an ultra-long-range survey class AUV. In *Oceans 07*, Aberdeen, UK

Gao, J., Bi, S., Li, J. & Liu, C. (2009) Design and experiments of robot fish propelled by pectoral fins. In *IEEE International Conference on Robotics and Biomimetics*, Guilin, China, December 19–23

Grémillet, D., Kuntz, G., Woakes, A. J., Gilbert, C., Robin, J.-P., Maho, Y. L., *et al.* (2005) Year-round recordings of behavioural and physiological parameters reveal the survival strategy of a poorly insulated diving endotherm during the Arctic winter. *Journal of Experimental Biology*, **208**, 4231–4241

Griffiths, G. (Ed.) (2003) *Technology and Applications of Autonomous Underwater Vehicles*. Ocean Science and Technology, Taylor & Francis, London

Griffiths, G., Jamieson, J., Mitchell, S. & Rutherford, K. (2004) Energy storage for long endurance AUVs. In *ATUV Conference*, London, March 16–17

Hammer, C. (1995) Fatigue and exercise tests with fish. *Comparative Biochemistry and Physiology Part A: Physiology*, **112**, 1–20

Hasvold, Ø., Størkersena, N. J., Forsetha, S. & Liana, T. (2006) Power sources for autonomous underwater vehicles. *Journal of Power Sources*, **162**, 935–942

Herr, H. & Dennis, R. G. (2004) A swimming robot actuated by living muscle tissue. *Journal of Neuroengineering and Rehabilitation*, **1**, 6

Heymsfield, S. B., Gallagher, D., Kotler, D. P., Wang, Z., Allison, D. B. & Heshka, S. (2002) Body-size dependence of resting energy expenditure can be attributed to nonenergetic homogeneity of fat-free mass. *American Journal of Physiology – Endocrinology and Metabolism*, **282**, E132–E138

Hinch, S. G. & Rand, P. S. (2000) Optimal swimming speeds and forward-assisted propulsion: Energy-conserving behaviours of upriver-migrating adult salmon. *Canadian Journal of Fisheries and Aquatic Sciences*, **57**, 2470–2478

Hoerner, S. F. (1965) *Fluid-dynamic Drag, 2nd Edition*. Published by the author

Huggins, R. A. (2010) *Energy storage*. Springer, New York

Humbeeck, J. V. (2001) Shape memory alloys: A material and a technology. *Advanced Engineering Materials*, **3**, 837–850

Iverson, S. J., Frost, K. J. & Lang, S. L. C. (2002) Fat content and fatty acid composition of forage fish and invertebrates in Prince William Sound, Alaska: Factors contributing to among and within species variability. *Marine Ecology Progress Series*, **241**, 161–181

Ixsea (2011) *IXSEA PHINS Surface Inertial Navigation System*, http://www.ixsea.com/en/navigation_motion/3/phins.html

Jones, E. A., Lucey, K. S. & Ellerby, D. J. (2007) Efficiency of labriform swimming in the bluegill sunfish (*Lepomis macrochirus*). *Journal of Experimental Biology*, **210**, 3422–3429

Jonsson, N., Jonsson, B. & Hansen, L. P. (1997) Changes in proximate composition and estimates of energetic costs during upstream migration and spawning in Atlantic salmon *Salmo salar*. *Journal of Animal Ecology*, **66**, 425–436

Kleiber, M. (1932) Body size and metabolism. *Hilgardia*, **6**, 315–353

Korsmeyer, K. E. & Dewar, H. (2001) Tuna metabolism and energetics. *Fish Physiology*, **19**, 35–78

Korsmeyer, K. E., Steffensen, J. F. & Herskin, J. (2002) Energetics of median and paired fin swimming, body and caudal fin swimming, and gait transition in parrotfish (*Scarus schlegeli*) *and triggerfish* (*Rhinecanthus aculeatus*). *Journal of Experimental Biology*, **205**, 1253–1263

Larminie, J. & Lowry, J. (2003) *Electric Vehicle Technology Explained*. John Wiley & Sons, Chichester

Leeuw, J. J. D., Butler, P. J., Woakes, A. J. & Zegwaard, F. (1998) Body cooling and its energetic implications for feeding and diving of tufted ducks. *Physiological Zoology*, **71**, 720–730

Liao, J. C., Beal, D. N., Lauder, G. V. & Triantafyllou, M. S. (2003) The Kármán gait: Novel body kinematics of rainbow trout swimming in a vortex street. *Journal of Experimental Biology*, **206**, 1059–1073

Licht, S., Hover, F. & Triantafyllou, M. S. (2004a) Design of a flapping foil underwater vehicle. *International Symposium on Underwater Technology*, IEEE, Taipei, pp. 311–316

Licht, S., Polidoro, V., Flores, M. & Hover, F. S. (2004b) Design and projected performance of a flapping foil AUV. *Journal of Oceanic Engineering*, **29**, 786–794

Lighthill, M. J. (1969) Hydromechanics of aquatic animal propulsion. *Annual Review of Fluid Mechanics*, **1**, 413–446

Lighthill, M. J. (1970) Aquatic animal propulsion of high hydromechanical efficiency. *Journal of Fluid Mechanics*, **44**, 265–301

Liversey, G. & Elia, M. (1988) Estimation of energy expenditure, net carbohydrate utilization, and net fat oxidation and synthesis by indirect calorimetry: Evaluation of errors with special reference to the detailed composition of fuels. *The American Journal of Clinical Nutrition*, **47**, 608–628

Long Jr, J. H., Schumacher, J., Livingston, N. & Kemp, M. (2006) Four flippers or two? Tetrapodal swimming with an aquatic robot. *Bioinspiration & Biomimetics*, **1**, 20–29

Luna-Jorquera, G. & Culik, B. M. (2000) Metabolic rates of swimming Humboldt penguins. *Marine Ecology Progress Series*, **203**, 301–309

Luo, N., Miley, G. H., Kim, K.-J., Burton, R. & Huang, X. (2008) $NaBH_4/H_2O_2$ fuel cells for air independent power systems. *Journal of Power Sources*, **185**, 684–690

Maxon (2011) *Maxon Motor*, http://www.maxonmotor.co.uk

Mclaughlin, R. L. & Noakes, D. L. G. (1998) Going against the flow: An examination of the propulsive movements made by young brook trout in streams. *Canadian Journal of Fisheries and Aquatic Sciences*, **55**, 853–860

Mussi, M., Summers, A. P. & Domenici, P. (2002) Gait transition speed, pectoral fin-beat frequency and amplitude In *Cymatogaster aggregata, Embiotoca lateralis* and *Damalichthys vacca. Journal of Fish Biology*, **61**, 1282–1293

Ohlberger, J., Staaks, G. & Hölker, F. (2006) Swimming efficiency and the influence of morphology on swimming costs in fishes. *Journal of Comparative Physiology B: Biochemical, Systemic, and Environmental Physiology*, **176**, 17–25

Oota, S. & Saitou, N. (1999) Phylogenetic relationship of muscle tissues deduced from superimposition of gene trees. *Molecular Biology and Evolution*, **16**, 856–867

Palstra, A. P. & Van Den Thillart, G. E. E. J. M. (2010) Swimming physiology of European silver eels (*Anguilla anguilla L.*): Energetic costs and effects on sexual maturation and reproduction. *Fish Physiology Biochemistry*, **36**, 297–322

Parsons, G. R. (1990) Metabolism and swimming efficiency of the bonnethead shark *Sphyrna tiburo*. *Marine Biology*, **104**, 363–367

Persistor Instruments Inc. (2010) *Persistor(R) CF2*, http://www.persistor.com/

Pettersson, L.B. & Hedenstrom, A. (2000) Energetics, cost reduction and functional consequences of fish morphology. *Proceedings of the Royal Society of London. Series B, Biological Sciences*, **267**, pp. 759–764

Philips, A. B., Blake, J. I. R., Smith, B., Boyd, S. W. & Griffiths, G. (2010) Nature in engineering for monitoring the oceans: Towards a bio-inspired flexible AUV operating in an unsteady flow. *Proceedings of the Institution of Mechanical Engineers, Part M: Journal of Engineering for the Maritime Environment*, **224**, 267–278

Phillips, A. B., Furlong, M. E. & Turnock, S. R. (2007) The use of computational fluid dynamics to assess the hull resistance of concept autonomous underwater vehicles. In *Oceans 2007 – Europe*, Aberdeen, UK, pp. 1–6

Phillips, A. B., Turnock, S. R. & Furlong, M. (2010) The use of computational fluid dynamics to aid cost-effective hydrodynamic design of autonomous underwater vehicles. *Proceedings of the Institution of Mechanical Engineers, Part M: Journal of Engineering for the Maritime Environment*, **224**, 239–254

Plaut, I. (2001) Critical swimming speed: Its ecological relevance. *Comparative Biochemistry and Physiology Part A: Physiology*, **131**, 41–50

PNI (2011) *FieldForce TCM,* http://www.pnicorp.com/products/fieldforce-tcm

Prior, S. D. & White, A. S. (1995) Measurements and simulation of a pneumatic muscle actuator for a rehabilitation robot. *Simulation Practice and Theory*, **3**, 81–117

Read, D. A., Hover, F. S. & Triantafyllou, M. S. (2003) Forces on oscillating foils for propulsion and maneuvering. *Journal of Fluids and Structures*, **17**, 163–183

Reijniers, J. & Peremans, H. (2007) Biomimetic sonar system performing spectrum-based localization. *IEEE Transactions on Robotics*, **23**, 1151–1159

Roper, D. T., Sharma, S., Sutton, R. & Culverhouse, P. (2011) A review of developments towards biologically inspired propulsion systems for autonomous underwater vehicles. *Proceedings of the Institution of Mechanical Engineers, Part M: Journal of Engineering for the Maritime Environment*, **225**, 77–96

Rosen, D. S. & Trites, A. (2002) Cost of transport in steller sea lions, *Eumetopias jubatus. Marine Mammal Science*, **18**, 513–524

Sato, K., Shiomi, K., Watanabe, Y., Watanuki, Y., Takahashi, A. & Ponganis, P. J. (2010) Scaling of swim speed and stroke frequency in geometrically similar penguins: They swim optimally to minimize cost of transport. *Proceedings of the Royal Society of London B: Biological Sciences*, **277**, 707–714

Schmidt, J. (1923) Breeding places and migration of the eel. *Nature*, **111**, 51–54

Schmidt-Nielsen, K. (1997) *Animal Physiology: Adaptation and Environment, 5th* Edition. Cambridge University Press, Cambridge, UK

Smith, R. R. (1976) *Studies on the energy metabolism of cultured fish*, PhD Thesis. Ithaca, NY, Cornell University Press, New York

SNAME (1957) *8th International Towing Tank Conference,* Madrid

Stefoff, R. (2006) *Submarines*. Benchmark Books, New York

Stevenson, P., Furlong, M. & Dormer, D. (2007) AUV shapes – combining the practical and hydrodynamic considerations. In *Oceans 2007– Europe*, Aberdeen, UK

Struntz, D. J., Mclellan, W. A., Dillaman, R. M., Blum, J. E., Kucklick, J. R. & Pabst, D. A. (2004) Blubber development in bottlenose dolphins (*Tursiops truncatus*). *Journal of Morphology*, **259**, 7–20

Suleman, A. & Crawford, C. (2008) Design and testing of a biomimetic tuna using shape memory alloy induced propulsion. *Computers and Structures*, **86**, 491–499

Svedang, H. & Wickstrom, H. (1997) Low fat contents in female silver eels: Indications of insufficient energetic stores for migration and gonadal development. *Journal of Fish Biology*, **50**, 475–486

Townsend, C. R. & Winfield, I. J. (1985) The application of optimal foraging theory to feeding behaviour in fish. In Tyler, P. & Calow, P. (Eds.), *Fish Energetics: New Perspectives*. Baltimore, MD, Johns Hopkins University Press

Tytell, E. D. & Lauder, G. V. (2004) The hydrodynamics of eel swimming I. Wake structure. *Journal of Experimental Biology*, **207**, 1825–1841

U.S. Department of Agriculture (2010) *USDA national nutrient database for standard reference, release 23. nutrient data laboratory home page*, http://www.ars.usda.gov/nutrientdata

Ura, T. & Obara, T. (1999) Twelve hour operation of cruising type AUV "R-One Robot" equipped with a closed cycle diesel engine system. In *Oceans'99*, Seattle, pp. 1188–1193

Van Ginneken, V. J. T., Antonissen, E., Müller, U. K., Booms, R., Eding, E., Verreth, J. *et al.* (2005) Eel migration to the Sargasso: Remarkably high swimming efficiency and low energy costs. *Journal of Experimental Biology*, **208**, 1329–1335

Van Ginneken, V. J. T. & Maes, G. E. (2005) The European eel (*Anguilla anguilla, Linnaeus*), its lifecycle, evolution and reproduction: A literature review. *Reviews in Fish Biology and Fisheries*, **15**, 367–398

Videler, J. J. (1993) *Fish Swimming*. Springer, New York

Videler, J. J. & Nolet, B. A. (1990) Costs of swimming measured at optimum speed: Scale effects, differences between swimming styles, taxonomic groups and submerged and surface swimming. *Comparative Biochemistry and Physiology Part A: Physiology*, **97**, 91–99

Webb, D. C., Simonetti, P. J. & Jones, C. P. (2001) SLOCUM: An underwater glider propelled by environmental energy. *IEEE Journal of Oceanic Engineering*, **26**, 447–452

Webb, P.W. (1975) Hydrodnamics and energetics of fish propulsion. *Bulletin Fisheries Research Board of Canada*, **190**, pp. 1–158

Webb, P. W. (1998) Entrainment by river chub *Nocomis micropogon* and smallmouth bass *Microtperus dolomieu* on cylinders. *Journal of Experimental Biology*, **201**, 2403–2412

Webber, D. M. & O'dor, R. K. (1986) Monitoring the metabolic rate and activity of free-swimming squid with telemetered jet pressure. *Journal of Experimental Biology*, **126**, 205–224

Weihs, D. (1989) Design features and mechanics of axial locomotion in fish. *American Zoology*, **29**, 151–160

Williams, R. & Noren, D. P. (2009) Swimming speed, respiration rate, and estimated cost of transport in adult killer whales. *Marine Mammal Science*, **25**, 327–350

Williams, T. M. (1999) The evolution of cost efficient swimming in marine mammals: Limits to energetic optimization. *Philosophical Transactions of the Royal Society B: Biological Sciences*, **354**, 193–201

Winberg, G. G. (Ed.) (1971) *Methods for the Estimation of Production of Aquatic Animals*. Academic Press, London and New York

Wolf, M. I., Licht, S. C., Hover, F. & Triantafyllou, M. S. (2006) Open loop swimming performance of 'Finnegan' the biomimetic flapping foil AUV. In *Sixteenth (2006) International Offshore and Polar Engineering Conference*, San Francisco, CA, USA, May 28–June 2

Yu, J., Hu, Y., Huo, J. & Wang, L. (2009) Dolphin-like propulsive mechanism based on an adjustable Scotch yoke. *Mechanism and Machine Theory*, **44**, 603–614

Zhou, C., Wang, L., Cao, Z., Wang, S. & Tan, M. (2007) Design and control of biomimetic robot fish FAC-1. In Kato, N. & Kamimura, S. (Eds.), *Biomechanisms of Swimming and Flying: Fluid Dynamics, Biomimetic Robots, and Sports Science*. Tokyo, Japan, Springer

Appendix 2.3. Mission based Optimum System Selector for Bio-inspired Unmanned Untethered Underwater Vehicles

Haroutunian M. and Murphy A.J. (2012). "Mission based Optimum System Selector for Bio-inspired Unmanned Untethered Underwater Vehicles". In: Autonomous Underwater Vehicles (AUV2012) conference, 24th -27th September 2012. Southampton, UK.

Mission based Optimum System Selector for Bio-inspired Unmanned Untethered Underwater Vehicles

Maryam Haroutunian
School of Marine Science and Technology,
Armstrong Bld.
Newcastle University, NE1 7RU
Newcastle upon Tyne - UK
maryam.haroutunian@ncl.ac.uk

Dr. Alan J Murphy
School of Marine Science and Technology,
Armstrong Bld.
Newcastle University, NE1 7RU
Newcastle upon Tyne - UK
a.j.murphy@ncl.ac.uk

***Abstract*—This paper is a part of the Nature in Engineering for Monitoring the Oceans (NEMO) project, investigating bio-inspiration to improve the performance of Unmanned Untethered Underwater Vehicles (UUUVs). Since biological systems (i.e. marine animals) are natives to the oceans, successfully surviving through time, they have been the source of this approach.**

NEMO's earlier investigations highlighted biological capabilities desirable for UUUV operations, including speed, speed range and manoeuvrability. These are significantly superior compared to current engineered systems. However, not all desirable characteristics are evident in the same species. Considering the mismatch between the "missions" of biological and engineered systems, no single specific biological system is able to fulfil all the desired UUUV mission requirements. Therefore, means are required to obtain the myriad of information from the biological world and adjust them to engineering needs.

This paper describes the algorithm of an Optimum System Selector (OSS) demonstrating its methodology and explaining modules such as estimating the drag of biological systems and indication of their propulsive efficiency. The OSS is implemented to output the appropriate combination for a bio-inspired UUUV design, based on its mission.

The OSS comprises missions as inputs, the decision maker, and the outputs. Mission profiles also account for capabilities unique to biological systems such as high manoeuvrability. The decision maker takes into account three main modules; speed and propulsion, manoeuvrability and upright stability. The fitness-for-purpose function of the selector consists of the energetic cost of the proposed combination, as well as the trade-off between the three modules due to the multi-functionality of the biological systems. The output consists of body and control surfaces design, propulsion and manoeuvring systems.

Through this method, OSS is an excellent guide to transform complex biological data for the future design and development of UUUVs.

Keywords-Bio-inspiration; AUV; Mission profile; Optimisation

Nomenclature and Abbreviations

AR……..	Aspect Ratio
AUV……..	Autonomous Underwater Vehicle
A_{WS}…….	Wetted Surface Area $[m^2]$
BH……..…	Body Height $[m]$
BMS……..	Biological Marine System
BUUUV….	Bio-inspired Unmanned Untethered Underwater Vehicle
BW…….…	Body Width $[m]$
C_D……..	Drag Coefficient
C_f……..	Friction Coefficient
CFD……....	Computational Fluid Dynamics
COT…..…...	Cost of Transport $\left[{}^{J}/_{kg.m}\right]$
D_{BB}……Bare Body Drag $[N]$	
D_e……...	Equivalent Diameter $[m]$
GA……..…	Genetic Algorithm
G/B……..…	Gearbox
EL……...	Elliptical Length $[m]$
FF……...	Fitness Function
M……...	Mass $[kg]$
MOGA…...	Multiple Objective Genetic Algorithm
NN………	Neural Network
OSS……....	Optimum System Selector
P_B……...	Brake Power $[W]$
P_E……...	Effective Power $[W]$
P_H……...	Hotel Load $[W]$
P_M……...	Muscle Power $[W]$
Re…….…...	Reynolds Number
R_{Yaw}……..	Yaw Radius$[m]$
TL……...	Total Length $[m]$
U_a……...	Advance Speed $[{}^{m}/_{s}]$
U_{Max}……...	Maximum Speed $[{}^{m}/_{s}]$
U_{opt}……...	Optimum Speed $[{}^{m}/_{s}]$
U_{Turn}……..	Turning Speed $[{}^{\circ}/_{s}]$
η_C……...	Conversion Efficiency
$\propto$……...	Added Drag Coefficient
η_B…….	Behind Efficiency
η_D……...	Delivered Efficiency
η_H…….	Hull Efficiency
η_{Ped}……...	Peduncle Efficiency
η_s……...	Shaft Efficiency
η_{Total}……..	Total Efficiency

I. INTRODUCTION

Mankind has a long history in ocean exploration and exploitation. The introduction of underwater vehicles in the past few decades - especially Autonomous Underwater Vehicles (AUVs) - facilitated these explorations and has made many scientific, military and industrial operations possible in previously unreachable waters. Nowadays expectations have increased and underwater vehicle users and clients are demanding faster, more manoeuvrable vehicles that are able to reach the deepest depths of the oceans with greater endurance at lower cost.

There are various approaches to investigate possible means of improving the performance of underwater vehicles. However, the longest surviving types of underwater systems are marine animals, which will be referred to as Biological Marine Systems (BMS) in this paper. Native to the oceans, they evolve and survive the harshest conditions underwater. Nature in Engineering for Monitoring the Oceans (NEMO) project is investigating novel technologies and generating bio-inspired design techniques & implementation methods based on these BMSs to improve current underwater vehicles performance. This is achieved by fulfilling two main objectives:

- Investigating bio-inspiration, and
- Application of bio-inspiration

The main focus is on increasing the speed, manoeuvrability and depth capability of unmanned underwater vehicles while reducing weight and energy consumption.

A. *Investigating bio-inspiration: The contrast between BMS and AUV capabilities*

As part of this research, studies were carried out on means to compare BMSs with engineered vehicles, to investigate whether bio-inspiration is a promising approach. However, originally, animals are studied by scientists whereas engineers study vehicles; in bio-inspiration, the two are combined. This is where the challenge stands; the key is to understand the mechanism of both systems and unify the definitions and measurements, in order to conduct a valid comparison. One significant challenge in this research was investigating the energetics comparison of animals and vehicles. For vehicles, energetic cost is calculated from knowledge of the energy stored in the batteries and its subsequent consumption, which is well defined and specified. However for BMSs with limited available data, the calculation is rather complicated. Therefore, a formulation of the physical factors associated with biological & engineered systems energy usage was presented for energetic cost comparison [1]. Since BMSs from many and various biological classes of species are investigated in this research, there were a number of principal challenges to be overcome. These challenges were unifying body measurements, comparing speed and depth capabilities which, due to size and taxonomy differences for BMSs, proved to be complicated also comparing scientific and engineered definitions, calculations and measurement of drag and power which are explained in Section IV.

B. *A general challenge in bio-inspiration*

Gathered data for BMSs is based on experiments carried out on each animal by external sources or the authors' observations and measurements from videos and photos taken from the animals. Unlike engineered vehicles, which have a well-defined capability, the performance of a specific species is a variable depending on the physical and environmental parameters of the samples, e.g. animal body size. Consequently for a given species every characteristic is specified over a range and not given as a specific value and therefore, in many cases values are an average of multiple experiments.

By overcoming the abovementioned challenges, a database of BMSs has been gathered and the parameters are shown Table I, Table II provides some explanatory notes to Table I.

TABLE I. KNOWN PARAMETERS FOR EACH BMS

Known Characteristics	***Parameters***	***Unit or description***
Body design	Body Form	General form of the body known for BMSs; e.g. Fusiform
	Cross Section Type	General shape of the body cross sectional area
	Average Mass	$[kg]$
	Maximum body height (BH)	Greatest height of the BMS along the body
	Maximum body width (BW)	Greatest width of the BMS along the body
	Elliptical Length	Length of the equivalent ellipsoid of the BMS body
	Peduncle Length	Length of the area connecting the elliptical BMS body to the rear fin
	Total Length (TL)	Overall length from the snout to the end of the rear fin
	"a" & "b" factors (*)	$\text{Mass} = \text{a}(\text{Length})^{\text{b}}$
Taxonomy (**)	Full name	Common Name & Binominal Name
	Family, Order, Class	-
Swimming	Swimming Mode	Various body & rear fin or paried fin swimming modes; e.g. Thunniform
	Optimum Speed	$Uopt\ [\frac{m}{s}]$
	Maximum Speed	$Umax\ [\frac{m}{s}]$

Known Characteristics	***Parameters***	***Unit or description***
Manoeuvring (***)	Turning (yaw) radius	R_{Yaw}
	Turning Speed	U_{Turn}
Control surfaces: Rear fin Side fins Top fin(s) Bottom fin (s) Side stabilising fins	Numbers or pairs	-
	Chord	$[m]$
	Span	$[m]$
	Area	$[m^2]$
	Aspect ratio	$AR = \frac{Span \times Chord}{Area}$
	Position from the snout	$[m]$
Diving	Maximum Depth	$[m]$
	Depth Range	$[m]$
Energetics	Cost of transport	$\left[\frac{J}{kg.m}\right]$
	Endurance (****)	$[km]$ or $[h]$
	Fat tissue storage	Can aid to estimate the energy reserve

TABLE II. EXPLANATORY NOTES TO TABLE I

Note	**Description**
*	Empirically obtained for each species based on measurements
**	All data is not available for every species, therefore taxonomy helps to relate data collected to similar animals. In this research taxonomy data are coded numerically for simplicity.
***	Turning speed is inversely proportional to the speed of the animal, therefore maximum turning speed and lowest yaw radius is usually achieved by unpowered turns. An example of conducted experiments on various marine mammals illustrates this fact [2].
****	Usually measured during long migration.
Note that all parameters are not known for the more than 200 animals in the database, therefore only the ones with available data are used when deriving calculations.	

A similar database was gathered for AUVs and the body design, speed and depth capabilities, manoeuvrability and energetics of various classes of marine species were compared with current AUVs. As a result of these comparisons, capabilities of BMSs with significant superiority over AUVs were identified; these characteristics, which include speed, speed range and manoeuvrability, were highlighted across a broad range of species [3]. The next step is to find a means to apply them to AUV design.

This paper explains the challenges involved in the application of bio-inspiration to AUV engineering. The rationale behind an Optimum System Selector (OSS) is explained and its algorithm described; this includes demonstrating its methodology and explaining its modules. The purpose of the described selector is to output the appropriate parameters required to aid the design of a bio-inspired UUUV, based on the vehicle's mission.

II. APPLICATION OF BIO-INSPIRATION

In order to apply the findings of this earlier research to Bio-inspired Unmanned Untethered Underwater Vehicle (BUUUV) design, the design procedure of BMSs must be understood and as for any other system the "purpose" or mission plays an important role. For an AUV user, "best" option is not always the vehicle that does the maximum in any single performance characteristic, but the one that fulfils the requirements of the user across a combination of speed capability and range, manoeuvrability, depth capability, endurance, energetic cost and weight. Therefore, the bio-inspired technology should attempt to find the optimum option that nature has to offer for a corresponding AUV mission.

While missions are not formally defined for BMSs, they are in fact a consequence of an evolutionary process, subject to highly varied evolutionary pressures. Consequently, some are highly manoeuvrable, e.g. black ghost, some exhibit high speed, e.g. sailfish, and some have high acceleration characteristics, such as the barracuda. Although animals are highly capable, their main aim is to survive and reproduce and the data gathered from them can always be biased by other factors such as the physical and mental condition of the BMS at the time of data collection.

However, AUV missions are varied and different to ones of an animal; in addition, the superiority of BMSs is spread over a wide range of marine animals and they use various methods and systems which are interrelated with their other functions; i.e. no specific BMS is able to fulfil all desired mission profiles of an AUV. In addition, unlike engineered vehicles, BMSs sub-systems are multi-functional, which makes it impossible to investigate them as stand-alone systems.

For an engineering perspective, therefore, it is not a complete BMS that is sought, rather particular sub-systems of BMSs; which of course is unnatural and defines the challenge that this research attempts to overcome.

In addressing this challenge a simple approach could be to search the database of BMSs and find a system which fulfils all engineering requirements.

As part of the research this simple approach was examined. Consider the algorithm in Figure 1 as the system selector for a BUUUV; for each mission scenario, mission requirements are input to the selector and the capabilities of BMSs is gathered in a large database as shown in Table I. These capabilities are then sorted based on fulfilling each mission requirement and the most capable BMSs are extracted; however:

1. Many of the BMSs will be excluded from the sorting system due to failing even a single mission requirement.

2. Since overall ranking is considered based on how much of the mission is fulfilled by the system, in many mission scenarios, systems with close ranks would vary in capabilities.

3. This system only selects the existing best option but cannot consider "optimisation".

This method therefore provided little useful insight to assist the design of a BUUUV. Therefore, means are required to output the appropriate combination for a bio-inspired design based on a particular mission profile. This is called the Optimum System Selector (OSS). OSS attempts to solve the abovementioned challenge of associating biological capability with engineering requirement.

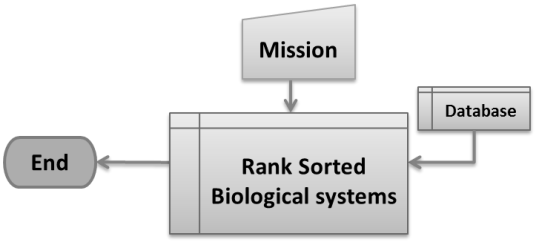

Figure 1 Simple algorithm to find best biological option

III. The Concept of an Optimum System Selector (OSS)

Figure 2 shows the algorithm modified for the OSS. In this algorithm, for every input, the BMS database is compared against the desired mission specifications; similar to the initial algorithm in Figure 1. If the requirements are met by any BMS, then the corresponding system is the output; however, for many mission profiles that is not the case and instead subsets of BMSs which meet at least one of the mission specifications are selected.

To optimise this initial subset, a decision maker is used. In nature, this is done through breeding and evolution; therefore being inspired by nature, the decision maker is designed to accelerate evolution by using a genetic algorithm (GA).

GAs take an initial potential group as parents and breed a new generation. The off-spring are then evaluated and ones with superior performance are used as new parents for the next generation. The cycle carries on until the desired performance characteristics are fulfilled or until the continuation of the GA will not improve the results any further. In this research, due to numerous influencing factors, there are multiple equations to be solved simultaneously; therefore a Multiple Objective Genetic Algorithm (MOGA) is implemented within the OSS.

The desired mission specifications are input as the GA constrains and the BMS subset from the database of existing species is input as the first generation.

The initial selection of the BMSs also ensures that animals that are by no means fit to fulfil any of the mission requirements are eliminated at an early stage to facilitate the task of the decision maker.

The decision maker then generates off-springs of the initial BMSs as a new generation, calculates their performance, and based on the mission input targets, decides which ones survive and the process continues until the desired results are achieved.

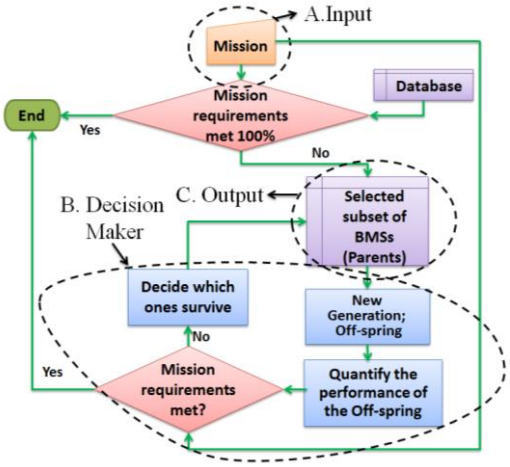

Figure 2 The algorithm modified for the OSS

The sub-algorithms of the OSS as indicated by dashed lines in Figure 2 are:

A. Missions

B. The Decision maker, and

C. Output;

These are explained next.

A. Missions

Desired AUV mission specifications are specified by the user. A manoeuvrability factor is included which may be achieved by using biological techniques as explained in Section IV. These mission specifications are shown in Table III.

The term "importance weight factor" for each mission specification is used to weight it against other inputs when evaluating the overall performance of systems and making the decision on the optimum off-spring. These are used to derive the weight factor, w_i, in (1).

TABLE III. Mission Inputs

Input	*Sub-input(s)*	*Unit(s)*
Size	Body length (EL)	$[m]$
	Mass (M)	$[kg]$
Speed	Optimum speed (U_{opt})	$[m/s]$
	Maximum speed (U_{Max})	$[m/s]$
Depth	Maximum Depth	$[m]$
Energetics	Energetic cost of Transport (COT)	$[J/kg.m]$
	Endurance	$[km$ or $h]$
Manoeuvrability	Turning Radius (R_{Yaw})	$[m]$
	Turning speed (U_{Turn})	$[°/s]$
Importance weight factors		

B. The decision maker

The decision maker takes the selected sub-set of BMSs and produces off-spring with optimised performance. Optimising the performance of the off-spring consists of minimising the energetic cost of the off-spring, as well as the trade-off between speed and propulsion, manoeuvrability, and stability due to the multi-functionality of the BMSs. As mentioned previously, these are known for the parents, but they must be calculated for the subsequent generations which are defined by the genetic algorithm. Since the decision maker makes the selection based on the estimated performance of the off-springs, it is crucial to minimise the calculation or estimation error.

However, due to the complexity of BMSs and data being sparse, for the purpose of this research a variety of methods are used. The parameters are divided into two groups as follows:

- Calculable Parameters which include body drag, energetic cost, efficiency, stability and body flexibility. These parameters are calculable by deriving formulae based on physical arguments or trends discovered by analysing the performance of BMSs from the data on existing species.

- Complex parameters which include manoeuvrability and defining propulsion mode. These parameters are a consequence of the multi-functionality of the systems; therefore it is necessary to understand the impact of each parameter to the overall performance of the system. However, some parameters are either dependent on multiple variables, various systems are involved to perform the task (multi-functionality) or the relations are non-linear. These parameters are difficult to estimate with a one-fits-all method. To solve this challenge, Neural Networks (NN) are being investigated to estimate the relation of the variables and predict the desirable parameters.

The details of the calculations and estimations are explained in Section IV. All the formulae defined and used in this research are tested against the first generation of BMSs to ensure their validity.

C. Output

The final off-spring generation produced by the decision maker is sorted in order by using linear programming which uses a Fitness Function (FF) [4] in the form of:

$$a_1 w_1 + a_2 w_2 + \cdots + a_n w_n = FF \qquad (1)$$

Where w_1 is the importance weight factor of each parameter and a_i is calculated as:

$$a_i = \frac{Value_{Obtained} - Value_{Desired}}{Value_{Desired}} \qquad (2)$$

e.g. for speed a_i is calculated as:

$$a_i = \frac{\mathrm{U}_{off-spring} - \mathrm{U}_{\mathrm{Desired}}}{\mathrm{U}_{\mathrm{Desired}}} \qquad (3)$$

The sorted collection will output specifications for body geometry, control surfaces & propulsion method and an estimate of speed and energetic cost. Outputs are shown in TABLE IV; the 2nd column is output directly generated by the OSS and the 3rd column can be then derived from these output parameters.

TABLE IV. OUTPUTS OF THE OSS

Categories	***Outputs from the OSS***	***Later stage output***
Size	EL, BH, BW $[m]$	Propulsion mode
	$Mass$ $[kg]$	
Speed	U [m/s]	
Maneouvrability	Flexibility No.	
	Turning Radius [m]	-
Body control surfaces (Important for stability, diving and surfacing, propulsion & manoeuvre)	Area of each control surface	Chord, span and length of the control surface
Energetics	Transport cost	-
Overall efficiency	Overall efficieny	-

IV. CALCULATION OF PARAMETERS

This section describes the details of calculations required to quantify the specifications of the off-spring generated by the decision maker. These are as follows:

A. Calculation of the energetic cost

B. Estimate of stability

C. Manoeuvrability assessment

D. Swimming mode selection

Each method will be explained next.

A. Calculation of the energetic cost

As explained by Phillips et al [1], the energetic cost of transport for biological and engineered vehicles is calculated as:

$$COT = \frac{P_H}{MU} + \frac{D_{BB}}{\xi M} \qquad (4)$$

where M is the mass,

U is the speed,

D_{BB} is the bare body drag,

P_H is the hotel load, and

$$\xi = \frac{\eta_{Total}}{\propto} \qquad (5)$$

where η_{Total} is the total efficiency and

$\propto$ is a coefficient which accounts for additional components of drag caused by

appendages such as control surfaces, body roughness and gills of BMSs.

It is evident from literature that the definition of total efficiency is inconsistent when applied to BMSs and in some cases unclear; therefore to elaborate further on the definition of η_{Total}, this is given special treatment in Section V.

To solve (4), U and M are known and P_H is estimated using an empirical formula in the form of $P_H = \mathrm{x}(Mass^{y})$ obtained from multiple sources as discussed by Phillips et al [1]. Drag and ξ must be calculated.

Although BMSs have a wide speed range, two specific speeds have significant importance when investigating the performance of systems; optimum speed, U_{opt}, and maximum speed, U_{max}, and COT is calculated for these two speeds. The optimum speed of a BMS is the speed at which the energetic cost is minimum and is marginally lower than cruising speed. In engineering terms this is referred to as the economic speed of the vehicles.

- Calculation of drag

In engineering bare body drag, D_{BB}, is calculated as:

$$D_{BB} = 0.5\rho C_D A_{WS} U^2 \tag{6}$$

Where:

C_D is the drag coefficient and A_{WS} is the wetted surface area and both must be estimated to calculate drag. As part of this research it has been concluded that, for the purposes of providing sufficiently accurate drag estimates, BMSs body forms can be idealised using a tri-axial ellipsoid [3], as illustrated in Figure 3. From this wetted surface area and drag coefficient can be estimated.

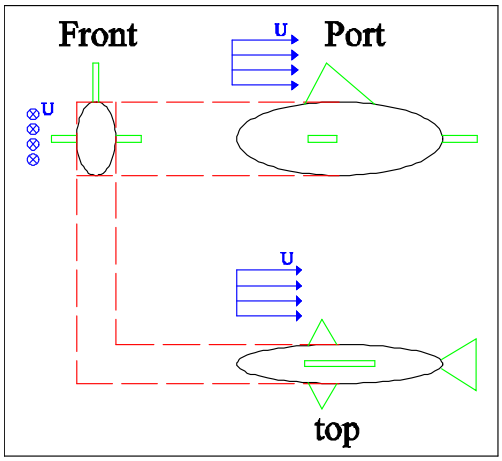

Figure 3 Three-view schematic design of a Marine Mammal

Although no analytical formula is defined to calculate the surface area of a tri-axial ellipsoid, a number of approximation formulae exist and the one used in this research is the Knud-Thomsen formula [5] which estimates A_{WS} with less than 1% error.

The Knud-Thomsen formula for a BMS is:

$$A_{WS} = \pi\left(\frac{\left(EL(BW+BH)\right)^{1.6075} + (BW \times BH)^{1.6075}}{3}\right)^{\frac{1}{1.6075}} \tag{7}$$

Where BW and BH are maximum body width and height and EL is elliptical length. EL is used as the length of the main body, instead of total length, TL, or standard length, SL. This is because TL includes the rear fin and SL includes the length of the peduncle.

The drag coefficient is in the form of:

$$C_D = C_f(1+k) \tag{8}$$

Where C_f is the friction coefficient and $(1+k)$ is the form factor.

To estimate C_f for vehicles the Prandtl-von Karman formula is used, that is:

$$C_f = 0.072Re^{-0.2} \tag{9}$$

Where Re is the Reynolds number.

The values obtained by using this formula were compared to examples tested in CFD software and the results show less than 4% error.

Hoerner, 1965 [6] estimates the $(1+\mathrm{k})$ value, for Spheroids:

$$1 + k = 1 + 1.5\left(\frac{BD}{EL}\right)^{\frac{3}{2}} + 7\left(\frac{BD}{EL}\right)^{3} \tag{10}$$

where BD and EL are the diameter and length of the spheroid respectively. The equivalent diameter for a tri-axial ellipsoid can be calculated from (11).

$$D_e = \sqrt{BH \times BW} \tag{11}$$

By substituting D_e in (11), for BD in (10), the results obtained using (10) closely correspond with results from CFD, therefore results from Hoerner, 1965 formula are valid estimates of the form factor for a tri-axial ellipsoid.

- Estimate of ξ_{Uopt}

As mentioned earlier, COT must be calculated for optimum and maximum speed (U_{opt}, and U_{max}), therefore ξ must be estimated for these two speeds.

To estimate ξ at optimum speed, ξ_{Uopt}, COT is differentiated with respect to U:

$$\frac{dCOT}{dU} = \frac{1}{M}\left(\frac{-P_H}{U^2} + \frac{1.8 \times bU^{0.8}}{\xi}\right) \tag{12}$$

The optimum COT is found at the speed, U_{opt}, when $\frac{dCOT}{dU} = 0$.

Therefore,

$$\xi_{Uopt} = \frac{1.8bU_{opt}{}^{2.8}}{P_H} \quad (13)$$

where b is:

$$b = 0.5\rho(1+k) \times 0.072\left(\frac{10^6 EL}{1.19}\right)^{-0.2} \times A_{WS} \quad (14)$$

- Estimate of ξ_{Umax}

For vehicles motor brake power is related to efficiency as follows:

$$P_B = U \times D_{BB} \times \frac{\propto}{\eta_{Total}} \quad (15)$$

Where P_B is the motor brake power; therefore:

$$\xi_{Umax} = \frac{Umax \times D_{BB_{Umax}}}{P_{B_{Umax}}} \quad (16)$$

To estimate ξ at maximum speed, ξ_{Umax}, the propulsion power at maximum speed must be quantified. For BMSs muscle power corresponds to the motor power and the power output of both red and white muscle fibres have been obtained from reference [7].

ξ_{Umax} is estimated by substituting the maximum available muscle powers in (16).

At this point all terms to calculate COT are known and (4) can be solved.

B. Estimate of stability

For the purpose of this research three main stabilities are considered for underwater vehicles as follows:

- **Yaw stability** is provided by the top and bottom fins and increases with increasing area of those fins. This improves manoeuvrability but increases appendage drag and hence ∝.
- **Pitch stability** is provided by a relatively flat body and is therefore increased with the value of $\frac{BW}{BH}$. This stability is useful when diving and surfacing but reduces the yaw stability.
- **Roll stability** is provided by side fins and increases with increasing area of those fins. This improves upright stability but increases appendage drag and hence ∝.

Based on the importance of each specification the OSS will select one of a few possible options for different missions; e.g. if pitch stability is more important than yaw stability, the off-spring with higher $\frac{BW}{BH}$ will be ranked higher.

C. Manoeuvrability assessment

Many parameters are involved in the manoeuvrability of a vehicle. One term which is specific to BMSs is flexibility. Although it is difficult to quantify flexibility, it is required to have an understanding of the effects of it on manoeuvrability. Therefore, investigations are being carried out to quantify the flexibility of a BMS by comparing their ability to turn with one of a solid body.

It is possible to estimate a flexibility number, however, predicting the manoeuvrability of a system is difficult because it depends on the area of the fins, the propulsion mode, the stability, the flexibility of the system, etc. For this purpose a neural network is being investigated to estimate the manoeuvrability of a system by predicting the turning radius based on known parameters.

D. Swimming mode selection

The resistance and propulsion characteristics are calculated numerically as discussed in this paper, and specifications of BUUUVs are selected by the OSS. From these calculations the swimming mode type can be determined by estimating what mode would be likely to achieve the outcomes of the OSS, based on observations from existing BMSs. This is achieved by using a categorising neural network. This particular network is trained by the available data for the BMSs and the existing data are categorised into various biological propulsion modes. The data of off-spring are then input into the trained neural network. The result is the swimming mode most appropriate for the off-spring.

V. DEFINITION OF EFFICIENCY

This section provides a detailed explanation of propulsion energy usage for BMSs and AUVs. This is to resolve the issue of inconsistent and unclear definitions and use of propulsive efficiency when applied to BMSs, as noted in Section II. This leads to a clear and consistent definition of propulsive efficiency.

Batteries are the energy store of AUVs which corresponds to food and fat for marine animals. As energy flows from the battery to eventually move the vehicle forward, some energy losses occur from the system. Figure 4.a illustrates the flow of power and efficiency relationships in an AUV propulsion system and Figure 4.b. is the equivalent concept presented for a BMS. Table V provides explanatory notes to Figure 4.

From the descriptions in Table V, it is realised that the total efficiency for BMSs, η_{Total}, is:

$$\eta_{Total} = \frac{DU_{BMS}}{\mathrm{P_M}} \quad (17)$$

Where D is the drag,

U_{BMS} is the BMS speed and

P_M is the muscle power.

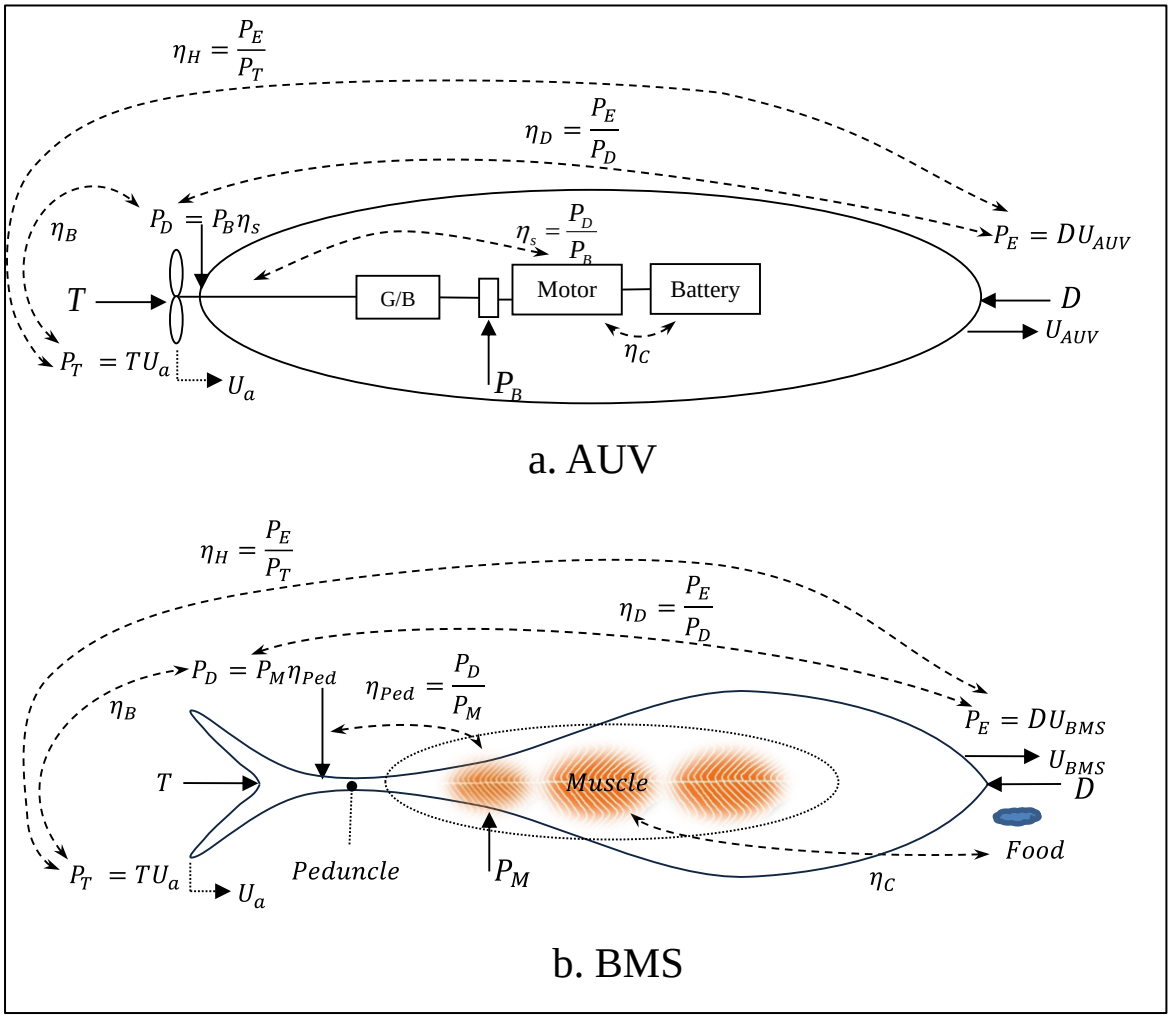

Figure 4 Comparison of power delivery in engineered vehicles and BMSs

TABLE V. EXPLANATORY NOTES TO THE POWER TRANSITIONS AND EFFICIENCIES ILLUSTRATED IN FIGURE 4

Process in AUV	Corresponding Process in BMS
Energy is lost when chemical energy in the battery is converted into electrical energy in the motor.	Energy loss when food and fat are converted into protein for muscle operation. (*)
In this research the efficiency associated with this this energy loss is called the conversion efficiency, η_C	Similar to an AUV
Energy is lost from friction when it is transferred through the drive chain to the propulsor.	Energy loss when energy is transferred from the muscle to the tail through the peduncle.(**)
The efficiency associated with this energy loss is known as the transmission, or shaft efficiency, η_s. $\eta_s = \frac{P_D}{P_B}$ Where P_D is the delivered power to the propeller and P_B is the brake power from the motor	The efficiency associated with this energy loss is the peduncle efficiency, η_{Ped}. $\eta_{Ped} = \frac{P_D}{P_M}$ Where P_D is the delivered power to the rear fin (the tail) and P_M is the muscle power
Energy is lost due to the propeller working in the flow field behind the AUV. In the desipline of naval architecture this is usually considered in two parts, namely with the propeller operating in the so-called open water condition with another adjustment for the effect of the wake behind the vehicle.[8]	Energy is lost due to the tail working in the flow field behind the BMS.
The efficiency associated with this energy loss is known as the "behind efficiency", η_B. $\eta_B = \frac{P_T}{P_D}$ Where P_T is the thrust power and is calculated as: $P_T = TU_a$ Where T is the thrust and U_a is the advance speed	In this research the efficiency associated with this energy loss is called the behind efficiency, η_B. $\eta_B = \frac{P_T}{P_D}$ Where P_T is the thrust power and is calculated as: $P_T = TU_a$ Where T is the thrust and U_a is the advance speed Note that T for a flapping tail is the mean net thrust derived over a complete oscillation.

<table>
<tr><td>There is a difference between the power developped at the propeller as compared to the effective power of the AUV overcoming drag at a given AUV speed.</td><td>There is a difference between the power developped at the tail compared to the effective power of the BMS overcoming drag at a given speed.</td></tr>
<tr><td>This power loss is referred as the hull efficiency, η_H.
$$\eta_H = \frac{P_E}{P_T}$$
Where $P_E$is the effective power and is calculated as:
$$P_E = DU_{AUV}$$</td><td>This power loss can be referred to as the hull or BMS body efficiency, η_H.
$$\eta_H = \frac{P_E}{P_T}$$
Where $P_E$is the effective power and is calculated as:
$$P_E = DU_{BMS}$$</td></tr>
<tr><td colspan="2">From the explanations given above:</td></tr>
<tr><td>$$\eta_{Total} = \eta_s \times \eta_B \times \eta_H$$
and in fact:
$$\eta_B \times \eta_H = \eta_D = \frac{P_E}{P_D}$$
Where η_D is the delivered efficiency, therefore:
$$\eta_{Total} = \eta_s \times \eta_D = \frac{P_E}{P_B} = \frac{DU_{AUV}}{P_B}$$</td><td>$$\eta_{Total} = \eta_{Ped} \times \eta_B \times \eta_H$$
And in fact:
$$\eta_B \times \eta_H = \eta_D = \frac{P_E}{P_D}$$
Where η_D is the delivered efficiency, therefore:
$$\eta_{Total} = \eta_{Ped} \times \eta_D = \frac{P_E}{P_M} = \frac{DU_{BMS}}{P_M}$$</td></tr>
<tr><td colspan="2">In BMS:
* Food corresponds to the battery and muscle to the motor of an AUV.
** Peduncle corresponds the propeller shaft and the propulsion fin; e.g. the tail to the propeller of an AUV</td></tr>
</table>

In much of the literature which considers the locomotive and/or propulsive efficiency of BMSs, it is often unclear where the starting point in the energy flow in Figure 4 is. Therefore, claims of very high propulsive efficiency are often quoted as being a "total" efficiency, whereas, in reality they are more likely one of the sub-set of the efficiency terms illustrated in Figure 4 and explained in Table V which by definition will be higher than the real total efficiency.

VI. CONCLUSION

The superior performance of BMSs is apparent compared to engineered vehicles; however, no specific system is able to completely fulfil desired AUV mission requirements.

In this paper an Optimum System Selector (OSS) is described which combines BMSs to find an optimised solution for specific desired mission specifications. Therefore, it is crucial to calculate accurately the performance of the off-spring generated by the MOGA. The use of these calculation methods were described and justified in this paper.

Through considering multi-functionality and interaction of various biological sub-systems, OSS is an excellent guide to transform complex biological data for future vehicle design.

To realise the full potential of bio-inspiration, research is continuing by resolving the flexibility and depth-capability challenges and estimating the efficiency of the systems accurately.

ACKNOWLEDGMENT

NEMO is a collaboration between Newcastle University (NCL), University of Southampton (UoS) and the National Oceanography Centre (NOC) and it is sponsored by the Engineering and Physical Sciences Research Council (EPSRC) - Funding reference: EP/F066767/1.

REFERENCES

[1] Phillips, A. B., Haroutunian, M., Man, S. K., Murphy, A. J., Boyd, S. W., Blake, J. I. R. & Griffiths, G. (2012-a). "Nature in Engineering for Monitoring the Oceans: Comparison of the energetic costs of marine animals and AUVs". In: Sutton, R. and Roberts, G. (Ed.) Further Advances in Unmanned Marine Vehicles. The Institution of Engineering and Technology (IET). ISBN: 978-1-84919-479-2

[2] Fish, F. E. (2002). "Balancing Requirements for Stability and Maneuverability in Cetaceans". In: Integrative and Comparative Biology. Vol. 42, no. 1, pp. 85-93. DOI: 10.1093/icb/42.1.85

[3] Murphy, A.J. and Haroutunian, M. (2011). "Using Bio-Inspiration to Improve Capabilities of Underwater Vehicles". In: 17th International Unmanned Untethered Submersible Technology Conference (UUST 2011), 21-24 August, Portsmouth-USA. Curran Associates, Inc. pp. 20-31. ISBN: 978-1-61839-927-4

[4] Kreyszing, E. (1999). "Advanced Engineering Mathematics". John Wiley & Sons. 8th Edition, p.994. ISBN-10: 047133328X.

[5] Michon, G. P. (2012). "Final Answers". URL: http://www.numericana.com/answer/ellipsoid.htm. [Accessed: 04.2012]

[6] Hoerner, S. F. (1965). "Fluid-Dynamic Drag. Theoretical, experimental and statistical information". Hoerner Fluid Dynamics.

[7] Altringham, J. D. and Johnston, I.A. (1990)."Modelling Muscle Power output in a Swimming fish". In: Journal of experimental biology.Vol.148, pp.395-402.

[8] Lewis, Edward V., Principles of Naval Architecture, Society of Naval Architects and Marine Engineers, 1989, Volumes II.